Stellar Polarimetry

David Clarke

WILEY-VCH

David Clarke

Stellar Polarimetry

Related Titles

Bohren, C. F., Clothiaux, E. E.

Fundamentals of Atmospheric Radiation
An Introduction with 400 Problems

2006
ISBN 978-3-527-40503-9

Stahler, S. W., Palla, F.

The Formation of Stars

2004
ISBN 978-3-527-40559-6

Foukal, P. V.

Solar Astrophysics

2004
ISBN 978-3-527-40374-5

Spitzer, L.

Physical Processes in the Interstellar Medium

1998
ISBN 978-0-471-29335-4

Thompson, A. R.

Thompson: Interferometry & Synthesis in Radio Astronomy

1986
ISBN 978-0-471-80614-1

David Clarke

Stellar Polarimetry

WILEY-
VCH

WILEY-VCH Verlag GmbH & Co. KGaA

The Author

Dr. David Clarke
Department of Physics and Astronomy
The University
Glasgow G12 8QQ
Scotland
United Kingdom

Library of Congress Card No.: applied for
British Library Cataloguing-in-Publication Data: A catalogue record for this book is available from the British Library.
Bibliographic information published by the Deutsche Nationalbibliothek
The Deutsche Nationalbibliothek lists this publication in the Deutsche Nationalbibliografie; detailed bibliographic data are available on the Internet at <http://dnb.d-nb.de>.

Printed in the Federal Republic of Germany
Printed on acid-free paper

Typesetting le-tex publishing services GmbH, Leipzig
Printing betz-druck GmbH, Darmstadt
Binding Litges & Dopf GmbH, Heppenheim

ISBN 978-3-527-40895-5

To Doreen Sara
With Thanks For An Ever Present Support Of Her
“Nutty Professor”

Contents

Stellar Polarimetry. David Clarke

ISBN: 978-3-527-40895-5

Preface

To many astrophysicists, *Stellar Polarimetry* is a Cinderella subject considered as being so insignificant and, at the same time, being so esoteric as to be ignored and left alone. Others have followed and developed the theme with an enthusiastic passion. There can be no doubt, however, that the study of polarization within Astronomy has a strong role to play either in its own right, or in combination with other observational tools, as a diagnostic for understanding the behaviour of celestial sources.

One problem is that the general topic of *Polarization* is frequently neglected in undergraduate teaching of Optics. It tends to be placed at the end of many basic courses and is then abandoned as time for presentation runs out. This may have a consequence that some Astronomers perhaps fight shy of becoming involved with its disciplines and connections to celestial sources. As time goes on, however, there is a more general awareness of what polarimetry can do for us in terms of gaining information on the geometry of astrophysical sources, and on the environments giving rise to polarized radiation. This treatise is offered to provide insight into the subject of *Stellar Polarimetry*, from a basic understanding of polarized light, to the instrumentation required to measure polarization, and to a simple overview of polarimetry as applicable to stellar radiation, particularly in the optical region of the spectrum.

From the outset it may be noted that, in general, stellar polarimetric signals are very small. Using a lax terminology, it might be said that the task of recording data is a matter of looking for an exceedingly small number of photons that are polarized amongst a very much larger number which have random relationships with respect to each other, both in terms of 'orientation' and 'phase'. With the right techniques, the task of teasing out the polarized photons can be accomplished with reward, leading to insight into some astrophysical objects that perhaps may not have been achievable by any other diagnostic technique.

In any book which aims to be a source text covering a fundamental scientific discipline, it is virtually impossible to introduce the subject and write about it without assuming that the reader is already familiar with some of the basic terms and concepts. This is certainly true of the text ahead. For example, the first chapter provides a historical overview of polarization, exploring its relationship with Astronomy, and it is impossible to do this without assuming that the reader already

Stellar Polarimetry. David Clarke

ISBN: 978-3-527-40895-5

has some inkling as to what polarization is about. It is not suggested, however, that the material presented there should be read first and digested to its full before advancing further. All that is required is that the reader has familiarity with the concepts associated with electromagnetic waves and their make-up within a beam of light. In fact the whole treatise is not one that needs to be read in the exact order of its presentation. It can be dipped into according to the interests and background of the reader.

The book comprises two parts. Chapters 1 to 9 of Part I relate to the broad history of polarization and its introduction to astronomy, to its understanding and mathematical description, to optical devices required in its measurement, to telescope practices and to some of the mechanisms that generate polarization in the radiation collected by telescopes. Part II, comprising Chapters 10 to 15, covers the observations and interpretations of the polarized light from stars. References are provided at the conclusion of each chapter or topic with their page locations given in square brackets following each citation.

When Hugo Schwarz, who tragically died so young, was undertaking a review of the literature on Astronomical Polarimetry in the early 1980s for his PhD presentation, he noted the annual growth of papers on the subject. He informed me that, by 2013, the length of library shelf space required to cope with the holding of the material would involve an annual expansion rate approaching the speed of light, and calculable only by including relativistic terms. Essentially he was correct as the numbers of papers referring to a contribution of polarimetry appear to grow exponentially. What has happened to relieve his predicted problem is the development of electronic productions giving access to papers by keyboard in the office, library, or even at the home PC.

Stellar Polarimetry has indeed blossomed with great effect over the last 25 years and it is now impossible for the subject to be given complete and comprehensive coverage with full revues of all matters. The material has been assembled with the aim of providing historical background to the development of the subject. It is now impossible to cover all aspects with a full listing of *References*. One of the remits is to present starting points for new research. Discussions on various stellar types are not full reviews for each kind of star, but are written with the aim of showing how polarization has contributed to the understanding of their nature.

There have been several giants who have pioneered and advanced Astronomical Polarimetry to the status it now holds in Astrophysics. These include the likes of Bernard Lyot, Yngve Öhman, Kris Serkowski, Jim Kemp and others and it is to their memory that this book is dedicated. One of the early inspirations for the author was the receipt of a compendium of notes produced by Öhman entitled 'Polarization Measurements in Astronomy' – Notes of Lectures presented at the University of Colorado during the Spring of 1949 – while he was a Research Fellow at Harvard University. Without those notes, imparting to me a life-long enthusiasm for all things '*Polarimetric*', this book would not have been written.

There are many others who have advanced the frontiers of *Stellar Polarimetry* and they also deserve special mention. Rather than listing them by name here, a cursory look at the citation index at the end of the text immediately reveals the presence of several key drivers who have made very substantial contributions to the subject. My admiration goes out to them, as without their inspiring work, this book would be very short of content.

Throughout my travels with *Polarimetry*, I have been accompanied by a host of colleagues, postgraduate students and friends of Glasgow University, expanding the joy of the journey, whether the times have been at the blackboard, or at the telescope. Several of them graciously accepted being harangued to don running shoes and to expand their lungs in the remote locations where astronomical observations were made. All experiences are not to be forgotten. In alphabetical order amongst those who deserve special mention are Victor Ameijenda, Andy Brooks, John Brown, Steven Fullerton, John Grainger (deceased), Paul McGale, Ian McLean, Jaber Naghizadeh-Khouei, Dirk Neumayer, Hugo Schwarz (deceased), John Simmons, Brian Stewart, Richard Smith and Alan Wyllie. I am very much in their debt in so many different ways.

Following the usual practice with the presentation of any document, this tome carries an *E* & *O* E clause – nothing to do with Ordinary and Extra-Ordinary Rays – but simply the abbreviation for Errors and Omissions Excepted. As far as the *O*missions go, apologies can only be given to those authors and researchers who feel that their work has been under-represented, or who are upset by not having particular papers referenced. By the nature of the text, it is impossible to include all the material that should rightly be discussed. The aim is to present an overview of ‘Stellar Polarimetry’, particularly from the viewpoint of its development. As for any *E*rrors, these are the sole responsibility of the author. Any suggestions for correction would be gratefully received.

Two hundred years ago, in 1808, the behaviour of light in respect of double refraction produced by Iceland Spar crystals was linked to that of its reflection from polished materials by a simple observation made by Malus at his Paris home, looking at reflections of the Sun in windows across the street. He discussed his finding by considering the corpuscular concepts of Newton and the wave theory of Huyghens. In his treatise published on 2 January 1810, he recorded his deliberations and, on page 239, coined the term ‘polarisée’, using it several times together with some of its derivatives, so introducing new words to language. These immediately jumped the channel as the work of Malus was reported in British journals. ‘Polarize’ and ‘Polarization’ were very readily used in the arena of optics from thereon. It is now apposite to celebrate the bi-centenary of the establishment of such words which are now in more common everyday use beyond the realm of optics.

Stellar Polarimetry was projected into Astrophysics in 1946 and became established in grand measure in 1948/49 through the discovery of interstellar polarization. Since then the subject has grown in many directions covering all types of stellar variables, binary stars and all manner of exotic systems. The birth of all these developments is now due for celebration as a Diamond Anniversary.

I hope that this text can be accepted at least partly in terms of a celebration marking the joint 200th and 60th anniversaries of two very importantly linked scientific events.

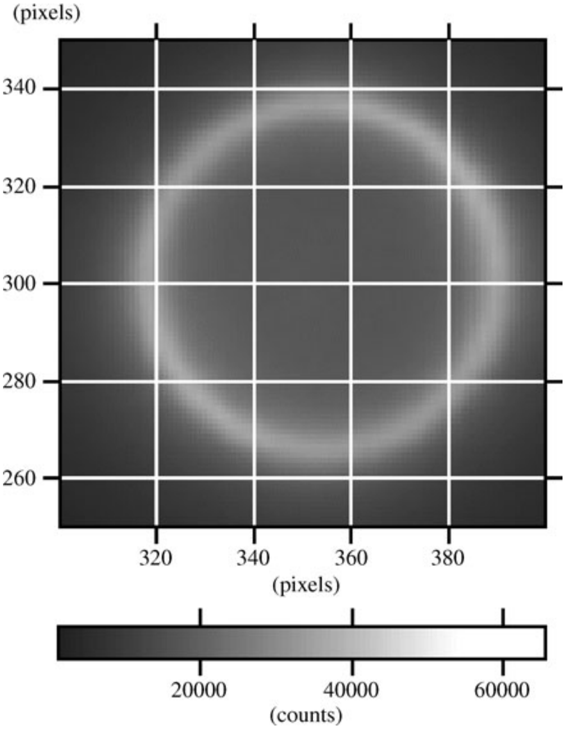

Fig. 1 An image of α Leo taken with an instrument designed for polarimetry by the detection of intensity variations around the annulus recorded by a CCD detector.

It may have been noted that one of the letters in the title of this text carries a strange font. The letter o was generated by an instrument developed to measure stellar polarization. The image was recorded and the symbol produced using the radiation from a star! (see Clarke, D. & Neumayer, D. (2002), *AA*, **383**, 360–366).

In some ways this single letter sums up the ingenuity of mankind of being able to express and write about ideas of the Universe simply by recording starlight.

Glasgow University Observatory, 1 Jan 2009 *David Clarke*

Part I History – Mathematics – Instruments – Observational Procedures – Polarigenic Mechanisms

Chapters 1–9

PROGRAMME: Astrometry and Photometry have been the basic disciplines of Observational Astronomy for centuries. Spectroscopy and Polarimetry were applied to the study of the heavens as the understanding of the nature of electromagnetic radiation grew within the scientific laboratory. The concept of polarization only emerged about 200 years ago and although it was immediately applied to celestial studies, it was just 60 years ago that it burgeoned on the stellar scene.

The history of the understanding of polarization is presented with new researched material. Mathematics related to the description of polarization is given together with the concepts associated with Stokes parameters, these being used quite generally to describe the measurements of stellar polarimetry. The expected statistical behaviour of repeated polarimetric measurements is described so that the accuracy and precision of any data can be formally assessed.

Some basic properties of optical elements are described followed by reference on how they are utilized to provide modulators within polarimetric instruments. The principles behind the measurements are described together with the required observational strategies. Finally, some of the polarigenic mechanisms likely to occur in astrophysical situations are presented.

Throughout Part I, details of all cited papers and references are collated at the end of each chapter.

Stellar Polarimetry. David Clarke

ISBN: 978-3-527-40895-5

1
Introduction and History

1.1
General History

Stellar polarimetry appeared as a green shoot in astrophysical diagnostic practice some 60 years ago. Following the early nineteenth-century discoveries of polarimetric phenomena in the physics and chemistry laboratories, and the establishment of the understanding of the transverse nature of the oscillatory disturbances within electromagnetic radiation, polarimetry lay dormant for over 100 years in its application to stars. Its dawning on the stellar scene awaited the combination of a prediction by Chandrasekhar (1946) related to the outcome of radiative transfer studies for early-type stellar atmospheres, and the simultaneous development of detector technology sufficient to make an observational response to the challenge set by theory.

With a degree of interpretive licence, the introduction of polarimetry to Astronomy may be set to an earlier millennium. Much of the early history of astronomy is bound up with application of celestial observations to determinations of local time and geographical position. It has been suggested that a navigational tool, or medieval GPS, in the form of the natural crystal (*cordierite*) with polarization properties, was used as an astrolabe by the Vikings as early as AD 1000 (see Walker, 1978). With such a device the position of the Sun, hidden by a cloud, or below the horizon, could have been determined to within 3°. It might be claimed, therefore, that polarimetry was utilised within Astronomy well in advance of the more readily appreciated diagnostic tool of spectroscopy! The concept of polarimetry as applied to the pursuit of physical understanding of the heavens did not emerge, however, until the turn of the nineteenth century, with application particularly to the Solar System, running hand in hand with the development of the subject in the optical laboratory.

The history of polarimetry within the physical sciences can be followed in a variety of optical texts and will not be expounded in detail here. A benchmark in its study was the discovery in 1669 of the birefringence of Iceland Spar by Erasmus Bartholinus (1669).[1] This phenomenon was investigated by Huyghens (1690)[2] and

---

[1] An excerpt from this work, translated into English, can be found in Swindell (1975).

[2] Again, relevant excerpts from Huygens' *Traité de la Lumière* can be found in Swindell (1975).

Stellar Polarimetry. David Clarke

ISBN: 978-3-527-40895-5

later by Malus, famous for his '$\cos^2\theta$ law', associated with the flux of light transmitted by two crystals or polarizers set with their principal axes at angle θ with respect to each other (see Malus, 1810a).

It was from an early description of the behaviour of the double refraction of Iceland Spar, and the orientational quality which appeared to be carried by light, that the connection with the root word 'pole', later to give rise to the word 'polarization', was made. In the writings of Sir Isaac Newton (see Newton, 1931), we find in 'Question 29' of Book III of his *Opticks*:

> . . . And lastly, the unusual Refraction of Island-Crystal looks very much as if it were perform'd by some kind of attractive virtue lodged in certain Sides both of the Rays and of the Particles of the Crystal . . . since the Crystal by this Disposition or Virtue does not act upon the Rays unless when one of their Sides of unusual Refraction look towards that Coast, this argues a Virtue or Disposition in those Sides of the Rays which answers to, and sympathizes with that Virtue or Disposition of the Crystal, as the poles of two Magnets answer to one another . . . I do not say that this Virtue is magnetical: It seems to be of another kind. I only say, that whatever it be, it's difficult to conceive how the Rays of Light, unless they be Bodies, can have permanent Virtue in two of their sides which is not in their other Sides, and this without any regard to their Position to the Space or Medium through which they pass.

The essential point that Newton made was that light appeared to *interact* differently with the crystal according to the orientation with respect to the crystal of some direction at right angles to the ray. It may be noted that Newton's use of the word 'Bodies' relates to his corpuscular theory for light. His reference to 'poles' was clearly an analogy to describe the observed behaviour.

In January 1808, the Paris Académie des Sciences promoted a prize for physics in 1810, the award being offered in response of a quest: 'To furnish a mathematical theory of double refraction and to confirm it by experiment'. Among those who took up the challenge was Étienne Louis Malus (1775–1812), a French army officer and engineer, who had returned in ill-health to Paris following Napolean's campaign in Egypt. The life and times of Malus have been graphically described in an essay by Kahr & Claborn (2008). With crystals of Iceland Spar to hand, Malus made a most momentous discovery related to the nature of light purely through simple curiosity.

One evening, in the autumn of 1808, while standing near a window in his home in the Rue d'Enfer in Paris, Malus looked through a crystal of Iceland Spar at the setting Sun, reflected in the windows of the Palais Luxembourg across the street. As he turned the crystal about the line of sight, the two images of the Sun seen through it became alternately darker and brighter, switching every 90° of rotation. After the Sun had set, Malus went indoors and pursued experiments with candle light reflected from the surface of water in a bowl and from a glass bottle. On that same night he was able to show that the strongest effect of intensity changes for the two refracted rays observed through the crystal occurred at particular angles of the reflecting surface, this property later being formulated by Sir David Brew-

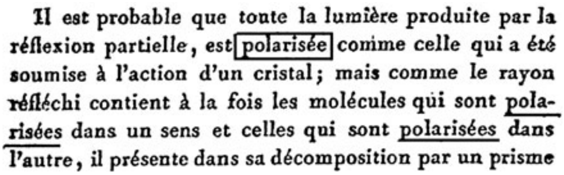

Il est probable que toute la lumière produite par la réflexion partielle, est polarisée comme celle qui a été soumise à l'action d'un cristal; mais comme le rayon réfléchi contient à la fois les molécules qui sont polarisées dans un sens et celles qui sont polarisées dans l'autre, il présente dans sa décomposition par un prisme

Fig. 1.1 The middle section of page 239 of the treatise of Malus published on 2nd January 1810 (see Malus, 1810a) records the introduction the word "polarisée" to language, three times within four consecutive lines.

ster. The fact that reflected light carried a similar property to beams produced by double refraction was presented by Malus at the Societé d'Arcueil on 12 December 1808 (see Malus, 1809a). After these preliminary discoveries, Malus investigated this peculiar orientational property associated with light by more substantial studies, including experiments on the behaviour of images seen through two crystals of Iceland Spar in sequence according to their relative orientation (Malus, 1809a, 1809b). Thus Malus had discovered the property of *polarization* associated with light, although in these early papers, use of words such as 'polarise' or 'polarisation' is absent.

According to the *Oxford English Dictionary – OED*[3] (1961), the introduction to the literature of the word *polarization* was by Malus. The etymological date provided by the 1961 Edition of *OED* is '11 March 1811', the citation taken from Malus (1811a, 1811b, 1811c), these three papers being commentaries on Malus' work. The date in the margin of the second and more important noted paper is '11 Mai 1811', later corrected to '11 Mars 1811' by an errata entry (see note in the Reference List relating to Malus, 1811b), this latter date being that referred to in the *OED*. General use of the word in the French scientific school appears prior to these dates, however. Arago had already used it and its derivatives on 18 February 1811, referring to Malus, in a paper delivered to "La Classe des Sciences Mathématiques et Physiques de L'Institut Impérial de France" (see Arago, 1858a).

The use of 'polar' as a stem word appears for the *first time* in Malus' treatise of *1810* published on *January 2nd* entitled: '*Théorie de la Double Réfraction de la Lumière dans les substances cristallisées*'. In this work, Malus (1810a) clearly describes the parallels of the properties of light reflected by optical surfaces at certain angles and the light beams produced by double refraction. The first use of the word 'polarisée' appears on page 239 of the treatise and the appropriate section is reproduced in Figure 1.1.

It is this coinage that introduces to language a term to describe the newly discovered property of light. Very shortly after, words such as 'polaris/zed' and 'polaris/zation' crossed the Channel into British scientific circles and journals. Now,

---

3) The Oxford English Dictionary intend to change the etymological details for the entry of polarization commencing with the online edition (Private Letter to the Author – 17 Dec. 2007).

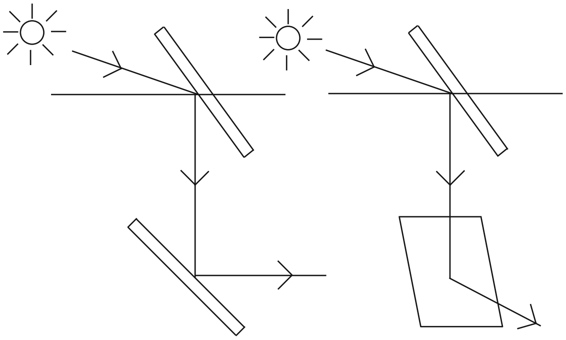

Fig. 1.2 The observational arrangement used by Malus to demonstrate the polarization property associated with light, the intensity reflected by the second mirror being dependent on its orientation relative to the first.

of course, these words appear in more general everyday use beyond their esoteric association with optics.

The reasoning for choosing these terms is apparent from three papers read before before the *Institut de France* on 11 March, 27 May and 19 August, 1811 – these being the basis of the citations included in the *Oxford English Dictionary* – but appearing in the *Mémoires de l'Institut* under the year 1810 (see Malus, 1810b, 1810c, 1810d). In the first of the papers, Malus describes an experiment using two mirrors with polished glass surfaces in the form of a heliostat (see Figure 1.2). The phenomenon relating to the polarizing effects of the surfaces was described in the following manner (translation of Malus, 1810b (pp. 105–106) by Lowry, 1964):

> Let us direct, by means of a heliostat, a ray of sunlight in the plane of the meridian, in such a way that it makes an angle of 19°10′ with the horizon. Then let us fix an untinned mirror in such a way as to reflect the beam vertically downwards. If we place a second mirror below the first and parallel to it, it will make an angle of 35°25′ with the downward ray, which will be reflected again parallel to its first direction. In this case one will not observe anything remarkable; but if this second mirror is turned so that it faces East or West, without changing its inclination to the vertical ray, it will no longer reflect a single molecule of light, either at its first or at its second surface. If, whilst keeping its inclination to the vertical ray unchanged, its face is turned towards the South, it will begin anew to reflect the ordinary proportion of incident light. In intermediate positions, the reflection will be more or less complete, according as the reflected ray approaches more or less to the plane of the meridian. In these circumstances, in which the reflected ray behaves so differently, its inclination to the incident ray is kept constant. Thus, we see a vertical ray of light which, falling on a transparent body, behaves in the same way when the reflecting surface is turned to the North or South, and in a different way when this surface is turned to the East or West, although these

> surfaces are always inclined at an angle of $35°25'$ to the vertical direction of the ray.
> These observations lead us to conclude that the light acquires in these circumstances properties which are independent of its inclination to the surface which reflects it, but are unique relatively to the sides of the vertical ray. These are the same for the South and North sides, and different from the East and West sides. Giving to the sides the names of poles, I will describe as *POLARISATION* the modification which gives to the light its properties relatively to these poles.

A translation and extension of the latter paragraph of the original article can also be found in Buchwald (1989):

> These observations lead us to conclude that light acquires in these circumstances properties that are independent of its direction with respect to the reflecting surface and that are the same for the south and north sides (of the ray), and different for the east and west sides. In calling these sides poles, I will call *polarization* the modification that gives light properties relative to these poles. I waited until now (two and a half years) before admitting this term in the description of the physical phenomena in question; I dared not introduce it in the *Mémoires* wherein I published my latest experiments; but their varieties presented by this new phenomenon and the difficulties in describing them force me to admit this new expression, which simply signifies the modification light is subject to on acquiring new properties that are related not to the direction of the ray, but only to its sides taken at right angles and a plane perpendicular to its direction.

The plane of the meridian, defined by the incident ray and the ray reflected from the first surface, was later selected to describe the 'plane of polarization'. Today we know that light has an electromagnetic nature and that the **E** component is usually the more important in general optical interactions rather than the **H** vector. According to Malus' experiments it turns out that the **E** vector oscillates *normal* to the plane of incidence and that the early definition of the *plane of polarization* corresponded to the **H** vector. Modern usage now has the *plane of polarization* at right angles to the plane of incidence as defined in Malus' experiment, although there are some texts, usually old ones, that carry the original definition.

In the second memoir, Malus (1810c) describes the partial polarization transmitted through glass being a mixture of unpolarized light and light polarized in a plane at right angles to the plane of polarization of the reflected ray. He also describes the use of a series of parallel plates, or pile-of-plates, to produce more complete polarization of the transmitted beam.

The third memoir (Malus, 1810d) describes the occurrence of double refraction in all crystals except those belonging to the cubic system, and in all vegetable and animal substances that were tested.

With his simple, but fundamental, observation in a Paris street, followed up with some simple laboratory experiments, Malus, in these great 'eureka' moments, had discovered that light contained an orientational property that was common to beams emerging from what we now refer to as birefringent crystals and to beams being reflected by material surfaces. He discussed the exciting discovery of the similarities of such beams in terms of the wave theory of Huyghens and the corpuscular theory of Newton. No doubt he was aware of Newton's description of double refraction (see above), and it was therefore natural to describe the phenomena in terms of forces acting on the corpuscules of light and to describe light beams subject to such forces in their modification by refraction or reflection as being *polarized*.

In the paper presented to La Classe des Sciences Mathématiques de l'Institut Impérial de France on 18 February 1811, Arago (1858a) neatly sums up the discovery of Malus by saying:

> La lumière se polarise non-selement dans l'acte de la double réfraction, mais encore dans d'autres circonstances très-remarquable que Malus a découvertes.

The Count Rumford Medal for 1810 was awarded by the Royal Society to Malus for his work on double refraction, it being noteworthy that excellent scientific interchange was able to exist between two countries suffering strong political divides. The letter of announcement to Malus written by Thomas Young was dated 22 March 1811.

The first usage of the term and its extension within an article in English is in *Nicholson's Journal* (1811), Volume: XXX – page 192, with a letter from Paris saying:

> Mr Malus is still pursuing with success
> his inquiries concerning *polarised* light.

Also noted in *Nicholson's Journal* (1812), Volume: XXXIII – page 345, is the fact that Malus coined the word 'polarisation' with the comment:

> By giving to these sides (of the vertical ray) the names of poles, he calls the modification which imparts to light properties relative to these poles, *polarization* ... This new expression ... signifies simply the modification that light has undergone in acquiring new properties, relative not to the direction of the ray, but solely to its *sides*, considered at a right angle, and in a plane perpendicular to its direction.

In 1801, Thomas Young firmly established that light had a wave nature through his interpretation of the phenomenon of Newton's rings. He proposed that the observed colours exist within the incident light and that wavelengths could be assigned to them through the principle of the constructive interference of waves. His double-slit experiment, again related to the interference of light, still remains a classical experiment for physics undergraduates to perform.

In the immediate years following the discovery of polarization, a major problem was the reconciliation of the behaviour of polarized light and the principles of wave theory, particularly in respect of the propagation by longitudinal disturbances. Young had pondered the problem but remained baffled by it. In 1816, he received a visit from Arago who told him of a result obtained with Fresnel in connection with the double-slit experiment, but working with polarized light. They had found that if the slits were illuminated separately using beams of polarized light with their planes at right angles, the interference phenomena were not present. (The discovery of this behaviour was not published until 1819 – see Arago & Fresnel, 1819.)

Soon after Arago's return to France, Young reflected on this result and discovered the long-sought key to the mystery. The solution turned out to have been a proposal which Bernoulli (the younger) had considered and rejected 80 years ago, of supposing that the vibrations of light are executed at right angles to the direction of propagation. According to Whittaker (1958):

> Young's ideas were first embodied in a letter to Arago dated 12 January 1817. – 'I have been reflecting,' he wrote, 'on the possibility of giving an imperfect explanation of the affection of light which constitutes polarisation, without departing from the genuine doctrine of undulations. It is a principle in this theory, that all undulations are simply propagated through homogeneous mediums in concentric spherical surfaces like the undulations of sound, consisting simply into direct and retrograde motions of the particles in the direction of the radius, with their concomitant condensation and rarefractions. And yet it is possible to explain in this theory a transverse vibration, propagated also in the direction of the radius, and with equal velocity, the motions of the particles being in a certain constant direction with respect to that radius; and this is *polarisation*.'
>
> In an article on 'Chromatics', which was written in September of the same year for the supplement to the *Encyclopaedia Britannica*, he says: 'If we assume as a mathematical postulate, on the undulating theory, without attempting to demonstrate its physical foundation, that a transverse motion may be propagated in a direct line, we may derive from this assumption a tolerable illustration of the subdivision of polarised light by reflection in an oblique plane,' by 'supposing the polar motion to be resolved' into two constituents, which fared differently at reflection.
>
> In a further letter to Arago, dated 29 April 1818, Young recurred to the subject of transverse vibrations, comparing light to the undulations of a cord agitated by one of its extremities. This letter was shown by Arago to Fresnel, who at once saw that it presented the true explanation of the non-interference of beams polarised in perpendicular planes, and that the latter effect could even be made the basis of a proof of the correctness of the Young's hypothesis; for if the vibration of each beam be supposed resolved into three components, one along the ray and the other two at right angles to it, it is obvious from the Arago–Fresnel experiment that the components in the direction of the ray must vanish; in other words, that the vibrations which constitute light are executed in the wave-front.

From thereon Fresnel took up the concept of transversality and wrote on it in very clear terms killing any idea that the vibrations could be longitudinal. Fresnel (1824a) later concluded that ‘the vibrations of a polarized beam must be perpendicular to what is called its *plane of polarization*’. Fresnel’s theory of the nature of polarized light was presented in *Mémoire sur la double Réfraction* and read before the *Académie des Sciences* on 26 November 1821, and 22 January and 22 April 1822 (see Fresnel, 1868). A most relevant passage to the advance in the understanding of the nature of polarized light is found in pages 265–266 of Fresnel (1825), and translated by Lowry (1964), reading as follows:

> . . . the luminous vibrations take place only in directions parallel to the surface of the waves . . . It suffices to admit in the ether a sufficient resistance to compression to understand the absence of longitudinal vibrations . . . Polarised light is that in which the transverse oscillations take place constantly in one direction, the ordinary light is bringing together and the rapid succession of an infinite number of systems of waves polarised in all directions. The act of polarisation does not consist in creating transverse vibrations, but in decomposing them along two fixed directions at right angles to one another, and separating the two systems of waves thus produced, either merely by their difference of velocity as in crystalline plates, or also by a difference of direction of the waves and of the rays, as in crystals cut into prisms or in thick plates of carbonate of lime; for, wherever there is a difference of velocity between the rays, refraction can make them diverge. Finally, according to the same theory, the plane of polarisation is the plane perpendicular to that in which the transverse vibrations take place.

Mention has already been made of Bernoulli (the younger) in relation to the notion that the transmission of light is accompanied by disturbances involving transverse vibrations. At the time, Bernoulli thought that all space was permeated by a fluid aether containing an immense number of excessively small whirlpools. According to Whittaker (1958), he thought that

> A source of light communicates to its surroundings a disturbance which condenses the nearest whirlpools; these by their condensation displace the contiguous corpuscles from their equilibrium position and these in turn produce condensations in the whirlpools next beyond them, so that vibrations are propagated in every direction from a luminous point. It is curious that Bernoulli speaks of these vibrations as *longitudinal*, and actually contrasts them with those of a stretched cord, which, ‘when it is slightly displaced from its rectilinear form, and then let go, performs *transverse* vibrations in a direction at right angles to the direction of the cord.’ When it is remembered that the objection to the longitudinal vibrations, on the score of polarisation, had already been clearly stated by Newton, and that Bernoulli’s aether closely resembles that which Maxwell invented in 1861–62 for the express purpose of securing

> transversality of vibration, one feels that perhaps *no man ever so narrowly missed a great discovery*.

Even more remarkable is a statement made by Thomas Hooke, 100 years previous to Bernoulli, in which he appears to have recognised that light may consist of some kind of wave disturbance with associated transversality. In his celebrated book known as *Micrographia* Hooke (1655) writes

> . . . ; for since by that Hypothesis the undulating pulse is always carried perpendicular, or at right angles with the Ray or Line of direction, it follows, that the stroke of the pulse of light, after it has been once or twice refracted (through a Prisme, for example) must affect the eye with the same kind of stroke as if it had not been refracted at all.

The nature of the Fresnel–Arago interference laws with respect to polarization has been appreciated for some considerable time, but occasionally they are re-iterated with mathematical descriptions (e. g. see Collett, 1971). It is only recently that their understanding has been expressed in erudite form by Mujat, Dogariu & Wolf (2004). In this paper the laws have been summarized as follows:

1. Two rays of light polarized at right angles do not produce any effect on each other under the same circumstances in which two rays of ordinary light produce destructive interference.
2. Rays of light polarized in the same plane interfere as rays of ordinary light, so in these two kinds of light the phenomena of interference are identical.
3. Two rays that were originally polarized at right angles may be brought to the same plane of polarization without thereby acquiring the ability to interfere.
4. Two rays of light polarized at right angles and afterwards brought into the same plane of polarization interfere as ordinary light provided that they were originally polarized in the same plane.

As it turns out, appreciation of the behaviour according to these laws is of importance to the understanding of some of the interference problems which appear in modern instruments designed to undertake spectropolarimetry, as discussed by Semel (2003), for example.

With respect to transversality, mention has been made in a quotation above to the work of Maxwell. Based on the experimental works of Faraday on electrical and magnetic phenomena, James Clerk Maxwell was able to link them through a mathematical formulation that predicts electromagnetic waves which travel with a velocity calculable from electric and magnetic constants measured in the laboratory. The predicted velocity matched the measurements of the velocity of light. In addition, Maxwell’s equations predict that the electric and magnetic oscillations associated with the progress of the waves are transverse to the direction of propagation. The nature of transversality was clearly described by Maxwell (1861) as follows:

> The velocity of transverse undulations in our hypothetical medium, calculated from the electro-magnetic experiments of MM Kohlrausch and Weber, agrees so exactly with the velocity of light calculated from the optical experiments of M. Fizeau, that we can

> scarcely avoid the inference that *light consists in the transverse undulations of the same medium which is the cause of electric and magnetic phenomena*.

Returning to the discoveries of Malus, Sir David Brewster in Edinburgh investigated reflection and refraction and, under the entry of polarization, the *Oxford English Dictionary* credits Brewster as being the first person to use the term ‘polarisation’ within a scientific paper (Brewster, 1814a). On page 188 of this paper he writes:

> A ray of light transmitted through a plate of agate cut by planes perpendicular to the laminae of which it is composed suffers *polarisation* like one of the pencils formed by double refraction.

The first scientific paper with the term ‘polarisation’ in its title also appears to have been written by Sir David Brewster (Brewster, 1814b), namely,

> ‘On the Polarisation of Light by oblique transmission through all Bodies, whether crystallized or uncrystallized.

It is interesting to note that within this paper he says:

> The celebrated discovery made by MALUS, of the polarisation of light by oblique reflection, is perhaps the most important that optics has received since the discovery of achromatic telescopes;...

Of course, such a simile would not be used today, the latter instruments now being classed as technological dinosaurs, but the resonant sentiment remains with polarization being a very important and essential aspect to our understanding of radiation. The application of polarimetry is now a well-established diagnostic in astrophysics with an ever continuing expansion of its use in both theory and observation.

A mathematical expression relating the particular angle of incidence, θ_B, for which full polarization occurs in the reflected beam was established by Brewster (1815a, 1815b) 1 year later. For an air–material interface, Brewster’s law may be expressed as $\theta_\mathrm{B} = \arctan(n)$, where n is the refractive index of the reflecting material.

Observations of the colours produced when various substances were placed following a pile-of-plates polarizer and then viewed through an Iceland Spar crystal were presented at the Institut de France on 11 August 1811 by Arago (1811, 1858b). Most of the investigated materials were birefringent crystals and he was exploring the effects of differential phase delays that they introduce between the resolved components of polarized light, although he would not have appreciated this at the time. It is noteworthy that he found that the behaviour of a plate of quartz cut with surfaces perpendicular to the principal axis of the crystal behaved very differently to plates of mica or gypsum. What he had unknowingly discovered was the fact that polarized light is rotated by some materials, this later being referred to as *circular birefringence*, and becoming the basis of a very important diagnostic in the field of molecular chemistry; the laws governing this phenomenon were investigated and established by Biot a few years later (see chemistry texts such as Lowry, 1964). Of more direct relevance to radio astronomy, rather than in the optical domain, the rotation of polarized radiation caused by the presence of a magnetic field in the transmitting medium was discovered by Faraday (1846).

Fresnel’s experiments related to total internal reflection, and the associated behaviour of polarization, led him to propose that orthogonal vibrations produce linear polarization when they are in phase, and circular polarization when they have a phase difference of $\pi/2$. In a paper (Fresnel, 1824b), he writes:

> . . . on aura une idée juste du genre de vibration lumineuse que j’ai proposé de nommer *polarisation circulaire*, en appelant *polarisation rectiligne* celle qui a été remarquée pour la première fois par Huygens dans la double réfraction du spath d’Islande, et que Malus a reproduite par la simple réflexion sur la surface des corps transparents.

In referring to polarization forms, the term ‘*circular*’ remains to this day but the word ‘*rectilinear*’ is normally reduced simply to ‘*linear*’.

In the above text, it may already have been noted that there is an alternative in spelling of the theme word and its derivatives, with both ‘s’ and ‘z’ being used. At its birth in the French language, Malus used the terms ‘polarisée’ and ‘polarisation’, the words incorporating ‘s’. Its introduction to papers written in English shows immediate spelling ambiguity. In two of Brewster’s papers (1814a, 1814b), the root word is spelled with ‘s’ whereas in a contemporaneous paper by Brewster (1814c), it employs an inconsistent mixture of both ‘s’ and ‘z’. In a paper by Faraday (1846), both the words ‘polarized’ and ‘polarising’ are used. Modern texts continue to use the alternative spellings – though usually more self-consistent. The *Oxford English Dictionary* refers only to the alternative with ‘z’; the *Collins English Dictionary* (1992) lists the use of ‘z’ with the alternative of ‘s’. Throughout this text, the ‘z’ spelling is preferred, except in verbatim quotations, and in titles of papers within the reference lists, originally using ‘s’.

More important than the arcane detail of the ‘correct’ spelling of *polarisation* is the fact that the word itself seems inapt for describing what are now known to be the statistical fluctuations of the electric vector in a beam of electromagnetic radiation. Again according to the *Oxford English Dictionary*, under the entry on the origin of the word *polarize*, it says:

> But this unfortunately assumed a sense of *pole*, quite different from its use in astronomy, geography, and magnetism with the consequence that *polarization* as applied to light and radiant heat has nothing in common with magnetic or electric polarization.

As already mentioned, the term ‘pole’ in relation to optical phenomena originates from Newton. Apart from not describing the underlying behaviour accurately, some of its derivatives such as *plane of polarization* are open to alternative interpretations. In Figure 1.3, two scenarios are depicted which cannot simply be differentiated by using the term ‘plane of polarization’. Lord Kelvin made pertinent comment on the terminology in 1884 in his Baltimore Lectures (see Lord Kelvin, 1904). In his discussions he referred to a confusing remark of Jamin’s as follows:

> . . . ‘vibrations polarisé dans le plan de l’incidence’ may have signified not that the plane of polarization but that the line of vibration, was in the plane of incidence.

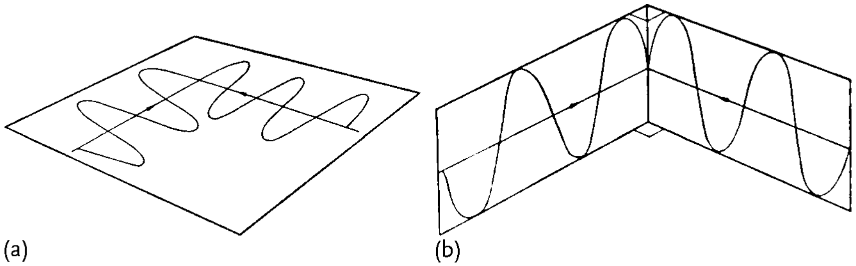

Fig. 1.3 Origins for confusion over the use of the term 'plane of polarization'. (a) depicts two light waves with the same plane of polarization, but perpendicular directions of vibration; (b) depicts two light waves with the same direction of vibration but perpendicular planes of polarization.

Lord Kelvin asterisked 'plane of polarization' and made the following comment in a footnote:

> Considering the inevitable liability to ambiguity of this kind, I have abandoned the designation 'plane of polarization' and resolved always to specify or describe with reference to vibrational lines. Abundant examples may be found … illustrating the inconvenience of the designation 'plane of polarization' were, as is now generally admitted, in the very beginning unhappily chosen words for differences of action in different directions around a ray of light. These differences are essentially not according to what we now understand by 'polar quality'.

The term 'polarization' is deemed to stay in the literature, however, there being little point in displacing it as there is no obvious alternative. It is perhaps ironic that the word associated with phenomena related to the wave nature of light should find its origin in Newton's now abandoned corpuscular theory. As for the usage of 'plane of polarization', alternatives such as *direction of vibration* appear in the literature. In astronomy the use of *position angle of the vibration*, *azimuth of the vibration* or *direction of vibration* is an attractive alternative, especially when measurements are being referred to projections against celestial coordinate systems. In addition to waves which vibrate in a particular plane (linear polarization) set at a given position angle relative to some preferred axial frame, the form of the polarization may be *elliptical* and the term 'position angle' or 'azimuth' may also be applied to the orientation of the major axis with respect to the reference frame.

1.2
Early Astronomical Polarimetry

It is interesting to note that running hand in hand with the development of the basic understanding of laboratory polarization phenomena, the light from celestial bodies was also investigated for the attribute. As it turns out, the eye by itself is virtually insensitive to polarized light, although under favourable circumstances, the effects of high levels of polarization can be apparent through the phenomenon of Haidinger's Brush – see Haidinger (1844). If the eye perceives a wide uniform field of strongly polarized light such as the sky viewed at 90° from the Sun, some people are able to detect a yellowish figure of eight, about 3° across, at the centre of the field. The figure has its long axis at right angles to the direction of polarization. Its origin results from the yellow pigment of the eye being dichroic. Details of how the appearance of Haidinger's Brush behaves according to both linear and circular polarization, and how the perception is induced in the eye are provided by Fairbairn (2001). Experiments on the eye's response to linear and circular polarization have been conducted by de Vries, Jielof & Spoor (1950). In order to make any polarization of a light beam more generally detectable by eye, some simple optical pieces are required. Such devices are, of course, also required to make the modern detectors used on telescopes sensitive to polarized light, their combinations comprising a polarimeter.

The first polarimetric observations in Astronomy were made by Arago in 1811 when he directed his visual instrument to the Moon to see if the reflected sunlight carried similar properties to those seen by Malus in reflections by glass surfaces (see Arago, 1855a, 1858c). Arago's equipment (see Arago, 1855b) comprised a quartz plate, cut to give a wavelength-dependent rotation of the direction of vibration of any linearly polarized light, and a Wollaston prism to resolve the orthogonal polarizations. Two images of differing colour were seen for incident polarized light. The original instrument has been restored and tested by Dougherty & Dollfus (1989).

At about the same time, Arago discovered that the light of the daytime sky was polarized, finding that the polarization maximum occurred at approximately 90° from the Sun. He also found that the light from a direction of about 25° above the antisolar direction was unpolarized. This point is referred to as Arago's neutral point. Two other neutral points were later found to be present in the sunlit sky. The Babinet point and the Brewster point were discovered in 1840 and 1842 respectively, both lying within 10° to 20° along the vertical circle through the Sun; the Brewster neutral point occurs below the Sun and the Babinet point occurs above it. Although it is very apparent to anyone who wears 'Polaroid' sunglasses that the light of the sky is generally polarized, it is difficult to detect the neutral points by eye because of the solar glare. They occur as a result of multiple scattering within the atmosphere and their position relative to the Sun is sensitive to the local turbidity.

In 1828, Arago (see Arago, 1855b) made measurements of solar light and, from his null result, concluded that the Sun was wholly gaseous, since, if solid or liquid, its surface would give rise to partial polarization near the limb. This conclusion was accepted by some later workers, but was criticised by Sir John Herschel (1869) who suggested that such a notion was only applicable to a smooth surface with observations showing that this latter condition did not apply. With the advance of modern technology and improved detectivity, measurements of limb polarization, particularly within spectral lines, have opened up a new exciting avenue of solar research. Records of spectropolarimetry of the Sun are referred as the '*second*' solar spectrum (see Stenflo, 1996 and Stenflo & Keller, 1997). Arago (see Arago, 1855c and Grant, 1852) is also credited with the discovery that cometary light (namely the comets of 1819 and 1835 (Comet Halley)) is polarized.

Unlike astrometry, photometry and spectroscopy, the advances of polarimetry in the nineteenth century were relatively slow being limited to the Moon, this being of interest only because of its extreme brightness accompanied with high levels of polarization. Notable contributions in the nineteenth century were by Secchi (1860) and Lord Rosse (see Parsons 1878). The key works related to lunar polarimetry from this period and the early part of the twentieth century have been referenced by Fielder (1961) and also described by Turner (1957, 1958). It may also be mentioned that the Moon's light, particularly from the dark maria at a phase $\sim 110^\circ$, provides a simple, but delicate, opportunity to observe polarization directly by eye by rotating a polarizer before it, with, or without, the use of a telescope.

Planetary work was also initiated at the turn of the century by Lyot (1929) through the ingenious design of a sensitive visual polarimeter. His observations were seminal, acting as reference for a whole range of later measurements of the Moon, planets, asteroids and rough scattering by laboratory samples. One of the highlights resulting from a development of this work is the determination of asteroid diameters by polarimetry. According to Umov (1912), the albedo of a rough surface is inversely proportional to the amount of polarization in the scattered light. With good calibration, partly obtained by laboratory measurements, and partly through telescope observations, polarimetry of asteroids over their phase angle range provides albedo values. For any asteroid, photometric measurement of its absolute magnitude, together with its 'polarimetric' albedo, then allows a cross-sectional area to be determined, from which a diameter is obtained. Early work in this area was undertaken by Bowell & Zellner (1974).

1.3
The Dawning of Stellar Polarimetry

The first attempt to measure polarization in the light from stars appears to have been made by Öhman (1934) when he used a photographic technique to investigate possible polarimetric variations within spectral lines of the famous eclipsing binary, β Lyr. At the time, tentative claims were made for positive results, but on reflection, some 30 years later, Öhman (1965) commented that he was now more cautious about his earlier detection levels and that the photographic method was probably not sufficiently sensitive to give conclusive answers in every respect. Encouragement to publish his results was offered by the Editor of the scientific journal *Nature*, following a visit by him and his wife to Stockholm Observatory.

The key paper which triggered observational activity in stellar polarimetry was that of Chandrasekhar (1946) who predicted that the continuous radiation of early-type stars should be polarized. By considering the opacity of the atmospheres of such stars to be the result of electron scattering, he demonstrated that the radiation emerging from the stellar limb would have a polarization of just over 11%, with the azimuth of vibrations tangential to the limb, the polarization becoming zero for radiation emerging from the centre of the disc. Quoting from his paper, he says:

> It is not impossible that this predicted polarization of the radiation of the early-type stars (in which scattering by free electrons is believed to play an important part in the transfer of radiation) would be detected under suitably favourable conditions.

Radial symmetry rules out there being a net polarization in the global radiation, but for an eclipsing binary in which a larger late-type companion partially masks the disc of the early-type star, the symmetry is broken and a polarization modulation is to be expected during the eclipse phase. It is of interest to note that, at about the same time as Chandrasekhar's work on radiative transfer, Kopal & Shapley (1946) suggested that polarization modulations might be expected in such stars as V 444 Cyg, comprising a Wolf–Rayet and O star eclipsing system, embedded in an extended dissociated atmosphere of free electrons.

As well as potentially revealing polarization by breaking the symmetry as consequence of eclipses, Öhman (1946) demonstrated by qualitative argument that, for stars with high values of $v \sin i$, a variation of polarization might be seen at all times across the Doppler rotationally broadened profiles, with the wings of the lines being weighted by radiation from the equatorial limb and the line core being weighted by light from the centre of the stellar disc. At the time of this proposal, measurement techniques were insufficient to explore the proposition.

1.4
The Discovery of Interstellar Polarization

The history of the serendipitous discovery that interstellar dust imposes polarization on starlight passing through it has been sketched out by Struve & Zebergs (1962). They comment that:

> The detection of interstellar polarization always will remain one of the most striking examples of purely accidental discovery, such as Wilhelm Röntgen's discovery of X-rays in 1885.

In response to Chandrasekhar's theoretical paper on the production of polarization by electron scattering in the atmospheres of early-type stars, the challenge of detecting polarimetric variability in eclipsing binaries was taken up, the first chosen star for investigation by Jansenn (1946) being U Sag. The exploratory technique employed a Wollaston prism placed before the photographic camera attached to the Yerkes 40″ refractor. In order to improve the detectivity, the resolved beams were spread over a large area of the plate by focussing the objective on the emulsion, rather than obtaining pin-point sharp stellar images. With this system, Hiltner (1947) investigated the eclipsing binary RY Per and suggested that a systematic change in polarization had been detected through the light-curve minimum.

The real breakthrough to the detection of stellar polarizations came with the application of the photomultiplier tube which, following World War II, fortuitously appeared on the scene at the right time to provide sufficient photometric sensitivity for the remarkable, but serendipitous, discovery of *interstellar polarization*. Rather than detecting the predicted intrinsic effects generated within stellar atmospheres, the new technology discovered a very unexpected phenomenon.

From two adjacent papers in the journal *Science*, it is apparent that William A. Hiltner (1949a) and John S. Hall (1949) originally had collaborated on stellar polarimetric observations, but that instrumental problems and other difficulties had prevented the completion of their joint study. These two papers describing the early results of independent work serve as a benchmark for the establishment that starlight becomes polarized by its passage through the interstellar medium.

Responding to Chandrasekhar's prediction, Hall designed a photoelectric polarimeter (see Hall, 1948 and Hall & Mikesell, 1950) in 1946 and independently measured the constant interstellar polarizations in the summer of 1948.

The description of how the phenomenon of interstellar polarization became established is clearly related by Hiltner (1949b). His photoelectric measurements of CQ Cep, also made in the summer of 1948, revealed a polarization of some 10% which was independent of the stellar phase. Other stars such as Z Lac and HD 211853 also provided substantial levels of polarization. Hiltner concluded:

> . . . that this polarization is not associated with the individual stars but is introduced to the stellar radiation in its passage through interstellar space.

In the penultimate paragraph of the paper, Hiltner listed a number of conditions that must be met to explain the presence of polarization in distant stars, namely

1. the mechanism must be independent of wavelength,
2. the mechanism must be operating over a large distance – stars within a small area on the sky exhibit polarization of different amounts but with the same position angle,
3. a positive colour excess is necessary but not sufficient and
4. the plane of polarization is associated with the galactic plane, i. e., stars of low galactic latitude tend to provide the electric vector maximum which is approximately parallel to the galactic plane.

Finally, Hiltner surmised:

> . . . if the polarization is a consequence of scattering by interstellar particles, it follows that these particles must be unsymmetrical, that is, elongated, and that these particles are subject to some alignment force. This force may take the form of magnetic fields,. . .

Hiltner and Hall continued to make measurements, both producing catalogues (Hiltner, 1951, 1954; Hall, 1958) which mapped the variations of interstellar polarization around the Galaxy, a task which was made more complete by Mathewson & Ford (1970) (see Figure 1.4).

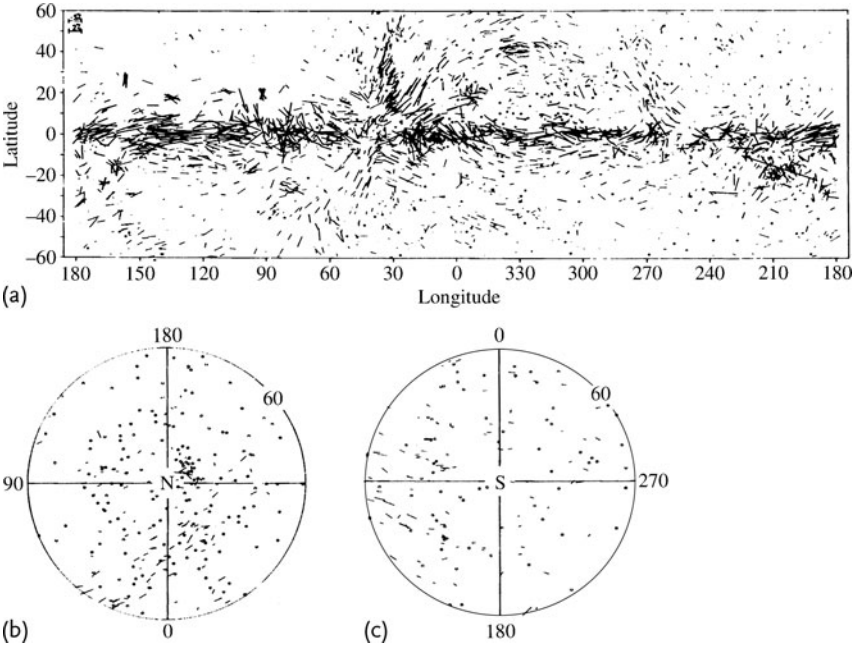

Fig. 1.4 Polarization vectors corresponding to measurements of individual stars set on a galactic map. (a) plots values for stars along the galactic equator covering a galactic latitude range of ±60°, while the circles (b,c) correspond to the galactic poles. The similarity of patterns akin to those of iron filings scattered on paper with a magnet placed on the underside is not fortuitous. (From Mathewson & Ford, 1970.)

It is perhaps of interest to note that Öhman (1949) also discovered interstellar polarization without realising it. One of the photometric instruments he developed involved the use of quartz plates following a rotating polarizer such that the modulated signal provided information on the stellar colour. For some reddened stars the photomultiplier produced a greater ‘dark current’ than expected. The excess was considered to result from the presence of polarization effects but was rejected as being improbable and was attributed to accidental variations in the dark signal. In this instance, the hand of serendipity was not grasped.

Photoelectric instruments immediately lent themselves to investigations of the wavelength dependence of polarization. Indeed early observations by Hiltner and Hall of the newly discovered interstellar polarization suggested that there was little or no wavelength dependence. Ten years later, as instrumental techniques and sensitivities improved, broadband spectropolarimetry became firmly established. Initial work on the wavelength dependence of the interstellar polarization was undertaken by Behr (1958) and Gehrels (1960). Adjacent to Behr’s paper is a discussion by Davis (1958) on the nature of interstellar dust and the form of the wavelength dependence of the generated polarization. It is of interest to note though that the majority of the stars measured by Behr have subsequently been proven to display intrinsic polarizations.

In the early 1960s, Gehrels & Teska (1963) were promoting the application of spectropolarimetry to a wide variety of astronomical sources. A series of papers under the running heading of 'Wavelength Dependence of Polarization' also began to appear at this time in *Astronomical Journal*; a full listing of these is given in Appendix B.

An important conclusion emerged around 1970 in respect of the wavelength dependence of interstellar polarization. By normalizing both the polarization measurements and the wavelength points of the observations, a unique curve emerged, this being independent of the galactic position of any star (see Chapter 10). This behaviour was established by Serkowski (1973), although formulated earlier by Serkowski (1971), but with an erroneous value for a constant term which the later paper confirmed as being a misprint. This algebraic representation of the behaviour of interstellar dust above is now referred to as *Serkowski's Law*.

Not only has Serkowski's Law been important in investigating the nature of interstellar dust grains within the Galaxy, it provides a useful diagnostic for decoupling intrinsic and interstellar contributions within individual stellar measurements. By the mid-1970s there was independent evidence – time-dependent variability and peculiar wavelength dependences – which confirmed that some stars have polarigenic[4] mechanisms operating within their atmospheres. Understanding the nature of these mechanisms and of their presence in astrophysical situations has grown as more and more measurements have accrued.

1.5
Intrinsic Polarization

Although the observational investigations had taken a completely different tack from the direction set by Chandrasekhar's theoretical work, it was only a few years later when variability of polarizations was reported, confirming that some stars exhibit intrinsic effects generated within their atmospheres. Indeed, hints of the presence of intrinsic polarization were indicated in the early catalogues of measurements. For example, Hall & Mikesell (1950) noted that ζ Tau displayed a polarization greater than expected according to its small colour excess. Later measurements of this star revealed a wavelength dependence very different from the curve associated with interstellar polarization (e. g. see Capps, Coyne & Dyck , 1973), and also a temporal variability (e. g. see Clarke & McLean, 1976).

---

[4] Some etymological purists might object to the use of such an engineered word, but 'polarigenic' describes very well the concept of the generation of polarized light by some physical mechanism. Its origin is uncertain, but the author became conscious of its use in the PhD thesis of Schwarz (1984). (Dr. Hugo E. Schwarz died tragically on 20 October 2006.)

In Behr's (1959) catalogue, γ Cas was highlighted as displaying variable polarization. Both ζ Tau and γ Cas are Be stars and, as it has since turned out, this spectral class has provided targets for one of the most fruitful fields of stellar polarimetric research. Serkowski (1970) demonstrated that measurements made with standard *UBV* filters were sufficient to reveal that Be stars behave differently from stars exhibiting polarization simply as a result of the interstellar medium.

The acceptance and establishment that some stars do indeed display intrinsic polarization was not without problems. An interpretation of measurements made by Thiessen (1961) was of a correlation existing between the amount of polarization and stellar luminosity, the notion that synchrotron radiation might occur in stellar atmospheres being mooted. Behr (1961) dismissed this suggestion, demonstrating the influence of observational selection; brighter supergiants are observed more readily, despite effects of interstellar absorption – but with increased interstellar polarization. Later, however, through the discovery of variable intrinsic polarization of OB supergiants (see, e. g. Coyne, 1971), the notion of polarization/luminosity relationships re-emerged, but not to the extent originally proposed by Thiessen.

At the other end of the spectral range, red supergiant stars such as μ Cep were reported as displaying variable polarization (e.g. see Grigoryan, 1958). Even in the late 1960s, however, Lodén (1967a, 1967b) suggested that such claims of intrinsic variations should be treated with some caution. Again, observations of both temporal fluctuation and spectral variation of the polarizations of this type of star have since become a profitable study.

Investigations of eclipsing binary stars which initiated the first stellar polarimetric observations were continued and have become productive as detection sensitivities have improved. Early notable work was by Shakhovskoi (1963) who observed the famous supergiant eclipsing binary, β Lyrae. Changes in polarization during the eclipse phase in about 12 other binary systems were discovered by Shakhovskoi (1965, 1969) and by Shulov (1967), with most of the examples displaying spectra indicating the presence of gas streams and rings, the polarigenic mechanism being scattering from detached material and not from the Chandrasekhar (1946) effect.

By the early 1970s the usefulness of studying polarization associated with circumstellar material gained significant momentum. A benchmark paper was presented by Zellner & Serkowski (1972) which highlighted situations whereby intrinsic polarization might be generated and also decrying the fact that very little work had been done on modelling the temporal or spectral behaviour of a plethora of observations. Nearly all of the various categories of stars known to be photometric and/or spectroscopic variables (e. g. T Tauri, RV Tauri stars, etc.) have now been detected as displaying polarimetric variability. It is not profitable here to cite all the early observations and to assign names of researchers associated with the discovery of intrinsic polarization for each kind of star, but a seminal paper describing such pioneering investigations was presented by Serkowski (1971). The latter chapters of Part II of the text are dedicated to presenting the polarimetry of the various kinds of variable star.

1.6
Circular Polarization

All the discussion above is essentially related to ‘linear polarization’. In the early 1970s James C. Kemp introduced a photoelastic modulator to the telescope, the system being ideally suited to the measurement of circular polarization (see Kemp & Barbour, 1981). With this instrument he detected circular polarization in the light of white dwarfs (Kemp, 1970a) and at the same time described (Kemp, 1970b) a new physical process of gray-body magneto-emissivity to explain the observed phenomena.

As interstellar grains are birefringent, on entering a dust cloud, any initial linear polarization will be modified by differential phase changes to produce a circular component. Thus, circular polarization may be generated by the interstellar medium if the stellar line of sight contains complex dusty regions. Linear polarization might be produced by the early part of an interstellar cloud and, if its alignment axis is set at an angle to the later part of the cloud, the twist produces a circular component. In addition, there may also be an intrinsic linear polarization from the star itself, prior to the light passing through a cloud. An effect of the handedness having opposite senses either side of the wavelength, $\lambda_{\max}$, at which the linear polarization has its maximum value, was discovered by Kemp & Wolstencroft (1972).

Following the interest in the optical identification of newly discovered X-ray sources, Tapia (1977) investigated the star AM Her and found remarkably large changes in both linear and circular polarization on a period of 0.128918 days. The source of the polarization was suggested as cyclotron emission by hot electrons in a magnetic field of the order of 10^8 G. These systems are perhaps the most exciting stellar objects in terms of their polarimetric behaviour. Several more have since been discovered and stars of this genre are sometimes referred to as *polars*.

Although not measuring polarization directly, Babcock (1958) used the diagnostic of spectral line splitting by the Zeeman effect to undertake a survey of magnetic fields associated with Ap stars. By forming two spectra comprising orthogonal circular polarizations, the longitudinal component of the magnetic field was measured from the line pair displacements in the photographic spectral records. His catalogue provided a table of 89 magnetic stars with measured field strengths and a table of 66 stars which probably show Zeeman effects. Many of the magnetic stars show periodic variability as a result of their rotation. The technique was advanced further by photoelectric determinations of the circular polarization in the red and blue wings of spectral lines (e. g., see Landstreet, 1980). Linear polarization studies have also been made of the continuum light of Ap stars (e. g., see Leroy, 1995).

1.7
Polarization and Geometry

The key attribute of polarization is the vectorial nature of the electromagnetic disturbances that is carried. The orientational properties that are encrypted in the received flux relate to aspects of the source geometry, whether the light has a direct route, or is redirected towards the observer as a result of scattering. By teasing out the polarizational characteristics of the light from any object, the reduced information may lead to the determinations of astrophysical geometry which could not be ascertained by ordinary photometry. The diagnostics associated with polarimetry provide unique information of source structures.

Perhaps the most readily appreciated aspect of this relates to the possible determination of the orientation of a magnetic field by measurements of the Zeeman effect. According to classical Lorentzian theory (see, for example, Jenkins & White, 1965, and Chapter 9), the light emitted by atoms radiating in a strong magnetic field will be polarized. When the field is longitudinal to the line of sight, the resultant emission line is split into two components, shifted in wavelength either side of the original value. The two generated lines are circularly polarized with opposite handedness. For a transverse field, the original line splits into three components, two found either side in wavelength of the original line value, the third being undisturbed in position. The two wavelength-shifted components are linearly polarized while the central component is also linearly polarized but with an orthogonal azimuth. In principle, by measuring the full polarizational behaviour, with sufficient spectral resolution, through Zeeman broadened lines, the longitudinal and transverse components of the magnetic field may be determined and compounded to provide the orientation of the field in the environment of the radiating atoms.

Reference has also been given to the behaviour of the polarization produced by particles in the interstellar medium (see Figure 1.4), indicating the presence of some alignment mechanism which is locally coherent. Mapping the effects of this polarization gives unique insight into interstellar cloud structures and into the variations of the direction of the alignment mechanism.

Finally, the special property of polarization may be highlighted by exploring a star which has a localized, optically thin, cloud of electrons orbiting about it. Some of the radiated light will be scattered into the line of sight, making the star appear slightly brighter, according to the cloud's distance from the star, the electron density and the phase angle of the scattering. This additional contribution to the apparent brightness will also be polarized according to the phase angle. Overall, the star would appear to exhibit an intrinsic polarization originating in the cloud, but diluted by the unpolarized radiation received directly from the stellar surface. In general, the star might appear to vary in brightness and in polarization, according to the orbital characteristics of the cloud.

Consider a special case for which the electron cloud is in a circular orbit with an inclination of 0°, so that its path is projected as a circle on the sky (see Figure 1.5). As the orbit progresses, the apparent brightness will not vary; the degree of polarization will also remain constant. The azimuth of the polarization will rotate, however, running through the angular positions of 0° through 90° to 180°, twice over the orbital cycle. The presence of the cloud would only be apparent from polarimetric studies monitoring the rotation of direction of vibration, there being neither brightness nor spectral variations. Such a star can be considered uniquely as a *polarimetric variable* with special characteristics. It goes without saying that

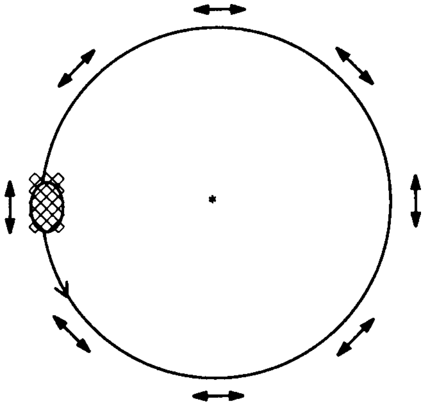

Fig. 1.5 As a cloud of electrons executes a circular orbit in the plane of the sky about a point source star, the azimuth of polarization vector rotates from 0° through 90° to 180° twice per orbit, but its strength maintains at a constant level with the overall brightness of the system also remaining constant.

any quest to find such a perfectly behaved object is likely to draw a blank. However, from phase-locked polarimetric variability detected in some stars, it has been possible to determine the geometry of orbiting material which could not be ascertained from the brightness variability alone. See Chapter 11 for a more incisive presentation on this point.

1.8
Chirality and the Origin of Life

Some 150 years ago, Louis Pasteur demonstrated that certain molecules with helical structures occur in two forms, or *enantiomers*, referred to as being either left- or right-handed. Such molecules are said to be *chiral*. In the laboratory, chemical reactions producing chiral molecules generally produce equal amounts of the two types. Organic compounds from living matter, however, are almost always of one handedness or the other. Amino acids that form the building blocks of proteins are all left-handed (L(aevo)-configuration), whereas the sugars including ribose and deoxyribose, important components of RNA and DNA, are always right-handed (D(extro)-configuration). A quest followed by Pasteur was the search for the asymmetric physical force that could account for the origin of biological homochirality which, according to him, was the only well-marked demarcation between the chemistry of dead matter and the chemistry of living matter. He considered circularly polarized light as being one such possible triggering source although he did not investigate this proposition by experiment. All explorations of this suggestion produced negative results until the experiments by Kuhn around the 1930s (see, for example, Kuhn & Braun, 1929) successfully demonstrated enantio-differentiating reactions with circularly polarized light in the UV region. Since then, numerous arrangements have been used involving circularly polarized light to selectively produce either left- or right-handed forms of particular molecules. The principle relies on one of the enantiomers preferentially absorbing circular polarized light of a specific handedness and exciting the molecule to a state which allows further constructive chemical reaction to take place more frequently than for the other form. The importance of chirality in respect of possible life beyond the Earth has been discussed by many researchers including Thiemann (1975), for example. The circular polarization present in the scattered light of the daytime sky has been considered by Wolstencroft (1985) as a local source for affecting a bias on the distribution of enantiomers on the Earth's surface.

The recent discoveries by radio and millimetre astronomy of so many signatures of different kinds of organic molecules demonstrate the abundance in the interstellar medium of the building blocks for life. It could well be that the origins of life on the Earth are from beyond our globe, and have been transported from space by comets, interstellar dust, or were already present in the protoplanetary material. Certainly an important finding is the excess of L-amino acids in the Murchison meteorite (see Cronin & Pizzarello, 1997; Engel & Macko, 1997). The basic path to our homochirality has been summarized by Cronin (1998). The starting point simply requires the setting of an imbalance within some particular astrophysical environment. Bonner (1991a, 1991b) suggested the scenario of electron plasmas in an orbit about a neutron star, with circular polarized light being generated over a wide range of wavelengths as synchrotron radiation. Such light would illuminate the organic matter in nearby molecular clouds. According to the geometry and depending on whether the light originated above or below the plane of the orbiting electrons, one of the enantiomers would preferentially emerge. The imbalance is therefore present in the protostellar systems and their planetesimals and cometary material. Following the discovery of high levels of infrared circular polarization in the Orion OMC-1 region, Bailey, Chrysostomou, Hough, *et al.* (1998) have proposed that enantiometric excesses can be established in organic molecules in protostellar clouds as a result of scattering of the UV radiation from a nearby star.

Although there are alternative mechanisms for the original trigger for our local biological homochirality, effects associated with polarized radiation are strong contenders. It is, of course, of great interest to the astrophysicist to explore the localities in the Universe where the original seeds were set. The diagnostic role of polarimetry may well provide an important contribution to unravelling this enigma.

1.9
Conclusion

The basic history of our understanding of *polarization* as an important attribute of light has been sketched out with particular reference to the discoveries of Malus. The importance of polarimetric measurements for gaining unique knowledge of the geometry of astrophysical systems has been emphasized.

The highlights of the first 50 years of stellar polarimetry have been described briefly in terms of telescopic discoveries and their phenomenology. Admittedly the citations are not complete and may have short-changed some of the important contributors to the field; selection is necessary, however, in striving to keep the introduction to reasonable length. References to many important developments have not been made, but this will be remedied to some degree later in the main body of the text. Little reference has been made to the contemporaneous advances made in understanding the polarigenic mechanisms and the modelling of astrophysical situations. Again coverage of these topics is reserved for fuller discussion in the later chapters. Before this can be done, it is first necessary to describe the concepts associated with polarization more fully, together with the formalism of the mathematical tools required to understand instrumental design, to appreciate the necessary telescope protocol and to decipher its connections with astrophysical phenomena.

In summary, here it might be said that, as well as being a supportive diagnostic to other kinds of observation in astrophysics, polarimetry has sufficient power and independence to be sometimes relied on alone through its own fundamental merits. It is interesting to note that what might be called the first Conference on Stellar Polarimetry was held at the Lowell Observatory, Flagstaff, Arizona, in 1960 (see Lowell Observatory, 1960). In 1972, a conference on *Photopolarimetry* covering *Stars, Planets and Nebulae* (and other topics) was held in Tucson, Arizona. The proceedings were edited by Gehrels (1974); the resulting collection of material is sometimes euphemistically referred to as the *Polarimetric Bible*. More recently a workshop was held at the Vatican Observatory, Castel Gandolfo, in 1987, resulting in the production of a range of papers under the umbrella title ‘Polarized Radiation of Circumstellar Origin’ (see Coyne, Magalhães, Moffat, *et al.*, 1988). Also the Royal Astronomical Society (London) has hosted a one day specialist discussion meeting entitled ‘Astronomical Polarimetry as a Source Diagnostic’ covering its application in various parts of the electromagnetic spectrum (see Clarke, 1992). The essentials of polarimetry which tend to be neglected in undergraduate courses on optics may be set with astrophysical context to provide the bases of postgraduate schools – see, for example, Trujillo-Bueno, Moreno-Insertis & Sánchez (2001). An International Conference on ‘Astronomical Polarimetry – Current Status and Future Directions’ was held in March 2004 in Hawaii (see Adamson, Aspin, Davis, *et al.*, 2005), followed by one in Malbaie, Québec, in 2008 (see Bastien & Manset, 2009).

Key papers on the understanding and mathematics associated with the descriptions of polarization have been collected by Swindell (1975), this work containing some material related to historic papers which are otherwise difficult to obtain for consultation. Descriptive books on the presence of polarization in nature have been produced by Können (1985) and Pye (2001). Other texts also available on Optical Polarimetry describing the physics of polarization phenomena and optical devices used are those of Shurcliff (1962), Clarke & Grainger (1971) and Huard (1997).

On the astronomical scene, polarimetry is the theme of works by Tinbergen (1996), Dolginov, Gnedin & Silant’ev (1995) and Leroy (1998, 2000). The rapidly expanding theme of spectropolarimetry is also supported by a text by del Toro Iniesta

(2003), this providing extensive material on the effects associated with polarization signatures within spectral lines, with particular reference to the Sun.

References

Adamson, A., Aspin, C., Davis, C.J., Fujiyoshi, T. (eds) (2005) Astronomical polarimetry: current status and future directions. *ASP Conf. Ser.*, No. 343, San Fransisco. [26]

Arago, D.F.J. (1811) Sur une modification remarquable qu'éprouvent les rayons lumineux dans leur passage à travers certains corps diaphanes, et sur quelques autres nouveaux phénomènes d'optique. *Mém. Inst.* **12**, Part I, 93–134. See also Arago (1858b). [12]

Arago, D.F.J. (1855a) Popular Astronomy, Vol. II, *Polarisation of the Moon's Light*, Longman, Brown, Green and Longmans, London, pp. 289–292. [15]

Arago, D.F.J. (1855b) Popular Astronomy, Vol. I, *Examination of the Theory of the Spots According to the Phenomena of Polarisation*, Longman, Brown, Green and Longmans, London, pp. 413–419. [15, 15]

Arago, D.F.J. (1855c) Popular Astronomy, Vol. I, *The Comets*, Longman, Brown, Green and Longmans, London, p. 629. [16]

Arago, D.F.J. (1858a) Mèmoire sur les Couleurs des Lames Minces. (Paper presented on 18 Feb. 1811 but published in 1817). *Œuvres Complètes de François Arago* **10** – Mémoires Scientifiques 1, 1–35. Gide, Éditeur, Paris; T.O. Weigel, Éditeur, Leipzig. [5, 8]

Arago, D.F.J. (1858b) Mémoire sur La Polarisation Colorée. *Œuvres Complètes de François Arago*. **10**, – Mémoires Scientifiques 1, 36–74. Gide, Éditeur, Paris; T.O. Weigel, Éditeur, Leipzig. (This is the same paper referenced as Arago (1811) but published in Mémoires of the Institut in 1812). [12]

Arago, D.F.J. (1858c) Observations sur la Lumière de la Lune *Œuvres de François Arago*, **10** – Mémoires Scientifiques 1, 564–570. Gide, Éditeur, Paris; T.O. Weigel, Éditeur, Leipzig. [15]

Arago, D.F.J. and Fresnel, L. (1819) Sur L'Action que les rayons de lumière polarisés exercent les uns sur les autres. *Ann de Chimie et de Physique* t X, 288–305. (See also Œuvres complètes de Fresnel – Eds H. de Senarmont, E, Verdet and L. Fresnel) (1866) Vol. I: 509–522. [8]

Babcock, H.W. (1958) A catalog of magnetic stars. *ApJS*, **3**, 141–210. [22]

Bailey, J.A., Chrysostomou, A., Hough, J.H., Gledhill, T.M., McCall, A., Clark, S., Ménard, F., Tamura, M. (1998) Circular polarization in star-formation regions: implications for biomolecular homochirality. *Science*, **281**, 672–674. [25]

Bartholinus, E. (1690) *Experimenta Crystalli Islandici Disdiaclastici Quibus mira et insolita Refractio detegetur Hafniae*, Copenhagen. A relevant excerpt translated into English is presented in Swindell (1975). [3]

Bastien, P., Manset, N. (eds) (2009). *Astronomical Polarimetry 2008: Science from Small and Large Telescopes. ASP Conf. Ser.*, San Francisco (in press). [26]

Behr, A. (1958) Beobachtungen zur Wellenlängenbhängigkeit de interstellaran Polarisation. *Zeit. für Astrophysik*, **47**, 54–58. Also, *Veröff. der Univ. – Sternwarte zu Göttingen*, **7** (Nr. 124), 175–180. [19]

Behr, A. (1959) Die interstellare Polarisation des Sternlichts in Sonnennumgebung. *Veröff. der Univ.– Sternwarte zu Göttingen*, **7** (Nr. 126), 199–256. [21]

Behr, A. (1961) Bemerkungen über den Ursprung der Polarisation des Sternlichts. (Remarks on the origin of polarization of starlight.) *Zeit. für Astrophysik*, **53**, 95–105. Also, *Veröff. der Univ. – Sternwarte zu Göttingen*, **7** (Nr. 133), 403–413. [21]

Bonner, W.A. (1991a) The origin and amplification of biomolecular chirality. *Origins of Life*, **21**, 59–111. [25]

Bonner, W.A. (1991b) Terrestrial and extraterrestrial sources of molecular homochirality. *Origins of Life*, **21**, 407–420. [25]

Bowell, E., Zellner, B. (1974) Polarizations of asteroids and satellites. pp. 381–404 in *Planets, Stars and Nebulae studied with Photopolarimetry*. (ed. T. Gehrels), University of Arizona, Tucson, AZ. [16]

Brewster, D. (1814a) On the affectations of light transmitted through crystallized Bodies. *Philos. Trans. R. Soc.*, **104**, 187–218. [12, 13]

Brewster, D. (1814b) On the polarisation of light by oblique transmission through all Bodies, whether crystallized or uncrystallized. *Philos. Trans. R. Soc.*, **104**, 219–230. [12, 13]

Brewster, D. (1814c) On the affectations of light transmitted through crystallized bodies. *Philos. Mag.*, **44**, 261–270. [13]

Brewster, D. (1815a) On the laws which regulate the polarisation of light by reflexion from transparent bodies. *Philos. Trans. R. Soc.*, **105**, 125–130. [12]

Brewster, D. (1815b) On the laws which regulate the polarisation of light by reflexion from transparent bodies. *Philos. Trans. R. Soc.*, **105**, 158–159. [12]

Buchwald, J.Z. (1989) pp. 54–55 in *The Rise of the Wave Theory of Light – Optical Theory and Experiment in the Early Nineteenth Century*. University of Chicago Press, Chicago, IL. [7]

Capps, R.W., Coyne, G.V., Dyck, H.M. (1973) A model for the observed polarized flux from zeta Tauri. *ApJ*, **184**, 173–179. [20]

Chandrasekhar, S. (1946) On the radiative equilibrium of a stellar atmosphere. X. *ApJ*, **103**, 351–370. [3, 16, 21]

Clarke, D. (1992) Summary of the RAS Specialist Discussion Meeting on "Astronomical Polarimetry as a Source Diagnostic". *The Observatory*, **122**, 268–276. [26]

Clarke, D., Grainger, J.F. (1971) *Polarized Light and Optical Measurement*. Pergamon, Oxford. [26]

Clarke, D., McLean, I.S. (1976) Linear polarization measurements at Hβ of early-type emission line stars. *MNRAS*, **174**, 335–343. [20]

Collett, E. (1971) Mathematical formulation of the interference laws of Fresnel and Arago. *Am. J. Phys.*, **39**, 1483–1495. [11]

Collins English Dictionary – Harper Collins Publishers, 3rd Edition (Reprint 1992). [13]

Coyne, G.V. (1971) Intrinsic polarization in the atmospheres of supergiant stars. *Proceedings of the Third Trieste Colloquium in Astrophysics*. pp. 93–107, Ed. M. Hack – Osservatorio Astronomico di Trieste [*Ric. Astron. Spec. Vaticana*, No: 53]. [21]

Coyne (SJ), G.V., Magalhães, A.M., Moffat, A.F.J., Schulte-Ladbeck, R.E., Tapia, S., Wickramasinghe, D.T. (eds) (1988) *Polarized Radiation of Circumstellar Origin – Workshop held at the Vatican Observatory*. University of Arizona, Tucson, AZ. [26]

Cronin, J. (1998) Pasteur, light and life. *Physics World*, October 1998, 23–24. [25]

Cronin, J., Pizzarello, S. (1997) Enantiomeric excesses in meteoritic amino acids. *Science*, **275**, 951–955. [25]

Davis L. Jr., (1958) The color dependence of the polarization of starlight. *Zeit. für Astrophysik*, **47**, 59–66. [19]

de Vries, Hl., Jielof, R., Spoor, A. (1950) Properties of the human eye with respect to linearly and circularly polarized light. *Nature*, **166**, 958–959. [15]

del Toro Iniesta, J.C. (2003) *Introduction to Spectropolarimetry*. Cambridge University Press, Cambridge. [27]

Dolginov, A.Z., Gnedin, Yu. N., Silant'ev, N.A. (1995) *Propagation and Polarization of Radiation in Cosmic Media*. Gordon & Breach, Basel. [26]

Dougherty, L.M., Dollfus, A. (1989) F.D. Arago's polarimeter and his original observations of extraterrestrial polarisation on 1811. *JBAS*, **99**, 183–186. [15]

Engel, M.H., Macko, S.A. (1997) *Nature*, **389**, 265–268. [25]

Fairbairn, M.B. (2001) Physical models of Haidinger's Brush. *J. R. Astron. Soc. Can.*, **95**, 248–251. [15]

Faraday, M. (1846) On the magnetic affection of light, and on the distinction between ferromagnetic and diamagnetic conditions of matter. *Philos. Mag.*, **29**, 153–156. [12, 13]

Fielder, G. (1961) *Structure of the Moon's Surface*. Pergamon, Oxford. [16]

Fresnel, A. (1824a) Considérations théoriques sur la polarisation de la lumière. *Bull. Soc. Philomat.*, p. 150.

Fresnel, A. (1824a) Considérations théoriques sur la polarisation de la lumière. *Bull. Soc. Philomat.*, p. 157.

Fresnel, A.J. (1825) D'un Mémoire sur la double Réfraction. *Ann. de Chimie et de Physique* [ii], **28**, 263–279. (See also Fresnel (1868), pp. 465–478). [10]

Fresnel, A. (1868) *Œuvres complètes D'Augustin Fresnel*, Vol. 2, Edited by Henri de Senarmont, Émile Verdet and Léonor Fresnel, Paris. See pp. 255–623: Théorie de la Lumiière – Quatrième Section – Double Réfraction. [10]

Gehrels, T. (1960) Measurements of the wavelength dependence of polarization. *Lowell Observatory Bulletin* No.105, Vol IV No.17, 300–301. [18]

Gehrels, T. (1974) (Ed.) *Planets, Stars and Nebulae studied with Photopolarimetry*. University of Arizona, Tucson, AZ. [26]

Gehrels, T., Teska, T.M. (1963) The wavelength dependence of polarization. *Appl. Opt.*, **2**, 67–77. [20]

Grant, R. (1852) p. 313 in *History of Physical Astronomy*, Henry G Bohn, London. [16]

Grigoryan, K. A. (1958) Polarization observations of μ Cephei. *Soob. Byurakan Obs.*, **25**, 45–48. [21]

Haidinger, W. (1844) Ueber das directe Erkennen des polarisirten Lichts und der Lage der Polarisationsebene. *Ann. Phys.*, **139** (9), 29–39. [15]

Hall, J.S. (1948) A photoelectric polarimeter. *AJ*, **54**, 39. [18]

Hall, J.S. (1949) Observations of the polarized light from stars. *Science*, **109**, 166–167. [18]

Hall, J.S., Mikesell, A.H. (1950) Polarization of the light in the galaxy as determined from observations of 551 early-type stars. *Publications of the US Naval Observatory*. Second Series Vol XVII – Part I, Washington. [18, 20]

Hall, J.S. (1958) Polarization of Starlight in the Galaxy. *Publications of the US Naval Observatory*. Second Series Vol XVII – Part VI, Washington. [18]

Herschel, J.F.W. (1869) *Outlines of Astronomy*. Longmans, Green, London. [15]

Hiltner, W.A. (1947) On the presence of polarization in the continuous radiation of early-type stars. *ApJ*, **106**, 231–234. [17]

Hiltner, W.A. (1949a) Polarization of light from distant stars by interstellar medium. *Science*, **109**, 165. [18]

Hiltner, W.A. (1949b) On the presence of polarization in the continuous radiation of stars II. *ApJ*, **109**, 471–478. [18]

Hiltner, W.A. (1951) Polarization of stellar radiation. III. The polarization of 841 stars. *ApJ*, **114**, 241–271. [18]

Hiltner, W.A. (1954) Interstellar polarization of 405 stars. *ApJ*, **120**, 454–463. [18]

Hooke, R. (1665) *Micrographia – Some Physiological Descriptions of Minute Bodies Made by Magnifying Glasses with Observations and Inquiries Thereupon*. Pub. under the auspices of The Royal Society, London. [11]

Huard, S. (1997) *Polarization of Light*. John Wiley & Sons Chichester, West Sussex. [26]

Huyghens, C. (1690) Traité de la Lumière – Leyden. Relevant excerpts can be found in Swindell (1975). [3]

Janssen, E.M. (1946) On the polarization of the continuous radiation of early-type stars. *ApJ*, **103**, 380. [17]

Jenkins, F.A., White, H.E. (1965) *Fundamentals of Optics – 3rd Edition*, McGraw-Hill, New York [23]

Kahr, B., Claborn, K. (2008) The lives of Malus and his bicentennial law. *ChemPhysChem.*, **9**, 43–58. [4]

Kemp, J.C. (1970a) Quantum magnetic features in the polarized light of Grw $+70^\circ$ 8247. *ApJ*, **162**, L69–L72. [22]

Kemp, J.C. (1970b) Circular polarization of thermal radiation in a magnetic field. *ApJ*, **162**, 169–179. [22]

Kemp, J.C., Barbour, M.S. (1981) A photoelectric polarimeter at Pine Mountain Observatory. *PASP*, **93**, 521–525. [22]

Kemp, J.C., Wolstencroft, R.D. (1972) Interstellar circular polarization: data for six stars and the wavelength dependence. *ApJ*, **176**, L115–L118. [22]

Können, G.P. (1985) *Polarized Light in Nature*. Cambridge University Press, Cambridge. [26]

Kopal, Z., Shapley, M.B. (1946) A study of the extended envelope surrounding the Wolf–Rayet component of V444 Cygni. *ApJ*, **104**, 160–176. [17]

Kuhn, W., Braun, E. (1929) Photochemische erzeugung optisch aktiver stoffe. *Naturwiss.*, **17**, 227–228. [24]

Landstreet, J.D. (1980) The measurement of magnetic fields in stars. *AJ*, **85**, 611–620. [22]

Leroy, J.-L. (1995) Linear polarimetry of Ap stars. V. A general catalogue of measurements. *A&AS*, **114**, 79–104. [22]

Leroy, J.-L (1998) *La polarisation de la lumière et l'observation astronomique*. Gordon & Breach, Amsterdam. [26]

Leroy, J.-L (2000) *Polarization of Light and Astronomical Observation*. Gordon & Breach, Amsterdam (an English translation of the previously referenced book). [26]

Lodén, L.O. (1967a) A study of possible variations in the polarization of starlight. *Ark. för Astron.*, **4**, 357–373. [21]

Lodén, L.O. (1967b) On the variability of starlight polarization. *The Observatory*, **87**, 294–295. [21]

Lord Kelvin (1904) p. 401 in *Baltimore Lectures* 1884. C.J. Clay & Sons, London. [13]

Lowell Observatory (1960) Polarization of starlight by the interstellar medium. *Lowell Observatory Bulletin* No. 105, Vol. IV, No. 17, pp. 264–321. [26]

Lowry, T.M. (1964) *Optical Rotatory Power*. Dover, New York (republication of the work first published (1935) by Longmans, Green and Co., London). [6, 10, 12]

Lyot, B. (1929) Recherches sur la polarisation de la lumière des planets et quelques substances terrestres. *Ann. de l'Observatoire de Paris – Section de Meudon* VIII, No:1. For an English translation see NASA TT F-187 (1964). [16]

Malus, E.L. (1809a) Sur une propriété de la lumière réfléchie. *Memoires de Physique et de Chimie de la Societé D'Arcueil*, **2**, 143–158. [5, 5]

Malus, E.L. (1809b) Sur une propriété de la lumière réfléchie par les corps diaphanes. *Nouveau Bull. de la Societé Philomatique*, **1**, 266–270. [5]

Malus, E.L. (1810a) Treatise: *Théorie de la Double Réfraction de la Lumière dans les substances cristallisées*, Paris. Mémoire couronné par l'Institut dans la séance publique du 2 Janvier 1810. [4, 5, 5]

Malus, E.L. (1810b) Mémoire sur de nouveaux Phénomènes d'Optique. *Mém. Inst.* **11**, Part II, 105–111. [6, 6]

Malus, E.L. (1810c) Mémoire sur les Phénomènes qui accompagnent la réflexion et la réfraction de la Lumière. *Mém. Inst.* **11**, Part II, 112–120. [6, 7]

Malus, E.L. (1810d) Mémoire sur l'axe de réfraction des Cristaux et des Substances organisées. *Mém. Inst.* **11**, Part II, 142–148. [6, 7]

Malus, E.L. (1811a) Mémoire sur la Lumière; par M. Malus. *Nouveau Bull. de la Societé Philomatique*, **2**, 252. [5]

Malus, E.L. (1811b) Mémoire sur de nouveaux phénomènes d'optique; par M. Malus. *Nouveau Bull. de la Societé Philomatique*, **2**, 291–295 (see Errata on p. 316 of the same publication). [5, 5]

Malus, E.L. (1811c) Mémoire sur les phénomènes qui accompagnent la réflexion et la réfraction de la lumière; par M. Malus. *Nouveau Bull. de la Societé Philomatique*, **2**, 320–325. [5]

Mathewson, D.S., Ford, V.L. (1970) Polarization observations of 1800 stars. *Mem. R. Astron. Soc.*, **74**, 139–182. [19, 18]

Maxwell, J.C. (1861) The Physical Lines of Force. In The London, Edinburgh, and Dublin Philosophical Magazine and Journal of Science. Vol. XXI, Fourth Series, January–June – London: Taylor and Francis, 1861. Also see p. 500 in *The Scientific Papers of James Clerk Maxwell*, Vol. I, Ed. Sir W.D. Niven, Cambridge University Press, Cambridge (1890). [11]

Mujat, M., Dogariu, A., Wolf, E. (2004) A law of interference of electromagnetic beams of any state of coherence and polarization and the Fresnel–Arago interference laws. *J. Opt. Soc. Am. A*, **21**, 2414–2417. [11]

Newton, Sir Isaac. (1931) The quotation is from *Opticks* by Sir Isaac Newton – taken from the edition published in 1931 by G. Bell & Sons, Ltd. [4]

Nicholson's Journal (1811) XXX, p. 192, Extract of a Letter from Dr. Francis Delaroche to F. Berger, Esq.; on Radiant Heat and other Subjects. Communicated by the latter Gentleman. [8]

Nicholson's Journal (1812) XXXIII, pp. 344–348, Popular Statement of the beautiful experiments of Malus, in which he has developed a new property of light. [8]

Öhman, Y. (1934) Effects of polarization in the spectrum of β Lyrae. *Nature*, **134**, 534. [16]

Öhman, Y. (1946) On the possibility of tracing polarization effects in the rotational profiles of early type stars. *ApJ*, **104**, 460–462. [17]

Öhman, Y. (1949) Photoelectric work by the Flicker method. *Stockholms Obs. Ann.*, **15** (8),1–46. [19]

Öhman, Y. (1965) Private communication – Letter to the Author dated 23 September 1965. [16]

Oxford English Dictionary, Oxford University Press (1933) – Reprinted 1961, Vol. VII. [5]

Parsons, W. (1878) (The 3rd Earl of Rosse). Preliminary Note on Some Measurements of the Polarization of the Light coming from the Moon and from the Planet Venus. *Sci. Proc. R. Soc. Dublin*, **1**, 19–20. [16]

Pye, D. (2001) *Polarised Light in Science & Nature*. Institute of Physics Publishing, Bristol. [26]

Schwarz, H. E. (1984) *Spectropolarimetry of cool giants and supergiants*. PhD Thesis, Department of Astronomy, University of Glasgow. [20]

Secchi, A. (1860) Letter from the Rev. Father Secchi to the Astronomer Royal. *MNRAS*, **20** 70–71. [16]

Semel, M. (2003) Spectropolarimetry and polarization-dependent fringes. *A&A*, **401**, 1–14. [11]

Serkowski, K. (1970) Intrinsic polarization of early-type stars with extended atmospheres. *ApJ*, **160**, 1083–1105. [21]

Serkowski, K. (1971) Polarization of variable stars. pp. 11–31 in *New Directions and New Frontiers in Variable Star Research*, IAU Colloquium No. 15, Bamberg. [20, 21]

Serkowski, K. (1973) Interstellar polarization. pp. 145–152 in *Interstellar Dust and Related Topics*. IAU Symp. No. 52. (eds J.M. Greenberg and H.C. van de Hulst). Dordtecht, The Netherlands. [20]

Shakhovskoi, N.M. (1963) Polarization observations of β Lyrae. *Sov. Astron.*, **6**, 587–589. [21]

Shakhovskoi, N.M. (1965) Polarization in variable stars II. Eclipsing binaries. *Sov. Astron.*, **8**, 833–842. [21]

Shakhovskoi, N.M. (1969) The spatial orientation of the orbit planes of close binary stars. *Sov. Astron.*, **13**, 303–305. [21]

Shulov, O.S. (1967) Polarimetric observations of close binary stars. *Trudy Astron. Obs. Leningrad*, **24**, 38–53. [21]

Shurcliff, W.A. (1962) *Polarized Light*. Harvard University Press, Harvard. [26]

Stenflo, J.O. (1996) Scattering physics. *Sol. Phys.*, **164**, 1–20. [16]

Stenflo, J.O., Keller, C.U. (1997) The second solar spectrum. A new window for diagnostics of the Sun. *A&A*, **321**, 927–934. [16]

Struve, O., Zebergs, V. (1962) pp. 368–372 in *Astronomy of the 20th Century*. MacMillan, New York. [17]

Swindell, W. (1975) *Polarized Light* – Benchmark Papers in Optics/1. Dowden, Hutchinson & Ross, Stroudsburg, PA, USA. [3, 26]

Tapia, S. (1977) Discovery of a magnetic compact star in the AM Herculis/3U 1809+50 System. *ApJ*, **212**, L125–L129. [22]

Thiemann, W. (1975) Life and Chirality Beyond The Earth. *Origins of Life*, **6**, 475–481. [25]

Thiessen, G. (1961) Über die Polarisation des Sternlichtes, die Strahlung der Sterne, Sowie Bemerkungen zur Galaktiscehn Struktur. *Astr. Abh. Hamburg Stern.*, Vol. V, No. 9. [21]

Tinbergen, J. (1996) *Astronomical Polarimetry*. Cambridge University Press, Cambridge. [26]

Trujillo-Bueno, J., Moreno-Insertis, F., Sánchez, F. (2001) *Astrophysical Spectropolarimetry*. Cambridge University Press, Cambridge. [26]

Turner, G. (1957) Nineteenth-century studies of the polarization of light reflected by the Moon. *JBAS*, **67**, 185–188. [16]

Turner, G. (1958) The polarization of light reflected by the lunar surface. *JBAS*, **68**, 253–263. [16]

Umov, N. (1912) Eine spektropolariskopische Methode zur Erforschung der Lichtapsorption und der Natur der Farbstoffe. *Phys. Zeitschr.*, **13**, 962–971. [16]

Walker, J. (1978) More about polarizers and how to use them particularly for studying polarized sky light. *Scientific American*, **238**, 132–136. [3]

Whittaker, E. (1958) *A History of the Theories of Aether and Electricity*. Thomas Nelson, London (first published 1910, Reprinted 1958). [9, 10]

Wolstencroft, R.D. (1985) The search of extra-terrestrial life: recent developments. pp. 171–175 in *Astronomical Sources of Circularly Polarized Light and Their Role in Determining Chirality on Earth*. IAU Symp. No: 112, Boston 18–21 June 1984. Ed. M.D. Papagiannis, Reidel, Dordrecht. [25]

Zellner, B.H., Serkowski, K. (1972) Polarization of light by circumstellar material. *PASP*, **84**, 619–626. [21]

2
The Polarization Ellipse

2.1
Electromagnetic Waves

It is taken for granted that the reader will already be familiar with classical electromagnetic theory. It will be remembered that in a region where there are no charges, or current distributions, other than those determined by Ohm's law, the electric (**E**) and magnetic (**H**) fields are described by Maxwell's equations (MKS units), namely

$$\operatorname{curl}\mathbf{E} = -\mu\mu_o\frac{\partial\mathbf{H}}{\partial t} \tag{2.1}$$

$$\operatorname{div}\mathbf{H} = 0 \tag{2.2}$$

$$\operatorname{curl}\mathbf{H} = \sigma\mathbf{E} + \epsilon\epsilon_o\frac{\partial\mathbf{E}}{\partial t} \tag{2.3}$$

$$\operatorname{div}\mathbf{E} = 0\,, \tag{2.4}$$

where ϵ, μ and σ are, respectively, the dielectric constant, permeability and conductivity of the medium in the region, and ϵ_0 and μ_0 are respectively the permittivity and permeability of free space. These relations give rise to wave equations in the form

$$\nabla^2\mathbf{E} - \sigma\mu\mu_0\frac{\partial\mathbf{E}}{\partial t} - \epsilon\epsilon_0\mu\mu_o\frac{\partial^2\mathbf{E}}{\partial t^2} = 0\,, \tag{2.5}$$

$$\nabla^2\mathbf{H} - \sigma\mu\mu_0\frac{\partial\mathbf{H}}{\partial t} - \epsilon\epsilon_0\mu\mu_o\frac{\partial^2\mathbf{H}}{\partial t^2} = 0\,, \tag{2.6}$$

which represent a set of six equations, one for each component of the appropriate vector. Since the equations are linear, any combination of solutions will also be a solution. Thus, any waveform which is capable of Fourier analysis will be a solution, provided sinusoids are solutions. When the most simple and special solution of a sinusoid in a non-conducting medium is considered, the velocity of the wave in the medium can be expressed as

$$v = \frac{1}{\sqrt{\epsilon\epsilon_0\mu\mu_0}}\,. \tag{2.7}$$

Stellar Polarimetry. David Clarke

ISBN: 978-3-527-40895-5

In free space, both ϵ and μ unity, and so the velocity under these conditions is given by

$$c = \frac{1}{\sqrt{\epsilon_0 \mu_0}} \,. \tag{2.8}$$

The ratio c/v is known as the *refractive index* of the medium and equals $\sqrt{\epsilon\mu}$. At optical frequencies, the value of μ is very close to unity for dielectrics and hence the refractive index is $\sqrt{\epsilon}$, where ϵ is the dielectric constant at the particular frequency of the wave.

Investigation of these solutions of the wave equations shows that the wave motion is transverse to the direction of propagation, and that **E** and **H** are perpendicular and in phase. In a medium of zero conductivity, the ratio $E/H = \sqrt{\mu\mu_0/\epsilon\epsilon_0} = Z$ has the dimensions of an impedance and is referred to as the *wave impedance* of the medium. In the case of free space, it is equal to $376 \cdot 6\Omega$.

The vector cross-product, or $\mathbf{E} \times \mathbf{H}$, can also be shown to represent the instantaneous energy flux density in the field and is known as *Poynting's vector*, giving the direction of propagation of the radiation. For sinusoidal waves, the time-averaged magnitude of this vector is $\frac{1}{2} E_0 H_0$, where E_0 and H_0 are the amplitudes of **E** and **H**. Since E and H are related by Z, we can say the time-averaged energy flux density or '*intensity*' of the wave is $\frac{1}{2}(E_0^2/Z)$ or $\frac{1}{2} Z H_0^2$, i. e. the intensity is proportional to the square of the wave's amplitude.

In order, then, to describe such a classical wave we need to know its

1. intensity ($\propto E_0^2$),
2. frequency,
3. direction of propagation (Poynting's vector) and
4. orientation of the vibrations relative to some axial frame.

The notions above can be translated to four main subject areas within observational astronomy all involving time-dependent measurements of the parameters, namely

photometry, **spectrometry**, **astrometry** and **polarimetry**.

It is the latter aspect, both of measurement and interpretation, which forms the theme of this text.

To specify the characteristic associated with (4) above, we could clearly choose either the electric or magnetic vector. Usually the *electric* vector is preferred to describe the various polarization phenomena, as it is this component of the radiation which generally has the greater interaction with matter. As the electric and magnetic disturbances are orthogonal, they mimic each other in terms of any polarizational characteristic. It may be noted that some older optical texts, and indeed some astronomical papers, use the magnetic vector to describe polarization states. Prior to the development of current electromagnetic theory, and the knowledge that both electric and magnetic components were involved, polarization phenomena were described in terms of a *light vector*. Malus' original definition for this relates to the observation of the component in the rays in the plane of incidence as reflected by the glass windows and viewed through his calcite prism when the sunlight was incident at Brewster's angle. Malus' definition was geared more to the nature of the geometry of the process generating the polarization rather than to the vector nature of light which, at the time, was not appreciated. Thus, the *light vector* corresponded to what subsequently emerged to be the magnetic component. It is the behaviour of the electric vector that is now preferred for the description of polarization and associated phenomena.

2.2
The Ellipse Figure

Mathematical descriptions of the concepts of polarization vary from one text to another, as do the symbols used and, even more importantly, the definitions. Generally the problems raised by this are fairly trivial and unimportant but may cause confusion, for example, in assigning the polarity of a magnetic field. In the discussion here, and throughout this text, a consistent set of concepts, definitions and nomenclature will be used. References will be occasionally made to the use of other definitions to highlight the problems and difficulties that occur in interpreting some material and discussions found in the literature.

The concepts of polarizational phenomena may be explored by considering classical electromagnetic waves travelling along the z-axis of a right-handed Cartesian frame. By considering the disturbances of the electric vector in the xz- and yz-planes, the components may be expressed as

$$E_x = E_{x_0} \mathrm{e}^{\mathrm{i}\left(2\pi[\nu t - z/\lambda] + \delta_x\right)} , \tag{2.9}$$

$$E_y = E_{y_0} \mathrm{e}^{\mathrm{i}\left(2\pi[\nu t - z/\lambda] + \delta_y\right)} , \tag{2.10}$$

where E_{x_0} and E_{y_0} are the respective amplitudes of the components, ν is the frequency of the radiation, λ its wavelength and δ_x, δ_y are the phases of the two components. By taking the real parts of these equations,

$$E_x = E_{x_0} \cos\left(2\pi[\nu t - z/\lambda] + \delta_x\right) , \tag{2.11}$$

$$E_y = E_{y_0} \cos\left(2\pi[\nu t - z/\lambda] + \delta_y\right) . \tag{2.12}$$

The situation is depicted in Figure 2.1. It may be noted that various optical texts use the complex conjugate equations with $i(=\sqrt{-1})$ set as $-i$, and some authors also set the phases δ_x, δ_y as $-\delta_x$, $-\delta_y$. All these conventions have been discussed by Muller (1969) with comments as to how they influence polarimetric definitions and other defined optical parameters, particularly with respect to ellipsometry. Discussion with reference to the problems over definitions used in astronomical polarimetry will emerge later. The convention used in (2.9) and (2.10) correspond to those determined at the International Ellipsometry Conference in Nebraska (see Muller, 1973).

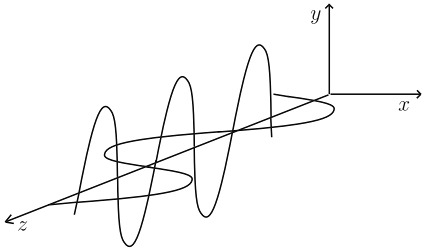

Fig. 2.1 Snapshots of the E disturbances of classical waves with differing wavelength values in the xz- and yz-planes travelling along the z-axis.

The form of the electrical disturbance in a plane normal to the direction of propagation can be readily determined by choosing a particular value of z, say $z = 0$. The above equations then reduce to

$$E_x = E_{x_0} \cos\left(2\pi\nu t + \delta_x\right), \tag{2.13}$$

$$E_y = E_{y_0} \cos\left(2\pi\nu t + \delta_y\right). \tag{2.14}$$

A *test* charged particle such as an electron in that plane would be subject to the oscillatory electric fields and it would execute an orbit. Its locus would be that of a Lissajou figure corresponding to the two orthogonal forces oscillating at the same frequency with a constant phase difference but having different amplitudes. In general, the executed figure is that of an ellipse, the *polarization ellipse*. The equation of the polarization ellipse is obtained by eliminating t from the two equations as follows. Equations (2.13) and (2.14) which represent the electric vibrations in the xz- and yz-planes at the value of $z = 0$ may be expanded and written in the form

$$\frac{E_x}{E_{x_0}} = \cos(2\pi\nu t)\cos\delta_x - \sin(2\pi\nu t)\sin\delta_x\,, \tag{2.15}$$

$$\frac{E_y}{E_{y_0}} = \cos(2\pi\nu t)\cos\delta_y - \sin(2\pi\nu t)\sin\delta_y\,. \tag{2.16}$$

By multiplying (2.15) by $\sin\delta_y$ and (2.16) by $\sin\delta_x$ and subtracting leads to

$$\frac{E_x}{E_{x_0}}\sin\delta_y - \frac{E_y}{E_{y_0}}\sin\delta_x = \cos(2\pi\nu t)\left[\sin\delta_y\cos\delta_x - \cos\delta_y\sin\delta_x\right]. \tag{2.17}$$

Similarly, by multiplying (2.15) by $\cos\delta_y$ and (2.16) by $\cos\delta_x$ and subtracting leads to

$$\frac{E_x}{E_{x_0}}\cos\delta_y - \frac{E_y}{E_{y_0}}\cos\delta_x = \sin(2\pi\nu t)\left[\sin\delta_y\cos\delta_x - \cos\delta_y\sin\delta_x\right]. \tag{2.18}$$

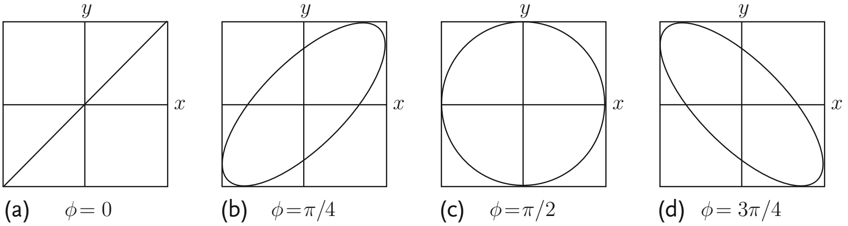

Fig. 2.2 Ellipse forms are depicted for phase differences $(\delta_y - \delta_x) = \phi$ of 0 (a), $\pi/4$ (b), $\pi/2$ (c) and $3\pi/4$ (d), with the orthogonal amplitudes, E_{x0}, E_{y0}, equal to each other. For $\phi = 0$, linear polarization ensues; for $\phi = \pi/2$, with equal component amplitudes, circular polarization results. The sense of description of the ellipse figures depends on the sign of the phase difference (see the text).

Squaring (2.17) and (2.18) and adding gives

$$\frac{E_x^2}{E_{x_0}^2} + \frac{E_y^2}{E_{y_0}^2} - \frac{2E_x E_y \cos\left(\delta_y - \delta_x\right)}{E_{x_0} E_{y_0}} = \sin^2\left(\delta_y - \delta_x\right). \tag{2.19}$$

This last equation represents the polarization ellipse and various forms demonstrating its behaviour according to the phases for the special condition with $E_{x_0} = E_{y_0}$ are depicted in Figure 2.2.

Thus the form of the polarization is described by the four parameters E_{x_0}, E_{y_0}, δ_x, and δ_y. Such quantities, however, are not directly measurable, but it will be demonstrated later that various combinations of them can be formed which are more convenient for describing the polarization ellipse.

It is important to remember that the polarization ellipse is not static in the xy-plane corresponding to $z = 0$; its locus is described at the frequency of the radiation.

The directional sense of 'drawing out' the ellipse carries an alternative depending on the magnitude of the phase difference between the orthogonally resolved amplitudes. According to the mathematics above, when $\pi > \left(\delta_y - \delta_x\right) > 0$, the **E**-vector would be seen to rotate in a clockwise direction as viewed by an observer receiving the radiation; when $0 > \left(\delta_y - \delta_x\right) > -\pi$, the **E**-vector would be seen to rotate in an anti-clockwise direction.

It is traditional to express this by the notion *handedness*, with the terms *right-handed* and *left-handed* being used. As it turns out, it is the conventions related to 'handedness' which are a troublesome thorn in general polarimetry (see Clarke, 1973), with the various scientific disciplines adopting their individual schemes, as does the International Astronomical Union (IAU) itself. At this stage it would be confusing to assign *handedness* to the outcome of the mathematics above for the following reasons.

Handedness depends on the viewpoint in which right-handed as 'seen' by an observer is left-handed from the point of view of the source. Terms such as *clockwise* and *anti-clockwise* suffer in the same way. The problem is further compounded by

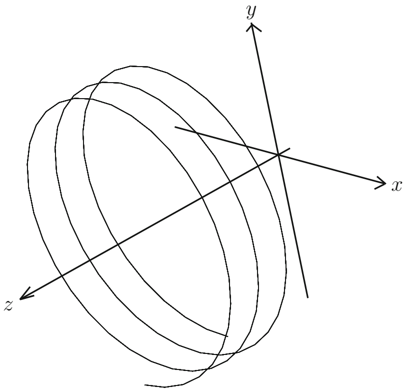

Fig. 2.3 A snapshot of the helical distribution (left-handed in the figure) of the electric disturbance. As time proceeds, the helix is carried along the z-axis without rotation. In any xy-plane, the vector will be seen to rotate with a particular sense according to the handedness of the helix. According to the viewpoint of the observer, the rotation would be anti-clockwise for the depicted case.

the fact that a 'sign' is sometimes added to the handedness and, across the various cross-disciplinary studies, a given elliptical polarization may be described by one of four differing definitions: right-handed positive (+), right-handed negative (−), with 'right-handed' having alternative definitions according to the viewpoint as just described. These issues will be discussed again later in Chapter 4 in respect of the definitions adopted by the IAU.

There is, however, a unique way of defining handedness (see Clarke & Grainger, 1970) for it can be readily demonstrated that an instantaneous snapshot of the electric vector, as it is distributed along the z-axis, traces out a helical pattern (see Figure 2.3). As a helix has a handedness which is defined independently of the observer's viewpoint, the polarization handedness may be labelled by the type of helix (left- or right-handed) which is present. If we consider the motion of the disturbance with time, we see that the helix moves along the direction of propagation *without rotation* and that its point of intersection with a plane transverse to its direction, say the xy-plane at $z = 0$, executes the polarization ellipse; the sense of execution, as seen by the observer, is clockwise for a right-handed helix and anti-clockwise for a left-handed helix, and hence the handedness of the helix corresponds to the common definition of polarization handedness used in general optics. In the literature there are, however, conflicting comments on this point. It is sometimes stated erroneously that when the handedness of the helix is used to describe the polarization handedness, a convention which is opposite to that of tradition results. Such a notion perhaps arises by considering the disturbance to be represented by a vector which is rotating as it is propagated. Its tip would again describe a helix, but this helix would be fixed in space, and not moving without rotation as the equations of the waves imply.

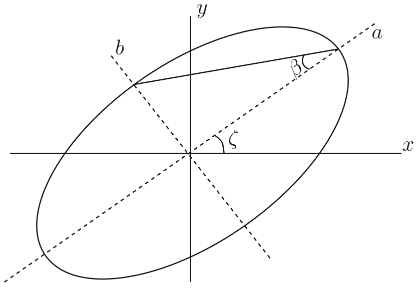

Fig. 2.4 The polarization ellipse is set with its major axis at an angle ζ to the *x*-axis. The value of $\tan\beta$ corresponds to the ratio of the minor to major axes of the ellipse.

The concept of handedness can also be considered from the description of the ellipse as follows. If the ratio of minor to major axes, $E_{b_0}/E_{a_0} = \tan\beta$ (see Figure 2.4) is defined as η, where $(1-\eta)$ defines the ellipticity, then it can be shown (see below) that

$$\sin 2\beta = \frac{2}{1+\eta^2} = \frac{2E_{x_0}E_{y_0}\sin\left(\delta_y - \delta_x\right)}{E_{x_0}^2 + E_{y_0}^2} \,. \tag{2.20}$$

The ratio, η, as defined is essentially positive, whereas (2.20) is quadratic and allows the algebraic possibility of negative roots. The significance of the sign of the deduced value of η is that positive indicates a clockwise rotation, as seen from the viewpoint of the observer, whilst negative indicates an anti-clockwise rotation. It is easily seen that the product of the roots of (2.20) is positive and equal to unity and so their signs must be the same. Since only one root can be numerically less than one, it follows from its definition that there is no ambiguity in determining the numerical value of η. Again it must be noted that any 'sign' convention depends on the way the equations for the classical waves are set with the signs associated with δ_x and δ_y, and on whether the phases are considered as being delays or advancements.

The presence of the cross-product in (2.19) simply reflects the fact that the major and minor axes of the ellipse do not coincide with the xy-axes of the reference frame. The situation is indicated in Figure 2.4.

Suppose that the axial frame is rotated positively through an angle, ζ, until it lies along the same directions as the major and minor axes of the ellipse, a, b. If E_a, E_b correspond to the vibration components with amplitudes and phases, E_{a_0}, E_{b_0}, δ_a and δ_b, along these directions, the form of the ellipse may be written as

$$\frac{E_a^2}{E_{a_0}^2} + \frac{E_b^2}{E_{b_0}^2} - \frac{2E_a E_b \cos\left(\delta_b - \delta_a\right)}{E_{a_0}E_{b_0}} = \sin^2\left(\delta_b - \delta_a\right) . \tag{2.21}$$

It may be noted that by using the coordinate frame a, b defined by the axes of the ellipse, the resolved disturbances have a phase difference of $\pi/2$, and (2.21) reduces to

$$\frac{E_a^2}{E_{a_0}^2} + \frac{E_b^2}{E_{b_0}^2} = 1\ . \tag{2.22}$$

The size of the ellipse may be described by the combination of the values of the major, E_a, and minor, E_b, axes in the form of $E_{a_0}^2 + E_{b_0}^2$ which is proportional to the intensity, I, of the beam. It is obvious that:

$$E_{a_0}^2 + E_{b_0}^2 = E_{x_0}^2 + E_{y_0}^2\ . \tag{2.23}$$

As the disturbances resolved in the coordinate frame defined by the axes of the ellipse have a relative phase difference of $\pi/2$, and by using the definition $E_{b_0}/E_{a_0} = \tan\beta$, they may be expressed by

$$E_a = E_{a_0}\cos(2\pi\nu t) = I^{1/2}\cos\beta\cos(2\pi\nu t)\,, \tag{2.24}$$

and

$$E_b = E_{b_0}\cos\left(2\pi\nu t + \frac{\pi}{2}\right) = E_{b_0}\sin(2\pi\nu t) = -I^{1/2}\sin\beta\sin(2\pi\nu t)\ . \tag{2.25}$$

Resolving these disturbances along the x- and y-axes gives

$$E_x = I^{1/2}\left\{\cos\beta\cos\zeta\cos(2\pi\nu t) + \sin\beta\sin\zeta\sin(2\pi\nu t)\right\}, \tag{2.26}$$

and

$$E_y = I^{1/2}\left\{\cos\beta\sin\zeta\cos(2\pi\nu t) - \sin\beta\cos\zeta\sin(2\pi\nu t)\right\}, \tag{2.27}$$

these equations being equivalent to (2.13) and (2.14).

By expanding (2.26) and (2.27), and equating the coefficients of $\cos(2\pi\nu t)$ and $\sin(2\pi\nu t)$, we have

$$\begin{aligned}
E_{x_0}\cos\delta_x &= I^{1/2}\cos\beta\cos\zeta\ , && \text{(a)}\\
E_{y_0}\cos\delta_y &= I^{1/2}\cos\beta\sin\zeta\ , && \text{(b)}\\
E_{x_0}\sin\delta_x &= -I^{1/2}\sin\beta\sin\zeta\ , && \text{(c)}\\
E_{y_0}\cos\delta_y &= I^{1/2}\sin\beta\cos\zeta\ . && \text{(d)}
\end{aligned}$$

By taking (**a**) × (**b**) and (**c**) × (**d**) and then adding gives

$$\begin{aligned}
&E_{x_0}E_{y_0}\left(\cos\delta_x\cos\delta_y + \sin\delta_x\sin\delta_y\right)\\
&\qquad = I\left(\cos^2\beta\cos\zeta\sin\zeta - \sin^2\beta\cos\zeta\sin\zeta\right),
\end{aligned}$$

which reduces to

$$2E_{x_0}E_{y_0}\cos\left(\delta_y - \delta_x\right) = I\cos 2\beta\sin 2\zeta\ . \tag{2.28}$$

Similarly by taking (**a**) × (**d**) with (**b**) × (**c**) and adding leads to

$$2E_{x0}E_{y0}\sin\left(\delta_y-\delta_x\right)=I\sin 2\beta\ . \tag{2.29}$$

Squaring (**a**) and (**c**) and adding gives

$$E_{x0}^2=I\left(\cos^2\beta\cos^2\zeta+\sin^2\beta\sin^2\zeta\right). \quad (\mathbf{e})$$

Squaring (**b**) and (**d**) and adding gives

$$E_{y0}^2=I\left(\cos^2\beta\sin^2\zeta+\sin^2\beta\cos^2\zeta\right). \quad (\mathbf{f})$$

By adding (**e**) and (**f**),

$$E_{x0}^2+E_{y0}^2=I\ . \tag{2.30}$$

By subtracting (**f**) from (**e**),

$$E_{x0}^2-E_{y0}^2=I\cos 2\beta\cos 2\zeta\ . \tag{2.31}$$

From (2.28), (2.29), (2.30) and (2.31):

$$\tan 2\zeta=\frac{2E_{x0}E_{y0}\cos\left(\delta_y-\delta_x\right)}{E_{x0}^2-E_{y0}^2} \tag{2.32}$$

and

$$\sin 2\beta=\frac{2E_{x0}E_{y0}\sin\left(\delta_y-\delta_x\right)}{E_{x0}^2+E_{y0}^2}\ . \tag{2.33}$$

Thus the orientation of the ellipse relative to the measurement axis can be found by applying (2.32); (2.33) is key to determining the ellipticity, and the sense of rotation of the **E**-vector (see earlier discussion) describing the ellipse. Thus, in summary, it can be seen that *four* parameters, E_{x0}, E_{y0}, δ_x and δ_y, originally describing the polarization ellipse, can be combined to provide an alternative set corresponding to the ellipse size, the azimuth of the major axis, the ellipticity and the sense of the rotation. These terms are physically more meaningful for the ellipse description, and have the additional advantage by comprising components with dimensions of intensity. The size proportional to the intensity of the beam of radiation may be written as

$$\underline{I=E_{x0}^2+E_{y0}^2}\ . \tag{2.34}$$

It is also convenient to define three intensities as

$$\underline{I_{\text{diff}}=E_{x0}^2-E_{y0}^2\equiv I\cos 2\beta\cos 2\zeta\ ,} \tag{2.35}$$

$$\underline{I_{\cos}=2E_{x0}E_{y0}\cos\left(\delta_y-\delta_x\right)\equiv I\cos 2\beta\sin 2\zeta} \tag{2.36}$$

and

$$I_{\sin} = 2E_{x_0}E_{y_0}\sin\left(\delta_y - \delta_x\right) \equiv I\sin 2\beta\ . \tag{2.37}$$

The azimuth of the major axis of the ellipse may then be calculated from

$$\tan 2\zeta = I_{\cos}/I_{\text{diff}}\ , \tag{2.38}$$

and its ellipticity ($\tan\beta - 1$) from:

$$\sin 2\beta = I_{\sin}/I\ , \tag{2.39}$$

and the sense of description from the sign of $\tan\beta$.

It may also be noted that

$$I^2 = I^2_{\text{diff}} + I^2_{\cos} + I^2_{\sin}\ . \tag{2.40}$$

2.3
The Poincaré Sphere

From above, it can be seen that any polarization form can be described in terms of the two double angles, 2ζ and 2β. These may then serve as polar coordinates, θ, ϕ, in conjunction with a radius value of $I = (E^2_{x_0} + E^2_{y_0})$, usually normalized to unity.

As a consequence, polarization forms may be mapped on the surface of a sphere with

$$\theta = 2\zeta \equiv \text{longitude}\ , \quad \text{within the range} \quad 0^\circ \le 2\zeta \le 360^\circ\ ,$$

and

$$\phi = 2\beta \equiv \text{latitude}\ , \quad \text{within the range} \quad -90^\circ \le 2\beta \le +90^\circ\ .$$

Each point on the sphere, $\mathbf{P}(2\zeta, 2\beta)$, corresponds to a unique polarization form, the system being referred to as the *Poincaré sphere* representation (see Poincaré, 1892, and Deschamps, 1951). The radius vector to a point on the sphere characterizing a particular polarization form is called the *eigenvector* of that form.

The longitude of any point reflects the azimuth of the major axis of the polarization ellipse, and the latitude expresses the ellipticity. For points around the equator, the value of $\phi = 2\beta$ is zero and the mapped polarizations are linear, the azimuth, ζ, of the vibration is given by the value $\theta/2$. From the mathematics used in the text, the upper hemisphere, with positive ϕ, corresponds to the elliptical polarization being described by a clockwise rotation of the **E**-vector, as seen by the observer receiving the radiation; the lower hemisphere depicts polarizations of the opposite sense. At the poles, $\theta = 2\beta$ is equal to 90°, and the polarization has circular form. A small circle, drawn at a fixed value of θ with ϕ running from 0° to 2π, gives

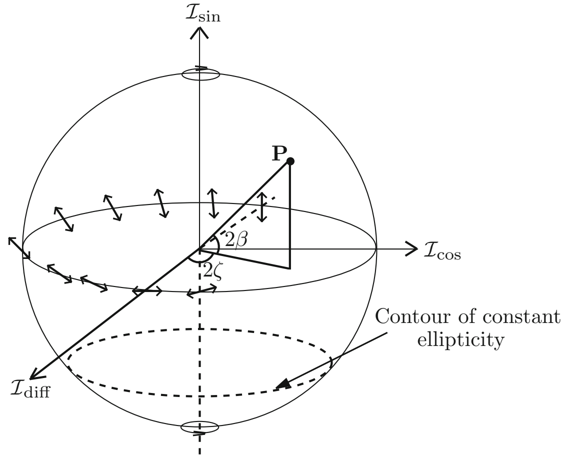

Fig. 2.5 The Poincaré sphere indicating the position of the eigen vector of one particular polarization form, **P**, described by the coordinates, $2\zeta, 2\beta$. Points around a small circle of fixed latitude, marked with a 'dashed' locus, describe polarization forms of identical ellipticity, their position in azimuth describing the azimuth of the ellipse major axis. The equator corresponds to linear polarization forms; an indication of the azimuths of these is portrayed around a portion of this great circle. The upper hemisphere pole represents elliptical polarization with the **E**-vector rotating clockwise, as seen by the observer receiving the radiation, while the lower hemisphere depicts elliptical polarization of the opposite sense; the poles correspond to circular polarization.

the locus of a set of polarization forms with identical ellipticity, but with azimuths running from 0° to π, depending on the value of ϕ. Polarization forms with characteristic points at opposite ends of a diameter of the Poincaré sphere, and hence with opposite eigenvectors, are said to be *orthogonal*. Orthogonal forms thus have perpendicular azimuths, opposite handedness but identical ellipticities. Mapping of polarizations on a sphere has special appeal, as the various forms are related by spherical trigonometry, with formulae familiar to the well-trained Astronomer. A Poincaré sphere is presented in Figure 2.5.

A Cartesian coordinate frame with axes corresponding to $\mathcal{I}_{\mathrm{diff}}$, $\mathcal{I}_{\cos}$ and $\mathcal{I}_{\sin}$ may be ascribed to the sphere of radius, I, such that the respective values I_{diff}, $I_{\cos}$ and $I_{\sin}$, describing a particular polarization form, relate to the polar angles by $\tan 2\zeta = I_{\cos}/I_{\mathrm{diff}}$ and $\sin 2\beta = I_{\sin}/I$.

As mentioned above, linear polarization forms run around the equator, and their vector behaviour of the azimuths for some are depicted in Figure 2.5 around part of the equatorial great circle; if the xz-plane (see Figure 2.1) corresponds to being horizontal, then horizontal linear polarization is represented by polar coordinates, $(0°, 0°)$, or Cartesian coordinates, $(I, 0, 0)$, and vertical polarization corresponds to $(180°, 0°)$, or $(-I, 0, 0)$.

It may be noted that **P** can also be described in terms of a spherical triangle formed by a great circle inclined at an angle of $(\delta_y - \delta_x)$ to the equator, the distance of **P** from $(I, 0, 0)$ given by 2α, where $\alpha = \tan^{-1}(E_{x0}/E_{y0})$. The situation is depicted

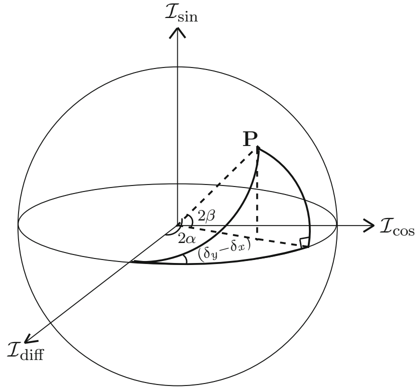

Fig. 2.6 The Poincaré sphere indicating the position of the eigenvector of one particular polarization form described by a spherical triangle. The angle 2α is the distance along the great circle from the reference $(I, 0, 0)$ to the point **P**, the circle being inclined to the equator at an angle of $(\delta_y - \delta_x)$.

in Figure 2.6. By using the sine formula of spherical trigonometry,

$$\frac{\sin 2\alpha}{\sin \pi/2} = \frac{\sin 2\beta}{\sin\left(\delta_y - \delta_x\right)}\,, \tag{2.41}$$

leading to

$$\sin 2\beta = \sin 2\alpha \sin\left(\delta_y - \delta_x\right) = \frac{2E_{x0}E_{y0}\sin\left(\delta_y - \delta_x\right)}{E_{x0}^2 + E_{y0}^2}\,, \tag{2.42}$$

so confirming the correctness of this description. It can be seen that to arrive at **P** from the linear polarization state denoted by $(I, 0, 0)$, the point on the $\mathcal{I}_{\text{diff}}$-axis, the sphere should be rotated in a positive direction through an angle $(\delta_y - \delta_x)$ about the diameter defined by the $\mathcal{I}_{\text{diff}}$-axis. Relationships between any two eigenvectors of polarization can be established using spherical trigonometry (see Chapter 3).

2.4
Conclusion

The description and discussion above of the polarization ellipse within a particular plane were developed by combining two orthogonal classical waves. Such waves can be considered as having a long-term phase coherence, with the form of the ellipse persisting over a long period of time. If the amplitudes and/or the phases of the waves are subject to a change, the form of the ellipse will change in sympathy. The behaviour of the changes can be described in terms of the Poincaré sphere representation, but this becomes complicated if the mechanism producing the change also attenuates the radiation. In order to determine any optical effects – astrophysical or instrumental – which alter the polarization ellipse as the radiation progresses from its source to the observer, it is useful to have a more general algebra to facilitate this. A discussion on such matters now follows with a description of the Jones calculus given in the next chapter.

References

Clarke, D. (1973) Nomenclature of polarized light: elliptical polarization. *Appl. Opt.*, **13**, 222–224. [37]

Clarke, D., Grainger, J.F. (1971) *Polarized Light and Optical Measurement*. Pergamon, Oxford. [38]

Deschamps, G.A. (1951) Geometrical representation of the polarization of a plane electromagnetic wave. *Proc. IRE*, **39**, 540–544. [42]

Muller, R.F. (1969) Definitions and conventions in ellipsometry. *Surface Science*, **16**, 14–33. [35]

Muller, R.F. (Ed.) (1973) *Advances in Electrochemistry and Electrochemical Engineering. Volume 9 – Optical Techniques in Electrochemistry*. John Wiley & Sons, New York. [35]

Poincaré, H. (1892) pp. 282–285 in *Théorie Mathèmatique de la Lumiére II*. Gauthiers Villars, Paris (it may be noted that this reference appears in Part II of the book and that the first part carries the date (1895)). [42]

3

The Algebra of Polarization

3.1

Introduction

There are a variety of ways for calculating how the polarization form is transformed when a beam of light passes through an optical element or suffers some scattering process. The most simple method for doing this is by application of the *Jones calculus*. With this algebra, it is readily seen how the resulting polarization ellipse can be calculated and appreciated following any transformation by an optical interaction. It should be noted immediately that the Jones calculus is only applicable to light beams that are *coherent* and should be used if knowledge of phase is important such as in the calculation of interference effects in optical devices when polarization is involved. It is more appropriate for dealing with wave amplitudes rather than fluxes or intensities. The algebra, therefore, has only limited use in respect of general astrophysical situations. For the latter, the polarization description is better expressed using *Stokes parameters* and the *Mueller calculus*, these algebras being adopted quite generally in stellar polarimetry. The physical concepts associated with Stokes parameters are presented in Chapter 4.

The Jones calculus is easy to apply, however, for expressing the characteristics of optical trains within instruments, although it is not amenable for describing the effects of depolarization. For completeness, and to give insight into the behaviour of polarization forms according to their interplay with optical interactions, the principles of this calculus are given below.

3.2

The Jones Calculus

When polarized light interacts with matter such as in a scattering process, or passes through optical elements, the polarization characteristics suffer change. Each scattering element or constituent of an optical train has properties which may alter the amplitudes of the waves, introduce phase delays or rotate the azimuth of the major axis of the polarization ellipse.

Stellar Polarimetry. David Clarke

ISBN: 978-3-527-40895-5

For the first two kinds of interaction, the affecting element has orthogonal reference axes which are used to define the amplitude coefficients for the scattering, or the transmission coefficients, or to describe the phase delays applied to the resolved beams. In order to calculate the effect of an optical interaction, the equations describing the oscillations ((2.13) and (2.14)) must first be rewritten to correspond to the axial frame of the element.

Suppose that in the xy-coordinate frame corresponding to $z = 0$, the electric disturbances are written as

$$E_x = E_{x_0} \mathrm{e}^{\mathrm{i}(2\pi\nu t + \delta_x)} \longrightarrow E_{x_0} \cos(2\pi\nu t + \delta_x)\,, \tag{3.1}$$

$$E_y = E_{y_0} \mathrm{e}^{\mathrm{i}\left(2\pi\nu t + \delta_y\right)} \longrightarrow E_{y_0} \cos\left(2\pi\nu t + \delta_y\right). \tag{3.2}$$

If these equations are now described in a new frame, $x'y'$, which is set at an angle, γ, relative to the original xy-frame, such that the angle is positive and measured anti-clockwise, as seen looking against the direction of propagation, and as depicted in Figure 3.1, the oscillations may be written as

$$E_{x'} = E_x \cos\gamma + E_y \sin\gamma\ , \tag{3.3}$$

$$E_{y'} = -E_x \sin\gamma + E_y \cos\gamma\ . \tag{3.4}$$

This transformation may be written in the matrix form as

$$\begin{bmatrix} E_{x'} \\ E_{y'} \end{bmatrix} = \begin{bmatrix} \cos\gamma & \sin\gamma \\ -\sin\gamma & \cos\gamma \end{bmatrix} \begin{bmatrix} E_x \\ E_y \end{bmatrix}. \tag{3.5}$$

Suppose that the radiation is subject to absorption and phase delay as it passes through some astrophysical medium, or through an optical device such that the amplitude transmission coefficients, $k_{x'}, k_{y'}$, and retardations, $\mathit{\Delta}_{x'}, \mathit{\Delta}_{y'}$, are defined in this new coordinate frame. By using the concept of *retardation*, this ensures that $\mathit{\Delta}_{x'}, \mathit{\Delta}_{y'}$ are amounts of phase to be *subtracted*. This convention provides a convenient notation and is in keeping with the declared polarimetric definitions. Using an asterisk (*) to indicate parameters referring to the emergent light, the

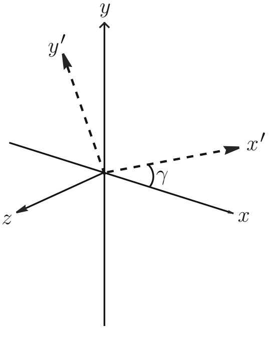

Fig. 3.1 The effect of rotating the reference frame, xy, to another, $x'y'$, by a positive angle, γ, so that the new frame corresponds with the principal axes of an optical device; z is the direction of propagation of the light beam.

equations representing the resulting polarization may be written as

$$E^*_{x'} = k_{x'} E_{x'_0} \cos(2\pi\nu t + \delta_{x'} - \varDelta_{x'}) \equiv E^*_{x'_0} \cos(2\pi\nu t + \delta^*_{x'}) \,, \tag{3.6}$$

$$E^*_{y'} = k_{y'} E_{y'_0} \cos(2\pi\nu t + \delta_{y'} - \varDelta_{y'}) \equiv E^*_{y'_0} \cos(2\pi\nu t + \delta^*_{y'}) \,. \tag{3.7}$$

The values of $E^*_{x'_0}$, $E^*_{y'_0}$, $\delta^*_{x'}$ and $\delta^*_{y'}$ may then be used to evaluate the four parameters I, I_{diff}, $I_{\cos}$ and $I_{\sin}$, as defined in Chapter 2, these being used in turn to determine the characteristics of the ellipse – its size, ζ, η and the sign of η.

The procedure of determining the characteristics of the modified ellipse in this manner is cumbersome, and completely unmanageable when the cumulative affect of several different optical elements in series requires calculation. The algebra describing the various interactions noted above can be simplified by using matrix notation. The situation represented by (3.6) and (3.7) may be expressed by using exponentials to describe the waves, and matrices to define the various effects that the optical elements, or media, have on the radiation. Thus,

$$\begin{bmatrix} E^*_{x'} \\ E^*_{y'} \end{bmatrix} = \underbrace{\begin{bmatrix} k_{x'} & 0 \\ 0 & k_{y'} \end{bmatrix}}_{\text{Transmission}} \underbrace{\begin{bmatrix} \mathrm{e}^{-\mathrm{i}\varDelta_{x'}} & 0 \\ 0 & \mathrm{e}^{-\mathrm{i}\varDelta_{y'}} \end{bmatrix}}_{\text{Phase Delay}} \underbrace{\begin{bmatrix} \cos\gamma & \sin\gamma \\ -\sin\gamma & \cos\gamma \end{bmatrix}}_{\text{Rotation}} \begin{bmatrix} E_x \\ E_y \end{bmatrix} , \tag{3.8}$$

i. e.

$$\begin{bmatrix} E^*_{x'} \\ E^*_{y'} \end{bmatrix} = \begin{bmatrix} k_{x'} & 0 \\ 0 & k_{y'} \end{bmatrix} \begin{bmatrix} \mathrm{e}^{-\mathrm{i}\varDelta_{x'}} & 0 \\ 0 & \mathrm{e}^{-\mathrm{i}\varDelta_{y'}} \end{bmatrix} \begin{bmatrix} E_{x'} \\ E_{y'} \end{bmatrix} . \tag{3.9}$$

This approach of formulation was first set out in a series of papers by R. Clark Jones (see Jones 1941a, 1941b, 1942, 1947a, 1947b, 1948, 1956 and Jones & Hurwitz 1941). The column vectors describing the components of the vibration are known as *Jones vectors*; the procedures of setting out the interaction of polarized light with optical devices is known as the *Jones calculus*.

For the general situation, the optical devices are usually linear, i. e. the frequency of the emergent radiation from the device is the same as that of the incident radiation. Thus, the time dependences of the incident and emergent Jones vectors cancel and we have

$$\begin{bmatrix} E^*_{x'_0} \mathrm{e}^{\mathrm{i}\delta^*_{x'}} \\ E^*_{y'_0} \mathrm{e}^{\mathrm{i}\delta^*_{y'}} \end{bmatrix} = \begin{bmatrix} k_{x'} & 0 \\ 0 & k_{y'} \end{bmatrix} \begin{bmatrix} \mathrm{e}^{-\mathrm{i}\varDelta_{x'}} & 0 \\ 0 & \mathrm{e}^{-\mathrm{i}\varDelta_{y'}} \end{bmatrix} \begin{bmatrix} E_{x'_0} \mathrm{e}^{\mathrm{i}\delta_{x'}} \\ E_{y'_0} \mathrm{e}^{\mathrm{i}\delta_{y'}} \end{bmatrix} . \tag{3.10}$$

We are rarely interested in the absolute phases of the individual components and it is advantageous to rewrite (3.10) in the form:

$$\begin{aligned} &\mathrm{e}^{\mathrm{i}\delta^*_{x'}} \begin{bmatrix} E^*_{x'_0} \\ E^*_{y'_0} \mathrm{e}^{\mathrm{i}(\delta^*_{y'} - \delta^*_{x'})} \end{bmatrix} \\ &= \begin{bmatrix} k_{x'} & 0 \\ 0 & k_{y'} \end{bmatrix} \mathrm{e}^{-\mathrm{i}\varDelta^*_{x'}} \begin{bmatrix} 1 & 0 \\ 0 & \mathrm{e}^{-\mathrm{i}(\varDelta_{y'} - \varDelta_{x'})} \end{bmatrix} \mathrm{e}^{\mathrm{i}\delta_{x'}} \begin{bmatrix} E_{x'_0} \\ E_{y'_0} \mathrm{e}^{\mathrm{i}(\delta_{y'} - \delta_{x'})} \end{bmatrix} . \end{aligned} \tag{3.11}$$

Since phase is only ever determined to within an additive constant, we can set $\delta_{x'} = 0$. Also, since the emergent x' component can only have acquired a non-zero phase as a result of its passage through the device, it follows that

$$\mathrm{e}^{\mathrm{i}\delta^*_{x'}} = \mathrm{e}^{-\mathrm{i}\Delta_{x'}} \,. \tag{3.12}$$

We thus have

$$\begin{bmatrix} E^*_{x'_0} \\ E^*_{y'_0}\mathrm{e}^{\mathrm{i}(\delta^*_{y'}-\delta^*_{x'})} \end{bmatrix} = \begin{bmatrix} k_{x'} & 0 \\ 0 & k_{y'} \end{bmatrix} \begin{bmatrix} 1 & 0 \\ 0 & \mathrm{e}^{-\mathrm{i}(\Delta_{y'}-\Delta_{x'})} \end{bmatrix} \begin{bmatrix} E_{x'_0} \\ E_{y'_0}\mathrm{e}^{\mathrm{i}(\delta_{y'}-\delta_{x'})} \end{bmatrix} . \tag{3.13}$$

It may be noted that only relative phase differences, or relative retardations, occur within the matrices of (3.13). They have been engineered to be written with respect to the y'-axis. By doing this, the values of $E^*_{x'_0}$, $E^*_{y'_0}$ and $(\delta^*_{y'} - \delta^*_{x'})$ are directly related to the determination of the form of the resultant ellipse by insertion into (2.19). The value of $(\Delta_{y'} - \Delta_{x'})$ represents the *differential retardation*, Δ, introduced by the element, with the wave resolved in the y' direction being more retarded than that defined by the x'-axis. If such a differential phase delay is produced by a wave plate, the direction of y' corresponds to the plate's slow axis.

The matrix product

$$\begin{bmatrix} k_{x'} & 0 \\ 0 & k_{y'} \end{bmatrix} \begin{bmatrix} 1 & 0 \\ 0 & \mathrm{e}^{-\mathrm{i}(\Delta_{y'}-\Delta_{x'})} \end{bmatrix} \tag{3.14}$$

represents the total effect of the optical element and can be multiplied out to give a single matrix specifying the element.

It is important to remember that this element matrix is written in terms of axes fixed in the element, and that to operate with it on the Jones vector of the incident beam of light, it is first of all necessary to multiply that vector by the appropriate rotation matrix, as was done above.

Suppose $[\mathcal{E}_1]$, $[\mathcal{E}_2]$, $[\mathcal{E}_3]$, etc. correspond to the characteristic matrices of a set of optical elements. If the rth and sth elements are inclined at a positive angle, γ_{rs}, the rotation matrix describing the coordinate change from the r-frame to the s-frame is

$$\begin{bmatrix} \cos\gamma_{rs} & \sin\gamma_{rs} \\ -\sin\gamma_{rs} & \cos\gamma_{rs} \end{bmatrix} , \tag{3.15}$$

and may be formally written $[\mathcal{R}_{rs}]$. If [J] is the Jones vector of a beam of light incident on the first element, written in terms of axes inclined to that element at an angle, $\gamma_{0,1}$, then the Jones vector $[\mathbf{J}^*]$ of the light emerging from the nth element written in terms of the coordinate frame to which [J] is referred is given by

$$[\mathbf{J}^*] = [\mathcal{R}_{n,0}][\mathcal{E}_n][\mathcal{R}_{n-1,n}][\mathcal{E}_{n-1}]\ldots[\mathcal{E}_3][\mathcal{R}_{2,3}][\mathcal{E}_2][\mathcal{R}_{1,2}][\mathcal{E}_1][\mathcal{R}_{0,1}][\mathbf{J}] \,. \tag{3.16}$$

Given the elements of a Jones vector, it is a simple matter to compute the intensity, azimuth, ellipticity and handedness of the ellipse by using relationships defined

Table 3.1 The Jones calculus. The simplest transforming effects operating on the amplitudes contained in a Jones vector are: (1) differential transmission for the orthogonal vibrations, (2) phase delays of different values affecting the orthogonal vibrations, and (3) rotation of the direction of vibration of the linear polarization or of the major axis of the polarization ellipse. The matrices representing these effects are summarized below.

Operation	**Matrix and notes**
Partial polarizer	$[\mathcal{PP}] = \begin{bmatrix} k_1 & 0 \\ 0 & k_2 \end{bmatrix}$ Subscripts 1 and 2 refer to two orthogonal directions; k_1 is the amplitude transmission coefficient of the element to light perfectly linearly polarized in direction 1, k_2 is a similar coefficient for direction 2. It is usual to choose directions 1 and 2 such that $\mid k_1 - k_2 \mid$ is maximized.
Perfect polarizer	$[\mathcal{P}] = \begin{bmatrix} 1 & 0 \\ 0 & 0 \end{bmatrix}$ The matrix assumes that the polarizer has perfect transmission but may be multiplied by a coefficient (< 1) to allow for this if necessary.
Pure retarder	$[\Delta] = \begin{bmatrix} 1 & 0 \\ 0 & \mathrm{e}^{-\mathrm{i}\Delta} \end{bmatrix}$ or $[\Delta] = \begin{bmatrix} \mathrm{e}^{\mathrm{i}\Delta/2} & 0 \\ 0 & \mathrm{e}^{-\mathrm{i}\Delta/2} \end{bmatrix}$ Δ is the differential retardation, or *retardance*. These matrices are not mathematically equivalent as the second should be multiplied by a factor of $\mathrm{e}^{-\mathrm{i}\Delta/2}$. This factor is normally ignored as the phase of the wave is only determined to within an additive constant. In other words, it is only the differential retardation that is of interest.
Rotation	$[\mathcal{R}(\gamma)] = \begin{bmatrix} \cos\gamma & \sin\gamma \\ -\sin\gamma & \cos\gamma \end{bmatrix}$ γ is a positive angle from the x-axis to the y-axis and measured anticlockwise as seen by the observer. This matrix can also be used to describe the effect of optical activity or Faraday rotation.

in (2.34), (2.38) and (2.39). The matrices describing various polarimetric elements are summarized in Table 3.1.

Clearly from its formulation, the Jones calculus deals with situations involving radiation with waves which have long-term phase coherence. It is important to remember that the algebra can deal with the combination of beams of radiation only if the phases of the component beams are taken into account. Thus, suppose that the disturbances within a beam of radiation can be expressed in the form of (2.13) and (2.14), i. e.

$$E_{1x} = E_{1x_0} \cos\left(2\pi\nu t + \delta_{1x}\right) , \tag{3.17}$$

$$E_{1y} = E_{1y_0} \cos\left(2\pi\nu t + \delta_{1y}\right) , \tag{3.18}$$

these giving rise to a particular polarization form. Suppose that a second polarized beam is added with classical waves expressed as

$$E_{2x} = E_{2x_0} \cos\left(2\pi\nu t + \delta_{2x}\right) , \tag{3.19}$$

$$E_{2y} = E_{2y_0} \cos\left(2\pi\nu t + \delta_{2y}\right) . \tag{3.20}$$

The combination gives rise to disturbances which are described as

$$E_x^* = E_{1x_0} \cos\left(2\pi\nu t + \delta_{1x}\right) + E_{2x_0} \cos\left(2\pi\nu t + \delta_{2x}\right), \tag{3.21}$$

$$E_y^* = E_{1y_0} \cos\left(2\pi\nu t + \delta_{1y}\right) + E_{2y_0} \cos\left(2\pi\nu t + \delta_{2y}\right). \tag{3.22}$$

These latter two equations can be contracted to

$$E_x^* = E_{x_0}^* \cos\left(2\pi\nu t + \delta_x^*\right), \tag{3.23}$$

$$E_y^* = E_{y_0}^* \cos\left(2\pi\nu t + \delta_y^*\right), \tag{3.24}$$

where,

$$\begin{aligned}
(E_{x_0}^*)^2 &= \{E_{1x_0} \cos\delta_{1x} + E_{2x_0} \cos\delta_{2x}\}^2 + \{E_{1x_0} \sin\delta_{1x} + E_{2x_0} \sin\delta_{2x}\}^2, \\
(E_{y_0}^*)^2 &= \{E_{1y_0} \cos\delta_{1y} + E_{2y_0} \cos\delta_{2y}\}^2 + \{E_{1y_0} \sin\delta_{1y} + E_{2y_0} \sin\delta_{2y}\}^2, \\
\tan\delta_x^* &= \{E_{1x_0} \sin\delta_{1x} + E_{2x_0} \sin\delta_{2x}\} / \{E_{1x_0} \cos\delta_{1x} + E_{2x_0} \cos\delta_{2x}\}, \\
\tan\delta_y^* &= \{E_{1y_0} \sin\delta_{1y} + E_{2y_0} \sin\delta_{2y}\} / \{E_{1y_0} \cos\delta_{1y} + E_{2y_0} \cos\delta_{2y}\}.
\end{aligned}$$

Thus, as can be seen from (3.23) and (3.24), combinations of orthogonally resolved classical coherent waves, with particular polarization forms, lead to a pair of classical waves with a new resultant polarization form.

3.3
The Description of Scattering

It is impossible here to provide all the material required to appreciate fully the physics and mathematics associated with scattering within astrophysical situations. There are several texts available which comprehensively cover these matters. However, it is important that scattering mechanisms are understood to some degree in respect of their polarigenic potential. As it turns out, some of the algebra used to formulate scattering processes has overtones with the Jones calculus.

When radiation encounters assemblies of small particles such as dust within circumstellar envelopes, electron clouds in extended dissociated stellar atmospheres, or dust in the interstellar medium, the interaction causes it to be scattered. Generally the scattering is not isotropic with the amplitudes of the waves being dependent on the angle of emergence with respect to the original direction of incidence. In addition, the scattering is also sensitive to polarization.

By defining some plane associated with any incoming radiation, the waves may be resolved in directions perpendicular (⊥) and parallel (||) to this plane. Thus, the orthogonal vibrations may be written as

$$E_\perp = E_{\perp_o} \cos\left(2\pi\nu t + \delta_\perp\right), \tag{3.25}$$

$$E_\parallel = E_{\parallel_o} \cos\left(2\pi\nu t + \delta_\parallel\right). \tag{3.26}$$

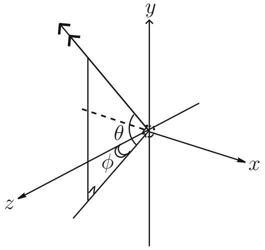

Fig. 3.2 Radiation travelling along the z-axis hits an assembly of scattering particles positioned in the xy-plane and is scattered in a direction given by θ, ϕ.

Following the scattering process, the magnitudes of the perpendicular and parallel vibrations may be represented by $E_{\perp_o}(\theta,\phi)$ and $E_{\|_o}(\theta,\phi)$, where θ and ϕ are the polar angles describing the direction of the emergence of the radiation (see Figure 3.2). These waves may be simply represented in terms of a linear transformation of the incident wave, and consequently the relationship can be described in terms of an interaction, much in the same way as is done by the Jones calculus. Hence the description of scattering may be written as

$$\begin{bmatrix} E'_{\perp_o}(\theta,\phi) \\ E'_{\|_o}(\theta,\phi) \end{bmatrix} = \begin{bmatrix} S_{1\perp}(\theta,\phi) & S_{2\|}(\theta,\phi) \\ S_{2\perp}(\theta,\phi) & S_{1\|}(\theta,\phi) \end{bmatrix} \begin{bmatrix} E_{\perp_o} \\ E_{\|_o} \end{bmatrix}, \tag{3.27}$$

where $E'_{\perp_o}$, $E'_{\|_o}$ are the resulting vibrations and $S_{1\perp}$, $S_{2\perp}$, $S_{1\|}$ and $S_{2\|}$ are the *amplitude scattering functions*, dependent on θ and ϕ. They comprise real and imaginary parts, in turn dependent on the refractive index, $\tilde{m} = m' - \mathrm{i}m''$, of the scattering particle, and on its size, a, in relation to the wavelength of the radiation being scattered; normally the size/wavelength relationship is expressed as $x = 2\pi a/\lambda = ka$, with $2\pi/k$ defining the *wavenumber*.

Generally in an astrophysical situation, the scattering is simple, corresponding to the equivalent of linear dichroism and linear birefringence, there being no circular dichroism and no circular birefringence. For mathematical simplicity, it is also convenient to assume that the principal axes of the tensor describing the particle anisotropy coincides with the frame defined by the $\perp$ and $\|$ directions. With these assumptions $S_{2\perp}$ and $S_{2\|} = 0$, and the unity subscript may be dropped leading to a description represented by

$$\begin{bmatrix} E'_{\perp_o}(\theta,\phi) \\ E'_{\|_o}(\theta,\phi) \end{bmatrix} = \begin{bmatrix} S_{\perp}(\theta,\phi) & 0 \\ 0 & S_{\|}(\theta,\phi) \end{bmatrix} \begin{bmatrix} E_{\perp_o} \\ E_{\|_o} \end{bmatrix}. \tag{3.28}$$

The amplitude scattering functions may comprise real and imaginary parts so that

$$S_{\perp} = a_{\perp} - ib_{\perp} \tag{3.29}$$

$$S_{\|} = a_{\|} - ib_{\|}\,, \tag{3.30}$$

where the terms $a_{\perp}$ and $a_{\|}$ dictate the absorptive effects, their combination describing the extinction; the terms $b_{\perp}$ and $b_{\|}$ also describe the linear birefringence. According to the type of scattering particle, the values of $a_{\perp}$, $a_{\|}$, $b_{\perp}$ and $b_{\|}$ may be assigned.

A very simple example of the scattering matrix is that for the free electron where, in the azimuthal plane, the function $S_\perp(\theta) \Rightarrow \cos(\theta)$ and $S_\parallel(\theta) \Rightarrow 1$. Simple consideration reveals that no radiation vibrating parallel to the scattering plane is found at an angle of 90° from the direction of the incident radiation. A more thorough and rigorous treatment of the mathematics and physics of scattering processes can be found in the classical text of van de Hulst (1957).

From a determination of the amplitude scattering functions, the intensity of the radiation scattered in any direction can be readily calculated. If a scattering particle is illuminated by incident unpolarized flux of I_0, the scattered fluxes received at a distance, r, from the particle may be written as

$$I_\perp = \frac{I_0 F_\perp(\theta,\phi)}{2r^2k^2} \quad \text{and} \quad I_\parallel = \frac{I_0 F_\parallel(\theta,\phi)}{2r^2k^2} \,. \tag{3.31}$$

The terms

$$\frac{F_\perp(\theta,\phi)}{k^2} \quad \text{and} \quad \frac{F_\parallel(\theta,\phi)}{k^2}$$

are referred to as the *angular scattering distributions*. The scattering cross-section of any particle may be determined by integrating these functions over the total solid angle and may be expressed as

$$C_{\text{sca}} = k^{-2} \int \left[F_\perp(\theta,\phi) + F_\parallel(\theta,\phi)\right] \mathrm{d}\omega \,. \tag{3.32}$$

The extinction cross-section comprises scattering and absorption components. Thus,

$$C_{\text{ext}} = C_{\text{sca}} + C_{\text{abs}} \,. \tag{3.33}$$

In most cases, the determined cross-sections do not correspond to the basic geometric values of the grain sizes but can be related by means of efficiency factors, Q. Hence we may write

$$\begin{cases} C_{\text{sca}} = \pi a^2 Q_{\text{sca}} \\ C_{\text{abs}} = \pi a^2 Q_{\text{abs}} \\ C_{\text{ext}} = \pi a^2 Q_{\text{ext}} \,. \end{cases} \tag{3.34}$$

If the imaginary part of the refractive index of the scattering grain is equal to 0, then $C_{\text{abs}} = 0$.

There is a relationship between the forward-scattered radiation and extinction. It is referred to as the *optical theorem* and results from the conservation of energy giving the identities

$$C_{\text{ext}(\perp)} = -\frac{4\pi}{k^2}\Re\left\{S_\perp(0)\right\}, \tag{3.35}$$

$$C_{\text{ext}(\parallel)} = -\frac{4\pi}{k^2}\Re\left\{S_\parallel(0)\right\}, \tag{3.36}$$

where $\Re S(0)$ is the real part of the complex forward scattering amplitude, with the $\perp, \parallel$ subscripts corresponding to the polarizations perpendicular to, and parallel to, the scattering plane.

Determination of the scattering phase functions and the Q values for different kinds of particles has been exercised by various techniques, both mathematical and empirical. Perhaps the most common reference is to Mie scattering which refers to solutions of the homogeneous sphere problem and solved exactly by Mie (1908). For many practical situations, the rigorous computation of efficiency factors for scattering and extinction can be by-passed.

For $x(= 2\pi a/\lambda) \le 1$, Q_{ext} and Q_{sca} may be expanded as the convergent power series in x as follows:

$$\begin{aligned} Q_{\text{ext}} \cong {} & -x\Im\left[4\left(\frac{\tilde{m}^2-1}{\tilde{m}^2+2}\right)\right] \\ & + x^3\Im\left[-\frac{4}{15}\left(\frac{\tilde{m}^2-1}{\tilde{m}^2+1}\right)\left(\frac{\tilde{m}^4+27\tilde{m}^2+38}{2\tilde{m}^2+3}\right)\right] \\ & + x^4\Re\left[\frac{8}{3}\left(\frac{\tilde{m}^2-1}{\tilde{m}^2+21}\right)^2\right] + \cdots \end{aligned} \tag{3.37}$$

$$Q_{\text{sca}} \cong \frac{8}{3}x^4\Re\left[\left(\frac{\tilde{m}^2-1}{\tilde{m}^2+2}\right)^2\right] + \cdots \tag{3.38}$$

where $\Re$ and $\Im$ refer to real and imaginary parts respectively.

Convergence of the series is expected to be quite rapid for $x \lesssim 0.6$. For $x \ll 1$, the first term with non-zero coefficient may suffice and the two formulae that are often quoted are

$$Q_{\text{ext}} \cong -4x\Im\left[\left(\frac{\tilde{m}^2-1}{\tilde{m}^2+2}\right)\right], \tag{3.39}$$

$$Q_{\text{sca}} \cong \frac{8}{3}x^4\Re\left[\left(\frac{\tilde{m}^2-1}{\tilde{m}^2+2}\right)^2\right]. \tag{3.40}$$

Another analytical solution relates to scattering by (infinitely) long cylinders which has application to the modelling of elongated grains, such forms required to explain interstellar polarization. For grains with complicated shapes and with mantle structures, their scattering cross-sections may be explored empirically by scaling a model grain, and conducting experiments on it in a microwave laboratory, it being noted that scattering behaviour depends on x, the ratio of the particle size to the wavelength of the incident radiation.

3.4
Poincaré Sphere

The Poincaré sphere has its main application in problems relating to phase changes affecting radiation such as those provided by retarders within some instrumenta-

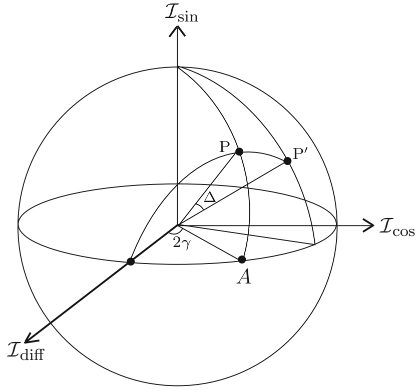

Fig. 3.3 The procedure for determining the effect of a retarder of phase, Δ, with its principal axis set at an angle, γ, to the reference frame defining **P**, is illustrated with the location of the resulting polarization form, **P′**, indicated.

tion. Any beam of perfectly polarized light represented by an eigenvector, **P**, will be modified to provide a resultant eigenvector, **P′**, its position depending on the orientation of the retarder axis and its phase delay. The relationship of **P′** with respect of **P** may be determined according to the following recipe.

Suppose that radiation described by **P** and defined by $(I_{\rm diff}, I_{\rm cos}, I_{\rm sin})$ is incident upon a retarder which introduces a retardance, Δ, between perpendicular directions (x', y') with the fast axis oriented at an angle, γ, to the x, y directions; the angle γ is measured anti-clockwise as seen by the observer from (x, y) to (x', y') – see Figure 3.1. The point representing the emergent beam $(I'_{\rm diff}, I'_{\rm cos}, I'_{\rm sin})$ can be determined by two simple steps. By considering Figure 3.3 and starting at the point where the $\mathcal{I}_{\rm diff}$-axis intersects the surface of the sphere, move round the great circle, which is the intersection of the sphere and the $(\mathcal{I}_{\rm diff}\mathcal{I}_{\rm cos})$-plane, through an angle, 2γ, in the direction $\mathcal{I}_{\rm diff}$ to $\mathcal{I}_{\rm cos}$. This defines a point, A. Regarding A as a pole, construct the latitude and longitude circles through the point $(I_{\rm diff}, I_{\rm cos}, I_{\rm sin})$ and then move clockwise as seen from A, round the latitude circle and through an angle, Δ, of longitude. This defines the point $(I'_{\rm diff}, I'_{\rm cos}, I'_{\rm sin})$.

Clearly the method can be extended to evaluate the effect of a series of retarders. It must be remembered that the γ's relating each of the devices must all be measured relative to the original frame of reference. The reverse procedure can be used to determine the necessary retarder to achieve a desired result from a known input. The normal rules of spherical geometry, as applied to the Poincaré representation, constitute an attractive method for investigating retarder problems. An excellent example of this is the work of Pancharatnam (1955a, 1955b) who explored the problems of the design of achromatic retarders by this mathematical method.

3.5
Conclusion

In simple summary, the term 'polarization' refers to the time-dependent behaviour of the electric and magnetic disturbances within some plane set normal to the direction of propagation of the electromagnetic radiation. Quantitatively it describes any asymmetry in the azimuthal distribution of the vectors in that plane or any persistent phase coherence between the resolved components of the fluctuations.

Generally in nature, a beam of radiation does not have a persistent classical form but comprises combinations of waves with disturbances persisting for a short time before being replaced by others. There are constant fluctuations in the phase relationships and in the position angles of the component vibrations. The radiation may also encompass a frequency spread as in '*white light*'. Amongst these statistical fluctuations, however, there may be some polarization forms during the integration time of the observation which occur more frequently than others and dominate in the time-averaging process during measurement. There are several mathematical formulations which deal with these situations. The most favoured involves the use of Stokes parameters and the Mueller calculus. These are introduced in the following chapter.

References

Jones, R.C. (1941a) A new calculus for the treatment of optical systems. I. Description and discussion of the calculus. *J. Opt. Soc. Am.*, **31**, 488–493. [49]

Jones, R.C. (1941b) A new calculus for the treatment of optical systems. III. The Sohncke theory of optical activity. *J. Opt. Soc. Am.*, **31**, 500–503. [49]

Jones, R.C. (1942) A new calculus for the treatment of optical systems. IV. *J. Opt. Soc. Am.*, **32**, 486–493. [49]

Jones, R.C. (1947a) A new calculus for the treatment of optical systems. V. A more general formulation, and description of another calculus. *J. Opt. Soc. Am.*, **37**, 107–110. [49]

Jones, R.C. (1947b) A new calculus for the treatment of optical systems. VI. Experimental determination of the matrix. *J. Opt. Soc. Am.*, **37**, 110–112. [49]

Jones, R.C. (1948) A new calculus for the treatment of optical systems. VII. Properties of the *N*-matrices. *J. Opt. Soc. Am.*, **38**, 671–685. [49]

Jones, R.C. (1956) A new calculus for the treatment of optical systems. VIII. Electromagnetic theory. *J. Opt. Soc. Am.*, **46**, 126–131. [49]

Jones, R.C., Hurwitz, H. Jr. (1941) A new calculus for the treatment of optical systems. II. Proof of three general equivalence theorems. *J. Opt. Soc. Am.*, **31**, 493–499. [49]

Mie, G. (1908) Beiträge zur Optik trüber Medien, speziell kolloidaler Metallösungen. *Ann. Phys.*, **330**, 377–445. [55]

Pancharatnam, S. (1955a) Achromatic combinations of birefringent plates. Part I. An achromatic circular polarizer. *Proc. Indian Acad. Sci. A*, **41**, 130–136. [56]

Pancharatnam, S. (1955b) Achromatic combinations of birefringent plates. Part II. An achromatic quarter-wave plate. *Proc. Indian Acad. Sci. A*, **41**, 137–144. [56]

Van de Hulst, H.C. (1957) *Light Scattering by Small Particles.* John Wiley & Sons, Inc., New York. [54]

4

The Stokes Parameters

4.1

Introduction

The form of the Jones vector, with its description of orthogonal classical waves maintaining a constant phase difference, obviously refers to beams of radiation which are perfectly coherent. Such coherence automatically means that the radiation is perfectly polarized, displaying a unique and long-term polarization form and figure.

In nature, such radiation is rarely met. Using a simplistic picture, it will be appreciated that within a beam of electromagnetic radiation, many waves and vibrations are simultaneously present, with their electric field disturbances providing a distribution of orientations and phases. As time progresses, some of the component vibrations die away to be replaced by others, without any phase coherence being maintained. This kind of radiation is sometimes referred to as *natural light*, but the more precise terminology of *unpolarized radiation* is to be preferred.

If snapshot pictures could be made of the resultant electric disturbance in the orthogonal plane through which the radiation passes, with exposures of the order of a few times the reciprocal of the frequency of the radiation, a series of ellipses would be recorded (see Figure 4.1). Successive frames would show figures that progressively change ellipticity and orientation of the major axis. Over longer experimental times, the ellipse patterns would appear to be more and more scrambled, and no preferred figure would emerge. According to a simple model for the behaviour, Hurwitz (1945) has shown that fairly thin ellipses dominate. For more than half the time, the ellipse being traced out has a major axis which is three and a half times larger than the minor axis; all orientations of the major axis are equally probable, as is the alternative choice of the handedness.

Suppose that the quantities which define the ellipse, $(E_{x0}^2 + E_{y0}^2)$, $(E_{x0}^2 - E_{y0}^2)$, $2E_{x0}E_{y0}\cos(\delta_y - \delta_x)$ and $2E_{x0}E_{y0}\sin(\delta_y - \delta_x)$, as given by (2.34), (2.35), (2.36) and (2.37), are determined in a normal experimental situation. The measurements correspond to expectation values of these quantities over the observational time. Thus, the recorded values correspond to time averages of the behaviour of the ellipses during the measurement integration time; the average also involves all the ellipses associated with the different wavelengths within the operating bandwidth

Stellar Polarimetry. David Clarke

ISBN: 978-3-527-40895-5

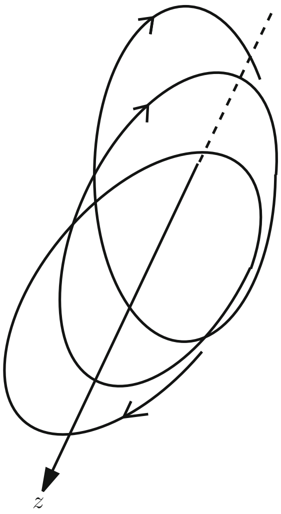

Fig. 4.1 The development of the polarization ellipse showing rotation of the major axis over a few cycles of the progression of an electromagnetic wave.

of the detected radiation. The values of the above terms may be expressed as

$$I = \langle E_{x0}^2 + E_{y0}^2 \rangle_{\lambda,t} \tag{4.1}$$

$$Q = \langle E_{x0}^2 - E_{y0}^2 \rangle_{\lambda,t} \tag{4.2}$$

$$U = \langle 2E_{x0}E_{y0} \cos\left(\delta_y - \delta_x\right) \rangle_{\lambda,t} \tag{4.3}$$

$$V = \langle 2E_{x0}E_{y0} \sin\left(\delta_y - \delta_x\right) \rangle_{\lambda,t} \,. \tag{4.4}$$

These definitions for I, Q, U, V are referred to as the *Stokes parameters*, following the classical paper of Stokes (1852). They may be written in the form of a column vector or *Stokes vector*. The elements of the vector are described in terms of *specific intensity*, when discussing theoretical ideas or astrophysical modelling problems, or *flux units*, when describing their measurement. According to Collett (1971), the impasse to a complete understanding of the Fresnel–Arago laws (see Chapter 1) remained for nearly 35 years until Stokes considered the problem, and successfully introduced a mathematical description of unpolarized light as contained within the concept of the parameters named after him.

It may be noted that some workers prefer to express the Stokes parameters in an alternative mathematical form as

$$I = \left\langle E_{x0}E_{x0}^* + E_{y0}E_{y0}^* \right\rangle_{\lambda,t} \tag{4.5}$$

$$Q = \left\langle E_{x0}E_{x0}^* - E_{y0}E_{y0}^* \right\rangle_{\lambda,t} \tag{4.6}$$

$$U = \left\langle E_{x0}E_{y0}^* + E_{y0}E_{x0}^* \right\rangle_{\lambda,t} \tag{4.7}$$

$$V = \left\langle \mathrm{i}(E_{x0}E_{y0}^* - E_{y0}E_{x0}^*) \right\rangle_{\lambda,t} , \tag{4.8}$$

where the superscript $*$ refers to the complex conjugate of the function.

It is interesting to note that, across a range of science disciplines, Stokes parameters have been 'reinvented' or 'rediscovered' at various times. In the field of chemistry, they were restated by Perrin (1942), and they were also described by Walker (1954). In his original paper, Stokes identified the parameters as $\{A, B, C, D\}$; Perrin (1942) used the variables $\{I, M, C, S\}$, while Walker (1954) referred to them as $\{I, Q, U, V\}$. They were finally introduced to Astronomy by Chandrasekhar (1947), defining them in relation to his studies on radiative transfer theory associated with stellar atmospheres. A disguised use of them was also made by Wesselink (1958). Chandrasekhar (1947) used the notation of $\{I, Q, U, V\}$ and this practice will be continued in this work.

If the makeup of the radiation comprises electrical fluctuations from waves appearing and dying with complete lack of time coherence, then $Q = U = V = 0$, and the light is said to be *unpolarized*. According to the degree of coherence that is maintained over the experimental time, Q, U and V may take values up to a maximum equal to I. For reference, in relation to the description of perfectly polarized light in Chapter 2 (see (2.40)), it will be noted that

$$I = (I_{\text{diff}}^2 + I_{\cos}^2 + I_{\sin}^2)^{1/2} , \tag{4.9}$$

or

$$I = (Q^2 + U^2 + V^2)^{1/2} . \tag{4.10}$$

Partial randomization of the phases of the contributing waves with the progress of time provides the condition of

$$I \geq \left(Q^2 + U^2 + V^2\right)^{1/2} . \tag{4.11}$$

Part of the contribution to the inequality may also arise from the fact that the waves are non-classical, comprising components with a range of frequencies, the averaging process taking this into account.

In the classical paper of Stokes (1852), it was demonstrated that when beams of radiation are combined, the parameters describing their individual polarizations are simply additive to provide a description of the resultant beam; there is no phase coherence that needs to be taken into account. By representing the parameters as column vectors, this additivity rule may be represented as

$$\begin{bmatrix} I_T \\ Q_T \\ U_T \\ V_T \end{bmatrix} = \begin{bmatrix} I_1 \\ Q_1 \\ U_1 \\ V_1 \end{bmatrix} + \begin{bmatrix} I_2 \\ Q_2 \\ U_2 \\ V_2 \end{bmatrix} + \cdots + \begin{bmatrix} I_n \\ Q_n \\ U_n \\ V_n \end{bmatrix} , \tag{4.12}$$

with

$$I_{\text{T}} = \sum_{j=1}^{n} I_j , \quad Q_{\text{T}} = \sum_{j=1}^{n} Q_j , \quad U_{\text{T}} = \sum_{j=1}^{n} U_j , \quad V_{\text{T}} = \sum_{j=1}^{n} V_j .$$

Unlike the situation for the addition of coherent beams, for which the relative phases are important, the total intensity is just the sum of the intensities of the individual beams. A consequence of the Stokes *additivity theorem* is the inverse notion that any given beam of radiation can be considered as being the resultant of combinations of component beams. If two sets of component beams provide the same resultant, they are said to be *optically equivalent*. This principle is sometimes referred to as the *theorem of optical equivalence*.

An important conceptual way of breaking down any Stokes vector is to consider it as the combination of two intensities, I_p, I_u, one completely polarized and the other unpolarized. Unfortunately for the observationalist, there is no optical device that physically enables such a dichotomy! Using the notation of the Stokes column vector, this conceptual process may be expressed as

$$\begin{bmatrix} I \\ Q \\ U \\ V \end{bmatrix} = \begin{bmatrix} I_\mathrm{p} \\ Q_\mathrm{p} \\ U_\mathrm{p} \\ V_\mathrm{p} \end{bmatrix} + \begin{bmatrix} I_\mathrm{u} \\ Q_\mathrm{u} \\ U_\mathrm{u} \\ V_\mathrm{u} \end{bmatrix}, \tag{4.13}$$

or, since $Q_\mathrm{u} = U_\mathrm{u} = V_\mathrm{u} = 0$ for unpolarized light, it may be simplified to

$$\begin{bmatrix} I \\ Q \\ U \\ V \end{bmatrix} = \begin{bmatrix} I_\mathrm{p} \\ Q_\mathrm{p} \\ U_\mathrm{p} \\ V_\mathrm{p} \end{bmatrix} + \begin{bmatrix} I_\mathrm{u} \\ 0 \\ 0 \\ 0 \end{bmatrix}. \tag{4.14}$$

With this dichotomy, it is possible to calculate the *degree of polarization* defined by

$$\begin{aligned} d &= \frac{\left(Q_\mathrm{p}^2 + U_\mathrm{p}^2 + V_\mathrm{p}^2\right)^{1/2}}{I_\mathrm{p} + I_\mathrm{u}} \\ &= \frac{\left(Q_\mathrm{p}^2 + U_\mathrm{p}^2 + V_\mathrm{p}^2\right)^{1/2}}{I}. \end{aligned} \tag{4.15}$$

It is more usual, however, to break this definition into two parts corresponding to the degrees of linear, p, and circular, v, polarizations separately. Thus,

$$p = \frac{I_\mathrm{p}}{I_\mathrm{u} + I_\mathrm{p}} = \frac{(Q_\mathrm{p}^2 + U_\mathrm{p}^2)^{1/2}}{I_\mathrm{u} + I_\mathrm{p}} = \frac{(Q_\mathrm{p}^2 + U_\mathrm{p}^2)^{1/2}}{I}, \tag{4.16}$$

and

$$v = \frac{V_\mathrm{p}}{I_\mathrm{u} + I_\mathrm{p}} = \frac{V_\mathrm{p}}{I}. \tag{4.17}$$

It can be seen from above that the degree of polarization is a measure of the flux of polarized radiation to that of the total flux. In some texts, the degree of linear polarization is written as

$$p = \frac{I_\mathrm{max} - I_\mathrm{min}}{I_\mathrm{max} + I_\mathrm{min}}, \tag{4.18}$$

where I_{max} and I_{min} are the maximum and minimum intensities, respectively, that are recorded when a polarizer is rotated in the beam. The expression is limited to partially linearly polarized light only. When the polarizer's axis is parallel to the direction of vibration, the transmitted intensity is $I_{\text{max}} = 1/2 I_{\text{u}} + I_{\text{p}}$, and when it is set at right angles, the transmitted intensity is $I_{\text{min}} = 1/2 I_{\text{u}}$. Expressing I_{u} and I_{p} in terms of I_{max} and I_{min}, (4.16) can be rewritten as

$$p = \frac{I_{\text{p}}}{I_{\text{u}} + I_{\text{p}}} = \frac{I_{\text{max}} - I_{\text{min}}}{I_{\text{max}} + I_{\text{min}}} \, . \tag{4.19}$$

4.2
The Mueller Calculus

When radiation interacts with matter, its polarization state is likely to suffer change. In the context of stellar polarimetry it is important to be able to formulate the effects within astrophysical situations such as the scattering of stellar radiation by localized dust, say, or to describe the role of various optical elements within a polarimetric instrument. Such Stokes parameter transformations can be conveniently performed by applying matrix multiplication to the original Stokes vector. The method of applying the various kinds of transformation is commonly known as the Mueller calculus (see Mueller, 1948). Thus the final Stokes vector, $\{I_{\text{o}}, U_{\text{o}}, Q_{\text{o}}, V_{\text{o}}\}$, is related to the initial vector, $\{I_{\text{i}}, U_{\text{i}}, Q_{\text{i}}, V_{\text{i}}\}$, by a 4×4 matrix such that

$$\begin{bmatrix} I_{\text{o}} \\ Q_{\text{o}} \\ U_{\text{o}} \\ V_{\text{o}} \end{bmatrix} = \begin{bmatrix} m_{11} & m_{12} & m_{13} & m_{14} \\ m_{21} & m_{22} & m_{23} & m_{24} \\ m_{31} & m_{32} & m_{33} & m_{34} \\ m_{41} & m_{42} & m_{43} & m_{44} \end{bmatrix} \begin{bmatrix} I_{\text{i}} \\ Q_{\text{i}} \\ U_{\text{i}} \\ V_{\text{i}} \end{bmatrix} . \tag{4.20}$$

In calculating the outcome of a particular situation, the calculus usually requires the application of several matrices in combination which must be organized in the *correct order*. It will be remembered, for example, that the Stokes vector is expressed in a particular reference frame and, to determine the effect of a partial polarizer, say, it is first necessary to set the description of the polarization to the frame corresponding to the principal axes of the device. Thus the operation of a partial polarizer may be represented by

$$\begin{bmatrix} I_{\text{o}} \\ Q_{\text{o}} \\ U_{\text{o}} \\ V_{\text{o}} \end{bmatrix} = [R(-\gamma)][PP][R(\gamma)] \begin{bmatrix} I_{\text{i}} \\ Q_{\text{i}} \\ U_{\text{i}} \\ V_{\text{i}} \end{bmatrix} . \tag{4.21}$$

The application of the third 4×4 matrix, $[R(-\gamma)]$, rotates the output Stokes vector back to the original reference frame. In Chapter 8, various designs of polarimeter are described and the application of the Mueller calculus is required to demonstrate the form of the signal that the polarimetric modulator produces. The more important matrices that are employed are listed in Table 4.1.

Table 4.1 The Mueller calculus. The simplest transforming effects operating on Stokes vectors are (1) differential transmission for the orthogonal polarization vibrations, (2) phase delays of different values affecting the orthogonal vibrations, and (3) rotation of the direction of vibration of the linear polarization or of the major axis of the polarization ellipse. The matrices representing these effects are summarized below.

Device	**Matrix and notes**
Partial polarizer	$[\mathcal{PP}] = \frac{1}{2}\begin{bmatrix} [K_1 + K_2] & [K_1 - K_2] & 0 & 0 \\ [K_1 - K_2] & [K_1 + K_2] & 0 & 0 \\ 0 & 0 & 2[K_1 K_2]^{1/2} & 0 \\ 0 & 0 & 0 & 2[K_1 K_2]^{1/2} \end{bmatrix}$ K_1, K_2 are the *intensity* transmission coefficients of the device to light perfectly linearly polarized in orthogonal directions 1 and 2; these are chosen so that $[K_1 - K_2]$ is maximized.
Perfect polarizer	$[\mathcal{P}] = \frac{1}{2}\begin{bmatrix} 1 & 1 & 0 & 0 \\ 1 & 1 & 0 & 0 \\ 0 & 0 & 0 & 0 \\ 0 & 0 & 0 & 0 \end{bmatrix}$ The matrix assumes that the polarizer has perfect transmission but may be multiplied by a coefficient (< 1) to allow for this if necessary.
Pure retarder	$[\varDelta] = \begin{bmatrix} 1 & 0 & 0 & 0 \\ 0 & 1 & 0 & 0 \\ 0 & 0 & \cos\varDelta & \sin\varDelta \\ 0 & 0 & -\sin\varDelta & \cos\varDelta \end{bmatrix}$ $\varDelta$ is the differential retardation or *retardance* of the device.
Rotation	$[\mathcal{R}(\gamma)] = \begin{bmatrix} 1 & 0 & 0 & 0 \\ 0 & \cos 2\gamma & \sin 2\gamma & 0 \\ 0 & -\sin 2\gamma & \cos 2\gamma & 0 \\ 0 & 0 & 0 & 1 \end{bmatrix}$ Positive γ is measured anti-clockwise from the x-axis towards the y-axis as seen looking against the z direction This matrix can also be used to predict the effect of optical activity or Faraday rotation.

In order to represent the effect, say of some scattering mechanism, then again a 4×4 matrix can also be applied, but containing geometric terms to represent the angular dependence of the scattered intensity and its polarization. The example below in (4.22) represents Thomson scattering for a free electron with cross-section σ_T according to the scattering phase angle χ given by the direction of the illuminating radiation and the line of sight from which the radiation is received:

$$\sigma_\mathrm{T}\begin{bmatrix} \frac{1}{2}(1+\cos^2\chi) & \frac{1}{2}\sin^2\chi & 0 & 0 \\ \frac{1}{2}\sin^2\chi & \frac{1}{2}(1+\cos^2\chi) & 0 & 0 \\ 0 & 0 & \cos\chi & 0 \\ 0 & 0 & 0 & \cos\chi \end{bmatrix}, \tag{4.22}$$

where $\sigma_\mathrm{T} = 8\pi r_\mathrm{e}^2/3$, with the classical electron radius given by r_e.

4.3
Normalized Stokes Parameters

It is the *normalized Stokes parameters* (NSPs) that are key to the description of all measurements of stellar polarization. The definitions in (4.15), (4.16) and (4.17) are combinations of Stokes parameters with units of specific intensity, or flux, which have been normalized by I to become dimensionless. In a similar fashion, the individual Stokes parameters may also be normalized such that

$$q = \frac{Q}{I}\,, \quad u = \frac{U}{I} \quad \text{and} \quad v = \frac{V}{I}\,. \tag{4.23}$$

The parameters q, u and v are referred to as *normalized Stokes parameters* or *NSPs*. Rather than measuring the individual Stokes parameters absolutely, it is generally the NSPs which are determined. It may be noted that in the astronomical literature, 'q' is sometimes used a symbol to define the degree of circular polarization, which is written as 'v' here, and throughout this text. According to the context, such differences in symbolism should not cause confusion.

When dealing with linear polarization, it is the values of q and u that are important. Comparison with (4.16) shows that the degree of polarization, p, is given by

$$p = (q^2 + u^2)^{1/2}\,. \tag{4.24}$$

Again, reference to either (2.32) or (2.38) shows that the position angle, ζ, of the direction of vibration may be calculated from

$$\zeta = \frac{1}{2}\arctan\left(\frac{u}{q}\right), \tag{4.25}$$

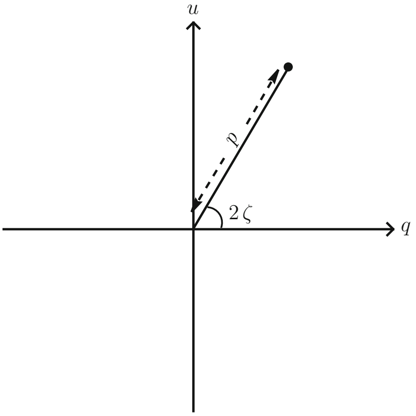

Fig. 4.2 A basic normalized Stokes parameter diagram indicating the relationship between the NSPs, q, u, the degree of polarization, p, and the direction of vibration, ζ. Note that in the diagram, the polar angle of p is marked as 2ζ.

with the quadrant in which ζ appears being dependent on the individual signs of q and u.

In order to represent graphically the NSPs corresponding to linear polarization measurements, a Cartesian frame may be used with q and u acting as the abscissa and ordinate respectively, as depicted in Figure 4.2. It will be readily appreciated that the vector addition of a q, u pair corresponds to the value of p. Care, however, must be taken with the interpretation of the value of the polar angle in this coordinate frame, the angle needing to be halved for the calculation of the direction of vibration. Mistakes on this point are usually made by novices to the subject, but researchers with experience also fall victim to this idiosyncrasy.

In summary, it may be noted that

$$q = p\cos 2\zeta \quad \text{and} \quad u = p\sin 2\zeta\ . \tag{4.26}$$

4.4
The Practicality of Stokes Parameters

Simple investigation of the forms of the Stokes parameters reveals an aspect very much related to their physical concept in terms of simple measurement. This is very apparent for the parameter Q. Inspection of (4.2) clearly shows that Q is simply the difference of intensities between the resolved components along the defining axes, x, y. To measure Q, all that is required is a device – a polarizer – which transmits just one direction of vibration, this defining its principal axis. By measuring the two intensities passed with the principal axis, first aligned to the x-axis and then rotated by 90° to be aligned to the y-axis, the difference provides the value of Q. A non-zero value indicates the presence of linear polarization.

A zero value for Q does not immediately mean that there is no linear polarization present, however. Suppose that the beam contains a linear polarization component but with its direction vibration at 45° to the x, y reference frame. Resolving it along the x- and y-axes provides equal fluxes in these directions; the measurement procedure, as above, would provide a value of $Q = 0$. To resolve the issue, an experimental strategy would be to make two further intensity measurements corresponding to the principal axis being set at angles of 45° and 135° to the xy-frame. The intensity difference now corresponds to the U parameter. Although this may not be immediately apparent from the algebra describing U (see (4.3)), its defining relationship is readily demonstrated as follows.

As expressed in (3.1) and (3.2), consider a beam of radiation with resolved amplitudes:

$$E_x = E_{x_0}\mathrm{e}^{\mathrm{i}(2\pi\nu t+\delta_x)} \tag{4.27}$$

$$E_y = E_{y_0}\mathrm{e}^{\mathrm{i}(2\pi\nu t+\delta_y)}\ . \tag{4.28}$$

By rotating the reference axis by 45°, these vibrations may now be expressed by

$$E_{x'} = \frac{E_{x0}}{\sqrt{2}} \mathrm{e}^{\mathrm{i}(2\pi\nu t+\delta_x)} + \frac{E_{y0}}{\sqrt{2}} \mathrm{e}^{\mathrm{i}(2\pi\nu t+\delta_y)} \,, \tag{4.29}$$

$$E_{y'} = -\frac{E_{x0}}{\sqrt{2}} \mathrm{e}^{\mathrm{i}(2\pi\nu t+\delta_x)} + \frac{E_{y0}}{\sqrt{2}} \mathrm{e}^{\mathrm{i}(2\pi\nu t+\delta_y)} \,. \tag{4.30}$$

By taking the above expressions and forming products with their complex conjugates, the intensities, $I_{x'}$, $I_{y'}$, associated with these waves are given by

$$I_{x'} = \frac{1}{2} \left\{ E_{x_0}^2 + E_{y_0}^2 + 2 E_{x_0} E_{y_0} \cos\left(\delta_y - \delta_x\right) \right\} \tag{4.31}$$

$$I_{y'} = \frac{1}{2} \left\{ E_{x_0}^2 + E_{y_0}^2 - 2 E_{x_0} E_{y_0} \cos\left(\delta_y - \delta_x\right) \right\} . \tag{4.32}$$

The difference of the two intensity values from (4.32) and (4.31) leads to the expression

$$2 E_{x_0} E_{y_0} \cos\left(\delta_y - \delta_x\right) , \tag{4.33}$$

so corresponding to the definition of U.

As for the fourth Stokes parameter, it is explored by inserting a quarter-wave plate in the beam to provide a differential phase delay of $\pi/2$, converting any circular polarization into linear form. (From Chapter 2, it will be appreciated that circular polarization requires a phase difference of $\pi/2$ between the E_x, E_y components and that an additional phase delay of $\pi/2$ to either component converts the phase difference to zero or π, so producing linear polarization (see Figure 2.2)). The strength of the produced linear polarization is then detectable by the two-position polarizer technique as above. Suppose the plate is set to provide the phase delay for the y-axis vibration. The vibrations resolved on the x, y axes may now be written as

$$E_x = E_{x_0} \mathrm{e}^{\mathrm{i}(2\pi\nu t+\delta_x)} \,, \tag{4.34}$$

$$E_y = E_{y_0} \mathrm{e}^{\mathrm{i}(2\pi\nu t+\delta_y-\pi/2)} \,. \tag{4.35}$$

Again by rotating the axis by 45°, these vibrations are now expressed in the new frame as

$$E_{x'} = \frac{E_{x0}}{\sqrt{2}} \mathrm{e}^{\mathrm{i}(2\pi\nu t+\delta_x)} + \frac{E_{y0}}{\sqrt{2}} \mathrm{e}^{\mathrm{i}(2\pi\nu t+\delta_y-\pi/2)} \,, \tag{4.36}$$

$$E_{y'} = -\frac{E_{x0}}{\sqrt{2}} \mathrm{e}^{\mathrm{i}(2\pi\nu t+\delta_x)} + \frac{E_{y0}}{\sqrt{2}} \mathrm{e}^{\mathrm{i}(2\pi\nu t+\delta_y-\pi/2)} \,. \tag{4.37}$$

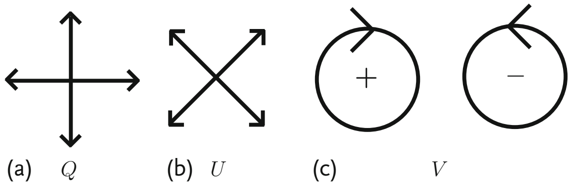

Fig. 4.3 A schematic depiction of the polarization forms that make up the Stokes parameters Q (a), U (b) and V (c), as seen from the viewpoint of the observer. For the alternative circular components, the sense of rotation with '+' and '−' relates to the mathematical descriptions in Chapter 2, and also the sign associated with $\sin(\delta_y - \delta_x)$ in (4.40). (N.B.: This is not the convention adopted by the IAU).

By determining the two associated intensities as above, the values may be written as

$$I_{x'} = \frac{1}{2}\left\{E_{x_0}^2 + E_{y_0}^2 + 2E_{x_0}E_{y_0}\cos\left(\delta_y - \delta_x - \pi/2\right)\right\}, \tag{4.38}$$

$$I_{y'} = \frac{1}{2}\left\{E_{x_0}^2 + E_{y_0}^2 - 2E_{x_0}E_{y_0}\cos\left(\delta_y - \delta_x - \pi/2\right)\right\}. \tag{4.39}$$

Subtraction of (4.39) from (4.38) leads to the expression

$$2E_{x_0}E_{y_0}\cos\left(\delta_y - \delta_x - \pi/2\right) = 2E_{x_0}E_{y_0}\sin\left(\delta_y - \delta_x\right), \tag{4.40}$$

which is the definition of V. The sign of the value of V indicates the sense of rotation of the circular component.

From the discussion above, a schematic for the nature of the Stokes parameters may be presented in a simple diagram as in Figure 4.3.

4.5
Additivity Theorem for Small Polarizations

In general, when two or more beams of radiation are combined, the resultant Stokes vector is derived by adding the absolute values of the corresponding Stokes parameters. For weak polarizers which act successively on originally unpolarized light, however, the resultant can be considered as the addition of the individually produced degrees of polarization, taking into account their relative orientations. It is as though each device acts independently and separately, with the subsequent devices ignoring the polarizations produced by the earlier devices in the optical train. In the calculation of the resultant polarization, the contributions of second-order terms are simply neglected.

Consider two such weak partial polarizers in turn. Using the first polarizer to act as a reference axis, its effect on unpolarized radiation can be written as

$$\begin{aligned}
&\begin{bmatrix} \mathcal{PP}(K_1, K_2) \end{bmatrix} \begin{bmatrix} 1 \\ 0 \\ 0 \\ 0 \end{bmatrix} \\
&= \frac{1}{2} \begin{bmatrix} [K_1 + K_2] & [K_1 - K_2] & 0 & 0 \\ [K_1 - K_2] & [K_1 + K_2] & 0 & 0 \\ 0 & 0 & 2[K_1 K_2]^{1/2} & 0 \\ 0 & 0 & 0 & 2[K_1 K_2]^{1/2} \end{bmatrix} \begin{bmatrix} 1 \\ 0 \\ 0 \\ 0 \end{bmatrix} \\
&= \frac{1}{2} \begin{bmatrix} [K_1 + K_2] \\ [K_1 - K_2] \\ 0 \\ 0 \end{bmatrix} = \frac{K_1 + K_2}{2} \begin{bmatrix} 1 \\ p_K \\ 0 \\ 0 \end{bmatrix},
\end{aligned} \tag{4.41}$$

where p_K is the polarizance of the device, given by $(K_1 - K_2)/(K_1 + K_2)$.

Now consider the effect of a second weak polarizer in turn with a polarizance given by

$$p_k = \frac{k_1 - k_2}{k_1 + k_2},$$

set an angle, α, to the direction of vibration of the above generated polarization. The situation can be represented as

$$\begin{aligned}
&\frac{K_1 + K_2}{2} \begin{bmatrix} \mathcal{PP}(k_1, k_2) \end{bmatrix} \begin{bmatrix} \mathcal{R}(\alpha) \end{bmatrix} \begin{bmatrix} 1 \\ p_K \\ 0 \\ 0 \end{bmatrix} \\
&= \frac{K_1 + K_2}{4} \begin{bmatrix} [k_1 + k_2] + [k_1 - k_2] p_K \cos 2\alpha \\ [k_1 - k_2] + [k_1 + k_2] p_K \cos 2\alpha \\ -2[k_1 k_2]^{1/2} p_K \sin 2\alpha \\ 0 \end{bmatrix}.
\end{aligned} \tag{4.42}$$

By neglecting small terms such as $[k_1 - k_2] p_K \cos 2\alpha$ and noting also that since $k_1 \approx k_2$, and $(-2[k_1 k_2]^{1/2})/(k_1 + k_2) \approx 1$, the resulting Stokes vector becomes

$$\frac{[K_1 + K_2][k_1 + k_2]}{4} \begin{bmatrix} 1 \\ p_k + p_K \cos 2\alpha \\ -p_K \sin 2\alpha \\ 0 \end{bmatrix}. \tag{4.43}$$

Rotation of this Stokes vector to the original reference frame may be expressed as

$$\frac{[K_1 + K_2][k_1 + k_2]}{4} \begin{bmatrix} 1 & 0 & 0 & 0 \\ 0 & \cos 2\alpha & -\sin 2\alpha & 0 \\ 0 & \sin 2\alpha & \cos 2\alpha & 0 \\ 0 & 0 & 0 & 1 \end{bmatrix} \begin{bmatrix} 1 \\ p_k + p_K \cos 2\alpha \\ -p_K \sin 2\alpha \\ 0 \end{bmatrix}$$

$$= \frac{[K_1 + K_2][k_1 + k_2]}{4} \begin{bmatrix} 1 \\ p_k \cos 2\alpha + p_K \\ p_k \sin 2\alpha \\ 0 \end{bmatrix} . \tag{4.44}$$

Thus the resultant degree of polarization is given by

$$p_{\text{tot}} = \left(p_k^2 + p_K^2 + 2 p_k p_K \cos 2\alpha\right)^{1/2} , \tag{4.45}$$

with its position angle, ζ, given by

$$\tan 2\zeta = \frac{p_k \sin 2\alpha}{p_k \cos 2\alpha + p_K} . \tag{4.46}$$

The outcome is demonstrated in the Stokes vector diagram depicted in Figure 4.4. Using this diagram, the conclusion obtained by the Mueller calculus above may be confirmed directly from the geometry described by the vectors.

For some situations, the converse of the *additivity theorem for small polarization* may also be appropriate, i. e. for low levels of polarization, it is sometimes convenient to consider breaking the resultant into two or more components.

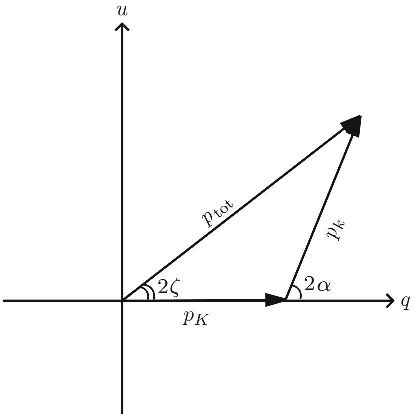

Fig. 4.4 The vector diagram using NSPs q, u, shows the resultant polarization, p_{tot}, obtained from the contribution of a degree of polarization, p_K, set along the reference axis (q) added to a degree of polarization, p_k, set at an angle, α, giving 2α in the diagram. Note again that in the diagram, the position angle, ζ, of the resultant is marked as 2ζ.

4.6
Conventions in Astronomical Polarimetry

4.6.1
Linear Polarization

For optical astronomical measurements, q and u are referred to a coordinate frame based on equatorial coordinates such that positive q corresponds to a direction of vibration parallel to the N/S direction or Declination; a negative value for q refers to the vibration being parallel to the E/W direction. The value of ζ increases positively as the position angle of the vibration rotates North through East, this being the same convention as for the description of position angles associated with visual binary stars. Thus a polarization measurement with a zero q component, but with positive u, describes a vibration set along the projection of NE/SW on the sky; negative u corresponds to the vibration being parallel to the NW/SE direction.

4.6.2
Circular Polarization – Handedness

For circular polarization, the definition of handedness is a thorny problem (see Chapter 2) and has a history of confusion with respect to its conventions. This need not have been so as Clarke & Grainger (1971) have pointed out. In their discussion related to circularly polarized light, they noted that a snapshot record of the behaviour of the **E**-vector along the direction of propagation corresponds to a helical figure; as time progresses, this helix moves along the direction of propagation without rotation and, in a given plane, the electric vector rotates in a direction according to the form of the helix. As the handedness of a helix is independent of viewpoint, describing the handedness of any circular polarization according to the sense of the helical pattern provides a unique descriptor.

Consider, for example, radiation containing say left-handed helical forms passing through a fixed plane as seen projected on the celestial sphere containing a right-handed coordinate frame, as is the case for equatorial coordinates. As the helices advance without rotation, the electric vector would appear to rotate with increasing angle, ζ, i. e. in an anti-clockwise sense as seen from the viewpoint of the observer (see Figure 2.3). According to the definitions adopted by the IAU (see later), this form of circular polarization, however, should be referred to as *right-handed* and *positive*. It may be noted that the sense of rotation depends on the viewpoint of the observer; a clockwise rotation as noted by an observer receiving the radiation corresponds to an anti-clockwise rotation as seen from the viewpoint of the source.

Even if the unique definition of the helical behaviour of the radiation were to be applied, ambiguity would occur if the assignation of a ‘+’ or ‘−’ sign is added. This issue related to astronomical polarimetry was exposed by Clarke (1974a). For a given handedness of circular polarization as defined by the contained helices, the sign of V depends on the sign conventions associated with δ_x and δ_y describing

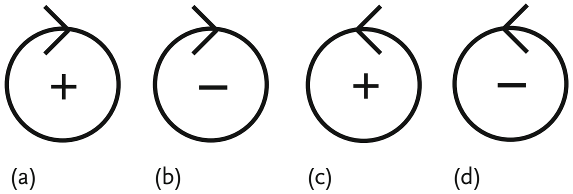

Fig. 4.5 Four possible definitions related to 'right-handed' circular polarization. The senses of the rotation of the **E**-vector correspond to the viewpoint of the observer receiving the radiation and may carry either a '+' or '−' sign. According to Gehrels (1972), (a) corresponds to right-handed polarization, this also being used by Avery, Michalsky & Stokes (1973); Serkowski (1973) described (b) as corresponding to right-handed, this also being the convention of Gnedin & Shulov (1971); Martin (1972) described (c) as being right-handed, this also being used by Kemp & Wolstencroft (1973). The IAU preferred definition corresponds to (c).

the **E** vibrations (see (2.11) and (2.12)), i. e. whether these phases are taken as advancements or retardations and whether they are written as $+\delta_x$, $+\delta_y$, or $-\delta_x$, $-\delta_y$ in the basic equations describing the orthogonally resolved waves. According to the definitions and development in Chapter 2, a positive value of V ensues for radiation carrying a right-handed helical forms. The problems and confusions of polarimetric definitions generally through optics and other disciplines have been discussed by Clarke (1974b, 1974c), the second paper including a quotation from the Bible – the Gospel according to St. Matthew 6:3. Perhaps a more appropriate text, however, may be taken from Jonah 4:11:

> ... Ninevah, that great city, wherein are more than six score thousand persons that cannot discern between their right-hand and their left-hand; ...

With a choice of two kinds of handedness which can be assigned with either a '+' or '−' sign, there are four permutations that can be considered to describe the 'sense' of elliptical polarization (see Figure 4.5); references to their use of three of them are readily found in the optical astronomical literature. The following examples show the diversity of the conventions that have been used.

The plus and minus signs for right- and left-handed circular polarization, respectively, were used by Gehrels (1972), right-handed corresponding to a clockwise rotation of the electric vector for the radiation approaching the observer; the sense was calibrated in the laboratory – see Figure 4.5a.

Serkowski (1973) commented that the sign of his circular polarization measurements was calibrated using metallic reflections as described by Swindell (1971). Right-hand polarization is denoted by considering the **E**-vector to rotate clockwise as seen by an observer looking against the direction of propagation. According to Swindell (1971), when the **E**-vector of some incident linearly polarized light is oriented in a direction given by a clockwise rotation, θ $(0 < \theta < \pi/2)$, from the plane of incidence when looking back into the source, then the reflected light is right-elliptically polarized. Conversely, when the **E**-vector of linearly polarized light is oriented in a direction given by a counterclockwise rotation, θ $(0 > \theta > \pi/2)$, from the plane when looking back into the source, then the reflected light is left-elliptically polarized. The result holds for any metal and any angle of incidence – see Appendix A. Right-handed polarization is denoted in Serkowski's paper as negative (see Figure 4.5b); for an observer facing the star, it corresponds to the **E**-vector rotating clockwise in a plane projected on the celestial sphere. Serkowski compares his results with those of Gehrels noting that the latter worker describes right-handed polarization as being positive.

The convention of Gnedin & Shulov (1971) was based on a '−ve' sign corresponding to a clockwise rotation of **E**, as seen by the observer looking at the star. To the contrary, Avery, Michalsky & Stokes (1973) used a '+ve' sign such that, for an observer facing the source, the rotation of the electric vector in a fixed plane was clockwise. They commented that this convention is the opposite to that used by Kemp. In Martin's (1972) analysis of the behaviour of interstellar grains, positive angles are measured counterclockwise on the sky and positive values of V correspond to right-handed polarization with a counterclockwise rotation of the electric vector (see Figure 4.5c). In their observations of Zeeman effects in newly discovered X-ray stars, Kemp & Wolstencroft (1973) considered circular polarization to be positive for counterclockwise rotations of the electric vector as seen by the observer.

For the measurements of AM Her, Tapia (1977) used the convention that the sign for handedness is determined according to the angular momentum convention. The handedness is *positive* when the optical electric vector carries positive angular momentum to the observer.

Michalsky, Swedlund, Stokes, *et al.* (1974) changed their convention to follow the sign convention adopted by the IAU Colloquium No. 23; positive polarization is taken to mean that for an observer facing the source the electric vector's rotation in a fixed plane is counterclockwise.

At the IAU General Assembly in Sydney in 1973, Commissions 25 and 40 proposed the adoption of the following terminology in polarimetry:

> The frame of reference for the Stokes parameters is that of Right Ascension and Declination with the position angle of electric vector maximum, ζ, starting from North and increasing through East. Elliptical polarization is defined in conformity with the definitions of the Institute of Electrical and Electronics Engineers (IEEE Standard, 211, 1969). This means that the polarization of incoming radiation, for which the position angle, ζ, of the electric vector, measured as a fixed point in space, increases with time, is described as right-handed and positive.

As seen by an observer, the rotation of the **E**-vector for such right-handed polarizations is counterclockwise, i. e. ζ is increasing continually.

The relevant definition from IEEE Standard 211 relates to left-handed polarization and is

> *Left-Handed (Counterclockwise) Polarized Wave.* An elliptically polarized electromagnetic wave in which the rotation of the electric field vector with time is counterclockwise for a stationary observer

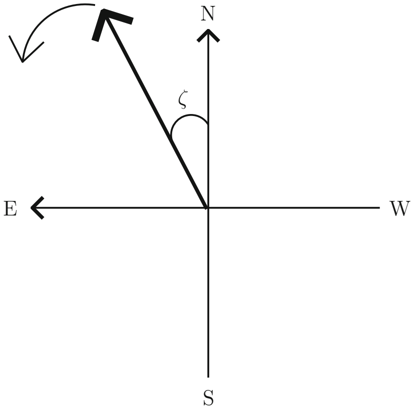

Fig. 4.6 The IAU preferred definitions for the description of polarization show the direction of vibration set at an angle, ζ, North through East. For circular polarization with the **E**-vector rotating with increasing ζ, the form is described as *right-handed* with a '+' sign also applied.

> looking in the direction of the wave normal. (Note: For an observer looking from a receiver toward the apparent source of the wave, the direction of rotation is reversed.)

Careful consideration of this latter definition of left-handed polarization shows that the angle defining the direction of vibration is decreasing in the right-handed frame of celestial coordinates, i. e. East through North. For *right-handed polarization*, the **E**-vector would be seen against the reference frame as rotating in the opposite direction, i. e. *anti-clockwise* or from North through East, with ζ continuously increasing (see Figure 4.6).

With such definitions, it turns out that sense of the helix that is associated with the radiation itself has the opposite convention, i. e. right-handed polarization comprises left-handed helical disturbances which travel without rotation along the direction of propagation. Relevant to radio astronomy, it may be noted that according to the IEEE definition, left-handed polarization would be best received by a left-handed helical antenna rather than by one of opposite sense. Thus the definition appears to be guided by the readily identifiable physical form of the receiving equipment rather than the physical behaviour within the radiation. For radio astronomy, a convention based on the unique handedness of helical antennae has been adopted (IRE, 1942, and Kraus, 1986). The largest reaction from a helical antenna occurs when it receives radiation carrying helical forms of the opposite sense. So, for example, a left-handed antenna has maximum response when the radiation received is in the form of radiation travelling as a right-handed helix and the radiation would be referred to as being left-handed.

Obviously it is preferable to accept some convention that everyone is familiar with and one which for any new instrument can be readily checked out. Whether it is the most logical one or not, the IAU definition should be followed.

Over and above the issue of definitions, there are sometimes problems in interpreting the sense of magnetic fields from observations of circular polarization or from measurements of Zeeman shifts. These will be discussed and resolved in Chapter 9.

Finally with respect to definitions, and turning to the description of the shape of the polarization ellipse, the term 'ellipticity' is often confused with the 'axial ratio' defined as $\eta = b/a$ (e. g. see Wolf, 1972). Ellipticity is a general term of geometry and is normally defined as the ratio of the difference between the major and minor axes to the major axis, i. e. $(a - b)/a$. With this definition, the value of ellipticity is very meaningful in that it increases as the ellipse departs more from a circle towards a straight line. According to the definition of axial ratio, immediately above, the ellipticity is given by $(1 - \eta)$, with the value of η being deducible from the modulus of the fourth Stokes parameter expressed as

$$|V| = \frac{2\eta}{1 + \eta^2} \,. \tag{4.47}$$

4.7
Polarization Magnitudes

In the first era of recording the measurements of stellar polarimetry, it was common to express the degree of linear polarization, p, in terms of a magnitude difference, Δm. Such practice soon faded, but we are left with catalogues – see, for example, Hiltner (1951, 1954), Hall (1958) and Behr (1959) – which tabulate the values of Δm only. Conversion of these early measurements to values following the modern conventional practice is straightforward.

Polarimetric measurements involve the determination of two intensities resolved in orthogonal directions. If these, for example, are given by $I(0°)$ and $I(90°)$, with the fiduciary of 0° corresponding to the direction of Q, they may also be expressed as a magnitude difference, m_q, given by

$$\begin{aligned} m(90°) - m(0°) = m_q &= -2.5 \log_{10} \frac{I(90°)}{I(0°)} \\ &= 2.5 \log_{10} \frac{I(0°)}{I(90°)} \,. \end{aligned} \tag{4.48}$$

Hence we have

$$\begin{aligned} \frac{I(0°)}{I(90°)} &= \exp\left(\frac{\log_e 10}{2.5} m_q\right) \\ &= \exp\left((0.921) m_q\right) . \end{aligned} \tag{4.49}$$

Now q is defined by

$$q = \frac{I(0°) - I(90°)}{I(0°) + I(90°)} \\ = \frac{I(0°)/I(90°) - 1}{I(0°)/I(90°) + 1} \,. \tag{4.50}$$

Now by substituting (4.49) into (4.50), we may write

$$\begin{aligned} q &= \frac{e^{(0.921)m_q} - 1}{e^{(0.921)m_q} + 1} \\ \text{or} \qquad &= \frac{e^{(0.46)m_q} - e^{-(0.46)m_q}}{e^{(0.46)m_q} + e^{-(0.46)m_q}} \\ &= \tanh[0.46\,m_q]\,, \\ \text{and for small } m_q\,, \quad q &\simeq 0.46\,m_q\,. \end{aligned} \tag{4.51}$$

Alternatively, by using (4.48) again,

$$\begin{aligned} q_m &= 2.5\log_{10}\frac{I(0°)}{I(90°)} \\ &= 2.5\log_{10}\frac{1+q}{1-q} \\ &= (2.5)(0.4343)\log_e\frac{1+q}{1-q} \\ &= 2.1717\left(\log_e(1+q) - \log_e(1-q)\right), \end{aligned} \tag{4.52}$$

and, after expanding the logarithmic terms as a Taylor series,

$$q_m = 2.1717\left(q + q^3/3 + q^5/5 + \cdots\right). \tag{4.53}$$

It may be noted that the same numerical scaling factor in (4.51) is applicable to the parameters expressed in magnitudes, m_u, m_v and m_p, for conversion to NSPs, u and v, and the degree of polarization, p.

References

Avery, R.W., Michalsky, J.J., Stokes, R.A. (1973) Circular polarization in the B stars X Persei, 5 Persei, 55 Cygnii and 30 Pegasi. *ApJ*, **180**, L127–L128. [73, 72]

Behr, A. (1959) Die interstellare Polarisation des Sternlichts in Sonnennumgebung. *Veröff. der Univ.-Sternwarte zu Göttingen*, **7** (Nr. 126), pp. 199–256. [75]

Chandrasekhar, S. (1947) On the radiative equilibrium of a stellar atmosphere XV. *ApJ*, **105**, 424–434. [61, 61]

Clarke, D., Grainger, J.F. (1971) *Polarized Light and Optical Measurement*. Pergamon, Oxford. [71]

Clarke, D. (1974a) Polarimetric Definitions. pp 45–53 in *Planets, Stars and Nebulae Studied with Photopolarimetry*. Ed. T. Gehrels, University of Arizona Press, Tucson, AZ. [71]

Clarke, D. (1974b) Nomenclature of polarized light: linear polarization. *Appl. Opt.*, **13**, 3–5. [72]

Clarke, D. (1974c) Nomenclature of polarized light: elliptical polarization. *Appl. Opt.*, **13**, 222–224. [72]

Collett, E. (1971) Mathematical formulation of the interference laws of Fresnel and Arago. *Am. J. Phys.*, **39**, 1483–1495. [60]

Gehrels, T. (1972) On the circular polarization of HD 226868, NGC 1068, NGC 4151, 3C 273, and VY Canis Majoris. *ApJ*, **173**, L23–L25. [72, 72]

Gnedin, Yu.N., Shulov, O.S. (1971) Observation of variable circular polarization in the optical emission of the X-ray source Sco X-1. *JETP Lett.*, **14**, 348–350. [73, 72]

Hall, J.S. (1958) Polarization of Starlight in the Galaxy. *Publications of the US Naval Observatory* – Second Series – Vol. XVII – Part VI. [75]

Hiltner, W.A. (1951) Polarization of stellar radiation. III. The polarization of 841 stars. *ApJ*, **114**, 241–271. [75]

Hiltner, W.A. (1954) Interstellar polarization of 405 stars. *ApJ*, **120**, 454–463. [75]

Hurwitz, H. Jr. (1945) The statistical properties of unpolarized light. *J. Opt. Soc. Am.*, **35**, 525–531. [59]

IRE (1942) Standards on Radio Wave Propagation. *Proc. IRE*, **30** (7), Pt. III (Suppl.) [74]

Kemp, J.C., Wolstencroft, R.D. (1973) Zeeman Effect in the X-ray Star Candidates HD 77581 and θ^2 Orionis. *ApJ*, **182**, L43–L46. [73, 72]

Kraus, J.D. (1966) *Radio Astronomy*. McGraw-Hill, New York, See Chapter 4. [74]

Martin, P.G. (1972) Interstellar circular polarization. *MNRAS*, **159**, 179–190. [73, 72]

Michalsky, J.J., Swedlund, J.B., Stokes, R.A., Avery, R.W. (1974) Interstellar circular polarization: a report of eight new positive results. *ApJ*, **187**, L13–L14. [73]

Mueller, H. (1948) The foundations of optics. *J. Opt. Soc. Am.*, **38**, 661. [63]

Perrin, F. (1942) Polarization of light scattered by isotropic opalescent media. *J. Chem. Phys.*, **10**, 415–427. [61, 61]

Serkowski, K. (1973) Infrared circular polarization of NML Cygni and VY Canis Majoris. *ApJ*, **179** L101–L106. [72, 72]

Stokes, G.G. (1852) On the Composition and Resolution of Streams of Polarized Light from Different Sources. *Trans. Cambridge Philos. Soc.* **IX**, 399–416 (See also: Stokes, G.G. (1901) *Mathematical and Physical Papers – Vol. 3*, pp 233–251, London: Cambridge University Press.) [60, 61]

Swindell, W. (1971) Handedness of polarization after metallic reflection of linearly polarized light. *J. Opt. Soc. Am.*, **61**, 212–215. [72]

Tapia, S. (1977) Discovery of a magnetic compact star in the AM Herculis/3U 1809+50 system. *ApJ*, **212**, L125–L129. [73]

Walker, M.J. (1954) Matrix calculus and the Stokes parameters of polarized radiation. *Am. J. Phys.*, **22**, 170–174. [61, 61]

Wesselink, A.J. (1958) On the reduction of polarization measures affected by instrumental polarization. *MNRAS*, **118**, 271–275. [61]

Wolf, G.W. (1972) A search for elliptical polarization. *AJ*, **77**, 576–583. [75]

5
Polarization Statistics and Data Treatment

5.1
Introduction

The levels of polarization that are generally observed from stellar sources are usually very small, and it is important to know how experimental noise affects measurements and their interpretation. This is particularly important in the assessment of detectivity, and in ascribing confidence levels to any data. Polarimetry is sometimes referred to as being a photon-intensive pursuit in that many detection counts need to be accumulated before the polarimetric signal emerges. In the limit, polarimetric detectivity and accuracy depend only on the statistical behaviour of the detection of photons. Most instruments claim to overcome all other generated noises and to achieve the fundamental accuracies imposed by the limits set by the number of photons recorded. For the purpose of discussing the statistics associated with polarimetry, it will be assumed that no sources of noise other than photon shot noise affect the measurements.

5.2
Basic Statistics

The formulation of the way that photon shot noise affects determinations of a normalized Stokes parameter, or p, depends on the modulation technique. Any measurement of an NSP is essentially one of differential photometry comprising the determination of intensities of a pair of orthogonal polarizations. The smaller the Stokes parameter, the smaller is this intensity difference, and the larger is the total photon count required to tease out the value of the parameter with statistical significance. Because of the nature of the observations, it is a normal practice to break down the total integration time needed to count the required number of photons in smaller intervals, with a series of measurements being undertaken. Thus, for example, these might correspond to a polarizer being set first parallel to some reference frame, say Q, and then perpendicular to the same frame, with the procedure repeated many times. The signals may comprise direct photon counts, say from a photomultiplier detector, or analogue-to-digital units (ADUs) from a CCD camera,

Stellar Polarimetry. David Clarke

ISBN: 978-3-527-40895-5

with each unit carrying a calibrated photon count conversion factor. If $n_{\|i}$ and $n_{\perp i}$ correspond to the recorded signals (photon counts) from a single measurement, then the NSP values are determined from

$$q_i = \frac{n_{\|i} - n_{\perp i}}{n_{\|i} + n_{\perp i}} \,. \tag{5.1}$$

For a situation with small polarization such that $q_i \sim 0$, and assuming that $n_{\|i}$ and $n_{\perp i}$ are independent variables, with 1σ values determined by photon counting Poisson statistics, and given by the square root of the signals themselves, manipulation of (5.1) provides a simple conservative estimate for the 1σ uncertainty of each NSP measurement as

$$\Delta q_i = \pm\sqrt{\frac{1}{n_o}} \,, \tag{5.2}$$

where $n_o = n_{o\|} + n_{o\perp}$, these identities corresponding to the 'true' underlying photon counts. Comparisons of papers in the literature suggest a minor confusion with respect to (5.2) in that it sometimes carries an additional factor of $1/\sqrt{2}$. Whether or not this numerical term occurs is purely a matter of definition in that some authors define $n_o = n_{o\|} = n_{o\perp}$, rather than as above. A similar formula also applies to the determination of the NSPs corresponding to u_i. It should be noted that ascribed uncertainties calculated by (5.2) are conservative estimates as the exact underlying true value of n_o is unknown, and is an estimate itself, based on the same measurements made to determine q_i.

For calculations of a mean value for q, Clarke, Stewart, Schwarz, *et al.* (1983) have commented on the various estimators that are used. For example, if the total observation time is divided so that N repeated samples represented by $n_{\|i}$, $n_{\perp i}$ are recorded, the individual values of q_i may be used to evaluate a mean given by

$$\tilde{q} = \frac{1}{N}\sum_{i=1}^{N} q_i = \frac{1}{N}\sum_{i=1}^{N}\left(\frac{n_{\|i} - n_{\perp i}}{n_{\|i} + n_{\perp i}}\right) . \tag{5.3}$$

Extending the general principle of the central limit theorem, the best value for a normalized parameter is obtained when the ratio is performed with the highest signal-to-noise ratio for the quotient parameters. If, for example, any noise introduces biasing to these parameters, its effects will be minimal when the signal-to-noise is a maximum. For this reason, Clarke, Stewart, Schwarz, *et al.* (1983) preferred an alternative estimator for the mean based on

$$\bar{q} = \frac{\sum_{i=1}^{N} n_{\|i} - \sum_{i=1}^{N} n_{\perp i}}{\sum_{i=1}^{N} n_{\|i} + \sum_{i=1}^{N} n_{\perp i}} \,. \tag{5.4}$$

It will be seen that for $\tilde{q}$, the repeated determinations of q_i carry the noises associated with the individual repeated measures of $n_{\|i}$ and $n_{\perp i}$, whereas for $\bar{q}$, the noises have better chance to average out within the summations before the final ratio is taken. Determination of $\bar{q}$, however, provides only one single estimate for the true underlying value, q_o, and its associated uncertainty must be obtained either from *a priori* knowledge of the accuracies of the summations, or by considering the scatter associated with the measurements for q_i.

Based on the definition of (5.1), Clarke, Stewart, Schwarz, *et al.* (1983) have also shown that the probability distribution for q may be expressed by

$$F(q) = \frac{B \exp\left(B^2/A - C\right)}{\sigma_{\|}\sigma_{\perp} A\sqrt{A\pi}(1+q)^2}\,, \tag{5.5}$$

where

$$\begin{cases} A = \dfrac{1}{2}\left(\dfrac{1}{\sigma^2_{\|o}} + \dfrac{1}{\sigma^2_{\perp o}}\left(\dfrac{1-q}{1+q}\right)^2\right) \\ B = \dfrac{1}{2}\left(\dfrac{n_{\|o}}{\sigma^2_{\|o}} + \dfrac{n_{\perp o}}{\sigma^2_{\perp o}}\left(\dfrac{1-q}{1+q}\right)\right) \\ C = \dfrac{1}{2}\left(\dfrac{n^2_{\|o}}{\sigma^2_{\|o}} + \dfrac{n^2_{\perp o}}{\sigma^2_{\perp o}}\right) \end{cases}$$

and where the terms $n_{\|o}$, $n_{\perp o}$, $\sigma^2_{\|o}$ and $\sigma^2_{\perp o}$, respectively, refer to underlying true values of the component signals and their variances, the latter themselves assumed to follow normal distributions.

It can be seen that the probability function for NSPs (5.5) is not a normal distribution. With the assumption that the achieved photon accumulations are reasonably high and their Poisson behaviour can be equated to Gaussian statistics, the form of $F(q)$ has been investigated by Clarke, Stewart, Schwarz, *et al.* (1983) and compared with a ‘perfect normal curve’ (PNC) expressed as

$$F_{\text{Nor}}(q) = \frac{1}{\sigma_q\sqrt{2\pi}} \exp\left(\frac{-(q-q_o)^2}{2\sigma_q^2}\right). \tag{5.6}$$

This exercise reveals that $F(q)$ is symmetrical about q_o, but that kurtosis is significant for very low photon counts, the curve having a sharper peak than the PNC, but with broader wings. For example, for $n_o = 100$, the kurtosis coefficient is 3.135 but, for $n_o = 5000$, it reduces to 3.002, it being remembered that for a PNC, this coefficient is exactly 3.0. When calculating confidence intervals associated with a mean NSP obtained from a sample of repeated measurements, such departures from normality should, in principle, be taken into account. It may be noted, however, that effects caused by small amounts of positive kurtosis have minor consequences on confidence intervals. In most cases of stellar polarimetry, the value of n_o is $> 10^6$, making the kurtosis effects virtually insignificant and, to all intents and purposes, NSPs can be considered to follow a normal distribution. Detail of the extreme behaviour of $F(q)$ for low photon accumulations with a Poisson statistical behaviour has been examined by Maronna, Feinstein & Clocchiatti (1993).

5.3
The Statistics of *p*

If the two Stokes parameters describing linear polarization are combined to provide values for the degree of polarization, p, then repeated determinations of p provide a biased distribution. By definition, the parameter, p, is a positive definite quantity. When determined by measurement, its component Stokes parameters carry noise and, as a consequence of the squaring procedure in calculating p, this always contributes in a positive way, thus producing biased results. The effect is at its most obvious for the case corresponding to measurements of zero polarization such that $p_o = (q_o^2 + u_o^2)^{1/2} = 0$. Although the true NSPs, q_o, u_o, are both zero, because of the experimental noise, individual records, q_i, u_i, will generally have non-zero values, which may be +ve or −ve; the evaluated individual polarization values calculated from $p_i = (q_i^2 + u_i^2)^{1/2}$ will always be positive and non-zero.

The bias can also be readily visualized by considering pairs of NSPs (q_i, u_i), both following normal distributions and with identical variances, giving rise to polarization values, p_i (see Figure 5.1). It can be seen that the mean value defined by $\bar{p} = \frac{1}{N}\sum_{i=1}^{N} p_i$ does not lie at the data centre of gravity defined by $p_\mathrm{c} = (\bar{q}^2 + \bar{u}^2)^{\frac{1}{2}}$, this latter quantity being frequently chosen to represent the determined value of p. When a pointer of length p_c, anchored at the origin is swept through the qu-plane, the generated arc does not divide the data into equal portions, i.e., $p_\mathrm{c} \neq \bar{p}$.

The degree of bias depends on the single-to-noise ratio of the measurements. Consequently any determination of p is better made by determining the mean values of the contributing Stokes parameters and using these to determine the best

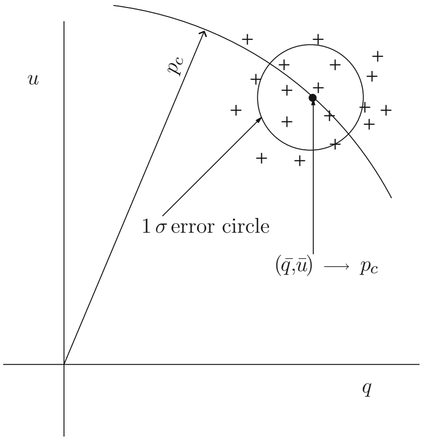

Fig. 5.1 A typical distribution of repeated NSP measurements is displayed with the centre of the distribution, $\bar{q}$, $\bar{u}$, providing a polarization value, p_c. In relation to the data distribution, it is obvious that if p_c is used as a radius to provide an arc through the data, its value is a biased estimator as there are more points outside the arc than on its nearside towards the origin; the arc does not divide the circle into equal areas.

value of p, rather than determining the mean value of a set of repeated measurements of p. From any assembly of repeated measurements, statistical tests to check out whether the recorded Stokes parameters can be considered as following a normal distribution can be readily applied; the quality of any data can be assessed in this way and the variance checked to see how closely it agrees with an estimate based on the number of recorded photons.

Many observers appear to be unaware of the statistical behaviour of p, and implicitly assume that its measurement values follow a normal distribution. In fact, all experimentally determined values of p are biased to a degree according to the signal-to-noise ratio of the basic records. Without bias being taken into account, comparison of data from various sources is hazardous. Mistaken polarimetric variability can all too easily be 'detected' in data embracing a variety of signal-to-noise conditions.

It is sometimes boasted that polarimetry with a fast modulator can be performed under adverse conditions of varying atmospheric transparency, which would be prohibitive for ordinary stellar photometry. What is usually meant by the statement is that reduced measurements from successive integrations have uncertainties strictly dependent on the photon shot noise associated with each particular result. The usefulness of operating under such difficult conditions is somewhat limited, however, as the determined values of p carry a range of bias according to the photon count and the individual signal-to-noise ratios, and calculation of any overall confidence limits is extremely difficult. Great care must be taken in assessing any temporal polarimetric changes in such data.

Serkowski (1958) was first to formulate the probability distribution for p and it has been since investigated by Vinokur (1965) and Simmons & Stewart (1985). In order to establish expressions for $F(p)$, initial assumptions are that q and u are independent variables, both distributed normally around true values of q_o and u_o, and that their associated variances are known and equal with values of σ_o^2. For most observational circumstances these assumptions are fairly reasonable but they are invalid when:

1. the recorded NSPs are not from a normal distribution, possibly as a result of observing with low signal-to-noise ratios (see above), or if the noise is dominated by atmospheric intensity scintillation, which itself has a non-normal distribution,
2. certain measurement techniques are used whereby a noise correlation is introduced between the recorded NSPs (see, for example, Stewart, 1985).

By considering random Gaussian noise with a variance, σ_o^2, superposed on a underlying fixed signal vector of length p_o, the probability distribution of the values of p is given by the well-known Rice (1944) distribution:

$$F(p; p_o, \sigma_o) = \frac{p}{\sigma_o^2} \exp\left(\frac{-(p^2 + p_o^2)}{2\sigma_o^2}\right) J_o\left(\mathrm{i}\frac{p\,p_o}{\sigma_o^2}\right), \tag{5.7}$$

where $J_o(ix)$ is the zero-order Bessel function of the imaginary argument. The probability curves are more conveniently represented by normalising the various

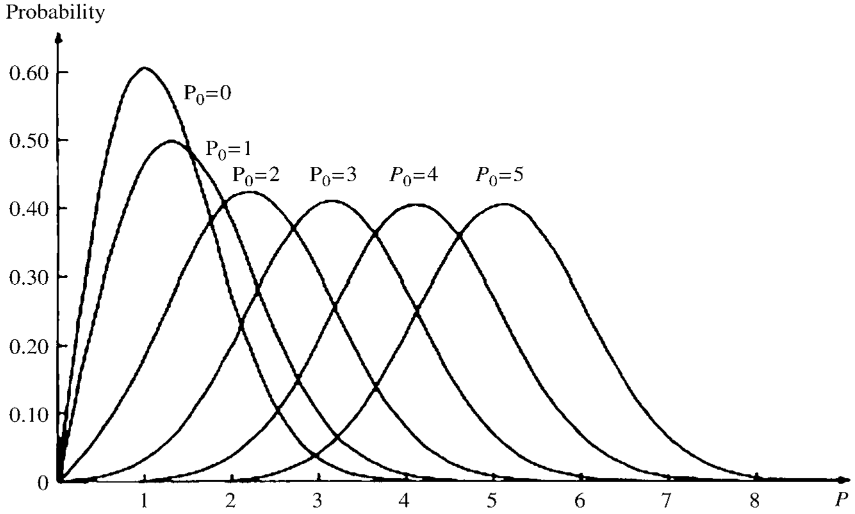

Fig. 5.2 The Rice distribution $F(P; P_o)$ as a function of P is displayed for values of $P_o = 1, 2, 3, 4$ and 5. (Taken from Simmons & Stewart, 1985.)

NSPs, q, u, q_o, u_o, by σ_o to produce the parameters $q_n = q/\sigma_o$, $u_n = u/\sigma_o$, $q_{on} = q_o/\sigma_o$ and $u_{on} = u_o/\sigma_o$, these leading to normalized polarization values of P with an underlying value of P_o. The distribution function for P is now written as

$$F(P; P_o) = P \exp\left(\frac{-(P^2 + P_o^2)}{2}\right) J_o(\mathrm{i}P P_o) \,. \tag{5.8}$$

Probability distribution functions of P for low signal-to-noise situations are depicted in Figure 5.2. It may be noted that for a situation with $P = 0$, the range of values that might be recorded runs from just greater than zero to a value of $P \approx 4$; the most probable recorded value is approximately just less than unity. Also as a result of distributions for a given P_o being asymmetric, with the tail extending to larger values of P, any assigned '± error bars' will be of unequal length either side of any determined value of P.

For run of the mill measurements, with $p \gg 0$, the reported values for p should be corrected for bias. The classical formula used is that of Serkowski (1958, 1962) whereby the revised estimate $\hat{p}_S$ is given by

$$\hat{p}_S = \left(p^2 - \sigma^2\right)^{1/2} . \tag{5.9}$$

When dealing with low levels of polarization ($p \approx 0$), or for measurements made with low signal-to-noise ratios, Serkowski (1962) provides a corrected estimate given by

$$\hat{p}_S = \left(p^2 - \frac{1}{2}\pi\sigma^2\right)^{1/2} . \tag{5.10}$$

Throughout optical polarimetry, for those observers who appreciate the problem, it is the formula given by (5.9) which is used to provide the declared value for the degree of polarization (see, for example, Poeckert & Marlborough, 1976). The same formula, but derived in a different way, is used by radio astronomers (see Wardle & Kronberg, 1974).

Although Serkowski (1962) suggests that the correction formulas ensue by considering the observed value to be the most probable, the study by Simmons & Stewart (1985) shows that it relates to the value for which the observed measurement is taken as the mean of the distribution $F(p; p_o, \sigma_o)$. In their work, Simmons & Stewart (1985) have studied the effects of bias on P, and various 'unbiased' estimators are defined and examined for their effectiveness. Comments are made on some of the astrophysical issues where the choice and application of the most appropriate estimator might be important. Adopting their nomenclature for the unbiased estimator, $\hat{P}_o$, they considered the Serkowski mean estimator, $\hat{P}_S$, the most probable value as considered by Wardle & Kronberg (1974), $\hat{P}_W$, the maximum likelihood estimator, $\hat{P}_{ML}$ and the median estimator, $\hat{P}_M$. These four estimators, along with the uncorrected, naive estimator, $\hat{P} = P$ are depicted in Figure 5.3.

Simmons & Stewart (1985) also considered the bias, $\langle \hat{P}_o \rangle - P_o$, and risk function (or square error), $\langle (\hat{P}_o - P_o)^2 \rangle$ for the various estimators. From this work, the following observations can be made:

1. For values of $p/\sigma > 4$, all the correcting estimators agree, with the estimated value of P_o approximately given by $\hat{P}_o = (P^2 - 1)^{\frac{1}{2}}$ – this corresponding to the formulas of Serkowski (1962) and of Wardle & Kronberg (1974).

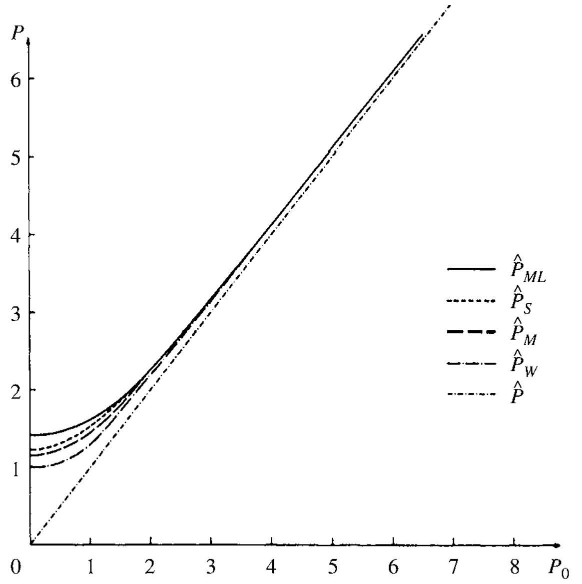

Fig. 5.3 Estimator curves for $\hat{P}_{ML}$, $\hat{P}_S$, $\hat{P}_M$, $\hat{P}_W$ and $\hat{P}$ are displayed according to the appropriate definition (see the text) and may be used to obtain an estimated value of P_o from the observed polarization. (Taken from Simmons & Stewart, 1985.)

2. $\hat{P}_{\mathrm{W}}$, and the naive $\hat{P}$, are always positively biased, while the other estimators display positive and negative bias, depending on the underlying value of P_o.
3. For small values of P_o ($P_o \lesssim 0.7$), $\hat{P}_{\mathrm{ML}}$ is the best estimator, having least bias and associated risk.
4. At larger values of P_o ($P_o \gtrsim 0.7$), $\hat{P}_{\mathrm{W}}$ becomes the best estimator.
5. The P_o region over which $\hat{P}_{\mathrm{S}}$ and $\hat{P}_{\mathrm{M}}$ are truly the best estimators is very small.
6. $\hat{P}_{\mathrm{ML}}$, $\hat{P}_{\mathrm{S}}$, $\hat{P}_{\mathrm{W}}$ and $\hat{P}_{\mathrm{M}}$ all yield an estimated value of P_o which is less than $\hat{P}$.

To allow ready calculation for point and confidence intervals for determined values of p, Stewart (1991) has provided polynomial fits to the curves describing the behaviour of the various estimators above. Another approach for applying confidence limits on polarization measurements has been presented by Vaillancourt (2006). Tests to consider whether a star exhibits polarization or not have been developed by Clarke & Stewart (1986) and tables are provided in this reference to allow confidence values on the decision.

Determination of a mean value of p can be obtained either by taking mean values of the contributing NSPs to form a single value, or the observed NSPs can each provide p values from which a mean is obtained. The latter is a mean of biased values with offsets from the true underlying value, according to the signal-to-noise ratios of the NSP measurements; the final bias offset is going to be the same order as that of the individual values. For the case of determining a single value of p from the mean NSP values, it will also carry bias, but the offset is likely to be reduced as it is determined with a better signal-to-noise ratio according to the square root of the number of NSP measurements. As in the case of the determination of NSPs (see (5.4)), it is the best policy to calculate a single value of p with the highest signal-to-noise ratio by lumping together all of the underlying photon counts, rather than by combining many individual determinations each made with a lower signal-to-noise ratio.

5.4
The Statistics of Position Angle

Some feeling for the behaviour of repeated determinations of the position angle, ζ, of linear polarization can be appreciated by considering the distribution of NSPs in a normalized Stokes vector diagram. When the underlying value of p is close to zero, or equal to it, the values spread around the origin are distributed in each quadrant and, in that case, the variance associated with ζ is independent of the signal-to-noise ratio of the measurements. For a circumstance with a significant value of p, the NSPs concentrate about their centre of gravity, predominantly in one quadrant such that the spread in ζ depends on the value of p and the accuracy of the determinations.

Serkowski (1958, 1962) presented formal error estimates ($1\sigma_\zeta$) for the two extreme cases for which the underlying value of the polarization, p_o, is very close to zero and when it has significant value, measured with a high signal-to-noise ratio. Based on the notion that the σ_p value is known perfectly, the appropriate formulas may be written as

$$\sigma_\zeta(p) = \begin{cases} \dfrac{\pi}{\sqrt{12}}\text{rad} = 51.^\circ 96 & p_o \simeq 0 \\ \dfrac{\sigma_p}{2p}\text{rad} = 28.^\circ 65 \dfrac{\sigma_p}{p} & p_o \gg \sigma_p \,. \end{cases} \tag{5.11}$$

The derivation of these expressions may be found in Naghizadeh-Khouei & Clarke (1993). Wardle & Kronberg (1974) have calculated the $1\sigma_\zeta$ confidence limits for more general values of p_o, presenting their results in graphical form. It will be appreciated that the distribution of ζ about ζ_o is symmetric, so that resultant mean from a set of measurements is an unbiased estimator. For large signal-to-noise ratios, the distribution for ζ tends towards being Gaussian; for small signal-to-noise ratios, the distribution becomes kurtose with appreciable wings (see Figure 5.4). As a consequence, the $2\sigma_\zeta$, $3\sigma_\zeta$ or other confidence values should not be calculated by applying simple proportional scaling factors to the $1\sigma_\zeta$ value above.

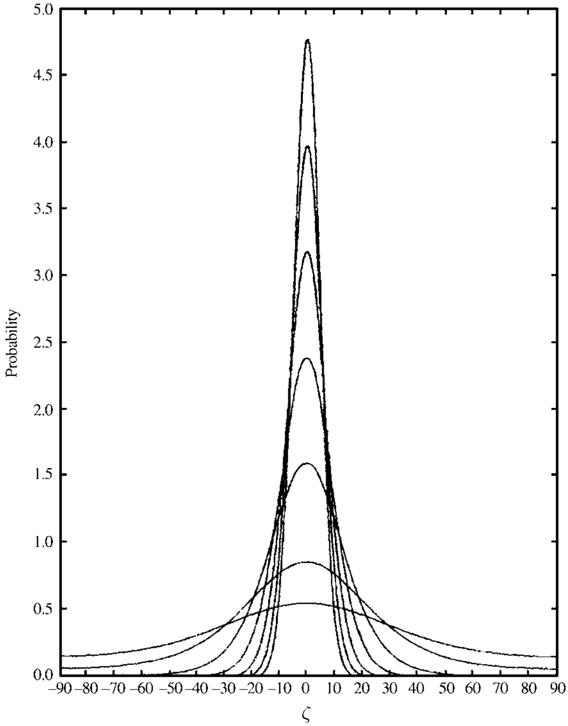

Fig. 5.4 The position angle distribution as a function of ζ for values of P_o (signal-to-noise ratio = 0.5, 1, 2, 3, 4, 5 and 6). (Taken from Naghizadeh-Khouei & Clarke, 1993.)

If the underlying variance of a set of NSPs is known exactly, the probability distribution for ζ may be expressed by

$$G(\zeta;\zeta_o,P_o)=\frac{1}{\sqrt{\pi}}\left[\frac{1}{\sqrt{\pi}}+\eta_o e^{\eta_o^2}\left[1+\operatorname{erf}(\eta_o)\right]\right]\exp\left(-\frac{P_o^2}{2}\right), \qquad (5.12)$$

where $\eta_o = P_o\cos(\zeta-\zeta_o)/\sqrt{2}$, $P_o = p_o/\sigma$, equivalent to the signal-to-noise ratio of the measurements of p, and 'erf' is the Gaussian error function. This equation is essentially a more organized version of that by Vinokur (1965) and its derivation can be found in Naghizadeh-Khouei & Clarke (1993), together with a calculations of the 95 and 99% confidence intervals for a range of signal-to-noise conditions.

5.5
Instrumental Correction

The collected stellar radiation is transferred by the telescope optics to the polarimetric modulator. As a result, the initial polarization may be altered before it is measured by the instrument attached at the telescope's focus. The most common spurious effect is that any collected unpolarized light becomes weakly polarized. The amount of polarization introduced is referred to as the *instrumental polarization*. There may be additional sources contributing to the instrumental polarization other than the telescope mirrors.

It is usual practice in any observing programme to investigate the instrumental polarization by making measurements of unpolarized standard stars. The mean values of the NSPs for these measurements may be represented by q_{I} and u_{I}, and the position of the instrumental polarization can be plotted in a normalized Stokes vector diagram. For measurement of other stars, the reduction procedure involves shifting the origin, O, of the measurements to that of the instrumental polarization position, O′ (see Figure 5.5). This is best done by subtracting the offset, q_{I}, u_{I}, from the q, u values of the program stars. The process corresponds to a vector subtraction of the instrumental offset by the inversion of the principle of the *Additivity Theorem for Small Polarizations* (see Section 4.5).

If the source of instrumental polarization is identifiable as occurring in the telescope fore-optics, and can be expressed as a Mueller matrix, a more accurate reduction would involve an inversion procedure to obtain revised values according to the elements of this matrix. In the simplest case, the matrix would be that of a weak polarizer; in some cases, there may also be a small phase change introduced by the optics and this would need to be incorporated into the matrix (see further discussion in Chapter 7).

It is also possible that the telescope optics effect a depolarization to any collected polarized light (see Section 7.4), this being a true reduction of a degree of polarization and not simply a linear-to-circular conversion. Depolarization is a difficult parameter to investigate, the best that can be done is to inter-compare results taken by different instrumental setups. If its effects on all the Stokes parameters are known, and are expressible in the form of a Mueller matrix, in principle, any

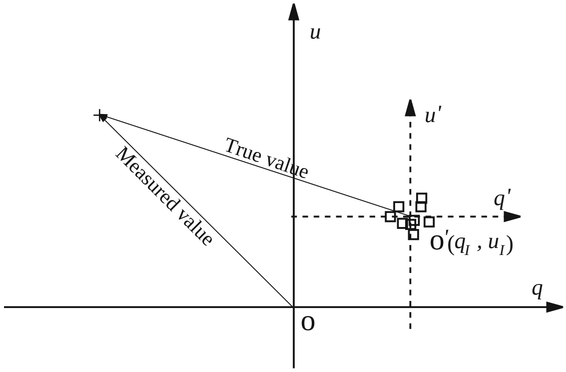

Fig. 5.5 A schematic normalized Stokes vector diagram illustrating that a set of measurements (☐) of unpolarized stars are not at the origin of the NSP vector diagram, but are offset at a mean value of q_{I}, u_{I}, corresponding to the instrumental polarization. Using this point as a revised origin, O′, a corrected value for the degree of polarization of a program star (+) may be determined.

measurements can be corrected by an inversion procedure. Setting a calibration polarizer in the beam passing through the instrument does not resolve the issue as it is placed after the telescope optics, and only allows the modulation efficiency to be checked.

5.6
Intrinsic/Interstellar Separation

One of the problems in considering discussion of any astrophysics from polarization measurements is that a measured value is often the resultant of processes in the atmosphere of a star, with the effects of some interstellar polarization added on. Thus the observed resultant may comprise intrinsic and interstellar components, and the latter must be removed in order to effect any model fit to the intrinsic polarigenic processes. The strength of the interstellar component can sometimes be estimated by making measurements of nearby field stars, particularly for those which are at the same distance as the target star. Generally, the interstellar component is removed by vector subtraction but again, if the highest accuracy is required, the effects of the interstellar medium should be represented as a Mueller matrix with an inversion process applied.

According to McLean & Clarke (1979), the presence of an intrinsic polarization component can be inferred from one, or more, of four characteristics. These may be summarized as

1. Temporal variability of the observed polarization (p, ζ),
2. A wavelength dependence of $p(\lambda)$ different to that of the established curve related to interstellar effects,

3. A wavelength variation of the polarization position angle, $\zeta(\lambda)$ – but with due care taken to resolve whether this is caused by complex structures in the interstellar material along the line of sight,
4. Changes of the polarization (p, ζ) across discrete spectral emission or absorption features of stellar origin.

For criterion (1) to be applied, instrumental stability must be of high order. It is also generally assumed that, for a given star, any interstellar component is constant with time. Such a notion has been challenged by Bastian, Drissen, Ménard, *et al.* (1988) although their conclusions, based on statistical arguments, were later found by Clarke & Naghizadeh-Khouei (1994) to have shortcomings. No doubt that in the future, as the time-base and polarimetric accuracy increase, the effects of changes of interstellar polarization may become apparent as stars move relative to the columns of dust along their line of sight. In order to apply criteria (2) and (3), measurements covering a wide spectral range are generally required.

In many cases, it can be considered that the intrinsic polarization is engendered by a global structure which remains constant in terms of its geometric characteristics but which varies in scattering strength. What this does is to provide a contribution to the observed polarization, which is set at some fixed position angle, but which varies in its vector length. This direction, as determined from the behaviour of the data in a normalized Stokes parameter diagram, has been described by Clarke & McGale (1987) as the *maximum principal axis* (MPA) or the *intrinsic line*.

In some cases, it is hard to differentiate between data distributions, which are dependent only on the noise associated with the observations, and those which represent low levels of variable intrinsic polarization. A statistical check as to whether the q, u values form a distribution with underlying circular symmetry, or whether they contain an intrinsic variability, can be made by first transforming the data to an axial frame with origin at the centre of gravity of the data distribution. Suppose there are N data points with values represented by q_i, u_i. A quantitative approach can be made by taking moments, $m^{(k)}$ about the centre of gravity defined as q_{c}, u_{c}, a moment being defined as

$$m_q^{(k)} = \frac{1}{N}\sum_{i=1}^{N}(q_i - q_{\mathrm{c}})^k \; ; \qquad m_u^{(k)} = \frac{1}{N}\sum_{i=1}^{N}(u_i - u_{\mathrm{c}})^k \; . \tag{5.13}$$

The first moment is automatically equal to zero by definition. The second, third and fourth moments may be used to test whether the data distributions can be considered as being statistical normal, and confidence intervals on the outcomes may then be applied from tables such as those developed by Brooks, Clarke & McGale (1994). When these tests are undertaken, it is usually assumed that the quality of the data is uniform. If accurate values for the uncertainty associated with each of the data points are known, it is best to undertake statistical tests based on measurements of q and u which have been normalized by their uncertainty.

The second moment provides a measure of the spread of the data, defining the population variance, and it can be used for assessing the presence of eigen directions. By progressively rotating the axial frame about the centre of gravity of

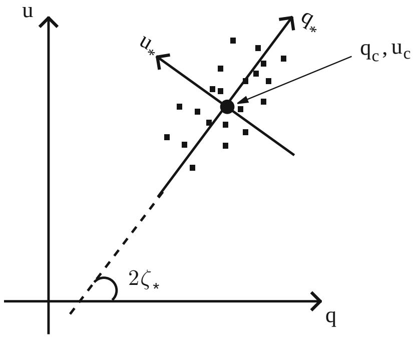

Fig. 5.6 Repeated measurements of a star provide a centre of gravity, q_c, u_c, for the data in an NSP diagram. By rotating a set of reference axes about this new origin, represented by q_*, u_*, the pairs of second moments may be compared to find the maximum disparity. If this is statistically different, the angle, $2\zeta_*$ corresponds to the MPA, and provides some preferred direction associated with the star, possibly a projection of the stellar equator, at an angle, ζ_*, on the sky.

the data, an angle may be found for which in the new reference frame, denoted by q_*, u_*, the pair of second moments have their maximum difference (see Figure 5.6). A check on whether such maximum and minimum variances pairs are significantly different can be made by the usual F-test (see Snedecor & Cochran, 1980). The axis set at $2\zeta_*$, which coincides with the direction of maximum variance, may be taken as the MPA (see above). According to appropriate models for given types of star, the MPA may, for example, coincide with the projection of the stellar equator set at ζ_* on the sky (see, for example, Figure 5.7).

For cases in which an obvious intrinsic line is found, or determined from statistical criteria, the interstellar polarization component for the given wavelength of the measurements is represented by a single point somewhere on the line. To find that point requires a knowledge of one of the following:

1. The direction of vibration of the interstellar polarization, ζ_i.
2. The amount of interstellar polarization, p_i, at the given wavelength, λ.
3. The true amount of intrinsic polarization, $p_\star$, at the given λ at some time.

A mean value for the orientation of interstellar polarization, $\bar{\zeta}_i$, can sometimes be inferred from observations of a common proper motion star, or a physical companion star positioned with sufficient angular separation, or by averaging the apparent position angles of 'normal stars', i. e. non-intrinsically polarized stars, lying at a similar distance as the program star, and within a few degrees of it. The latter method of course assumes a certain homogeneity of the interstellar effects, which is by no means assured, and a statistically large enough sample of stars is not always available. Data for the reference stars exhibiting interstellar polarization may only be obtained from catalogues, or at the time of measurement of the program star.

The amount of interstellar polarization is generally not easily estimated. For stars near the galactic plane, and with colour excesses greater than $E_{B-V} \sim 0.1$ mag,

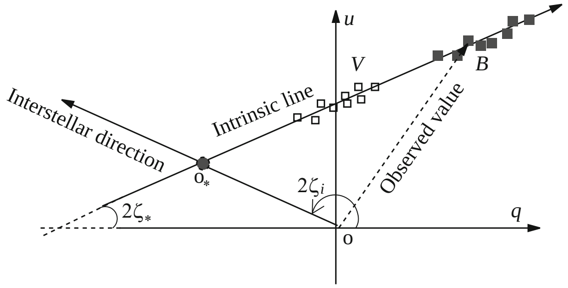

Fig. 5.7 A schematic normalized Stokes vector diagram of *B* and *V* data of a polarimetric variable star. The intrinsic line is obtained by taking the best fit to the direct measurements; the interstellar direction is obtained from the polarization vectors for stars in the neighbourhood of the program star. The origin ($O_\star$) for the degree of intrinsic polarization corresponds to the intersection of the intrinsic and interstellar lines. Following the construction, the vector length, $O - O_\star$, should be checked to see if it matches the estimated value for degree of interstellar polarization affecting the star.

Serkowski, Mathewson & Ford (1975) have shown that the maximum in the wavelength dependence of the interstellar polarization, $p_{\max}(\%)$, lies in the range $3E_{B-V} \leq p_{\max}(\%) \leq 9E_{B-V}$. For nearby stars, and those at high galactic latitudes, the limits are less certain; as a rough guide, typical values of $\bar{p}_i \sim 5E_{B-V}$ occur for stars within ±15° of the galactic plane; for nearby and high-latitude stars, $\bar{p}_i \sim 3E_{B-V}$ may be taken.

In the schematic example shown in Figure 5.7, polarization data for the *B* and *V* spectral bands indicate that the variability follows an intrinsic line with a position angle on the sky at $\zeta_\star$ – N.B., the line is set at $2\zeta_\star$ in the normalized Stokes vector diagram. From data associated with neighbourhood stars exhibiting interstellar polarization only, an underlying interstellar direction with position angle, ζ_i, is obtained, and this is seen to intersect the intrinsic line at $O_\star$, giving an origin from which the amount of intrinsic polarization can be deduced. If the interstellar direction is not well defined but the degree of polarization, p_i, is estimated to reasonable certainty, then two possible positions for $O_\star$ might be obtained. Rotation of a vector of length, p_i, about the origin, O, should yield two coordinate points or intercepts on the intrinsic line, one of which lies along ζ_i.

Separation of the intrinsic component from the interstellar contribution is generally improved if the exercise is performed with measurements obtained in a range of wavebands. An example of the success of such an analysis is provided by Pfau, Piirola & Reiman (1987) for the star HD 200775.

High-resolution studies sometime reveal sharp changes in $p(\lambda)$ across individual spectral lines, this indicating the presence of intrinsic polarization. If such data are represented in an NSP diagram, the locus of the changes may indicate the intrinsic line for the star. For the case of Be stars, the Balmer emission lines usually display a reduction in the polarization. In the early studies of this effect, it was thought that the degree of reduction was directly linked to the strength of the emission feature, as though this additional radiation was essentially unpolarized (see McLean & Clarke, 1979). As higher spectral resolution was applied to spectropolarimetry of

Be stars, the situation was found to be more complicated with the locus performing looped patterns in the qu-plane. Nonetheless, the spectral behaviour of the line polarization across emission features can be useful in establishing the intrinsic line especially in conjunction with any monitored time variability of the star. Measurements at the Balmer jump of Be stars have been used by Quirrenbach, Bjorkman, Bjorkman, *et al.* (1997) to remove contaminations of interstellar polarization. In some late-type stars, polarization changes are sometimes noted in molecular absorption lines and again these may help in establishing the intrinsic line.

5.7
Interpreting Measurements

5.7.1
Polarization and Small Samples

In the earlier presentation on the theoretical distributions of p and ζ, and on discussion of the confidence intervals associated with assigned values, it is assumed that the variances of the underlying NSP values are known perfectly, or at least have been well estimated from a large sample of measurements. Also, it has been assumed that the uncertainties of the NSPs, σ_q, σ_u, are the same and equal to σ. This ideal situation holds, or is very close to pertaining, in most observational circumstances. When $\sigma_q \neq \sigma_u$, however, the resulting distribution functions for p and ζ are complicated and do not depend explicitly on p, p_0, ζ and ζ_0, making the point and interval estimation of p and ζ very involved. As an added difficulty, experiments are often conducted with only a small sample of repeated NSP measurements being obtained, in which case the derived σ_u, σ_q values strictly represent estimates rather than being true values. A mathematical derivation of the distributions of p and ζ in these circumstances would be a formidable task.

Determining the *best* estimator for the value of p_0, and prescribing accurate confidence levels is a thorny problem. Without an analytic expression for the distribution function for p related to the experimental conditions, the behaviour of small sample estimators and confidence intervals might be investigated and compared using computer generated data of the same ‘ quality’ as those obtained directly from observation.

When the determined values of p and σ have been obtained from a small set of repeated NSP measurements, with $p/\sigma \gtrsim 6$, it may be possible to assume that p comes from a normal distribution. The best estimate for p_0 would then perhaps be given by $\hat{p}_0 = (p^2 - \sigma^2)^{\frac{1}{2}}$. Confidence intervals on $\hat{p}_0$ could therefore be assigned by using the sample-dependent Student-t modification on the value of σ. It must, however, be pointed out that, for low values of p/σ, this method will produce only approximate estimates on the point and interval values of p.

Conservative confidence intervals for p and ζ, taking into consideration sample size and the condition that $\sigma_q \neq \sigma_u$, can be constructed through the method of projection on the qu-plane. In the large sample case, for example, repeated NSP

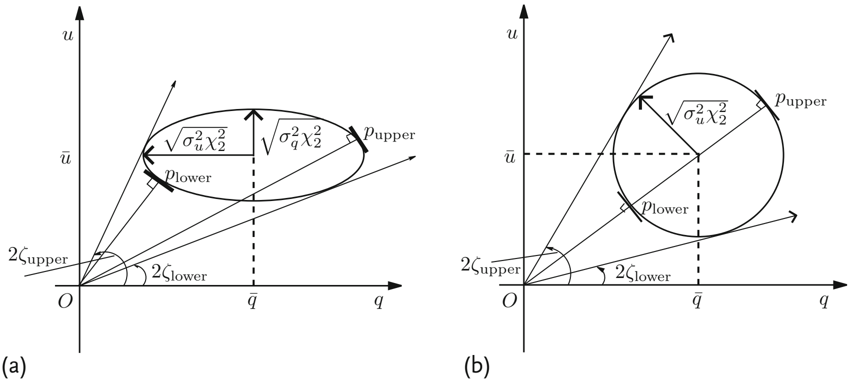

Fig. 5.8 The construction of confidence regions for the degree of polarization and position angle using projection techniques on the qu-plane. (a) shows the elliptical case with $\sigma_q^2 \neq \sigma_u^2$; (b) illustrates the circular case with $\sigma_q^2 = \sigma_u^2 = \sigma^2$.

measurements would produce the mean values, $\bar{q}$, $\bar{u}$, and standard mean errors, σ_q and σ_u. Confidence regions for the true NSPs, q_0, u_0, can be constructed by noting that

$$\frac{(\bar{q} - q_0)^2}{\sigma_q^2} + \frac{(\bar{u} - u_0)^2}{\sigma_u^2} \sim \chi_2^2 \,. \tag{5.14}$$

The left-hand side of (5.14) is distributed in the form of a χ-square distribution with two degrees of freedom. The values of χ_2^2 at the 67, 95 and 99%, confidence levels are 2.22, 5.99 and 9.21, respectively. Using the appropriate value for χ_2^2, the appropriate elliptical confidence regions are obtaining for q_0, u_o, with semi-major and/or semi-minor axes given by $\sqrt{\sigma_q^2\chi_2^2}$ or $\sqrt{\sigma_u^2\chi_2^2}$. This region can be transformed into $p, 2\zeta$ space and intervals instructed for p and 2ζ as indicated in Figure 5.8a. The interval for p is obtained by drawing two perpendiculars from the axial frame origin to the ellipse, the intercepted values representing the upper and lower levels for p_0. The confidence intervals for 2ζ are similar but are constructed by drawing tangent lines from the axial frame origin to the ellipse.

In Figure 5.8b, the circular case with $\sigma_q = \sigma_u = \sigma$ is depicted showing that the corresponding intervals are symmetrical around the estimated values of p, which are biased, and 2ζ.

5.7.2
Detection of Polarizational Differences

A problem that frequently occurs, but is generally inadequately treated, involves the assessment of detecting polarizational differences between two or more meaned values. An astrophysical study might be related to deciding if a star has changed its polarization with time, or if two stars have differing polarizations, or if one star can be considered as being a member of a group representing a particular polarization state, or if the polarization of a star varies with wavelength. In all these cases, because of differing intensity levels and observing conditions, the values for comparison are means based on data with different sample sizes (usually small) and different variances. In these circumstances, using a simple procedure of applying formal error combination formulas is inadequate for the decision-making process.

A suitable quantitative statistical approach which takes into account sample size and variance has been described by Welch (1951). From analyses by Brown & Forsythe (1974) and Kohr & Games (1974), in terms of size and power (power being the probability of rejecting the hypothesis of equality of means when it is indeed false), application of the *Welch test*, is a recommended statistical procedure.

For a given set of g assemblies of data points for the NSP q (and/or u), each may have different sample sizes, $n_1 \neq n_2 \neq \ldots \neq n_g$, and estimated variances, $\widehat{\sigma_1}^2 \neq \widehat{\sigma_2}^2 \neq \ldots \neq \widehat{\sigma_g}^2$, the Welch statistic, W, is calculated from

$$W = \frac{\sum_{i=1}^{g} w_i (q_i - \tilde{q})^2/(g-1)}{\left[1 + \frac{2(g-2)}{(g^2-1)} \sum_{i=1}^{g} (1 - w_i/z)^2/(n_i - 1)\right]} , \tag{5.15}$$

where

$$w_i = \frac{1}{\widehat{\sigma_i}^2} , \qquad z = \sum_{i=1}^{g} w_i , \qquad \tilde{q} = \sum_{i=1}^{g} w_i q_i / z .$$

When all population means are equal (the estimated variances being equal or unequal), W is approximately distributed as an F-statistic with $(g-1)$ and f degrees of freedom, where f is defined by

$$\frac{1}{f} = \left(3/(g^2-1)\right) \sum_{i=1}^{g} \left(1 - \frac{w_i}{z}\right)^2 /(n_i - 1) . \tag{5.16}$$

The hypothesis of equality of population means is rejected at the usual 95% or 99% confidence levels by consulting the appropriate F-statistic tables (see, for example, Snedecor & Cochran, 1980)). When little or no correlation exists between the measurements of multivariate parameters (in this case the NSPs), according to Timm (1975), testing of differences between the means of several data points should employ univariate rather than multivariate techniques. In other words, Welch tests should be applied to q and u separately. The Welch test has been applied successfully in astrophysical situations as described in Clarke & Brooks (1985) and Clarke, Schwarz & Stewart (1985).

5.7.3
Data Assemblies

For some discussions on the interpretations of measurements, it is sometimes relevant to consider assemblies of data to examine their behaviour relative to some expectation. For example, if a star is suspected to exhibit variable polarization, the first approach might be to take the repeated NSP measurements and check whether they can be considered as being a representative sample from a normal distribution, with a variance defined by the experimental errors.

There are various ways of testing whether a sample of measurements comes from a given or known population distribution. When a sample is large enough, the observed polarizations can be *binned* to form a histogram. This immediately gives a good picture of the behaviour and leads to a comparison with the theoretical distribution, the goodness of fit perhaps being investigated using the well-known χ-square test. This procedure has two drawbacks, however. Firstly, the number of bins and the bin sizes are arbitrary. Secondly, it breaks down when the number of measurements is small.

A more suitable procedure is the *Kolmogorov test*, as presented by Conover (1980), for example. A pictorial assessment of the data behaviour can be made from comparison of the continuous theoretical cumulative distribution function (CDF) with the empirical cumulative distribution (ECD), these being defined by

$$\mathrm{CDF}(P) = \int_0^P f(P : P_0)\,dP \Big/ \int_0^\infty f(P : P_0)\,dP \tag{5.17}$$

and

$$\mathrm{ECD}(P) = \frac{\text{Number of observed values} < P}{\text{Total number of measurements}}\,. \tag{5.18}$$

The values of the modulus of any differences between the two functions at each sample point has a known distribution regardless of the underlying form of the probability curve; tables are available to determine the significance of any observed departure. Although the χ-square test is strictly valid only for large samples, the Kolmogorov test has the advantage of being exact for all samples no matter the size; evidently the significance of any result will increase with the size of the sample. The test has wide application and, for example, it might be used to test if data follow a normal distribution with some given variance. The example presented in Figure 5.9 demonstrates its application to the catalogue of Piirola (1977) to check whether his listed values are representative of the stars being unpolarized.

In Figure 5.9a, the smooth curve presents the CDF of the Rice distribution for p_0 equal to zero, using normalized polarization values, as in (5.8). It can be seen that the ECD departs to the larger values of P indicating a broadening of its distribution. According to the tables provided by Conover (1980), the departure is statistically significant at the 99% confidence level. This does not automatically mean that the measurements do not correspond to those expected from unpolarized stars. It will be appreciated that depicted CDF does not take account of the fact that the normalizing values of σ used for each star are not exact, but are themselves estimates. In a study by Clarke, Naghizadeh-Khouei, Simmons, *et al.* (1993), on the assessment of several *zero-polarization catalogues*, they demonstrate the effect of how experimental estimates for σ alters the behaviour of the CDF for P.

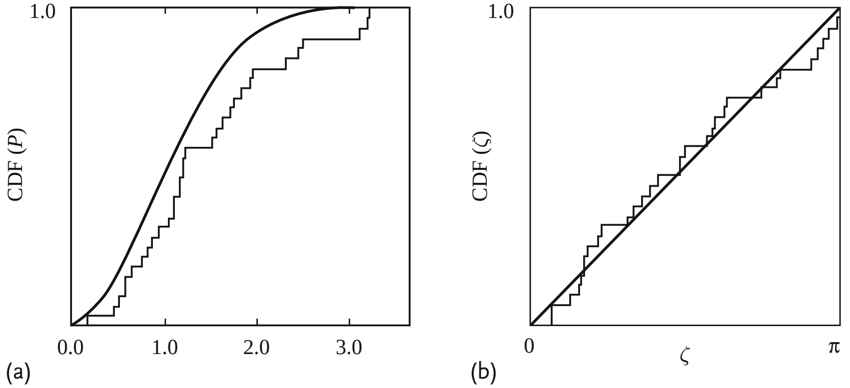

Fig. 5.9 In (a) the CDF(P) curve for the Rice distribution describing the expected measurement behaviour of unpolarized stars is used for comparison with the catalogue of Piirola (1977). (b) refers to the CDF, ECD behaviours of the the position angle, ζ.

In Figure 5.9b, the CDF for the expected behaviour of ζ is shown as a diagonal line, corresponding to a uniform distribution running from 0 to π. Piirola's data used to generate the ECD reveal no significant departures from the CDF.

5.7.4
Polarimetric Period Searches

If it is thought that a polarimetric data set contains a periodic element, this can be searched for by any of the standard techniques normally used in stellar photometry considering each NSP in turn. A simple approach might be one of Fourier analysis, say by the Deeming (1975) algorithm.

An extension of the Lafler–Kinman statistic to explore for periodicities in q and u simultaneously has been promoted by Clarke (2002). In this method, the data points are re-ordered according to their phase with respect to a selected period, and the vector length, or 'string length', joining the points in sequence in the qu-plane is then determined. By applying a grid of periods, any detected period shows as a minimum in the periodogram of string lengths and confidence intervals can be applied as to its significance.

For some Be stars, the intrinsic polarization is found to vary on long time scales along a preferred direction, suggesting the presence of an MPA as outlined above. If an axial frame is rotated so that the revised q parameter axis coincides with the MPA, it may be noted that, on shorter time scales, the revised u values may fluctuate about the q-axis. Whether there is periodicity in this behaviour can be explored simply by comparing the predicted signs of u with the recorded values, according to a selected period with a given phase. The outlines of the technique are given by Clarke & McGale (1987) and an example of its application is that by Clarke (1990) in respect of the star, γ Cas.

If it is suspected that the variability is caused by scattering from material between two stars of a binary system, the canonical model of Brown, McLean & Emslie (1978) suggests that the behaviour of normalized Stokes parameters should comprise a constant term plus variations described by the fundamental and first harmonic of the orbital period (see Chapter 11). Determination of the amplitudes and phases of these components leads to an evaluation of the inclination, i, of the binary system, the orientation, Ω, of the system projected on the sky and the phase, ϵ, of the executed orbit. In order to match the data with the canonical binary model, Kemp's group (Kemp, Southwick & Rudy, 1976, Kemp, Barbour, Herman, *et al.*, 1978) used an autocorrelation technique to determine the polarization power periodogram. Significant periods were then fitted by least squares to allow determination of the Fourier coefficients which were then translated into geometric parameters describing the stellar system (see Kemp & Barbour, 1983). A similar scheme was used by Clarke & McGale (1988) in connection with measurements of σ Ori E, with the F-statistic being applied to the outcome, so obtaining the significance of the suggested period.

References

Bastien, P., Drissen, L., Menard, F., Moffat, A.F.J., Robert, C., St Louis, N. (1988) The variability of polarized standard stars. *AJ*, **95**, 900–910. [90]

Brooks, A., Clarke, D., McGale, P.A. (1994) Investigating stellar variability by normality tests. *Vistas Astron.*, **38**, 377–399. [90]

Brown, M.B., Forsythe, A.B. (1974) The small sample behaviour of some statistics which test equality of several means. *Technometrics*, **16**, 129–132. [95]

Brown, J.C., McLean, I.S., Emslie, A.G. (1978) Polarisation by Thomson scattering in optically thin stellar envelopes. II – Binary and multiple star envelopes and the determination of binary inclinations. *A&A*, **68**, 415–427. [98]

Clarke, D. (1990) Temporal polarization variations of Be stars – V. Comments on the similar behaviour of γ Cassiopeiae and κ Draconis. *A&A*, **227**, 151–155. [97]

Clarke, D. (2002) String/Rope length methods using the Lafler–Kinman statistic. *A&A*, **386**, 763–774. [97]

Clarke, D., Brooks, A. (1985) Narrow-band polarization measurements of late-type stars. *MNRAS*, **212**, 211–218. [95]

Clarke, D., McGale, P.A. (1987) Temporal polarization variations of Be stars – II. Model fitting of polarimetric data. *A&A*, **178**, 294–300. [90, 97]

Clarke, D., McGale, P.A. (1988) Temporal polarization variations of Be stars - IV. The polarimetric behaviour of σ Orionis E. *A&A*, **205**, 207–214. [98]

Clarke, D., Naghizadeh-Khouei, J. (1994) A reassessment of polarization standard stars. *AJ*, **108**, 687–693. [90]

Clarke, D., Naghizadeh-Khouei, J., Simmons, J.F.L., Stewart, B.G. (1993) A statistical assessment of zero-polarization catalogues. *A&A*, **269**, 617–626. [96]

Clarke, D., Schwarz, H.E., Stewart, B.G. (1985) Polarimetric measurements of late-type stars at Hβ and CaII K. *A&A*, **145**, 232–240. [95]

Clarke, D., Stewart, B.G., Schwarz, H.E., Brooks, A. (1983) The statistical behaviour of normalised Stokes parameters. *A&A*, **126**, 260–264. [80, 80, 81, 81]

Clarke, D., Stewart, B.G. (1986) Statistical methods of stellar polarimetry. *Vistas Astron.*, **29**, 27–51. [86]

Conover, W.J. (1980) Chapter 6 in *Practical Non-Parametric Statistics*. 2nd Ed. Wiley, New York. [96, 96]

Deeming, T.J. (1975) Fourier Analysis with unequally-spaced data. *Astrophys. Space Sci.*, **36**, 137–158. [97]

Kemp, J.C., Barbour, M.S., Herman, L.C., Rudy, R.J. (1978) Discovery of synchronous binary polarization in Cygnus X-1. *ApJ*, **220**, L123-L126. [98]

Kemp, J.C., Barbour, M.S. (1983) X Persei – Optical polarization variation on the 580 day binary-like period. *ApJ*, **264**, 237–250. [98]

Kemp, J.C., Southwick, R.G., Rudy, R.J. (1976) The variable linear polarization of Cygnus X-1, 1974–1975 observations. *ApJ*, **210**, 239–249. [98]

Kohr, R.L., Games, P.A. (1974) Robustness of the analysis of variance, the Welch procedure, and a box procedure to heterogeneous variances. *Journal of Experimental Education*, **43**, 61–69. [95]

Maronna, R., Feinstein, C., Clocchiatti, A. (1993) Optimal estimation of Stokes' parameters. *A&A*, **260**, 525–532. [81]

McLean, I.S., Clarke, D. (1979) Separation of the intrinsic and interstellar linear polarization components of Southern Hemisphere early-type emission-line stars. *MNRAS*, **186**, 245–263. [89, 92]

Naghizadeh-Khouei, J., Clarke, D. (1993) On the statistical behaviour of the position angle of linear polarization. *A&A*, **274**, 968–974. [87, 87, 88]

Pfau, W., Piirola, V., Reiman, H.-G. (1987) Interstellar extinction and polarimetric properties of the star HD 200775. *A&A*, **179**, 134–140. [92]

Piirola, V. (1977) Polarization observations of 77 Stars within 25 pc from the Sun. *A&AS*, **30**, 213–216. [96, 97]

Poeckert, R., Marlborough, J.M. (1976) Intrinsic linear polarization of Be stars as a function of $V \sin i$. *ApJ*, **206**, 182–195. [85]

Quirrenbach, A., Bjorkman, K.S., Bjorkman, J.E., Hummel, C.A., Buscher, D.F., Armstrong, J.T., Mozurkewich, D., Elias Ii, N.M., Babler, B.L. (1997) Constraints on the geometry of circumstellar envelopes: optical interferometric and spectropolarimetric observations of seven Be stars. *ApJ*, **479**, 477–496. [93]

Rice, S.O. (1944) Mathematical analysis of random noise. Part III. Statistical properties of random noise currents. *Bell Systems Tech. J.*, **24**, 46–108. [83]

Serkowski, K. (1958) Statistical analysis of the polarization and reddening of the double cluster in Perseus. *Acta Astron.*, **8**, 135–170. See Appendix 1, pp. 163–164. [83, 84, 86]

Serkowski, K. (1962) Polarization of Starlight. pp. 289–352 in *Advances in Astronomy and Astrophysics*, **1**. Ed. Z. Kopal, Academic Press, NY & London. [84, 84, 85, 85, 86]

Serkowski, K., Mathewson, D.S., Ford, V.L. (1975) Wavelength dependence of interstellar polarization and ratio of total to selective extinction. *ApJ*, **196**, 261–290. [92]

Snedecor, G.W., Cochran, W.G. 1980 *Statistical Methods* (7th Edition), Iowa State University Press, Oxford, UK. [91, 95]

Simmons, J.F.L., Stewart, B.G. (1985) Point and interval estimation of the true unbiased degree of linear polarization in the presence of low signal-to-noise ratios. *A&A*, **142**, 100–106. [83, 84, 85, 85, 85, 85]

Stewart, B.G. (1985) The correlation between normalised Stokes parameters in a sinusoidally modulated intensity polarimeter. *A&A*, **143**, 235–240. [83]

Stewart, B.G. (1991) Polynomial fits for polarization estimation. *A&A*, **246**, 280–282. [86]

Timm, N.H. (1975) *Multivariate Analysis with Application in Education and Psychology*, Brooks-Cole, Monterey, CA. [95]

Vaillancourt, J.E. (2006) Placing confidence limits on polarization measurements. *PASP*, **118**, 1340–1343. [86]

Vinokur, M. (1965) Optimisation dans la recherche d'une sinusoïde. *Ann. d'Astr.*, **28**, 412–445. [83, 88]

Wardle, J.F.C., Kronberg, P.P. (1974) The linear polarization of quasi-stellar radio sources at 3.71 and 11.1 centimeters. *ApJ*, **194**, 249–255. [85, 85, 85, 87]

Welch, J.B. (1951) On the comparison of several mean values: An alternative approach. *Biometrica*, **38**, 330–336. [95]

6
The Basics of Polarimetric Elements

6.1
Introduction

The optical elements used in instruments for the measurement of the state of polarization are normally *polarizers* and *retarders*, although other elements, such as polarization rotating or depolarizing devices, may sometimes be employed. Most elements operate by a controlled application of birefringence, a property of some materials having alternative refractive indices according to the orientation of the electric vector of the incoming radiation. Most of the devices used in astronomical polarimetry have been described by Serkowski (1974).

Many of the elements within a polarimeter are constructed from natural or man-made birefringent crystals. When a beam of light enters such a crystal, it splits into two and, on rotation of the crystal, the behaviour of one beam (the ordinary ray or o-ray) is unaffected while the other (extraordinary ray or e-ray) alters its direction of travel. Common materials are calcite, quartz and magnesium fluoride (MgF_2). Some older systems employed wave plates made of mica, which are now used infrequently. When different devices are compared for usefulness, several criteria have to be considered before the best choice can be made. These may include: the efficiency of fulfilling the desired purpose, the transmittance, the angular acceptance, the wavelength range of use, the purity in terms of producing detrimental internal scattering within the instrument, ghost images by reflections within the optical interfaces, and interference effects.

Reflections from materials are also sensitive to polarization and this property is sometimes employed to provide polarimetric elements. In other circumstances, reflections can be deleterious to a polarimetric exercise. All current stellar measurements are performed using reflector telescopes with metallic coated mirrors, usually vacuum deposited aluminium. As a result of imperfections in the coatings, polarizing patches may occur over the mirror surfaces. Also the fact that the mirror surfaces are curved implies that the various beam reflections are not exactly normal to their directions of travel; the state of polarization of the collected light must therefore be altered to some degree by the time it arrives at the telescope focus.

Stellar Polarimetry. David Clarke

ISBN: 978-3-527-40895-5

In order to be able to describe the various devices used in stellar polarimetry, and to discuss other important effects, recall of some optical principles will be made where necessary. For reference, the behaviour of reflection and refraction at optical surfaces, in particular, a fuller description of the Fresnel laws, can be found in Appendix A. The discourse there is particularly important for checking out the behaviour of the reflection and transmission coefficients and on handedness changes that may occur within optical elements.

6.2
Polarizers

A perfect polarizer is a device which the emergent beam is linearly polarized, regardless of the state of polarization of the incident beam. It may operate either in transmission or by reflection. The direction of vibration of the emergent linearly polarized light is a property of the polarizer and it relates to the polarizer's *principal axis*. Since most elements operate in transmission, another frequently met term describing a polarizer is its *transmission axis*.

For a single-beam polarizer, any component of the incident beam whose direction of vibration is at right angles to the polarizer's axis is rejected. A perfect polarizer, as defined above, is not realizable in practice, as the rejection of the component orthogonal to the polarizer's axis is never complete. Thus, if unpolarized light is incident on an actual polarizer, the emergent light will only be partially linearly polarized. The degree of polarization of this light is a measure of the efficiency of the polarizer and is known as its *polarizance*, p_K (see (4.41)). All devices with polarizances less than unity (i. e. all real polarizers) should strictly be referred to as 'partial polarizers'. Clearly, knowledge of the polarizance is all that is necessary to assess the effect of the device on any type of polarized light, say by the application of the Mueller algebra.

Many polarizers rely on birefringence and sometimes two refracted beams emerge. These are orthogonally linearly polarized, and their directions of vibration are referred to as the *polarizer's axes*. Such a double-beam device may be thought of as two independent perfect polarizers simultaneously present in the same device with their axes at right angles, and each operating as if the other were not there. A polarizance and transmittance can be defined for each of the outcoming beams; the beams may behave differently in these regards.

Several independent principles have been used in the construction of polarizers, and their polarizances are usually almost independent of wavelength throughout the visible spectrum. The list of polarizers discussed below does not pretend to be comprehensive, but most of the principles which have been employed are mentioned. Throughout the discussion, it will be assumed that the polarizers, though partial, are 'pure', i. e. they do not introduce any differential retardation between the components which they pass.

6.2.1
Dichroic Polarizers

In the early 19th century, dichroism was discovered, an effect later found to have important associations with respect to polarization. Wollaston (1804) reported that light transmitted by potassium chloropalladite (K_2PdCl_4) appeared red or green according to the direction of travel of the light in relation to the crystal axes. The phenomenon became known as *dichroism*; some crystals are found to show several colours and these are said to exhibit *pleochroism*.

If white light is passed through a dichroic crystal, and then through a suitably oriented doubly refracting crystal, the two emerging beams have different colours. Babinet (1837, 1838) realized that the phenomenon was a result of different functional dependencies of absorption on wavelength for the two directions of vibration which subsequently became the ordinary (o-) and extraordinary (e-) rays in a doubly refracting crystal. Nowadays, substances are known for which the absorption coefficient for one direction of vibration is essentially 100% over the whole visible spectrum, whilst for the orthogonal direction it is non-zero and reasonably constant. If white light is viewed through such a substance and then through a doubly refracting crystal, the 'colours' are 'black' and 'white', i. e. the beams have zero and non-zero, wavelength-independent intensities. The phenomenon is still referred to as dichroism, and it is used in the manufacturing of sheet polarizers, the material used being described as the *dichromophore*.

One crystal that exhibits dichroism is tourmaline and this material was used to make polarizers for some time in the 19th century. Instead of using a single crystal, the principle of dichroism was incorporated into the industrial production of large format polarizers. Various forms have been developed by the Polaroid Corporation in the USA and the sheet product is commonly known as 'Polaroid'. The material involves the use of tiny dichroic particles which are embedded and aligned in a plastic sheet or similar material. The main classes of *Polaroid* are the H-type, iodine fixed in stretched polyvinyl alcohol, and the K-type, produced by heating sheets of polyvinyl alcohol in the presence of the catalyst to produce polyvinylene which acts as the dichromophore. The type of *Polaroid* may be further labelled by N, denoting that it has a neutral colour. The fact that the success of *Polaroid* depends on the principle of dichroism is readily demonstrated. A polarizing filter in itself is usually clear and greenish for the direction of vibration parallel to its principal axis. For the orthogonal axis, the transmittance has a very dark, deep blue hue, appearing when one filter is crossed with another. *Polaroid* has a very large acceptance angle and so can be used in convergent light. Typical values for the orthogonal transmittances to fully polarized light in the mid-visual part of the spectrum for HN-22 *Polaroid* are $\mathcal{T}_{\parallel} = 0.50$, $\mathcal{T}_{\perp} = 2 \times 10^{-6}$.

Polaroid devices were used in many of the early photoelectric polarimeters but were later superseded by polarizing prisms offering better transmittance, a higher degree of polarizance and broader wavelength coverage. They are sometimes still used when a large acceptance area is required or are incorporated into devices for the calibration of the reference axis of a polarimeter.

6.2.2
Birefringent Polarizers

Two forms of birefringent polarizer are in common use in astronomical polarimeters. The first achieves beam separation simply by differences in the amount of refraction for the orthogonal vibrations; the second involves total internal reflection (TIR) of one of the components at an interface involving birefringent materials.

The simplest forms of refracting polarizers are the Rochon and Wollaston prisms, each being made of two components cemented together. Typical materials are quartz or calcite. The schematics of an all-calcite Rochon prism are illustrated in Figure 6.1. The first prism has its optic axis parallel to the direction of propagation, and the second prism has its optic axis perpendicular to this. As a result, the o-ray is transmitted without deviation while the e-ray is first deviated by the calcite–calcite interface and then further refracted by the calcite–air exit face. The total deviation is only of the order of 1° or 2°, the exact value depending on the angle of the prism and the refractive index of the material. As a consequence of the latter parameter, the deviated beam is subject to a small amount of spectral dispersion. If quartz is used instead of calcite, the e-ray is deviated towards the base of the second prism instead of the apex.

A less frequently used polarizer, with a performance very similar to that of the Rochon, is the Senarmont prism (Figure 6.2). It again comprises two prisms; the first has its optic axis in the direction of propagation, while the second has its optic axis perpendicular to this direction and to its base.

A larger deviation of the emergent beams can be produced by using a Wollaston prism (Figure 6.3). For this compound prism, the optic axes of both the sections are perpendicular to each other, and to the direction of propagation. At the internal interface, the resolved components are refracted in opposite directions, and they are further refracted at the exit faces. The angular separation of the components depends again on the angle of the prisms and on the wavelength. The deviations of the two emerging beams exhibit small amounts of dispersion but by differing de-

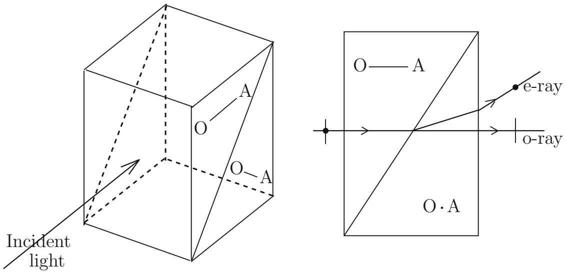

Fig. 6.1 A Rochon prism comprising two calcite elements: the separation of the emergent o- and e-rays is greatly exaggerated. The directions of the optic axes are shown as O—A, or as O · A when it is perpendicular to the page. The directions of vibration are depicted as ⟶–|– and ⟶–•– being, respectively, in the plane of the page or perpendicular to it.

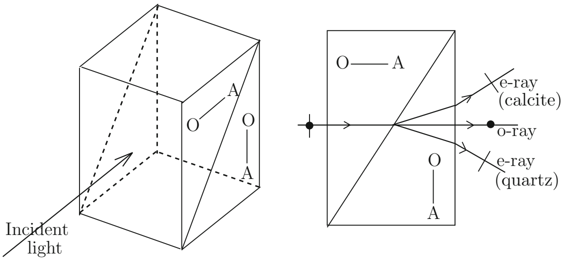

Fig. 6.2 A Senarmont prism. The directions of the emergent rays depend on whether the crystal materials have positive (quartz) or negative (calcite) birefringence. The key to the symbols is given in the caption of Figure 6.1. The separations of the various beams are greatly exaggerated in the drawing.

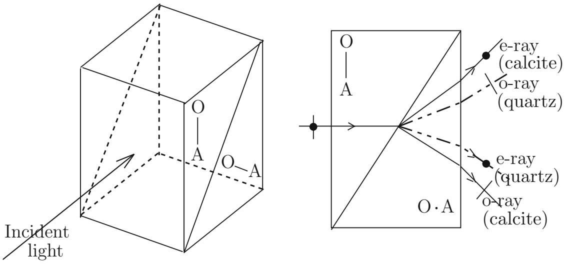

Fig. 6.3 A Wollaston prism. The directions of the emergent rays depend on whether the crystal materials have positive (quartz) or negative (calcite) birefringence. The key to the symbols is given in the caption of Figure 6.1. Again, the separations of the various beams are greatly exaggerated in the drawing.

gree. Three-element Wollaston prisms are also available with better image quality than a standard two-element system for a given beam divergence.

By applying the Fresnel equations to the various interfaces of either the Rochon or Wollaston prism, it is immediately apparent that the transmission coefficients for the orthogonally resolved beams are not the same. This means that if an unpolarized beam is passed through the device, the intensities of the polarized emergent beams will differ. Such a difference can be a disadvantage in some instances.

The small angular separation between the o-rays and e-rays produced by the above devices can be a serious drawback if the intensities of both beams are to be measured using separate detectors. This is sometimes remedied by the insertion of a triangular prism with its apex set between the two beams so that the rays reflected by its outer surfaces emerge $\sim 180°$ with respect to each other.

Considerably larger angular separations can be produced within two-beam polarizers, however, by allying the phenomenon of total internal reflection to that of birefringence. Historically, this was done to facilitate the interposition of an absorbing surface, as it was usual to use only one of the two resolved beams. There are many advantages in utilizing both components, and this is best achieved by using

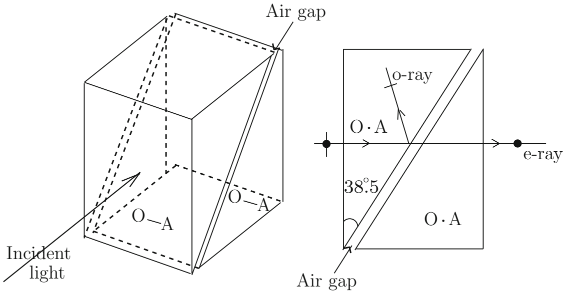

Fig. 6.4 A Glan–Foucault prism comprising two calcite elements with an air gap.

polarizing prisms which offer a large angular separation between the emerging beams.

One of the first polarizers to ally TIR to birefringence was invented by Nicol (1829) in 1828. It used the birefringence of calcite and rejected one of the resulting components of the incoming beam by TIR and absorption. The Nicol prism has been described in many earlier textbooks on optics and, as it has been superseded by other and much better polarizers, it will not be discussed here. Its main defects are that its entrance and exit faces are inclined to the optical path of the beam, and that the transmitted component is displaced laterally and is slightly elliptically polarized. The acceptance angle of the Nicol is of the order of 25°.

A commonly used polarizing prism is the Glan–Foucault type (see Figure 6.4) in which the light enters and leaves normally to the entrance and exit faces, these being parallel to each other. Here, the optic axes of the two calcite prisms are parallel to the entrance and exit faces, and TIR is achieved by using an air gap instead of cement. This allows the prism to be used in the ultraviolet, but restricts the acceptance angle to about 7°. The angle of the prism is approximately 38.°5; the transmitted component is again the e-ray. This type of prism has the disadvantage that the transmitted intensity of the utilized component is low (~ 0.5) because of the multiple reflection losses at the calcite–air–calcite interfaces. It has been shown by Archard & Taylor (1948) that the prism can have improved transmittance of approximately 0.90 by having the optic axis of the components parallel to the entrance face, i. e. at right angles to the original Glan–Foucault design. Their design is quite economical in the use of calcite when cut from the original crystal rhomb. If ultraviolet transmission is not important, the angular acceptance of the Glan–Foucault polarizer can be improved ($\sim 40°$) by using a cement layer instead of an air gap. This is done, however, at the expense of increasing the length-to-width ratio and involves wasteful cutting of calcite crystals.

Many of the old designs of prism can be adapted so that both of the resolved components can be utilized. Other prisms relying on birefringence and TIR have also been constructed specifically with this in mind. Figure 6.5 illustrates such a design. This compound prism is made up of two pieces of calcite, cemented with a non-birefringent material whose refractive index is as close as possible to the ordinary refractive index of calcite. The component prisms are cut so that their

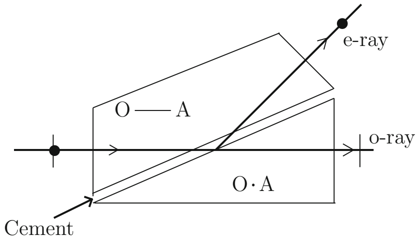

Fig. 6.5 A double-beam polarizer giving a separation of 45° between resolved beams. The composite prisms are made of calcite and glued with a cement matching the n_o refractive index of the crystal material. The marked emergent e-ray is from the lower prism; it travels as an o-ray in the upper prism.

optic axes are in the same directions as for the Rochon prism (see Figure 6.1), but the angle of incidence at the interface between the cement and the second prism is sufficiently large for the e-ray to suffer TIR, while the o-ray passes through undeviated. With this design, it is easily possible to achieve an angular separation of $\sim 45°$ between the o- and e-rays. It is also easy, as can be seen from the diagram, to arrange for these rays to pass normally through their respective exit faces.

In order to reduce the amount of calcite used, the first prism may be replaced by the one made from a glass having refractive index which matches that of the o-ray for calcite. Another device, based on a modification of the Foster (1938) prism, and used by Clarke (1965), involved two prisms made of such glass separated by, but cemented to, a sliver of calcite. Although successful, this design is subject to effects of multiple reflections at the interface within the prism.

The polarization properties associated with the reflection at a dielectric interface can be enhanced by applying thin film coatings. Successful double-beam polarizers are commercially available based on reflection and transmission at the hypotenuse surface of a 45° prism. Two such prisms can be combined to form a polarizing cube with the thin film trapped between the hypotenuse faces, which are cemented together. One beam is transmitted without deviation while the orthogonal beam emerges at right angles.

Another device that is sometimes used to separate the orthogonally resolved components of a light beam is the Savart plate (Figure 6.6). It comprises two birefringent beam splitting plates with their optic axes orthogonal to each other. An incident beam propagating through the first plate is resolved into ordinary and extraordinary beams, which are displaced from each other in the first principal plane. Upon entering the second plate, the ordinary beam becomes the extraordinary beam, while the extraordinary beam becomes the ordinary beam. Further splitting takes place in the second principal plane which is orthogonal to the first. The effect of the combination is to provide two emerging beams displaced along a diagonal relative to the edges of the square entrance face. The overall displacement is $\sqrt{2}$ times that of each plate. One of the attractions of the device is the fact that the optical path difference between the two emergent beams is zero for normal incidence.

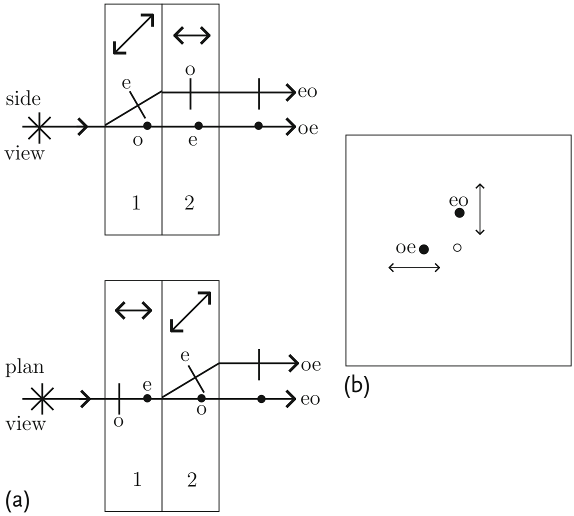

Fig. 6.6 The Savart plate comprises two plates (a) made of identical material cut with their optic axes as shown. The emergent orthogonally polarized beams are both displaced relative to the incoming rays (b). The behaviour of the rays passing through the system is described in the text.

When a Savart plate is placed between parallel or crossed polarizers, a collimated input beam produces a set of parallel fringes. Based on this, the device was used as a component within astronomical visual polarimeters, the eye being quite sensitive in detecting whether fringes are present or not. A basic instrument incorporates a Savart plate followed by a polarizer, the input light producing fringes if it carries polarization. The contrast of the fringes is indicative of the degree of polarization. In these old instruments, a null principle was used whereby the fringes were made to disappear by the inclusion of a tiltable calibration plate. The modern usage of Savart plates involves the comparison of simultaneously recorded images for the two resolved components as imaged on a two-dimensional detector such as a CCD. They are also used to produce two images with resolved polarizations for placement along the slit length of a spectrometer. At 500 nm, the beam displacement produced by Savart plate is 0.075 times the total thickness of both plates for calcite, and 0.0042 times the total thickness for quartz.

A specially constructed wedged double Wollaston prism has been designed by Oliva (1997). By placing this device at an image of the telescope aperture (pupil image), four beams emerge such that both q and u can be determined simultaneously from a single CCD frame.

6.2.3
Reflection Polarizers

When light is incident on any dielectric material the intensity of the reflected and transmitted beams are sensitive to polarization. If a dielectric plate is set at Brewster's angle relative to some incident light, the degree of polarization of the reflected beam should be unity (see Appendix A). Thus, it can act as a perfect polarizer. It is, however, usually inconvenient to use such a reflecting plate as a polarizer because of the angle at which the polarized light beam emerges; the emergent beam also describes a cone as the polarizer is rotated. The transmitted light is partially polarized, and by using a succession of plates set at Brewster's angle, the transmitted light becomes progressively more polarized. This type of device is referred to as a *pile-of-plates* polarizer and, although it is not often used in the optical region, the principle still finds application in the infrared. In optical texts, there is some confusion on the formulas promoted to describe the polarizance of the device and care should be taken in predicting the behaviour of any pile-of-plates system. The problem has been addressed by Tuckerman (1947).

By simply extending the number of involved plates to N, each of refractive index n and set at Brewster's angle, the polarizance, p_K, of the device is

$$p_K = \frac{1 - \left(\dfrac{2n}{n^2+1}\right)^{4N}}{1 + \left(\dfrac{2n}{n^2+1}\right)^{4N}} \,. \tag{6.1}$$

This equation relates to a system with all the reflected components absorbed before they meet another plate of the system. Although reference to the formula describing the polarizance may be found in earlier papers, the standard derivation is generally ascribed to De la Provostage & Desains (1850). In this more realistic treatment, the rays which have been reflected an even number of times are also included in the calculation of the polarizance of the emergent beam, and this may be expressed by

$$p_K = \frac{N}{N + \left(\dfrac{2n}{n^2-1}\right)^2} \,. \tag{6.2}$$

It can easily be seen that the polarizance is higher for the first condition (6.1) than for the second (6.2). For a device used in the polarimetric calibrations of measurements of the Zodiacal Light, Weinberg (1964) has drawn attention to the distinct differences of the behaviour of a pile-of-plates polarizer depending on whether multiple beam reflections are taken into account or not. The more efficient design is hard to achieve in practice without the device becoming long in comparison with its aperture. Conn & Eaton (1954) have pointed out that in some systems, only a small number of the multiple reflected rays pass through, and p_K may be larger than that given by (6.2).

The value of p_K for the pile-of-plates polarizer is also affected by absorption in the materials. This problem was investigated by Stokes (1862) and again by Tuckerman (1947). Interference effects are also likely to be present according to the optical quality of the plates but references as to how this affects the polarizance behaviour are elusive.

Drawbacks of the pile-of-plates polarizer are that the reflected components are lost, the emerging beam does not lie on the same axis as the entering beam, and surface films on the plates alter the polarizing characteristics from those predicted by the Fresnel equations as applied to simple plates. Growth of surface films with time consequently changes the polarizance and transmittance of the system.

6.3
Retarders

The purpose of a retarder is to alter the phase relation between orthogonally resolved components of a beam of light. Such a change is generally necessary when light is being analysed to determine its complete state of polarization. Devices that are able to produce a phase change are known as *retarders*. If the effect of the device is simply that of retardation, then it is known as a *pure retarder*. However, in some cases, the very mechanism which is utilized to bring about differential retardation also introduces a small polarizance which can affect the quest of high accuracy polarimetry. These devices might be classed as *impure retarders*.

Although retarders of any desired phase delay can be constructed, the most common types introduce phase delays of either $\pi/2$ or π, and are called *quarter-wave* and *half-wave retarders*, respectively. The differential retardation is produced between components resolved along two particular orthogonal directions fixed in the device. The directions with respect to which retardation is produced are referred to as the *fast* and *slow* axes, and the amount of retardation produced with respect to the axes is known as the *retardance*.

Quarter-wave retarders are often used to produce circularly polarized light from linearly polarized light and vice versa. Half-wave retarders are often used to produce linearly polarized light from already linearly polarized light, but with a different direction of vibration, i. e. the direction of vibration is rotated. The components of the incident linearly polarized light, along and perpendicular to the reference axis of the half-wave retarder, emerge with one of them changed in phase by π with respect to the other. They, therefore, recombine to give linear polarization again, but with the direction of vibration being inclined to that of the incident beam by twice the angle which the latter makes with reference axis of the retarder. This is readily confirmed by multiplying out the appropriate Mueller matrices representing the situation.

Relative phase changes can be brought about by passing a beam through a birefringent material, or by making it suffer a reflection which produces phase change effects. Retarders have been designed depending on both these principles, and it is convenient to discuss them accordingly. This is done in the following subsections.

6.3.1
Birefringent Retarders

Retarders using the phenomenon of birefringence are commonly known as *phase plates* or *wave plates*. They consist of a plane-parallel plate of birefringent material whose optic axis is parallel to the faces of the plate. For a plane wavefront incident normally, the resolved components progress at different velocities according to the refractive indices associated with the birefringence. A differential phase delay is introduced between the emergent e- and o-wavefronts without any refraction.

Retardation devices in the form of wave plates alter the polarization state of light transmitted through them. The affect of a plate is described in terms of principal axes, fast and slow, in the plane of its entrance aperture. Generally wave plates are manufactured from uniaxial birefringent crystals cut so that the principal axes offer the ordinary, n_o, and the extraordinary, n_e, refractive indices associated with the material. Common materials are cleaved mica or crystalline quartz. The ascribed phase delay relates the difference in optical path length for the transmitted electric components resolved parallel to these axes. Any required phase delay, Δ, is achieved by cutting and polishing the plate to a thickness, *d*, according to the operating wavelength, and the values of the refractive indices, n_o, n_e, at that wavelength. The nominal phase value of a wave plate, as provided in standard optical texts, is given by

$$\Delta = \frac{2\pi d}{\lambda}(n_e - n_o) . \tag{6.3}$$

In most polarimetric instruments, any included wave plate is likely to have a retardation of either $\pi/2 \equiv \lambda/4$, or $\pi \equiv \lambda/2$ based on this equation, although other phase values are sometimes encountered. Wave plates based on (6.3) are said to be of zero order. Thicker, and mechanically more robust retarders, may be considered to act as quarter-wave or half-wave plates by increasing the basic thickness by factors of 3, 5, 7, etc. Such multi-order plates, however, are more susceptible to wavelength-dependent efficiency problems.

Like most materials, the refractive indices of wave-plate materials display significant dispersion. However, dispersion of the birefringence, i. e. the difference between the refractive indices, is usually quite small. For a given wave plate, therefore, it is obvious from (6.3) that the phase delay is close to being inversely proportional to wavelength. A phase plate designed to be a quarter-wave at 800 nm will be close to providing a half-wave retardation at 400 nm. Any simple wave plate will only be operable over a limited range of the spectrum, this being set according to the purpose of the device and the required accuracy of the subsequent measurements. Much in the same way that achromatic lenses are achievable by the combination of two or more lenses made of different materials, achromatic wave plates are also readily available.

By constructing a compound wave plate from two different birefringent materials, it is possible to produce a desired phase delay at two wavelength values, and with a smaller spectral variation of the delay than for a plate made from a single material. Such a combination is referred to as being achromatic, and $\lambda/4$ and $\lambda/2$ achromatic devices are frequently employed. The most common materials used are the positive uniaxial crystals of quartz and magnesium fluoride (MgF_2), with their fast axes crossed. One approach to the achromatic design is to choose the thicknesses of the components so that each acts as a multi-order plate at a particular wavelength with their difference corresponding to the zero order of the required phase delay. Such a strategy is described by Hodgkinson & Wu (1997). An alternative approach is based simply on the choice of the two wavelength values for which exact achromatism is desired, with thicknesses of the materials manufactured to achieve this. The solution to this design problem is given in Clarke (1967) and for a $\lambda/2$ plate, the required thicknesses, d_1, d_2, may be calculated from

$$d_1 = \frac{\lambda_b \Delta n_{2a} - \lambda_a \Delta n_{2b}}{2(\Delta n_{1b}\Delta n_{2a} - \Delta n_{1a}\Delta n_{2b})}\,, \qquad d_2 = \frac{\lambda_a \Delta n_{1b} - \lambda_b \Delta n_{1a}}{2(\Delta n_{1b}\Delta n_{2a} - \Delta n_{1a}\Delta n_{2b})}\,, \tag{6.4}$$

where λ_a, λ_b are the chosen wavelengths for achromatism and $\Delta n_{1a}, \Delta n_{1b}, \Delta n_{2a}, \Delta n_{2b}$ are the birefringences of the two materials at the wavelengths denoted as a and b.

For the examples discussed here, the latter strategy has been followed with the achromatic wavelength values being arbitrarily selected at 425 and 575 nm. To achieve this design for an achromatic $\lambda/2$ plate, the required thicknesses of quartz and MgF_2 are 157.029 µm and 116.285 µm, respectively. The behaviour of such a plate is depicted in Figure 6.7. These thicknesses are simply halved to produce an achromatic $\lambda/4$ plate.

Other important design developments involve compound plates whose components have their axes set at angles which are neither 0° nor 90° with respect to each other. In the Pancharatnam (1955) configuration, three wave plates are used.

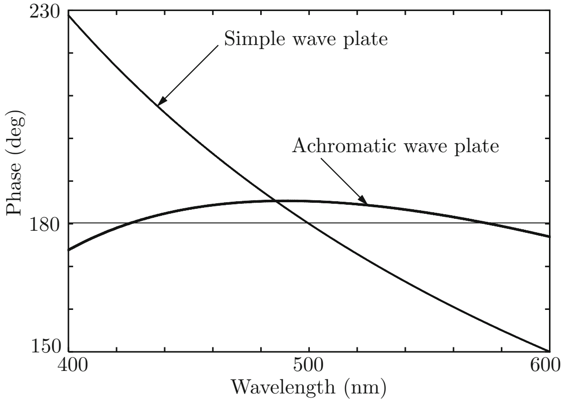

Fig. 6.7 The phase delay of a compound half-wave plate made of quartz and MgF_2, designed to be achromatic at 425 and 575 nm, is compared with a simple plate of quartz cut to be half-wave at 500 nm.

The outer plates are identical, with their axes set parallel to each other; the centre plate is of half-wave retardation, made of the identical material but with its axis set at some angle relative to the outer plates. The solution for an achromatic half-wave plate, for example, uses three half-wave plates, the middle element set with its fast axis at $\sim 57°$ to the outer plates. Although Pancharatnam designs have excellent properties in terms of the achromatization of the phase delay, they have a drawback in that the effective reference axis is not parallel to the fast axes of any of the individual plates, and this is exacerbated by the fact that it varies with wavelength, oscillating by a few degrees over the spectral range for which the achromatism of the phase delay is designed. In the measurement of the polarization of the light from stars, this axial dispersion results in changes in the orientation of the instrumental reference frame used for the determination of the Stokes parameters according to the operating wavelength passband; the measurements are later transformed to equatorial coordinates. In practice, the dispersion of the instrumental frame is calibrated from observations of standard stars, but the whole transformation process is susceptible to errors when very high accuracy polarimetry is pursued. By using a Pancharatnam design with elements which themselves are achromatic, a device that may be described as being superachromatic ensues.

In addition to its chief function of introducing a relative phase delay, a wave plate also acts as a weak partial polarizer and this may have repercussions in the pursuit of high accuracy polarimetry. Reflection losses at the entrance and exit faces depend on the refractive indices of the plate. As the device is made of birefringent material, the reflection losses, and hence the transmittances, $\mathcal{T}_{\mathrm{f}}, \mathcal{T}_{\mathrm{s}}$, for the fast and slow orthogonal axes defining the phase delay, have different values. A common design for a polarimetric modulator comprises a rotatable wave plate prior to a fixed polarizer. The small polarizance that the wave plate possesses introduces a spurious signal that may affect the determined Stokes parameters (see Clarke, 2005). The polarizance can be reduced, but not removed completely, by applying anti-reflection coatings to the wave plate surfaces. The true nature of a wave plate may be summarized by the Mueller matrix:

$$\begin{bmatrix} \mathcal{T}_{\mathrm{f}}+\mathcal{T}_{\mathrm{s}} & \mathcal{T}_{\mathrm{f}}-\mathcal{T}_{\mathrm{s}} & 0 & 0 \\ \mathcal{T}_{\mathrm{f}}-\mathcal{T}_{\mathrm{s}} & \mathcal{T}_{\mathrm{f}}+\mathcal{T}_{\mathrm{s}} & 0 & 0 \\ 0 & 0 & 2\sqrt{\mathcal{T}_{\mathrm{f}}\mathcal{T}_{\mathrm{s}}}\cos\varDelta & 2\sqrt{\mathcal{T}_{\mathrm{f}}\mathcal{T}_{\mathrm{s}}}\sin\varDelta \\ 0 & 0 & -2\sqrt{\mathcal{T}_{\mathrm{f}}\mathcal{T}_{\mathrm{s}}}\sin\varDelta & 2\sqrt{\mathcal{T}_{\mathrm{f}}\mathcal{T}_{\mathrm{s}}}\cos\varDelta \end{bmatrix}, \tag{6.5}$$

or

$$\begin{bmatrix} k_1 & k_2 & 0 & 0 \\ k_2 & k_1 & 0 & 0 \\ 0 & 0 & k_3\cos\varDelta & k_3\sin\varDelta \\ 0 & 0 & -k_3\sin\varDelta & k_3\cos\varDelta \end{bmatrix}, \tag{6.6}$$

where $k_1 = \mathcal{T}_{\mathrm{f}}+\mathcal{T}_{\mathrm{s}}$, $k_2 = \mathcal{T}_{\mathrm{f}}-\mathcal{T}_{\mathrm{s}}$ and $k_3 = 2\sqrt{\mathcal{T}_{\mathrm{f}}\mathcal{T}_{\mathrm{s}}}$. Account of the full properties of this matrix must be taken, with an inversion procedure applied for data reductions of high precision polarimetry involving the use of a rotating wave plate modulator.

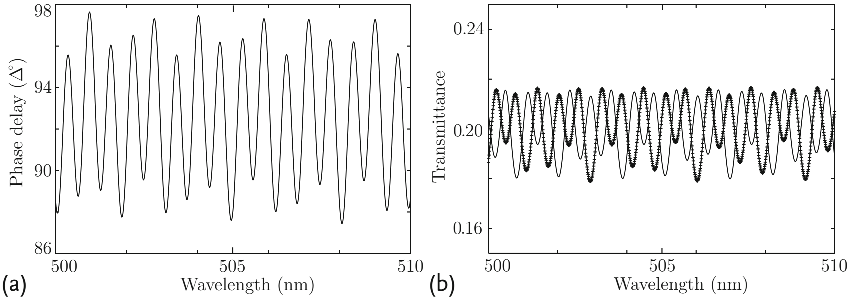

Fig. 6.8 (a) displays fringes associated with the phase delay over an interval of 10 nm of an achromatic quarter-wave plate made of quartz and MgF_2. Note that the mean level is greater than 90°, the plate designed to be exactly quarter-wave at 425 nm and 575 nm. It may be noted that the amplitude of the fringes is greater than the secular departure of the mean from being exactly 90°. The variations of the transmittances of the fast axis, $\mathcal{T}_f$, (heavy curve with marked points) and the slow axis, $\mathcal{T}_s$ (light curve) of the same achromatic plate are displayed in (b). Over the spectral interval of 10 nm, the fringes for the orthogonal axes are nearly in anti-phase, giving rise to polarizance fringes of large amplitude (after Clarke, 2005).

With the development of high-precision spectropolarimetry, a further problem has emerged with wave plate devices in that they may suffer from multiple beam interference within their entry and exit faces. The effect of this is to generate wavelength-dependent fringes for all the parameters k_1, k_2, k_3 and Δ. An example of the expected fringe behaviours of the transmittances and phase delay of an achromatic quarter-wave plate are displayed in Figure 6.8. The presence of fringes in the immediate data reductions for the determination of the Stokes parameters has been highlighted by Tinbergen (1994) and discussed by Harries & Howarth (1996) and Donati, Catala, Wade, *et al.* (1999). The more general problem associated with interference and polarization has been presented by Semel (2003). It may be noted that Donati, Catala, Wade, *et al.* (1999) used achromatic wave plates made by Halle of Berlin but later found that the ripple problem was very much reduced for those constructed by Optique Jean Fichou of Paris. In a spectropolarimeter designed by Matsuda, Ikeda, Akitaya, *et al.* (2005), a superachromatic half-wave plate manufactured by the Astropribor Company in Ukraine, and constructed of five polymethyl-methacrylate layers, was employed and the system appears to be little affected by fringes. The origin of the fringe problems within wave plates, with possible strategies to alleviate their influence in polarimetric practice, has been discussed by Clarke (2005) (see also Section 8.8).

Wave plates constructed from natural crystals may have entry and exit faces which are not perfectly parallel. Accordingly, on rotation, this can induce intolerable image wobble on the detector, or on the entrance slit of a spectrometer. It is sometimes possible to redress the problem by reworking the faces to remove any wedge to an acceptable tolerance as was done by Schwarz & Guisard (1995).

In some experimental arrangements, it is useful to employ a wave plate whose phase delay can be controlled. For example, in telescope systems that employ a

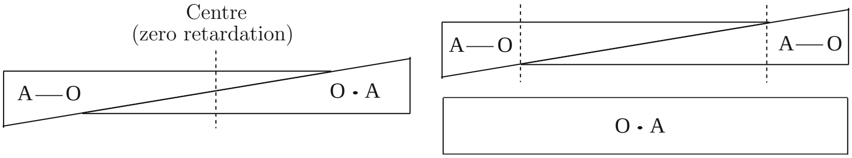

(a) (b)

Fig. 6.9 (a) shows the principle of the Babinet compensator involving two birefringent wedges with the optical axes set orthogonally. (b) is for the Soleil–Babinet compensator with two birefringent wedges set with their axes aligned but with their overall multi-order phase delay reduced by a rectangular prism of the same material with its optic axis set orthogonally. Constant retardance covers the area between the wedge apexes and is marked by the dotted lines.

tertiary mirror set at an angle to the incident beam, the reflected radiation is made elliptically polarized by the induced phase delay. This may be reverted by applying a phase delay of the opposite sense. A device producing a controlled variable phase delay might comprise two opposed quartz wedges of equal angle, one wedge being movable along its length by a micrometer screw. The wedges need to be cut so that their fast directions are along, and perpendicular to, the direction of motion. Such a simple arrangement is the *Babinet compensator* as shown in Figure 6.9. The phase delay for this basic system varies across its aperture. A more useful design is the *Soleil–Babinet compensator* in which the wedges are cut and placed together with their axes parallel, effecting a multi-order wave plate. By introducing a third element in the form of a rectangular prism of thickness matching that of the wedge combination, but with its axis set orthogonally, a zero-order wave plate is produced with an adjustable retardation from 0° to 2π which is constant over the aperture defined by the interval between the wedge apexes.

6.3.2
Reflection Retarders

It is well known that there are phase delays associated with TIR and that these are unequal for the orthogonal vibrations relative to the plane of incidence. According to the geometry of the angles involved and the refractive index of the more dense material in which the TIR takes place, devices can be constructed for the production of some desired differential phase delay. The most common device of this type is the *Fresnel rhomb*.

If a consistent sign convention is used to deal with the effects of TIR (see Clarke & Grainger, 1971, and Appendix A), it can be shown that the phase difference between components vibrating perpendicular to, and parallel to, the plane of incidence is greater than $\pi/2$ throughout the range of angles for which TIR takes place within all dielectrics of refractive index less than 2.414. If it is desired to produce a quarter-wave retarder, based on the difference in phase of the orthogonal vibrations defined above, this is not possible using only one TIR in normal glasses. Two such reflections, however, providing they are arranged so that the phase delays they produce are cumulative, will produce a delay ranging between 2π and $\tan(3\pi/16)$. Thus glasses with refractive indices equal to or greater than 1.496 can produce a retardation of the parallel component with respect to the perpendicular component of $3\pi/2$ or more, i. e. an effective *advance* of the parallel component of $\pi/2$ or less.

The Fresnel rhomb provides a phase delay of $3\pi/2$ using two identical TIRs. It consists of a parallelopiped of glass, the light passing normally through the entrance and exit faces. If the glass has a refractive index of exactly 1.496, then the $3\pi/2$ phase difference occurs for only one angle of incidence (see Appendix A), namely

$$\chi_i = \arccos\sqrt{\frac{1-n^2}{1+n^2}} \quad \text{or} \quad 52^\circ 10' \,. \tag{6.7}$$

If the refractive index is greater than 1.496, then two angles of incidence give a phase difference of $3\pi/2$. Fresnel pointed out that the larger of these angles is preferred, as the effects of dispersion are smaller. It is also preferred because the phase change of $3\pi/2$ is less seriously affected by any small departures in the angle of incidence. For the same reason, the less the refractive index exceeds 1.496 the better. Fresnel's first rhomb was made of glass of refractive index 1.51, which required angles of incidence of $54^\circ 37'$.

If the whole entrance face is illuminated and all this light is to emerge, the ratio of a long to short side of the parallelogram must be $2\sin\chi_i \tan\chi_i$, which, for $\chi_i = 54^\circ 37'$, is 2.3. Thus the original device is anything but a rhombus (see Figure 6.10). In fact, it is impossible for a rhombus to satisfy the condition that all the light entering normally should emerge and preserve the phase delay of $3\pi/2$.

One of the advantages of the Fresnel rhomb is that the phase delay is nearly achromatic. Stress birefringence and surface films may, however, reduce its performance. It has been shown by King (1966) that the desired retardance can be restored and made more achromatic by coating the reflecting surfaces of the rhomb with magnesium fluoride.

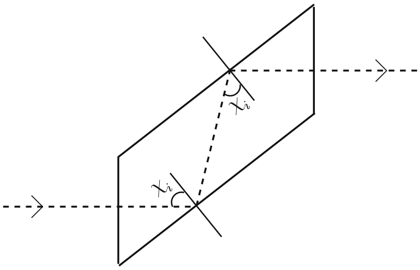

Fig. 6.10 A basic Fresnel rhomb three quarter-wave retarder with the angle of incidence at TIR of $\chi_i = 52.^\circ 1$. Note that the long side to short side ratio is ~ 2.3 so that parallel rays entering the device are reflected with all of them passing through the exit face.

Two of the disadvantages of the simple Fresnel rhomb are that the light does not emerge along the same axis as the incident beam, and the retardance produced varies with the angle of incidence. These problems are overcome by a system of two parellopipeds in series as suggested by Kizel, Krasilov & Shamraev (1964). They also describe a system using three TIRs in a five-sided prism. For a quarter-wave retardance, the angle of incidence is high in both devices and consequently, for the entrance aperture to be a reasonable size, the components must be long. They are thus prone to the effects of stress birefringence in the direction of propagation, and the performance of the retarders is consequently impaired.

In its application, it must be remembered that, despite it sometimes being referred to as a quarter-wave device, the Fresnel rhomb has a phase delay of 3/4-wave. This is confirmed by the statement of Wood (1947) who writes:

> In the case of TIR, the phase of the component of vibration parallel to the plane of incidence is retarded 135°, or a total retardation of 270° for two reflections. This is virtually the equivalent of an *acceleration* of 90° and we can so consider it in all experimental work.

Knowledge of the true value of its retardance is important when it comes to the interpretation of the handedness of any investigated circular polarization. An error in interpreting the sense of handedness will ensue if the device is treated as introducing a quarter-wave retardation, rather than three-quarters of a wave, in its circular-to-linear conversion. It is the sign of U from conversion of V that is taken to give the handedness of the original V. Application of the appropriate Mueller matrix on a Stokes column vector shows that a phase delay of $\pi/2$ converts positive V to positive U, whereas a retardation of $3\pi/2$ converts positive V to negative U.

An example of the use of Fresnel rhombs on the telescope is found in the instrument described by Miller, Robinson & Schmidt (1980) who used two of them to perform double-beam circular spectropolarimetry.

6.3.3
Tunable Wave Plates

Birefringence can be generated in some crystals by the application of electric fields. The Pockels effect, whereby the birefringence is in the direction of the field, has been utilized to produce retarders. A device is commercially available in the form of a cell with electrodes on its ends made of a mesh of transparent material to provide the field. The crystal normally used is potassium di-hydrogen phosphate, or KDP. The retardance of the Pockels cell can be tuned by adjusting the voltage applied to the electrodes. This voltage can be made to follow any desired waveform and the relationship between voltage and phase delay is linear. Typical frequency responses can be as high as 100 kHz. Because of the sensitivity of inefficient operation of the device to off-axis rays, the cells are best operated in a collimated beam. Problems with the device when used to provide phase delays which are maintained for long periods have been found in some applications (see Chapter 8).

An important invention by Kemp (1969), particularly suited to the investigation of high accuracy circular polarimetry, is the photoelastic modulator (PEM). It comprises a block of glass that is made to resonate in its natural vibrational mode. The oscillations of the bulk material induce a time-varying stress birefringence. By controlling the amplitude of the applied stimulus, the birefringence can be controlled to produce a variable phase delay of $\pm\lambda/4$, adjustable to any wavelength in the optical spectrum. Linear polarization may be investigated by the prior insertion of a quarter-wave plate. The resonant frequency is ∼50 kHz and, by applying synchronous gating techniques, the polarimetric signal produced at this very high frequency modulation can be readily recorded without it being subject to intensity scintillation noise produced by the Earth's atmosphere. Because the birefringence is small (only of the order of 1 part in 40 000) the glass plate is thick to achieve the value of phase delay, but there is an advantage in that the device's spurious polarizance by reflection at the entry face is small.

Recently, tunable wave plates have become available involving nematic liquid crystals. They operate with low driving voltages in the range of 0 to ∼15 V. Within a transparent cell, the anisotropic liquid crystals form uniaxial birefringent layers. The properties of nematic materials are such that the molecules tend to align with their long axes parallel and pointing in the same direction. Unlike a solid crystal, they do not settle in regular planes and the molecule centres are distributed at random. Electrical contacts are bonded to the windows of the cell which have a layer to align the molecules when no voltage is applied. On applying an AC voltage, the molecules tend to tip with the long axis becoming parallel to the oscillating electric field, this reducing the birefringence of the cell. The degree of birefringence is controllable by the size of the applied voltage amplitude. A minor disadvantage is the small residual retardance when the voltage is at its maximum as a result of some molecules being effectively pinned to the internal alignment layer of the cell window, but its effect can be removed by the addition of a fixed compensation plate with its fast axis parallel to the slow axis of the cell. The range of phase shift of the basic cell is just greater than $\lambda/2$. Typical response times are about 5 ms to switch from one-half to zero waves (low-to-high voltage change) and about 20 ms to switch from zero to one-half wave (high-to-low voltage change).

Liquid crystal wave plates have potential in that a series of them in combination could provide a modulator, with an appropriate switching sequence, to record the Stokes parameters in turn without the need of mechanical rotations of any optical devices within the optical train. A further improvement might be considered whereby the axes of the wave plates are orientated to follow a Pancharatnam configuration with a provision for achromatic switching of the phase delay.

6.3.4
Axis Determination of Wave Plates

In the application of wave plates in any optical system, it is important to be able to identify the orientation of the fast/slow axes of the device. For the conversion of linear to circular polarization, the axes of the applied quarter-wave plate need to be known in order to establish which handedness of circular polarization will be generated. Conversely, if the handedness of some circular polarization is being investigated, the result will be ambiguous unless it is known whether a phase delay of $+\pi/2$ or $-\pi/2$ has been applied relative to the instrumental polarimetric axes.

Determining which is the fast or slow axis of a wave plate can sometimes cause problems. It is useful to have devices available that have already been calibrated in terms of which are the fast and slow axes. It is often convenient to have a device whose fast and slow axes are known so that it can be overlaid on any other retarder to see whether the phase delay of the combination increases or decreases. In this way the fast and slow axes of the second retarder may be distinguished. In the field of optical crystallography, such a calibrating device is referred to as an *accessory plate*.

A simple means of producing such a device is to use 'Scotch tape' or 'Selotape' which has been adhered to a glass slide. In the manufacturing process of the tape, the substrate is stretched with the introduction of stress birefringence. According to Wood (1964), the long direction of the tape corresponds to the slow ray. Experience shows that, in some cases, the slow axis may not be exactly aligned to the edge of the tape as the slicing of rolls from the bulk material may be misaligned to the original stretch direction.

Although mica is now not generally used in instrumentation, it can be applied as an accessory plate. Any problem in deciding which are the fast and slow axes of a mica plate can be resolved quite easily as follows. Set up crossed polarizers – light from the exit face of the system will be extinguished. Insert a mica plate between them, preferably a square one with its axes parallel to its edges, and rotate it, keeping it normal to the beam, so that the maximum intensity is achieved. Now first tilt it about one of the axes parallel to an edge and then about the orthogonal edge; the edge corresponding to the fast axis is revealed as that producing a blackening at a tilt of about 35°.

6.4
Metallic Reflection

Many of the pieces employed in optical instrumentation rely on reflections by metallic surfaces. Most mirrors in telescope systems, for example, are coated with vacuum deposited aluminium. Spectrometers attached to telescopes invariably employ metallic coated mirrors.

Both the optical and the astronomical literature reveal ambiguities and inconsistences in relation to the definition of phase changes associated with metallic reflections. Many papers suggest that there is a phase difference of π between the resolved components for reflections at normal incidence. This, of course, cannot be the case since, at normal incidence, the components are indistinguishable. For this geometry, the phase difference must be zero. The effect of reflection, however, affects the descriptive coordinate frame and imposes a handedness change such that the U and V parameters are subject to sign changes, making the optical interaction 'equivalent' to there being a relative phase shift of π between the components. A more complete discussion of this is provided in Appendix A. Following the conventions there, the matrix describing reflection from a metal surface may be written as

$$\frac{1}{2}\begin{bmatrix} R_\perp + R_\| & R_\perp - R_\| & 0 & 0 \\ R_\perp - R_\| & R_\perp + R_\| & 0 & 0 \\ 0 & 0 & -2\sqrt{R_\perp R_\|}\cos\varDelta & -2\sqrt{R_\perp R_\|}\sin\varDelta \\ 0 & 0 & 2\sqrt{R_\perp R_\|}\sin\varDelta & -2\sqrt{R_\perp R_\|}\cos\varDelta \end{bmatrix}. \tag{6.8}$$

At normal incidence, with $\varDelta = 0$, the matrix of (6.8) reduces to

$$R\begin{bmatrix} 1 & 0 & 0 & 0 \\ 0 & 1 & 0 & 0 \\ 0 & 0 & -1 & 0 \\ 0 & 0 & 0 & -1 \end{bmatrix}, \tag{6.9}$$

where R is the reflection coefficient.

Thus, for any incoming radiation, the signs of U and V are flipped, the latter indicating that there is a change in handedness of any circularly polarized light. This obviously occurs if observations are made at primary focus of a single mirror in a telescope system, so requiring correction when the records are expressed in a standard celestial coordinate frame. For telescopes involving two on-axis mirrors, such as a regular Cassegrain system, there is a second flip of the U and V parameters, returning them to their original signs.

Typical variations of $R_\perp$, $R_\|$ and $\varDelta = \delta_\perp - \delta_\|$ are illustrated in Figure A.6 of Appendix A in respect of the optical coefficients determined by Capitani, Cavallini, Ceppatelli *et al.* (1989) for the mirrors of a coelostat. For 6500 Å they derived values for the real and imaginary parts of the refractive index of $n = 1.036$ and $\kappa = 5.89$ for the metallic coating, assuming that the behaviour of the reflection with angle of incidence followed the classical theory.

If the fore optics contain mirrors set at an angle, the matrix of (6.8) may be applied with appropriate values for the reflection coefficients and phase change according to the optical constants of the reflecting material. For example, for a reflection at 45°, as in a Newtonian or Nasmyth configuration, the derived polarization parameters show that $R_\perp = 0.93$, $R_\| = 0.87$ and $\varDelta = 6.^\circ 5$, according to the values of n and κ above.

If a compensator is employed to correct this, a phase of $-6.^\circ 5$ adjustment might be applied, with the recorded U, V corrected for sign to allow for the reflection of the reference axes. Alternatively, the applied phase compensation might be set for $(180^\circ - 6.^\circ 5)$, without sign corrections being required for the recorded U, V values.

6.5
Depolarizers

Although their application in polarimetric instruments is no longer a means of calibration, depolarizing devices are occasionally used in instruments to remove the sensitivity of an optical element or detector to polarized light. The depolarizer designed by Lyot (1929) comprises two thick wave plates made of the same material with their axes set at 45°; one plate is twice the thickness of the other. A typical depolarizer comprises quartz plates of 1 mm and 2 mm thick. Over a broad wavelength passband, any polarization present in a beam which it passes is scrambled both in polarization form and direction of vibration. The efficiency to which this is done has been explored comprehensively by Serkowski (1974).

For narrow spectral passbands the scrambling process of the Lyot depolarizer is insufficient for it to be effective. In such a situation, an alternative principle relies on the notion of performing the scrambling with respect to time, the resulting output polarization changing rapidly within the experimental integration interval of the measurement. Several monochromatic depolarizers were suggested by Billings (1951). One of them, involving the rotation of a quarter-wave plate followed by a half-wave plate rotating at twice the speed of the first, was tested by Clarke & Ameijenda (2000). Although successful, the system was subject to image wobble as a result of the wave plate surfaces not being exactly normal to the rotational axis.

6.6
Detectors

Descriptions of detector technology may be found in other texts. The main stay of stellar polarimetry for 40 years has been the photomultiplier, but as is the case with regular stellar photometry, this detector and its associated data reduction procedures have been replaced by CCD-type systems.

Photomultipliers that have cathodes inclined to the received illumination would be expected to be sensitive to the direction of vibration of polarized light. Clancey (1952) investigated several tubes of this design, measuring their effective polarizance, which was very significant. Hoenig & Cutler III (1966) suggested making such an effect a virtue in respect of the RCA 6903 tube; by its rotation about the optic axis, the detector itself could act as polarimetric modulator. Instrumental problems that might be introduced by detector sensitivity to polarized light can be alleviated by not allowing the direction of vibration of any polarization in the flux arriving at the sensitive area to rotate, or by using a depolarizer. End-on type photomultipliers are not immune to polarizational sensitivity.

Another effect that caused spurious signals in some early polarimeters was the changes in response to unit illumination according to the orientation of the detector in the Earth's magnetic field. This problem had been noted for IP21 photomultipliers in stellar photometry by Eggen (1951) and was encountered by the author as a problem in instruments for which the detectors are attached to the rotatable modulator system; changes in relative response of the detectors in double-beam polarimeters with this kind of arrangement require very careful calibration. Good design of the detector housing with magnetic field shielding overcomes such issues; modulator systems involving movement of the detectors at the back end of the instrument, however, were abandoned.

The photomultiplier is limited in dynamic range and, in photon counting mode, this corresponds to photoelectron recording of the order of 10^6 s^{-1}. For the brighter stars, with the use of large telescopes, this limit is readily reached and neutral filters need to be introduced in the optical train to provide lower flux levels on the detection photocathode. Also a polarimetric precision for p of 1 part in 10^4 requires the recording of just more than 10^8 photoelectrons, so requiring integration times of at least several minutes. Increasing the precision by a factor of 10 requires extension of the integration time by a factor of 100, with observing times of several hours required for a single determined value. This restriction does not occur with solid-state devices such as photodiodes. The requirement for these detectors is that records must be made with sufficient resolution of flux levels by using analogue-to-digital converters with adequate bit number. In an instrument constructed by Hough, Lucas, Bailey,*et al.* (2006) to achieve precisions for p of 1 part in 10^6, the detector system comprises cooled avalanche photodiodes with the output signal processed by 16-bit analogue-to-digital converters.

Various 2D detectors have been applied to polarimetry for measurements of star fields, extended objects and for spectropolarimetry. In the optical region, the CCD chip has obvious applications in polarimetry. In order to make assessment of the potential polarimetric accuracy relative to the number of photons registered, calibration of the number of photoelectrons per analogue-to-digital unit (ADU) is required. In determining possible polarimetric precision, the issue of the 'full well capacity' also needs to be considered. Saturation of an individual pixel occurs when $\sim 10^5$ electrons have been produced locally. To obtain polarimetric precision of 1 part in 10^4, the information of $\sim 10^3$ pixels, each exposed close to saturation, needs to be combined, i. e. the spread of the stellar image requires the 'seeing disc' to occupy an area comprising 10^3 pixels. For measurements of individual stars, one approach is to image the telescope aperture on the chip, as was explored by Clarke & Naghizadeh-Khouei (1997). It is generally assumed that the sensitivity of CCDs does not depend on the polarization characteristics of the illumination arriving on the chip. Experiments by Clarke & Neumayer (2002) provided null results for the chip they used, but polarizational sensitivity may emerge to be a problem as improved technologies reduce the pixel size to become closer to the wavelength dimension of the detected radiation.

An alternative concept of applying a CCD to the detection of low levels of polarization is employed in the ZIMPOL (Zurich Imaging Polarimeter). It is based on a fast polarization modulator such as a piezo- or ferroelectric retarder operating in the kHz range. A special CCD on which every second row is masked and the charges are shifted back and forth in phase with the modulator during an integration. For the case of solar measurements, images are recorded in two orthogonal polarization states in rapid succession; the charge created by illumination of the first mode is shifted to the adjacent masked row, which is used as a temporary buffer, while the intensity of second half of the modulation is being recorded. After many thousands of modulation cycles, the CCD is read out in less than 1 s. The sum of the two images is proportional to the intensity, which is used to normalize the difference of image intensities, to provide an NSP. ZIMPOL has had excellent success in the fields of solar spectropolarimetry and basic solar polarimetric imaging. It is also being considered by Schmid, Gisler, Joos, *et al.* (2005) as a means for the detection of extra-solar planets in stellar systems.

6.7
Notes on Polarization and Related Observations

Astronomical photometry is normally performed by comparing the response of an instrument to the radiations of some source to a standard object. If the two sources have different polarization characteristics, a photometer sensitive to polarization may give anomalous results. The situation may be exacerbated if the photometer is attached to a telescope at various orientations during the sets of observations. Such problems may arise as a result of the instrument containing reflection optics, or if the detector has a polarizational sensitivity.

In order to appreciate the magnitude by which photometric measurements can be distorted, consider the simple case of a photometer which, within its optical system, has no polarizing properties, but has a detector whose response depends on the position angle of the polarization of the light incident on the photocathode. An example is an RCA photomultiplier type 931A whose response changes by a factor of the order of ~ 1.15 as the direction of vibration of polarized light is rotated from being perpendicular to the length of the tube to being along the length of the tube (see Clancey, 1952). The system behaves as though it is a partial polarizer and by applying the Mueller calculus, the extreme levels of the output may be evaluated as

$$S = K(2.15 \pm 0.15p) \ ,$$

where p is the degree of polarization and K relates to the sensitivity of the photometer. If, for example, a star under scrutiny has a value of $p = 0.05$, a typical level associated with interstellar polarization, it might be assigned magnitudes differing by as much as $\sim 0.^{\text{m}}0076$, according to whether the position angle of the polarization is parallel or perpendicular to the detector tube's length. Such discrepancies are significant in terms of the accuracies that are claimed in photoelectric photometry. For other designs of photometer using optical elements with polarizing properties, the distortions in ordinary photometry may, in fact, be more severe. Obviously it is a good photometric practice to check out whether any instrument, including its optical components, is sensitive to polarization.

Care must also be taken in any kind of comparative spectrophotometry as the radiation being analysed may be polarized with characteristics which are wavelength dependent and the spectrometer may have polarizing properties which are also wavelength dependent. As an example of the way the particular measurement can be distorted by such effects, Lipskii (1958) has considered the measurement of the equivalent widths of coronal spectral lines; the continuous spectrum of the solar corona is partially polarized with a degree depending on the angular distance from the Sun, while the radiation from the coronal line may not be polarized. In comparing the relative strength of the continuous spectrum and the coronal line, allowance must be made for the effective difference in the transmittance of the polarizing spectrometer to differently polarized radiations.

For observations involving CCD detectors in spectrometry and spectropolarimetry, it is sometimes the practice to obtain calibration frames using the twilight sky as a source. Although it is generally appreciated that the sky brightness has a wavelength dependence close to following the λ^{-4} Rayleigh scattering law, careful study of the spectra of the daytime sky reveals that the Fraunhofer lines are filled in relative to the original solar line depths. This filling-in effect, or the Ring effect, discovered by Grainger & Ring (1962) results from rotational Raman scattering by the air molecules. If the calibration frames are being used to provide a reference for determination of a wavelength scale, consideration must be given to shifts of the line minimum position when the original line is asymmetric. In addition, it was discovered by Clarke & McLean (1975), and explored again by Clarke & Naghizadeh-Khouei (2000), that the filling-in was accompanied by polarizational changes across the Fraunhofer lines, the strength of the effect depending on the scattering angle given by the Sun's location and the monitored sky position. If CCD twilight sky frames are undertaken for the purpose of photometric calibration across spectral line profiles and the spectrometer carries polarization properties, or if the frames are used for polarimetric calibration purposes, account must be taken of the polarizational sensitive line filling-in effects related to the source.

It may be noted that both prism and grating spectrometers have strong polarization effects which are wavelength dependent. Grating instruments are subject to there being sudden changes in their polarizational characteristics at particular wavelengths as a result of Wood's anomalies (see, for example, Breckinridge, 1974).

Finally, it may be noted that the overall transmittance of any optical system depends on the relative orientation of the various polarizationally sensitive elements it comprises. It is of importance, for example, in the design of grating spectrometers which employ flat metallic coated mirrors to 'fold' the optical beam within the system. Sequential folding by two mirrors to turn a beam by 90° relative to the original plane of travel may form a system equivalent to crossed partial polarizers. As spectrometers generally possess a polarizance, their orientation at the focal plane of a coudé telescope affects the overall transmittance of the collected radiation. This problem has been discussed by Clarke (1973).

References

Archard, J.F., Taylor, A.M. (1948) Improved Glan–Foucault prism. *J. Sci. Inst.*, **25**, 407–409. [106]

Babinet, J. (1837) Précis d'un mémoire sur les caractères optiques des minéraux. *CR*, **4**, 758–766. [103]

Babinet, J. (1838) Sur l'absorption dans les milieux colorés biréfringents. *CR*, **7**, 832–833. [103]

Billings, B.H. (1951) A monochromatic depolarizer. *J. Opt. Soc. Am.*, **41**, 966–975. [121]

Breckinridge, J.B. (1974) Diffraction grating polarization. pp. 232–236 in *Planets, Stars and Nebulae Studied with Photopolarimetry,* (ed. T. Gehrels), University of Arizona, Tucson, AZ. [124]

Capitani, C., Cavallini, F., Ceppatelli, G., Landi Degl'innocent, E., Landi Degl'innocent, M., Landolfi, M., Righini, A. (1989) Polarization properties of a 'Zeiss-type' coelostat: the case of the solar tower in Arcetri. *Sol. Phys.*, **120**, 173–191. [120]

Clancey, E.P. (1952) Polarization effects in phototubes. *J. Opt. Soc. Am.*, **42**, 357. [121, 123]

Clarke, D. (1965) Studies in astronomical polarimetry. II. A double beam polarimeter. *MNRAS*, **130**, 75–81. [107]

Clarke, D. (1967) Achromatic half wave plates and linear polarization rotators. *Optica Acta*, **14**, 343–350. [112]

Clarke, D. (1973) Effects of polarization on the transmission of Coudé-spectrometer systems. *A&A*, **24**, 165–170. [124]

Clarke, D. (2005) Effects in polarimetry of interference within wave plates. *A&A*, **434**, 377–384. [113, 114, 114]

Clarke, D., Ameijenda, V. (2000) Hα polarimetry of the solar limb. *A&A*, **355**, 1138–1145. [121]

Clarke, D., Grainger, J.F. (1971) *Polarized Light and Optical Measurement.* Pergamon, Oxford. [115]

Clarke, D., McLean, I.S. (1975) Polarization measurements of the Hβ line in blue sky light. *Planet. Space Sci.*, **23**, 557–559. [124]

Clarke, D., Naghizadeh-Khouei, J. (1997) Polarimetry using CCD detectors. pp. 303–308 in *Sensors and their Applications VIII,* (eds A.T. Augousti & N.M. White), Institute of Physics Publishing, Bristol. [122]

Clarke, D., Naghizadeh-Khouei, J. (2000) Polarimetric studies of rotational Raman scattering (the Ring effect) in the zenith sky. *Planet. Space Sci.*, **48**, 285–295. [124]

Clarke, D., Neumayer, D. (2002) Experiments with a novel CCD stellar polarimeter. *A&A*, **383**, 360–366. [122]

Conn, G.K.T., Eaton, G.D. (1954) On polarization by transmission with particular reference to selenium films in the infrared. *J. Opt. Soc. Am.*, **44**, 553–557. [109]

De la Provostage, M.F., Desains, P. (1850) Mémoire sur la polarisation de la Chaleur par réfraction simple. *Ann. de Chimie et de Physique*, **30**, 158–178. [109]

Donati, J.-F, Catala, C., Wade, G.A., Gallou, G., Delaigue, G., Rabou, P. (1999) A dedicated polarimeter for the MuSiCoS échelle spectrograph. *A&AS*, **134**, 149–159. [114, 114]

Eggen, O.J. (1951) Photoelectric studies VIII. Positional effect in photomultipliers and some revised magnitudes in the North Polar Sequence and Harvard region C12. *ApJ*, **114**, 141–144. [121]

Foster, L.V. (1938) A polarizing vertical illuminator. *J. Opt. Soc. Am.*, **28**, 124–126. [107]

Grainger, J.F., Ring. J. (1962) Anomalous Fraunhofer line profiles. *Nature*, **193**, 762. [124]

Harries, T.J., Howarth, I.D. (1996) Linear spectropolarimetry of the Hα emission line of ζ Puppis. *A&A*, **310**, 533–546. [114]

Hodgkinson, I.J., Wu, Q.H. (1997) *Birefringent Thin Films and Polarizing Elements.* World Scientific Publishing, Singapore. [112]

Hoenig, S.A., Cutler III, A. (1966) Polarization sensitivity of the RCA 6903 photocathode tube. *Appl. Opt.*, **5**, 1091–1092. [121]

Hough, J.H., Lucas, P.W., Bailey, J.A., Tamura, M., Hirst, E., Harrison, D., Bartholomew-Biggs, M. (2006) PlanetPol: a very high sensitivity polarimeter. *PASP*, **118**, 1302–1318. [122]

Kemp, J.C. (1969) Piezo-optical birefringence modulators: new use for a long-known effect. *J. Opt. Soc. Am.*, **59**, 950–954. Reprinted in 1990 – *Selected Papers on Polarimetry.* Ed. B.H. Billings – SPIE Milestone Series **MS23**, SPIE, Bellingham. [118]

King, R.J. (1966) Quarter-wave retardation systems based on the Fresnel rhomb principle. *J. Sci. Inst.*, **43** 617–622. [116]

Kizel, V.A., Krasilov, Yu. I., Shamraev, V. N. (1964) Achromatic $\lambda/2$ device. *Optics & Spectroscopy*, **17**, 248–249. [117]

Lipskii, Iu. N. (1958) The dependence of the equivalent widths of coronal lines on the degree of polarization of the continuous spectrum of the corona. *Sov. Astron.*, **2**, 615–619. [123]

Lyot, B. (1929) Recherches sur la polarisation de la lumière des planets et quelques substances terrestres. *Ann. de l'Observatoire de Paris – Section de Meudon* VIII, No:1 (for an English translation see NASA TT F-187 (1964)). [121]

Matsuda, K., Ikeda, Y., Akitaya, K.S., Seki, M., Okazaki, A., Hirata, R. (2005) High resolution spectropolarimeter, LIPS: its performance and observational results. pp. 87–88 in *Astronomical Polarimetry: Current Status and Future Directions – ASP Conf. Ser.*, No: **343**, (eds A. Adamson, C. Aspin, C.J. Davis & T. Fujiyoshi), San Fransisco. [114]

Miller, J.S., Robinson, L.B., Schmidt, G.D. (1980) The remote-controlled spectrograph, area scanner, and spectropolarimeter for the Lick 3-m telescope. *PASP*, **92**, 702–712. [117]

Nicol, W. (1829) On a method of so far increasing the divergency of the two rays in calcareous spar that only one image may be seen at a time. *Edinburgh New Philos. J.*, **6**, 83–84. [106]

Oliva, E. (1997) Wedged double Wollaston, a device for single shot polarization measurements. *A&AS*, **123**, 589–592. [108]

Pancharatnam, S. (1955) Achromatic combinations of birefringent plates Part II. An achromatic quarter-wave plate. *Proc. Indian Acad. Sci.*, **A 41**, 137–144. [112]

Schmid, H.M., Gisler, D., Joos, F., Povel, H.P., Stenflo, J.O., Feldt, M., Lenzen, R., Brandner, W., Tinbergen, J., Quirrenbach, A., Stuik, R., Gratton, R., Turatto, M., Neuhäuser, R. (2005) ZIMPOL/CHEOPS: a polarimetric imager for the direct detection of extra-solar planets. pp. 89–91 in *Astronomical Polarimetry: Current Status and Future Directions – ASP Conf. Ser.*, No: **343**, (eds A. Adamson, C. Aspin, C.J. Davis & T. Fujiyoshi), San Fransisco. [123]

Schwarz, H., Guisard, S. (1995) Rotating half wave plate for EFOSC1 refurbished. *The Messenger*, **81**, 9–10. [114]

Semel, M. (2003) Spectropolarimetry and polarization-dependent fringes. *A&A*, **401**, 1–14. [114]

Serkowski, K. (1974) Polarization techniques – Chapter 8 from *Methods of Experimental Physics*, (eds M.L. Meeks & N.P. Carleton) **12**, Astrophysics: Part A – Optical & Infrared, Academic Press, New York. [101, 121]

Stokes, G.G. (1862) On the intensity of the light reflected from or transmitted through a pile of plates. *Proc. R. Soc. London*, **11**, 545–556; *Philos. Mag.*, **[4]24**, 480–489. (See also – pp. 145–156 in Mathematical and Physical Papers – G.G. Stokes. Vol IV. Cambridge University Press, Cambridge, 1904). [110]

Tinbergen, J. (1994) Ripples we have seen. *Spectrum: Newsl. R. Obs.*, **1**, 26–28. [114]

Tuckerman, L.B. (1947) On the intensity of the light reflected from or transmitted through a pile of plates. *J. Opt. Soc. Am.*, **37**, 818–825. [109, 110]

Weinberg, J.L. (1964) On the use of a pile-of-plates polarizer – The transmitted component. *Appl. Opt.*, **3**, 1057–1061. [109]

Wollaston, W.H. (1804) On a new metal, found in crude platina. *Philos. Trans. R. Soc.*, **94**, 419–430. [103]

Wood, E.A. (1964) *Crystals and Light – An Introduction to Optical Crystallography*. Van Nostrand, Princeton, NJ. [119]

Wood, R.W. (1947) *Physical Optics*, p. 270. Macmillan, New York. [117]

7

Pre-measurement Distortions

7.1

Introduction

Before stellar radiation is analysed by polarimetry, it first passes through the Earth's atmosphere, and is then collected and focussed by a telescope. Both these media may alter the polarizational information, particularly the collector fore-optics, so affecting the assessment of the true normalized Stokes parameters related to the source. So far, passage through the atmosphere of the light from stars, other than the introduction of intensity scintillation noise, has been deemed to be unimportant in producing polarimetric distortions, but, as accuracy and sensitivity increase, it will prove necessary to reconsider several problems which must affect the measurements at some level.

7.2

The Earth's Atmosphere

It is well known that the Earth's atmosphere directly affects both astrometry and photometry in significant ways. Procedures for refraction corrections, and removal of the effects of atmospheric extinction, form regular reduction exercises for all ground-based work. In the case of polarimetry, the situation is somewhat different in that direct distortions of normalized Stokes parameters by the atmosphere are extremely small, and, as yet, have not been considered to any significant degree.

Atmospheric extinction brings no polarimetric problems other than flux loss, therefore reducing the potential accuracy in a given observational time. Also, if intensity scintillation dominates over photon shot noise, then the accuracy of any polarimetry may be affected relative to the full potential carried by the total photon count. Problems of this latter kind can be avoided by employing a modulator working at high frequency, or by using a system that simultaneously records the orthogonally resolved components. The fact that intensity scintillation is coherent in orthogonally resolved beams, as demonstrated experimentally by Hiltner (1951, 1952), is of no surprise in that the atmosphere is essentially neither dichroic nor birefringent.

Stellar Polarimetry. David Clarke

ISBN: 978-3-527-40895-5

Possible problems that may be significant in upsetting the recorded results in terms of the true underlying values, are induced polarizations, depolarization effects, Faraday rotation and the sky background brightness, which itself is likely to be polarized, causing further complications.

7.2.1
Induced Polarization

When radiation encounters a medium with a change of refractive index, the Fresnel laws allow calculation of the polarization that is induced by the interface. It is easy to show (see Appendix A) that the degree of polarization of a refracted beam, originally unpolarized, is given by

$$p = \frac{1 - \cos^2(\chi_i - \chi_t)}{1 + \cos^2(\chi_i + \chi_t)} , \tag{7.1}$$

where χ_i and χ_t are the angles of incidence and refraction, respectively.

In the case of the Earth's atmosphere, the transmitting medium changes continuously with depth, and it is a difficult task to predict the value of any induced polarization in the radiation collected by the telescope. An estimate of the extreme effect can be obtained by considering the atmosphere to act as a uniform slab, as though the refraction is caused by a single interface. Again, by considering the maximum effect close to the horizon, which provides a refraction value of $(\chi_i - \chi_t) \sim 35'$, the resulting value of p is $\sim$ 0.000052. This figure is generally smaller than the uncertainties achieved in current regular polarimetric practice and hence refraction should not introduce disturbing systematic errors; the situation may, however, require reassessment as accuracies and detectivities improve. It is noteworthy that Hough, Lucas, Bailey, *et al.* (2006) have discovered low levels of induced polarization that are detectable for stars at a large zenith distance, and suggest that aligned dichroic particles of Saharan dust are the cause, the dust being prevalent at their observing site.

7.2.2
Depolarization Effects

Related to telecommunications, experimental tests have been undertaken to investigate possible depolarization of radiation passing through the Earth's atmosphere. Fried & Mevers (1965) used a laser source and investigated its transmission over a long path length, claiming that polarization fluctuations were readily detectable. This was refuted by later experiments of Bradford & Tucker (1969) who showed that any depolarization was less than 1 part in 10^{-8} over a path length of over 600 m; they suggested that the earlier result arose from effects associated with random and continuously varying illumination of the collection aperture, in similar fashion to the cause of stellar intensity scintillation. To some degree, fluctuations in the evenness of aperture illumination, giving rise to intensity scintillation, must affect stellar polarimetric measurements, but there are no reports in the literature on these issues (but see Section 7.4).

7.2.3
Faraday Rotation

Perhaps the most significant effect distorting ground-based polarimetry is Faraday rotation. Lyot (1929) made comment that Becquerel had suggested that the atmosphere can rotate the direction of vibration, the effect being maximum along the magnetic meridian, reaching 45′ at 5° above the horizon. In a model by Finkel (1964), the effects of O_2 and N_2 have been combined and integrated according to their molecular concentrations and temperature with height, with the Earth's field approximated by a centred dipole. Calculations suggest that the maximum effects, with the field along the line of sight, are $\sim$ 10.5, 6.8, 2.9 arcminutes per oersted ($\equiv$ gauss in air) at 4000, 5000 and 8000 Å respectively. Hsu & Breger (1982) have also calculated that for a star 5° above the horizon and located on the geomagnetic meridian, Faraday rotation is $\sim$ 40′. At air masses less than 1.5, any rotation is always less than $0.^\circ 1$.

Equation (5.11) suggests that with an underlying polarization of say 0.01, measured to an accuracy of ± 0.0001, so providing a signal-to-noise ratio $(p/\sigma_p) \sim 100$, the uncertainties in ζ are $\sim \pm 18'$. Hence Faraday rotations produced by the Earth's atmosphere are close to being detectable, according to the source's position in the sky. If signal-to-noise ratios $p/\sigma_p \sim 1000$ are achieved, then Faraday rotation effects need to be considered in data reductions.

7.2.4
Sky Background

When measuring stellar polarizations photoelectrically, the field stop in the focal plane of the telescope also allows light from the background sky to be detected at the same time as that of the target star. Depending on the brightness of the star relative to that of the sky background, and on the planned accuracy of the polarimetry, the contaminating signal needs to be accounted for. This might be done by making measurements of a nearby empty field, or by instrumental design so that the sky background is automatically removed (see, for example, Piirola, 1973, Metz, 1984). With 2D detectors, sky background can usually be dealt with by exploring pixels adjacent to that of the target. It must be remembered that the light from the night sky is not just a background brightness but may itself be significantly polarized, particularly if the Moon is the chief source.

In a theoretical study by Fox (1992), various issues with respect to sky background contamination were explored, the biggest problem being scattered moonlight. There have been several episodes whereby an *exciting* polarimetric result has been published, which later has been challenged, or even retracted, when the problem of sky background interference was more fully assessed.

7.2.5
Effects of a Variable Equivalent Wavelength

Investigations of stellar polarimetry are always conducted according to some specified wavelength passband. Although the equivalent wavelength of any instrumental system is controlled by the filter/detector, the convolution required to determine the *effective* wavelength, λ_{eff}, of the measurement also includes a contribution of $I(\lambda)$, describing the wavelength dependence of the received flux from any individual star. Unfortunately, as for photometry, the spectral distribution of the received energy is distorted by atmospheric extinction, making λ_{eff} dependent on zenith distance. Such colour-dependent extinction can also affect the precision of stellar polarimetry.

For any star subject to interstellar polarization, this component has a wavelength dependence according to its location in the Galaxy. If the effective wavelength of a set of repeated measurements changes during some observations, this will be reflected in the stability of the results. Thus, it is expected that repeated determined values of p will be subject to a drift, or scatter, according to the zenith distance. A simple calculation demonstrates the typical magnitude of such variations.

Suppose that the true underlying values for a star are $p = 0.9\%$ in B and 1% in V. With a difference in bandpass position $\sim$1000 Å, the polarization changes by 0.1%. For a conservative small shift of say 10 Å for the λ_{eff} of B, as a result of zenith angle change between two observations, the recorded difference in p would be

$$\sim \frac{0.1\% \times 10}{1000} \sim 0.00001 \,,$$

this being about a factor of 10 smaller than the uncertainties that are quoted for high accuracy measurements. For studies of intrinsic polarizations for which the behaviour of $p(\lambda)$ is more pronounced across the optical spectrum, shifts in λ_{eff} are, however, likely to have greater effect, making the noise on the determinations of p more apparent. As precision advances for some particular studies, say the polarimetric detection of planetary systems about stars, or in establishing the stability of standard stars, variability of the effective wavelength should be considered which results from the spectral behaviour of atmospheric extinction, this being dependent on zenith distance.

7.3
The Telescope Optics

Stellar radiation collected by a telescope is brought to a focus before analysis by an attached polarimeter. In the transmission, or reflection, by the various elements of the fore-optics, any collected radiation may have its polarization characteristics altered by small amounts. Generally to the accuracies that are regularly achieved, the main considered effect is that of systematic *instrumental polarization*. This shows itself by unpolarized radiation accruing a small polarization. Its effect on the data is generally removed by calibrations, and, by applying the inverse of the *Additivity Theorem of Small Polarizations* (see Section 4.5), the raw measurements being considered as the simple addition of the true underlying value plus the instrumental polarization. For very high accuracy measurements, this simple approach is inadequate and the source of the contamination needs to be identified more carefully. Although the incoming radiation may carry only a small polarization, the second-order effects of the action on this by the small polarizance and phase shifts associated with the instrumental polarization need to be taken into account. By summarizing the instrumental effects as a Mueller matrix, an inversion process should be applied in data reductions.

The two main effects of the telescope optics are that the mirrors may offer a weak polarizance and/or may introduce phase changes which affect the incoming radiation. These effects are expressable in terms of Mueller matrices, with a reference axis that may be set at some arbitrary angle, α, relative to the coordinate frame describing the Stokes parameters of the radiation. Any polarizance effect may be expressed as

$$\begin{bmatrix} I' \\ Q' \\ U' \\ V' \end{bmatrix} = \frac{R}{2} \begin{bmatrix} M_{11} & M_{12} & 0 & 0 \\ M_{21} & M_{22} & 0 & 0 \\ 0 & 0 & M_{33} & 0 \\ 0 & 0 & 0 & M_{44} \end{bmatrix} \begin{bmatrix} 1 & 0 & 0 & 0 \\ 0 & \cos 2\alpha & \sin 2\alpha & 0 \\ 0 & -\sin 2\alpha & \cos 2\alpha & 0 \\ 0 & 0 & 0 & 1 \end{bmatrix} \begin{bmatrix} I \\ Q \\ U \\ V \end{bmatrix} . \tag{7.2}$$

where R is an 'average' reflection coefficient. It is expected that $M_{11} \simeq M_{22} \simeq M_{33} \simeq M_{44} \simeq 1$, and $M_{12} \simeq M_{21}$, these carrying very small values. By multiplying out (7.2):

$$\begin{bmatrix} I' \\ Q' \\ U' \\ V' \end{bmatrix} = \frac{R}{2} \begin{bmatrix} M_{11} I + M_{12}(Q \cos 2\alpha + U \sin 2\alpha) \\ M_{21} I + M_{22}(Q \cos 2\alpha + U \sin 2\alpha) \\ -M_{33}(Q \sin 2\alpha + U \cos 2\alpha) \\ M_{44} V \end{bmatrix} , \tag{7.3}$$

and this may be rewritten as

$$\begin{bmatrix} I' \\ Q' \\ U' \\ V' \end{bmatrix} = \frac{RI}{2} \begin{bmatrix} M_{11} + M_{12}(q \cos 2\alpha + u \sin 2\alpha) \\ M_{21} + M_{22}(q \cos 2\alpha + u \sin 2\alpha) \\ -M_{33}(q \sin 2\alpha + u \cos 2\alpha) \\ M_{44} v \end{bmatrix} . \tag{7.4}$$

The standard procedure to deal with this induced polarizance effect is to observe a selection of unpolarized standard stars to determine the value of M_{21}. Its value is simply treated as an offset and subtracted from all subsequent measurements – see Chapter 5. In the measurement of linear polarization, such an approach assumes that $M_{11} = M_{22} = M_{33} = 1$, and that the second-order effects associated with them not being exactly equal to unity are neglected. When the high accuracy polarimetry is being pursued, their values need to be determined by observing a variety of precise polarized standard stars, and then used in an inversion procedure to determine the true values of q and u of any other source. Such a treatment is required to remove the polarizance fringes, described in Chapter 6, that can affect spectropolarimetry conducted by instruments using a wave-plate modulator.

For the case of telescope mirrors carrying phase changes, their effects may be included by considering values for M_{34} and M_{44} which are not zero. The resultant changes to the incoming radiation may now be expressed as

$$\begin{bmatrix} I' \\ Q' \\ U' \\ V' \end{bmatrix} = \frac{RI}{2} \begin{bmatrix} M_{11} + M_{12}(q\cos 2\alpha + u\sin 2\alpha) \\ M_{21} + M_{22}(q\cos 2\alpha + u\sin 2\alpha) \\ -M_{33}(q\sin 2\alpha + u\cos 2\alpha) + M_{34}v \\ M_{44}v - M_{43}(q\sin 2\alpha + u\cos 2\alpha) \end{bmatrix} . \tag{7.5}$$

It can be seen that there is cross-talk within the U' and V' parameters as a result of both circular-to-linear and linear-to-circular conversions. The latter effect is generally more troublesome than the former, as the incoming radiation is likely to carry linear polarization, which is much larger than any circular component being measured. In principle, values for M_{34} and M_{44} can be determined from observations of standard stars and they can be applied in reduction procedures by inversion.

In the study by Miller (1963), the effects of telescopes on astronomical measurements have been formulated in terms of the existence of polarization eigenstates associated with the collector mirrors. In addition to a discussion on the need to establish zero-polarization standard stars, the paper also discussed the proposal to develop a rotatable telescope (see further) to remove disturbing effects of the mirrors. Attention was drawn to some of the problems that a rotatable telescope system cannot solve, particularly in relation to the measurement of circular polarization.

From measurements made using standard stars, Gehrels (1960) investigated the instrumental polarization of three different telescopes. The polarization produced by the aluminized mirrors was wavelength dependent, generally increasing in the ultraviolet. Some of the possible origins of the cause of the effects were discussed in terms of the aluminizing processes.

For axi-symmetric collectors such as a Cassegrain system, it might be expected that the telescope instrumental polarization would be zero. It is suspected that in some aluminizing procedures, the sputtering process gives rise to crystalline-type growths with a preferred direction on the optical surface, this introducing an instrumental polarization. To counteract such a problem, Gehrels & Meltzer (1966) suggested that, at the time of aluminizing telescope mirrors, the secondary might be mounted in the hole of the primary and on completion, it should be mounted after rotation by 90° with respect to the primary. Even if the mirrors are in perfect condition, problems may arise with photomultiplier detectors. In instruments employing these, an image of the telescope collector aperture is usually focussed on the cathode by means of a Fabry lens. Different regions of the aperture may be given unequal weights because of non-uniform sensitivity of the photocathode over its area. Polarization may also be introduced as a result of non-uniformities over the mirror surfaces. Protective coatings can cause polarization contaminations as well.

Severe telescope instrumental polarization is obviously to be expected in Newtonian and coudé systems employing plane mirrors with the optical rays impinging at large angles of incidence. With a coudé–spectrometer system, differential polarization measurements say across spectral features remain feasible, but absolute measurements are problematic, even if additional optics are included to compensate for the effects of the coudé mirrors. Relevant to this, the overall transmittance of a coudé telescope feeding a spectrometer with polarizational characteristics has been analysed and discussed by Clarke (1973). One conclusion from this work was that, in general, it is better to place the length of the spectrometer entrance slit to run parallel to the Declination Axis, the common practice, however, usually sets the slit to be parallel to Right Ascension.

Serkowski (1974) has commented on the effects of plain mirrors in Newtonian, coudé telescopes and heliostats in that their effects depend in a complicated way on the state of polarization of the incident light, the angles of incidence and the ageing properties of the aluminium coatings. He suggests that 'eliminating these effects by compensating plates is a hopeless task'. The enormity of the problem is readily appreciated by considering the analysis undertaken by Ruben (1959), for example, in respect of a coelostat system. The problem of compensating for the large polarizing effects in telescope using mirrors at high angles of incidence has been investigated by Cox (1976). This study showed that effects resulting from construction errors and differences between mirrors outweigh those related to the lack of collimation in converging beams, with their associated range of angles of incidence, as they progress through the system.

By adding a compensating mirror, however, crossed with the flat in a Newtonian system, van P. Smith (1956) was able to undertake a successful study of interstellar polarization. Marin (1964) has used a coudé system successfully. High spectral resolution of the polarimetric behaviour of magnetic variable stars was explored by Borra & Vaughan (1977) using the coudé focus of the 2.5 m Mount Wilson telescope. While producing a linear polarization, the flat mirror in the telescope system introduces a phase shift to any linear polarization originally carried in the light of the star, both effects being dependent on the declination of the observed star. Corrections for the phase shift were effected by a Babinet compensation plate whose phase delay was adjusted according to the stellar declination. At the same time as a resolved element within a spectral line was being measured, the polarization of the nearby continuum was also recorded, thus allowing application of differential processes in the data reductions. By applying the Mueller calculus to the situation, it was shown that systematic errors in the circular polarization measurements were likely to be very small with respect to depolarization effects, but that great care was required in setting up the compensator to prevent cross-talk among the Stokes parameters. For linear polarization measurements, one of the Stokes parameters, Q, is unaffected by errors introduced by incorrect phase delay compensation. For U, depolarization is negligible but the cross-talk from V was dependent to first order. This has ramifications in determining the transverse Zeeman effect in the presence of fields with a longitudinal component.

Many of the new and projected large telescopes operate with a Nasmyth focus using a tertiary mirror at 45°. The problem that this introduces to polarimetry with discussion on the measures that can be taken to address the issues has been presented by Tinbergen (2007).

It may be noted that an alt-azimuth mounting can be advantageous because any telescope instrumental polarization can be determined by comparing the results obtained for the same star either side of the meridian, the whole optical system suffering rotation around the observed direction as the hour angle changes sign. This is common practice in radio astronomy. For equatorially mounted telescopes, any polarization produced by the mirrors can be explored and eliminated by rotating the entire telescope tube together with the mirrors. In the 1960s, two 24″ Cassegrain rotatable telescopes were specially designed for polarimetric use (see Hiltner & Schild, 1965), and these were instrumental in setting up set of unpolarized standard stars. In the Northern Hemisphere (Yerkes Observatory), Appenzeller (1968) made use of the instrument in his survey of the galactic pole and in the Southern Hemisphere (Siding Spring in Australia), an important study was made by Serkowski, Mathewson & Ford (1975). The project established a number of nearby stars of intermediate spectral types for which no linear polarization was detectable within the limits of the measurement error.

It may also be noted that some of the early investigations of interstellar polarization were conducted with large refractor telescopes. Again it would be expected that the circular symmetry of the collection aperture in the form of an objective lens should not introduce any spurious instrumental polarization. However, Serkowski (1960) drew attention to the effects of stress birefringence that can occur in the glass material of the lenses. The small phase changes that are produced effectively decrease the measured values for the degree of linear polarization. Using the 26-inch refractor in Belgrade, Krzemiński (1959) measured the polarization of 23 stars with known interstellar 4430 Å band intensities. Comparison with the measurements by Hiltner of the same stars showed that the values were systematically smaller, but that they were reconcilable by considering the Belgrade objective to act as a phase plate with a retardance of 1/14 of a wave. According to Serkowski (1960), in view of the thickness of the lenses, such a value of phase delay is not unexpected.

In some cases, instrumental polarization may have components generated in the optics of the modulator itself, or in the electronic gating of the signal. For example, if a rotating wave plate is employed as part of the modulator, as well as its phase delay, it also acts as a weak partial polarizer, this affecting the signal to some degree. The opening and closing of gates synchronously with the modulator's position to allow sampling over sections of the oscillatory signal needs to be timed to high accuracy and be free from drift.

For high accuracy and precision in polarimetric observations, stability of operation is important. Such aims are best achieved by having telescopes that are dedicated solely to polarimetry. The results published by Kemp's group at the University of Oregon and by the Wisconsin group (see Nordsieck, Babler, Bjorkman, *et al.*, 1992) owe their success to this. Unfortunately, this means that available apertures will inevitably be fairly small, limiting such polarimetric studies to the brighter stars.

7.4
Optical Depolarization

The fact that all optical elements depolarize radiation that they transmit, or reflect, is not generally appreciated. Because of the curvatures of the optical surfaces of mirrors and lenses, some of the rays contributing to any image are reflected, or transmitted, at non-zero angles of incidence. As a consequence, the Fresnel coefficients for the various rays resolved parallel to, and perpendicular to, the local plane of incidence will be unequal. Also, for metallic coated mirrors, the phase changes for different rays will not be exactly 0°. These two effects induce a *depolarization*, the phenomenon being *fundamental* to the passage of radiation through any instrument system.

The principles related to the effects have been described by Sen & Kakati (1997) with respect to polarimetric field imaging, but their thesis is also important in high-precision measurements of individual stars. A simple approach to estimate depolarizing effects can be made by considering light rays impinging on a circular mirror, assuming that elemental portions of its surface act independently so that there is no phasal coherence for the various ray paths in coming to a focus.

Suppose I is the flux per unit area falling on the telescope aperture. For an annular zone of width $\mathrm{d}r$, at a distance, r from the axis of the mirror, the flux entering a small area bounded by ψ to $\psi + \mathrm{d}\psi$ is given by

$$I\, r\, \mathrm{d}r\, \mathrm{d}\psi \ , \tag{7.6}$$

the variable, ψ, describing the angular position around the annulus relative to some arbitrary fiduciary position.

If the light entering the primary mirror carries a Stokes vector $\{I, Q, U, V\}$, the emergent vector from the small defined area is determined from

$$\begin{bmatrix} I' \\ Q' \\ U' \\ V' \end{bmatrix} = r\, \mathrm{d}\psi\, \mathrm{d}r \left[\mathrm{Rot}(-\psi)\right][M]\left[\mathrm{Rot}(\psi)\right] \begin{bmatrix} I \\ Q \\ U \\ V \end{bmatrix} . \tag{7.7}$$

The Stokes vector transformer $[M]$ corresponds to that for metallic reflection and is given by (6.8).

Following the matrix multiplication, and by integrating around an annulus from $\psi = 0$ to 2π, the emergent Stokes vector from the annulus at distance, r, from the centre of the mirror, may be written as

$$\begin{bmatrix} I_r \\ Q_r \\ U_r \\ V_r \end{bmatrix} = \frac{\pi\, r\, \mathrm{d}r}{2} \begin{bmatrix} 2(R_\perp + R_\parallel) I \\ Q[(R_\perp + R_\parallel) + 2\sqrt{R_\perp R_\parallel} \cos \Delta)] \\ -U[(R_\perp + R_\parallel) + 2\sqrt{R_\perp R_\parallel} \cos \Delta] \\ -4\sqrt{R_\perp R_\parallel} \cos \Delta \end{bmatrix} . \tag{7.8}$$

Quantitatively, the Q and U parameters suffer in an identical way, as might be expected from the circular symmetry of the telescope optics, but the sign of U is reversed as it is also for V. For a perfect mirror, there is no cross-talk between the parameters.

If the telescope aperture is directed to a polarized source with a Stokes vector given by $\{I, Q, 0, 0\}$, the measured degree of polarization, p_r, from the annulus is given by

$$p_r = \frac{Q[(R_\perp + R_\|) + 2\sqrt{R_\perp R_\|}\cos \Delta]}{2I(R_\perp + R_\|)} , \tag{7.9}$$

rather than simply

$$p = \frac{Q}{I} . \tag{7.10}$$

At exactly normal incidence, i. e. for rays arriving at the centre of the mirror, it can be seen that (7.9) reduces to Q/I. Comparing (7.9) with (7.10) shows that there is an effective depolarization for rays arriving in any annulus surrounding the mirror centre.

For an $f/3$ mirror, for example, the angle of incidence for rays arriving towards the outer edge is of the order of 10°. Using the values of n and κ obtained by Capitani, Cavallini, Ceppatelli *et al.* (1989) from experiments with aluminium-coated coelostat mirrors, values for $R_\perp$, $R_\|$ and Δ may be calculated for any angle of incidence. By considering $i = 10°$, the outer annulus of an $f/3$ primary mirror is likely to reduce the linear polarization for the measurement to $p_r \sim 0.999993 \times p$. The outer annulus of the secondary mirror accepting the same rays from the primary provides a further depolarizing factor. Although the overall effect is small, it is an important issue to consider as polarimetric accuracy is advanced. It may be also noted that the degree of circular polarization is also reduced. Effects of lenses in the subsequent optical system also introduce a depolarization which can be estimated for each surface depending on the behaviour of the Fresnel coefficients according to the angle of incidence presented to the curved surfaces. For light in transmission, the value of Δ is equal to zero.

It may be noted that the illumination of a telescope mirror is not uniformly static, but suffers fluctuations over its area as a result of turbulence in the Earth's atmosphere. Rather than there being a constant depolarization factor associated with any telescope, a fluctuating depolarization noise will ensue, this being further complicated by the spread of angles of incidence according to the seeing conditions. Depolarization variations will also be present as a result of telescope tracking inaccuracies.

Regarding the development of telescopes for improving solar polarimetry, with the aim of designing a polarization-free system, Sánchez Almeida & Martìnez Pillet (1992) modelled the polarization structure likely to appear in the diffraction pattern of a point source in the telescope focal plane. They considered the behaviour for on-axis and off-axis sources and the seeing-induced instrumental polarization. For an unpolarized source, in addition to the known intensity behaviour of the diffraction patch, patterns for both Q and U revealed peaks at a level ~0.01% with their orientations set at 45° with respect to each other; no V parameter polarization was generated. For a polarized source, complicated cross-talk patterns between the various parameters clearly emerged. This study was extended by Sánchez Almeida & Martìnez Pillet (1994) by modelling the effects of seeing, with the conclusion that the atmosphere produces a sort of noise which randomly changes the crosstalk between the Stokes parameters. For the case of stellar telescope systems with a spider supporting the secondary mirror, the effects of its associated diffraction pattern are likely to complicate the issue further. Effects on high accuracy measurements may depend on the direction of the spider arms with respect to the position angle of the polarization of the incoming light.

Although refractor telescopes are generally no longer used, as described earlier, stress birefringence in the lenses of the objective converts linear polarization to elliptical, effectively introducing a depolarization. As the stress may depend on the orientation of the telescope, the depolarizing factor may be variable. Catadioptric systems are also likely to suffer similar problems. It may be noted that any lens system prior to the modulator may suffer from stress birefringence, or other effects resulting from its anti-reflection coatings.

References

Appenzeller, I. (1968) Polarimetric observations of nearby stars in the directions of the galactic poles and the galactic plane. *ApJ*, **151**, 907–918. [134]

Borra, E.F., Vaughan, A.H. (1977) High-resolution polarization observations inside spectral lines of magnetic Ap stars. I. Instrumentation and observations of β coronae Borealis. *ApJ*, **216**, 462–478. [133]

Bradford, J.N., Tucker, J.W. (1969) A sensitive system for measuring atmospheric depolarization of light. *Appl. Opt.*, **8**, 645–647. [128]

Capitani, C., Cavallini, F., Ceppatelli, G., Landi Degl'innocent, E., Landi Degl'innocent, M., Landolfi, M., Righini, A. (1989) Polarization properties of a 'Zeiss-type' coelostat: the case of the solar tower in Arcetri. *Sol. Phys.*, **120**, 173–191. [136]

Clarke, D. (1973) Effects of polarization on the transmission of Coudé-spectrometer systems. *A&A*, **24**, 165–170. [133]

Cox, L.J. (1976) The compensation of instrumental polarization by inclined mirrors. *MNRAS*, **176**, 525–532. [133]

Finkel, J. (1964) Optical faraday rotation in the atmosphere. *J. Atmos. Terr. Phys.*, **26**, 297–299. [129]

Fox, G.K. (1992) A preliminary investigation of the effects of the background sky upon polarimetric measurements. *MNRAS*, **258** 533–542. [129]

Fried, D.L., Mevers, G.E. (1965) Atmospheric optical effects – polarization fluctuation. *J. Opt. Soc. Am.*, **55**, 740–741. [128]

Gehrels, T. (1960) The wavelength dependence of polarization. I. Instrumental polarization. *AJ*, **65**, 466–469. [132]

Gehrels, T., Meltzer, A.S. (1966) Wavelength dependence of polarization. VII. Interstellar polarization. *AJ*, **71**, 111–113. [132]

Hiltner, W.A. (1951) Compensation of seeing in photoelectric photometry. *The Observatory*, **71**, 234–237. [127]

Hiltner, W.A. (1952) Compensation of seeing noise in photoelectric polarization photometry. *AJ*, **57**, 13. [127]

Hiltner, W.A., Schild, R. (1965) A rotatable telescope for polarization studies. *Sky & Telescope*, **XXX**, 144–147. [134]

Hough, J.H., Lucas, P.W., Bailey, J.A., Tamura, M., Hirst, E., Harrison, D., Bartholomew-Biggs, M. (2006) PlanetPol: a very high sensitivity polarimeter. *PASP*, **118**, 1302–1318. [128]

Hsu, J-C., Breger, M. (1982) On standard polarized stars. *ApJ*, **262**, 732–738. [129]

Krzemiński, W. (1959) Photoelectric polarization measurements of 23 stars with known interstellar λ 4430 band intensities. *Acta Astron.*, **9**, 231–236. [134]

Lyot, B. (1929) Recherches sur la polarisation de la lumière des planets et quelques substances terrestres. *Ann. de l'Observatoire de Paris – Section de Meudon* VIII, No:1 (for an English translation see NASA TT F-187 (1964)). [129]

Marin, M. (1964) Measures photoélectriques de polarisation à l'aide d'un télescope coudé de 1 mètre. *Th. Sciences Physiques, Paris* Série A, No: 897. See also: *Rev. d'Opt.*, **44**, 115–144. [133]

Miller, R.H. (1963) The effects of telescopes on astronomical polarization measurements. *Appl. Opt.*, **2**, 61–65. [132]

Metz, K. (1984) A polarimeter with a new polarizer and a new device for eliminating the sky background polarization. *A&A*, **136**, 175–177. [129]

Nordsieck, K.H., Babler, B., Bjorkman, K.S., Meade, M.R., Schulte-Ladbeck, R.E., Taylor, M.J. (1992) Stellar Spectropolarimetric Monitoring at The University of Wisconsin. pp. 114–117 in *Nonisotropic and Variable Outflows from Stars – ASP Conf. Ser.*, **22**, (eds L. Drissen, C. Leitherer & A. Nota), San Francisco. [134]

Piirola, V. (1973) A double image chopping polarimeter. *A&A*, **27**, 383–388. [129]

Ruben, G. (1959) Die Polarisation des Lichtes an aluminisation Coelostaten-Spieglen. *Zeit. Optik*, Bd. **16**, Heft 6, 326–338. – *Mitt. des Astro. Obs. Potsdam* No: 77. [133]

Sánchez Almeida, J. (1994) Instrumental polarization in the focal plane of telescopes II. Effects of induced seeing. *A&A*, **260**, 543–555. [137]

Sánchez Almeida, J., Martìnez Pillet, V. (1992) Instrumental polarization in the focal plane of telescopes. *A&A*, **260**, 543–555. [136]

Sen, A.K., Kakati, M. (1997) Instrumental polarization caused by telescope optics during wide field imaging. *A&AS*, **126**, 113–119. [135]

Serkowski, K. (1960) Influence of the instrumental circular polarization on the measurements of linear polarization. pp. 296–299, in *Bulletin Lowell Observatory* No: 105, Vol. IV – No. 17 – Polarization of Starlight by the Interstellar Medium – A Conference Sponsored by the NSF and the Lowell Observatory. [134, 134]

Serkowski, K. (1974) Polarization Techniques – Chapter 8 from *Methods of Experimental Physics*, (eds M.L. Meeks & N.P. Carleton) **12**, Astrophysics: Part A – Optical & Infrared. Academic Press, New York. [133]

Serkowski, K., Mathewson, D.S., Ford, V.L. (1975) Wavelength dependence of interstellar polarization and ratio of total to selective extinction. *ApJ*, **196**, 261–290. [134]

Tinbergen, J. (2007) Accurate optical polarimetry on the Nasmyth platform. *PASP*, **119**, 1371–1384. [134]

van P. Smith, E. (1956) Interstellar polarization in the Southern Milky Way. *ApJ*, **124**, 43–62. [133]

8
Polarimetric Principles and Instruments

8.1
Introduction

Polarization phenomena are related to orientational qualities of the electromagnetic waves making up a beam of radiation. In order to explore these and to make quantitative measurements of the polarization, a modulator and detector system requires to be fitted in an instrument for the attachment to a telescope. In most cases, some of the included optical elements need to be rotatable in order to tease out the polarimetric information. Not all polarimeters are designed to measure simultaneously all the Stokes parameters of the collected light. By far the majority of polarimetry concerns the measurement of the linear parameters: $\{Q, U\}$, or $\{q, u\}$, or $\{p, \zeta\}$. Most instruments are specifically designed to do so using a modulator that alters the flux passed to the detector according to the strength of Q and U in the collected radiation. The values of the parameters describing the linear polarization are calculated from measurements of the modulations in the recorded signal produced by the detector. The circular parameter, V or v, may be measured using an instrument designed for linear polarization studies, but with the appropriate insertion of a quarter-wave plate prior to the modulator. Other designs are immediately better suited for measuring V or v, alone in isolation. Again, these latter instruments can be adapted to measure the linear parameters by the addition of a quarter-wave plate prior to the modulator. Occasionally, instruments are designed to measure both the linear and circular components simultaneously. In any instrument, particularly as higher and higher accuracy is demanded, care must be taken to check out any deleterious effects of cross-talk between the various Stokes parameters. This is particularly important when measuring circular polarization, as it is usually very small, and is subject to contamination by linear-to-circular conversions within the instrument. Also, the very requirement of having rotatable elements may in itself be a source of spurious signals, or an instrumental polarization, as a result of displacements of the light beams. The effects of such disturbances must be calibrated out and compensation applied.

The last element of any modulator system is a polarizer and, as a consequence, the subsequent optical train receives radiation which is completely polarized. Any polarizing properties of the later optics are irrelevant in terms of biasing or distort-

Stellar Polarimetry. David Clarke

ISBN: 978-3-527-40895-5

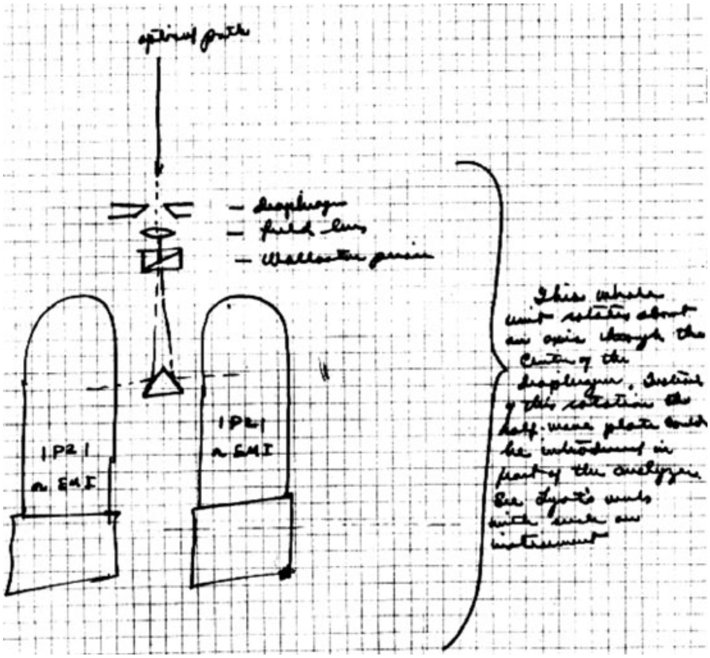

Fig. 8.1 A sketch of a basic double-beam polarimeter of the late 1950s era. (Communication to the author by W. Hiltner in 1959.)

ing the measurement of the original collected radiation. The relevant orientations of the various optical parts in the overall train are important, however, in determining the flux level arriving at the detector and in controlling the strength of the output signal. As discussed earlier (Section 7.3), in reference to instrumental polarization associated with the telescope, any optics can introduce distortion to the measurement and for this reason the modulator is placed early in the system, usually immediately after the field stop. The basic parts of the simplest kind of double-beam photoelectric polarimeter are sketched in Figure 8.1.

In general, a modulator comprises either rotatable elements or devices whose retardation is adjustable by some controlled external stimulus, or a combination of both. For those instruments employing rotatable components, the modulation may be achieved by continuous rotation, or by adjustment to click-stop preferred orientations. Just as in the discipline of spectrometry, with its plethora of optical systems, various kinds of polarimetric elements have been incorporated within instruments, and a range of techniques has developed for determining the Stokes parameters of any collected radiation. A simple descriptive overview, although not complete, has been provided by Oetken (1970). A survey of techniques, polarimetric devices and instruments has also been made by Serkowski (1974a, 1974b). While comparing the performance and different designs of astronomical polarimeters, Cox (1983) has used the concept of information capacity.

Most designs of polarimeter operate with converging, or diverging, beams passing through the modulator as the elements are usually capable of accepting reasonably large cone angles without losing efficiency. There may be concerns over the operation of wave plates with such arrangements, and it is sometimes better if the transmitted beams are first collimated. In the case of the design by Clarke & McLean (1975), sketched out in Figure 8.4, a collimated beam was employed to avoid spectral passband spread of the narrow-band interference filters placed after the polarizer.

The principles of polarimetric techniques are readily appreciated in terms of the signals generated by the modulator. For some forms of detector, the information may be apparent in real time, the output keeping pace with the generated modulation. Other detectors may accumulate the signal before presenting a read-out at appropriate times. As described in the the following sections, the forms of the signals are generally schematic and may need to be interpreted according to the design of particular equipment.

8.2
Rotation of a Polarizer or Wave Plate

The most obvious polarimetric technique is to use a modulator which contains rotatable elements whose transmittances are directly sensitive to the vibration directions of the electric disturbances within the incoming beam. In the early days of experimentation, this was done by introducing sheet *Polaroid* into the conventional photoelectric photometers and taking brightness readings at specific orientations of its principal axis. The observational scheme is essentially the same as that used for multi-filter photometry and, for that reason, early reported measurements of the degree of polarization were expressed as magnitude differences. Several of the early catalogues (e. g. Hiltner, 1951a, Behr, 1959) list p in magnitudes and these require conversion to fractional, or percentage, values to correspond with modern convention (see Section 4.7).

The behaviour of an instrument based on the rotation of a polarizer may be expressed in terms of Mueller matrices, set out in their correct order, operating on the input Stokes vector $\{I, Q, U, V\}$ of the incoming light. According to the orientation, α, of the principal axis of the polarizer with respect to the axial frame describing the original Stokes parameters, as in Figure 8.2, the output Stokes vector $\{I', Q', U', V'\}$ may be determined from

$$\begin{bmatrix} I' \\ Q' \\ U' \\ V' \end{bmatrix} = \frac{1}{2} \begin{bmatrix} 1 & 1 & 0 & 0 \\ 1 & 1 & 0 & 0 \\ 0 & 0 & 0 & 0 \\ 0 & 0 & 0 & 0 \end{bmatrix} \begin{bmatrix} 1 & 0 & 0 & 0 \\ 0 & \cos 2\alpha & \sin 2\alpha & 0 \\ 0 & -\sin 2\alpha & \cos 2\alpha & 0 \\ 0 & 0 & 0 & 1 \end{bmatrix} \begin{bmatrix} I \\ Q \\ U \\ V \end{bmatrix} . \qquad (8.1)$$

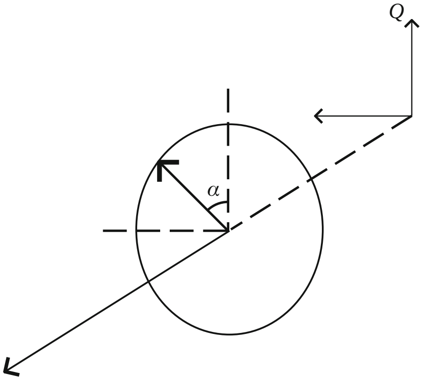

Fig. 8.2 The rotation of a polarizer through a positive angle, α, relative to the reference axis defining Q.

It is the parameter, I', and its dependence on α that is measured by the detector, and, following the matrix multiplication, it may be expressed as

$$I'(\alpha) = \frac{1}{2}\left[I + Q\cos 2\alpha + U\sin 2\alpha\right]. \tag{8.2}$$

Remembering that $Q/I = q = p\cos 2\zeta$, and $U/I = u = p\sin 2\zeta$ (see (4.26)), the above equation may be rewritten as

$$I'(\alpha) = \frac{1}{2}I\left[1 + p\cos 2(\alpha - \zeta)\right]. \tag{8.3}$$

Generally the reference axis of the polarimeter is described with respect to equatorial coordinates, i. e. the fiduciary of the instrument is such that, when ζ is zero, the polarizer's transmission axis runs N/S, and aligned with Declination.

Thus, it can be seen that the variation of intensity produced by a rotating polarizer modulator comprises a mean level, on which a modulation is superimposed, with amplitude dependent on the degree of polarization, and with the phase dependent on the direction of vibration of the incoming light. Essentially, there are three unknowns requiring quantification.

In fact, the actual signal, $S_{\|}(\alpha)$, involves additional parameters to describe it, and should be written as

$$S_{\|}(\alpha) = \frac{1}{2}G_{\|}(\alpha)T(t)\left[I + Q\cos 2\alpha + U\sin 2\alpha\right], \tag{8.4}$$

where $G_{\|}(\alpha)$ expresses the detector's response to unit intensity, also showing that it might perhaps be affected according to the rotational position of the polarizer as a result of beam wobble, or to the detector's sensitivity with respect to the direction of vibration of the polarized light which illuminates it; the symbol, $\|$, refers to the fact that the intensity with vibration parallel to the polarizer's principal axis is being measured. The coefficient, $T(t)$, describes the variation of the signal with time caused either by the Earth's atmosphere as a result of intensity scintillation, or by the slower, secular changes in atmospheric extinction.

The signal for measurement as written in (8.4) may also be expressed as

$$S_{\parallel}(\alpha) = \frac{1}{2} G_{\parallel}(\alpha) T(t) I \left[1 + p \cos 2(\alpha - \zeta)\right] . \tag{8.5}$$

In order to prevent the noise associated with $T(t)$ affecting the determination of the NSPs – q, u or p, ζ, the waveform needs to be sampled faster than variations associated with intensity scintillation, and this can be done if the rotational speed of the polarizer is high ($\gtrsim$500 Hz). By exploring the simultaneous signals from orthogonally resolved beams, Hiltner (1951b) demonstrated the coherence of the intensity scintillation which they both carry. A résumé of this finding is also provided in Hiltner (1952). Taking the ratio of the orthogonal signals allows the elimination of scintillation noise. It was noted that the ratio is generally close to unity, and so it is possible to 'eliminate' the noise by directly measuring the difference of the signals, as in Behr's (1956) polarimeter, using the occasional insertion of a depolarizer in the beam to serve as a reference for zero polarization. Although the difference signal itself carries intensity scintillation noise, the disturbance affecting the polarimetric determinations is very much less when it is recorded directly, rather than recording the two signals in succession and then determining their difference. These issues were explored by Clarke (1965). In many of the early instruments involving photomultiplier tubes, photometric signals were recorded using DC amplifiers and pen recording systems. Such electronic practice performed well while recording the individual signals, or the directly formed difference signal, but was inconvenient for determining the ratio of the two outputs. It was not until later, when photon-counting systems were developed, that the two digital outputs were recorded simultaneously over a matched integration interval, and ratios obtained by computer calculation. With the advent of two-dimensional detectors such as CCDs, orthogonally resolved images may be recorded simultaneously, and ratios of their intensities determined automatically in the computerized data reduction procedures.

Consider the principles of the two-beam system. If in (8.4) the value of α is replaced by $\alpha + \pi/2$, the signal recorded for the second beam may be written as

$$S_{\perp}(\alpha) = \frac{1}{2} G_{\perp}(\alpha) T(t) \left[I - Q \cos 2\alpha - U \sin 2\alpha\right] , \tag{8.6}$$

or,

$$S_{\perp}(\alpha) = \frac{1}{2} G_{\perp}(\alpha) T(t) I \left[1 - p \cos 2(\alpha - \zeta)\right] , \tag{8.7}$$

where $S_{\perp}(\alpha)$ corresponds to the orthogonal component resolved by a two-beam polarizer. It can be seen that the records, $S_{\parallel}(\alpha)$ and $S_{\perp}(\alpha)$, are in anti-phase with each other. Hence, by taking the ratio of the two signals, we get

$$\frac{S_{\parallel}(\alpha)}{S_{\perp}(\alpha)} = \frac{G_{\parallel}(\alpha)[1 + p \cos 2(\alpha - \zeta)]}{G_{\perp}(\alpha)[1 - p \cos 2(\alpha - \zeta)]} . \tag{8.8}$$

With the insertion of a depolarizer in the beam, if it is assumed that its transmittance is identical for the orthogonal beams, the ratio of the two outputs may then be represented by

$$\frac{S_{\parallel D}(\alpha)}{S_{\perp D}(\alpha)} = \frac{G_{\parallel}(\alpha)}{G_{\perp}(\alpha)} \,. \tag{8.9}$$

Hence, with calibrations of the relative responses for the two beams provided by the depolarizer as in (8.9), the value of p and ζ may be readily determined from (8.8) by performing measurements at various values of α. With the later establishment of calibration stars, including a set representative of unpolarized standards, the practice of using a depolarizer was eventually abandoned.

It will be appreciated that an NSP is essentially the difference between the intensities of orthogonally resolved beams, normalized by their sum. Thus, NSPs may be determined directly by recording the difference and summation of the intensities of the two beams. In systems which used photomultipliers as detectors, taking the difference of signals directly, and displaying them on a chart recorder was relatively easy. A very simple practical way of doing this has been documented, for example, by Thiessen (1958).

If the difference signal for the two beams is recorded directly, it may be represented as

$$D(\alpha) = I\,T(t)\left\{G_{\parallel}(\alpha) - G_{\perp}(\alpha) + p\cos 2(\alpha - \zeta)[G_{\parallel}(\alpha) + G_{\perp}(\alpha)]\right\}. \tag{8.10}$$

With the inclusion of a depolarizer in the beam prior to the polarizer, the difference signal may then be written as

$$D_{\mathrm{D}}(\alpha) = I\,T_{\mathrm{D}}(t)\tau\left\{G_{\parallel}(\alpha) - G_{\perp}(\alpha)\right\}, \tag{8.11}$$

where τ is the the transmittance of the depolarizer, again assumed to be identical for the resolved beams.

By also combining the two output signals electronically at the same time as the difference signals are recorded, the records, without and with depolarizer, may be expressed as

$$A(\alpha) = I\,T(t)\left\{G_{\parallel}(\alpha) + G_{\perp}(\alpha) + p\cos 2(\alpha - \zeta)[G_{\parallel}(\alpha) - G_{\perp}(\alpha)]\right\}, \tag{8.12}$$

$$A_{\mathrm{D}}(\alpha) = I\,T_{\mathrm{D}}(t)\tau\left\{G_{\parallel}(\alpha) + G_{\perp}(\alpha)\right\}. \tag{8.13}$$

By manipulating (8.10) to (8.13), values of $p\cos 2(\alpha - \zeta)$ may be determined from

$$p\cos 2(\alpha - \zeta) = \frac{D(\alpha)A_D(\alpha) - A(\alpha)D_D(\alpha)}{A(\alpha)A_D(\alpha) - D(\alpha)D_D(\alpha)}\,, \tag{8.14}$$

with the effects of atmospheric generated noise removed by taking the ratio. For low levels of polarization, accuracy may not be compromised by doubling either of the individual signals to obtain a value for the summation signal. The principles of the method as summarized in (8.14) have been used by Fessenkov (1959) and by Clarke (1965).

It is well known that a half-wave plate flips the direction of vibration of the incoming light from one side of its principal axis to the other. (This can be readily checked by applying the Mueller calculus). Thus, the position angle of any linearly polarized light is rotated through twice the angle set by the original position angle and the wave plate's axis. As a consequence, this device provides an alternative to the rotation of a polarizer to provide a modulator for the investigation of linearly polarized light. A system is achieved by rotating a half-wave plate prior to a fixed polarizer. This principle was employed by Lyot (1948a) in prototype instruments using photoelectric cells as early as 1922. The signal has the same form as that of the rotating polarizer, as described above, but the modulation frequency is doubled, running at four times the mechanical rotation rate of the wave plate. The system has the advantage of alleviating the problems of spurious signals that might be generated by the detector's sensitivity to the direction of polarization that illuminates it, this now being set by the fixed polarizer. A disadvantage of using a simple wave plate is that its phase delay suffers from spectral dispersion, and can only be considered as providing a half-wave retardation over a limited spectral range. This limitation can be removed, however, by using achromatic devices.

The effects of the optical elements comprising a Lyot-type modulator may by summarized by

$$\begin{bmatrix} I' \\ Q' \\ U' \\ V' \end{bmatrix} = \begin{bmatrix}\text{Pol}\end{bmatrix} \begin{bmatrix}\text{Rot} \\ (-\alpha)\end{bmatrix} \begin{bmatrix}\text{Wave} \\ \text{Plate}\end{bmatrix} \begin{bmatrix}\text{Rot} \\ (\alpha)\end{bmatrix} \begin{bmatrix} I \\ Q \\ U \\ V \end{bmatrix}, \tag{8.15}$$

where $\{I', Q', U', V'\}$ is the Stokes column vector describing the emergent light falling on the detector. The angle, α, is the rotational setting of the axis of the wave plate relative to the principal axis of the polarizer, the latter remaining fixed in the instrument and used as the reference axis for describing the Stokes vector, $\{I, Q, U, V\}$, of the incoming light. Again, it is the intensity, $I'(\alpha)$, that is measured as the polarimetric signal.

In (8.15) describing the instrument, $[\text{Rot}(\alpha)]$ is the standard matrix representing rotation of the Stokes vector to the coordinate frame describing the wave plate, and $[\text{Rot}(-\alpha)]$ is a similar matrix involving the same angle, but of opposite sign, returning the Stokes vector to the original coordinate frame of the polarizer; [Pol] is the standard matrix describing the operation of the fixed polarizer.

The matrix written as [Wave Plate] represents the effect of the wave plate that, for a pure device, simply comprises terms describing the effects of the phase delay. It is written as

$$\begin{bmatrix} 1 & 0 & 0 & 0 \\ 0 & 1 & 0 & 0 \\ 0 & 0 & \cos\Delta & \sin\Delta \\ 0 & 0 & -\sin\Delta & \cos\Delta \end{bmatrix} \text{and, with } \Delta = \pi, \text{ becomes} \begin{bmatrix} 1 & 0 & 0 & 0 \\ 0 & 1 & 0 & 0 \\ 0 & 0 & -1 & 0 \\ 0 & 0 & 0 & -1 \end{bmatrix}. \tag{8.16}$$

By multiplying out the matrices of (8.15), and following the same development as for the rotating polarizer modulator, the signal for measurement may be written as

$$S_{\parallel}(\alpha) = \frac{1}{2} T(t) G_{\parallel}(\alpha) \left[I + Q \cos 4\alpha + U \sin 4\alpha \right], \tag{8.17}$$

or

$$S_{\parallel}(\alpha) = \frac{1}{2} T(t) G_{\parallel}(\alpha) I \left[1 + p \cos 4(\alpha - \zeta) \right]. \tag{8.18}$$

A similar signal, $S_{\perp}(\alpha)$, is also available with an anti-phase modulation for measurements made with a two-beam fixed polarizer.

Any linear polarization present in a light beam is seen to produce a sinusoidal modulation as in (8.18) by the rotation of a half-wave plate prior to a fixed polarizer. More efficient modulation can be achieved by constructing a disc with sectors of wave-plate material arranged so that adjacent elements have phase delays of zero and $\lambda/2$. By passing the light beam through the periphery of the disc which is rotated about its centre, the handedness of any circularly polarized light alternates its sense as the consecutive sectors interrupt the beam. By placing quarter-wave plates either side of the disc, any linear polarization is modulated to provide a square-wave signal. This kind of system was employed by Lyot (1948b) and later by Dollfus (1958), Marin (1964) and Tinbergen (1972, 1973).

8.3
Fixed Position Records

In many polarimeters involving the rotation of either a polarizer or a wave plate, the output signal may be recorded with the rotatable element set at some preferred, fixed angular settings. The underlying form of the signals for such modulators comprises a sinusoidal variation, superimposed on a mean level. Three independent parameters therefore describe it – the mean level, the amplitude of the sinusoidal variation and its phase. With three unknowns, the characteristics of the polarization may be obtained by recording the signal at a minimum of three specific angular positions. This is the essence of *Fessenkov's method* – see Fessenkoff (1935), his name later transcribed as Fessenkov, whereby signals, $S_{\parallel 1}$, $S_{\parallel 2}$ and $S_{\parallel 3}$, are recorded for polarizer positions of 0°, 60° and 120°, relative to the fiduciary axis. From such measurements, the characteristics of a linear polarization in terms of the degree of polarization, p, and the direction of vibration, ζ, may be written as

$$p = \frac{2 \left\{ S_{\parallel 1}(S_{\parallel 1} - S_{\parallel 2}) + S_{\parallel 2}(S_{\parallel 2} - S_{\parallel 3}) + S_{\parallel 3}(S_{\parallel 3} - S_{\parallel 1}) \right\}^{1/2}}{S_{\parallel 1} + S_{\parallel 2} + S_{\parallel 3}}, \tag{8.19}$$

and[5]

$$\tan 2\zeta = \frac{\sqrt{3}(S_{\|2} - S_{\|3})}{2S_{\|1} - S_{\|2} - S_{\|3}} . \tag{8.20}$$

Other similar formulae may be generated by choosing three alternative values of α, or by using a modulator involving a rotating half-wave plate prior to a fixed polarizer with selected angles of 0°, 30° and 60°.

The Fessenkov operational scheme has had occasional use (e. g. see Clarke 1971, Dorotovič, Pintér & Rybanský, 2003) but a more common technique employs four positions of the polarizer at values of 0°, 90°, 45° and 135°, these being more directly relatable to the determination of the Stokes parameters. From the form of the modulation expressed as

$$S_{\|}(\alpha) \longrightarrow I + p\cos 2(\alpha + \zeta) , \tag{8.21}$$

the records may be written as

$$\begin{aligned}
\alpha &= 0^\circ & &\longrightarrow & S_{\|1} &= I + p\cos 2\zeta \\
\alpha &= 90^\circ & &\longrightarrow & S_{\|2} &= I - p\cos 2\zeta \\
\alpha &= 45^\circ & &\longrightarrow & S_{\|3} &= I - p\sin 2\zeta \\
\alpha &= 135^\circ & &\longrightarrow & S_{\|4} &= I + p\sin 2\zeta .
\end{aligned} \tag{8.22}$$

The first two measurements lead to a value of $p\cos 2\zeta = q = (S_{\|1} - S_{\|2})/2$, while the last two measurements provide a value of $p\sin 2\zeta = u = (S_{\|4} - S_{\|3})/2$. By combining these two values, the degree of polarization is given by

$$p = \frac{1}{2}\left\{(S_{\|1} - S_{\|2})^2 + (S_{\|4} - S_{\|3})^2\right\}^{1/2} = \sqrt{p^2\cos^2 2\zeta + p^2\sin^2 2\zeta} , \tag{8.23}$$

the latter form being that given by Pickering (1874). This measurement procedure may therefore be referred to as *Pickering's method*. For instruments involving the rotatable half-wave plate option, the chosen angular settings for the measurements are 0°, 45°, 22.°5 and 67.°5.

Taking the ratio of the recorded intensities of the two resolved beams removes the noise generated by the Earth's atmosphere. In order to obtain the values of the NSPs, the relative response of the two detectors needs to be calibrated. This might be done by using a depolarizer, but may also be achieved if the beams can be switched from one detector to the other. In principle, the switch might be made by rotating the double-beam polarizer independently of the two detectors, but generally the geometry of the arrangement negates this. An equivalent way is to use

---

[5] For the record, it has been pointed out by Öhman (1971), who also cites the concurrence of Dr Hack of Trieste, that a misprint appears in Fessenkov's paper. In the original formula for $\tan 2\zeta$, a 'sign' error is carried in the numerator; the formula as it appeared in Fessenkoff (1935) is correct if $S_{\|1}$, $S_{\|2}$ and $S_{\|3}$ correspond to angular polarizer positions of 0°, 120° and 60°, respectively.

a modulator comprising a rotatable half-wave plate prior to the fixed polarizer and detector system. Consider now applying the Pickering method to such an instrument. The two signals may be represented by

$$S_{\parallel}(\alpha) = \frac{1}{2} G_{\parallel}(\alpha) T(t) \left[I + Q \cos 4\alpha + U \sin 4\alpha \right] , \tag{8.24}$$

$$S_{\perp}(\alpha) = \frac{1}{2} G_{\perp}(\alpha) T(t) \left[I - Q \cos 4\alpha - U \sin 4\alpha \right] . \tag{8.25}$$

By making records at angular settings of the wave plate of 0° and 45°, with ratios of the signals subsequently taken at each of these positions, the pair of measurements may be represented by

$$R_0 = \frac{\frac{1}{2} T_0(t) G_{\parallel}(I + Q)}{\frac{1}{2} T_0(t) G_{\perp}(I - Q)} = \frac{G_{\parallel}(I + Q)}{G_{\perp}(I - Q)} , \tag{8.26}$$

$$R_{45} = \frac{\frac{1}{2} T_{45}(t) G_{\parallel}(I - Q)}{\frac{1}{2} T_{45}(t) G_{\perp}(I + Q)} = \frac{G_{\parallel}(I - Q)}{G_{\perp}(I + Q)} . \tag{8.27}$$

By taking the ratios of these determined values, the problem of the different sensitivities of the two detectors is then eliminated, i. e.

$$R_q = \frac{R_0}{R_{45}} = \frac{G_{\parallel}(I + Q)}{G_{\perp}(I - Q)} \bigg/ \frac{G_{\parallel}(I + Q)}{G_{\perp}(I - Q)} = \left(\frac{I - Q}{I + Q} \right)^2 , \tag{8.28}$$

from which the NSP may be calculated as

$$q = \frac{\sqrt{R_q} - 1}{\sqrt{R_q} + 1} . \tag{8.29}$$

A similar expression for the u parameter may be developed by using the polarizer at settings of 22.°5 and 67.°5, leading to

$$u = \frac{\sqrt{R_u} - 1}{\sqrt{R_u} + 1} , \tag{8.30}$$

$$\text{where} \qquad R_u = \frac{R_{22.5}}{R_{67.5}} = \left(\frac{I + U}{I - U} \right)^2 . \tag{8.31}$$

Thus, the linear polarization parameters are determinable without calibrating the relative sensitivities of the detectors; compensation for atmospheric effects is also automatically achieved. This is of great importance to the application of CCDs to polarimetry. Tinbergen & Rutten (1992) promoted the concept of this method in their *User Guide for Spectropolarimetry* for the William Herschel Telescope. In their general use, CCDs require the time-consuming procedure of flat-fielding, which would also be necessary if single-beam polarimetry were to be attempted. A strict requirement of the modulator system as described above is that the image pairs should not wander over the CCD pixels as the wave plate is rotated to the designated positions.

Various data reduction strategies are applied to the observations made by instruments which record intensity values at fixed positions of the rotatable wave plate. Statistically rigorous methods for doing this have been presented by von der Heide & Knoechel (1979).

8.4
Continuous Rotation Records

With records made at fixed positional angles of the modulator, two-beam polarizers allow for the removal of atmospheric generated noise by taking the ratio of the simultaneously recorded signals. Such noise can be overcome by rotating the modulator at high speed; the process can be enhanced further by taking ratios if orthogonal beams are available. There are many techniques for recording the waveform with a continuously rotating modulator. In the instrument (MINIPOL) designed by Frecker & Serkowski (1976), which has had extensive use at the University of Arizona, the sinusoid generated by a half-wave plate rotated at 20 Hz, was sampled over 12 equal angular spaced sections; least-squares sine fits were performed on the records to determine q and u. Another successful recording scheme involves the integration of the signal over three angular sections as the modulator rotates. For the case of a rotating polarizer modulator, a minimum of three channels are required to obtain a measurement. Following Klare, Neckel & Schnur (1974), the first channel records the signal continuously, while the the second integrates over the intervals of 0° $\rightarrow$ $\pi/2$ and π $\rightarrow$ $3\pi/2$ and the third from $\pi/4 \rightarrow 3\pi/4$ and $5\pi/4 \rightarrow 7\pi/4$. Thus, the three recorded measurements over N complete cycles may by written as

$$S_{\|1} = N \int_0^{2\pi} S_{\|}(\alpha) d\alpha = N\pi I \ , \tag{8.32}$$

$$\begin{aligned} S_{\|2} &= N \int_0^{\frac{\pi}{2}} S_{\|}(\alpha) d\alpha + N \int_{\pi}^{\frac{3\pi}{2}} S_{\|}(\alpha) d\alpha \\ &= 2N \int_0^{\frac{\pi}{2}} S_{\|}(\alpha) d\alpha = N\left(\frac{\pi}{2} I + U\right) , \end{aligned} \tag{8.33}$$

$$\begin{aligned} S_{\|3} &= N \int_{\frac{\pi}{4}}^{\frac{3\pi}{4}} S_{\|}(\alpha) d\alpha + N \int_{\frac{5\pi}{4}}^{\frac{7\pi}{4}} S_{\|}(\alpha) d\alpha \\ &= 2N \int_{\frac{\pi}{4}}^{\frac{3\pi}{4}} S_{\|}(\alpha) d\alpha = N\left(\frac{\pi}{2} I - Q\right) . \end{aligned} \tag{8.34}$$

The NSPs may then be derived as

$$q = \frac{Q}{I} = \pi\left(\frac{1}{2} - \frac{S_{\|3}}{S_{\|1}}\right) , \tag{8.35}$$

$$u = \frac{U}{I} = \pi\left(\frac{S_{\|2}}{S_{\|1}} - \frac{1}{2}\right) . \tag{8.36}$$

Terms involving the integration of the angular dependence of the detector's sensitivity to unit intensity, $G_{\|}(\alpha)$, over the appropriate interval have been neglected in the above summary, but their influence can be calibrated out by reference to standard stars. One of the advantages of this method of recording the polarimetric information in this way is that the system behaves as a heterodyne detector, responding only to the even harmonics of $G_{\|}(\alpha)$ described by $f(2 + 4n)$, with $n = 0, 1, 2, 3 \ldots$, the signal of interest corresponding to $n = 0$. All the odd harmonics which may be present, particularly that directly related to the mechanical rotational frequency, $f(1)$, and its harmonics, disappear in the integration process. A similar scheme involving three integrations over sectors of the waveform generated by a rotating wave plate has been described by Clarke & Fullerton (1996).

8.5
Variable Phase Delay Modulators

Instruments with polarimetric modulators involving Pockels cells have been described by Angel & Landstreet (1970), Miller, Robinson & Schmidt (1980) and McLean, Heathcote, Paterson, *et al.* (1984), for example. In the instrument described by the last authors, the applied voltage was tuned to produce a phase delay of $\pi/2$. Switching the polarity of the field, reverses the sense of the phase delay, and by applying a field which alternated, the cell was made to behave as a square-wave reversible quarter-wave plate, with a switching rate of 1 Hz. The following polarizer was placed with its principal axis set at 45° to that of the Pockels cell. By considering the Mueller algebra for the arrangement, it is readily shown that the signals corresponding to the alternate modes of the cell are $\frac{1}{2}G_{\|}(I + V)$ and $\frac{1}{2}G_{\|}(I - V)$; another pair of signals given by $\frac{1}{2}G_{\perp}(I - V)$ and $\frac{1}{2}G_{\perp}(I + V)$ is available if the polarizer provides both the orthogonally resolved beams. In order to determine the linear polarization, it must be converted to circular prior to the modulator, and this can be done by inserting a fixed quarter-wave plate. In the instrument designed by McLean, Heathcote, Paterson, *et al.* (1984) for the Anglo-Australian Telescope, alternative quarter wave plates with differing orientations were included, one to convert $Q \longrightarrow V$ and the second to convert $U \longrightarrow V$.

An alternative kind of phase-switching device is the photoelastic modulator (PEM), involving a thick quartz plate which is made to vibrate, the induced stress producing an oscillating phase delay. It operates best when tuned to provide a phase delay of $\pm\pi/2$, again making it an ideal device for the detection of circular polarization. Its resonant frequency is very high (~50 kHz) so that the switching rate readily overcomes the effects of atmospheric intensity scintillation. The original PEM instrument has been described by Kemp, Wolstencroft & Swedlund (1972) and again by Kemp & Barbour (1981). The form of the signal for measurement may be considered by applying the Mueller algebra with the appropriate matrices for the optical elements, and their relative orientations; the value of Δ, corresponding to the phase of the PEM, may be expressed as $\sin(\omega t)$ with the signal involving such terms as $\sin(\sin \omega t)$. By writing

$$\Delta = \frac{\pi}{2} \sin \omega t \tag{8.37}$$

then

$$\begin{cases} \cos \Delta = J_0\left(\frac{\pi}{2}\right) + 2J_2\left(\frac{\pi}{2}\right) \cos 2\omega t + \cdots \\ \sin \Delta = 2J_1\left(\frac{\pi}{2}\right) \sin \omega t \ , \end{cases} \tag{8.38}$$

where J_n is a Bessel function of the first kind and nth order. The complex output signal may be recorded by gating sections of it according to the stimulus signal applied to the cell. Details of the complex form of the polarimetric signal can be found in Hough, Lucas, Bailey, *et al.* (2006). An example of details of an arrangement within an instrument designed for spectropolarimetry, using a sequential scanning monochromator, is given in Wolstencroft, Cormack, Campbell, *et al.* (1983). It may be noted that if a sinusoidal switching signal is applied to a Pockels cell, the form of the output modulation is the same as that of the PEM.

8.6
Simultaneous NSP Measurements

By rotating a quarter-wave plate prior to a fixed polarizer, the signal for measurement is represented by

$$I'(\alpha) = \frac{1}{2}\left[I + \frac{Q}{2} + \frac{1}{2}(Q \cos 4\alpha + U \sin 4\alpha) - V \sin 2\alpha\right]. \tag{8.39}$$

Thus, the Q and U parameters are modulated four times per cycle while the V parameter is modulated twice per cycle; the mean level comprises the value of I plus half the Q intensity. In principle, by recording this waveform, all of the NSPs may be determined, although there appears to be no reference to the use of this simple method.

A successful technique to measure both linear and circular polarization simultaneously by the continuous rotation of a quarter- and half-wave plate in opposite senses was suggested by Serkowski (1974b); it has been developed and implemented at the University of Cape Town (see Cropper, 1985). With this design, any circular component is modulated at six times the rotation rate, and the linear is split equally between four and eight times the rotation rate. In the Cape Town instrument, the mechanical rotation was 10 Hz with the signal for each rotation split into 100 memory sectors. At the end of the integration scheme, the data are fitted to the 4th, 6th and 8th harmonics of the rotational frequency by least squares, and the Stokes parameters are calculated from the amplitudes and phases of the recorded harmonics.

8.7
Spatial Recording of the Polarimetric Modulation

In Chapter 1, it was suggested that stellar polarimetry began to flourish through the advent of the photomultiplier and it is fair to say that most of the accumulated data of interstellar and circumstellar polarization have been obtained using such detectors. The advent of 2D detectors has now allowed observational research into polarimetry of individual stars, star fields, extended objects and stars at high spectral resolution, in a more efficient way. Using these detectors has also offered the challenge that measurements of improved accuracy might be pursued for broadband measurements.

Equation (5.2) shows that the ultimate accuracy of any measurement of an NSP, such as q, depends simply on the number of photons, n_o, registered during the integration with the uncertainty (1σ), Δq, given by $\pm 1/\sqrt{n}_o$. Unfortunately, the photomultiplier carries a dead-time limitation when photon counting techniques are applied. If the photon arrival rate is too high, counts are lost as a result of pulse overlap and, because of non-linearities, corrections for this can only be applied successfully when count rates are only just above the critical value. Discussion on this problem is provided in Clarke & Naghizadeh-Khouei (1994). Generally, photon detection rates should not be allowed to be much greater than $10^5\,\mathrm{s}^{-1}$. At such a rate, an uncertainty of $\Delta q \sim \pm 0.0001$, requiring a photon count of 10^8, can only be achieved by an integration $\sim$1000 s.

For large aperture telescopes and for the measurement of brighter stars, the potential photoelectron rate is embarrassingly high for photon counting techniques. In some observational studies, the dead-time problem has been avoided by using neutral density filters to reduce the detectable flux, and then extending the experimental time to accumulate the necessary photon count – a somewhat defeatist solution.

One approach for gleaning the maximum information from the collected photons and improving polarimetric detection limits is to use a solid-state detector such as a PIN diode. The output requires digitization of the analogue signal by a voltage-to-frequency converter with the appropriate linearity and dynamic range (see Hough, Lucas, Bailey, *et al.*, 2005, Hough, Lucas, Bailey, *et al.*, 2006). An alternative is to consider the application of CCDs.

In accumulating the necessary large photoelectron counts, it is important that the pixel records of the CCD are well below saturation ($\sim 5 \times 10^5$ electrons) to prevent non-linear effects, thus limiting the accuracy per pixel to Δq or $\Delta u \sim \pm 0.01$. For stellar images, atmospheric seeing spreads out the flux over several tens of pixels allowing more photoelectrons to be recorded in an image in any one frame. Photometric experience shows that differential stellar brightness values can be achieved fairly readily to an accuracy $\sim \pm 0.^{\mathrm{m}}001$. By recording orthogonally resolved images simultaneously, the immediate potential accuracy of Δq or Δu is $\sim \pm 0.0005$ per frame. For brighter sources, to prevent saturation, the images may be defocussed to spread the flux over a larger number of pixels, with the potential of further increasing polarimetric accuracy.

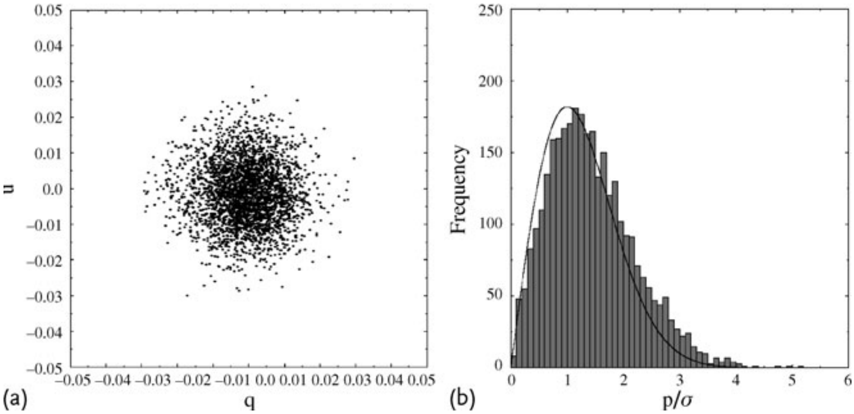

Fig. 8.3 (a) shows the distribution of ~ 3000 q, u pixel measurements centred on the origin of an NSP diagram for the unpolarized standard star, θ Boö, the data obtained from four CCD frames of the image of the telescope aperture. (b) displays the histogram of (p/σ) values for the adjacent data showing that it closely follows a Rice distribution corresponding to $p_0 = 0$. The slight displacement of the histogram pattern indicates the presence of a very small polarization which is generated by the outer annuli of the telescope mirror. (The material is taken from Clarke & Naghizadeh-Khouei, 1997.)

The ultimate way of using CCDs to achieve the highest polarimetric accuracy for a single star is to consider a design whereby the source is isolated in the telescope focal plane, and then the radiation passed through the modulator and an imaging system so that the telescope aperture is focussed on the chip. This has the advantage of the illuminated patch being fixed, even if there is image movement in the telescope focal plane. A further advantage of the system is that any patchy polarizing effects of the telescope mirrors contributing to the instrumental polarization can be explored by observing standard unpolarized stars and, in the subsequent data reductions, applying appropriate corrections to each pixel within the aperture image.

A prototype aperture imaging polarimeter of this kind was tested by Clarke & Naghizadeh-Khouei (1997). By using a Savart plate, the instrument was designed to produce two images of the telescope aperture on the same CCD chip. Switching the orthogonally resolved polarizations was achieved by a rotatable half-wave plate. For each stellar polarimetric measurement some 3000 pixels were used, and final accuracies in NSPs of ±0.0001 were readily achieved. An example of measurements of a standard unpolarized star is shown in Figure 8.3. When the data are grouped together in zones across the image of the aperture, mean values of the measurements clearly indicated that the telescope mirror introduced small amounts of polarization with the outer annuli being the most affected in this way. Also in Figure 8.3, a histogram of the p/σ values is depicted relative to the Rice distribution for $p_0 = 0$; the small disparity of the data relative to the theoretical distribution curve relates to a mirror-induced polarization.

Another novel approach to spatial imaging for recording stellar polarizations is by a method pioneered by Treanor (1968). Using a very simple arrangement, he demonstrated that polarimetric information might be encoded as a spatial record for registration by a two-dimensional detector such as a photographic plate. In his instrument, a polarizer was rotated together with a glass wedge prior to the telescope focus. Stellar images were then recorded in the form of annuli. If the light from a star is polarized, the corresponding annulus carries an intensity modulation with a variation of the form given by (8.3), i. e.

$$S(\theta) = I\{1 + p\cos 2(\theta - \zeta)\}, \tag{8.40}$$

where θ defines the angular position around the annulus. The principle was applied to star fields with many stars being recorded simultaneously on a single photographic plate. The technique appeared to have been abandoned because of the poor quantum efficiency of emulsion photography, and other problems associated with calibrations and data reduction procedures.

With the advent of CCD detectors, Treanor's idea has been reconsidered by Clarke & Neumayer (2002) and a system has been developed by Steele, Bates, Carter, *et al.* (2006) for use on an automated telescope for immediate optical follow up of gamma-ray burster events. As well as undertaking polarimetry of stellar fields, the technique can be applied to individual stars. Using a large number of pixels near to full well capacity, a very large number of photons can be accumulated to achieve high accuracy for the measured value. The modulator may be simply a rotating tilted disc of high quality sheet polarizer. A rotating Rochon prism, with its weak spectral dispersion, might also be used to provide high accuracy, low spectral resolution spectropolarimetry, the annuli having a radial spread according to wavelength.

Oliva (1997) has designed a specially constructed wedged double Wollaston prism. For the simple case of recording the polarization of star fields, by using the appropriate optics, it can be placed at the image of the telescope aperture. By re-imaging the field on a CCD chip, four images are produced simultaneously corresponding to the polarization directions 0°, 90°, 45° and 135°, from which both q and u can be determined. Thus all the linear polarization characteristics can be measured from a single CCD frame. By placing it at a pupil image within a spectrometer, single frame spectropolarimetry may also be undertaken.

8.8
Spectropolarimetry

In many polarimeters, spectral measurements can be made by the insertion of filters in the system. The best location to do this is after the modulator system so that the filter does not introduce any spurious polarization into the measurements. The spectral bandpass is dictated by the choice of filters and, in some instruments, high resolution has been achieved by narrow-band interference filters. By tilt-tuning these devices (see Clarke, McLean & Wyllie 1975), it was possible to obtain $p(\lambda)$ measurements across line profiles. Instruments involving this technique have had particular success at Hβ and Hα (see, for example, Clarke & McLean, 1975, 1976).

With the advent of 2D detectors such as CCDs, measurements can be made simultaneously at multi-wavelength positions, and single-point sequential scanning has now been abandoned. It is now possible to conduct spectropolarimetry at high resolution and over a broad spectral range. By using a Savart plate prior to the entrance slit of a spectrometer, two spectra corresponding to the orthogonal beams can be produced which may be recorded side by side. Insertion of an achromatic rotatable half-wave plate prior to the polarizing beam splitter allows the NSPs to be determined across the recorded spectra.

With the accuracies that such systems provide, problems of the wave plate polarizance and 'fringing' have become apparent in the raw data. The matrix written as [Wave Plate] in (8.15) describes the effect of the wave plate that, for a pure device, simply includes terms describing the effects of the phase delay. In reality, as discussed in Chapter 6, it also needs to include the effects of a polarizance. Its form is therefore represented by (6.5) or (6.6). Using the latter equation, and following multiplying out the matrices in (8.15), the signal for measurement, $\mathcal{S}(\alpha)$ may be organized to be written as

$$\begin{aligned} 2\mathcal{S}(\alpha) = {} & k_1(I + Q\cos 4\alpha + U\sin 4\alpha) \\ & - k_3 V \sin\varDelta \sin 2\alpha \\ & + k_2(I\cos 2\alpha + Q\cos 2\alpha + U\sin 2\alpha) \\ & + (k_1 + k_3\cos\varDelta)\left(Q\sin^2 2\alpha - \frac{U}{2}\sin 4\alpha\right) . \end{aligned} \tag{8.41}$$

In exploring the behaviour of (8.41), it is expected that k_1 and k_3 are both close to unity, with $k_2 \approx 0$. If linear polarization is being measured, it can be seen that, in addition to the expected α modulation of the Stokes parameters, the polarizance introduces a spurious signal according to 2α, however. This problem is exacerbated by the effects of 'fringing' caused by multiple beam interference within the wave plate. The modulation efficiency, dependent on the value of $\cos\varDelta$, is also subject to fringing.

In considering these issues, Clarke (2005) has provided observing strategies that help to alleviate the various troublesome effects. For linear polarization measurements, the polarizance of the wave plate and its fringe structure can be calibrated out by making measurements at $\alpha = \pi/2$ and $3\pi/4$, in addition to $\alpha = 0$ and $\pi/4$, for the determination of q (see (8.29)). Similarly, measurements made at $\alpha = 5\pi/4$ and $7\pi/4$, in addition to those at $\alpha = \pi/8$ and $3\pi/8$, allow the polarizance calibration with respect to the u parameter (see (8.30)). As a result of linear-to-circular cross-talk with fringe structures, the spectral measurement of circular polarization is particularly prone to misinterpretations. If 'fringing' remains evident in the raw data, the reduction problem can only be dealt with properly by determining the elements of the matrix of the wave plate for each spectral point and performing inversion procedures rather than simple off-set subtractions. Stability of the 'fringe' structures is also an issue and it is important to operate with a modulator that is temperature stabilized.

8.9
Polarimetric Instruments

A basic stellar polarimeter comprises a modulator and detector system. The units are usually mounted within a box for attachment to the telescope. This self-contained polarimetric head may provide observer support devices such as retractable transfer optics for inspection of the telescope image prior to the measurements. Instruments using photomultiplier detectors require the use of a field stop or field-limiting diaphragm, in similar fashion to a regular photometer. According to Pospergelis (1965), the field stop must have a knife edge of strictly circular shape, with minimal reflecting surface at its edge. The aperture should be made with non-metallic material such as ebonite, and the beam must pass through the hole symmetrically. If these conditions are not met, spurious linear polarization of up to 0.1% may arise.

The simplest form of modulator is a rotatable polarizer prior to a detector. As described at the beginning of the chapter, an early polarimeter of this type, used by Hiltner (1951a), was a standard photometer with a *Polaroid* inserted whose orientation was adjustable to selected positions. In a system described by Hall (1951), a continuous rotating Glan–Thompson prism was employed. With this instrument, the probable error of the measurements was typically $\sim$0.2%, one of the chief problems being atmospheric intensity scintillation noise.

A pioneering double-beam polarimeter using a Wollaston prism was constructed by Gehrels & Teska (1960). The output signals for the two channels with photomultiplier detectors were simply recorded by DC amplifiers and pen recorder systems. An early design of double-beam polarimeter was also used by Serkowski & Chojnacki (1969). The system comprised a Wollaston prism, with further separation of the resolved components by the apex of an aluminized 97° prism. The instrument was rotatable in steps of 45° on the telescope mounting plate. Signals were obtained from photomultipliers illuminated via Fabry lenses so that the telescope pupil was imaged on them. Difference signals were recorded, and detector imbalances were calibrated using a depolarizer.

Many of the early instruments involving stepped rotation of wave plates or polarizers were controlled by hand. As computer control became an eventuality, such operations were performed by using stepper motors. An early automated system was described by Kinman & Mahaffey (1974), this being similar to the design of Visvanathan (1972).

In order to reduce sky background contamination that is prevalent at high latitude observatories, Piirola (1973, 1975) designed an instrument with built-in compensation. Two diaphragms were placed in the focal plane of the telescope and by a mechanical chopping arrangement, the detector was alternatively illuminated by star plus sky background and then just by an equal area of the sky alone; in this way the contaminating signal from the sky was automatically subtracted. The same principle was also incorporated by Korhonen, Piirola & Reiz (1984) and Piirola (1988) in a more sophisticated instrument allowing simultaneous five-band multi-colour observations.

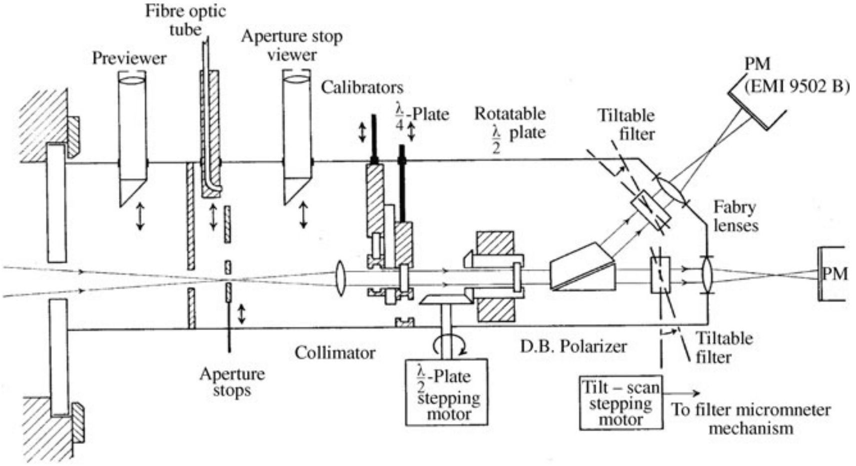

Fig. 8.4 An early double-beam polarimeter of the 1970s capable of making measurements at selected positions in the Hα and Hβ lines. Note that within the instrument, the beam is collimated. (Taken from Clarke & McLean, 1975.)

A system using a variation of a Foster prism as the polarizer and means for eliminating the contaminating signal from the sky background has been described by Metz (1984). In a later development, Metz (1986) discussed the remedy for the problem of instrumental polarization introduced by the fixed superachromatic wave plate which is incorporated after the rotatable one to counter spectral dispersion of the instruments reference axis. Compensation for sky contamination was effected in an instrument used by Jain & Srinivasulu (1989) by rotating an eccentrically placed aluminium plate with two semi-circular slots in it, prior to the focal plane of the telescope.

The principle of the rotating half-wave plate polarimeter has been described earlier in this chapter. An instrument using a rotatable achromatic wave plate prior to a Wollaston prism, followed by further geometric separation of the beams, with the signals recorded by photomultipliers and photon counting techniques, has been described by Appenzeller (1967). The design for this is based on that of Hiltner (1959), and is shown in Figure 8.1, which is in the form of an original sketch by him. A dual-beam polarimeter, as sketched out in Figure. 8.4, incorporating a rotatable achromatic wave plate, and capable of spectral studies within stellar line profiles, has been described by Clarke & McLean (1975). For multi-band work, the problem of dispersion of the phase delay of the rotating element was overcome by using a superachromatic design. As described in Frecker & Serkowski (1976) such an instrument can be operated over the wavelegth range of 300 nm to 1.1 µm. Their system known as 'MINIPOL', and mentioned earlier, formed the basis of an instrument described by Benedetti (1982) and Magalhães, Benedetti & Roland (1984) which also incorporated a facility for tilt-scanning narrow-band interference filters, following the principles used by Clarke, McLean & Wyllie (1975).

In the design of Bailey & Hough (1982), the two beams emerging from the double-beam polarizer were fed to detectors of different spectral sensitivity. One arm was capable of making measurements through the visual range, while the other allowed near infrared observations. By using a rotating superachromatic retarder prior to the polarizer, the instrument was able to make $UBVRIJHK$ measurements, according to the filter selection. Using a rotating achromatic wave plate modulator, followed by dichroic filters, a system allowing the monitoring in eight different passbands simultaneously has been described by Kikuchi (1988).

The Dollfus design of modulator was developed by Tinbergen (1972) to incorporate achromatic wave plates. Tinbergen's prototype used plastic components for the compound wave plates, and the instrument, even in this primitive form, proved to be successful. A further improvement was suggested by Chen (1979), which involved a Pancharatnam type wave plate with uniform retardation and no variation of reference axis orientation over the range 0.35–1 µm.

Most of the early spectropolarimeters incorporated filters to achieve spectral resolution. A significant development in terms of spectral resolution and flexibility of selected passbands was made by Wolstencroft & Nandy (1971). They converted a wavelength scanning spectrometer to allow polarimetry at sequential positions in the spectrum; the single pixel nature of the photomultiplier detector, however, necessitated long observing runs to achieve data with good spectral coverage.

The PEM is particularly clean in that it produces an oscillating phase delay with little or no polarizance, making it very suitable for the detection and measurement of circular polarization. The pioneering work of producing this device and applying it to Astronomy was undertaken by J. C. Kemp. An early successful instrument that provided measurements of 15 objects was described by Kemp, Wolstencroft & Swedlund (1972); its development formed the basis of the production of many papers involving new astrophysical scenarios, and it was described again in Kemp & Barbour (1981). A PEM system was also used by Wolstencroft, Cormack, Campbell, *et al.* (1983) prior to a standard spectrometer, with a photomultipler as the detector. The instrument was able to explore $p(\lambda)$ structure by sequential scanning through the spectrum. An instrument of very high sensitivity using a PEM has recently been developed by Hough, Lucas, Bailey, *et al.* (2006) with the aim of discovering extrasolar planets by polarimetry.

An early form of spectropolarimeter was devised by Nordsieck (1974) whereby fringes were imposed on the recorded spectra, their modulation carrying information on the Stokes parameters. The optical system included two thick multi-order quartz wave plates, the first 1 mm thick, the second 3 mm thick, and adjustable in orientation relative to the first.

One of the best sets of data related to polarimetric structure across the Balmer lines of Be stars, and still remaining so, is that presented by McLean, Coyne, Frecker, *et al.* (1979). Their spectropolarimeter used a 'Digicon' as the detector, the device offering a photon counting system with 200 silicon diodes in two parallel rows, all contained in the same glass envelope. The records were obtained without sequential scanning through the spectrum. Unfortunately the Digicon systems had short working life-times because of outgassing problems associated with the very large number of connection wires emerging from the glass envelope.

By the end of the 1970s, the development of 2D linear response detectors with quantum efficiencies considerably greater than photographic plates began to displace single pixel photomultipliers. The impact of the change, with new data logging techniques, is clearly seen in the papers collected in McCarthy (1980), and, in particular, in the presentation of McLean (1980).

A simple modulator made from inexpensive optical components to allow spectropolarimetry through the visual spectrum from 430 to 800 nm has been described by Walker, Dinshaw, Saddlemyer, *et al.* (1993). The telescope/spectrometer arrangement was of long standing, and included an image slicer. Because of the polarization characteristics of the latter, a quarter-wave plate was inserted converting any linear polarization to circular. Differential polarization values were obtained and structure across stellar spectral lines was sensed at levels ~0.01%.

A spectropolarimeter using a Pockels cell modulator, prior to a standard Cassegrain spectrometer, with an intensifier-dissector-scanner type detector has been described by Tomaszewski, Symonds & Landstreet (1980). The instrument was capable of recording $p(\lambda)$ over a spectral window of 2000 Å with a resolution of 15–20 Å. A similar scheme was also developed by McLean, Heathcote, Paterson, *et al.* (1984) for the Anglo-Australian Telescope, but using an Image Photon Counting System (IPCS) detector. A Pockels cell modulator was also used in an instrument constructed by Miller, Robinson & Schmidt (1980).

In the system described by Östreicher & Schulte-Ladbeck (1985), the modulator comprised a rotatable $\lambda/2$ plate followed by two perpendicular orientated sheet polarizers with a mechanism to chop between them. The system was then connected to the spectrometer by a fibre optic link.

As CCDs can store and shift the charge produced by the illuminating photons, Miller, Robinson & Goodrich (1987) have described a spectropolarimeter and discussed several strategies for the polarimetric modulation using a Pockels cell, and for the assembly of the data. One approach involved the recording of orthogonal polarization states in repeated succession. By using a three-phase CCD, a short exposure may be made for one of the polarization forms, followed by an image shift. Another exposure is then made for the orthogonal form on the same part of the chip, followed by an image shift in the opposite direction. The process is then repeated until sufficient photons have been accumulated and the record is then read out. In summary, two images are recorded with orthogonal polarization states but recorded on the exact same pixels so that non-uniform response of the CCD is not important in the data reduction. However, problems associated with the image transfer processes caused the scheme to be abandoned. It was also found that if the modulation rate was very slow, the Pockels cell could not withstand DC operation and gradually became cloudy. The final arrangement involved the use a rotatable superachromatic wave plate prior to a specially constructed double-beam polarizer which provided two images on the spectrometer slit. Observations were made at fixed orientations of the wave plate. In a later design, Goodrich (1991) has considered the use of a superachromatic wave plate prior to a novel polarizer beamsplitter, the modulator being very efficient and compact, the latter property usually being an issue in retrofitting a unit to an existing spectrometer.

The behaviour of Zeeman split spectral lines over the rotational cycle of stars holds the potential to undertake magnetic topography. Following Babcock's pioneering work, several instruments have been designed for such studies. An example is that described by Vogt, Tull & Kelton (1980). After making compensation for the phase change introduced by the telescope coudé mirror, the modulator comprised a $\lambda/4$ plate and a calcite beam-splitter. The problems of operating with coudé spectrometers have generally been phased out with the development of modern spectrometer designs. High spectral resolution can now be achieved using echelle gratings with the instrument at the Cassegrain focus, thereby introducing the minimum of disturbing effects by the telescope mirrors.

A modulator designed for the MuSiCos èchelle spectrograph has been described by Donati, Catala, Wade, *et al.* (1999). This design is capable of studying magnetic topologies of active and chemically peculiar stars over the rotational cycle for linearly and circularly polarized Zeeman signatures in line profiles. The issue of polarimetric fringes being generated within wave plates was discussed, it being noted that their severity depended on the particular manufacturer.

Several instruments have been developed using a scheme promoted by Öhman (1939). In a review by Scarrott (1991), the principle is elaborated whereby a mask comprising slits is placed in the focal plane of the telescope (see Figure 8.5). The focal plane is re-imaged onto a CCD chip. By using a double-beam polarizer, the images for the orthogonal beams are recorded so that one of them is deviated into the areas corresponding to blanked off zones in the telescope's focal plane, while

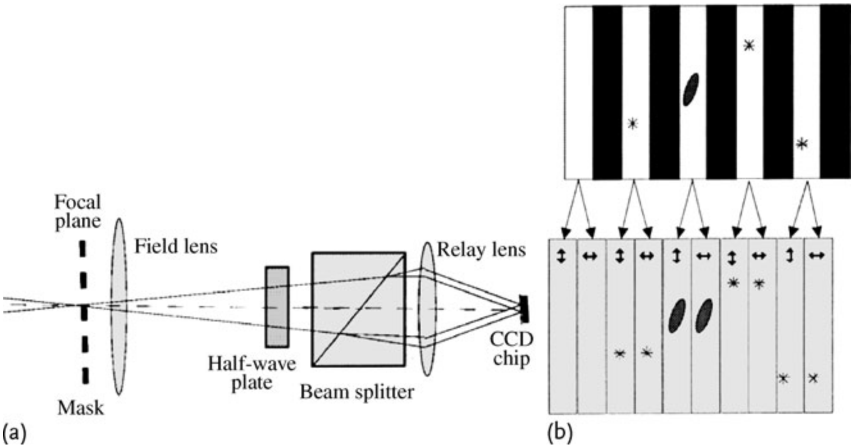

Fig. 8.5 (a) sketches the basic optical layout of an imaging polarimeter with the mask of parallel rulings in the focal plane of the telescope; the half-wave plate, prior to the Savart plate, is rotatable. Images of the transparent strips in the focal plane are split to form orthogonal pairs on the CCD camera (b). (Taken from Scarrott, 1991.)

the other beam is imaged in what would have been a transparent zone. On the CCD frames, pairs of images are recorded side by side for the orthogonal polarizations. The modulator is completed by having a rotatable wave plate prior to the double-beam polarizer. Half of the field is lost because of the blanking out strips of the mask, but two sets of observations can be considered by off-setting the telescope by the appropriate angle according to the mark-to-space ratio of the mask. Generally an instrument of this kind is used for measurements of extended objects such as reflection nebulae but it can be used for investigating star fields – see, for example, Magalhães, Rodrigues, Margoniner, *et al.* (1996). An imaging polarimeter based on this design has also been described by Ramaprakash, Gupta, Sen, *et al.* (1997).

The WUPPE instrument (Wisconsin Ultraviolet Photo-Polarimeter Experiment) had unprecedented success when it was aboard the Astro-1 mission on the Space Shuttle Columbia in December 1990. An example of its notable achievements in performing UV spectropolarimetry of Be stars can be found in Bjorkman, Nordsieck, Code, *et al.* (1991). A polarimeter designed to operate in the far ultraviolet at wavelengths from 135 to 260 nm for the launch as sounding rocket payloads has been described by Nordsieck, Marcum, Jaehnig, *et al.* (1993).

8.10
Instrument Calibrations

8.10.1
Reference Frame

Most instruments are designed so that, when they are attached to the telescope, their reference frames used to describe measurements of the Stokes parameters are set with positive q running parallel with Declination. To check on this, or to determine the axes of an instrument bolted to the telescope focus at some arbitrary orientation, several experimental strategies are available. It should be noted that, according to Hsu & Breger (1982), systematic differences of the order of 1° are not uncommon when measurement of stars made by different authors are compared, despite claims by them that the absolute zero point of the position angle has been determined to some fraction of a degree.

Gehrels & Teska (1960) used a large sheet of *Polaroid* which was loosely hung in the light path of a laboratory lamp with the telescope pointed horizontally and set at 0° in hour angle. The instrument box was rotated to be crossed with the suspended *Polaroid* to obtain the minimum signal. The *Polaroid* was rotated about the plumb-line axis by 180° and the 'crossing' procedure repeated. The mean value of the two position angles of the instrument gives the orientation of the polarizer in the instrument with respect to the meridian vertical. On each occasion, this calibration exercise was performed twice either on both sides of the pier, or with the telescope pointed north and south; the probable error of the calibrations was $\pm 0.^{\circ}06$. The same procedural principle has been described for the optical laboratory by Rowell, Levit & Ghaffer (1969), who described a method of setting the axis of a polarizer in a rotatable mount calibrated in angular measure by suspending it in a beam of polarized light. The exercise requires that the extinction is obtained, and the angular setting noted; after rotating the mount by 180° about the suspension axis, extinction is obtained again, and the setting noted on the mount. The mid-point between the two noted angular measurements corresponds to the axis of the polarizer. According to Aspnes (1970), however, small systematic errors can occur with this technique when determining the axis of prism polarizers such as the Glan–Taylor air-gap calcite device. It has also been noted by Serkowski (1974a) that some *Polaroids* are not perfect in that they may rotate the direction of vibration by as much as $0.^\circ 2$.

To secure the reference axis of a *Polaroid* with respect to equatorial coordinates, Serkowski (1965) directed the telescope to the daylight cloudy sky with the telescope exactly in the meridian. By placing a glass plate in a perfectly horizontal position, the telescope was adjusted in Declination so that the sky was viewed through it and the *Polaroid* after reflection at Brewster's angle. Extinction was achieved by rotation of the *Polaroid* to an angular setting with uncertainty not exceeding $0.^\circ 3$.

In the exercise to establish a set of polarization standard stars for the Hubble Space Telescope, Schmidt, Elston & Lupie (1992) measured lunar light scattered by the Earth's atmosphere in the Sun–Moon–Earth plane, the polarization azimuth being normal to this.

The direction of vibration of the polarization of light from planets or asteroids is either perpendicular or parallel to the scattering plane, according to the phase angle. Calibration of the instrumental axis relative to equatorial coordinates can be obtained by observing these objects at suitable phase angles as suggested by Serkowski (1974a), following an earlier description of the process by Gehrels & Teska (1960).

In the scheme devised by Dolan & Tapia (1986), a Glan–Thompson prism was insertable in a slide so that its principal axis was aligned with cross-hairs of the eyepiece used to view the field around any target star. The polarimeter was then rotated on its mounting plate so that the cross-hairs were parallel to the N/S and E/W directions, this being checked by moving the telescope in these directions via the guidance controls. When inserted, the polarizing prism converts any targeted star to act as a reference source with $p = 100\%$, and with the position angle parallel to the N/S axis of equatorial coordinates. For this arrangement the reference axis was determined with an uncertainty $< 0.^\circ 1$. Another possibility might involve the use of an insertable Savart plate so that a pair of stars produces four images. By rotating the plate, these images may be adjusted so that they are co-linear. Each of the four pencils will comprise light with $p = 100\%$, with directions of vibration set at 45° to the line joining the images; one pair of images will carry a direction of vibration orthogonal to that of the other pair. Measurement of the polarizations allows the directions of vibration to be referred to the line joining the images which in turn can be related to equatorial coordinates via the catalogued coordinates of the pair of stars.

Most new polarimetric studies do not undertake fundamental observational procedures as outlined above, but determine the instrumental axis by reference to concurrent measurements of stars which are known to display high values of interstellar polarization, these assumed to be constant with time.

8.10.2
Standard Stars

8.10.2.1 **Polarized Standards**

For all new observational polarimetric studies, it is important to have standard stars available for concurrent measurement. These should comprise stars with a constant, high level of polarization – *polarized standards* – with values of p and position angle, known to high levels of accuracy, to provide a reference axis for the instrument on the telescope, and to allow calibration of its modulation efficiency. Another set of stars known to be stable with polarization so small as not to be detectable – *unpolarized standards* – should also be available to allow investigation of any instrumental polarization (see Section 5.5). For the polarized standards, it may also be important to know their wavelength-dependent behaviour. A problem associated with the provision of standards for position angle was exposed by Gehrels & Silvester (1970) who discovered that many stars exhibit spectral dispersion in this parameter, possibly as a result of complications in the interstellar clouds along the line of sight. Many observationalists refer to tables within Serkowski (1974b), which provide a selection of standard stars; his *Polarized Standards* are re-listed in Table 8.1 and the *Unpolarized Standards* are given in Table 8.2, with his supplementary list in Table 8.3.

A self-inherent problem concerns the stability of measurements of stars with relatively high values of polarization, and it is likely that variability of some *Polarized Standards* is inherent to some degree. In order for large interstellar polarization to accrue, a considerable line of sight dust column is required. The accompanying interstellar absorption imposes that for stars to have a reasonable apparent brightness to allow easy measurement, they tend to be intrinsically bright early-type supergiants. Several nearby stars of this type, with little or no interstellar polarization, are known to exhibit variable polarization (e. g. see Hayes, 1984, 1986). If the poligenic sources involve a combination of intrinsic stellar atmospheric effects and the interstellar medium, small levels of variability may be recorded, if the star is itself variable.

With respect to the values of position angle, Dolan & Tapia (1986) conducted a special study on stability and found that 9 of 11 selected stars from Serkowski's Table of *Standard Stars with Large Interstellar Polarization* exhibited significant spectral dispersion of position angle, primarily caused by the vector combinations of intrinsic and interstellar effects. Their summary concludes that $\Delta\zeta/\Delta\lambda$ is generally not linear but complex, and that no stars can be taken as satisfactory standards at the $0.^\circ1$ level of accuracy. Hsu & Breger (1982) have discussed some of the problems associated with the establishment of standard stars and suggest that 55 Cyg (HD 198478), 9 Gem (HD 43384) and HD 183143, sometime taken as polarized standards, all display variability. Viråghalmy (1986) also provides evidence that 55 Cyg, a well-known supergiant spectrum variable, is polarimetrically vari-

Table 8.1 Standard stars with large interstellar polarization as in Appendix 3 of Serkowski (1974b). The column headed λ_{max} corresponds to the wavelength (μm) at which the polarization is a maximum and is taken from Serkowski, Mathewson & Ford (1975). The list of p values (%) and position angles, ζ°, refer to values at λ_{max}.

HD	Star	α_{2000}	δ_{2000}	m_V	Sp Type	λ_{max}	p_{max}	ζ°
7927	ϕCas	01 20.1	+58 14	5.0	F0 Ia	0.51	3.4	94
14433	+56° 568	02 21.9	+57 15	6.4	A1 Ia	0.51	3.9	112
21291	2H Cam	03 29.1	+59 57	4.2	B9 Ia	0.53	3.5	115
23512	+23° 524	03 46.6	+23 38	8.1	A0 V	0.61	2.3	30
43384[a]	9 Gem	06 16.9	+23 44	6.2	B3 Ia	0.53	3.0	170
80558	HR 3708	09 18.7	−51 33	5.9	B7 Iab	0.61	3.3	162
84810	l Car	09 45.3	−62 31	3.3–4.0	FO – K0 Ib	0.57	1.6	100
111613	HR 4876	12 51.3	−60 20	5.7	A1 Ia	0.56	3.2	81
147084	oSco	16 20.6	−24 10	4.6	A5 II–III	0.68	4.3	32
154445	HR 6553	17 05.6	−00 53	5.7	B1 V	0.55	3.7	90
160529	−33° 12361	17 41.9	−33 30	6.7	A2 Ia +	0.54	7.3	20
183143	+18° 4085	19 27.4	+18 17	6.9	B7 Ia	0.56	6.4	0
187929	ηAql	19 52.5	+01 00	3.5–4.3	F6–G2 Ib	0.56	1.8	93
198478[b]	55 Cyg	20 48.9	+46 07	4.9	B3 Ia	0.53	2.8	3
204827	+58° 2272	21 29.0	+58 44	7.9	B0 V	0.47	5.7	60

[a] Exhibits variable polarization according to Hsu & Breger (1982).

[b] Exhibits variable polarization according to Hsu & Breger (1982) and Viråghalmy (1986).

Additional Notes summarized from Dolan & Tapia (1986).

HD 927 Known to display $\zeta(\lambda)$ with inflection at 7000 Å (Gehrels & Silvester, 1965, Coyne & Gehrels, 1966, Hsu & Breger, 1982); ζ also time dependent – a poor standard.
HD 21291 Displays $\zeta(\lambda)$ – best interpretation being ‘intrinsic + interstellar’.
HD 43384 Displays $\zeta(\lambda)$; behaviour agrees with Serkowski & Robertson (1969) and Serkowski, Mathewson & Ford (1975) – interpreted as two interstellar clouds with different alignments.
HD 80558 Little or no $\zeta(\lambda)$ – no significant differences between various workers.
HD 111613 Little or no $\zeta(\lambda)$ – but small variations with time.
HD 147084 No $\zeta(\lambda)$ – no differences noted between various workers.
HD 160529 $\zeta(\lambda)$ has an inflection similarly recorded by various workers – difficult to reconcile by two cloud model.
HD 183143 Flat $\zeta(\lambda)$ on some nights, variation on others – no pattern in qu-plane.
HD 187929 Marked $\zeta(\lambda)$ with an inflection; differences in ζ values are apparent with respect to Hsu & Breger (1982). A marked $\zeta(\lambda)$ was recorded by Clarke (1986).
HD 198478 The $\zeta(\lambda)$ is significant and there is a 3° difference with respect to Hsu & Breger (1982), but consistent with Coyne (1974).
HD 204827 Time variability of ζ on a scale of a month.

able. Berdyugin, Snåre & Teerikorpi (1995) have used HD 161056 as a high polarization standard, as its position angle, according to Bastien, Drissen, Ménard, *et al.* (1988), appears to be constant to within 1°.

Table 8.2 Unpolarized nearby standard stars observed with rotatable tube telescopes as listed in Appendix 1 of Serkowski (1974b). The spectral bandpass of the measurements is ∼ 0.4 to 0.6 µm. The numbers under the heading of Ref refer to: 1. Appenzeller (1966); 2. Serkowski, Mathewson & Ford (1975); Serkowski (1968); 4. Walborn (1968).

HD	Star	α_{2000}	δ_{2000}	m_v	Sp type	r (pc)	p	$\zeta°$	Ref
432	βCas	00 09.0	+59 09	2.2	F2 IV	14	0.009±0.009	32	1
10476	107 Psc	01 42.6	+20 17	5.2	K1 V	8	0.016±0.006	175	2
20630	κCet	03 19.3	+03 22	4.8	G5 V	10	0.006±0.008	135	3
38393	γ Lep A	05 44.5	−22 26	3.6	F6 V	8	0.005±0.008	130	2,3
39587	χ^1Ori	05 54.4	+20 17	4.4	G0 V	10	0.013±0.007	20	2
43834	αMen	06 10.2	−74 45	5.1	G5 V	9	0.009±0.010	142	2,3
61421	αCMi	07 39.4	+05 15	0.3	F5 IV	4	0.005±0.009	145	2,3
100623	−32°8179	11 34.6	−32 51	6.0	K0 V	10	0.016±0.012	57	2
102870	βVir	11 50.6	+01 47	3.6	F8 V	10	0.017±0.014	162	2
114710	βCom	13 12.0	+27 51	4.3	G0 V	8	0.018±0.014	116	2
115617	61 Vir	13 18.6	−18 17	4.8	G6 V	9	0.010±0.006	132	2,3
142373	χHer[a]	15 52.6	+42 26	4.6	F9 V	18	0.012±0.009	31	4
155885/6	36 Oph AB	17 15.4	−26 34	4.3	K1 V	5	0.005±0.007	61	3
165908	99 Her AB	18 07.0	+30 34	5.0	F7 V	17	0.002±0.007	39	4
185395	θ Cyg	19 36.5	+50 12	4.5	F4 V	15	0.003±0.007	139	4
188512	βAql	19 55.3	+06 25	3.7	G8 IV	14	0.012±0.005	154	4
198149	ηCep	20 45.3	+61 49	3.4	K0 IV	14	0.006±0.005	101	4
209100	ϵInd	22 02.5	−56 43	4.7	K5 V	4	0.006±0.008	88	2,3
210027	ιPeg	22 07.0	+25 20	3.8	F5 V	14	0.002±0.006	45	4
216956	αPsA	22 57.6	−29 37	1.2	A3 V	7	0.006±0.009	89	3

[a] Exhibits polarization according to Piirola (1977).

In an effort to establish a set of *Polarization Standards* suitable for use with the emerging polarimetric star-field instrumentation involving CCD detectors, Clemens & Tapia (1990) have reinvestigated 16 stars previously measured by Mathewson & Ford (1970) and have promoted 12 which might be used as standards. Proposals with respect to the establishment of polarimetric standard stars have been made by Bolkvadze & Sigua (1986).

In addition, to concerns of variable intrinsic polarization, the stability of the constancy of interstellar polarization itself has been challenged by Bastien, Drissen, Ménard, *et al.* (1988). From their analysis of repeated measurements of some standard stars, they suggested that the interstellar line of sight dust columns might be fluctuating on time scales of a few weeks. Their statistical analysis of the suspected variability was later shown by Clarke & Naghizadeh-Khouei (1994) to be flawed, but the original contention of the temporal variability within the interstellar medium,

Table 8.3 Nearby stars of spectral type G fainter than 6.5 mag as listed in Appendix 2 of Serkowski (1974b) (these stars may be useful for determining any instrumental polarization and were selected from the catalogue by Gliese (1969). They have not been fully checked out by rotatable telescopes and have not been heavily monitored for stability).

HD	BD CoD	α_{1975}	δ_{1975}	m_v	Sp type (MK)	Distance (pc)
9540	−24°658	1 32.1	−24 18	7.0	G8 V	16
9407	+68°113	1 32.7	+68 37	6.5	G6 V	20
18803	+26°503	3 01.0	+26 31	6.7	G6 V	18
42807	+10°1050	6 11.8	+10 39	6.5	G6 V	18
65583	+29°1664	7 59.0	+29 18	7.0	G8 V	17
90508	+49°1961	10 26.5	+48 56	6.5	G1 V	19
98281	−04°3049	11 17.0	−04 55	7.3	G8 V	20
102438	−29°9337	11 46.0	−30 09	6.5	G5 V	18
103095[a]	+38°2285	11 51.4	+37 56	6.5	G8 VI	9
125184	−06°3964	14 16.7	−07 25	6.5	G8 V	16
144287	+25°3020	16 03.0	+25 19	7.1	G8 V	19
144579	+39°2947	16 04.1	+39 16	6.7	G8 V	12
154345	+47°2420	17 01.9	+47 06	6.8	G8 V	16
202573[b]	+24°4357	21 14.9	+25 20	7.0	G5 V	18
202940	−26°15541	21 18.4	−26 29	7.6	G5 V	19

[a] $p = 0.005\% \pm 0.037\%$ (m.e.), $\zeta = 137°$ according to Appenzellar (1968).

[b] This star carries a small amount of polarization according to Berdyugin, Snåre & Teerikorpi (1995).

being of sufficient scale as to affect polarimetric measurements, is important for future studies.

With the launch of the HST, a new enterprise was undertaken to establish a set of polarimetric calibration objects with data collated by Turnshek, Bohlin, Williamson II, *et al.* (1990). Their preparations involved a programme of check measurements, and they comment that some target stars have been retained which were listed as variable by Bastien, Drissen, Ménard, *et al.* (1988), as there was no evidence of variability in their new survey. A resumé of the results of the programme, providing a set of *polarized* and *unpolarized standards* for the Northern Hemisphere, has been given by Schmidt, Elston & Lupie (1992).

Several other workers have thrown suspicions on the stability of some of the commonly used stars. Whether any apparent variability is intrinsic to the light from the star itself, or related to an some unappreciated noise, are issues requiring further investigation as polarimetric accuracy improves, with the application of larger telescopes and solid state detectors, enabling larger numbers of photons to be accumulated in shorter experimental times.

It should also be remembered that catalogued measurements of position angle are referred to equatorial coordinates of a particular epoch. It has been noted by Hsu & Breger (1982) that the secular changes of precession need to be considered while recording the position angles. As time advances, the orientation of the equatorial coordinate system is subject to rotation relative to any fixed vibration direction in the polarization of a celestial source. For stars at $\delta \sim 60^\circ$, the apparent change of position angle can be as high as 1° in 100 years, and allowance should be made for this if new measurements are compared with older catalogued values.

8.10.2.2 Unpolarized Standards

In setting up any catalogue of *unpolarized standards*, experience shows that stars in the mid-part of the spectral sequence are less likely to display intrinsic effects relative to early-type and late-type objects. As a consequence, most catalogues promoting unpolarized stars usually comprise solar types. In addition, to avoid effects of interstellar polarization, the objects are usually in the local solar neighbourhood and away from the galactic plane. Stars in the solar environment were measured by Behr (1959), with later work by Walborn (1968), Piirola (1977), Krautter (1980) and Leroy (1993).

Piirola (1977) showed that dust in the solar vicinity is inhomogeneous with some parts being dust free. He also suggested that χ Per, sometimes used as an unpolarized reference (see Walborn, 1968), exhibits variation. A preliminary collection of data for a catalogue of zero-polarization standards, combining previous material and new observations of his own from different observing stations was presented by Tinbergen (1979) and later extended (see Tinbergen, 1982). A careful assembly of honed data for 1000 stars within 50 pc of the Sun has been provided by Leroy (1993), this based on 401 stars observed by himself, with 395 measured to an accuracy better than 0.03%, and the remainder taken from records of earlier work by others.

The statistical behaviour of an assembly of measurements of *zero-polarization* stars was established by Clarke, Naghizadeh-Khouei, Simmons, *et al.* (1993), and they demonstrated that the catalogue of Tinbergen (1979) does not correspond to one for measurements of unpolarized stars, with differences depending on the choice of stellar spectral type, and on the particular observing station. They also found small disparities associated with the Piirola's (1977) data. Statistical tests applied to the repeated measurements of a few selected G- and K-dwarf stars by Leroy & Le Borgne (1989) show that these data are indistinguishable from those of a set of unpolarized stars. The stars HD 65583 and HD 144287 have been measured over a number of years at the Crimean Observarory and are confirmed by Berdyugin, Snåre & Teerikorpi (1995) as zero-standards.

8.10.3
Other Useful Catalogues

A synthesis of general measurements from a variety of sources was made by Axon & Ellis (1976), producing a catalogue containing information for 5070 stars. The source material is from Hall (1958), Hiltner (1951a, 1954a, 1954b, 1956), van P. Smith (1956), Behr (1959), Appenzeller (1966, 1968), Mathewson & Ford (1970), Klare, Neckel & Schnur (1972), Schröder (1976) – some of the included citations being corrected here. With the aim of studying interstellar polarization at high and intermediate galactic latitudes, Korhonen & Reiz (1986) have provided a catalogue of *B*-band measurements of 358 A- and F-type stars, combining data from Mathewson & Ford (1970) with their new measurements. By far the most comprehensive catalogue is that of Heiles (2000) who has collected data from a variety of sources making careful checks on the entries and removing errors that have arisen elsewhere. This data base contains the results for 9286 stars.

Other useful tables of measurements for reference include:

1. Coyne & Gehrels (1966) – Table VI: Various data on the stars observed in this program.
2. Coyne & Gehrels (1967) – Table V: Various data on the stars observed in this program.
3. Serkowski (1968) – Table 1: Polarimetric Observations with One-Channel Glan–Foucault Polarimeter at Lowell Observatory.
4. Serkowski (1968) – Table 2: Polarimetric Observations with Two-Channel Polarimeter attached to the 24-in. Rotatable Telescope at Siding Spring Observatory.
5. Serkowski (1968) – Table 3: Polarization of Stars Nearer Than 10 Parsecs Observed with the 24-in. Rotatable Telescope at Siding Spring Observatory.
6. Serkowski (1968) – Table 5: The Stars with Known Wavelength Dependence of Polarization and *VRI* Photometry Available.
7. Serkowski, Gehrels & Wiśniewski (1969) – Table V: The stars with known wavelength dependence of polarization and *VRI* photometry available.
8. Coyne & Wiśniewski (1969) – Table II: Various data on the stars observed.
9. Serkowski (1970) – Table 1: Polarimetric Observations in *UBV* Spectral Regions.
10. Coyne (1971) – Table I: Stars which lie below the maximum of the $p(\lambda)$ curve.
11. Coyne (1971) – Table II: Early-type supergiants with variable polarization.
12. Dyck & Jennings (1971) – Table I. Program Stars.
13. Appenzeller (1974) – Table 1: Observational Results – The data cover the zone containing the Barnard Loop Nebula.
14. Mathewson, Ford, Klare, *et al.* (1978) Polarization Catalogue. (Microfiche).
15. Schmidt, Elston & Lupie (1992) The Hubble Space Telescope Northern-Hemisphere Grid of Stellar Polarimetric Standards.
16. Bel, Lafon & Leroy (1993) – Table 1: New polarization measurements in Cassiopeia and Cepheus clouds.
17. Berdyugin, Snåre & Teerikorpi (1995) Table 2: Measurements of 52 stars at high galactic latitudes.
18. Reiz & Franco (1998) – *UBV* polarimetry of 361 A- and F-type stars in selected areas (Original material available in electronic form via anonymous ftp at cdsarc.u-strasbg.fr (130.79.128.5))

References

Angel, J.R.P., Landstreet, J.D. (1970) Magnetic observations of white dwarfs. *ApJ*, **160**, L147–L152. [150]

Appenzeller, I. (1966) Polarimetrische, photometrische und spektroskopische Beobachtungen von Sternen im Cygnus und Orion. *Zeit. für Astrophysik*, **64**, 269–295. [168, 165]

Appenzeller, I. (1967) A new polarimeter for Feint Astronomical Objects. *PASP*, **79**, 136–139. [157]

Appenzeller, I. (1968) Polarimetric observations of nearby stars in the directions of the galactic poles and the galactic plane. *ApJ*, **151**, 907–918. [168, 166]

Appenzeller, I. (1974) Interaction between the Barnard Loop Nebula and the interstellar magnetic field. *A&A*, **36**, 99–105. [168]

Aspnes, D.E.(1970) Comments on the determination of absolute alignment of a polarizer. *Appl. Opt.*, **9**, 1708–1709. [162]

Axon, D.J., Ellis, R.S. (1976) A catalogue of linear polarization measurements for 5070 stars. *MNRAS*, **177**, 499–511. [167]

Bailey, J., Hough, J.H. (1982) A simultaneous infra red/optical polarimeter. *PASP*, **94**, 618–623. [158]

Bastien, P., Drissen, L., Ménard, F., Moffat, A.F.J., Robert, C., St-Louis, N. (1988) The variability of polarized standard stars. *AJ*, **95**, 900–910. [164, 165, 166]

Behr, A. (1956) Eine differentielle Methode der lichtelektsrischen Polarisationmessung des Sternlichts. *Veröff. der Univ.-Sternwarte zu Göttingen*, **7** (Nr. 114), pp. 401–435. [143]

Behr, A. (1959) Die interstellare Polarisation des Sternlichts in Sonnennumgebung. *Veröff. der Univ.-Sternwarte zu Göttingen*, **7** (Nr. 126), pp. 199–256. [141, 167, 168]

Bel, N., Lafon, J.-P. J., Leroy, J.-L. (1993) Visual polarization measurements in the Cepheus Flare. *A&A*, **270**, 444–450. [168]

Benedetti, E.J. (SJ) (1982) An achromatic polarimeter for spectral scanning across atomic lines and molecular bands. *Vat. Obs. Pubs.*, **2** (2), 15–19. [157]

Berdyugin, A., Snåre, M.-O., Teerikorpi, P. (1995) Interstellar polarization at high galactic latitude for distant stars: First results for Z less than or equal to 600 pc. *A&A*, **294**, 568–574. [164, 167, 168, 166]

Bjorkman, K.S., Nordsieck, K.H., Code, A.D., Anderson, C.M., Babler, B.L., Clayton, G.C., A. M. Magalhães, A.M., Meade, M.R., Nook, M.A., Schulte-Ladbeck, R.E., Taylor M, Whitney, B.A. (1991) First ultraviolet spectropolarimetry of Be stars from WUPPE. *ApJ*, **383**, L67–L70. [161]

Bolkvadze, O.R., Sigua, L.A. (1986) On possible stellar standards to be used in polarization studies. *Abastumanskaya Astrofiz. Obs. Byull*, **61**, 147–150 (in Russian). [165]

Chen, P.C. (1979) Suggestions for modifying the linear Dollfus polarimeter. *A&A*, **74**, 118–120. [158]

Clarke, D. (1965) Theoretical considerations in the design of an astronomical polarimeter. *MNRAS*, **129**, 71–84. [143, 144]

Clarke, D. (1971) Polarization measurements of the head of comet Bennett (1969I), *A&A*, **14**, 90–94. [147]

Clarke, D. (1986) The wavelength dependence of the interstellar polarization of o Sco, σ Sco and η Aql. *A&A*, **156**, 213–216. [164]

Clarke, D. (2005) Effects in polarimetry of interference within wave plates. *A&A*, **434**, 377–384. [155]

Clarke, D., Fullerton, S.R. (1996) The Sun as a polarimetric variable star. *A&A*, **310**, 331–340. [150]

Clarke, D., McLean, I.S. (1975) A dual narrowband wavelength scanning polarimeter. *MNRAS*, **172**, 545–556. [141, 154, 157, 157]

Clarke, D., McLean, I.S. (1976) Linear polarization measurements at Hβ of early-type emission line stars. *MNRAS*, **174**, 335–343. [154]

Clarke, D., Naghizadeh-Khouei, J. (1994) A Reassessment of some polarization standard stars. *AJ*, **108**, 687–693. [152, 165]

Clarke, D., Naghizadeh-Khouei, J. (1997) Polarimetry using CCD detectors. pp. 303–308, in *Sensors and their Applications VIII*, (eds A.T. Augousti & N.M. White), Institute of Physics Publishing, Bristol. [153, 153]

Clarke, D., Neumayer, D. (2002) Experiments with a novel CCD stellar polarimeter. *A&A*, **383**, 360–366. [154]

Clarke, D., McLean, I.S, Wyllie, T.H.A. (1975) Stellar line profiles by tilt-scanned narrow band interference filters. *A&A*, **43**, 215–221. [154, 157]

Clarke, D., Naghizadeh-Khouei, Simmons, J.F.L., Stewart, B.G. (1993) A statistical assessment of zero-polarization catalogues. *A&A*, **269**, 617–626. [167]

Clemens, D.P., Tapia, S. (1990) Toward selection of intermediate-magnitude polarization standards. *PASP*, **102**, 179–182. [165]

Cox, L.J. (1983) The design of polarimeters for astronomy. *MNRAS*, **203**, 571–579. [140]

Coyne (SJ), G.V. (1971) Intrinsic polarization in the atmospheres of supergiant stars. pp. 93–107 in *Proceedings of the Third Trieste Colloquium in Astrophysics*, (ed. M. Hack) – Osservatorio Astronomico di Trieste (also as *Spec Vat.* No: 53). [168, 168]

Coyne (SJ), G.V. (1974) Wavelength dependence of polarization. XXV. Rotation of the position angle by the interstellar medium. *AJ*, **79**, 565–580. [164]

Coyne (SJ), G.V., Gehrels, T. (1966) Wavelength dependence of polarization. VIII. Interstellar polarization. *AJ*, **71**, 355–363. [168, 164]

Coyne (SJ), G.V., Gehrels, T. (1967) Wavelength dependence of polarization. X. Interstellar polarization. *AJ*, **72**, 887–898. [168]

Coyne (SJ), G.V., Wiśniewski, W. (1969) Wavelength dependence of polarization. XVII. Be-type stars. *AJ*, **74**, 528–532. [168]

Cropper, M. (1985) Simultaneous linear and circular polarimetry of EF Eri. *MNRAS*, **212**, 709–721. [151]

Dolan, J.F., Tapia, S. (1986) Wavelength dependence of position angle in polarization standards. *PASP*, **98**, 792–802. [163, 163, 164]

Dollfus, A. (1958) Un Polarimétre Photoelectric très sensible pour l'étude du Soleil. *CR*, **246**, 2345–2347. [146]

Donati, J.-F, Catala, C., Wade, G.A., Gallou, G., Delaigue, G., Rabou, P. (1999) A dedicated polarimeter for the MuSiCoS échelle spectrograph. *A&AS*, **134**, 149–159. [160]

Dorotovič, I., Pintér, T., Rybanský, M. (2003) Polarization of the solar corona in the 530.3 nm emission line. pp. 493–496 in *Solar Polarization 3 – ASP Conf. Ser.*, **307**, (eds J. Trulillo Bueno & J. Sánchez Almeida), San Francisco. [147]

Dyck, H.M., Jennings, M.C. (1971) Intrinsic polarization in K and M giants and supergiants. *AJ*, **76**, 431–444. [168]

Fessenkoff, B. (1935) Détermination de la Polarisation de la Couronne Solaire. *Astronomicheskii Zhurnal*, **12** (4), 309–321. [146, 147]

Fessenkov, V.G. (1959) A 2-channel polarimeter and its application in atmospheric optics and astrophysics. *Sov. Astron.*, **3**, 1007–1022. [144]

Frecker, J.E., Serkowski, K. (1976) Linear polarimeter with rapid modulation, achromatic in the 0.3 – 1.1 μm range. *Appl. Opt.*, **15**, 605–606. [149, 157]

Gehrels, T., Silvester, A.B. (1965) Wavelength dependence of polarization. V. Position angles of interstellar polarization. *AJ*, **70**, 579–580. [163, 164]

Gehrels, T., Teska, T.M. (1960) A Wollaston Photometer. *PASP*, **72**, 115–122. [154, 161, 162]

Gliese, W. (1969) Catalogue of nearby stars. *Veröff. Astr. Rechen-Inst. Heidelberg* **22**, 1–117. [166]

Goodrich, R.W. (1991) High efficiency "superachromatic" polarimetry optics for use in optical astronomical spectrographs. *PASP*, **103** 1314–1322. [159]

Hall, J.S. (1951) Some polarization measurements in astronomy. *J. Opt. Soc. Am.*, **41**, 963–966. [156]

Hall, J.S. (1958) Polarization of starlight in the galaxy. *Pubs. of the US Naval Observatory* – Second Series, Vol. XVII, Part VI. [168]

Hayes, D.P. (1984) Variable polarization observations of the early type supergiants κCas and αCam. *AJ*, **89**, 1219–1228. [163]

Hayes, D.P. (1986) Rigel's circumstellar envelope structure. *ApJ*, **302**, 403–409. [163]

Heiles, C. (2000) 9286 Stars: an agglomeration of stellar polarization catalogs. *AJ*, **119**, 923–927. [168]

Hiltner, W.A. (1951a) Polarization of stellar radiation. III. The polarization of 841 stars. *ApJ*, **114**, 241–271. [141, 156, 168]

Hiltner, W.A. (1951b) Compensation of seeing in photoelectric photometry. *The Observatory*, **71**, 234–237. [143]

Hiltner, W.A. (1952) Compensation of seeing noise in photoelectric polarization photometry. *AJ*, **57**, 13. [143]

Hiltner, W.A. (1954a) Interstellar polarization of 405 Stars. *ApJ*, **120**, 454–463. [168]

Hiltner, W.A. (1954b) Early-type stars in the direction of the galactic center. *ApJ*, **120**, 41–47. [168]

Hiltner, W.A. (1956) Photometric, polarization and spectrographic observations of O and B stars. *ApJS*, **2**, 389–462. [168]

Hiltner, W.A. (1959) Private communication – Letter to the Author dated 10 August 1959. [140, 157]

Hough, J., Lucas, P., Bailey, J., Hirst, E., Tamura, M., Harrison, D. (2005) PlanetPol: a high sensitivity polarimeter for the direct detection and characterisation of scattered light from extra-solar planets. *ING Newsl.*, 9, pp. 26–27. [152]

Hough, J.H., Lucas, P.W., Bailey, J.A., Tamura, M., Hirst, E., Harrison, D., Bartholomew-Biggs, M. (2006) PlanetPol: a very high sensitivity polarimeter. *PASP*, **118**, 1302–1318. [151, 152, 158]

Hsu, J-C., Breger, M. (1982) On standard polarized stars. *ApJ*, **262**, 732–738. [161, 163, 167, 164, 164, 164, 164]

Jain, S.K., Srinivasulu, G. (1989) A fast star-and-sky chopping polarimeter. *Indian Inst. Astrophys. Newsletter*, **4**, No: 2, 7–9. [157]

Kemp, J.C., Barbour, M.S. (1981) A photoelectric-modulator at Pine Mountain Observatory. *PASP*, **93**, 521–525. [150, 158]

Kemp, J.C., Wolstencroft, R.D., Swedlund, J.B. (1972) Circular Polarimetry of fifteen interesting objects. *ApJ*, **177**, 177–189. [150, 158]

Kikuchi, S. (1988) The present status of the multi-channel polarimeter at Dodaira. *Tokyo Astron. Bull.* Second Series No: 281. 3267–3277. [158]

Kinman, T.D., Mahaffey, C.T. (1974) A computer-controlled photometer and polarimeter. *PASP*, **86**, 336–339. [156]

Klare, G., Neckel, Th., Schnur, G. (1972) Polarization measurements of 1600 Southertn OB-Stars. *A&AS*, **5**, 239–262. [149, 168]

Korhonen, T., Piirola, V., Reiz, A. (1984) Polarization measurements at La Silla. *The Messenger*, **38**, 20–24. [156]

Korhonen, T., Reiz, A. (1986) Interstellar polarization from observations of A and F stars in high and intermediate galactic latitudes, and from stars in the Mathewson and Ford polarization catalogue. *A&AS*, **64**, 487–494. [168]

Krautter, J. (1980) Polarization measurements of 313 nearby stars. *A&AS*, **39**, 167–172. [167]

Leroy, J.L. (1993) Optical polarization of 1000 stars within 50 pc from the Sun. *A&AS*, **101**, 551–562. [167, 167]

Leroy, J.L., Le Borgne, J.F. (1989) Polarimetry of solar-type stars and magnetic field diagnostics. *A&A*, **223**, 336–342. [167]

Lyot, B. (1948a) Un polarimètre photoélectrique. *CR*, **226**, 25–28. [145]

Lyot, B. (1948b) Un polarimètre photoélectrique intégrateur utilisant des cellules á multiplicateurs d'électrons. *CR*, **226** 137–140. [146]

Magalhães, A.M., Benedetti, E., Roland, E.H. (1984) A photoelectric polarimeter with tilt-scanning capability. *PASP*, **96**, 383–390. [157]

Magalhães, A.M., Rodrigues, C.V., Margoniner, V.E., Pereyra, A., Heatcote, S. (1996) High precision CCD imaging polarimetry. pp. 118–122 in *Polarimetry of the Interstellar Medium – ASP Conf. Ser.*, **97**, (eds W.G. Roberge & D.C.B. Whittet), San Francisco. [161]

Marin, M. (1964) Measures photoélectriques de polarisation à l'aide d'un télescope coudé de 1 mètre. *Th. Sciences Physiques, Paris* Série A, No: 897. See also: *Rev. d'Opt.*, **44**, 115–144. [146]

Mathewson, D.S., Ford, V.L. (1970) Polarization observations of 1800 stars. *Mem. R. Astron. Soc.*, **74**, 139–182. [165, 168, 168]

Mathewson, D.S., Ford, V.L., Klare, G., Neckel, Th., Krautter, J. (1978) Polarization Catalogue. Strasbourg: Centre de Données Stellaires. (Microfiche). [168]

McCarthy, M.F. (SJ) (1980) New techniques in stellar photometry and polarimetry (Scientific Session of Commission 25 XVII General Assembly of IAU) *Ric. Astron. Spec. Vaticana*, **10**, Special Issue. pp. 1–2[159]

McLean, I.S. (1980) Multichannel detectors in polarimetry. pp. 71–100, in *New Techniques in Stellar Photometry and Polarimetry* (Scientific Session of Commission 25 XVII General Assembly of IAU) (ed. McCarthy, M.F.) (SJ) *Ric. Astron. Spec. Vaticana*, **10**, Special Issue. [159]

McLean, I.S., Coyne, G.V., Frecker, J.E., Serkowski, K. (1979) High resolution polarization structure of Hβ in Be-Shell stars measured with a new digicon spectropolarimeter. *ApJ*, **228**, 802–808. [158]

McLean, I.S., Heathcote, S.R., Paterson, M.J., Fordham, J., Shortridge, K. (1984) A multichannel Pockels cell spectropolarimeter for the Anglo-Australian Telescope. *MNRAS*, **209**, 655–664. [150, 150, 159]

Metz, K. (1984) A polarimeter with a new polarizer and a new device for eliminating the sky background polarization. *A&A*, **136**, 175–177. [157]

Metz, K. (1986) A polarimeter with a new device for eliminating the instrumental phase plate polarization. *A&A*, **159**, 333–335. [157]

Miller, J.S., Robinson, L.B., Goodrich, R.W. (1987) A CCD spectropolarimeter for the Lick Observatory 3-meter telescope. From: *Instrumentation for Ground-Based Optical Astronomy*, (ed. L.B. Robinson). Springer, Berlin. [159]

Miller, J.S., Robinson, L.B., Schmidt, G.D. (1980) The remote-controlled spectrograph, area scanner, and spectropolarimeter for the Lick 3-m telescope. *PASP*, **92**, 702–712. [150, 159]

Nordsieck, K.H. (1974) A simple polarimetric system for the Lick Observatory image-tube scanner. *PASP*, **86**, 324–329. [158]

Nordsieck, K.H., Marcum, P., Jaehnig, K.P., Michalski, D.E. (1993) New techniques in ultraviolet astronomical polarimetry: wide-field imaging and far-ultraviolet spectropolarimetry, in *X-Ray and Ultraviolet Polarimetry*, (ed. Silvano Fineschi), Proc. SPIE 2010, 28–36. [161]

Oetken, L. (1970) Polarimetric methods in astrophysics. *Jena Review*, **6**, 330–334. [140]

Öhman, Y. (1939) On some observations made with a modified Pickering polarigraph. *MNRAS*, **99**, 624–633. [160]

Öhman, Y. (1971) Private Communication to the author dated 26 May 1971. [147]

Oliva, E. (1997) Wedged double Wollaston, a device for single shot polarization measurements. *A&AS*, **123**, 589–592. [154]

Östreicher, R., Schulte-Ladbeck, R. (1985) A spectropolarimeter for low polarization. *A&A*, **148**, 179–182. [159]

Pickering, E.C. (1874) Applications of Fresnel's formula for the reflection of light. *Proc. Am. Academy Arts Sci.*, **IX**, 1–29. (See p. 14). [147]

Piirola, V. (1973) A double image chopping polarimeter. *A&A*, **27**, 383–388. [156]

Piirola, V. (1975) The double beam chopping photometer-polarimeter. *Ann. Acad. Sci. Fennicae*. Series A, VI Physica No: 418. [156]

Piirola, V. (1977) Polarization observations of 77 Stars within 25 pc from the Sun. *A&AS*, **30**, 213–216. [165, 167, 167, 167]

Piirola, V. (1988) Simultaneous five-colour (UBVRI) Photopolarimeter. pp. 735–746 in *Polarized Radiation of Circumstellar Origin*. (eds G.V. Coyne (SJ), A.M. Magalhães, A.F.J. Moffat, R.E. Schulte-Ladbeck, S. Tapia & W. Wickramasinghe). University of Arizona, Tucson, AZ. [156]

Pospergelis, M.M. (1965) The "Taimyr" electronic polarimeter. *Sov. Astron.*, **9**, 398–408. [156]

Ramaprakash, A.N., Gupta, R., Sen, A.K., Tandon, S.N. (1999) An iImaging polarimeter (IMPOL) for multi-wavelength observations. *A&AS*, **128**, 369–375. [161]

Reiz, A., Franco, G.A.P. (1998) UBV polarimetry of 361 A- and F-type stars in selected areas. *A&AS*, **130**, 133–140. [168]

Rowell, R.L., Levit, B.A., Ghaffer, M.A. (1969) Determination of the absolute alignment of a polarizer. *Appl. Opt.*, **8**, 1734. [161]

Scarrott, S.M. (1991) Optical polarization studies of astronomical objects. *Vistas Astron.*, **34** 163–177. [160, 160]

Schmidt, G.D., Elston, R., Lupie, O.L. (1992) The Hubble space telescope Northern-Hemisphere grid of stellar polarimetric standards. *AJ*, **104**, 1563–1567. [162, 166, 168]

Schröder, R. (1976) Optical polarization of stars of galactic latitudes $b < -45°$. *A&AS*. **23**, 125–137. [168]

Serkowski K. (1965) Polarization of galactic clusters M 25, NGC 869, 884, 1893, 2422, 6823, 6871, and association VI Cygni. *ApJ*, **141**, 1340–1361. [162]

Serkowski, K. (1968) Correlation between the regional variations in wavelength dependence of interstellar extinction and polarization. *ApJ*, **154**, 115–134. [168, 168, 168, 168, 165]

Serkowski, K. (1970) Intrinsic polarization of early-type stars with extended atmospheres. *ApJ*, **160**, 1083–1105. [168, 164]

Serkowski, K. (1974a) Polarization techniques, Chapter 8 from *Methods of Experimental Physics*, (eds M.L. Meeks & N.P. Carleton) **12**, Astrophysics: Part A – Optical & Infrared. Academic Press, New York. [140, 162, 162]

Serkowski. K. (1974b) Polarimeters for optical astronomy. pp. 135–174 in *Planets, Stars and Nebulae Studied with Photopolarimetry*, (ed. T. Gehrels), University of Arizona Press, Tucson, AZ. [140, 151, 163, 164, 165, 166]

Serkowski, K., Chojnacki, W. (1969) Polarimetric observations of magnetic stars with two-channel polarimeter. *A&A*, **1**, 442–448. [156]

Serkowski, K., Gehrels, T., Wiśniewski, W. (1969) Wavelength dependence of polarization XIII interstellar extinction and polarization correlation. *AJ*, **74**, 85–90. [168]

Serkowski, K., Mathewson, D.S., Ford, V.L. (1975) Wavelength dependence of interstellar polarization and ratio of total to selective extinction. *ApJ*, **196**, 261–290. [164, 164, 165]

Serkowski, K., Robertson, J.W. (1969) Regional variations in the wavelength dependence of interstellar polarization *ApJ*, **158**, 441–447. [164]

Steele, I.A., Bates, S., Carter, D., Clarke, D., Melandri, A., Mottram, C.J., Mundell, C., Scott, A., Smith, R.J., Swindlehurst, J. (2006) RINGO: a novel ring polarimeter for rapid GRB followup. *SPIE Conference*: 6296M, 14 pages. [154]

Thiessen, G. (1958) On Photoelectric polarization photometry. *The Observatory*, **78**, 256–257. [144]

Tinbergen, J. (1972) Precision spectropolarimetry of starlight: development of a wide-band version of the Dollfus polarization modulator. PhD Thesis, University of Leiden, Holland. [146, 158]

Tinbergen, J. (1973) Precision spectropolarimetry of starlight: development of a wide-band version of the Dollfus polarization modulator. *A&A*, **23**, 25–48. [146]

Tinbergen, J. (1979) A list of zero-polarization standards. *A&AS*, **35**, 325–326. [167, 167]

Tinbergen, J. (1982) Interstellar polarization in the immediate solar neighbourhood *A&A*, **105**, 53–64. [167]

Tinbergen, J., Rutten, R.G.M. (1992) A User Guide to WHT Spectropolarimetry (La Palma User Manual No: 21, Royal Greenwich Observatory). [148]

Tomaszewski, L., Symonds, G.R., Landstreet, J.D. (1980) Spectropolarimetry with an intensified-dissector-scanner. *PASP*, **92**, 518–527. [159]

Treanor, P.J. (1968) A new technique for stellar polarimetry. *MNRAS*, **138**, 325–336. [153]

Turnshek, D.A., Bohlin, R.C., Williamson,II, R.L., Lupie, O.L., Koornneef, J., Morgan, D.H. (1990) An atlas of hubble space telescope photometric, spectrophotometric, and polarimetric calibration objects. *AJ*, **99**, 1243–1261. [166]

van P. Smith, E. (1956) Interstellar polarization in the Southern Milky Way. *ApJ*, **124**, 43–60. [168]

Viråghalmy, G. (1986) Linear polarimetric measurements of 55 Cygni. *IBVS*, No: 2938, Budapest. [163, 164]

Visvanathan, N. (1972) An automatic fast digital-photoelectric photometer and polarimeter. *PASP*, **84**, 248–253. [156]

Vogt, S.S., Tull, R.G., Kelton, P.W. (1980) Performance of the Zeeman analyzer system of the McDonald Observatory 2.7 m telescope. *ApJ*, **236**, 308–317. [160]

von der Heide, K., Knoechel, G. (1979) Statistically rigorous reduction of stellar polarization measurements. *A&A*, **79**, 22–26. [149]

Walborn, N.R. (1968) Twenty-five polarimetric standard stars within twenty parsecs of the Sun. *PASP*, **80**, 162–164. [167, 167, 165]

Walker, G., Dinshaw, N., Saddlemyer, L., Younger, F. (1993) Spectropolarimetry with a cube beamsplitter. *Expt. Astron.*, **2**, 391–398. [159]

Wolstencroft, R.D., Nandy, K. (1971) A study of wavelength dependence of interstellar polarization using a scanning spectropolarimeter. *Astrophys. Space Sci.*, **12**, 158–164. [158]

Wolstencroft, R.D., Cormack, W.A., Campbell, J.W, Smith, R.J. (1983) High precision spectropolarimetry of stars and planets – I. The ROE spectropolarimeter. *MNRAS*, **205**, 23–38. [151, 158]

9
Some Polarigenic Mechanisms

9.1
Introduction

In applying polarimetry as a diagnostic tool in astrophysics, there are two aspects of information that can be gleaned. Firstly, polarization measurements offer direct insight into the properties and conditions of the materials generating the radiation, or on the material scattering it into the line of sight. Secondly, the Stokes parameters carry the descriptions of the orientational properties of the electrical disturbances in the waves, and these in turn may reflect information on the astrophysical geometries associated with the production, or the scattering, of the radiation. Preferred directions of vibration within the measured flux result from particular geometries associated with the regions where the polarization is generated.

There are many processes that can generate polarized radiation in astrophysical situations, and it would be impossible to discuss them all in this chapter. Many of them will be presented at the appropriate times when the polarimetric behaviours of the various types of star are described. However, important polarigenic mechanisms relate to the emission or absorption of atoms in the presence of a magnetic field, or to the scattering of radiation by particles, such as free electrons, or dust grains. Examples from these areas will be described here to provide simple demonstration of the usefulness of polarimetry as an important astrophysical diagnostic and, in the case of magnetic fields, to give reminder of the importance of handedness in providing interpretation of field directions.

9.2
The Presence of Magnetic Fields

9.2.1
Zeeman Effect

The most commonly met mechanism linking polarization to magnetic fields is the Zeeman effect. This can be readily appreciated and understood in terms of a classical approach which treats any atom as a potential light source. It is instructive to set

Stellar Polarimetry. David Clarke

ISBN: 978-3-527-40895-5

out the basic behaviour of radiating atoms in a magnetic field, if for no other reason than to confirm the sense of handedness of any produced circular polarization, V, and how this relates to determining the direction of the underlying magnetic field, $\vec{B}$. The basic atomic model assumes that one or more electrons orbit a fixed centre with an attractive force proportional to the displacement. A standard treatment of this approach, whereby atoms are considered to behave as classical oscillators, can be found in Jenkins & White (1965).

Suppose that the atoms are seen in the projected xy-plane with the radiation travelling to the observer along the z direction of a right-handed Cartesian frame. In the absence of a magnetic field, the elliptical motion associated with a given electron within an atom may be regarded as the superposition of three linear harmonic oscillations, two occurring in the xy-plane along the x and y directions, and the third along the z direction. The first two components can be taken as combining in the xy-plane to produce an elliptical motion, which, in turn, may be considered as two counter rotating circular motions, generally with different amplitudes. In summary, each electron motion can be thought of as comprising three coherent oscillations, one executing linear oscillations along the z-axis, while the other two comprise circular oscillations of opposite sense in the xy-plane.

For simplicity, it may be assumed that, without the field, the atoms emit monochromatic light. This means that the proportionality constant, k, between the elastic force and the displacement, is the same for all electronic oscillators. For the circular oscillations, the particles rotate on a radius, r, with constant angular velocity, ν_0, and there is an equality between the elastic force, kr, and the centripetal force, $m\nu_0^2 r$, i. e.

$$kr = m\nu_0^2 r \,, \tag{9.1}$$

where m is the electron mass. Hence,

$$\nu_0 = \sqrt{\frac{k}{m}} \,. \tag{9.2}$$

When spectral analysis is made of the light emitted by the source, in the absence of the field, unpolarized light of a single frequency, ν_0, is observed no matter the viewpoint. In the presence of the field, however, the result is modified according to the direction of observation.

Any magnetic field acts on each moving electron of charge, $-e$, and velocity, $\vec{v}$, with a force $\vec{F}_\mathrm{B}$ given by

$$\vec{F}_B = -e\vec{v} \times \vec{B} \,. \tag{9.3}$$

Assuming that the light source is placed in a magnetic field, $\vec{B}$, parallel to the z-axis and pointing in the positive z-direction, the force is zero if v is parallel to B – i. e. parallel to the z-axis. Hence electrons vibrating in the direction of the z-axis are unaffected by the magnetic field and continue to execute linear oscillations with their characteristic frequency, ν_0. The motions of electrons describing circular

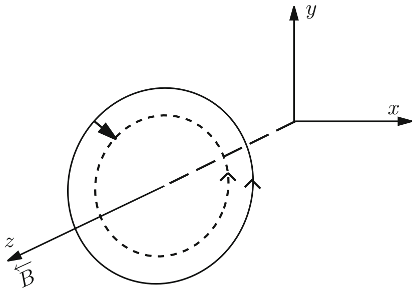

Fig. 9.1 The schematic displays the original anti-clockwise circular orbit (as seen by the observer) of an electron contracted to a smaller one by the presence of a magnetic field running parallel to the travel direction of the radiation along the *z*-axis.

orbits in the xy-plane are modified, however, with the angular velocity changing from ν_0.

For an electron rotating from x to y, i. e. counterclockwise as seen looking against z, as depicted in Figure 9.1, the new radius, r, of the orbital circle gives rise to an angular velocity, ν_1, so that the linear velocity may be expressed as $\nu_1 r$. The magnetic field acts on the electron with a force of $eB\nu_1 r$, pointing toward the centre of the circle. The resultant of this force and the elastic force is $kr + eB\nu_1 r$, which is balanced by the centripetal force so that

$$kr + eB\nu_1 r = m\nu_1^2 r \, ,$$

or, by recalling (9.1):

$$eB\nu_1 = m(\nu_1^2 - \nu_0^2) \, . \tag{9.4}$$

Similarly, if ν_2 is the angular velocity of an electron rotating with a clockwise rotation, the resultant balance of forces may be expressed by

$$eB\nu_2 = m(\nu_0^2 - \nu_2^2) \, . \tag{9.5}$$

Equations (9.4) and (9.5) determine the new angular velocities of the two electronic oscillators such that $\nu_1 > \nu_0$ and $\nu_2 < \nu_0$. If B is sufficiently small, the summations $(\nu_1 + \nu_0)$ and $(\nu_0 + \nu_2)$ may be written as $2\nu_1$ and $2\nu_2$, respectively. From (9.4) and (9.5), the changes in angular frequency may then be written as

$$\nu_1 - \nu_0 = \nu_0 - \nu_2 = \Delta\nu = \frac{eB}{2m} \, . \tag{9.6}$$

Thus, for a longitudinal magnetic field with vector $\vec{B}$ pointing along the direction of propagation of the radiation, the angular velocity of the electrons rotating counterclockwise increases by $\Delta\nu$; a decrease by the same amount applies to the electrons rotating in the clockwise direction. Two spectral lines, referred to as 'σ' components, due to the electrons rotating counterclockwise and clockwise in the

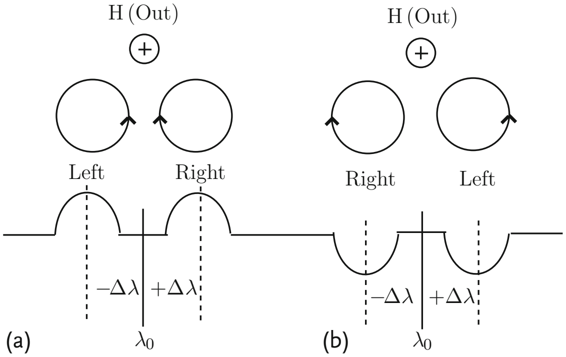

Fig. 9.2 The handedness difference associated between emission lines and absorption lines as a result of a longitudinal magnetic field, with field lines emerging in a direction towards the observer. In (a) the lines are in emission with the blue-shifted component displaying a left-handed polarization. In (b) the lines are in absorption; for the blue shifted line, left-handed polarization is removed leaving an excess of the right-handed form. All the senses of handedness would be reversed if the magnetic field displays the opposite polarity.

xz-plane will be observed; the third linear oscillator vibrating along the z-axis does not radiate in the direction of its motion. The spectral line corresponding to the higher angular frequency $\nu_0 + \Delta\nu$, with blue-shifted wavelength, will show left-handed circular polarization according to the IEEE definition (see page 4.5); the line for angular frequency $\nu_0 - \mathit{\Delta}\nu$ (red-shifted) will show right-handed circular polarization. These outcomes are depicted in Figure 9.2a. The handedness assignations reverse if the longitudinal field is in the opposite direction, pointing against the radiation flow.

For a situation involving a transverse field, three spectral lines should be recorded. In the sketched arrangement of Figure 9.1, if the radiation is received along the x-axis, the middle line, unshifted in wavelength and referred to as the 'π' component, is due to light waves of angular frequency, ν_0, emitted by the electrons vibrating in the direction of the z-axis. This light is linearly polarized, with the plane of vibration parallel to the magnetic field. The other two lines are due to light waves of angular frequencies $\nu_0 + \Delta\nu$ and $\nu_0 - \Delta\nu$ emitted by the electrons rotating counterclockwise and clockwise in the plane perpendicular to the magnetic field. As the circular motions are seen edge-on, their radiations are linearly polarized, with a direction of vibration perpendicular to the magnetic field.

It is noteworthy that because of the inverse relationship between ν and λ, i. e. $c = \nu\lambda$, the line splitting expressed in terms of wavelength is $\propto \lambda^2$. Consequently magnetic fields should be more readily detected by using Zeeman sensitive spectral lines of longer wavelength.

The shift in wavelength for the normal triplet may be expressed numerically as

$$\Delta\lambda = \pm 4.67 \times 10^{-13} \lambda^2 H \ \text{Å} , \tag{9.7}$$

where the field, H, is expressed in gauss and the wavelength, λ, in Ångstrom units.

The classical theory outlined above is only partially borne out by observation. When excited atoms are placed in a magnetic field, some spectral lines split into a triplet, as theoretically predicted, and the separations of the components, as well as their states of polarization, agree accurately with the results of theory, with the behaviour referred to as the *normal Zeeman effect*. Many spectral lines, however, behave in a more complicated manner, with splitting into multiple lines, the behaviour referred to as the *anomalous Zeeman effect*. Such disagreement between theory and observation is due to a fundamental limitation of the simple model, and can be removed only by the more exact quantum-mechanical treatment of the phenomenon.

The effect of an electric field on the emission lines of gases is qualitatively similar to that of a magnetic field. Here, too, a single spectral line splits into multiples with polarized components. However, a discussion of this effect on the basis of the classical model is not profitable here.

In an attempt to maintain continuity in the description of the senses of magnetic fields already ascribed to magnetic stars through the work of Babcock (1958), in a footnote of the preprint of their paper (but removed from the final version), Kemp, Wolstencroft & Swedlund (1972) comment: 'We do not know whether positive H_e, in the convention of the magnetic-star spectroscopists, means that the H field is inclined toward or away from us. After asking three of them and after reading Babcock's original papers we remain confused. This will eventually have to be settled in order to relate the sign of our q (v, in the nomenclature of this book) to their field signs'. According to Kemp (1970), positive V for grey-body magneto-emission from electrons means H is *towards* the observer, but again this does not clarify the issue unless the chosen sign convention can be related to the helix handedness, or to the IEEE definition.

According to Babcock (1962):

> If one observes a source in which there is a magnetic field directed towards the observer (+ polarity), then the electrons revolving in a counter clockwise direction and resulting in left-hand circularly polarized radiation will produce the higher frequency σ component, or components, of the pattern, and these components either in emission or in absorption (the inverse Zeeman effect) will be transmitted by a left-hand analyzer. The right-hand polarized components, of lower frequency, will be totally suppressed by the analyzer.

Unfortunately, this description is again not exactly clear. Although the sense of polarization generated in relation to the emission and absorbed components is consistent with the outcomes based on the simple classical model described above, and the IEEE definition, the interpretation of what is measured is confusing. If the component is 'in absorption', how can it be 'passed' by an analyser? What is the polarization form of the *remaining* light that is passed? This issue is more clearly presented by Bray & Loughhead (1964) in relation to the behaviour of the inverse Zeeman effect as observed in sunspots.

The circular polarizations associated with the split emission lines, with reference to their handedness, are depicted in Figure 9.2. If the atoms in the magnetic field are absorbing radiation from a continuum, then the polarization forms absorbed will have the same description as for emission. For absorption spectra, what is recorded, however, is the remaining unabsorbed light and, in the cores of split stellar absorption lines, orthogonal forms with opposite handedness to the descriptions above for emission will be noted, (see Figure 9.2b) and this is sometimes carelessly forgotten. Proper interpretation of this process is important in determining the vector directions of a magnetic field. The overall situation for emission and absorption is summarized in Figure 9.2.

Two other issues can also cause problems with the interpretation of the directional sense of magnetic fields.

1. The handedness of any circular polarization is reversed by any mirror reflection and this would be the case if observations are made at the telescope prime focus. Most measurements are recorded using Cassegrain systems, however, and handedness reversals are cancelled out by reflections by the primary and secondary mirrors in sequence.
2. The situation is more complex using coudé or Nasmyth telescopes. Generally the first two mirrors are at normal incidence with the straightforward handedness changes cancelling out. The third mirror, usually introduces a phase change that can be compensated for according to the source's Hour Angle and Declination. Care must be exercised in establishing the overall behaviour of such a system as, although the phase change is usually small, the third mirror imposes an additional handedness change. It is also important to make sure that the compensating phase delay has opposite sense to that introduced by the telescope mirrors and that its value is interpreted without an error of $\sim \pi$, as might occur if a Fresnel rhomb is used, and considered to have a quarter-wave retardation rather than being a 3/4-wave device (see Chapter 6).

9.2.2
Hβ Magnetography

By measuring the circular polarization in the wings of spectral lines, it is possible to determine the magnitude of longitudinal fields in some stars. This can be done using the broad Balmer lines such as Hβ and, in the early observational schemes, sequential measurements of the two wings were made.

Suppose $p(\lambda)$ represents the polarimetric line profile in the spectrum of a star. For the simple Zeeman doublet produced by the field longitudinal component of $H_e = H\cos\gamma$, where γ is the angle of the direction of field direction relative to the line of sight, the two line profiles can be represented by

$$p(\lambda + \Delta\lambda) \quad \text{and} \quad p(\lambda - \Delta\lambda)\,, \tag{9.8}$$

where $\Delta\lambda = 4.67 \times 10^{-13} g\lambda^2 H_e$, the shift is expressed in Å; the term, g, is the Landé splitting factor. The profiles are circularly polarized with opposite handedness. Hence, the fourth Stokes parameter for each component is given by

$$V(\lambda + \Delta\lambda) = p(\lambda + \Delta\lambda) \quad \text{and} \quad V(\lambda - \Delta\lambda) = -p(\lambda - \Delta\lambda) \,. \tag{9.9}$$

For a completely unresolved doublet, the intensity and circular polarization may be expressed by

$$I(\lambda) = p(\lambda + \Delta\lambda) + p(\lambda - \Delta\lambda) \,, \tag{9.10}$$

$$V(\lambda) = p(\lambda + \Delta\lambda) - p(\lambda - \Delta\lambda) \,. \tag{9.11}$$

Since $\Delta\lambda \ll \lambda$, a first-order Taylor expansion can be applied to p so that

$$p(\lambda + \Delta\lambda) = p(\lambda) + \Delta\lambda \frac{\mathrm{d}p}{\mathrm{d}\lambda} \,. \tag{9.12}$$

A similar expansion is also applicable to $p(\lambda - \Delta\lambda)$. We may, therefore, express $I(\lambda)$ and $V(\lambda)$ as

$$I(\lambda) \simeq 2p(\lambda) \,, \tag{9.13}$$

$$V(\lambda) \simeq 2\Delta\lambda \frac{\mathrm{d}p(\lambda)}{\mathrm{d}\lambda} \,. \tag{9.14}$$

By forming the normalized Stokes parameter:

$$v(\lambda) = \frac{V(\lambda)}{I(\lambda)} = \Delta\lambda \frac{\mathrm{d}p(\lambda)/\mathrm{d}\lambda}{p(\lambda)} \,. \tag{9.15}$$

Hence,

$$v(\lambda) \simeq 4.67 \times 10^{-13} g\lambda^2 H_e \frac{\mathrm{d}p(\lambda)/\mathrm{d}\lambda}{p(\lambda)} \,. \tag{9.16}$$

Assuming $g = 1$, and taking $\lambda = 4861.3$ Å, we have

$$v(\lambda) \simeq 1.104 \times 10^{-5} H_e \frac{\mathrm{d}p(\lambda)/\mathrm{d}\lambda}{p(\lambda)} \,. \tag{9.17}$$

If the field is non-uniform over the star, and the star is a fast rotator, with the Doppler effect being the chief line profile broadening agent, an appropriate Doppler-shifted average of the above equation will be required, and the polarization profile may differ considerably. This process is referred to as the *crossover effect*. However, for low resolution, corresponding say to the width of one line wing, a simple fitting procedure is useful, namely

1. Calculate the *mean* fractional circular polarization of the two line wings, red (R) and blue (B) from the measured values:

$$\bar{v} = \frac{1}{2}(q_R - q_B) \,. \tag{9.18}$$

2. Calculate the *mean* normalized gradients of the polarization in the line wings such that

$$G = \frac{1}{2}\left[\left(\frac{\mathrm{d}p/\mathrm{d}\lambda}{p}\right)_{\mathrm{R}} - \left(\frac{\mathrm{d}p/\mathrm{d}\lambda}{p}\right)_{\mathrm{B}}\right]. \tag{9.19}$$

3. Then

$$\bar{v}/G = 1.104 \times 10^{-5} H_{\mathrm{e}} . \tag{9.20}$$

By a similar argument, the degree of linear polarization, p, for the transverse field, $H_\perp$, is:

$$p \propto (\Delta\lambda)^2 \frac{\mathrm{d}^2 p(\lambda)}{\mathrm{d}\lambda^2} \propto H_\perp^2 . \tag{9.21}$$

It can be seen that, for transverse fields, the generated linear polarization variations across spectral lines depend on second-order terms, and are very much smaller than those related to v. The value of p is very much smaller than v for given H.

9.2.3
Differential Saturation of Zeeman Components

When considering the behaviour of stellar spectra under the influence of strong magnetic fields, Babcock (1949) noted that anomalous Zeeman patterns could be much wider than the thermal Doppler patterns. For absorption lines that are strongly saturated, this may lead to additional radiation being absorbed and he coined the term 'magnetic intensification of stellar absorption lines'. He suggested that if equivalent widths of lines are measured, this could lead to estimations of magnetic field strengths by comparison of lines selectively intensified by Zeeman splitting.

It was later suggested by Warwick (1951) that broadband linear polarization might be detectable in magnetic stars as a result of the same mechanism and the idea was developed by Leroy (1989) who showed that a non-zero polarization is generated across the overall spectrum, with the cumulative effects of all the lines controlling the behaviour of $p(\lambda)$. His calculations involved a treatment for each individual line based on an analytic solution of the transfer equation, carefully adjusted to solar conditions, to provide a good fit to the actual curve of growth of photospheric lines. The exercise was conducted for the case of weak magnetic fields, with the Zeeman splitting being much smaller than the line-width ($B = 500\,\mathrm{G}$), and for strong fields, with most of the photospheric lines completely split ($B = 10\,000\,\mathrm{G}$). The resulting polarization spectra, as displayed in Figure 9.3, show a variation which behaves approximately as $1/\lambda^{-4}$, but with a dip at 4800 Å and bump at 5200 Å, providing distinctive features for differentiating the mechanism relative to Rayleigh scattering.

In a following paper, Leroy (1990) refers to this form of generation of polarization as the effect of *differential saturation* of Zeeman components, and that it is noticeably reduced in blended lines. Any polarization signal does not increase very much

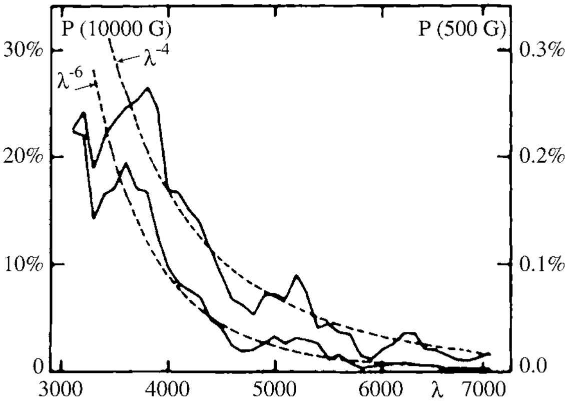

Fig. 9.3 Predicted $p(\lambda)$ curves for magnetic patches on solar type stars have been calculated by Leroy (1989) for fields of 500 G (upper curve and right hand scale) and 10 000 G with the effects of the photospheric lines smoothed out over spectral intervals of 100 Å. Curves for λ^{-4} or λ^{-6} give a good approximation to the general but the dip at 4800 Å and the bump at 5200 Å are clearly seen.(Taken from Leroy, 1989.)

in a crowded spectrum, therefore, even though the fraction of the continuum subtracted by the lines is larger. This natural limitation exists in the solar spectrum where the maximum polarization is reached in the blue region. The influence of line crowding is shown to be more pronounced in K-type stars as revealed in Leroy's worked example of Arcturus (α Boö).

9.2.4
Zeeman–Doppler Imaging

The information on magnetic fields of stars generally relates to an average picture of field strengths. A recent important observational development is the application of spectropolarimetry to the determination of the distribution of magnetic features over the surfaces of rapidly rotating stars by the principle of Zeeman–Doppler imaging (ZDI).

By performing high spectral resolution polarimetry, features may be detected in rotationally broadened lines and followed, as they migrate across the profile, according to the rotational phase. By dividing the projected image of a star into strips of apparent equal line of sight velocity, the light from any zone carries a particular Doppler shift. For a magnetic spot found in a zone, its associated polarization signatures will appear within the overall broadened line at some wavelength position defined by its Doppler shift.

In the first of a series of papers, Semel (1989) described the principle, and outlined the scheme whereby the average of the measurements of many lines may be used to improve the signal-to-noise ratio, and the quality of the field imaging. The feasibility of applying the technique was investigated numerically by Donati,

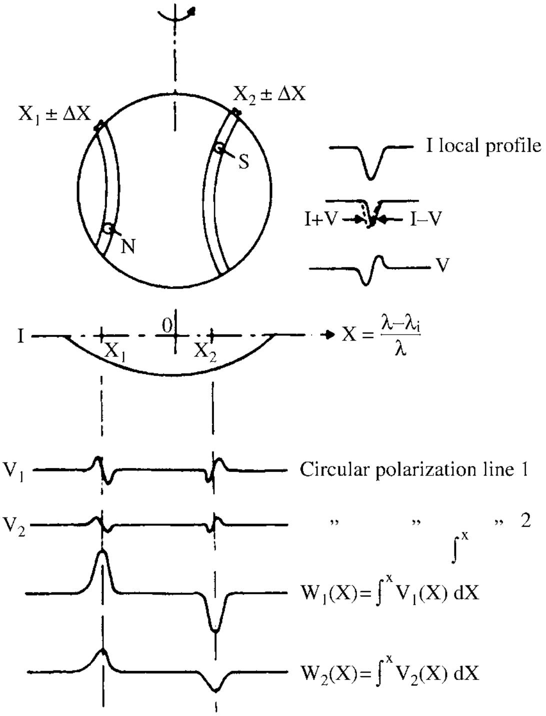

Fig. 9.4 Two magnetic spots of opposite polarity are placed such that their polarization effects appear at blue-shifted and red-shifted positions within the overall Doppler broadened line. The detailed circular polarization signatures are depicted together with their integration at the localized positions within the broadened line. (After Semel, 1989.)

Semel & Praderie (1989). The principle behind the measurements is outlined in Figure 9.4 which shows the effects for two spots of opposite polarity, one suffering a blue shift, and the other a red shift.

Problems associated with spurious signals that occur in the collection of data are discussed in Semel, Donati & Rees (1993), together with a listing of field detections which have been achieved by instrumentation on three different telescopes. Donati, Semel, Carter, *et al.* (1997) have enhanced the sensitivity of ZDI by sophisticated reduction techniques. The procedure, or least-squares deconvolution (LSD), embraces an idea outlined immediately above involving the simultaneous analysis of many spectral lines. LSD assumes that all spectral features in a given Stokes parameter $\{I, Q, U, V\}$ spectrum have identical shape, but may differ in amplitude by known scaling factors.

9.2.5
Resonance Radiation – The Hanle Effect

The phenomenon of resonance scattering was discovered in the laboratory by Wood (1905) in respect of the sodium D lines. By illuminating sodium vapour with radiation at the wavelength of the D lines, it was found that the absorption raises the scattering atom from the normal state of lowest energy to a higher state, and that, at low pressure, the atom very quickly returns to its normal state, re-emitting the radiation, the process being referred to as *resonance scattering*. It was later found that resonance scattering is not confined to absorption and re-emission of radiation at the same wavelength. The spectrum of sodium contains a fairly close pair of lines with wavelengths at approximately 3303 Å. It was discovered by Lord Rayleigh (see Strutt, 1915) that if sodium vapour is illuminated with radiation at these wavelengths, some of the re-emitted energy also appears at the wavelength of the sodium D lines ($\sim$5890 Å) in addition to a fraction showing at the original wavelength. The energy level that has been excited by the incident radiation can emit at the same wavelengths as it returns to the original ground state, or it may de-energise via a cascade of energy levels, each downward jump emitting at particular wavelengths. This phenomenon has been detected in symbiotic stars – see Schmid (1989) and Schmid & Schild (1994), for example.

Polarization effects associated with resonance scattering in the laboratory have an intriguing history, with repercussions on the early development of quantum theory through the discovery and explanation of the *Hanle effect*. Rayleigh (1922) performed a series of experiments involving the scattering of light by mercury vapour. He observed that the 2537 Å line could be linearly polarized, but with puzzling results in that the degree of polarization can change significantly between experiments. Subsequently, Wood & Ellett (1923) found that the observed polarization was sensitive to the orientation of the experimental setup with respect to magnetic fields, including the Earth's field. It was Hanle (1924) who was the first to interpret correctly the observations, using a classical description of a damped atomic oscillator.

Suppose, as in Figure 9.5, the scattering medium is at O, and is illuminated along the direction of Oz, and that part of the scattered radiation is viewed along the direction of Oy. The resonance emission is polarized in direction and amount according to the direction of polarization of the exciting radiation, and to both the direction and strength of the local magnetic field. Sometimes a strong polarization can be observed when an essentially unpolarized line would appear in the field-free case. Consider a few simple scenarios:

1. When the direction of vibration of the electric vector in the exciting radiation is parallel to the x-axis, and the scattering atoms are in the presence of a magnetic field (25–100 G) in the same direction, the observed polarization of the resonance-scattered light will be in the same direction as in the field-free case. Thus a high degree of incident polarization along the x-axis produces scattered light that has strongly enhanced vibrations in the x-direction. This

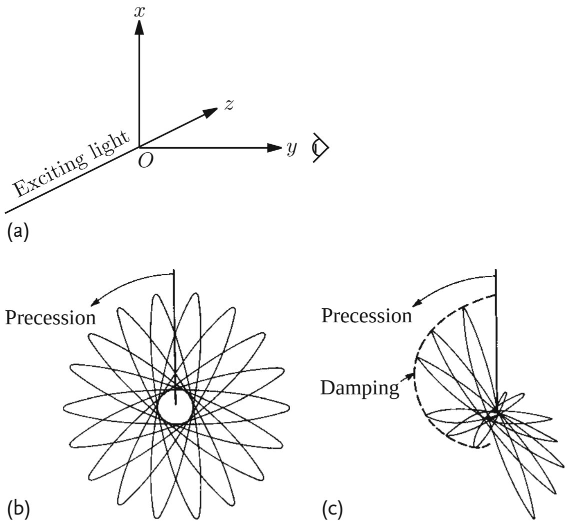

Fig. 9.5 (a) illustrates a reference frame in respect of resonance scattering. (b) depicts the oscillator pattern precessing in the presence of a magnetic field such that the time-averaged observed polarization would reduce to zero. With the effects of damping, as (c) shows, a polarization ensues but with the azimuth of vibration rotated with respect to the original direction. The rosette depictions can be found in Hanle (1924).

follows directly from classical theory for an atom with the scatterer behaving like a classical oscillator.

2. For a weak magnetic field ($<$ a few gauss) parallel to the y-axis, the strong resonance-scattered line still has strongly enhanced vibrations in the x-direction. If the field strength increases, the observed percentage polarization decreases. As long as the field is weak, the direction of vibration only deviates slightly from that of the field-free case, but as the field increases and the polarization continues to decrease, the observed direction of vibration of the polarization rotates by large angles.

The explanation of the behaviour of the observed polarization to the magnetic field orientation can be appreciated in the framework of the classical oscillator. The electronic orbits in the atom precess about the magnetic vector with the atomic oscillator emitting circularly polarized light along the magnetic field, and linearly polarized light normal to the field.

If the atom is considered as a damped oscillator, the dependence of the polarization behaviour to the strength of field is also explained. Due to the effects of precession, the direction of vibration will deviate from the original direction, thus causing the polarization azimuth of the emitted light to be rotated. The oscillator describes the pattern of a rosette when viewed along the magnetic field; the shape of the rosette and consequently the nature of the polarization, will depend on the ratio between the angular velocity of precession, ω, and the radiative damping constant, the latter being the reciprocal of the radiative lifetime, τ, of the oscillator.

If $\omega\tau \gg 1$, the rosette will have central symmetry as the atom will have ample time to precess before being damped out (see Figure 9.5b). Consequently, there is no polarization observed along the magnetic field. If the field is such that $\omega\tau \approx 1$, an asymmetrical rosette would be described by the oscillator (see Figure 9.5c) giving a reduced polarization relative to the field-free case, with a vibration direction rotated with respect to that of the exciting beam. Finally, for $\omega\tau \ll 1$, the oscillator has no time to precess before it is damped out, thus explaining the weak-field behaviour.

The described polarization behaviour was first summarized by Breit (1925) who derived expressions for the degree of polarization and the angle of rotation of the azimuth of vibration. When the magnetic field direction is along the line of sight, the observed polarization is given by

$$p = \frac{p_0}{1 + (g\,\omega_e\tau)^2}\,, \tag{9.22}$$

where p_0 is the degree of polarization for the field-free case, and

$$\omega_e = \frac{eB}{2mc} \tag{9.23}$$

is the Larmor precession velocity for the electron of mass, m, and charge, e, in the presence of a magnetic field, B. The angle of rotation affecting the observed direction of vibration is given by

$$\tan 2\phi = g\omega_e\tau\,. \tag{9.24}$$

The adjustment factor, g, is necessary to obtain the observed results from classical theory. It has since been shown that classical and quantum-mechanical results agree if this correction factor is Landé's g factor for the upper-level (ul) of the transition in question.

A fundamental parameter governing the Hanle effect is the ratio of the Larmor frequency to the A value of the transition:

$$\frac{\omega_e}{A_{ul}} \propto \frac{B}{A_{ul}}\,.$$

Inspection of A values for resonance lines of astrophysical interest indicates that the Hanle diagnostic can be useful for the detection and investigation of magnetic fields in the range of 1–1000 G.

The first astrophysical observation of the Hanle effect was that of Redman (1941) who detected polarization effects near the Sun's limb in the calcium line at 4227 Å. Although the Hanle effect was considered as a diagnostic for investigating solar emission lines (see, for example, Tanberg-Hanssen, 1974) it was not until the 1980s that the subject blossomed in respect of the solar photosphere by the seminal work of Sentflo, Twerenbold & Harvey (1983) and Stenflo, Twerenbold, Harvey, *et al.*

(1983). By the 1990s, solar spectropolarimetry became referred to as the study of *The Second Solar Spectrum* – see Stenflo & Keller (1997), the subject warranting a series of international conferences in its own right – see, for example, Casini & Lites (2006).

The nature of the Hanle effect suggests that it can also have potential as a diagnostic for exploring weak fields in stars, at a threshold much lower than provided by the Zeeman effect. Modelling of the Hanle effect operating within some simple stellar geometries has been undertaken by Ignace, Nordsieck & Cassinelli (1997). They have considered an optically thin ring illuminated by a stellar point source, and applied the results to derive the polarization from polar plumes, equatorial discs and spherical shells. The integrated line polarization was calculated for axisymmetric rings with a variety of magnetic field orientations, and, in all cases, it was found that the polarization is proportional to $\sin^2 i$, where i is the viewing inclination, just as in the zero-field case. It was also found that the Hanle effect can alter the integrated line polarization very significantly. For some cases, the position angle of the polarization within a line can be rotated by 90° relative to the zero field case.

In a later paper, Ignace, Cassinelli & Nordsieck (1999) considered the effects on line profiles for axial and toroidal magnetic fields in optically thin axisymmetric equatorial discs, and for a dipole field in a spherical wind. The magnetic field can cause significant deviations of the polarized line profile from that obtained in the absence of magnetic fields, including flattening of the profile, position angle flips and asymmetries for the profile shape. The occurrence, and degree of these effects, depends on the magnetic geometry, the surface-field strength, and the viewing perspective. In relation to the earlier work (Ignace, Nordsieck & Cassinelli, 1997), this study showed clearly that more information about the magnetic field structure is available from well-resolved resonance lines. As with modelling associated with Thomson scattering in Be stars, the early exercises considered the illuminating star to be a point source. To illustrate the way a finite star effectively reduces the polarization that might otherwise be observed, Ignace (2001) has examined how depolarization factors, and the magnetic field distribution, affect the spatial sensitivity of the Hanle effect as a magnetic diagnostic.

The hot stellar winds as in P Cygni stars have been modelled by Ignace, Nordsieck & Cassinelli (2004). From a given set of scattering lines, stronger fields will lead to higher line polarizations, with the field topology also influencing the polarization profiles. In order to explore the potential of the Hanle affect as a diagnostic for investigating the nature of stellar winds, spectropolarimetry should be at its most powerful in the far ultraviolet and it is anticipated that the required observations will be undertaken in the near future.

9.2.6
Synchrotron Radiation

When charged particles move in a magnetic field their orbits are changed. The Lorentz force on the particles acts perpendicular to both the magnetic field lines and the particle motion. For particles entering the environment of a magnetic field with velocity parallel to the field, the force causes them to spiral around the field as they progress. The acceleration associated with this spiraling motion causes the particles to radiate. For non-relativistic velocities, the nature of the process is very straightforward leading to the production of *cyclotron radiation*. The generated radiation frequencies correspond directly to the gyration frequencies around the field lines. Similar to the description related to the Zeeman effect earlier, the observed polarization depends on the viewpoint relative to the field direction. If the magnetic field is parallel to the line of sight, circular polarization would be observed. If the viewpoint is normal to the field, linear polarization would be apparent. For intermediate viewpoints, elliptical polarization would be recorded.

For particles with relativistic velocities, the gyration frequency takes on its relativistic form given by

$$\omega = \frac{eB}{\gamma mc}\,, \tag{9.25}$$

where γ is given by

$$\gamma = \left(1 - \frac{v^2}{c^2}\right)^{-\frac{1}{2}}\,. \tag{9.26}$$

The frequency spectrum of the radiation does not have a one-to-one relationship with ω and is complex, and may extend to many times the gyration frequencies. In this situation the emitted energy is referred to as *synchrotron radiation*. The emitted radiation is compressed into a small range of angles around the instantaneous velocity vector of the particle. This effect is referred to as *beaming*, and it results in a spreading of the energy spectrum in a way that depends on the momentum of the particle in the direction perpendicular to the field. In such a situation, there is still a maximum photon energy that can be radiated which is proportional to the field strength and inversely proportional to the particle momentum. Synchrotron spectra have a power law shape (flux $\propto$ photon energy to some power) simply due to the particle momenta having a power law distribution. In most astrophysical situations, any synchrotron radiation is generated by free electrons. Most observational studies are related to the detection and interpretation of synchrotron radiation in the radio or X-ray domains, but it has an important polarimetric role to play in the optical spectrum in relation to exotic stars such as AM Her objects, or *polars* (see Chapter 11). It is not expected that synchrotron radiation plays any general role in the generation of polarization within stellar atmospheres, but is very apparent in the material surrounding supernova remnants such as the Crab Nebula.

A discourse on the polarization associated with synchrotron radiation would be out of place here, but the ground work of the physical platforms associated with the topic can be found in the texts of Rybicki & Lightman (1979) and Longair (1994). As described in the latter reference, any elliptical polarization tends to be generated with opposite handednesses which cancel out, leaving the radiation to be dominated by linear polarization. An important factor in determining the degree of polarization is the power-law distribution of the electron energies described by $N(E) = \kappa E^{-u} \mathrm{d}E$. To determine p at a given frequency, averaging over the range of energies that contribute to the intensity at the observed frequency is made, leading to

$$p = \frac{u+1}{u+7/3} \, . \tag{9.27}$$

For a typical value of the exponent describing the energy spectrum of the electrons, say $u = 2.5$, the value of $p \sim 0.72$, an extremely high value relative to all other astrophysical polarigenic effects.

9.3
Electron Scattering – A Simple Stellar Model

An excellent example of how polarimetry offers a distinct advantage of astrophysical diagnosis with respect to regular photometry is readily demonstrated by considering the behaviour of a localized scattering cloud in the cis-stellar environment. An extreme case has already been highlighted in Chapter 1.

Consider the scenario of a single star illuminating an optically thin cloud of electrons. Simply to demonstrate the outcome, it is assumed that both the star and the electron cloud act as a point source and a point scattering centre, respectively, following the model of Brown, McLean & Emslie (1978), as modified by Clarke & McGale (1986).

Figure 9.6a depicts the globule, P, in orbit at a co-latitude, θ, about the star at O, at an arbitrary longitude, ϕ, ($\equiv$ orbital phase). Two sets of Cartesian coordinates can be considered, one, X, Y, Z, associated with the preferred axes of the local stellar geometry, e. g. Z might correspond to the spin axis of the star with X, Y being the equatorial plane, the other, X', Y', Z', describing the observer's position such that $X'O$ corresponds to the line of sight to the star.

The relative orientation of the two frames (see Figure 9.6) is given by the great circle arc, XX′, which may be resolved into the great circle arcs, XM and MX′. The outcome of the behaviour of the model is independent of the fiduciary azimuthal angle corresponding to the arc, XM, only affecting the phase of the variations of brightness and polarization, and, for convenience, it may be taken as zero. The arc, MX′, corresponds to $(\pi/2 - i)$ where i is the inclination of the stellar pole to the line of sight.

The total flux scattered by the globule towards the Earth, and its associated polarization, is determined by applying the scattering matrix for the electron as given in (4.22). If the original stellar radiation is unpolarized, the situation is represented by

$$\begin{bmatrix} I \\ Q \\ U \\ V \end{bmatrix} = \frac{n\sigma_T}{r^2} \begin{bmatrix} \frac{1}{2}(1+\cos^2\chi) & \frac{1}{2}\sin^2\chi & 0 & 0 \\ \frac{1}{2}\sin^2\chi & \frac{1}{2}(1+\cos^2\chi) & 0 & 0 \\ 0 & 0 & \cos\chi & 0 \\ 0 & 0 & 0 & \cos\chi \end{bmatrix} \begin{bmatrix} I_\star \\ 0 \\ 0 \\ 0 \end{bmatrix} , \tag{9.28}$$

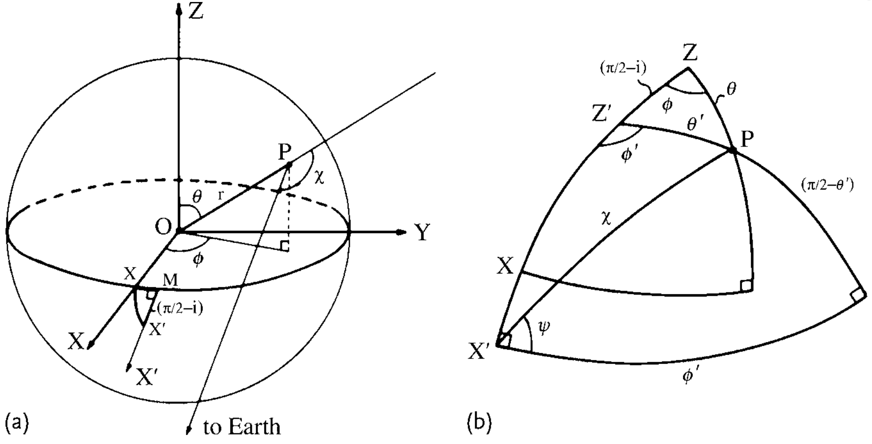

Fig. 9.6 (a) The stellar point source is at O, and P is a general region providing a scattering angle, χ. Stellar (X, Y, Z) and observer (X', Y', Z') coordinates have O as common origin and are uncoupled by the inclination i (arc XZ') of the star's rotation axis (OZ), whilst OX' is the direction to Earth. (b) The stellar coordinates (r, θ, ϕ) can be related to χ through the observer spherical coordinates (r', θ', ϕ').

where n is the number of electrons, each with Thomson cross-section, σ_{T}, in the globule at P, at a distance, r, from the star, providing a scattering angle, χ; $I_\star$ is the unpolarized isotropic intensity of the point source star. Hence the total flux, and the polarized component scattered in the direction of the Earth, may be expressed respectively as

$$I_* \tau_{\mathrm{e}}(1+\cos^2\chi) \qquad \text{and} \qquad I_* \tau_{\mathrm{e}} \sin^2\chi \,, \tag{9.29}$$

where τ_{e} corresponds to the total solid angle subtended by the electrons, as seen from the star. By referring these components to the reference plane that is set at an angle, ψ, to the local scattering plane, the reduced Stokes vector describing the linear polarization is of the scattered light is

$$\begin{bmatrix} I \\ Q \\ U \end{bmatrix} = I_* \tau_{\mathrm{e}} \begin{bmatrix} 1+\cos^2\chi \\ \sin^2\chi\cos 2\psi \\ \sin^2\chi\sin 2\psi \end{bmatrix} , \tag{9.30}$$

with the direction of Q corresponding to the projection of the stellar equator on the sky.

From the geometry depicted in Figure 9.6, the following relationships are readily established:

$$\frac{X'}{r} = \sin\theta'\cos\phi' = \cos\chi \,, \tag{9.31}$$

$$B = \frac{Y'}{r} = \sin\theta'\sin\phi' = \sin\chi\cos\psi \,, \tag{9.32}$$

$$C = \frac{Z'}{r} = \cos\theta' = \sin\chi \sin\psi\ . \tag{9.33}$$

Using the identities above, having related them to the local stellar frame through spherical triangle, $ZZ'P$, the reduced Stokes vector for the scattered contribution to the received flux from the globule may be written as

$$\begin{bmatrix} I \\ Q \\ U \end{bmatrix} = I_* \tau_\mathrm{e} \begin{bmatrix} 2 - (B^2 + C^2) \\ (B^2 - C^2) \\ 2BC \end{bmatrix}, \tag{9.34}$$

where $B = \sin\theta \sin\phi$ and $C = \cos\theta \sin i + \sin\theta \cos\phi \cos i$.

Thus, the variation of the apparent brightness of the system may be explored by considering the first element of the matrix above leading to the expression

$$\frac{I_\star \tau_\mathrm{e}}{2} \left(\sin^2\theta \sin^2 i \cos(4\pi\nu t) - \sin 2\theta \sin 2i \cos(2\pi\nu t)\right), \tag{9.35}$$

where ϕ has been replaced by $2\pi\nu t$, with ν corresponding to the rotational frequency of the globule about the star.

Comment has been made by Clarke & McGale (1987a) on the fact that the expected brightness variations follow the fundamental orbital frequency, but with the harmonic, 2ν, also present, such waveforms being recorded for several Be stars. Equation (9.35) shows that the geometric factors, i and θ, are interchangeable and cannot be decoupled from simple brightness measurements.

In addition to the scattered flux, the observer also receives the direct unpolarized flux from the star, thus reducing the overall degree of polarization that would otherwise be measured. When estimating the degree of polarization of the system, the normalizing total intensity may be taken as that of the star, with that from the scattered component being neglected. Hence, (9.34) may be written as

$$\begin{bmatrix} I \\ Q \\ U \end{bmatrix} = I_* \begin{bmatrix} 1 \\ \tau_\mathrm{e}(B^2 - C^2) \\ 2\tau_\mathrm{e} BC \end{bmatrix}. \tag{9.36}$$

Using this representation, the polarimetric behaviour of this scenario has also been discussed by Clarke & McGale (1987b). It can be readily shown that the normalized Stokes parameters may be written as

$$q = \tau_\mathrm{e}\left[q_o + q_1 \cos(2\pi\nu t) + q_2 \cos(4\pi\nu t)\right], \tag{9.37}$$

$$\text{and} \qquad u = \tau_\mathrm{e}\left[u_1 \sin(2\pi\nu t) + u_2 \sin(4\pi\nu t)\right]. \tag{9.38}$$

The coefficients in the expression describing q and u are given by

$$q_0 = \sin^2 i \left(\frac{3\sin^2\theta}{2} - 1\right); \qquad \tau_\mathrm{e} = \frac{n\sigma_T}{r^2} \tag{9.39}$$

$$q_1 = -\frac{1}{2}(\sin 2\theta \sin 2i); \qquad u_1 = \sin 2\theta \sin i \,, \tag{9.40}$$

$$q_2 = -\frac{1}{2}\left(\sin^2 \theta (1 + \cos^2 i)\right); \qquad u_2 = \sin^2 \theta \cos i \,. \tag{9.41}$$

Hence, the time-dependent behaviour of the NSPs may be written as

$$q(t) = \tau_{\mathrm{e}}\left[q_o - \frac{1}{2}\sin 2\theta \sin 2i \cos(2\pi\nu t) - \frac{1}{2}\sin^2\theta (1 + \cos^2 i)\cos(4\pi\nu t)\right] \tag{9.42}$$

and

$$u(t) = \tau_{\mathrm{e}}\left[\sin 2\theta \sin i \sin(2\pi\nu t) + \sin^2 \theta \cos i \sin(4\pi\nu t)\right]. \tag{9.43}$$

It may be noted that both NSPs carry variations with components at the orbital frequency and its harmonic. In principle then, by recording the temporal polarimetric behaviour of the system, the separate, individual values of i and θ can be determined, thus providing a means of decoupling the affects associated with the system's geometry and its aspects, highlighting the power of polarimetry over photometry. Further expansion and discussion on this theme in relation to binary stars is reserved for Chapter 11.

References

Babcock, H.W. (1949) Magnetic intensification of stellar absorption lines. *ApJ*, **110**, 126–142. [182]

Babcock, H.W. (1958) A catalog of magnetic stars. *ApJS*, **3**, 141–210. [179]

Babcock, H.W. (1962) Measurement of stellar magnetic fields – Chapter 5 in *Stars and Stellar Systems. II Astronomical Techniques*. (ed. W.A. Hiltner), University of Chicago Press, Chicago. [179]

Bray, R.J., Loughhead, R.E. (1964) *Sunspots*. Chapman and Hall, London (see Chapter 5). [179]

Breit, G. (1925) Polarization of resonance radiation in weak magnetic fields. *J. Opt. Soc. Am.*, **10**, 439–452. [187]

Brown, J.C., McLean, I.S., Emslie, A.G. (1978) Polarisation by Thomson scattering in optically thin stellar envelopes II. Binary and multiple star envelopes and the determination of binary inclination. *A&A*, **68**, 415–427. [190]

Casini, R., Lites, B.W. (eds) (2006) *Solar Polarization 4 – ASP Conf. Ser.*, **358**, San Francisco. [188]

Clarke, D., McGale, P.A. (1986) Temporal polarization variations of Be stars I. Models based on stochastic behaviour. *A&A*, **169**, 251–258. [190]

Clarke, D., McGale, P.A. (1987a) Double periodicity in Be stars. pp 197–198 in *Physics of Be Stars*, Proc. IAU Coll. No: 92, (eds A. Slettebak & T. P. Snow), Cambridge University Press, Cambridge. [192]

Clarke, D., McGale, P.A. (1987b). Temporal polarization variations of Be stars II. Model fitting of polarimetric data. *A&A*, **178**, 294–300. [192]

Donati, J.-F., Semel, M., Carter, B.D., Rees, D.E., Cameron, A.C. (1997) Spectropolarimetric observations of active stars. *MNRAS*, **291**, 658–682. [184]

Donati J.-F., Semel, M., Praderie, F. (1989) Zeeman–Doppler imaging of active stars II.

Numerical simulation and first observational results. *A&A*, **225**, 467–478. [184]

Hanle, W. (1924) Über magnetische Beeinflussung der Polarisation der Resonanzfluoreszenz. *Zeit. Phys.* **30**, 93–105. [185, 186]

Ignace, R. (2001) The Hanle Effect as a diagnostic of magnetic fields in stellar envelopes III. Including the finite star depolarization effect. *ApJ*, **547**, 393–401. [188]

Ignace, R., Nordsieck, K.H. Cassinelli, J.P. (1997) The Hanle Effect as a diagnostic of magnetic fields in stellar envelopes: I. Theoretical results for integrated line profiles. *ApJ*, **486**, 550–570. [188, 188]

Ignace, R., Cassinelli, J.P., Nordsieck, K.H. (1999) The Hanle Effect as a diagnostic of magnetic fields in stellar envelopes: II. Some theoretical results for resolved line profiles. *ApJ*, **520**, 335–346. [188]

Ignace, R., Nordsieck, K.H., Cassinelli, J.P. (2004) The Hanle Effect as a diagnostic of magnetic fields in stellar envelopes. IV. Applications to polarized P Cygni wind lines. *ApJ*, **609**, 1018–1034. [188]

Jenkins, F.A., White, H.E. (1965) *Fundamentals of Optics*, 3rd Edition (International Student Edition), McGraw-Hill, New York. [176]

Kemp, J.C. (1970) Circular polarization of thermal radiation in a magnetic field. *ApJ*, **162**, 169–179. [179]

Kemp, J.C., Wolstencroft, R.D., Swedlund, J.B. (1972) Circular polarimetry of fifteen interesting objects. *ApJ*, **177**, 177–189. [179]

Leroy, J.L. (1989) The spectral variation of polarization due to magnetic intensification. *A&A*, **215**, 360–370. [182, 183]

Leroy, J.L. (1990) Broad-band polarization in crowded spectra. *A&A*, **237**, 237–242. [182]

Longair, M.S.(1994) *High energy astrophysics* Vol: 2 *Stars, the Galaxy and the Interstellar Medium*, 2nd edition, Cambridge University Press, Cambridge. [189]

Rayleigh, Lord (1922) Polarization of light scattered by mercury vapour near the resonance periodicity. *Proc. R. Soc. London*, **102**, 190–196. [185]

Redman, R.O. (1941) Observational search for polarisation in the calcium line λ 4227 near the Sun's limb. *MNRAS*, **101**, 266–272. [187]

Rybicki, G.B., Lightman, A.P. (1979) *Radiative Processes in Astrophysics*, John Wiley & Sons, New York. [189]

Schmid, H.M. (1989) Identification of emission bands $\lambda\lambda$ 6830, 7088. *A&A*, **211**, L31–L34. [185]

Schmid, H.M., Schild, H. (1994) Raman scattered emission lines in symbiotic stars: a spectropolarimetric survey. *A&A*, **281**, 145–160. [185]

Semel M. (1989) Zeeman–Doppler imaging of active stars I. Basic principles. *A&A*, **225**, 456–466. [184, 183]

Semel, M., Donati, J.-F., Rees, D.E. (1993) Zeeman–Doppler imaging of active stars III. Instrumental and technical considerations. *A&A*, **278**, 231–237. [184]

Stenflo, J.O., Keller, C.U. (1997) The second solar spectrum. A new window for diagnostics of the Sun. *A&A*, **321**, 927–934. [188]

Sentflo, J.O., Twerenbold, D., Harvey, J.W. (1983) Coherent scattering in the solar spectrum: survey of linear polarization in the range 3165–4230 Å. *A&AS*, **52**, 161–180. [187]

Stenflo, J.O., Twerenbold, D., Harvey, J.W., Brault, J.W. (1983) Coherent scattering in the solar spectrum: survey of linear polarization in the range 4200–9950 Å . *A&AS*, **54**, 505–514. [188]

Strutt, R.J. [Lord Rayleigh] (1915) Observations on the fluorescence and resonance of sodium vapour – II. *Proc. R. Soc. London*, **91**, 511–523. [185]

Tanberg-Hanssen, E. (1974) Polarization of solar emission lines pp. 730–751 in *Planets, Stars and Nebulae studied with Photopolarimetry*, Ed. T. Gehrels, University of Arizona, Tucson, AZ. [187]

Warwick, J.W. (1951) Absorption-line polarization in magnetic stars. *AJ*, **56**, 50–51. [182]

Wood, R.W. (1905) The fluorescence of sodium vapour and the resonance radiation of electrons. *Proc. Phys. Soc. London*, **19**, 764–778. [185]

Wood, R.W., Ellett, A. (1923) On the influence of magnetic fields on the polarization of resonance radiation. *Proc. R. Soc. London, Series A*, **103**, 396–403. [185]

Part II The Interstellar Medium – Binary Stars – Early and Late Type Stars – Variable Stars

Chapters 10–15

PROGRAMME: The first major impact of Stellar Polarimetry was the discovery that galactic dust has polarizing properties, forcing a realization that the grains are not spherical, and are subject to alignment forces. Observational follow-up has provided a wealth of information on the dust's optical properties, and on the potential causes of the alignment. Although magnetic processes are favoured, the exact mechanism remains under debate. The story of interstellar polarization is presented in Chapter 10.

As the techniques and sensitivities of polarimeters have improved, phase-locked variability has been discovered in binary stars, and polarimetric measurements of these systems have provided information on mass transfer, and on the geometry of the binary orbits. The progress on these topics is described in Chapter 11.

Because of the multivariate attributes of some stars engendering intrinsic polarization, it is impossible for any scheme to place discussion of them under unique labels. Some stars, for example, may be considered as being binaries and, at the same time, exhibiting a magnetic field, or being simply designated as being of late-type. Although the divisions are a little artificial, for the purposes of presentation of their polarimetric behaviour here, Chapter 12 has been set aside to cover stars with strong magnetic fields. Chapters 13 and 14 relate to Early-Type and Late-Type stars, respectively. Finally Chapter 15 presents material for a range of stellar behaviours that do not readily fit into the above categories, and it also highlights other topics which are important to Stellar Polarimetry.

In the last chapters it is important to note that polarization can act as a diagnostic for determining evolutionary state, an outcome not envisaged when polarimetry was first applied to the stellar scene. Stars settling onto the main sequence can have magnetic fields and/or cis-stellar clumpy dust distributions, and older stars leaving the main sequence tend to exhibit asymmetry in their shell structures.

Again, all the cited papers in Part II are fully referenced at the conclusions of the appropriate chapters but, in some cases, the listings have been sub-divided according to the section heading dealing with a particular stellar type.

Stellar Polarimetry. David Clarke

ISBN: 978-3-527-40895-5

10
Interstellar Polarization

10.1
Introduction

The history associated with the revelation of interstellar polarization by Hall (1949) and Hiltner (1949) has already been presented in Chapter 1. Both Hiltner and Hall continued to make polarimetric observations following their momentous discovery. Hall & Mikesell (1949) reported on some 175 measurements of early-type stars. They also attempted to measure circular polarization, but concluded that the polarization form was essentially linear. Hiltner (1950) also extended his measurements to the infrared to see how they behaved relative to the photometric interstellar extinction law. Both Hiltner and Hall provided catalogues of their measurements and these have been extended by a host of workers (see the last section of Chapter 8).

As instrumental sensitivities have improved, explorations of the wavelength dependence of interstellar polarization have progressed, and detections of circular polarization have been pursued. All these studies have lead to improvements on the large scale, with respect to mapping structures within the Galaxy, and, on the small scale, to the understanding of the properties of interstellar dust grains, of their growth, and the role they play in respect of interstellar chemistry.

A popular discourse on interstellar polarization has been given by Greenberg (1967). Several citations on the relationship between polarimetry and our knowledge of the interstellar magnetic field are given in Heiles (1976). For the developments related to the measurements, their basic interpretation and the elements of scattering theory, a resumé to $\sim$ 1980 on the usefulness of polarization as a diagnostic for understanding the nature of interstellar dust has been provided by Greenberg (1978).

10.2
Polarization Growth with Distance

Lodèn (1961a, 1961b) made both photographic and photoelectric studies, investigating the relationships between p and different parameters, especially that of

Stellar Polarimetry. David Clarke

ISBN: 978-3-527-40895-5

stellar distance. Polarization and colour excess, and the growth of polarization with distance, have been investigated in 35 Kapteyn's selected areas by Reiz & Franco (1998).

As the accumulated mass of dust along any line of sight grows with distance, it is expected that the degree of polarization associated with any star will also depend on its distance. In fact, measurements of polarization can act as a crude means of determining a distance modulus; such a simple strategy has been used by Clarke (1964) and McLean (1976) in respect of novae. It may be noted, however, that the polarization–distance modulus is not a perfect correlation in that extinction grows as an algebraic summation, according to the number of grains along the line of sight, while the polarization growth depends on the orientations of the grains en route, with the resultant involving vector additions.

Lloyd & Harwit (1973) have analysed the growth of p with distance around the galactic equator in $10^\circ \times 10^\circ$ zones by calculating mean values of p up to some given distance, subtracting this from the measured value, and then repeating the procedure to a new distance. Their preliminary results clearly showed that starlight is systematically polarized in passing through spiral arms. Later, Fowler & Harwit (1974) completed this study by performing the incremental polarizational growth analysis at higher galactic latitudes, rather than simply around the galactic equator. The work provided maps of the p vector for a range of stepped distances from the Sun. Within the spiral arms, the orientations of the incremental p vector is correlated with the directions of the arms. Krautter (1980) performed similar analyses around the galactic plane out to a distance of 3 kpc with additional data, but came to the conclusion that no obvious correlation between the dust distribution and spiral arm indictors could be found.

In relation to the solar environment, Piirola (1977) provided a catalogue of 77 Stars within 25 pc showing a growth of interstellar polarization with distance given by $\overline{p_0}/\overline{r} = 0.0004\%\,\mathrm{pc}^{-1}$, suggesting that the measured stars could be used as zero polarization standards. Using the most accurate determinations of polarization, with more than 700 stellar measurements accurate to better than 0.02%, Leroy (1993) has performed an analysis on the presence of interstellar dust within 50 pc of the Sun. There appears to be a complete depletion of dust within 35 pc, with the dust signature beginning at 40–50 pc in a few directions, but more frequently at 70–100 pc, which seems to be the boundary of the local bubble. The existence of a nearby dusty region around $l = 0^\circ$, $b = -20^\circ$, as reported by Tinbergen (1982), was not confirmed. Later, Leroy (1999) used the Hipparcos stellar parallaxes in a re-analysis of the interstellar polarization in the local solar neighbourhood. The chief conclusions of the study were that the nearest patches of dust are at about 70 pc in some directions, in others beyond 150 pc. The region devoid of dust, commonly referred to as the *Local Hot Bubble,* is irregular in shape. The interstellar magnetic field revealed by the nearest polarized stars is certainly not a smooth, uniform field along the galactic equator; the structure is complex and this cannot be dismissed as an artefact of using inaccurate values of stellar distance.

10.3
Polarization and Extinction

10.3.1
p/A_V

From the early discoveries relating to interstellar polarization, it was obvious that for p to have a significant value, it must be associated with photometric extinction. As a consequence, there have been many studies whereby the relationship between p and A_V, have been explored.

The clustering of OB stars in Cygnus was investigated by Hiltner (1954a). No strong correlation between polarization and absorption emerged. It was suggested that the variation in the polarization in the group was not a consequence of polarization and depolarization within a series of clouds, but rather as a result of non-uniformity in orientation of the particles within the cloud or clouds. Hiltner (1954b) measured nine stars in M 29 in Cygnus and recorded a twist in the position angle across this galactic cluster. A strong correlation was found between polarization and extinction; the growth of polarization with extinction was about one half the rate as found in the direction of Cas–Per, where the rate is at its maximum. A catalogue of photometric, polarimetric and spectroscopic observations was provided by Hiltner (1956a). This work was key to the determination of polarization/extinction ratios. A selection of such data for eight zones around the galactic equator is presented in Figure 10.1. A maximum value for the ratio of polarization/absorption, p/A_V, was determined as ~ 0.06 (p expressed in magnitudes), this being equivalent to $p \sim 2.76\%$ per magnitude of extinction. A maximum polarization of 0.22 mag ($\sim$10%) was found in Cygnus, where the absorption is in excess of 10 mag.

10.3.2
$p/E_{(B-V)}$

In a short review paper, Hiltner (1956b) provided vector maps of zones in Cassiopeia and Cygnus. In the former region, the polarizations were relatively large with well correlated position angles; for the latter region, the polarization was generally smaller, with the position angles well less correlated. For M 29 (Cygnus), a strong correlation was observed between p and the colour excess, $E_{(B-V)}$. For Cassiopeia, $p/E_{(B-V)} = 0.18$ provides the observable maximum values for p (expressed in magnitudes). A group of OB stars in the direction of the galactic centre was also observed by Hiltner (1954c). Again it was found that the interstellar polarization was greatest for the more highly reddened stars.

Several star clusters have been investigated by Serkowski (1965). Quite generally, the directions of vibration associated with each star of the particular cluster are very much co-aligned. Study of the connection between p_V and E_{B-V} shows that there are fairly distinct differences in cluster behaviours. For example, comparisons are made of the behaviour of NGC 2422 with NGC 2437 (= M 46), the latter being more

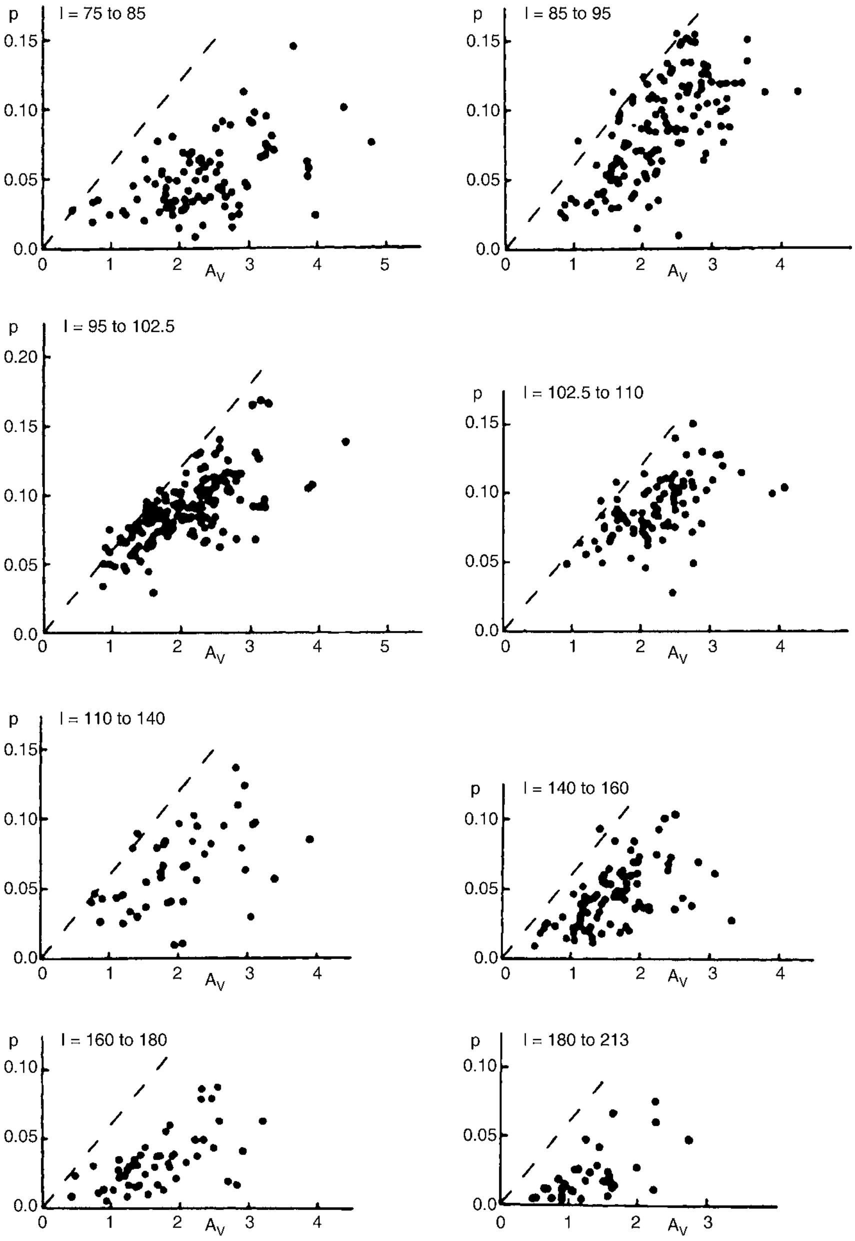

Fig. 10.1 Measurements of p (mags) plotted against A_V for six regions along the galactic equator. The dashed line, given by $p/A_V = 0.06$, represents an upper limit of the envelope. In the galactic longitude region of $l = 75°$ to $85°$, the p, A_V values are dispersed but, in the region $l = 95°$ to $102.5°$, the data are more compact and closer to the envelope boundary, this latter region offering alignment of position angles with small dispersion. (From Hiltner, 1956a.)

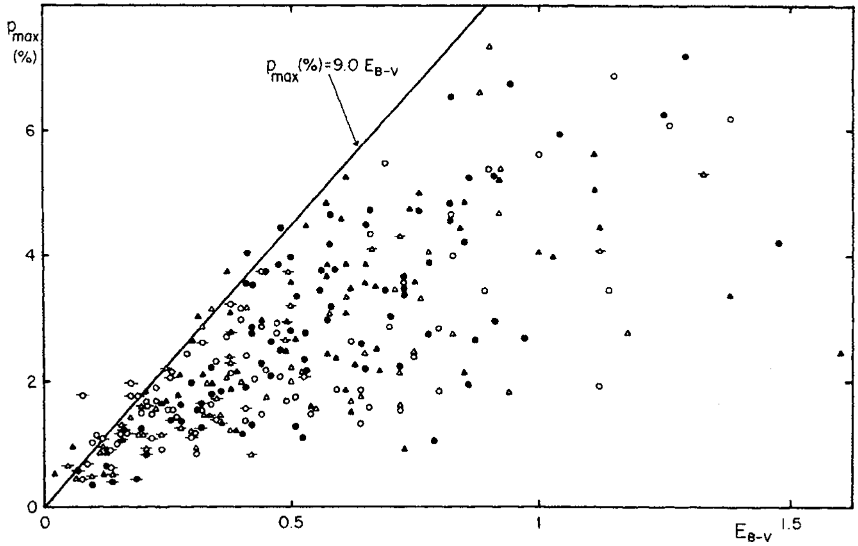

Fig. 10.2 The relationship between the maximum interstellar polarization, $p_{\max}$ (%), and colour excess, $E_{(B-V)}$, is depicted for a variety of stars. A straight line denoting the upper limit of the data spread corresponds to $p_{\max}/E_{(B-V)} = 9.0$. The symbols ▲, ●, ○ and △ correspond to $\lambda_{\max}$ values, $\leq 0.51\,\mu$m, 0.52–0.54 μm, 0.55–0.57 μm and $\geq 0.58\,\mu$m, respectively. Symbols for stars nearer than 0.4 kpc are crossed with a horizontal bar. (From Serkowski, Mathewson & Ford, 1975.)

strongly reddened and three times more distant, but without exhibiting larger polarization; the angular distance between the two clusters is only 1.°3. From all of the data, it is suggested that the maximum ratio of polarization to reddening is given by $p_V/E_{(B-V)} = 0.195$. From polarimetric studies, Dyck & McClure (1969) were able to show that, by using an upper limit for the polarization-reddening ratio given by $p/E_{(B-V)} \leq 0.195$, any reddening of the clusters M 3 and M 13 is insignificant.

Broadband measurements of stars exhibiting interstellar polarization display a smooth variation with a peak, $p_{\max}$, somewhere within the visual range of the spectrum. In Figure 10.2, values of $p_{\max}$ are plotted against the colour excess, $E_{(B-V)}$, for stars measured by Serkowski, Mathewson & Ford (1975). The boundary marked by $p_{\max}\,(\%) = 9.0\,E_{(B-V)}$ is clearly defined.

Serkowski (1968) found that the ratio p_V/p_B was well correlated with the ratio of colour excesses, $E_{(V-I)}/E_{(V-R)}$. Later, Serkowski, Gehrels & Wiísniewski (1969) presented clear correlations of polarization ratios measured in different colours with respect to colour excess ratios.

10.3.3
Relationship between *p* and *R*

As colour measurements became more precise, it was found that, for each star, $p(\lambda)$ displays a maximum value at some point in the middle part of the optical spectrum. In discussions of the spectral behaviour of p, it became convenient to describe the maximum value for any star as $p_{\max}$, occurring at some wavelength given by $\lambda_{\max}$.

From early measurements made by Serkowski (1968), it was found that $p_{\max}$ is shifted towards longer wavelengths for higher values of R, the ratio of total to selective extinction ($A_V/E_{(B-V)}$). Later, Serkowski, Mathewson & Ford (1975) reported on $UBVR$ measurements for 180 stars, mainly in the Southern Hemisphere. They found a correlation between R and $\lambda_{\max}$, with the relationship that $R = 5.5\lambda_{\max}$. They commented that polarimetry seems to be the most practical method of estimating R in any region of the sky. Several of the observed stars revealed a wavelength dispersion of the position angle, and two stars (No. 12 in association VI Cygni and HD 204827) displayed high levels of circular polarization.

Partly by noting that R is correlated with $\lambda_{\max}$, Whittet (1977) has shown that its value is systematically higher in the Southern Milky Way. He has shown that its dependence on galactic longitude has sinusoidal form and expressible as $R(l) = R_0 + R_1 \sin(l + \theta)$, where $R_0 = 3.08 \pm 0.03$, $R_1 = 0.17 \pm 0.06$ and $\theta = 175° \pm 20°$. The effect can be explained simply by there being a variation in the mean size of the dust grains in the local spiral arm. This work was followed by a research note by Whittet (1979) in which the analysis was conducted in a little more detail, showing that the $\lambda_{\max}$ variation with galactic longitude is a local phenomenon produced by grains within 500 pc of the Sun, with the high $\lambda_{\max}$ stars very likely being associated with Gould's belt.

The properties of the ISM along lines of sight known to have high values of $\lambda_{\max}$ have been studied by Cohen (1977), and she confirmed the hypothesis that these regions contain particles where the grain size is abnormally large, corresponding to the densest parts of the interstellar medium. It was suggested that the grains grow by accretion from the gas, and not by coalescence of previously existing grains.

Vrba, Coyne & Tapia (1993) have made a comprehensive study of the ρ Ophiuchi dark cloud, including polarimetric measurements. It was found that R scales with $\lambda_{\max}$ at the rate of $R = 5.7\lambda_{\max}$, this being consistent with other studies. They conclude that the grain size, as deduced from $\lambda_{\max}$, increases with optical depth in a manner consistent with a simple model of turbulence-driven coagulative grain growth.

A study of the Chamaeleon I dark cloud by Whittet, Gerakines, Carkner, *et al.* (1994) revealed that the highest values of $\lambda_{\max}$ are found in lines of sight that intercept the dense central region of the cloud. The value of R was only weakly correlated with $\lambda_{\max}$, suggesting a degree of independence among the populations of grains responsible for optical extinction and polarization. The ratio of $p_{\max}/A_V \simeq 4.5\,\%$ mag^{-1} is unusually high in some lines of sight, indicating a remarkable degree of alignment efficiency in comparison with other dark clouds. The mean direction of the magnetic field in the plane of the sky is perpendicular to the long axis of the cloud and parallel to the external field in the galactic neighbourhood, suggesting that the cloud formed by uniform collapse along field lines.

Special attention has been given by McMillan (1977) to polarimetry of the star Walker No. 67 in NGC 2264. The value of $p_{\max}$ of this star is very high at 5.5% with

$\lambda_{\max} = 0.88\,\mu\text{m}$. Both the infrared colour excess and distance modulus imply a high value of R, between 4 and 5, this being consistent with the large $\lambda_{\max}$, all suggesting the presence of large interstellar gains in a dense dust cloud near the centre of the cluster which has not been dispersed by the local, hot, luminous stars. The direction of vibration also displays a strong dispersion, $\sim 14°$ per µm. This star has been promoted by McMillan (1977) as a prime candidate for investigation by circular polarimetry. The birefringence of the interstellar medium can be determined by comparing the value of $\lambda_{\max}$ with the wavelength at which sign reversal of circular polarization occurs. The suggestion has not yet been followed, it requires circular polarimetry in the near infrared, a problem which is now resolvable by application of CCD detectors.

From measurements of 21 stars near the Orion nebula, Breger (1977) has shown that their behaviour generally corresponds to the characteristics of the interstellar law, but with some stars having high values of $\lambda_{\max}$. For two stars (BR 545 and BR 885), the large values of $\lambda_{\max}$ were found to be associated with unusually large values of R. Most of the observed polarization appears to arise from intracluster dust aligned by a magnetic field. McCall (1981) found that the stars located within the bounds of the great nebula in Orion have $\lambda_{\max}$ values larger than those of surrounding stars. Because the polarization can be attributed primarily to intracluster dust, it was concluded that grains located inside the nebula are larger than grains outside. Further polarimetric observations were made by Breger, Gehrz & Hackwell (1981) in combination with infrared photometry. For stars lying outside the two main regions of nebulosity, normal values of R and $\lambda_{\max}$ ($\sim$ 3 and 0.55 µm, respectively) occur, with normal grain sizes indicated. For stars carefully selected as being inside the nebulosity, extinction is characterized by large grains ($R \sim 5$, $\lambda_{\max} \sim 0.75\,\mu\text{m}$). In Orion, large interstellar grains are found in, and restricted to, regions of nebulosity.

10.4
The $p(\lambda)$ Curve

Some early colour measurements of the recently discovered interstellar polarization were made by Behr (1959). As it has turned out, several of his target stars were later shown to exhibit intrinsic polarization with a different wavelength dependence to that produced by the interstellar medium. Nonetheless differences in p were recorded between the three colour filter measurements. Mention of a variable polarization associated with γ Cas was also made. Observations to explore the wavelength dependence of interstellar polarization were later conducted by Treanor (1963). Early measurements were also presented by Gehrels (1960). From the eight stars observed, the maximum polarization occurred at $\sim$ 6500 Å. Comparisons with theoretical calculations provided good fits to the $p(\lambda)$ curves for both metallic and dielectric grain types without any strong distinction. Gehrels (1961) noted that reddening, and the $p(\lambda)$ curve, indicated interstellar particles with sizes $\sim$0.3 µm, and suggested that extending measurements to the UV would help in establishing the nature of the grains. He proposed that, by using instruments on balloons at 100 000 ft, decisive studies might be made at 2200 Å. The Polariscope Programme involving a balloon-borne instrument for ultraviolet measurements has been referenced by Gehrels (1972). Other early colour dependent observations were presented by Gehrels & Meltzer (1966).

Although the paper of Coyne & Gehrels (1967) is subtitled ‘interstellar polarization’, seven of the discussed stars are noted as displaying variable polarization, indicating that at least some elements of the measured values were intrinsically generated. Striking differences from the then current mean interstellar $p(\lambda)$ curve were found near Orion. Wickramasinghe (1969) proposed mixtures of graphite–silicate grains, the model giving rise to a broad maximum in the $p(\lambda)$ curve at 5000 Å. Further colour measurements were made by Coyne & Wickramasinghe (1969) with the general behaviour being discussed in terms of a composite interstellar grain model with a graphite core and dielectric mantle.

Early colour measurements by Serkowski (1968) demonstrated the correlation between regional variations in the wavelength dependence of interstellar extinction and polarization. Again by using standard UBV filters, data assembled by Serkowski & Robertson (1969) showed that the ratio of p_V/p_B depends on galactic longitude. In a review paper, Serkowski (1973) showed that there are well defined regions in the sky where $\lambda_{\max}$ is higher than average. As noted earlier, values of $\lambda_{\max}$ correlate well with R, the ratio of total to selective extinction. In the same paper, the law, now referred as the *Serkowski law*, describing the general behaviour of the wavelength dependence of interstellar polarization was presented.

By taking the $p(\lambda)$ values of individual stars and normalising them to their determined maximum value, $p_{\lambda_{\max}}$, occurring at some wavelength, $\lambda_{\max}$, and by normalising the wavelength values, λ, to $\lambda_{\max}$, an overall plot of $p/p_{\lambda_{\max}}$ against $\lambda_{\max}/\lambda$ produces a unique curve (Figure 10.3) described by an empirical formula of the form

$$\frac{p(\lambda)}{p(\lambda_{\max})} = \exp\left[-K \ln^2\left(\frac{\lambda_{\max}}{\lambda}\right)\right], \tag{10.1}$$

with $K \cong 1.15$ being the same for all stars. The algebraic representation above was originally proposed by Serkowski (1971),but with an erroneous value for K which the later paper (Serkowski, 1973) confirmed as being a misprint.

The method of fitting data to Serkowski’s law by a least-squares procedure is given by Coyne, Gehrels & Serkowski (1967). In this same paper, values of $\lambda_{\max}$ and $p_{\max}$ are listed for 202 stars, and the form of Serkowski’s law is compared with models based on dielectric cylinders subject to the Davis–Greenstein (see later) orientation mechanism.

The value of K used in Serkowski’s law is a mean taken from measurements of many stars. Codina-Landaberry & Magalhães (1976) have considered the role that it takes in relation to the individual value of each star, suggesting that it can act as an estimator of the discrepancy among particle sizes along the line of sight.

Differences in determined values of K are clearly shown in the observations of Clarke (1986) for the stars o Sco and σ Sco. With the advent of 2D detectors, it has

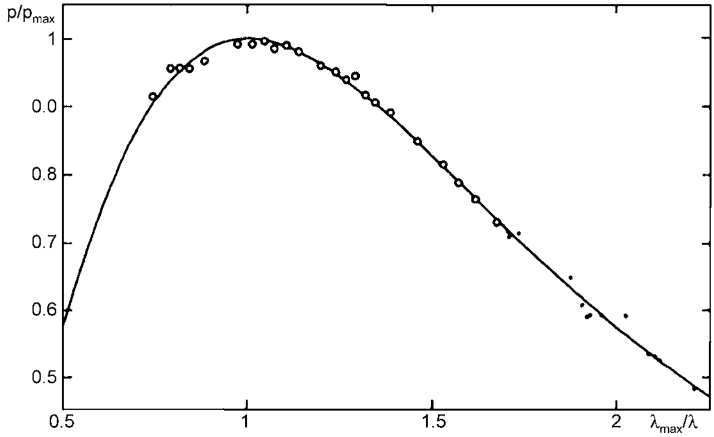

Fig. 10.3 An early form of the normalized wavelength dependence of interstellar polarization compares data with the basic Serkowski law as expressed in (10.1) with $K = 1.15$. Each open circle is based on 20 stars; each dot represents measurements of an individual star with a particular filter. (From Serkowski, Mathewson & Ford, 1975.)

become possible to record the $p(\lambda)$ curve at higher spectral resolution with the behaviour sampled at more wavelength points. Improved values for $p_{\max}$ and $\lambda_{\max}$ are then obtained with any variations of K being assessed better. In addition, such data provide more sensitive discrimination in the detection of any small intrinsic contributions to the resultant polarimetric signal (see Weitenbeck, 1999, 2004, for example).

By extending observations of *o* Sco into the infrared, Cox, Hough, Adams, *et al.* (1976) found that the values were larger than expected, based on the predicted behaviour according to Serkowski's law using optical-band measurements. Also, Dyck & Jones (1978) extended the colour measurements of interstellar polarization to the *JHK* bands and, for seven observed stars, noted that p fell less rapidly longward of $\lambda_{\max}$ than predicted by Serkowski's relation, with the measurements behaving according to there being a mixture of graphite and silicate grains. Observations of polarization combined with extinction were made at 2.2 µm by Jones (1989). He found an excellent correlation over a range of optical depths of 100, these being independent of physical path length. This behaviour was modelled involving equal contributions from a uniform component and a random component to the interstellar magnetic field, with the two components maintaining roughly the same proportions and strength in most phases of the interstellar medium.

Following new observations made in the near-infrared, Wilking, Lebofsky, Martin, *et al.* (1980) found that there is a broadening of the $p(\lambda)$ curve as $\lambda_{\max}$ decreases. They proposed a new form of the Serkowski empirical relation whereby the value of K depends on the value of $\lambda_{\max}$. According to this development:

$$\frac{p}{p_{\max}} = \exp\left[-1.7\lambda_{\max}\ln^2\left(\frac{\lambda_{\max}}{\lambda}\right)\right]. \tag{10.2}$$

The most simple explanation for the observed behaviour may be ascribed to prolate grains becoming more spherical (or oblate grains becoming flatter) as the mean grain size increases, or to a progressive narrowing of the size distribution of polarizing grains as the mean grain size increases. Both of these mechanisms are consistent with models for grain growth in interstellar clouds in which grains have accreted mantles in proportion to the heavy-element depletion of the gas. Further observations and analysis by Wilking, Lebofsky & Rieke (1982) suggest that the description of the variation of K with $\lambda_{\max}$ may be more accurately expressed as

$$K = (-0.10 \pm 0.05) + (1.86 \pm 0.09)\lambda_{\max} . \tag{10.3}$$

By considering the behaviour of grain growth, Aannestad (1982) demonstrated that the narrowing of the $p(\lambda)$ curve with $\lambda_{\max}$ can be explained by the shifting and steepening of the grain size distribution as would happen by size-independent accretion. In a further paper, Aannestad & Greenberg (1983) showed that the observed correlation of the width of the normalized polarization curve with $\lambda_{\max}$ is most likely caused by the accretion of dielectric mantles forming on grains with an initial power-law size distribution, and not by size modification of the power-law distribution by subsonic turbulent coagulation.

The behaviour of the correlation between K and $\lambda_{\max}$ was shown by Clarke & Al-Roubaie (1983) to be susceptible to the choice of filter passbands for the observations and to the signal-to-noise ratios of the measurements. Clarke & Al-Roubaie (1984) also demonstrated how K and $\lambda_{\max}$ may be affected by the presence of complex cloud structures along the line of sight. The difficulties of fitting newly acquired infrared polarization values to the Serkowski law have also been discussed by Clarke (1984).

Extensions of observations by Gehrels (1974) to the ultraviolet for a couple of stars were made by a balloon platform, and, in the same paper, he reported on measurements made in the infrared. The measurements of κ Cas provided wavelength extension to its $p(\lambda)$ associated with interstellar polarization, whereas those of γ Cas indicate an origin by the extended hydrogen shell surrounding the star.

Shulz & Lenzen (1983) performed a study of three stars with high precision using *UBVRI* observations to investigate the Wilking, Lebofsky, Martin *et al.* (1980) relation given in (10.2). They discuss the importance of separating out the effects of multiple clouds along the line of sight with differing gain alignments. The star, Cyg OB2 Sch. No:12, is an example showing that the observed $p(\lambda)$ is broadened as a result of its light passing through two clouds, the dissociation being achieved by modelling such that the observed wavelength dependence of the direction of vibration is accounted for (see also references to this star under the section on Circular Polarization).

Clayton, Anderson, Magalhães, *et al.* (1992) measured the ultraviolet behaviour of the interstellar polarization of six stars using the Wisconsin Ultraviolet Photopolarimeter Experiment (WUPPE) on the Astro-1 Mission. Three stars provided a good fit to the extrapolated Serkowski curve while one displayed an excess polarization in the ultraviolet. The star HD 197770 clearly showed a bump in $p(\lambda)$ closely matching the 2175 Å extinction feature. A more detailed discussion of the results was given by Wolff, Clayton & Meade (1993). Their general conclusion was that the MRN-bare silicate grain model (see below) was most successful in fitting the data. The polarization bump at the extinction dip was considered in terms of a graphite grain component. The apparent necessity of aligning both small silicate and graphite grains seems to raise questions about theories of grain alignment mechanisms.

The interstellar extinction over the wavelength range $0.11\,\mu\text{m} < \lambda < 1\,\mu\text{m}$ was modelled by Mathis, Rumpl & Nordsieck (1977) using a conglomeration of particle types with a size distribution (MRN distribution) described by a power law expressed as $f(a) = f_0 a^{-q}$, the value of q being in the range -3.3 to -3.6. It was found that graphite was a necessary component of any satisfactory mixture. Assuming the Davis–Greenstein alignment mechanism, the expected polarization was calculated by considering cylinders made of various dielectric materials mixed with spherical graphite particles. Although the extinction behaviour provided satisfactory fits to observations, the linear polarization displayed maxima in the deep ultraviolet. To fit both the polarization and extinction, it was necessary for the material generating the polarization to comprise fairly large, well-aligned particles, contributing little to the extinction. Dielectric particles with coatings were also considered as satisfactory. This approach to model fitting was expanded further by Mathis (1979).

In a study by Martin & Whittet (1990), by including measurements in the infrared, the universality of the spectral behaviour of both the extinction and polarization has been examined in a range of astrophysical situations. They found that the polarization curve in the infrared seems independent of the wavelength, λ_{max}, at which the value of p peaks in the optical region of the spectrum, implying that local variations in λ_{max}, like the correlated variations in the ratio of R_V, are caused by optical properties of the particles in the blue-visible domain of the spectrum rather than at infrared wavelengths.

10.5
Rotation of Position Angle

From a selection of stars, Gehrels & Silvester (1965) showed that several displayed appreciable wavelength dependence of position angle, these generally at distances greater than 0.6 kpc. The basic interpretations require either intrinsic effects related to the star combining with the interstellar component, or the lines of sight contain clouds comprising grains of various size, and with differing mean alignment directions. A prediction of the latter effect being important had already been made by Treanor (1963).

By extending their measurements into the ultraviolet and infrared, Coyne & Gehrels (1966) were able to confirm that, for some stars, the position angle of the polarization exhibited dispersion, the effect being explained by considering the light to traverse two or more discrete clouds with differing grain characteristics and alignments.

The effect of rotation of position angle was again referred to by Serkowski, Gehrels & Wiśsniewski (1969), the trend of the directions of rotation reversing at a galactic longitude of 144°. At smaller longitudes, the position angles increase, and at longer longitudes, they decrease with increasing wavenumber, although there are deviations to the rule. Using their polarization survey of the Southern Hemisphere with catalogued values from the Northern Hemisphere, Klare, Neckel & Schnur (1971) found that the dispersion in alignment of the polarization has well defined minima at $l = 140°$ and 320°. In these directions where the p vectors for the stars are more regularly aligned, the line of sight is vertical to the magnetic field.

Further colour observations of early-type stars in the galactic plane by Coyne & Wiskramasinghe (1969) revealed that about 25% of the stars in their survey exhibit a rotation of the position angle of the polarization with wavelength. A dedicated observing programme to investigate the rotation of the position angle by the interstellar medium was undertaken by Coyne (1971). Of the 105 measured stars, 24 predominantly carried interstellar polarization with dispersion of the position angle. A number of stars within 1 kpc of the Sun, and in the direction of the Perseus arm, exhibited dispersion; they formed two groups, locally separated, with rotation in opposite senses, the effect appearing to be a curiously local phenomenon.

10.6
Circular Polarization

The possibility that circular polarization might be generated by the ISM was first suggested by van de Hulst (1957). In a study of the polarization of galactic clusters, Serkowski (1965) made attempts to measure circular polarization with null results at limits of detection at the 0.05% level. Later, in a study of magnetic stars, Serkowski & Chojnacki (1969) measured nine with large linear interstellar polarization, but were unable to detect any elliptical component greater than 0.02%. As part of a general investigation of circular polarization within the radiation of a variety of objects, Wolf (1972) also was unable to measure definite detections of v to any significance. All of the 54 stars investigated gave zero detections, although it was suggested that HD 23060 and HD 23180 might exhibit ellipticity.

Following observations of X Per by Baud & Tinbergen (1972), Stokes, Avery & Michalsky (1973) improved the accuracy of the investigation of this object by some ten times, with marginal circular polarization detections in the B- and V-bands, but with questions of whether its source was intrinsic to the star, or caused by the ISM. Further reports on results of X Per were provided by Avery, Michalsky & Stokes (1973). Their measurements of 55 Cyg agreed with a positive detection made earlier by Kemp & Wolstencroft (1972). Stokes, Swedlund, Avery, *et al.* (1974) reported on a survey of 84 selected stars with the conclusion that thirteen of them exhibited circular polarization.

From theoretical work by Martin (1972, 1974) on various kinds of particles, it was suggested that better distinction as to whether they are dielectric or metallic might be made by investigating circular polarization effects if the incoming light to a cloud already has linear polarization with a direction of vibration set at an angle to the axes of the grains; such a situation might arise, for example, if the light passes through two clouds with differing alignments. For dielectric particles, it was demonstrated that the handedness of the circular polarization produced in this way should reverse at some point in the visible spectrum. The role that circular polarization might play in yielding information on the grain material has also been discussed by Martin (1973). At the same IAU symposium at which the previous paper was delivered, Kemp (1973) reported that the presence of circular polarization had been established in two reddened stars, o Sco and σ Sco A, this also being reported by Kemp (1972). In a following paper Kemp & Wolstencroft (1972) confirmed the suspicion that HD 15445 exhibited v and added a further three stars with positive detections, together with measurements of $v(\lambda)$. With typical measurement uncertainties $\sim$0.003%, they were able to show the sign of v reversing at the λ_{max} value associated with the linear polarization, and the 'plus' and 'minus' maximum values at wavelengths corresponding to positions $\sim 3/4p_{\text{max}}$, as predicted from a simple slab model with a continuous twist of grain alignment. The angle of twist may be estimated from the value of $-3v/p^2$ as measured in the blue part of the spectrum. Measurements of $v(\lambda)$ were also obtained by Avery, Michalsky & Stokes (1973) for four B stars, these showing similar behaviour to the results of Kemp, again indicating an interstellar origin.

Positive detections of circular polarization produced by the interstellar medium were described by Michalsky, Swedlund, Stokes, *et al.* (1974) with changes in handedness across the visible spectrum. For the star, HDE 226868, Michalsky, Swedlund & Avery (1975) also measured a circular polarization confirming the case for interstellar dust as the source of the effect.

Further investigations of $v(\lambda)$ were undertaken by Martin & Angel (1976) who demonstrated the connection between the wavelength of handedness crossover, λ_c, and λ_{max}, with the selected stars providing a wide range of the latter variable covering 0.45–0.80 µm. The correlated changes in λ_{max} and λ_c are explained qualitatively by differences in mean grain size along the line of sight column to the given star, or by changes of mean refractive index of the grains. The effect of the inferred size changes agrees with the behaviour of the extinction curves for the investigated stars. A functional formula for linear birefringence is obtained which is independent of the crossover wavelength. For the star VI Cyg No. 12, they obtained a value of $\lambda_{\text{max}}/\lambda_c = 1.02$, this being consistent with a nearly pure dielectric material.

By compensating for the polarization produced by material in the foreground to the Cygnus OB2 association, McMillan & Tapia (1977) have shown that the alignment of the position angles is improved, as well as better agreement with the $p(\lambda)$ standard curve and the value of λ_{max}, with the regional extinction law. For star No. 12, Martin's two-slab model was applied and, using a known value of v, a value for the wavelength λ_c was determined, so providing a ratio of $\lambda_{\text{max}}/\lambda_c = 1.02 \pm 0.05$, a result which is consistent with Martin & Angel (1976), and indicating a nearly pure dielectric medium with non-magnetic grains.

According to Kramers–Kronig relationships, the interstellar linear dichroism and the birefringence are related so that there should be a unique wavelength dependence of circular polarization to accompany the observed linear polarization. Martin (1975) has argued, however, that the relationship is hard to apply because of the limited wavelength range over which interstellar polarization has been studied.

10.7
Origin and Alignment Mechanism

During the period when an interstellar origin for the polarization was being firmly established, Thiessen (1961) proposed that the polarigenic mechanism was intrinsic to the stellar atmosphere and generated partly by synchrotron radiation. His thesis was discussed by Struve (1961) who noted that the proposal would drastically change the current theories of stellar structure. Although Behr (1961) showed that the foundations of Thiessen's arguments were erroneously based on observational selection, a repost was presented by Thiessen (1962), this being published after his tragic death. It may be noted that Thiessen's predicted variability of polarization in magnetic stars was observed by him for HD 71866.

Cernuschi, Marsicano & Kimel (1965) have studied the evolution of stellar matter resulting from supernovae explosions with the resulting grains developing a large magnetic moment. Under the local conditions, pairs of spherical grains may coalesce, to produce ellipsoidal particles. Their scenario, in terms of the produced numbers of particles, and the fraction which are orientated by the magnetic field, is tenable in relation to observed values of interstellar polarization.

As for the mechanism by which the elongated grains are preferentially aligned, there have been several proposals, none of which is perfectly satisfactory. Those which require the presence of a magnetic field have special appeal as the polarization vector maps provide interpretations of galactic magnetic field structures. The issues related to the various proposed mechanisms have been presented by Lazarian (2003). This reference summarises the the roles of the various players in alignment theory including paramagnetic dissipation experienced by rotating grains (*Davis–Greenstein process*), mechanical alignment by bombarding atoms (*Gold process*), and radiative torques (*Dolginov process*). His thesis promotes the notion that the latter mechanism was not fully appreciated when it was first suggested some 25 years ago, but is now a strong contender for being the chief process whereby grains are aligned. Lazarian & Cho (2005) claim that the bulk of existing observational data related to molecular clouds is consistent with the radiative torque alignment mechanism.

The *Davis–Greenstein mechanism* (see Davis & Greenstein, 1951) requires the grains to have paramagnetic properties. The interstellar field, say with the flux density $\vec{B}$, induces a field within the particle, the strength depending on the magnetic susceptibility. In a static situation, the internal and external fields would be parallel. For a spinning grain, however, adjustment of the internal field lags so that there is always a slight misalignment. This results in a dissipative torque about an axis perpendicular to $\vec{B}$, bringing the angular momentum of the grain in alignment with $\vec{B}$.

The process may also be described as follows. The field induces a *magnetic moment* and this changes continuously as the grain rotates. These internal changes of the magnetic moment require expenditure of energy taken from the rotational energy of the grain. The energy release appears as heat, the efficiency of the process depending on the value of the imaginary part of a magnetic susceptibility. The drag on the motion is greatest when the grain is rotating about an axis perpendicular to the direction of the external field and least when the axis is parallel to $\vec{B}$. The produced polarization is orthogonal to the grain alignment axis. The alignment mechanism cannot be perfect as the effects of collisions will tend to randomize the spin axes of the grains. Collisions will succeed in randomizing the orientations, unless the gas and grain temperatures are different. This polarigenic scenario has been described and summarized by Ireland (1961).

The sketches in Figure 10.4a illustrate spins of elongated dust grains which tend to be damped out from distribution of orientations with respect to the local magnetic field direction; Figure 10.4b shows the spin modes which will tend to dominate, with the lower cartoon depicting how polarization is generated with the vibrations resolved parallel to the grain axis suffering more absorption. Irrespective of the alignment mechanism, the dominant transmitted vibration is at right angles to the long axes of the grains.

An analytical treatment of the behaviour of the degree of alignment of dust grains when magnetic effects become greater than collisional effects has been given by Cugnon (1983). The paper raises concerns that the required magnetic field remains

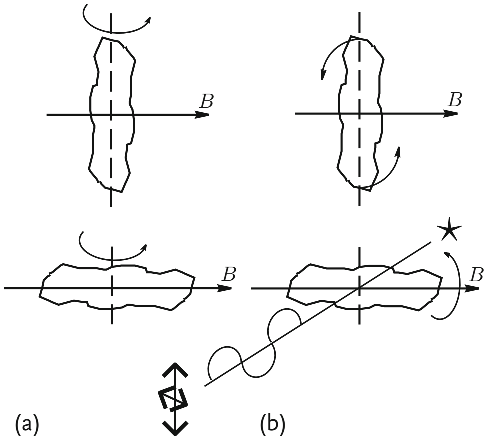

Fig. 10.4 For paramagnetic grains with their spinning axis normal to the local magnetic field, as depicted in (a), dissipative torques tend to remove them from the distributions of orientation in favour of grains with spins with the axis parallel to the field as in (b). The lower part of (b) shows that dust with this alignment absorbs more of the radiation from a star along the grain's length, so producing a polarization at right angles to the magnetic field.

too high when considering simple Davis–Greenstein alignment under realistic interstellar conditions.

The *Gold mechanism* relates to the supersonic impact between the dust and the gas molecules. As there was no other evidence of magnetic fields of sufficient strength to affect the alignment of grains, Gold (1952a, 1952b) proposed this alternative mechanism. For it to be tenable, a preferred direction in the interstellar medium is given by a process of double streaming such as by dust particles penetrating through the tenuous galactic gas. It seems likely that, in many circumstances, the relative velocity between the dust and gas by far exceeds the thermal velocities of the gas molecules. The spin of elongated dust particles can be calculated when it is principally due to impacts with gas molecules at supersonic speeds. All such impacts impart angular momentum about lines lying normal to the relative velocity. The elongated particles will spin with their long dimension remaining mainly in planes which all contain the direction of the relative velocity. Such a motion implies an anisotropy of the probability distribution of the instantaneous directions of the particles.

According to Lazarian (2003), there is an issue in providing supersonic drifts by collisions of dust clouds, and that the process could only align grains over limited zones of interstellar space; the process cannot account for the ubiquitous grain alignment in the diffuse medium throughout the Galaxy.

Salpeter & Wickramasinghe (1969) proposed that the alignment of interstellar grains may result from the combined effects of radiation pressure from the central bulge of the Galaxy, gas collisions and isotropic bombardment by cosmic rays. Harwit (1970a, 1970b) proposed that the alignment of dust grains is possible by the absorption of the angular momentum of photons from the radiation field produced by nearby stars. Following this theme, however, King & Harwit (1973) have demonstrated that neither photon nor magnetic alignment are plausible mechanisms, either in co-operation or alone.

Carrasco, Strom & Strom (1973) have used polarimetric diagnostics with extinction measurements to investigate the properties of the dust in the Rho Ophiuchi Dark Cloud with the conclusion that the mean particle size increases in the denser parts of the cloud. They conclude that grain alignment, either by photon angular momentum or by stellar radiation pressure, is difficult to promote; also, if the alignment results from paramagnetic relaxation, the magnetic field must increase towards the denser, central regions of the cloud.

For the *Dolginov mechanism*, alignment is achieved by anisotropic corpuscular flow or radiation fluxes, with consideration for the influence of a magnetic field. Dolginov (1972) suggested that quartz grains may acquire spin very readily as they possess an optical rotatory power. Later Dolginov & Mytrophanov (1976) showed that irregular grain shape offers differential scattering for incident left- and right-handed polarization. Helical grains are readily spun up by the scattering of unpolarized light which can be thought of as comprising equal amounts of these handednesses. Lazarian (2003) has made note that this radiative torque mechanism and Harwit's radiative emission/absorption are very different in that the former acts in a continuous way and increases the grain rotational velocity in proportion to time, while the latter is based on stochastic spin-up and is therefore subdominant.

10.8
DIBS

It is well known that the radiation from stars, on passing through the interstellar medium, is subject to discrete absorptions across the spectrum, these referred to as diffuse interstellar absorption bands, or DIBS. The strengths of these have been shown to be correlated with the magnitude of the interstellar polarization. Assuming that the atoms or molecules producing an absorption are imbedded in the grains, Greenberg & Stoeckly (1971) made predictions for the polarimetric behaviour that might occur across the 4430 Å feature. According to Martin & Angel (1974), if the interstellar dust grains carry the mechanism for the production of the diffuse bands, it is expected that there will be a fractional change in polarization, $\Delta p/p$, approximately equal to the factional change in optical depth, $\Delta\tau/\tau$, across the feature. Several observational studies have been made to see if there are spectral variation of $p(\lambda)$ within absorption structures, but the consensus is that of a null result. Measurements made of the star HD 183143 revealed no polarimetric structure at the predicted level. Walker (1963) noted that the measurement of polarization in the 4430 Å band might provide an increase in polarization relative to the nearby continuum, but his preliminary observational investigation was inconclusive.

It may be noted that Nandy & Sneddon (1970) claimed detection of a strong effect for 55 Cyg using photographic techniques, while A'Hearn (1972) found no significant polarization variation for 55 Cyg, HD 183143 and three other stars. At the IAU Symposium 52, Nandy & Sneddon (1973) presented their suggestion of there being structure in $p(\lambda)$ across the 4430 Å feature for 55 Cyg, but in the discussion, A'Hearn makes reference to his photoelectric filter measurements placing severe limits on the possible amplitude of any dispersion-like polarization curve. Gammelgaard & Rudkjøbing (1973) have made measurements of the strength of the 6180 Å absorption band for 49 stars in the Northern Milky Way with the inclusion of a polarizing filter in their instrument. They claim that the absorption index has a tendency to be maximum for electric vector position angles which are about orthogonal to those corresponding to maximum absorption connected with continuous polarization. Round about this era there were reports of broad structures being seen in the interstellar $p(\lambda)$ curve. Mavko, Hayes, Greenberg, *et al.* (1974), for example, reported the presence of humps and depressions which broadly agreed with predictions of Hayes, Mavko, Radick, *et al.* (1973) based on the behaviour of extinction curves. More recent data appear to display smooth curves without structure. Features in the $p(\lambda)$ curve have also been reported by Wolstencroft & Smith (1984a, 1984b). It may be mentioned that these measurements were obtained by sequential scanning systems which give rise to problems when data from different runs are pieced together. The features have not been substantiated by more recent measurements using 2D detectors with the spectral record obtained in a unified way. A discussion on structures within the $p(\lambda)$ curve can be found in Somerville (1996).

It would be of interest to explore possible $p(\lambda)$ structure across interstellar NaI absorption features which, by resolved Doppler shifts, indicate the presence of two or more clouds along the line of sight. A good candidate star for this would be HD 174632 (see Crawford, 1988).

10.9
Particle Types and Galactic Structure

The smoothness of the changes of polarization parameters around the sky was investigated by a simple correlation exercise by Kaplan & Klimishin (1959) between the observed difference in p and the angular distance (α in degrees) of pairs of stars on the celestial sphere. By considering values of $(p_1 - p_2)^2$, they found a weak correlation represented by $\overline{(p_1 - p_2)^2} \approx 5.2\alpha^{0.24}$.

From a statistical analysis of the data in the early polarimetric catalogues, Shain (1957) showed that the position angles of the polarization had uniform distributions at $l = 35^\circ \rightarrow 65^\circ$ and $l = 345^\circ \rightarrow 355^\circ$, corresponding to the directions of the galactic spiral arms. The variation of the mean value of the position angle around the galactic equator was well represented by a sine wave suggesting that the plane of the field is inclined to the galactic plane. The angle between the planes was $\sim 18^\circ$, with their intersection at $l \sim 15^\circ$ and 195°. This geometry has no connection with the local system (Gould's belt), nor with any other system. The derived plane cannot be associated with that of the plane of the magnetic field of the Galaxy as a whole. It evidently characterizes the fluctuations in the direction of the field on a scale of the order of 1000 pc.

In the analysis by Serkowski (1962), the catalogued polarization values were expressed in terms of galactic coordinates, and it was clearly demonstrated that q_G followed a double sine wave around the galactic equator, with minima at $l^{\mathrm{II}} \sim 50^\circ$ and $\sim 230^\circ$, corresponding to the longitudes towards which is directed the mean axis of symmetry of the mechanism aligning the interstellar dust grains. These positions coincide quite closely with the directions of the galactic spiral arms.

In exploring the process of the growth of p along the line of sight, Nee & Jokipii (1979) considered that there are random fluctuations along the local field directions. One specific result is that p saturates at a value which can be much less than unity, the value being a characteristic of the particular fluctuating medium. Both rotation of the position angle with wavelength, and the development of circular polarization are expected from the model. In Nee (1980), the model, based on fluctuation theory, was developed further to provide estimates of the average and the variance of values p according to distance. The form of growth was shown to match curves from zero to a plateau, according to distance. By comparing data for a zone on the galactic equator, estimates of correlation length of $\sim$225 pc were obtained with a fluctuating angle of $22.^\circ5$. Jokipii, Lerche & Schommer (1969) have considered the mean polarization and the variance of polarization about the mean, as functions of distance R from the Sun. Using the concept of a turbulent interstellar medium, they have shown that the mean increases linearly with R. For R less than the correlation length L, the variance increases as R^2, whereas for $R \gg L$, the variance increases linearly with R. From a collection of catalogued stars, the observed mean polarization and the variance were found to be in excellent agreement with their simple statistical theory with the conclusion that the ISM fluctuates irregularly with a correlation length of 150 pc. The problem of calculating the behaviour of polarization and extinction associated with mixtures of partially aligned grains has been considered by Mishchenko (1990), with the application of the Waterman's T-matrix approach to develop a rigorous analytical method to average the extinction matrix over orientations of non-spherical grains.

The analysis of the polarization vectors as projected on a galactic map have been analysed by Ireland (1961) in terms of a helically twisted model of the spiral arm magnetic field, the underlying alignment mechanism being that proposed by Davis & Greenstein (1951). According to Stępień (1964), neither the model of the galactic magnetic field with lines of force parallel to the axis of the spiral arm nor that of Ireland above, explained the observed behaviour of the Stokes parameters along the galactic equator. The behaviour is best explained by the model of the helical field with windings appropriately inclined. His conclusions, however, were not decisive.

The polarization in the Southern Milky Way was investigated by van P. Smith (1956) and it was found that the amount of polarization per unit extinction is lower than in the Northern hemisphere. Although the possibility of a difference in the optical properties of the grains was not ruled out, it was suggested that the particles are more rigidly aligned in the centre of the spiral arm, through which the line of sight passes in the northern direction, than in the periphery of the arm. Individual regions such as Vela, Carina and the Coal Sack were also made.

A sample of 308 stars within 200 pc of the Sun was measured by Appenzeller (1968) in directions of the galactic poles and the galactic plane. He found that the galactic longitude of the direction of the magnetic field observed at the N/S galactic poles was significantly different ($19^\circ \pm 4^\circ$). Further studies of the North Galactic Pole have been undertaken by Berdyugin, Snåre & Teerikorpi (1995) out to a distance of 600 pc.

Using polarization measurements of 70 stars, Markkanen (1979) has investigated a lower limit for the interstellar extinction in the area of the North Galactic Pole. A general extinction of $A_V \gtrsim 0.^{\mathrm{m}}03$ is found; in the quadrant of $l = 270^\circ$–360°, there is a dust cloud, or complex of clouds, at a distance of 100–200 pc, with $A_V \gtrsim 0.^{\mathrm{m}}1$. The galactic centre was observed in the infrared by Maihara & Sato (1973); p was $<5\%$, much less than that expected for an interstellar generated polarization.

Bel, Lafon & Leroy (1993) have presented accurate measurements of polarization of a stellar sample located in a large area in Cepheus. At large scales, they find that the galactic magnetic field, as given by the direction of vibration is, roughly speaking, parallel to the galactic plane in the Cassiopeia cloud, with a scale size of the order of 100 pc, while it is turned by about 90° in the Cepheus cloud. On small scales, in both the Cassiopeia and Cepheus clouds, the CO content has little correlation with p. Appenzeller (1974) has used polarimetric diagnostics to investigate the Barnard Loop Nebula in Orion. The observations revealed a complex field structure.

Bhatt & Jain (1993) have mapped the behaviour of the polarization vectors relative to two molecular clouds, B 227 and L 121. The magnetic field associated with B 227 appears to be more or less parallel to the long axis of the cloud, having the same direction as the local interstellar field. The field behaviour for L 121 was very much less ordered.

From measurements of the interstellar polarization in the direction of the Crab Nebula, Martin, Illing & Angel (1973) conclude that the particles are dielectric, with metallic particles being ruled out.

10.10
Stellar Clusters

Krzemiński & Serkowski (1967) have surveyed the polarization of the strongly reddened open cluster Stock 2, combining the data with colour photometry. The alignment of the position angle of the polarization is very coherent across the cluster and analysis of the variations indicated a microscale of 0.3 pc for the fluctuation in the polarizing medium. A region where the values of p were smaller than average was also highlighted.

The open galactic cluster, Mel 111 in Coma Berenices was observed by Markkanen (1974a), the group studied because of its evolutionary state, its proximity (80 pc), and its location near the North Galactic Pole. The very low levels of polarization were assumed to have an interstellar origin from which law limits of extinction and colour excesses were estimated. The colour excesses corrections were of the same order as deblanketing effects in the metal-line stars.

The Praesepe cluster was also investigated by Markkanen (1974b). Again the levels of polarization were low, but the position angles were very well aligned with a mean direction that fitted well into the helical model of the local magnetic field. Assuming that the polarization had an interstellar origin, low limits of extinction and colour excesses were estimated.

Markkanen (1977a) conducted a polarimetric survey of the galactic magnetic field and interstellar dust in the direction of the α Persei cluster. His analysis shows that, in this direction, the field is homogeneous to a distance of several 100 pc. A magnetic pocket of linear dimension $\sim$10 pc is noted in this direction, and at the distance of the cluster. In combination with photometric data, it is shown that there is a concentration of dust, about 30–40 pc in diameter, associated with the cluster. The increase of p and extinction at the cluster distance shows that the dust is concentrated in one cloud.

The α Persei star cluster has also been studied by Coyne, Tapia & Vrba (1979). The pattern of the position angle over the cluster shows very uniform alignment, and no discontinuity can be seen in the magnetic field as it passes through the region of star formation. The forms of the $p(\lambda)$ curves are also indistinguishable from those describing the general interstellar medium. The polarization data are used to determine polarization-to-absorption ratios, and to make better estimates of the distance, size and mass of the cluster.

The Pleiades have also been studied in combination with reddening effects. Using *UBV* filters, Markkanen (1977b) measured 12 of the brighter stars and found that the position angles coincided with the filament directions of the nebulosity. Several of the stars showed indications of intrinsic polarization, Pleione exhibiting a growth in p during the observations. Later measurements by Breger (1984) failed to confirm suspicions in the literature concerning a high incidence of intrinsic polarization. He found that the polarization/extinction ratio was compatible with an interstellar origin. A set of stars suspected as being pre-main-sequence was examined by Breger (1985). He was unable to confirm previously reported abnormal wavelength dependencies of polarization; the high polarization values of some faint stars were shown to be caused by high interstellar reddening in the molecular cloud region southwest of Merope. Based on polarimetry, 10 suspected pre-main-sequence stars were explored to see if their apparent high reddening, causing their abnormal positions in the HR diagram, could be related to interstellar material. For nine of the candidates, the determined interstellar reddening could not account for their offset from the main sequence. A more complete picture of the polarimetry of the Pleiades was given by Breger (1986), with the measurements being linked to colour measurements and millimetre and radio data. From the eastern part of the cluster, the interstellar material is uniform, resulting in constant values of $p(V) = 0.27\%$, $\theta = 114°$, $E_{(B-V)} = 0.03$ mag, the region coinciding with a 21 cm HI minimum. Light from the northwestern part passes through the foreground material in addition to a patchy intracluster cloud, and depolarization occurs due to the different magnetic field directions in the two clouds. A high reddening of ~0.30 mag and polarization ~2% in much of the southwestern region coincides with the position of a CO molecular cloud.

Corso, Shatzel, Lange, *et al.* (1993) have described a photographic survey and CCD technique for measuring stars with high polarization in the x Cas region. The average value of p is between 3 and 5%, with a few stars in excess of 6%. There is a tendency for the stars of highest polarization to occur south of the galactic equator in this region.

Determination of the intracluster polarization properties of the dust in the Carina nebula was reported by Marraco, Vega & Vrba (1993). In combination with photometric data, colour polarization measurements were modelled in terms of a foreground interstellar component which was then subtracted to provide intracluster values. It was concluded that the latter were generated with lower efficiency relative to the interstellar medium. The intracluster dust was characterized by a ratio of $E_{(V-K)}/E_{(B-V)}$ to $\lambda_{\max}$ higher than the canonical value for the interstellar medium.

The reddened open cluster, NGC 1502, has been studied by Weitenbeck, Halstead & Carver (2008). The polarization grows from being less than 1% at a distance of 100–200 pc to over 6% for the cluster stars; the directions of vibration are uniform to within about 10° of each other from the nearest, to the most distant stars. The $\lambda_{\max}$ value for the most distant field stars is about 5000 Å, and about 4800 Å for the cluster stars, implying that R is significantly less than 3 in this region of the Galaxy.

In respect of globular clusters, Martin & Shawl, (1981) presented a simple model showing that, under certain circumstances, polarization of light scattered by dust particles within globular clusters should engender observable effects. A search was made for polarization of radiation from dark patches within three clusters, the measurements avoiding the presence of stars, with a tentative detection in M 15 of $p = 0.22 \pm 0.06\%$.

Seven metal-poor globular clusters were investigated by Minniti, Coyne & Claria (1992), most of the measured stars being red giants. They found strong spatial variations of the polarization in the fields of NGC 4372, NGC 4833, M 4 and NGC 6266, concluding that differential reddening is important in these clusters. Mild extinction variations were found across ω Cen and M 22, while the interstellar medium towards NGC 6397, appeared fairly uniform. After taking the foreground polarization component into account, there was no evidence for significant intrinsic polarization in any of the observed stars. It was argued that an extreme Population II environment is very dust deficient.

10.11
Simple Models

Along any line of sight, the interstellar medium can be considered to act as a birefringent material. Consequently, it carries a polarizance and can also introduce phase delays. Serkowski (1962) set out the optical principles whereby the dust affects the polarization of the radiation passing through the medium.

The grains may be considered as producing a complex refractive index, $\tilde{m} = m' - im''$, for the interstellar medium. If classical waves are considered in the form of (2.9) and (2.10) entering a uniform cloud, then, at some distance, l, the orthogonal electric disturbances may be represented as

$$\begin{aligned} E_{\|} &= E_{\|0} e^{i(2\pi[\nu t]+\delta_{\|})} e^{-ilk\tilde{m}_{\|}} \Rightarrow E_{\|0} e^{-ilk\tilde{m}_{\|}} \,, \\ E_{\perp} &= E_{\perp 0} e^{i(2\pi[\nu t]+\delta_{\perp})} e^{-ilk\tilde{m}_{\perp}} \Rightarrow E_{\perp 0} e^{-ilk\tilde{m}_{\perp}} \,. \end{aligned} \tag{10.4}$$

where k is the wavenumber $= 2\pi/\lambda$.

The associated intensities may be expressed as

$$I_{\|} \Rightarrow |E_{\|}^2| \qquad \text{and} \qquad I_{\perp} \Rightarrow |E_{\perp}^2| \,. \tag{10.5}$$

An originally unpolarized light beam of intensity, I_0, may be considered to comprise orthogonal intensity components, $I_{\|0} = I_{\perp 0} = I_0/2$, and at a distance, l, within the medium may be represented as

$$I_{\|} = \frac{I_0}{2} e^{-2ikl\tilde{m}_{\|}} \qquad \text{and} \qquad I_{\perp} = \frac{I_0}{2} e^{-2ikl\tilde{m}_{\perp}} \,. \tag{10.6}$$

Hence,

$$I_{\|} = \frac{I_0}{2} \mathrm{e}^{-2\mathrm{i}kl(m'_{\|} - \mathrm{i}m''_{\|})} \qquad \text{and} \qquad I_{\perp} = \frac{I_0}{2} \mathrm{e}^{-2\mathrm{i}kl(m'_{\perp} - \mathrm{i}m''_{\perp})} \,, \tag{10.7}$$

leading to

$$I_{\|} = \frac{I_0}{2} \mathrm{e}^{-2kl(m''_{\|} + \mathrm{i}m'_{\|})} \qquad \text{and} \qquad I_{\perp} = \frac{I_0}{2} \mathrm{e}^{-2kl(m''_{\perp} + \mathrm{i}m'_{\perp})} \,. \tag{10.8}$$

The imaginary part of the refractive index gives rise to absorption, and the real part controls the phase delays effected by the medium. Thus the optical depth is proportional to $2km''l$. The extinction may also be written as $N_\mathrm{g} C_\mathrm{e} l$, where N_g is the number density of the grains and C_e the extinction cross section, this latter term comprising scattering and absorption components. Hence,

$$m''_{\|} = \frac{N_\mathrm{g} C_{\|\mathrm{e}}}{2k} \qquad \text{and} \qquad m''_{\perp} = \frac{N_\mathrm{g} C_{\perp\mathrm{e}}}{2k} \,. \tag{10.9}$$

From the optical theorem (conservation of energy):

$$C_{\|\mathrm{e}} = \frac{4\pi}{k^2} \Re[S_{\|}(0)] \qquad \text{and} \qquad C_{\perp\mathrm{e}} = \frac{4\pi}{k^2} \Re[S_{\perp}(0)] \,, \tag{10.10}$$

where $S_{\|}(0)$ and $S_{\perp}(0)$ are the complex forward amplitude scattering functions of the dust grains.

Hence,

$$m''_{\|} = \frac{2\pi N_\mathrm{g}}{k^3} \Re[S_{\|}(0)] \qquad \text{and} \qquad m''_{\perp} = \frac{2\pi N_\mathrm{g}}{k^3} \Re[S_{\perp}(0)] \,. \tag{10.11}$$

The phase changes, relative to what they would have been simply by travelling a distance, l, in vacuo, are proportional to $2k(m' - 1)l$ which, by analogy with the formalism of the extinction, may be written as $N_\mathrm{g} C_\mathrm{p} l$, where C_p is the cross section associated with phase delay. Hence,

$$m'_{\|} = 1 + \frac{N_\mathrm{g} C_{\|\mathrm{p}}}{2k} \qquad \text{and} \qquad m'_{\perp} = 1 + \frac{N_\mathrm{g} C_{\perp\mathrm{p}}}{2k} \,, \tag{10.12}$$

leading to

$$m'_{\|} = 1 + \frac{2\pi N_\mathrm{g}}{k^3} \Im[S_{\|}(0)] \qquad \text{and} \qquad m'_{\perp} = 1 + \frac{2\pi N_\mathrm{g}}{k^3} \Im[S_{\|}(0)] \,. \tag{10.13}$$

The orthogonal refractive indices may therefore be written in terms of the amplitude scattering functions as

$$\begin{aligned} \tilde{m}_{\|} &= 1 + \frac{2\pi N_\mathrm{g}}{k^3} \left[\Im\{S_{\|}(0)\} - \mathrm{i}\Re\{S_{\|}(0)\}\right] , \\ \tilde{m}_{\perp} &= 1 + \frac{2\pi N_\mathrm{g}}{k^3} \left[\Im\{S_{\perp}(0)\} - \mathrm{i}\Re\{S_{\perp}(0)\}\right] . \end{aligned} \tag{10.14}$$

Both $\tilde{m}_{\|}$ and $\tilde{m}_{\perp}$ are close to unity as N_{g} is very small.

Each grain may therefore be considered as carrying:

$$\begin{aligned}
&\text{Extinction characterized by:} && \kappa = \frac{1}{2}(C_{\|\mathrm{e}} + C_{\perp\mathrm{e}}) \, , \\
&\text{A differential extinction of:} && \sigma = \frac{1}{2}(C_{\|\mathrm{e}} - C_{\perp\mathrm{e}}) \, , \\
&\text{A differential phase delay of:} && \epsilon = \frac{1}{2}(C_{\|\mathrm{p}} - C_{\perp\mathrm{p}}) \, .
\end{aligned}$$

The passage of light of wavelength, λ, through a layer of elemental thickness, $\mathrm{d}s$, containing N_{g} scattering grains per unit volume (see Figure 10.5) may be described in the form of a Mueller matrix with the form

$$\begin{aligned}
&\begin{bmatrix} 1 - N_{\mathrm{g}}\kappa\mathrm{d}s & -N_{\mathrm{g}}\sigma\mathrm{d}s & 0 & 0 \\ -N_{\mathrm{g}}\sigma\mathrm{d}s & 1 - N_{\mathrm{g}}\kappa\mathrm{d}s & 0 & 0 \\ 0 & 0 & 1 - N_{\mathrm{g}}\kappa\mathrm{d}s & N_{\mathrm{g}}\epsilon\mathrm{d}s \\ 0 & 0 & -N_{\mathrm{g}}\epsilon\mathrm{d}s & 1 - N_{\mathrm{g}}\kappa\mathrm{d}s \end{bmatrix} \\
&= \begin{bmatrix} 1 & 0 & 0 & 0 \\ 0 & 1 & 0 & 0 \\ 0 & 0 & 1 & 0 \\ 0 & 0 & 0 & 1 \end{bmatrix} + N_{\mathrm{g}}\mathrm{d}s \begin{bmatrix} -\kappa & -\sigma & 0 & 0 \\ -\sigma & -\kappa & 0 & 0 \\ 0 & 0 & -\kappa & \epsilon \\ 0 & 0 & -\epsilon & -\kappa \end{bmatrix} . \qquad (10.15)
\end{aligned}$$

The elements of the resultant Stokes vector $\{I', Q', U', V'\}$ of a light beam which enters with a vector of $\{I, Q, U, V\}$ may be written as

$$\begin{aligned}
I' &= I - N_{\mathrm{g}}\mathrm{d}s\,(\kappa I + \sigma Q) \\
Q' &= Q - N_{\mathrm{g}}\mathrm{d}s\,(\sigma I + \kappa Q) \\
U' &= U - N_{\mathrm{g}}\mathrm{d}s\,(\kappa U - \epsilon V) \\
V' &= V - N_{\mathrm{g}}\mathrm{d}s\,(\epsilon U + \kappa V) \, . \qquad (10.16)
\end{aligned}$$

From these equations, the rate of change of the normalized Stokes parameters with the progression of a light beam through the cloud are determined as

$$\begin{aligned}
\frac{1}{I}\frac{\mathrm{d}I}{\mathrm{d}s} &= -N_{\mathrm{g}}\,(\kappa + \sigma[Q/I]) \\
\frac{\mathrm{d}[Q/I]}{\mathrm{d}s} &= -N_{\mathrm{g}}\sigma\left(1 - [Q/I]^2\right) \\
\frac{\mathrm{d}[U/I]}{\mathrm{d}s} &= +N_{\mathrm{g}}\,(\epsilon[V/I] + \sigma[Q/I][V/I]) \\
\frac{\mathrm{d}[V/I]}{\mathrm{d}s} &= -N_{\mathrm{g}}\,(\epsilon[U/I] - \sigma[Q/I][V/I]) \, . \qquad (10.17)
\end{aligned}$$

From the above equation, it can be seen that if the light is already polarized on entering the cloud, with a direction of vibration parallel to the the reference frame defining the grain alignment, the growth of the polarization is given by

$$\frac{\mathrm{d}p}{\mathrm{d}s} = -N_{\mathrm{g}}\sigma\left(1 - p^2\right) . \qquad (10.18)$$

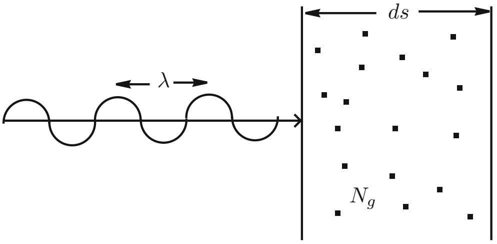

Fig. 10.5 Radiation of wavelength, λ, entering a dust cloud of length, ds, with a dust grain number density, N_g.

It is also obvious that circular polarization can only be generated if the light entering the cloud is already linearly polarized. Very generally, the levels of polarization under discussion are small, and the right-hand terms of (10.17) can be neglected so that

$$\begin{aligned}
\frac{1}{I}\frac{\mathrm{d}I}{\mathrm{d}s} &= -N_{\mathrm{g}}\kappa = -\frac{N_{\mathrm{g}}}{2}(C_{\|\mathrm{e}} + C_{\perp\mathrm{e}}) \\
\frac{\mathrm{d}[Q/I]}{\mathrm{d}s} &= -N_{\mathrm{g}}\delta = -\frac{N_{\mathrm{g}}}{2}(C_{\|\mathrm{e}} - C_{\perp\mathrm{e}}) \\
\frac{\mathrm{d}[U/I]}{\mathrm{d}s} &= +N_{\mathrm{g}}\epsilon[V/I] = +\frac{N_{\mathrm{g}}}{2}(C_{\|\mathrm{p}} - C_{\perp\mathrm{p}})[V/I] \\
\frac{\mathrm{d}[V/I]}{\mathrm{d}s} &= -N_{\mathrm{g}}\epsilon[U/I] = -\frac{N_{\mathrm{g}}}{2}(C_{\|\mathrm{p}} - C_{\perp\mathrm{p}})[U/I]\,.
\end{aligned} \tag{10.19}$$

If one commences with zero polarization, both the extinction and Q/I grow as the light passes through a regular cloud; U/I and V/I can only grow if the beam already contains V/I and U/I components. These might be present, however, because of intrinsic polarization generated by the star itself or, if there are two clouds along the line of sight, but with different angles of alignment of the dust.

It is unlikely that the effects of the grains will be uniform along any line of sight as a result of either twists in the preferred alignment through the cloud, or of the path involving a series of clouds with distinct differences in the direction of the dust alignment. Such situations have been modelled by Martin (1974). In particular his two-cloud model has proved to be instructive as to how the second cloud effects a *depolarization* relative to the potential polarization that the combination of the two clouds could provide, and on the wavelength dispersion of the observed direction of vibration (see Section 10.5).

According to the measurements, the optical properties of various types of dust grain can be considered to explore how the observed extinction and polarization growth is matched. All that is required is the knowledge of the amplitude forward amplitude scattering functions of the dust grains. It may be noted that within (10.19), there are four equations with five unknowns. The situation is better resolved by including wavelength dependence in the observations that also requires matching by the optical properties of the grains. The situation is generally more

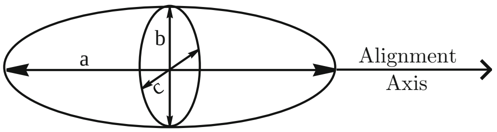

Fig. 10.6 A schematic of an ellipsoidal grain. The axis, *a*, may be considered as the alignment axis but, depending on the nature of the controlling mechanism, the grain may tend to be parallel to or perpendicular to the alignment direction.

complex than depicted here. Not all the grains will be preferentially aligned. An alignment distribution needs to be considered and also a particle-type distribution. The sophistication of modelling has developed to include mixtures of graphite and silicate particles, some coated with ice mantles, so as to reproduce all the important features associated with polarimetric and spectrometric observations over the spectral range of $2 \lesssim \lambda \lesssim 13\,\mu\mathrm{m}$. This has been done, for example, by Lee & Draine (1985) for the Becklin–Neugebauer (BN) object for which it may be noted that $p = 23\%$ at $2\,\mu\mathrm{m}$.

In order for polarization to be generated, the grain distribution requires that some of the particles are non-spherical. Grains may be considered as being ellipsoidal with principal axes *a*, *b* and *c* (see Figure 10.6). The longest axis, *a*, relates to that controlled by the alignment mechanism defined by the vector **A**, whether or not the grain tends to align with this direction or sets itself normal to it. For a grain viewed along the direction of alignment, the optical cross section of a grain may be denoted as σ_a, this being very different from either σ_b or σ_c associated with the orthogonal axes, the latter pair being close in value.

A strategy for investigating how distributions in the alignment of dust grains relative to the line of sight affect extinction and polarization was proposed by Davis (1959). The axes of symmetry for the distribution of the grain axes can be considered as being in the direction of **A**. A distribution parameter, *F*, can be applied to the grain orientations with a value lying between $-2/3$ and $1/3$. Extreme values refer to

$$\begin{array}{ll} \text{Orientation completely random:} & F = 0 \\ \text{All grains} \parallel \text{to the mechanism:} & F = -\dfrac{2}{3} \\ \text{All grains} \perp \text{to the mechanism:} & F = \dfrac{1}{3}\,. \end{array}$$

According to Davis & Greenstein (1951), who promoted magnetic fields as the alignment mechanism affecting small prolate spheroidal grains, the same polarization and extinction is produced as though the grains have a alignment dominance along **A**, with equal distribution factors associated with the two orthogonal axes.

In order to estimate the effect that the grains have according to their orientational distributions, the axial system set by the alignment direction needs to be transformed to a frame represented by $\mathbf{x}, \mathbf{y}, \mathbf{z}$, where $\mathbf{z}$ corresponds to the direction of propagation of the light from the star, and $\mathbf{x}, \mathbf{y}$ are in the plane of the sky.

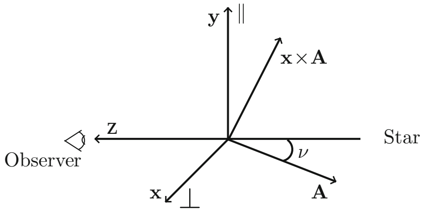

Fig. 10.7 Definition of the angle and vector directions associated with grain alignment distributions; **z**, **y**, **x** × **A** and **A** are in the same plane.

If ν is the angle between **A** and **z**, **y**, it may be judiciously chosen to correspond to $\mathbf{x} \times \mathbf{A}$, and **x**; the vector directions of **z**, **y**, $\mathbf{x} \times \mathbf{A}$ and **A** are in the same plane (see Figure 10.7). The directions of **x** and **y** now provide a reference system for the direction of vibration of the polarization.

According to the description above, the proportion of grains aligned along **A** is given by $(1/3 - F)$, with the remainder being distributed in equal proportion along any pair of orthogonal axes, in turn orthogonal to **A**. Thus the fractions orientated in the directions **A**, $\mathbf{x} \times \mathbf{A}$ and **x** are in the ratio

$$f_{\mathbf{A}} : f_{\mathbf{x} \wedge \mathbf{A}} : f_{\mathbf{x}} = \left(\frac{1}{3} - F\right) : \left(\frac{1}{3} + \frac{1}{2}F\right) : \left(\frac{1}{3} + \frac{1}{2}F\right) . \tag{10.20}$$

Again, following Davis (1959), the distributions associated with **A** and $\mathbf{x} \times \mathbf{A}$ can be transformed to be orientated along **z** and **y** by taking a factor of $\cos^2 \nu$ of the grains along **A** to **z**, and $\sin^2 \nu$ of them to **y**. These factors are plausible and give a tractable result. Thus the fractions orientated along **z**, **y** and **x** become

$$\begin{aligned}
\text{Along } \mathbf{z} : f_z \quad &= \left(\frac{1}{3} - F\right) \cos^2 \nu + \left(\frac{1}{3} + \frac{1}{2}F\right) \sin^2 \nu \\
&= \left[\frac{1}{3} + F\left(\frac{3}{2}\sin^2 \nu - 1\right)\right] \\
\text{Along } \mathbf{y} : f_y \quad &= \left(\frac{1}{3} - F\right) \sin^2 \nu + \left(\frac{1}{3} + \frac{1}{2}F\right) \cos^2 \nu \\
&= \left[\frac{1}{3} - F\left(\frac{3}{2}\sin^2 \nu - \frac{1}{2}\right)\right] \\
\text{Along } \mathbf{x} : f_x \quad &= \left[\frac{1}{3} + \frac{1}{2}F\right] .
\end{aligned} \tag{10.21}$$

Extinction cross sections, $C_{\parallel}$ and $C_{\perp}$, may now be defined relating to the **x** and **y** axes. For each axis, there is an identical component from the fraction of grains giving rise to a cross section of σ_a. For each axis, there are two additional components dependent on σ_b and σ_c, and on their fractions aligned with x and y. It is the difference between σ_b and σ_c that gives rise to any polarization. The two cross sections may be written as

$$\begin{aligned}
C_{\|} &\equiv f_z\sigma_a + f_y\sigma_b + f_x\sigma_c \\
&= \left[\frac{1}{3} + F\left(\frac{3}{2}\sin^2\nu - 1\right)\right]\sigma_a \\
&\quad + \left[\frac{1}{3} - F\left(\frac{3}{2}\sin^2\nu - \frac{1}{2}\right)\right]\sigma_b + \left[\frac{1}{3} + \frac{1}{2}F\right]\sigma_c \\
&= \frac{\sigma_a + \sigma_b + \sigma_c}{3} - F\left[3\left(\frac{\sin^2\nu}{2} - \frac{1}{3}\right)(\sigma_b - \sigma_a)\right] + \frac{F}{2}(\sigma_c - \sigma_b).
\end{aligned} \tag{10.22}$$

$$\begin{aligned}
C_{\perp} &\equiv f_z\sigma_a + f_y\sigma_c + f_x\sigma_b \\
&\left[\frac{1}{3} + F\left(\frac{3}{2}\sin^2\nu - 1\right)\right]\sigma_a \\
&\quad + \left[\frac{1}{3} - F\left(\frac{3}{2}\sin^2\nu - \frac{1}{2}\right)\right]\sigma_c + \left[\frac{1}{3} + \frac{F}{2}\right]\sigma_b \\
&= \frac{\sigma_a + \sigma_b + \sigma_c}{3} - F\left[3\left(\frac{\sin^2\nu}{2} - \frac{1}{3}\right)(\sigma_c - \sigma_a)\right] - \frac{F}{2}(\sigma_c - \sigma_b)\,.
\end{aligned} \tag{10.23}$$

Hence the total cross section for extinction can be written as

$$C_{\|} + C_{\perp} = \frac{2}{3}(\sigma_a + \sigma_b + \sigma_c) + F\left(1 - \frac{3}{2}\sin^2\nu\right)(\sigma_b + \sigma_c - 2\sigma_a)\,, \tag{10.24}$$

with the differential extinction written as

$$C_{\|} - C_{\perp} = F\frac{3}{2}\sin^2\nu(\sigma_c - \sigma_b)\,. \tag{10.25}$$

These terms may be inserted into (10.19) to evaluate the rate of growth of extinction and polarization with distance through any interstellar dust cloud. More realistic modelling may be effected by also applying an assembly of dust grains with a distribution of values for σ_a, σ_b and σ_c, or with a size distribution based on the three cross sections maintaining a constant ratio.

Polarization and extinction data are not uniquely correlated as can be seen in Figure 10.1, for example. Around galactic longitudes of $l \sim 85^\circ - 95^\circ$ (Perseus), the p/A_V ratio is high and the polarization vectors related to individual stars are closely aligned. On the other hand, for $l \sim 40^\circ - 50^\circ$ (Cygnus), the p/A_V ratio is low with the alignment of polarization vectors being more random. In the first case, the line of sight is across a spiral arm while, for the latter, it is more along the direction of the spiral arm. The differences in p/A_V values might be brought about by changes in the associated values of ν, perhaps also there being variations in the values of F, according to the galactic location. Differences in the interstellar reddening curve according to galactic longitude could also be influenced by the value of F (see, for example, Greenberg & Meltzer, 1960 and Wilson, 1960).

10.12
Beyond the Galaxy

A selection of stars in the Large Magellanic Cloud were observed by Visvanathan (1966). From the p/A_v ratio, he concluded that the system is seen nearly face on with the alignment of electric vectors uniform over large distances of the order of kiloparsecs, and with the magnetic field as indicated by electric vectors being related to the structure of the cloud. The study was later extended by Mathewson & Ford (1970) to cover 215 stars in the LMC and 77 stars in the SMC. The wavelength dependence of the polarization of the LMC was investigated by Clayton, Martin & Thompson (1983). After allowing for foreground contamination, they concluded that the typical $p(\lambda)$ behaviour was no different than that of our own Galaxy, this outcome being independent of the any issue associated with allowance for local dust along the line of sight.

Polarimetric measurements for about 15 spiral galaxies were discussed by Elvius (1978) in terms of their magnetic fields. The spirals observed included NGC 4216, as well as the peculiar galaxies NGC 3718 and NGC 2685. It was found that (1) light transmitted through the dust clouds of the dark lane in the spiral structure to the east of the nucleus in NGC 4216 exhibited polarization, with the strongest electric vector along the dark band, indicating large-scale magnetic fields in the direction of the spiral arms; (2) light was rather strongly polarized in the dark band believed to pass through the nucleus of NGC 3718, and (3) polarization effects caused by selective absorption were detected in the dark bands crossing over the NE part of the main body of NGC 2685, indicating the presence of magnetic fields along the observed filaments. These results show that the galaxies studied seemed to possess large-scale magnetic fields along the spiral arms, similar to the fields indicated in the Galaxy by the observed interstellar polarization of starlight. Some edge-on galaxies exhibiting polarization parallel to their dark bands were identified.

In a report by Magalhães, Loiseau & Piirola (1987), comment is made on the controversial existence of a Pan-Magellanic magnetic field, connecting the two Magellanic Clouds. They discuss the contribution that polarimetric observations might make and comment on the difficulties of removing effects of foreground polarization.

The wavelength dependence of the polarization in M 31 has been studied by Clayton, Wolff, Gordon, *et al.* (2004) by making measurements of globular clusters within this galaxy. The Serkowski law provides good fits to the variation, although the relationship between K and $\lambda_{\max}$ may be different from that for our own Galaxy. When curves for a given $\lambda_{\max}$ are compared, those for M 31 are significantly narrower than those in the Galaxy, and could be explained using extreme modifications to the size distributions of silicate particles. The average size of interstellar grains in M 31 appear to be smaller than for our Galaxy, if the general nature of the grains is the same.

The optical polarization of spiral galaxies has been modelled by Simmons & Audit (2000) by considering scattering of starlight by dust, molecules and electrons. By assuming the distribution of scatterers to be optically thin, semi-analytic expressions for the resolved intensity and polarized intensity for Thomson, Rayleigh and more general scattering mechanisms were obtained. For Thomson and Rayleigh scattering, and when scatterers and stars are distributed with rotational symmetry, the total polarized flux depends on the inclination, i, of the galactic axis to the line of sight according to a simple $\sin^2 i$ law. By using a method based on spherical harmonics for the more general scattering mechanisms, it was found that the $\sin^2 i$ law still holds, to a good approximation.

Not all the polarization generated in galaxies results from scattered starlight by dust. For example, Knacke & Capps (1974) made observations in the infrared of the Seyfert galaxy, NGC 1068, making comment that its ultraviolet excess was identified as synchrotron radiation after the discovery of linear polarization. The expectation that p should increase at wavelengths greater than 1 μm, as dilution from stellar radiation becomes less, was qualitatively borne out by observations at 3.5 and 10.2 μm.

References

Aannestad, P.A. (1982) On interstellar linear polarization and grain growth. *A&A*, **115**, 219–222. [206]

Aannestad, P.A., Greenberg, J.M. (1983) Interstellar polarization, grain growth, and alignment. *ApJ*, **272**, 551–562. [206]

A'Hearn, M.F. (1972) Polarization observations of the λ4430 diffuse interstellar absorption feature. *AJ*, **77**, 302–305. [213]

Appenzeller, I. (1968) Polarimetric observations of nearby stars in the directions of the galactic poles and the galactic plane. *ApJ*, **151**, 907–918. [216]

Appenzeller, I. (1974) Interaction between the Barnard Loop Nebula and the interstellar magnetic field. *A&A*, **36**, 99–105. [215]

Avery, R.W., Michalsky Jr, J.J., Stokes, R.A. (1973) Circular polarization in the B stars X Persei, 5 Persei, 55 Cygni and 30 Pegasi. *ApJ*, **180**, L127–L128. [208, 209]

Baud, B., Tinbergen, J. (1972). Optical polarization of X Per. *Nature*, **237**, 29–30. [208]

Behr, A. (1959) Beobachtungen zur Wellenlängenabhängigkeit der interstellaren Polarisation. *Zeit. für Astrophysik*, **47**, 54–58. [203]

Behr, A. (1961) Bemerkungen über den Ursprung der Polarisation des Sternlichts. *Zeit. für Astrophysik*, **53**, 95–105. [210]

Bel, N., Lafon, J.-P. J., Leroy, J.-L. (1993) Visual polarization measurements in the Cepheus Flare. *A&A*, **270**, 444–450. [221]

Berdyugin, A., Snåre, M.-O., Teerikorpi, P. (1995) Interstellar polarization at high galactic latitude for distant stars: first results for Z less than or equal to 600 pc. *A&A*, **294**, 568–574. [215]

Bhatt, H.C., Jain, S.K. (1993) Polarization maps for the dark clouds B227 and L121. *A&A*, **276**, 507–510. [216]

Breger, M. (1977) Intracluster Dust, circumstellar shell, and the wavelength dependence of polarization in Orion. *ApJ*, **215**, 119–128. [203]

Breger, M. (1984) The Pleiades cluster I. Polarization and reddening of the brighter stars. *A&A*, **137**, 145–148. [217]

Breger, M. (1985) The Pleiades Cluster II. Does it contain pre-main-sequence stars? *A&A*, **143**, 455–457. [217]

Breger, M. (1986) The Pleiades Cluster III. Polarization, reddening, and the unusual distribution of interstellar matter. *A&A*, **309**, 311–320. [217]

Breger, M., Gehrz, R.D., Hackwell, J.A. (1981) Interstellar grain size II. Infrared photometry and polarization in Orion. *ApJ*, **248**, 963–976. [203]

Carrasco, L., Strom, S.E., Strom, K.M. (1973) Interstellar dust in the Rho Ophiuchi dark cloud. *ApJ*, **182**, 95–109. [212]

Cernuschi, F., Marsicano, F.R., Kimel, I. (1965) On polarization of stellar light. *Ann. d'Astr.*, **28**, 860–866. [210]

Clarke, D. (1964) The polarization of Nova Herculis (1963) *The Observatory*, **84**, 28–29. [198]

Clarke, D. (1984) On the fitting of infrared data to the interstellar polarization law. *MNRAS*, **206**, 739–744. [206]

Clarke, D. (1986) The wavelength dependence of interstellar polarization of o Sco, σ Sco and η Aql. *A&A*, **156**, 213–216. [204]

Clarke, D., Al-Roubaie, A. (1983) Effects of noise and interstellar polarization law. *MNRAS*, **202**, 173–182. [206]

Clarke, D., Al-Roubaie, A. (1984) Effects of complex clouds on the interstellar polarization law. *MNRAS*, **206**, 729–738. [206]

Clayton, G.C., Anderson, C.M., Magalhães, A.M., Code, A.D., Nordsieck, K.H., Meade, M.R., Wolff, M.J., Babler, B., Bjorkman, K.S., Schulte-Ladbeck, R.E., Taylor, M.J., Whitney, B.A. (1992) The first spectral study of the wavelength dependence of interstellar polarization in the ultraviolet. *ApJ*, **385**, L53–L57. [207]

Clayton, G.C., Martin, P.G., Thompson, I. (1983) The wavelength dependence of interstellar polarization in the Large Magellanic Cloud. *ApJ*, **265**, 194–201. [225]

Clayton, G.C., Wolff, M.J., Gordon, K.D., Smith, P.S., Nordsieck, K.H., Babler, B.L. (2004) Interstellar polarization in M31. *AJ*, **127**, 3382–3387. [225]

Codina-Landaberry, S., Magalhães, A.M. (1976) On the polarizing interstellar dust. *A&A*, **49**, 407–413. [204]

Cohen, J.G. (1977) The interstellar medium near stars with peculiar interstellar polarization. *ApJ*, **214**, 86–91. [202]

Corso, G.J., Shatzel, A.V., Lange, W.F., Fox, R. (1993) Highly polarized stars in Cassiopeia. pp. 281–282 in *Massive Stars: Their Lives in the Interstellar Medium – ASP Conf. Ser.*, No: **35**, (eds J.P. Cassinelli & E.B. Churchwell), San Francisco. [217]

Cox, L.J., Hough, J.H., Adams, D.J., Jameson, R.F. (1976) Linear polarization measurements of o Sco in the near infrared. *MNRAS*, **176**, 131–133. [205]

Coyne (SJ), G.V. (1971) Wavelength dependence of polarization. XXV. Rotation of the position angle by the interstellar medium. *AJ*, **79**, 565–580. [208]

Coyne (SJ), G.V., Gehrels, T. (1966) Wavelength dependence of polarization. VIII. Interstellar polarization. *AJ*, **71**, 355–363. [207]

Coyne (SJ), G.V., Gehrels, T. (1967) Wavelength dependence of polarization. X. Interstellar polarization. *AJ*, **72**, 887–898. [204]

Coyne (SJ), G.V., Gehrels, T., Serkowski, K. (1967) Wavelength dependence of polarization. XXVI. The wavelength of maximum polarization as a characteristic parameter of interstellar grains. *AJ*, **79**, 581–589. [204]

Coyne, G.V., Tapia, S., Vrba, F.J. (1979) Wavelength dependence of polarization. XXXIII. The α Persei star cluster. *AJ*, **84**, 356–369. [216]

Coyne (SJ), G.V., Wickramasinghe, N.C. (1969) Wavelength dependence of polarization. XVIII. Interstellar polarization and composite interstellar particles. *AJ*, **74**, 1179–1190. [204, 208]

Crawford, I.A. (1988) High-resolution observations of interstellar Na I towards HD 174632. *MNRAS*, **233**, 923–928. [214]

Cugnon, P. (1983) Magnetic alignment of interstellar dust grains for dominating magnetic fields. *A&A*, **120**, 156–163. [211]

Davis, Jr., L. (1959) The color dependence of the polarization of starlight. *Zeit. für Astrophysik*, **47**, 59–66. [222, 223]

Davis, Jr., L., Greenstein, J.L. (1951) The polarization of starlight by aligned dust grains. *ApJ*, **114**, 206–240. [210, 215, 222]

Dolginov, A.Z. (1972) Orientation of interstellar and interplanetary grains. *Astrophys. Space Sci.*, **18**, 337–349. [212]

Dolginov, A.Z., Mytrophanov, I.G. (1976) Orientation of cosmic dust grains. *Astrophys. Space Sci.*, **43**, 291–317. [212]

Dyck, H.M., Jones, T.J. (1978) Near-infrared observations of interstellar polarization. *AJ*, **83**, 594–597. [205]

Dyck, H.M., McClure, R.D. (1969) Interstellar polarization in the directions of globular clusters M 3 and M 13. *AJ*, **74**, 1177–1178. [201]

Elvius, A. (1978) Magnetic fields in galaxies as revealed by the polarization of light. *Astrophys. Space Sci.*, **55**, 49–57. [225]

Fowler, L.E., Harwit, M. (1974) Incremental polarization of starlight at different locations in the galaxy. *MNRAS*, **167**, 227–236. [198]

Gammelgaard, P., Rudkjøbing, M. (1973) Observations of linearly polarized light of the intensity of the diffuse λ 6180 absorption band in 49 O, B and A stars. *A&A*, **27**, 261–271. [213]

Gehrels, T. (1960) Wavelength dependence of polarization. II. Interstellar polarization. *AJ*, **65**, 470–473. [203]

Gehrels, T. (1961) A short note on $p(\lambda)$ on UV Proposal. *AJ*, **66**, 44. [203]

Gehrels, T. (1972) The polariscope program. *Space Sci. Rev.*, **13**, 319. [204]

Gehrels, T. (1974) Wavelength dependence of polarization. XXVII. Interstellar polarization from 0.22 to 2.2 μm. *AJ*, **79**, 590–593. [206]

Gehrels, T., Meltzer, A.S. (1966) Wavelength dependence of polarization. VII. Interstellar polarization. *AJ*, **71**, 111–113. [204]

Gehrels, T., Silvester, A.B. (1965) Wavelength dependence of polarization. V. Position angles of interstellar polarization. *AJ*, **70**, 579–580. [207]

Gold, T. (1952a) Polarization of starlight. *Nature* **169**, 322. [212]

Gold, T. (1952b) The alignment of galactic dust. *MNRAS* **112**, 215–218. [212]

Greenberg, J.M. (1967) Interstellar grains. *Scientific American*, **217** (4), 106–114. [197]

Greenberg, J.M. (1978) Interstellar dust, Chapter 4 (pp. 187–284) in *Cosmic Dust.* Ed. J.A.M. McDonnell, Wiley, New York. [197]

Greenberg, J.M., Stoeckly, R. (1971) Shape of the diffuse interstellar bands. *Nature (Phys. Sci.)*, **230**, 15–16. [213]

Greenberg, J.M., Meltzer, A.S. (1960) The effect of orientation of non-spherical particles on interstellar extinction. *ApJ*, **132**, 667–671. [224]

Hall, J.S. (1949) Observations of the polarized light from stars. *Science*, **109**, 166–167. [197]

Hall, J.S., Mikesell, A.H. (1949) Observations of polarized light from stars. *AJ*, **54**, 187–188. [197]

Harwit, M. (1970a) Is magnetic alignment of interstellar dust really necessary? *Nature*, **226**, 61–62. [212]

Harwit, M. (1970b) Alignment of interstellar grains by starlight. *Bull. Astron. Inst. Czech.*, **21**, 204–211. [212]

Hayes, D.S., Mavko, G.E., Radick, R.R., Rex, K.H., Greenberg, J.M. (1973) Broadband structure in the interstellar extinction curve. pp. 83–90 in IAU Sym No: 52 *Interstellar Dust and Related Topics*, Reidel, Dordrecht, The Netherlands. [213]

Heiles, C. (1976) The interstellar magnetic field. *Ann. Rev. Astron. Astrophys.*, **14**, 1–22. [197]

Hiltner, W.A. (1949) Polarization of light from distant stars by interstellar medium. *Science*, **109**, 165. [197]

Hiltner, W.A. (1950) On polarization of radiation by interstellar medium. *Phys. Rev.*, **78**, 170–171. [197]

Hiltner, W.A. (1954a) Polarization of a heavily obscured clustering of OB stars in Cygnus. *ApJ*, **120**, 178–179. [199]

Hiltner, W.A. (1954b) Polarization of the cluster M29. *ApJ*, **120**, 367–368. [199]

Hiltner, W.A. (1954c) Early-type stars in the direction of the galactic center. *ApJ*, **120**, 41–47. [199]

Hiltner, W.A. (1956a) Photometric, polarization and spectrographic observations of O and B stars. *ApJS*, **2**, 389–462. [200, 199]

Hiltner, W.A. (1956b) Interstellar polarization. *Vistas Astron.*, **2**, 1080–1091. [199]

Ireland, J.G. (1961) On the effect of a helical magnetic field on the polarization of starlight. *MNRAS*, **122**, 461–472. [211, 215]

Jones, T.J. (1989) Infrared polarimetry and the interstellar magnetic field. *ApJ*, **346**, 728–734. [205]

Jokipii, J.R., Lerche, I., Schommer, R.A. (1969) Interstellar polarization of starlight and turbulent structures of the galaxy. *ApJ*, **157**, L119–L124. [214]

Kaplan, S.A., Klimishin, I.A. (1959) On the correlation between the observed difference in the degree of interstellar polarization and the angular distance of corresponding points on the celestial sphere. *Sov. Astron.*, **3**, 362. [214]

Kemp, J.C. (1972) Circular polarization of omicron Scorpii: possible interstellar origin. *ApJ*, **175**, L35–L37. [209]

Kemp, J.C. (1973) Interstellar polarization of upper Scorpius stars. pp. 181–185. IAU Symp. No: 52. Interstellar Dust and Related Topics, (eds J.M. Greenberg and H.C. Van de Hulst). Reidel, Dordrecht, The Netherlands. [209]

Kemp, J.C., Wolstencroft, R.D. (1972) Interstellar circular polarization: data for six stars and the wavelength dependence. *ApJ*, **176**, L115–L118. [208, 209]

King, L.W., Harwit, M.O. (1973) Photon and magnetic alignment of interstellar dust grains. pp. 197–202 in IAU Symp. No: 52. Interstellar Dust and Related Topics, (eds J.M. Greenberg and H.C. Van de Hulst). Reidel, Dordrecht, The Netherlands.. [212]

Klare, G., Neckel, Th., Schnur, G. (1971) Polarization of southern OB-stars. *A&A*, **11**, 155–158. [208]

Knacke, R.F., Capps, R.W. (1974) Infrared polarization of NGC 1068. *ApJ*, **192**, L19–L22. [226]

Krautter, J. (1980) The distribution of the interstellar dust in the galactic plane within 3 kpc. *A&A*, **89**, 74–79. [198]

Krzemiński, W., Serkowski, K. (1967) Photometric and polarimetric observations of the nearby strongly reddened open cluster stock 2. *ApJ*, **147**, 988–1002. [216]

Lazarian, A. (2003) Magnetic fields via polarimetry: progress on grain alignment theory. *J. Quant. Spectrosc. Radiat. Transf.*, **79**, 881–902. [210, 212, 212]

Lazarian, A., Cho, J. (2005) Grain alignment in molecular clouds. pp. 333–344 in *Astronomical Polarimetry: Current Status and Future Directions – ASP Conf. Ser.* No: **343**, (eds A. Adamson, C. Aspin, C.J. Davis & T. Fijiyoshi), San Francisco. [210]

Lee, H.M., Draine, B.T. (1985) Infrared extinction and polarization due to partially aligned spheroidal grains: models for the dust toward the BN object. *ApJ*, **290**, 211–228. [222]

Leroy, J.-L. (1993) A polarimetric investigation on interstellar dust within 50 pc from the Sun. *A&A*, **274**, 203–213. [198]

Leroy, J.-L. (1999) Interstellar dust and magnetic field at the boundaries of the Local Bubble – Analysis of polarimetric data in light of Hipparchos parallaxes. *A&A*, **346**, 955–960. [198]

Lodén, L.O. (1961a) A polarimetric investigation of 1300 stars. *Stockholms Obs. Ann.*, **21** (7), 1–94. [197]

Lodén, L.O. (1961b) Contribution to the discussion of interstellar polarization. *Stockholms Obs. Ann.*, **Bd.22** (1). [197]

Lloyd, S., Harwit, M.O. (1973) The Differential Polarization of Starlight as a Function of Distance. pp. 203–207. IAU Symp. No: **52**. Interstellar Dust and Related Topics, (eds J.M. Greenberg and H.C. Van de Hulst). Reidel, Dordrecht, The Netherlands. [198]

Magalhães, A.M., Loiseau, N., Piirola, V. (1987) Optical polarimetric survey of the Small Magellanic cloud. pp. 1–4 in *Proceedings Workshop "Magnetic Fields and Extragalactic Objects"* – Carsgèse, Corsica, June 1987. [225]

Maihara, T., Sato, S. (1973) A Search for Infrared Polarization in the Galactic Center. pp. 191–196 in IAU Symp. No: 52. Interstellar Dust and Related Topics, (eds J.M. Greenberg and H.C. Van de Hulst). Reidel, Dordrecht, The Netherlands. [215]

Markkanen, T, (1974a) Polarization observations in the coma cluster Mel 111. *A&A*, **32**, 89–91. [216]

Markkanen, T, (1974b) Polarization observations in Praesepe. *A&A*, **35**, 297–299. [216]

Markkanen, T. (1977a) The Magnetic Pocket – An Observational Study of the Structure of the Galactic Magnetic Field and of Interstellar Dust in the Direction of the α Persei Cluster. Report 1/1977 – Observatory and Astrophysics Laboratory, University of Helsinki, Helsinki. [216]

Markkanen, T. (1977b) Wavelength dependence of the polarization in the Pleiades. *A&A*, **56**, 83–89. [217]

Markkanen, T. (1979) Polarization measurements and extinction near the North Galactic Pole. *A&A*, **74**, 201–205. [215]

Marraco, H.G., Vega, E.I., Vrba, F.J. (1993) Intracluster dust polarization in the Carina Nebula. *AJ*, **105**, 258–270. [217]

Martin, P.G. (1972) Interstellar circular polarization. *MNRAS*, **159**, 179–190. [208]

Martin, P.G. (1973) Interstellar circular polarization and the composition of interstellar dust. pp. 161–167 in IAU Symp. No: 52. *Interstellar Dust and Related Topics*, (eds J.M.

Greenberg and H.C. Van de Hulst). Reidel, Dordrecht, The Netherlands. [209]

Martin, P.G. (1974) Interstellar polarization from a medium with changing grain alignment. *ApJ*, **187**, 461–472. [208, 215]

Martin, P.G. (1975) On the Kramers–Kronig relations for interstellar polarization. *ApJ*, **202**, 389–392. [210]

Martin, P.G., Angel, J.R.P. (1974) A study of interstellar polarization at the $\lambda\lambda$ 4430 and 5780 features in HD 183143. *ApJ*, **188**, 517–522. [213]

Martin, P.G., Angel, J.R.P. (1976) Systematic variations in the wavelength dependence of interstellar circular polarization. *ApJ*, **207**, 126–130. [209, 209]

Martin, P.G., Illing, R., Angel, J.R.P. (1973) Discovery of interstellar polarization in the direction of the Crab Nebula. pp. 169–179 in IAU Symp. No: 52. *Interstellar Dust and Related Topics*, (eds J.M. Greenberg and H.C. Van de Hulst). Reidel, Dordrecht, The Netherlands. [216]

Martin, P.G., Shawl, S.J. (1981) Polarization of scattered light in globular clusters. *ApJ*, **251**, 108–112. [218]

Martin, P.G., Whittet, D.C.B. (1990) Interstellar extinction and polarization in the infrared. *ApJ*, **357**, 113–124. [207]

Mathewson, D.S., Ford, V.L. (1970) Polarization measurements in the Magellanic Clouds. *AJ*, **75**, 778–784. [225]

Mavko, G.E., Hayes, D.S., Greenberg, J.M., Hiltner, W.A. (1974) Observations of structure in the interstellar polarization curve: preliminary results. *ApJ*, **187**, L117–L119. [213]

Mathis, J.S. (1979) The size distribution of interstellar articles. II Polarization. *ApJ*, **232**, 747–753. [207]

Mathis, J.S., Rumpl, W., Nordsieck, K.H. (1977) The size distribution of interstellar grains. *ApJ*, **217**, 425–433. [206]

Mathewson, D.S., Ford, V.L., Hiltner, W.A. (1974) Observations of structure in the interstellar polarization curve: preliminary results. *ApJ*, **187**, L117–L119. [212]

McCall, M.L. (1981) Big grains in the Orion Nebula. *MNRAS*, **194**, 485–502. [203]

McLean, I.S. (1976) Optical polarimetry and distance estimate for nova Cygni 1975. *MNRAS*, **176**, 73–80. [198]

McMillan, R.S. (1977) Walker No.67 in NGC 2264: A candidate for strong interstellar circular polarization. *ApJ*, **216**, L41–L43. [202, 203]

McMillan, R.S., Tapia, S. (1977) The wavelength dependence of polarization in the Cygnus OB2 Association. A new determination of interstellar birefringence. *ApJ*, **212**, 714–722. [209]

Michalsky Jr, J.J., Swedlund, J.B., Stokes, R.A., Avery, R.W. (1974) Interstellar circular polarization: a report of eight new positive results. *ApJ*, **187**, L13–L14. [209]

Michalsky Jr, J.J., Swedlund, J.B., Avery, R.W. (1975) Circular polarization of HDE 226868. *Nature*, **254**, 39–40. [209]

Minniti, D., Coyne, G.V., Claria, J.J. (1992) Linear polarization of stars in seven metal-poor globular clusters. *AJ*, **103**, 871–890. [218]

Mishchenko, M.I. (1990) Extinction and polarization of transmitted light by partially aligned nonspherical grains. *ApJ*, **367**, 561–574. [215]

Nandy, K., Seddon, H. (1970) Polarization-wavelength profile of the interstellar 4430 Å absorption band. *Nature*, **227**, 264–265. [213]

Nandy, K., Seddon, H. (1973) Polarization profile near the 4430 band. pp. 79–81 in IAU Symp. No: 52, *Interstellar Dust and Related Topics*, (eds J.M. Greenberg and H.C. Van de Hulst). Reidel, Dordrecht, The Netherlands. [213]

Nee, S.F., Jokipii, J.R. (1979) Interstellar polarization in an irregularly fluctuating medium. *ApJ*, **234**, 140–153. [214]

Nee, S.F. (1980) Fluctuation theory of starlight polarization. *ApJ*, **237**, 471–481. [214]

Piirola, V. (1977) Polarization observations of 77 stars within 25 pc from the Sun. *A&AS*, **30**, 213–216. [198]

Reiz, A., Franco, G.A.P. (1998) UBV polarimetry of 361 A- and F-type stars in selected areas. *A&AS*, **130**, 133–140. [198]

Salpeter, E.E., Wickramasinghe, N.C. (1969) Alignment of interstellar grains by cosmic rays. *Nature*, **222**, 442–444. [212]

Serkowski, K. (1962) Polarization of starlight. In *Advances in Astronomy and Astrophysics*, **1**, pp. 289–352. Ed. Z. Kopal, Academic Press, New York, London. [214, 218]

Serkowski K. (1965) Polarization of galactic clusters M 25, NGC 869, 884, 1893, 2422, 6823, 6871, and association VI Cygni. *ApJ*, **141**, 1340–1361. [199, 208]

Serkowski, K. (1968) Correlation between the regional variations in wavelength dependence of interstellar extinction and polarization. *ApJ*, **154**, 115–134. [201, 202, 204]

Serkowski, K. (1971) Polarization of variable stars. pp. 11–31 in *New Directions and New Frontiers in Variable Star Research*, IAU Colloquium No: 15. (Bamberg). [204]

Serkowski, K. (1973) Interstellar polarization. pp. 145–152 in IAU Symp. Vol. **52**, *Interstellar Dust and Related Topics*. (eds J.M. Greenberg and H.C. van de Hulst). Reidel, Dordrecht, The Netherlands. [204, 204]

Serkowski K., Chojnacki, W. (1969) Polarimetric observations of magnetic stars with two-channel polarimeter. *A&A*, **1**, 442–448. [208]

Serkowski, K., Gehrels, T., Wiśniewski, W. (1969) Wavelength dependence of polarization. XIII. Interstellar extinction polarization correlations. *AJ*, **74**, 85–90. [201, 208]

Serkowski, K., Mathewson, D.S., Ford, V.L. (1975) Wavelength dependence of interstellar polarization and ratio of total to selective extinction. *ApJ*, **196**, 261–290. [201, 201, 202, 205]

Serkowski, K., Robertson, J.W. (1969) Regional variations in the wavelength dependence of interstellar polarization. *ApJ*, **158**, 441–447. [204]

Shain, G.A. (1957) The inclination to the galactic equator of the general magnetic field of the Galaxy in the solar vicinity. *Sov. Astron.*, **1**, 1–7. [214]

Shulz, A., Lenzen, R. (1983) New polarization measurements of HD 183143, HD 204827 and Cyg OB2 Sch. No. 12. *A&A*, **121**, 158–161. [206]

Simmons, J.F.L., Audit, E. (2000) The optical polarization of spiral galaxies. *MNRAS*, **319**, 497–509. [225]

Somerville, W.B. (1996) Spectropolarimetry of optical and ultraviolet extinction features. pp. 143–158 in *Polarimetry of the Interstellar Medium – ASP Conf. Ser.*, **97**, (eds W.G. Roberge and D.C.B. Whittet), San Francisco. [213]

Stępień, K. (1964) Discussion of several models of the galactic magnetic field explaining the interstellar polarization. *Acta Astron.*, **14**, 81–95. [215]

Stokes, R.A., Avery, R.W., Michalsky J.J. Jr, (1973) Optical circular polarization of X Persei. *Nature (Phys. Sci.)*, **241**, 5. [208]

Stokes, R.A., Swedlund, J.B., Avery, R.W., Michalsky, J.J. (1974) Interstellar circular polarization: results from a survey of 84 stars. *AJ*, **79**, 678–681. [208]

Struve, O. (1961) Why is starlight polarized? *Sky & Telescope*, **21** (6), 317–320. [210]

Thiessen, G. (1961) Über die Polarisation des Sternlichts, die Strahlung der Sterne, Sowie Bemerkungen zur Galaktischen Strukter. *Astr. Abh. Hamburg Stern.*, Band V: Nr. 9. [210]

Thiessen, G. (1962) Zur Arbeit von A. Behr: “Bemerkungen über den Ursprung der Polarisation des Sternlichts”. *Zeit. für Astrophysik*, **54**, 287–288. [210]

Tinbergen, J. (1982) Interstellar polarization in the immediate solar neighbourhood. *A&A*, **105**, 53–64. [198]

Treanor (SJ), P.J. (1963) Wavelength dependence of interstellar polarization. *AJ*, **68**, 185–189. [203, 207]

van de Hulst, H.C. (1957) p. 452 in *Light Scattering by Small Particles*, Wiley/Chapman, New York/London. [208]

van P. Smith, E. (1956) Interstellar polarization in the Southern Milky Way. *ApJ*, **124**, 43–62. [215]

Visvanathan, N.V. (1966) Interstellar polarization in the large magellanic cloud. *MNRAS*, **132**, 423–432. [225]

Vrba, F.J., Coyne (SJ), G.V., Tapia, S. (1993) An investigation of grain properties in the ρ Ophiuchi Dark Cloud. *AJ*, **105**, 1010–1237. [202]

Walker, G.A.H. (1963) Photoelectric measures of the 4430Å diffuse interstellar band. *MNRAS*, **125**, 141–167. [213]

Weitenbeck, A.J. (1999) Stars with ISM Polarization observed with HPOL. *Acta Astron.*, **49**, 59–71. [205]

Weitenbeck, A.J. (2004) Stars with ISM oolarization observed with HPOL. II. *Acta Astron.*, **54**, 87–102. [205]

Weitenbeck, A.J., Halstead, E.A., Carver, A.J. (2008) ISM Polarization toward NGC 1502. *Acta Astron.*, **58**, 41–54. [217]

Whittet, D.C.B. (1977) The dependence of the extinction ratio of galactic longitude. *MNRAS*, **180**, 29–35. [202]

Whittet, D.C.B. (1979) Anomalous extinction and Gould's belt. *A&A*, **72**, 370–373. [202]

Whittet, D.C.B., Gerakines, P.A., Carkner, A.L., Hough, J.H., Martin, P.G., Prusti, T., Kilkenny, D. (1994) A study of the Chamaeleon I dark cloud and T-association. VI. Interstellar polarization, grain alignment and magnetic field. *MNRAS*, **268**, 1–12. [202]

Wickramasinghe, N.C. (1969) Interstellar polarization by graphite–silicate grain mixtures. *Nature*, **224**, 656–658. [204]

Wilking, B.A., Lebofsky, M.J., Martin, P.G., Rieke, G.H., Kemp, J.C. (1980) The wavelength dependence of interstellar linear polarization. *ApJ*, **235**, 905–910. [205, 206]

Wilking, B.A., Lebofsky, M.J., Rieke, G.H. (1982) The wavelength dependence of interstellar linear polarization: stars with extreme values of $\lambda_{\max}$. *AJ*, **87**, 695–697. [206]

Wilson, R. (1960) The relation between interstellar extinction and polarization. *MNRAS*, **120**, 51–63. [224]

Wolf, G.W. (1972) A search for elliptical polarization. *AJ*, **77**, 576–583. [208]

Wolff, M.J., Clayton, G.C., Meade, M.R. (1993) Ultraviolet interstellar linear polarization. I. Applicability of current dust grain models. *ApJ*, **403**, 722–735. [207]

Wolstencroft, R.D., Smith, R.J. (1984a) High precision spectropolarimetry of stars and planets – III. The wavelength dependence of interstellar polarization. *MNRAS*, **208**, 461–480. [213]

Wolstencroft, R.D., Smith, R.J. (1984b) Structure in the interstellar polarization curve and the nature of polarizing grains. pp. 167–170 in *Laboratory & Observational Infrared Spectra of Interstellar Dust*, Hilo Workshop, July 1983, (eds R.D. Wolstencroft and J.M. Greenberg). [213]

11
Binary Stars

11.1
Introduction

As seen in Chapter 1, it was the notion that early-type eclipsing binary stars should exhibit polarization variability that encouraged observationalists to construct equipment to investigate the issue. As it turned out, the first results immediately opened up polarimetric research related to the interstellar medium but, as instrumental techniques improved, the original sort for effects were detected and followed in a variety of systems. In addition, other binary systems that do not exhibit eclipses were also found to exhibit variable polarization as a result of scattering from gas streams between the stars, and, in some cases, this has led to understanding of the geometry of their orbits. Descriptions of the polarimetric behaviour of all the various kinds of binary star systems are presented below. As it turns out, many binary systems exhibit temporal polarizational signatures both by eclipse events and by scattering from detached material, and it is somewhat artificial to discuss their behaviour under the individual section headings as designated below. For convenience, however, the material is presented according to the nature of the system which initially brought itself to the attention of polarimetry.

11.2
Eclipsing Binaries

The detection of polarization signatures occurring in eclipsing binary stars, the original drive for the establishment of stellar polarimetry, was pursued by Hiltner. Although a possible detection of the *Chandrasekhar effect* had been reported for RY Per, Hiltner (1947) remained cautious. In a later investigation of possible candidates, Hiltner (1949) described the difficulties of making the necessary delicate measurements, but concluded that some of the strong, and apparently constant polarizations, were not associated with the individual target stars, being introduced to the stellar radiation in its passage through interstellar space. It is noteworthy that one of the cited stars, CQ Cep (HD 214419), has since had variable polarization recorded, analysed and modelled by Drissen, Moffat, Bastien, *et al.* (1986).

Stellar Polarimetry. David Clarke

ISBN: 978-3-527-40895-5

One of the most studied stellar objects is β Lyrae, its 13-day binary period known as early as 1784. In summary, it comprises a B-type primary that has transferred as much as 10 solar masses of its material to its darker, and now more massive, companion embedded within a toroidal disc. It attracted attention of Öhman (1934) for spectropolarimetry as early as 1934. Shakhovskoi (1963) was the first to observe polarization variability of the system, producing a p-curve for its cycle. From the amplitude of the changes, he was able to calculate the mass of material giving rise to the scattering that produces the polarization. A fuller report of his observations and of 16 other eclipsing binary systems, including RY Per, is provided in Shakhovskoi (1965). Appenzeller (1965) observed β Lyr and obtained a p-curve displaying differences relative to the behaviour recorded by Shakhovskoi. Serkowski (1965) also made measurements over the cycle; he commented that β Lyrae was the first object for which changes in the period p-curve were confirmed when the observations are repeated with different instruments.

UBV p-curves were obtained by Appenzeller & Hiltner (1967) with the interstellar component subtracted. The spectral coverage of the p-curve behaviour was extended by Coyne (1970a). A further paper by Coyne (1970b) suggested that the polarization observed at primary minimum was not due solely to the decrease in the unpolarized light by the eclipse. The increase in p at this phase was attributed to scattering by the material undergoing mass transfer, the same material explaining the asymmetry in the light-curve during primary eclipse.

The polarization behaviour of the Hα and Hβ emission lines was studied by McLean (1977) who confirmed orbital variations of p that did not follow those of the continuum. It was also concluded that the intrinsic polarization contribution is almost aligned to that of an interstellar component.

In the summary description of β Lyr above, it is noted that the system supports a toroidal disc. Such discs are accompanied by bipolar outflows. From measurements made by the Wisconsin Ultraviolet Photo-Polarimeter (WUPPE), Hoffman, Nordseick & Fox (1998) have found that the position angle in the UV is orthogonal to that in visible light, the former polarization being engendered by scattering from the polar regions rather than from around the equator.

Changes of p during eclipse phase for about 12 binaries were recorded by Shakhovskoi (1965, 1969) and Shulov (1967). The most prominent examples discovered as displaying variable p included the Wolf-Rayet binary, V 444 Cygni, (Shulov, 1966 and Hiltner & Mook, 1966) and U Sge and RY Per. For the latter star, temporal changes in p had already been suspected by Hiltner (1947) and then studied by Shakhovskoi (1965) and by Shulov & Goudcova (1969). A listing of some of the eclipsing binary stars displaying intrinsic polarization is provided by Kruszewski (1974). Serkowski (1970) investigated some 14 southern eclipsing binaries but found changes in only two, TT Hya and V 453 Sco.

A search for polarization changes in U Cep was made by Coyne (1974) near primary eclipse. This star is an Algol-type semi-detached binary with a B7 V primary and a G8 III–IV secondary which fills the Roche lobe. Observations were made just before first contact to just after third contact, but no intrinsic polarization was evident, although it should have been expected from the predicted densities and configuration of circumstellar material. It was concluded that the negative result might have arisen from the fact that the gas stream from the secondary, and the flattened disc about the primary, is not permanent, this confirmed by spectroscopy. A later study by Piirola (1980, 1981) reported that U Cep had given evidence of intrinsic p in 1972, but in early 1973, some 6 months prior to Coyne's study, the star was polarimetrically quiet. In late 1975, when Piirola performed his observations, large increases in p were measured, these following other indications of mass transfer events. The conclusion from polarimetry is that the effective radius of the primary star had increased during the period of high mass transfer and that the inclination of the orbit is about 83°.

Phased-locked polarimetric variability of AO Cas was recorded by Rudy & Kemp (1976). The polarization was explained by light scattered from a gas stream between the O-star binary, with the main scattering region being on the advancing side of the secondary star. Later, phased-locked linear polarization was also recorded by Rudy & Kemp (1977) in *u* Her, a partial eclipsing system. The peak-to-peak amplitude was very small (~0.06%) with the principal variation corresponding to the second harmonic of the known 2.05 day orbital period. Their favoured explanation of the behaviour involves the reflection of light from the primary by the facing hemisphere of the secondary.

Polarimetric determinations of the inclinations of five binary systems (AO Cas, u Her, β Per, U Sag and V 444 Cyg) were reported by Rudy & Kemp (1978). Observations of u Her were also made by Koch & Pfeiffer (1977) and compared with those of the Oregon team; colour measurements were also presented, indicating a fairly flat variation.

A later study of the most famous of all eclipsing binaries, Algol, or β Per, was conducted by Kemp, Barbour, McBirney, *et al.* (1981) with single measurement accuracies of ±0.003%, revealing a *B*-band variation with amplitude ~0.01%. From the q, u locus, an eigen direction was found which matches that of the major-axis direction of the third component star ($AB - C$) orbit, as measured by speckle interferometry. Various kinds of polarigenic mechanism were considered to explain the observed behaviour including reflections, Roche lobe internal scattering, and reflections from an optically thick flattened gas cloud near the L_1 point.

For the star AW UMa, classified as a W UMa eclipsing variable, Oshchepkov (1974) obtained a polarization curve. Relative to its light-curve, it displays maximum p at a phase of $0.^{\mathrm{P}}26$, resembling the behaviour of YY Eri. The position angle of the polarization carries little or no variation. Taking into account its light variation, its spectral behaviour and the polarization waveform, the system can be modelled qualitatively by either the presence of gaseous streams emerging from one component which is ahead of the primary minimum or the system possessing a common atmosphere, but with prolongated shape from the phase of $0.^{\mathrm{P}}25$. Four W UMa-type eclipsing binaries were observed by Piirola (1977). Changes in p over the orbital periods were very small, if any, and there was no evidence of gas streams, nor discs, nor any kind of detached matter in the systems.

Using the data of Koch & Pfeiffer (1989), Fox (1994) has made an analysis of the polarimetric variations of Y Cyg. This system comprises two similar B0 stars in an eccentric orbit ($e \sim 0.12$) with a period of $2.^{\mathrm{d}}996$, and a significant apsidal motion with an $\sim 42.^{\mathrm{y}}7$ cycle. No significant period was discernable from the polarimetric data spanning almost 13 years, but the polarization does change around the eclipse phases, but not in a regular way from period to period, suggesting that the primary star displays a variable stellar wind.

Coyne (1972) made measurements over a 4-year period of the eclipsing system ϵ Aur with an F2Ia spectrum and period of $27.^{\mathrm{y}}1$. An increase in p was noted beginning at a phase of about 0.4, remaining at this higher level through the non-eclipse conjunction. Encouragement was given to monitor this star over its long period, but no further measurements are available.

With reference to a photometric period of $0.^{\mathrm{d}}5914264$, Luna (1980) presented polarimetric data for ϵ CrA, showing a variation containing the second harmonic. From the standard model of Brown, McLean & Emslie (1978), he determined an inclination of 71°, agreeing well with the deduction from photometry.

The possibility of detections of circular polarization during eclipses of β Lyr and BM Ori has been investigated by Kemp, Wolstencroft & Swedlund (1972), but with null results.

11.3
Close Binaries

A summary of the usefulness of polarimetry to the investigation of close binary systems was provided by McLean (1980). The discussion relates to both the scattered light from material co-rotating in the system, and to effects occurring in the emission lines associated with gaseous streams and stellar winds.

Rudy & Herman (1978) monitored the O star Binary HD 47129 (Plaskett's star). The maximum levels of polarization appeared at quadratures which is explainable by the presence of co-rotating scattering material lying between the stars. After applying a regression analysis to the variations of the q, u parameters, the determined amplitudes of the first and second harmonics, based on the orbital period, provided an inclination of 71°. By applying this figure to the known mass function of the system, and using a mass ratio of unity, masses of $59 M_{\odot}$ were obtained for the component stars.

The double-lined spectroscopic binary LZ Cep, comprising O8.5 III and O9.5 V components, was discovered by Berdyugin & Harries (1999) to display phase-locked polarization variations. The most probable explanation of the behaviour is reflection of radiation from each binary component off the facing hemisphere of its companion.

The peculiar Ae-type hydrogen-deficient spectroscopic binary ν Sgr = HD 181615 was noted by Coyne & Gehrels (1967), in a table of stellar measurements, as displaying variability, and, according to Serkowski (1971), has been studied in more detail by Coyne & Kruszewski. Although Coyne & Kruszewski (1969) make reference to future publication of numerous measurements made of ν Sgr, published details of these data remain illusive.

Many of the newly discovered X-ray sources were investigated by optical polarimetry. A classic example is that of the X-ray binary, Cygnus X-1. Any determination of the orbital inclination has consequences on whether one of the components might be interpreted as being a black hole. Following an intensive programme of observations, Kemp, Southwick & Rudy (1976) showed that their data had a distribution in the qu-plane which was dispersed to a greater degree than formal errors suggested. When phase-folded on the $5.^{d}6$ photometric period, however, the apparent variations did not offer a recognisable undulation. With the addition of further measurements, Kemp, Barbour, Herman, *et al.* (1978) detected a stable polarization variation in the V-band with a period of $5.^{d}600$. From determination of the Fourier coefficients of the variation, a surprisingly large inclination of $i = 76° \pm 8°$ was determined. With further accumulation of data Kemp, Barbour, Parker, *et al.* (1979) extended their interpretation of the system, suggesting effects associated with an extension to the secondary envelope with an eclipsing region. The interpretation of such polarimetric data has not been without contention, however. A critique of the evidence on the interpretation of Cygnus X-1 has been given by Simmons, Aspin & Brown (1980).

In relation to close X-ray binaries, Gnedin, Silant'ev & Shibanov (1976) considered the behaviour of potential phase-locked curves for ellipsoidal distorted stars with the addition of a hot spot generated by the impact of transferred material. They suggested that, for the Cyg X-1 system, the ellipsoidal star should have an axial ratio of at least 0.85. From polarimetric measurements, Dolan & Tapia (1988) determined the inclination of the X-ray binary HD 77581 (= 4U 0900-40) providing a value of $i = 76°[+5°/-9°]$, using the method described in Section 11.4.

Kemp & Barbour (1983) also performed an extended observational study of X Per with the conclusion that part of its variability was correlated with a 580^{d} radial velocity (RV) cycle that had been recently proposed, and the harmonic of 290^{d}. These polarimetric data were also analysed by Clarke & McGale (1988a) who suggested that these long periods are associated with beats generated by the stellar rotation and the data sampling intervals, and that they have no astrophysical significance. The same suggestion was also made regarding the promoted orbital period deduced from the RV measurements.

A cursory investigation of criteria required for binary systems to exhibit polarization variability was presented by Pfeiffer & Koch (1977). The production of the signal is commonly scattering from circumstellar material, but in some systems, the same mechanism which causes polarization variability in single cool giants may be operating. With one exception (U Oph), un-evolved binaries do not exhibit intrinsic polarization, and it is relatively easy to detect variability among evolved pairs whose photospheres are separated by at least 10 solar radii.

11.4
Binary Orbit Theory

The polarimetry of close binary systems has been modelled by Buerger & Collins II (1970) by considering the distortions on the distribution of scattering material by axial rotation and gravitational interactions. The method allows calculation of intrinsic polarization in and out of eclipse. Predictions are for polarization variations of several tenths of a per cent.

By investigating the effects of Thomson scattering in optically thin stellar envelopes, Brown, McLean & Emslie (1978) established the fundamental polarimetric behaviour associated with binary systems with co-rotating steady state electron clouds. This paper is frequently cited, and the model will be referred to here as the *BMcLE model*. The form of the variation, as plotted in the qu-plane, is dependent on the inclination, i, of the system and may be expressed in terms of the fundamental period and its first harmonic. It was demonstrated how the formulation may be formally inverted to provide a systematic diagnostic for inferring the characteristics of a binary and its envelope. This seminal work has provided the basis of studies of a variety of binary types. Simmons (1983) later extended the BMcLE model by considering arbitrary scattering mechanisms other than Thomson scattering, with the results illustrated by Mie scattering. An alternative approach to modelling of the effects of scattering material in binary systems has been made by Dolan (1984) using regularized Monte Carlo calculations.

Aspin, Simmons & Brown (1981) performed an analysis of the required accuracy of q, u measurements to allow their variation to provide useful estimates of i. The procedure comprised evaluation of the confidence interval of i for a model involving single Thomson scattering in a co-rotating envelope which yields an acceptable χ^2 fit to simulated data when optimized over the free parameters involved in the model. The required accuracy of polarimetric observations was found to be significantly higher for low values of inclination. A later paper by Simmons, Aspin & Brown (1982) showed that fitting the canonical model to binary star data will tend to yield values of inclination greater than the true value. The statistical bias is most pronounced for data with higher noise values when the inferred value, and the formal linear error, have no bearing on the actual value. As the noise increases, the inferred inclination approaches 90°. Errors for inclination which are established by formal techniques are seriously over optimistic, except for data with high signal-to-noise ratios. It was also demonstrated by Brown, Aspin, Simmons, *et al.* (1982) that if the binary orbits are eccentric, third harmonics are generated in the polarimetric variation, making a clear diagnosis of noisy data more problematic.

The polarimetric behaviour of binary systems embedded in electron shells of various geometries has been explored by Manset & Bastien (2000). It was shown that the polarimetric variations should be more apparent for systems with the low inclination, a high optical depth, a flat envelope, a small cavity, or an orbit that brings the stars close to the inner edge of the cavity. They also demonstrated that the BMcLE model remains powerful in finding orbital inclinations $\gtrsim 45°$ for a variety of distribution forms for optically thin Thomson scattering clouds; the flatness of the envelope, the size of any central cavity and the size of the orbit have no significant influence on the inclination deduced by the BMcLE model.

Returning to the BMcLE model, the polarimetric effect of Thomsom scattering by material between a pair of stars can be considered by applying the simple approach as summarized in (9.34) and (9.35), i. e.

$$q = \tau_{\mathrm{e}} \left[q_0 + q_1 \cos(2\pi \nu t) + q_2 \cos(4\pi \nu t) \right] , \tag{11.1}$$

$$\text{and} \qquad u = \tau_{\mathrm{e}} \left[u_1 \sin(2\pi \nu t) + u_2 \sin(4\pi \nu t) \right] . \tag{11.2}$$

with the coefficients in the expression describing q and u given by

$$q_0 = \sin^2 i \left(\frac{3\sin^2 \theta}{2} - 1 \right) ; \qquad \tau_{\mathrm{e}} = \frac{\sigma_0 n}{r^2} , \tag{11.3}$$

$$q_1 = -\frac{1}{2} \left(\sin 2\theta \sin 2i \right) ; \qquad u_1 = \sin 2\theta \sin i , \tag{11.4}$$

$$q_2 = -\frac{1}{2} \left(\sin^2 \theta (1 + \cos^2 i) \right) ; \qquad u_2 = \sin^2 \theta \cos i . \tag{11.5}$$

With consideration to the theorem of optical equivalence, the effect of the light from the two stars, scattered by a complicated geometric optically thin distribution of electrons, will have the same form as the equations above. The coefficients, however, result from the sum or integrations of the scattering of the light from the pair of stars by the complex geometry associated with distribution of the scattering centres, and, in the first place, it is assumed that the stars move in circular orbits and that the envelope material co-rotates in a fixed fashion.

The scattering integrals may be expressed as products in the form of $\tau_0 \gamma_j$, where the term τ_0 is the effective Thomson scattering optical depth integrated over all directions. The five terms, given by $\tau_0 \gamma_0$ to $\tau_0 \gamma_4$, correspond to optical depths integrated over solid angle with various weightings associated with direction, and averaged for the two stars according to their brightnesses. These expressions summarize the scattering and polarigenic geometry. In keeping with an extension to (11.1) and (11.2), the expressions for the intensity and the NSPs, may be written, according to Brown, McLean & Emslie (1978), as

$$\begin{aligned} I = {} & I_0 \left[1 + \tau_0 \left\{ 2(1 + \gamma_0) + (1 - 3\gamma_0) \sin^2 i \right\} \right. \\ & \left. + \tau_0 \left\{ \sin 2i (\gamma_1 \cos \phi - \gamma_2 \sin \phi) + \sin^2 i (\gamma_3 \cos 2\phi - \gamma_4 \sin 2\phi) \right\} \right] , \end{aligned} \tag{11.6}$$

$$\begin{aligned} q = {} & \tau_0 \left[\left\{ (1 - 3\gamma_0) \sin^2 i \right\} \right. \\ & \left. + \left\{ \sin 2i (\gamma_1 \cos \phi - \gamma_2 \sin \phi) - (1 + \cos^2 i)(\gamma_3 \cos 2\phi - \gamma_4 \sin 2\phi) \right\} \right] , \end{aligned} \tag{11.7}$$

$$u = 2\tau_0 \left[\sin i (\gamma_1 \sin \phi + \gamma_2 \cos \phi) - \cos i (\gamma_3 \sin 2\phi + \gamma_4 \cos 2\phi) \right] , \tag{11.8}$$

where ϕ now describes the longitude of the second star with respect to the first.

For convenience in developing the notation for expressing the expected temporal behaviour, and for making analyses of data, (11.6), (11.7) and (11.8) may be rewritten as

$$\begin{aligned} I = I_0 \big[& 1 + \tau_0 \left\{ 2(1+\gamma_0) + (1-3\gamma_0)\sin^2 i \right\} \\ & + \tau_0 \left\{ G \sin 2i \cos(\phi + \phi_1) + H \sin^2 i \cos 2(\phi + \phi_2) \right\} \big] , \end{aligned} \tag{11.9}$$

$$\begin{aligned} q = \tau_0 \big[& \left\{ (1-3\gamma_0)\sin^2 i \right\} \\ & + G \sin 2i \cos(\phi + \phi_1) - H(1+\cos^2 i)\cos 2(\phi + \phi_2) \big] , \end{aligned} \tag{11.10}$$

$$u = 2\tau_0 \left[G \sin i \sin(\phi + \phi_1) - H \cos i \sin 2(\phi + \phi_2) \right] , \tag{11.11}$$

where

$$\tan \phi_1 = \frac{\gamma_2}{\gamma_1} ; \qquad G = (\gamma_1^2 + \gamma_2^2)^{1/2} , \tag{11.12}$$

$$\tan 2\phi_2 = \frac{\gamma_4}{\gamma_3} ; \qquad H = (\gamma_3^2 + \gamma_4^2)^{1/2} . \tag{11.13}$$

By replacing ϕ by $2\pi\nu t$, where ν is the orbital frequency, it can be seen from the equations describing the behaviour of the NSPs that they exhibit variability at the fundamental frequency, or first harmonic, and at the second harmonic. The equations also show that the global extended atmosphere generates a constant polarization with magnitude $\tau_0(1-3\gamma_0)\sin^2 i$, independent of ϕ, and contained in the q parameter. This is similar to the outcome of the model of Brown & McLean (1977) who explored the polarization produced by axisymmetric extended electron atmospheres around single stars. As the constant term affects the q parameter only, it is this polarization vibration that corresponds to the envelope axis projected on the sky. The bracketed term $(1-3\gamma_0)$ is essentially a shape factor, decreasing from unity for a plane envelope to -2 for a prolate envelope, with the material concentrated in the polar direction, and passing through 0 for a spherically symmetric distribution of electrons. It may be noted that the magnitude of the constant component is very sensitive to the inclination, i, of the system. Also, it must be remembered that both q and u may carry constant components, q_I, u_I, as a result of interstellar polarization.

The behaviour and variations of the electron number density, n, within the geometric system obviously have bearing on the interpretation of the values of G and H, but, nonetheless, some general comments have been made by Brown, McLean & Emslie (1978). Firstly the term G is a measure of the effective degree of asymmetry about the orbital plane, with the values of γ_1 and γ_2, separately and respectively, describing the asymmetry about the plane for material near the line connecting the two stars, and in directions normal to this line. Secondly, H relates to the effective concentration of scattering material to the orbital plane; the values of γ_4 and γ_3 separately measure this concentration at the particular pairs of longitudes, ($\pi/4$ or $3\pi/4$) and (0 or $\pi/2$), respectively.

11.4.1
Data Analysis by a Geometric Method

A sample of expected qu-loci that the BMcLE model predicts is presented in Figure 11.1 and reference to such patterns is a preliminary exercise that might be undertaken to explore the geometry of any polarimetric binary according to the recorded data. It may be noted that the sense of execution of such patterns indicates the direction in which the orbits are executed, in the same way that is apparent in the recording of visual binaries. In exploring data behaviour relative to a predicted pattern, it will be appreciated that the coordinate frame related to the star and its geometry is likely to be set at some angle, Ω, to the measurement frame of the data. For such comparisons, the NSP values from the models should be progressively rotated to explore the best match with the data loci.

If the data are numerous, and the orbital period is known, the value of Ω and the geometry related to the binary orbit may be obtained by geometric principles. Separation of the behaviour of the first and second harmonics can be achieved by forming from the original data, $q(\phi) \equiv q(2\pi\nu t)$, $u(\phi) \equiv u(2\pi\nu t)$, a new subsidiary set defined by

$$q_+(\phi) = \frac{1}{2}\left[q(\phi) + q(\phi + \pi)\right], \tag{11.14}$$

$$q_-(\phi) = \frac{1}{2}\left[q(\phi) - q(\phi + \pi)\right], \tag{11.15}$$

$$u_+(\phi) = \frac{1}{2}\left[u(\phi) + u(\phi + \pi)\right], \tag{11.16}$$

$$u_-(\phi) = \frac{1}{2}\left[u(\phi) - u(\phi + \pi)\right]. \tag{11.17}$$

If any of the chosen original data pairs are not separated exactly by a phase difference of π, then interpolations can be applied to obtain the required two values with the correct phase difference. Considering (11.14) and (11.16), they may be re-written as

$$q_+(\phi) = q_c + q_2 \cos 2(\phi + \phi_2)\,, \tag{11.18}$$

$$u_+(\phi) = u_c + u_2 \sin 2(\phi + \phi_2)\,, \tag{11.19}$$

where the numerical subscript, 2, refers to variations associated with the second harmonic.

Elimination of $(\phi + \phi_2)$ from (11.18) and (11.19) shows that the locus for the revised data follows an ellipse, centred on $q_\mathrm{c} = q_\mathrm{I} + \tau_0(1 - 3\gamma_0)\sin^2 i$, $u_\mathrm{c} = u_\mathrm{I}$, with semi-major axis, $|q_2| = \tau_0 H(1 + \cos^2 i)$, and with semi-minor axis, $|u_2| = 2\tau_0 H \cos i$. The ellipse has eccentricity given by $\sin^2 i/(2 - \sin^2 i)$, and is swept out twice per orbit from a fiduciary point determined by ϕ_2. The major axis is orientated at Ω to the q-axis of the celestial coordinates used for the measurements, so yielding the previously unknown orientation of the system. This elliptical lo-

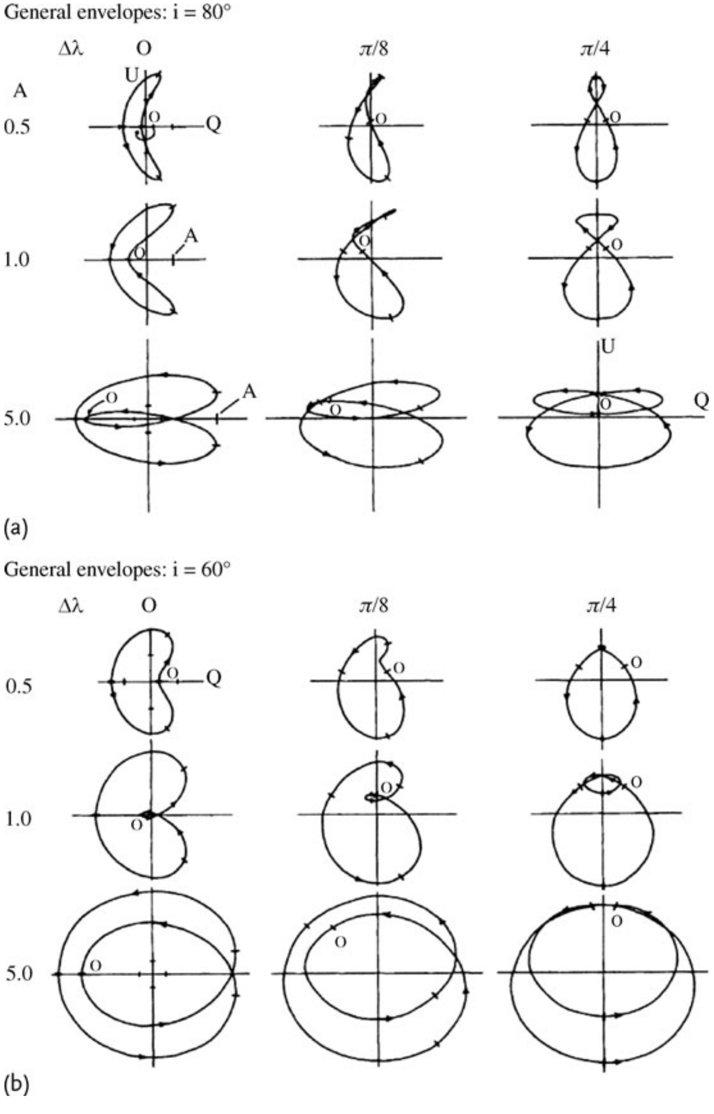

Fig. 11.1 A sample of expected polarimetric loci in the form of Lissajou figures for values of **A** $= H/G$ of 0.5, 1.0, 5.0 and $\Delta\lambda = \lambda_1 - \lambda_2$ of 0, $\pi/8$ and $\pi/4$. (a) is for $i = 80^\circ$ and (b) for $i = 60^\circ$. It may be noted that there are changes in scale according to the value of **A**. The direction of execution of the loci reflects the direction of the stellar orbit projected on the sky. (Taken from Brown, McLean & Emslie, 1978.)

cus corresponds to that for an envelope symmetric about the orbital plane with the same values for γ_3 and γ_4. Measurement of the ellipse allows determination of i, the integrals, $\tau_0\gamma_3$, $\tau_0\gamma_4$, and the interstellar component, u_{I}. The value of q_{c}, however, does not allow separation of q_I from the constant intrinsic polarization, $\tau_0(1-3\gamma_0)\sin^2 i$.

Likewise from (11.15) and (11.17), the equations

$$q_+(\lambda) = q_1 \cos(\lambda + \lambda_1) , \tag{11.20}$$

$$u_+(\lambda) = u_1 \sin(\lambda + \lambda_1) , \tag{11.21}$$

describe an ellipse centred on the origin of the qu-plane, with semi-major axis, $|u_1| = 2\tau_0 G \sin i$, oriented along the u direction, and the semi-minor axis, $|q_1| = \tau_0 G \sin 2i$, the unity subscript relating to the first harmonic of the variations. The eccentricity provides a value of $\sin i$, and the ellipse is described once per binary orbit, the starting point being determined by ϕ_1. From this ellipse, values of $\tau_0\gamma_1$, $\tau_0\gamma_2$ and i can be determined.

By applying this geometric approach, the behaviour of the basic measurements have been decoupled into the fundamental and first harmonic terms describing the cyclic polarimetric variations, i. e. γ_1, γ_2 are separated from γ_3, γ_4. The form of the two ellipses are not independent as their eccentricities depend on i, and their major axes are orthogonal, so providing self-consistency checks.

11.4.2
Analysis of Data by Fourier Methods

Applying a rotation matrix involving an angle, Ω, to the theoretical behaviour of the NSPs as given in (11.10) and (11.11), and assuming that the longitude angle, ϕ changes at a constant rate, $2\pi\nu t$, according to the orbits being circular, the polarimetric temporal behaviour of the model as described in the celestial coordinate frame, used as reference for the measurements, may be written as

$$q(t) = a_0 + a_\mathrm{c}\cos 2\pi\nu t + a_\mathrm{s}\sin 2\pi\nu t + A_\mathrm{c}\cos 4\pi\nu t + A_\mathrm{s}\sin 4\pi\nu t , \tag{11.22}$$

$$u(t) = b_0 + b_\mathrm{c}\cos 2\pi\nu t + b_\mathrm{s}\sin 2\pi\nu t + B_\mathrm{c}\cos 4\pi\nu t + B_\mathrm{s}\sin 4\pi\nu t . \tag{11.23}$$

There are various approaches to interpreting data which exhibit phase-locked variations to see how they can be matched to (11.22) and (11.23). In some cases a suspected value of a periodicity from photometric, or spectroscopic, observations might be used to evaluate the magnitudes of the coefficients, but this approach may be considered as carrying prejudice. In the case of HDE 226868, the optical counterpart of Cygnus X-1, Nolt, Kemp, Rudy, *et al.* (1975) used the period of $5.^\mathrm{d}60$, associated with its photometric variation, to see if it was reflected in their polarimetry. A curve fitting procedure involving a four parameter fit of the sine and cosine terms for this period, and the second harmonic, was applied with the outcomes compared with a direct Fourier analysis, giving good agreement. Some simple statistical tests were applied giving the significance of the determined amplitudes of the oscillatory components, although the behaviour of determined amplitudes, using other values of period for the fit, was not investigated as the number of data points was considered to be too small.

Again, in respect of an observational study of σ Ori E, Kemp & Herman (1977) used the photometric period to make a Fourier analysis to obtain the amplitudes of the polarimetric variations. The same data were later explored to provide a periodogram by Clarke & McGale (1988b) using the *F*-statistic with [4;N] degrees of freedom, based on fitting the four free parameters for the cosine and sine amplitudes of the first and second harmonics, with *N* data values. Statistical significance levels were placed across the periodogram according to the standard tables for *F*-tests, making it easy to highlight the period of the binary.

The determined Fourier coefficients can be translated into geometric parameters describing the stellar system according to the BMcLE model. They can be related to i, Ω, ϕ_1 and ϕ_2, and, according to the nomenclature here, may be written as

Fundamental:

$$\left[\frac{1+\cos i}{1-\cos i}\right]^2 = \frac{(b_c+a_s)^2+(a_c-b_s)^2}{(b_c-a_s)^2+(a_c+b_s)^2}\,, \tag{11.24}$$

$$\Omega = \frac{1}{4}\left[\tan^{-1}\left(\frac{b_c-a_s}{b_s+a_c}\right)+\tan^{-1}\left(\frac{b_c+a_s}{a_c-b_s}\right)\right], \tag{11.25}$$

$$\phi_1 = \frac{1}{2}\left[\tan^{-1}\left(\frac{b_c-a_s}{b_s+a_c}\right)-\tan^{-1}\left(\frac{b_c+a_s}{a_c-b_s}\right)\right]. \tag{11.26}$$

Harmonic:

$$\left[\frac{1+\cos i}{1-\cos i}\right]^4 = \frac{(B_c+A_s)^2+(A_c-B_s)^2}{(B_c-A_s)^2+(A_c+B_s)^2}\,, \tag{11.27}$$

$$\Omega = \frac{1}{4}\left[\tan^{-1}\left(\frac{B_c-A_s}{B_s+A_c}\right)+\tan^{-1}\left(\frac{B_c+A_s}{A_c-B_s}\right)\right], \tag{11.28}$$

$$2\phi_2 = \frac{1}{2}\left[\tan^{-1}\left(\frac{B_c-A_s}{B_s+A_c}\right)-\tan^{-1}\left(\frac{B_c+A_s}{A_c-B_s}\right)\right]. \tag{11.29}$$

It may be noted that the alternative expressions associated with the fundamental and harmonic serve as a consistency check on determined values of i and Ω. Drissen, Lamontagne, Moffat, *et al.* (1986) provide an excellent example of how data may be investigated for the determination of orbital parameters.

In later papers, the fitting of the canonical model above to data have been investigated by Simmons, Aspin & Brown (1980) and Aspin, Simmons & Brown (1981) in terms of the χ^2 statistic; these works show that normal experimental noise produces uncertainties to the model parameters which are larger than those predicted by the formal error treatment and, in addition, the determined system values carry bias.

In a paper concerned on the accuracy of polarimetric determinations of inclination, Aspin & Simmons (1982) re-examined the values obtained by Kemp and colleagues for 7 binaries. For five systems, they found the uncertainties in the orbital inclination were significantly larger than the previously quoted formal values, but with the optimum values of i coinciding with those given earlier. For Algol and σ Ori E (B-filter), the model was found to be unacceptable carrying only a 10% significance.

11.5
AM Her Stars – Polars

The star AM Her drew attention to itself as a possible optical counterpart of a variable soft X-ray source catalogued as 3U 1809+50. As part of its investigation, Tapia (1977) undertook both linear and circular polarization observations and discovered remarkable changes which proved to be cyclic, with a $3.^{\mathrm{h}}094$ period. Using the V-band, on the rising section, p_V increased from about 1% to a maximum, $\sim$5.3%, in about 30 min, followed by a near symmetrical fall. The circular polarization, v_V, displayed a more complicated behaviour over the period, with swings in level from $\sim +3\%$ to $\sim -9\%$.

Krzemiński & Serkowski (1977) also detected an extremely high circular polarization for AN UMa, with changes over a $1.^{\mathrm{h}}9$ period from -9% to -35% in the blue spectral region (see Figure 11.2). Pronounced variations in p were also recorded achieving a peak of 9%, near the time of minimum v, and maximum brightness. They proposed that, with the similarity of behaviour with AM Her, a distinct set of objects had been discovered with the polarimetry providing strong evidence of cyclotron emission from hot electrons in a magnetic field $\sim 10^8$ G. Direct evidence of the strength of the magnetic field of AN UMa was obtained from the polarimetric spectra of Schmidt, Stockman & Margon (1981). The behaviour could not be explained by the canonical models available for close X-ray binary stars, and gave rise to a new genre of cataclysmic variables emitting strongly polarized light, and proposed by Krzemiński & Serkowski (1977) to be called *polars*, although this term is not universally applied. Early reports on the polarimetric behaviour of AN UMa and HZ Her were given by Shakhovskoi (1978). Michalsky, Stokes & Stokes (1977) confirmed the polarimetric behaviour of AM Her and presented a preliminary geometrical model.

The basic model for a *polar* involves accretion from a low-mass secondary star onto a highly magnetic ($B \sim$ 20–50 MG) white dwarf. The strong field prevents the formation of an accretion disc with the stream of material being channelled along the field lines. High amounts of polarized light are generated by cyclotron emission. The polarimetric behaviour is orbitally phase-locked, and, as a starting point, a centred dipole field may be considered. The polarization waveforms depend on the angle β of the magnetic axis relative to the rotation axis of the white dwarf, and on the inclination, i, of the binary system to the line of sight. Monitoring their form leads to determinations of magnetic and binary geometries. With this simple model geometry, the angle, α, between the magnetic field and the line of sight is given by

$$\cos\alpha = \cos i \cos\beta - \sin i \sin\beta \cos[2\pi(\phi - s)] \,, \tag{11.30}$$

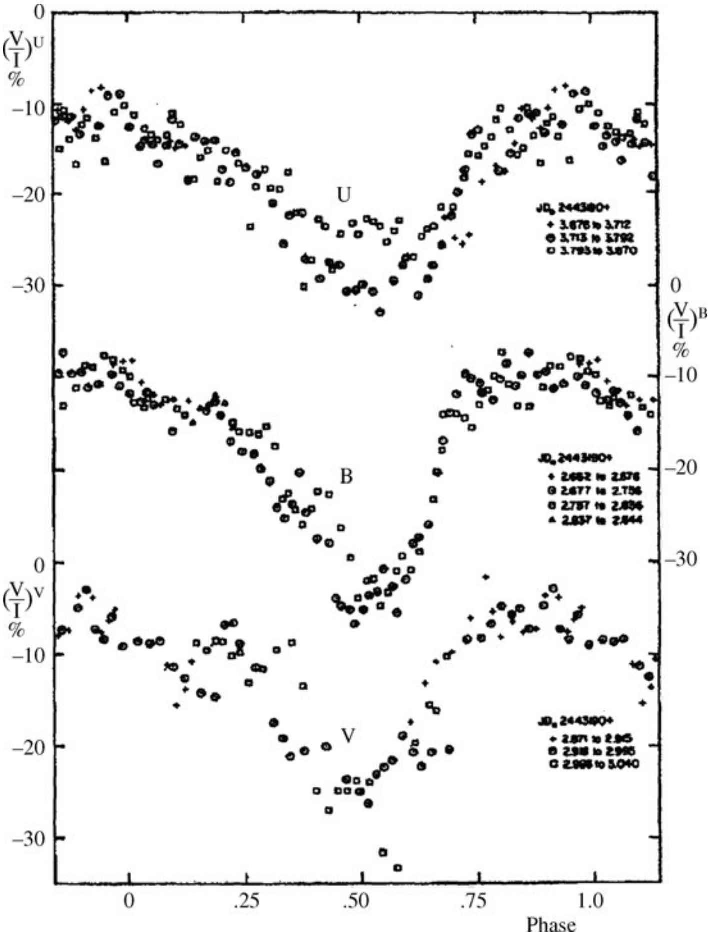

Fig. 11.2 Circular polarization of AN UMa in the *U*, *B* and *V* bands phased on a period of $1.^h9$, with phase zero given by the time of maximum linear polarization. Note that $v \sim 30\%$ at maximum is extraordinarily high. (Taken from Krzemiński & Serkowski, 1977.)

where ϕ is the orbital phase and s the phase at which the magnetic and rotation axes and the line of sight are in the same plane, the active magnetic pole being on the far side of the rotation axis. If the system is such that α can advance through 90°, and the circular polarization thus changes sign, a further relation (Bailey & Axon, 1981) between β and i ensues in the form

$$\cos(2\pi\phi_0) = \frac{1}{\tan i \tan\beta}, \tag{11.31}$$

where $2\phi_0$ is the length of the phase interval over which the sign of the circular polarization is reversed.

Since the direction of the linearly polarized component of cyclotron emission is perpendicular to the field, its position angle on the sky, up to some constant value, can be determined from:

$$\tan\zeta = \frac{\sin\beta\sin 2\pi(\phi - s)}{\sin\beta\cos i\cos\left(2\pi(\phi - s)\right) + \sin i\cos\beta}\,. \tag{11.32}$$

Using the recorded duration of the circular polarization reversal, a family of curves involving β and i can be established from (11.31), and their values then selected by checking the behaviour of the position angle of the polarization, ζ, with respect to (11.32). A simple relationship allowing determination of i also emerges from the rate of rotation of the position angle at the the time of the linear polarization pulse. According to Meggitt & Wickramasinghe (1982), at this particular phase:

$$\cos i = \frac{d\zeta}{d\phi} \sim \frac{\dot{\zeta}P}{2\pi}\,. \tag{11.33}$$

If $\beta < i$, the centre of the apparent disc of the white dwarf will be outside the projected path of the magnetic pole, and the resulting position angle curve will have one maximum and one minimum during the cycle, corresponding to the maximum tilt of the projected magnetic axis in opposite directions with respect to the rotation axis. For the remainder of the cycle, the position angle curve will vary smoothly between these two extremes. If $i < \beta < 90^\circ$, the centre of the white dwarf will lie inside the projected loop drawn by the magnetic pole, and a full rotation of the position angle through 360° is observed in each orbital cycle.

Measurements of the circular polarization waveform matching the photometric period of AM Her were made by Stockman, Schmidt, Angel, *et al.* (1977). Blueward of 4100 Å the modulation is reduced dramatically. The correlation of the photometric and circular polarization variations was confirmed by Priedhorsky, Krzemiński & Tapia (1978) over the period, and also for the flickering events. Five-colour polarimetry of AM Her has been performed by Piirola, Vilhu, Kyröläinen, *et al.* (1985), revealing a strong wavelength dependence of both the linear and circular periodic behaviours. According to the simple model fit, the determined co-latitude of the magnetic pole is wavelength dependent. Higher spectral resolution of the linear polarization variation was performed by Schaich, Wolf, Östreicher, *et al.* (1992) (see earlier announcement by Friedrich, Östreicher, Schaich, *et al.*, 1990) with the conclusion that the field has different strengths at the two accretion spots, and that the dipole field is off-centred. The strong depolarization feature around $\lambda \approx 6200$ Å was suggested to arise from $H_\alpha\sigma^-$ absorption.

Wickramasinghe, Reid & Bessell (1984) reported circular spectropolarimetric measurements of VV Pup, when the system was in a high excitation state. A broad minimum was present at 5040 Å which could be interpreted as cyclotron harmonic number $n = 7$, in a magnetic field of 3.2×10^7 G.

Another X-ray object investigated by Bailey, Hough & Axon (1980) was 2A 0311–227, later to be renamed EF Eri. Bailey, Hough, Axon, *et al.* (1982) applied the simple model to obtain its basic geometric parameters. Polarimetric waveforms were again obtained by Cropper (1985). Modelling was explored, but no substantive conclusions emerged on the geometrical parameters for inclination and magnetic co-latitude; many details of the light-curve and polarization curves remained unexplained, but it was suggested that larger i and smaller β are required than had been assumed earlier.

Simultaneous five-colour photometry and polarimetry of EF Eri was performed by Piirola, Reiz & Coyne (1987a) with a strong wavelength dependence of the polarization position angle being found, this being ascribed to Faraday rotation. A significant change in the circular polarization waveform was noted, indicating a change in geometry since the observations of previous workers. A fuller discussion of these data is given in Piirola, Reiz & Coyne (1987b) where the general model was applied. The phase dependence of the position angle of the polarization requires field and accretion geometries more complicated than a simple centred dipole, there being a second emitting region producing a weaker intermediate pulse. A value of $i = 55^\circ \pm 5^\circ$ is suggested, with the co-latitude, β, of the active pole at $38^\circ \pm 5^\circ$, and the second emitting region at $\beta = 145^\circ \pm 5^\circ$, both nearly at the same longitude, facing the main accretion stream.

Five-colour polarimetry of RX J0203.8+2959 was undertaken by Katajainen, Scaltriti, Piirola, *et al.* (2001) with the behaviour of its $4.^h6$ period favouring a geometry with two pole accretion, and allowing an inclination of $i \approx 70^\circ$ to be assigned.

Bailey, Axon, Hough, *et al.* (1983) made both photometric and polarimetric observations of the AM Herculis-type binary, E 1405-451, and detected circular polarization at wavelengths beyond 1 μm. The form of the polarization curve indicted that the accretion column is always in the hemisphere of the white dwarf towards the observer, and that the field becomes almost parallel to the line of sight at the phase of the minimum.

For BL Hyi, Piirola, Reiz & Coyne (1987c) found the cyclotron emission peaking in the near infrared (>0.8 μm), with the rotation rate of the position angle of the polarization during the bright phase, and the duration of the circular polarization sign reversal, being consistent with $i = 70^\circ \pm 10^\circ$, and co-latitude of the magnetic pole $\beta = 133^\circ \pm 10$. The basic geoemtry of BL Hyi was also determined by Schwope & Beuermann (1989). A brief description of the polarimetric behaviour of VV Pup was given by Piirola, Reiz & Coyne (1987d), and later by Piirola, Reiz & Coyne (1990), with discussion on the size of the emitting region, and how it appears to change dramatically in size according to wavelength. These two stars, together with AM Her, EF Eri and ST LMi, were discussed by Piirola (1988), their behaviour not being adequately explained in terms of the simple model of one narrow emitting region or two diametrically located opposite regions. In particular, the behaviour of the position angle of the polarization strongly suggests the existence of more than one discrete emission region, and shows deviations from the simple dipole field and emission geometry in these systems. A more sophisticated approach of modelling, with its application to AM Her, was described by Wickramasinghe, Bailey & Meggitt (1991).

Mason, Liebert & Schmidt (1989) made a study of H 0538+608, later to be called BY Cam by Mason, showed the system to have extremely large fluctuations from cycle to cycle, declaring it to have the most erratic behaviour of any *polar*. Further observations of BY Cam, with extensive modelling, are given by Piirola, Coyne, Takalo, *et al.* (1994). Over an interval of a few months, the changes in the polarimetric behaviour have promoted the notion that they arise from effects of precession, with a period of 100 to 150 days. The flickering, and longer term changes in both photometry and polarimetry, suggests a complex magnetic geometry, and that the simple dipole field notion cannot apply.

Particularly from the study of V 834 Cen, Cropper (1989) noted complicated changes in behaviour which the emerging extended models do not provide resolution, and he also suggested caution on accepting the values of i and β that have been promoted from simple model fitting to AM Her systems.

Cropper, Mason, Allington-Smith, *et al.* (1988) have developed the model for the cyclotron emission showing that the magnetic field strength of the accreting star may be determined from analyses of the spacing of wavelength dependent hump structures appearing in the polarization spectrum.

In connection with RE 0751+14, Pirrola, Hakala & Coyne (1993) discovered a circular polarization variation over the 13.9-min period. Their analysis suggested the presence of cyclotron emission from two extended regions near the opposite magnetic poles of a white dwarf with a field strength >5 MG.

References

References to Binary Stars and Models

Appenzeller, I. (1965) The polarization of Beta Lyrae. *ApJ*, **141**, 1390–1392. [234]

Appenzeller, I., Hiltner, W.A. (1967) True polarization curves for Beta Lyrae. *ApJ*, **149**, 353–362. [234]

Aspin, C., Simmons, J.F.L., Brown, J.C. (1981) Polarimetric accuracy required for the determination of binary inclinations. *MNRAS*, **194**, 283–291. [238, 244]

Aspin, C., Simmons, J.F.L. (1982) Reappraisal of the polarimetric data for seven binaries. *MNRAS*, **199**, 601–609. [244]

Berdyugin, A.V., Harries, T.J. (1999) Discovery of the variable phase-locked polarization in LZ Cephei. *A&A*, **353**, 177–181. [236]

Brown, J.C., Aspin, C., Simmons, J.F.L., McLean, I.S. (1982) The effect of orbital eccentricity on polarimetric binary diagnostics. *MNRAS*, **198**, 787–794. [238]

Brown, J.C., McLean, I.S. (1977) Polarisation by Thomson Scattering in optically thin stellar envelopes. I. Source star at centre axisymmetric envelope. *A&A*, **57**, 141–149. [240]

Brown, J.C., McLean, I.S., Emslie, A.G. (1978) Polarisation by Thomson scattering in optically thin stellar envelopes II. Binary and multiple star envelopes and the determination of binary inclinations. *A&A*, **68**, 415–427. [236, 238, 239, 240, 242]

Buerger, P.F., Collins II, G.W. (1970) Intrinsic polarization in close-binary systems. *ApJ*, **161**, 1025–1032. [238]

Clarke, D., McGale, P.A. (1988a) Temporal polarization variations of Be stars III. The polarimetric behaviour of X Persei. *A&A*, **190**, 93–102. [237]

Clarke, D., McGale, P.A. (1988b) Temporal polarization variations of Be stars IV. The polarimetric behaviour of σ Ori E. *A&A*, **205**, 207–214. [244]

Coyne (SJ), G.V. (1970a) Multi-color polarimetry of Beta Lyrae. *Ric. Astron. Spec. Vaticana*, **8** N. 13, 85–102. [234]

Coyne, G.V. (1970b) Mass exchange in Beta Lyrae. *ApJ*, **161**, 1011–1014. [234]

Coyne (SJ), G.V. (1972) Preliminary observations of variable polarization in Epsilon

Auriga. *Ric. Astron. Spec. Vaticana*, **8**, N. 13, 311–318. [236]

Coyne (SJ), G.V. (1974) A search for polarization in U Cephei. *Ric. Astron. Spec. Vaticana*, **8**, N. 24, 475–479. [234]

Coyne (SJ), G.V., Gehrels, T. (1967) Wavelength dependence of polarization. X. Interstellar polarization. *AJ*, **72**, 887–898. [236]

Coyne (SJ), G.V., Kruszewski, A. (1967) Wavelength dependence of polarization. XVII. Be-type stars. *AJ*, **74**, 528–532. [237]

Dolan, J.F. (1984) Regularized Monte Carlo calculations of the optical polarization induced by scattering in X-ray binaries. *A&A*, **138**, 1–9. [238]

Dolan, J.F., Tapia, S. (1988) Variable polarization in X-ray binaries: HD 77581. *A&A*, **202**, 124–132. [237]

Drissen, L., Lamontagne, R., Moffet, A.F.J., Bastien, P., Segvin, M. (1986) Spectroscopic and polarimetric parameters of the runaway WN7 binary system HD 197406. Is the secondary an X-ray-quiet black hole? *ApJ*, **304**, 188–200. [244]

Drissen, L., Moffat, A.F.J., Bastien, P., Lamontagne, R. (1986) Polarimetric observations of the WN7 binary CQ Cephei. *ApJ*, **306**, 215–224. [233]

Fox, G.K. (1994) On the polarimetric variability of Y Cygni. *PASP*, **106**, 370–375. [236]

Gnedin, Yu.N., Silant'ev, N.A., Shibanov, Yu.A. (1976) Ellipsoidality effects and linear polarization in close X-ray binaries. *Sov. Astron.*, **20**, 530–535. [237]

Hiltner, W.A. (1947) On the presence of polarization in the continuous radiation of early-type stars. *ApJ*, **106**, 231–234. [233, 234]

Hiltner, W.A. (1949) On the presence of polarization in the continuous radiation of early-type stars. II. *ApJ*, **109**, 471–478. [233]

Hiltner, W.A., Mook, D.E. (1966) Variable polarization in V444 Cygni. *ApJ*, **143**, 1008–1009. [234]

Hoffman, J.L., Nordsieck, K.H., Fox, G.K. (1998) Spectroplarimetric evidence for bipolar flow in β Lyrae. *ApJ*, **115**, 1576–1591. [234]

Kemp, J.C., Barbour, M.S., Herman, L.C., Rudy, R.J. (1978) Discovery of synchronous binary polarization in Cygnus X-1. *ApJ*, **220**, L123–L126. [237]

Kemp, J.C., Barbour, M.S., Parker, T.E., Herman, L.C. (1979) Cygnus X-1: Polarization evidence for an extended secondary envelope with an eclipsing region. *ApJ*, **228**, L23–L27. [237]

Kemp, J.C., Barbour, M.S., McBirney, R.E., Rudy, R.J. (1981) Algol: a further study of the optical polarization. *ApJ*, **243**, 557–566. [235]

Kemp, J.C., Barbour, M.S. (1983) X-Persei: Optical polarization variation on the 580 day binary-like period. *ApJ*, **264**, 237–250. [237]

Kemp, J.C., Herman, L.C. (1977) The polarization of Sigma Orionis E: A curious eclipsing binary. *ApJ*, **218**, 770–775. [244]

Kemp, J.C., Southwick, R.G., Rudy, R.J. (1976) The variable linear polarization of Cygnus X-1, 1974–1975 observations. *ApJ*, **210**, 239–249. [237]

Kemp, J.C., Wolstencroft, R.D., Swedlund, J.B. (1972) Circular polarimetry of fifteen interesting objects. *ApJ*, **177**, 177–189. [236]

Kock, R.H., Pfeiffer, R.J. (1977) The linear polarization of u Herculis. *IBVS*, No: 1326, Budapest. [235]

Koch, R.H., Pfeiffer, R.J. (1989) Properties of the circumstellar environment of Y Cygni as deduced from polarimetry. *PASP*, **101**, 279–285. [236]

Kruszewski, A. (1974) Circumstellar polarizations of early-type stars and eclipsing binary systems. pp. 845–857 in *Planets, Stars and Nebulae studied with Photopolarimetry*, Ed. T. Gehrels, University of Arizona, Tucson, AZ. [234]

Luna, H.G., (1980) Polarimetric observations of ϵ Coronae Austrinae. *PASP*, **92**, 79–80. [236]

Manset, N., Bastien, P. (2000) Polarimetric variations of binary stars. I. Numerical simulations for circular and eccentric binaries in Thomson scattering envelopes. *AJ*, **120**, 413–429. [238]

McLean, I.S. (1977) Intrinsic linear polarization in Hα, Hβ emission lines of the eclipsing binary beta Lyrae. *A&A*, **55**, 347–359. [234]

McLean, I.S. (1980) Polarimetry of close binary systems; Observations and interpretations. pp. 65–70 in *Close Binary Stars; Observations and Interpretations*, (eds M.J. Plavec, D.M. Popper and R.K. Ulrich). [236]

Nolt, I.G., Kemp, J.C., Rudy, R.J., Southwick, R.G., Radostitz, J.V., Caroff, L.J. (1975) Linear polarization variations modulo 5.6 days in HDE 226868. *ApJ*, **199**, L27–L29. [243]

Öhman, Y. (1934) Effects of polarization in the spectrum of β Lyrae. *Nature*, **134**, 534. [234]

Oshchepkov, R. A. (1974) Polarimetric observations of AW UMa. *IBVS*, No: 884, Budapest. [235]

Pfeiffer, R.J., Koch, R.H. (1977) On the linear polarization of close binaries. *PASP*, **89**, 147–154. [237]

Piirola, V. (1977) Polarization observations of four W UMa-type eclipsing binaries. *A&A*, **56**, 105–109. [235]

Piirola, V. (1980) A polarimetric study of U Cephei. Part I. *A&A*, **90**, 48–53. [235]

Piirola, V. (1981) A polarimetric study of U Cephei. Part II (Observations). *A&AS*, **44**, 461–466. [235]

Rudy, R.J., Herman, L.C. (1978) The variable linear polarization of the O star binary HD 47129 (Plaskett's star). *PASP*, **90**, 163–166. [236]

Rudy, R.J., Kemp, J.C. (1976) AO Cassiopeiae: Phase-locked polarization and geometry of the gas stream. *ApJ*, **207**, L125–L128. [235]

Rudy, R.J., Kemp, J.C. (1977) Phase-locked polarization in *u* Herculis: Evidence for the reflection mechanism. *ApJ*, **216**, 767–775. [235]

Rudy, R.J., Kemp, J.C. (1978) A polarimetric determination of binary inclinations: results for five systems. *ApJ*, **221**, 200–210. [235]

Serkowski, K. (1965) The polarization of Beta Lyrae. *ApJ*, **142**, 793–795. [234]

Serkowski, K. (1970) Intrinsic polarization of early-type stars with extended atmospheres. *ApJ*, **160**, 1083–1105. [234]

Serkowski, K. (1971) Polarization of variable stars. *New Directions and New Frontiers in Variable Star Research – IAU Coll. No. 15*, Bamberg. 11–31. [237]

Shakhovskoi, N.M. (1963) Polarization observations of β Lyrae. *Sov. Astron.*, **6**, 587–589. [234]

Shakhovskoi, N.M. (1965) Polarization in variable stars. II. Eclipsing binaries. *Sov. Astron.*, **8**, 833–842. [234, 234, 234]

Shakhovskoi, N.M. (1969) The spatial orientation of the orbit planes of close binary stars. *Sov. Astron.*, **13**, 303–305. [234]

Shulov, O.S. (1966) *Astr. Circ. USSR* No. 365. [234]

Shulov, O.S. (1967) Polarimetric observations of close binary stars. *Trudy Astron. Obs. Leningrad*, **24**, 38–53. [234]

Shulov, O.S., Guodcova, G.A. (1969) On the intrinsic polarization of RY Persei. *Astrofizika*, **5**, 477–485. [234]

Simmons, J.F.L. (1983) Analytic treatment of polarization by arbitrary scattering mechanisms in circumstellar envelopes – II. Binary Stars. *MNRAS*, **205**, 153–170. [238]

Simmons, J.F.L., Aspin, C., Brown, J.C. (1980) A critique of polarimetric evidence of the nature of Cygnus X-1. *A&A*, **91**, 97–107. [237, 244]

Simmons, J.F.L., Aspin, C., Brown, J.C. (1982) Bias of polarimetric estimators for binary star inclinations. *MNRAS*, **198**, 45–57. [238, 240]

References to AM Her Stars – Polars

Bailey, J., Axon, D.J. (1981) Multicolour polarimetry of AM Herculis. *MNRAS*, **194**, 187–194. [246]

Bailey, J., Hough, J.H., Axon, D.J. (1980) IR Photometry and polarimetry of 2A0311–327. *Nature*, **285**, 306–308. [247]

Bailey, J., Hough, J.H., Axon, D.J., Gatley, I., Lee, T.J., Szkody, P., Stokes, G., Berriman, G. (1982) A multiwavelength study of AM Herculis type binary 2A 0311-227. *MNRAS*, **199**, 801–815. [247]

Bailey, J., Axon, D.J., Hough, J.H., Watts, D.J., Giles, A.B., Greenhill, J.G. (1983) The AM Herculis-type binary E 1405-451. *MNRAS*, **205**, 1P–7P. [248]

Cropper, M. (1985) Simultaneous linear and circular polarimetry of EF Eri. *MNRAS*, **212**, 709–721. [248]

Cropper, M. (1989) The accretion region in AM Her systems: insights from polarimetry of V834 Cen. *MNRAS*, **236**, 935–957. [249]

Cropper, M., Mason, K.O., Allington-Smith, J.R., Branduardi-Raymont, G., Charles, P.A., Mittaz, J.P.D., Mukai, K., Smale, A.P. (1988) The magnetic field in four AM Her systems: measurements from cyclotron humps. *MNRAS*, **236**, 29P–38P. [249]

Friedrich, S., Östreicher, R., Schaich, M., Wolf, D.H. (1990) Linear and circular spectropolarimetry of AM Her. *Astron. Gesellschaft Abstract Series*, **4**, March 27–29, 45. [247]

Katajainen, S., Scaltriti, F., Piirola, V., Lehto, H.J., Anderlucci, E. (2001) *UBVRI*-polarimetry of the AM Herculis star RX J0203.8+2959. *A&A*, **372**, 945–951. [249]

Krzemiński, W., Serkowski, K. (1977) Extremely high circular polarization of AN Ursae Majoris. *ApJ*, **216**, L45–L48. [245, 245, 246]

Mason, P.A., Liebert, J., Schmidt, G.D. (1989) H 0538 +608: A long-period AM Her system exhibiting extreme variations in accretion geometry. *ApJ*, **346**, 941–949. [248]

Meggitt, S.M.A., Wickramasinghe, D.T. (1982) The polarization properties of magnetic accretion columns. *MNRAS*, **198**, 71–82. [247]

Michalsky, J.J., Stokes, G.M., Stokes, R.A. (1977) Multicolor linear and circular polarization of AM Herculis. I. A preliminary geometrical model. *ApJ*, **216**, L35–L39. [245]

Piirola, V. (1988) On the evidence for discreet emission regions in AM Her type objects. pp 261–279 in *Polarized Radiation of Circumstellar Origin* (eds G.V. Coyne (SJ), A,M. Magalhães, A.F.J. Moffat, R.E. Schulte-Ladbeck, S. Tapia, W. Wickramasinghe). University of Arizona, Tucson, AZ. [248]

Piirola, V., Coyne (SJ), G.V., Takalo, L., Larsson, S., Vilhu, O. (1994) UBVRI polarimetry of AM Herculis-type binaries V. The asynchronous (?) polar BY Cammmelopardis (H0538+608). *A&A*, **283**, 163–174. [249]

Pirrola, V., Hakala, P., Coyne (SJ), G.V. (1993) The discovery of variable polarization over the 13.9 minute spin period of the intermediate polar RE 0751 +14. *ApJ*, **410**, L107–L110. [248]

Piirola, V., Reiz, A., Coyne (SJ), G.V. (1987a) Simultaneous five color (UBVRI) polarimetry of EF Eri. *Astrophys. Space Sci.*, **130**, 197–201. [248]

Piirola, V., Reiz, A., Coyne (SJ), G.V. (1987b) Simultaneous five-color (UBVRI) polarimetry of EF Eri. *A&A*, **186**, 120–128. [248]

Piirola, V., Reiz, A., Coyne (SJ), G.V. (1987c) Five-color (UBVRI) polarimetry of H 0139–68 = BL Hydri. *A&A*, **185**, 189–195. [248]

Piirola, V., Reiz, A., Coyne (SJ), G.V. (1987d) Simultaneous five color (UBVRI) polarimetry of VV Puppis. *Astrophys. Space Sci.*, **130**, 203. [248]

Piirola, V., Reiz, A., Coyne (SJ), G.V. (1990) Multicolor photopolarimetry of magnetic cataclysmic variables. *Astrophys. Space Sci.*, **169**, 133–138. [248]

Piirola, V., Vilhu, O., Kyröläinen, J., Shakhovskoi, N., Efimov, Y. (1985) Five-colour pPolarimetry of AM Herculis. *Proc. ESA Workshop: Recent Results on Cataclysmic Variables*, Bamberg, 17–19, ESA SP–236 (April 1985). [247]

Priedhorsky, W.C., Krzemiński, W., Tapia, S. (1978) Correlated photometric and polarimetric phenomena in AM Herculis. *ApJ*, **225**, 542–547. [247]

Schaich, M., Wolf, D., Östreicher, R., Ruder, H. (1992) Phase resolved linear polarization spectra of AM Herculis. *A&A*, **264**, 529–535. [247]

Schmid, H.M. (1989) Identification of the emission bands at $\lambda\lambda$ 6830, 7088. *A&A*, 211, L31–L34. [248]

Schmidt, G.D., Stockman, H.S., Margon, B. (1981) A direct measurement of the magnetic field in AM Herculis. *ApJ*, **243**, L157–L161. [245]

Schwope, A.D., Beuermann, K. (1989) A polarimetric study of the magnetic cataclysmic binary BL Hydri. *A&A*, **222**, 132–140. [248]

Shakhovskoi, N.M. (1978) Polarimetric Observations of AN UMa and HZ Her. *Nauch. Inf. Ser. Astrofiz.*, **45** (88). [245]

Stockman, H.S., Schmidt, G.D., Angel, J.R.P., Liebert, J., Tapia, S., Beaver, E.A. (1977) New observations and a slow rotation model of the X-ray binary AM Herculis. *ApJ*, **217**, 815–831. [247]

Tapia, S. (1977) Discovery of a magnetic compact star in the AM Herculis/3U 1809+50 system. *ApJ*, **212**, L125–L129. [245]

Wickramasinghe, D.T., Bailey, J., Meggitt, S.M.A., Ferrario, L., Hough, J., Tuohy, I.R. (1991) New polarimetric observations and a two pole model for the cyclotron emission from AM Herculis. *MNRAS*, **251**, 28–45. [248]

Wickramasinghe, D.T., Reid, I.N., Bessell, M.S. (1984) Circular spectropolarimetry of VV Puppis. *MNRAS*, **210**, 37P–41P. [247]

12
Stars With Magnetic Fields

12.1
Introduction

Any process associated with the generation, or absorption, of radiation in the presence of a magnetic field will introduce polarization signatures in one way or another. An important mechanism which immediately comes to mind is the Zeeman effect associated with the behaviour of atomic transitions. The polarigenic effects are normally associated with spectral lines, but they may also influence the behaviour of the stellar continuum.

It is of interest to note that stellar magnetic fields were first detected by observations of resolved spectral lines, and most of the early research involved either measurements of the displacement of these features within a recorded spectrum or the recording of circular polarization in the line wings. It is only more recently that broadband linear polarizations have been detected and applied to the study of field distributions over stellar surfaces. A review of the available techniques of the time for measuring magnetic fields in non-degenerate stars was presented by Landstreet (1980), particularly dealing with the comparison of classical photographic techniques of measuring the displacement of Zeeman split lines, and the measurement of circular polarization in the wings of the Hβ line. A useful short, but incomplete, early presentation on the history of the detection of stellar magnetic fields has been given by Huovelin, Tuominen & Shcherbakov (1989).

There are many stellar spectral types that are known, or are likely, to carry magnetic fields, with their geometries engendering measurable polarization. By recording the spectral and temporal behaviour of the polarization signals, field geometries, field strengths, rotation periods, etc., may be determined. In this chapter, the behaviour of stars with particularly strong magnetic fields, permeating their whole structure, will be discussed. One such spectral type, Ap, relates to stars with peculiar spectral abundances; another stellar group with objects supporting enormous magnetic fields come under the umbrella of white dwarfs. Other variable stars, whose polarimetric behaviour may also be affected by the presence of localized magnetic fields, will be discussed in later chapters, as appropriate.

Stellar Polarimetry. David Clarke

ISBN: 978-3-527-40895-5

12.2
Magnetic and Ap Stars

An early observation by Babcock (1947), using a differential circular analyser prior to the slit of the coudé spectrograph of the 100-in. telescope at Mt.Wilson, revealed the Zeeman line displacements in the spectrum of the Ap star, 78 Vir, suggesting the presence of a magnetic field $\sim$ 1500 G. A 11-year study of stars of this type by Babcock (1958) resulted in the production of his grand catalogue of magnetic stars. The presentation of this work was followed by detailed reports of investigations of individual magnetic objects. For example, HD 125248 was studied by Babcock (1951), showing that the field varied from $+7000$ G to -6200 G, with the various monitored lines behaving in slightly different ways, indicating uneven distributions of the rare earth elements such as *Eu* and *Cr* over the stellar surface. Studies of α^2 CVn were made by Babcock & Burd (1952); HD 153882 was investigated by Gjellestad & Babcock (1953). HD 188041 was monitored by Babcock (1954) for 7 years, the field varying from 600 to 4800 G, with a period of 226 days; its polarity sign was always positive. The same star was later studied by Wolff (1969) who showed that the derived amplitudes of the field variations depended on the chemical element selected for measurement. This behaviour was again explained by the elements being unevenly distributed over the stellar surface. Perhaps the most famous cited magnetic star is HD 215441, found by Babcock (1960) to have the largest recorded magnetic field. It is now referred to as Babcock's Star, the field being $\sim$34 kG.

Preston & Pyper (1965) constructed a similar differential analyser arrangement for the 120-in. coudé spectrograph at the Lick Observatory and noted that, although the field curves of a couple of magnetic stars displayed the same signatures as recorded by Babcock, the magnetic field strengths appeared to be 30–40% higher. This difference may reflect the difficulties in calibrating and compensating out the problems associated with polarization effects of inclined mirrors in coudé systems.

It appears a little odd, perhaps, that despite the field strength, Babcock's star has proved to be elusive in exhibiting detectable polarimetric variations in broadband. After some earlier results by Polosukhina (1964) and Polosukhina & Lebedeva (1966), indicating that it displayed rapid and large ($\sim$1%) polarimetric variations, Berdyugin, Breger & Polosukhina (1992) concluded that the value of p was constant over its rotational period ($9.^{d}49$), and over an interval of 5 years. The individual measurements of p were made with typical uncertainty of ±0.04%. The observed high constant polarization appears to result from interstellar effects. Reasons for the null detection of any intrinsic polarization related to this star have been discussed by Leroy (1995).

The stars 17 Com and κ Cnc were observed by Preston, Kazimierz & Wolff (1969), the former star exhibiting a near sinusoidal magnetic field variation with a period of $5.^{d}0808$; the field variation of κ Cnc was less well defined, but a period of $5.^{d}0035$ was deduced. Both stars had also been monitored for photometric variability with periods matching the magnetic variation. The star, HD 32633, was studied by Preston & Stępień (1968) and they found that the period ($6.^{d}431$) of magnetic variations and light-curves matched, with the field strength being in anti-phase with the brightness. For 49 Cam, Bonsack, Pilachowski & Wolff (1974) measured a cyclic field between the limits of ±1.7 kG, with a period of $4.^{\mathrm{d}}285$. The light curves revealed complex variations, but with double minima occurring at the magnetic extrema.

Preston (1969b) also made a comprehensive study of the Zeeman spectrum of 53 Cam. Its surface field was ~ -15 kG at a phase 0.12 cycles prior to the polarity crossover. At this epoch the field produced only partially resolved patterns in the spectrum, with the then current observational technology.

Borra & Dworetsky (1973) re-measured the collection of Zeeman spectrographic plates obtained at the Hale Observatories to study the long-term behaviour of β CrB. They investigated one of the technical problems of converting photographic density to magnetic field strength, with the conclusion that some of the reports related to non-periodic variations in this star may be an artefact of the reduction method.

The principles of an instrument used as a solar magnetograph were applied by Severny (1970) to investigate the possibility of detecting magnetic fields in bright stars. He recorded weak longitudinal fields of 30–300 G. At about the same time, there had been claims that magnetic fields had been detected by Sargent, Sargent & Strittmater (1967) in two early peculiar B stars in Orion, but these results could not be reproduced by Conti (1970). In attempts to improve on the sensitivity of Babcock's photographic techniques, Borra & Landstreet (1973) devised a photoelectic spectropolarimeter employing a Pockels cell modulator prior to a spectrometer. Some 21 stars were investigated. A field was found for 53 Cam and possibly for γ Cyg; upper limits were set for the other 19 observed stars. The same modulator was later linked to a Fabry-Pérot interferometer, and Borra, Landstreet & Vaughan (1973) reported on the instrument's capabilities. Field measurements were reported for β CrB, while null results were found for α CMa, α^2 Lib and ι CrB.

Wood & Campusano (1975) made some preliminary Zeeman observations of Southern Hemisphere stars of Ap and F0Vp type. In their paper, a note was made that Canopus (HR 2326) surprisingly showed effects of Zeeman shifts in some of its lines. However, this finding has not been confirmed.

An early detection of linear polarization associated with the magnetic Ap stars HD 215441 and 53 Cam was provided by Kemp & Wolstencroft (1973) who showed that variability occurred in the Hβ line with the continuum almost constant, the effects in the line probably being caused by the transverse Zeeman effect. According to Borra (1973), the theoretical values for linear polarization in $H\beta$, based on the effects of a magnetic field, are two orders of magnitude smaller than that observed by Kemp & Wolstencroft (1973) for 53 Cam.

For objects exhibiting magnetic variability, it is generally considered that any periodicity is linked to stellar rotation. In the first place, the field curve may be considered in terms of the magnetic oblique rotator model, the basic concept illustrated in Figure 12.1.

According to the most simple dipole situation, any magnetic star may have its rotational axis set at an angle, i, to the line of sight, with the magnetic axis set

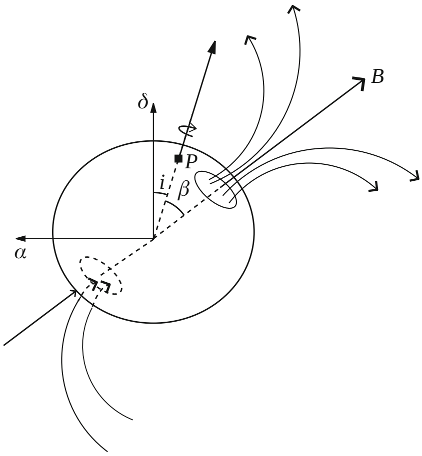

Fig. 12.1 A schematic of a magnetic oblique rotator indicates that the rotational pole, *P*, is projected at an angle, *i*, against equatorial celestial coordinates, α, δ. The dipole magnetic field, *B*, has its axis set at angle β to the rotational pole; as the star rotates, the magnetic poles are presented alternatively in the line of sight, with the view of the pole changing according to the rotational phase.

at angle, β, to this. As the star rotates, the form of the apparent field strength variation is essentially sinusoidal. If B_e represents the effective field seen from the observed hemisphere, its variation may be represented by $B_e = B_0 + B_1 \sin \omega t$, where $B_0 = (B_e^+ + B_e^-)/2$ and $B_1 = (B_e^+ - B_e^-)/2$. If we take r to be the ratio of the smaller of B_e^+ and B_e^-, to the larger, $(1 \geq r \geq -1)$, then:

$$\tan \beta = \frac{(1-r)}{(1+r)} \cot i \ . \tag{12.1}$$

The origins of this formula can be found in Stibbs (1950) who, from the above simple geometric picture, showed that the aspect angle, α, of the magnetic pole, when apparent on the stellar disc, may be written as

$$\cos \alpha = \cos i \cos \beta + \sin i \sin \beta \cos \theta \ , \tag{12.2}$$

where $\theta = 2\pi\times$ the phase associated with the rotation. By considering the alternative presentations of the polarity of the field, (12.1) was obtained by Preston (1967). This latter paper was related to the investigation of the statistical distribution of the determined values of β, the topic later discussed by Borra (1974a). Since then, more magnetic stars have been monitored with values for β being deduced, but studies on their statistical behaviour appear to have been neglected.

In general, if i is known, β may be determined, its value being well defined for sinusoidal signals. Correction factors may be applied to describe the effects of the dipole being off-centred, and also for the the magnetic field not being an exact dipole. In a study of Zeeman spectrograms of Babcock's Star, Preston (1969a) found that its magnetic field could not be simply considered as being dipolar; one of the features of its behaviour was the fact that the field did not reverse its polarity during the rotational cycle. Many stars present phase-locked signals with features imposed on a simple sine wave, suggesting that there is patchy structure of the fields over the stellar surface. In a comprehensive analysis of Zeeman spectra of α^2 CVn, Pyper (1969) showed that the magnetic configuration could be modelled by a combination of dipole and quadrupole fields, with their common axis inclined at $\sim 50^\circ$ to the rotational axis.

Using the Hβ magnetograph technique, Landstreet & Borra (1977) detected fields in three short-period Ap stars, θ Aur, CU Vir and ϕ Dra, the variability matching the known rotational periods of these stars. The recorded magnetic curves were compatible with dipole field geometries and the oblique rotator model. For CU Vir, the region of helium deficiency and silicon excess appear to lie near the magnetic equator. Similar measurements were also made by Borra & Landstreet (1977) of 53 Cam and α^2 CVn. These observations did not show the strong anharmonic behaviour found in the magnetic curves of these stars as determined by the older Zeeman spectra photographic technique. The photoelectric magnetic curves are fitted very satisfactorily by oblique rotator models with modestly decentred magnetic dipole geometries. The data suggest that the anharmonic effective field curves obtained photographically for these stars arise mainly because of the difficulty of visually measuring the separation of the centroids of the right and left circularly line profiles, as suggested by Borra (1974b), although non-uniform distribution of the metals may also contribute significant effects in α^2 CVn.

Following their discovery of intrinsic polarization in two magnetic Ap stars, 53 Cam and α^2 CVn, Kemp & Wolstencroft (1974) made intensive studies to provide values of p over the stars' rotational periods. A broadband variation was apparent for 53 Cam, but not for α^2 CVn, but the effect of rotation on the polarization within the Hβ line was clearly recorded. The behaviour of 53 Cam was compatible with the star being an oblique rotator, with the angular parameters in the range $50^\circ \lesssim (180^\circ - i) \lesssim 60^\circ$ and $\beta \sim 90^\circ$, values which agree with those deduced by other workers using different observational diagnostic techniques. On the basis of the classical Hanle effect, Finn & Kemp (1974) have modelled the polarimetric behaviour of 53 Cam, considering the scattering by a layer of elementary electric dipoles lying on the stellar surface. According to any selected geometry, the components of the Stokes vector were integrated analytically over the frequencies of a normal Zeeman triplet and numerically over the visible disc. In order to get a good agreement with the observed behaviour, it was necessary to involve a combined longitudinal and transverse displacement of the magnetic field from the centre of the star.

High-resolution polarization observations inside spectral lines of magnetic Ap stars were conducted through the development of an instrument by Borra & Vaughan (1977). Although the equipment was set at a coudé focus, an adjustable compensator was included to counter the polarization introduced by the inclined mirror of the telescope. The star, β CrB, was observed over its rotational cycle, and inferences were drawn regarding the magnetic geometry; the system appeared to be devoid of any symmetry, but could probably still be approximated by a decentred dipole model. The same instrument was applied by Borra & Vaughan (1978) to α^2 CVn, with the circular polarization and line profile of the FeII line at 4520.2 Å monitored over its $5.^{d}4694$ period. Modelling of the observed behaviour proved to be difficult.

By making measurements of the circular polarizations across the same FeII line of 78 Vir, Borra (1980a) followed its magnetic cycle, the behaviour agreeing with previous polarimetric studies of the Hβ line, and the straight forward technique of Zeeman line shifts recorded by a photographic spectrometer. In a following paper, Borra (1980b) analyzed his data in respect of an oblique rotator model, and the observations were mimicked well by an inclined dipolar geometry, and a moderate quadrupolar component.

The Ap Si star, 108 Aqu, has been extensively photometrically monitored by North, Brown & Landstreet (1992) with a period determination of $3.^{d}735239$, the light-curve shapes varying slightly according to the selected passband. In addition, magnetic data were obtained from measurements of circular polarization in the wings of Hβ. The field appears stronger at maximum brightness. From the simple oblique rotator model, a value of $\beta = 36° \pm 20°$ was determined, based on supporting evidence that $i = 61°$.

Landstreet (1982) has also conducted a survey to search for magnetic fields in normal upper main sequence stars. Some 31 stars in the spectral range 0 9.5 to F 6 were measured using a line profile scanner with a Balmer-line analyser. No magnetic fields were detected for any of the survey stars. The smallest standard error was ±7 G and the median error of the sample was ±65 G. It appears that longitudinal effective fields of more than 150 G are uncommon in general upper main sequence stars.

Bagnulo, Szeifert, Wade, *et al.* (2001) have described the early results of circular spectropolarimetric measurements relevant to A-type stars, using the VLT unit telescope at ANTU. The blue and red wings of the Balmer lines clearly show polarization of opposite handedness for the test target star, HD 94660. By using a least squares technique to allow combination of data from both Balmer and metallic lines, a longitudinal field of -2110 ± 50 G was derived, the determination providing a substantial gain in terms of the signal-to-noise ratio of the previous simple photopolarimetric technique of Hβ wing measurements.

As well as measurements of the Zeeman effect within stellar lines, linear polarization effects generated by magnetic fields may be present in continuum observations. Using more general linear and circular polarization measurements of the continuum, a sample of magnetic stars was observed by Serkowski & Chojnacki (1969), but no firm detections of intrinsic effects were reported. Kemp, Wolstencroft & Swedlund (1972) investigated six Ap stars for circular polarimetry, and tantalising results were obtained, the most significant associated with HD 215441.

It is interesting to note that such detections have been very dependent on the development of the detectivity of polarimeters. As support to a hypothesis that stellar polarizations did not have an interstellar origin, Thiessen (1961) cited the behaviour of the magnetic variable HD 71866. His measurements suggested a polarization maximum of about 0.0055 mag when the field strength was zero, and a

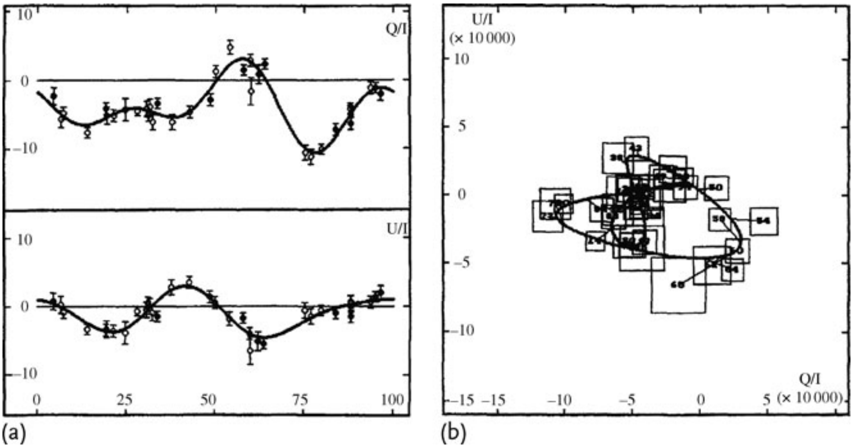

Fig. 12.2 (a) displays the q and u variations of HD 71866, with individual measurement uncertainties of $\sim \pm 0.0001$, phased on the star's rotational period; (b) plots the same data in the qu-plane revealing a complicated phase-locked locus, suggesting that the magnetic field is not simply dipolar in form; the boxes carry information of the phase of the included data point. (Taken from Leroy, 1995.)

minimum of about 0.0015 mag at the field maximum. Zappala & Hiltner (1966) later conducted a more intensive observational study of this star with individual measurements carrying an uncertainty of $\sim \pm 0.0008$ mag, or $\Delta p \sim \pm 0.0004$, and found no variations. With further instrumental improvements providing measurement uncertainties $\sim \Delta p \pm 0.0001$, Piirola & Tuominen (1981) detected polarization variability, and these data, together with later high-accuracy measurements of Leroy (1995), are presented in Figure 12.2.

As already described in Chapter 9, following the description of magnetic intensification by Babcock (1949), Warwick (1951) suggested that linear polarization might be detectable in magnetic stars as a result of the mechanism. Demkina & Obridko (1973) estimated that polarization of the radiation in the continuum of magnetic stars from the Zeeman effect cannot exceed 1%. They computed the $p(\lambda)$ variation in the range 4152–4262 Å for ϵ UMa, according to the spectral line behaviour in that wavelength window, following the same principles of calculations made for the Sun by Leroy (1962).

By considering saturated absorption lines which are subject to the transverse Zeeman effect, Leroy (1989) has shown that a non-zero polarization is generated with the cumulative effects of all the lines controlling an overall spectral behaviour, $p(\lambda)$. His calculations, initially related to middle- to late-type stars, involved a treatment for each individual line based on an analytic solution of the transfer equation, carefully adjusted to solar conditions, to provide a good fit to the actual curve of growth of photospheric lines. The exercise was conducted for the case of weak magnetic fields with the Zeeman splitting being much smaller than the line-width

($B = 500$ G), and for strong fields with most of the photospheric lines completely split ($B = 10\,000$ G). The resulting polarization spectra show a variation which behaves approximately as $1/\lambda^4$, but with a dip at 4800 Å, and bump at 5200 Å, these features possibly allowing distinctions to be made relative to Rayleigh scattering. In a later paper, Leroy (1990) showed that the polarization due to differential saturation of Zeeman components is noticeably reduced in blended lines. Any polarization signal, therefore, does not increase very much in a crowded spectrum, even though the fraction of the continuum subtracted by lines is larger. This natural limitation exists in the solar spectrum where the maximum polarization is reached in the blue region. The influence of line crowding is shown to be more pronounced in K-type stars as revealed in the worked example of Arcturus (α Boö).

The Ap star, γ Equ (HD 201601), is famous for its very long rotation period, a value $\sim$ 70 years being promoted by several photometric studies. Leroy, Bagnulo, Landolfi, *et al.* (1994) have performed polarimetry over three years and their study is consistent with system being an oblique rotator. With such a long period, issues are raised about braking mechanisms and whether the star's magnetic nature results from dynamo effects or represents the survival of a fossil field. Because of the slow rotation rate, the latter proposal is favoured.

At the other range of the period spectrum, Leroy, Landstreet & Bagnulo (1994) have recorded the polarimetric variations of 49 Cam, with a period determined as $4.^{\mathrm{d}}2866 \pm 0.^{\mathrm{d}}0005$. The variation of p is the largest of any Ap star, and the form of its behaviour makes it difficult to interpret in the customary framework of the oblique rotating model. By making some ad hoc changes to the field structure which modify its symmetry with respect to the magnetic axis, and introducing peculiarities to the polar regions, the observed behaviour is well replicated.

To allow determinations of magnetic field parameters from an observational study of broadband polarimetry of Ap stars, Landolfi, Landi Degl'Innocenti, Landi Degl'Innocenti *et al.* (1993) have developed a model based on the geometry of the oblique rotator which provides simple analytical solutions to the inversion problem. Their paper limits the discussion to classical dipole and quadrupole fields but, in principle, any analysis could be extended to more complex configurations. Although the field strength determination requires both knowledge of the line content within the passband, and a numerical integration over the stellar disc, determination of the field geometry, i. e. i and β, may be well specified.

In the second of a series of papers employing the inversion principles of the above canonical model, Leroy, Landolfi & Landi Degl'Innocenti (1993) have examined the behaviours of four stars (HD 137909 = β CrB, HD 65339 = 53 Cam, HD 71866, and HD 115708), with values of i and β being proposed. The third paper expanded the diagnostic method for modelling the results of broadband observations with Bagnulo, Landi Degl'Innocenti, Landolfi, *et al.* (1995) analysing measurements of HD 24712 and HD 71866, so providing more robust information on their magnetic field structures. In a fourth paper, Leroy, Landolfi, Landi Degl'Innocenti, *et al.* (1995) explored effects that might introduce magnetic anomalies with respect to the dipolar model, such as there being local abundance inhomogeneities. The notion of such a scenario was applied to data for 49 Cam, β CrB and HD 71866.

None of the spatial modulations was able to reproduce the observations of the latter star. Although satisfactory fits resulted for the other two stars, the magnitudes of the required inhomogeneities would also generate substantial photometric variations in the spectral lines, these not being observed. It was therefore concluded that the peculiarities of the executed loci in the qu-plane mainly result from departures of the magnetic configuration from being simply dipolar.

Adopting the oblique rotator model, Landolfi, Bagnulo, Landi Degl'Innocenti, *et al.* (1997) have compared the various diagnostics whereby the magnetic configuration of an Ap star is determined. Measurements of the splitting of lines leads to determination of the so-called mean magnetic field modulus or mean surface field, B_s; the circular polarization in individual lines leads to the so-called mean longitudinal field, B_l; broadband linear polarization measurements provide information of the differential saturation effects in all of the magnetic lines contained in the passband. Their study establishes the relationships between the three diagnostics in defining the constraints on magnetic field configurations. In a further paper, Leroy (1995) has brought together his broadband measurements of 55 Ap stars measured over a 4-year period, with data collected by other workers to provide a reference point catalogue for any future studies that might be undertaken. An example of the behaviour of a well-studied star, β CrB (= HD 137909), is depicted in Figure 12.3. Although the polarimetric behaviour looks very simple and readily interpretable, Leroy (1995) has noted that the fitted q- and u-phased curves require third-order Fourier expansions to describe them, this indicating significant departures to a standard dipolar configuration.

In the final paper of this series related to the behaviour of continuum polarization, Leroy, Landolfi & Landi Degl'Innocenti (1996) addressed the problem again

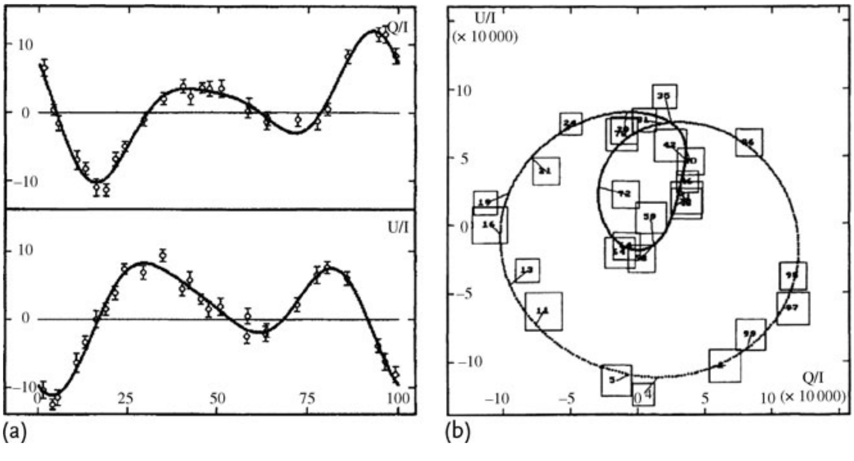

Fig. 12.3 (a) displays the q and u variations of β CrB (= HD 137909), phased on the star's rotational period of $18.^{d}4868$; (b) plots the same data in the qu-plane revealing a renal-shaped locus, the boxes carrying the phase values. (Taken from Leroy, 1995.)

of a dipole field model, and the departures from the expected behaviour of the executed path that the data reveal when plotted in the qu-plane. They were able to reconcile the issue by considering there to be inclination changes of the lines of force within their meridian plane. Keeping the magnetic equator as a plane of symmetry, they have shown that it is sufficient to assume slightly expanded lines of force, over some parts of the magnetic equator, to explain the peculiarities in the polarization curves. Such regions, where the lines of force expand outwards, seem to occur preferentially in the vicinity of the rotational poles for those stars having an angle of β not far from 90°.

Magnetic field determinations may be improved by combining the circular polarization signals within many spectral lines. In a simulation exercise, Stift (1986) has shown that such statistical techniques are sensitive to macroscopic velocity fields. Although multi-line combination methods may be useful for survey purposes, it was suggested that they do not provide a sound basis for detailed modelling of magnetic field geometries of individual stars.

By applying spectropolarimetry, Donati, Howarth, Bouret, *et al.* (2006) have recorded Zeeman signatures for the O f?p spectrum variable star, HD 191612, suggesting that it displays a large-scale field with a polar strength of about -1.5 kG. The star is the second magnetic O star to have been discovered. Its signature was essentially stable over four nights, indicating a slow rotation period. They suggest that HD 191612 is an evolved version of the near-zero-age main-sequence magnetic O star, θ^1 Ori C, but with an even stronger field; the rotation rate which is exceptionally slow by accepted O-star standards, could have been caused by angular momentum dissipation through a magnetically confined wind.

A recent important observational development is the detection of patchy magnetic fields on rapidly rotating stars by the principle of Zeeman–Doppler imaging (ZDI). By performing high spectral resolution polarimetry, features displaying polarization may be detected in rotationally broadened lines and followed, as they migrate across the profile as the star rotates. In the first of a series of papers, Semel (1989) has described the principle and outlined the scheme whereby the average of the measurements of many lines may be used to improve the signal-to-noise ratio of the determined magnetic fields, and their location on the stellar surface. A numerical simulation of the model was undertaken by Donati, Semel & Praderie (1989), and some preliminary results were presented for the magnetic Ap star, α^2 CVn.

Some of the problems associated with spurious signals which occur in the collection of data are discussed in Semel, Donati & Rees (1993), together with a listing of field detections which have been achieved by instrumentation on three different telescopes.

Donati, Semel, Carter, *et al.* (1997) have enhanced the sensitivity of ZDI by sophisticated reduction techniques to a selection of active stars, and have reported on the detection of magnetic fields for 14 objects. The procedure, or least-squares deconvolution (LSD), involves the simultaneous analysis of many spectral lines. LSD assumes that all spectral features in a given Stokes parameter $\{I, Q, U, V\}$ spectrum have identical shape, but may differ in amplitude by known scaling factors.

An example of its application to spectropolarimetry of Ap stars is provided by Wade, Donati, Mathys, *et al.* (1998). The very active K0 dwarf, AB Dor, has been studied by the ZDI technique by Donati & Cameron (1997) with excellent success, revealing differential rotation affecting the imaging of its magnetic polarity patterns. A short note of this work has also been given by Cameron, Donati & Semel (1997).

Waite & Marsden (2007) have reported on ZDI at the Anglo-Australian Telescope, with results on two solar-type stars, one of them, HD 106506 exhibiting a giant spot region encircling a pole. The reasons for its location is not fully known, but it is believed that the increased Coriolis force, due to rapid rotation, may have the effect of deflecting the spot features to higher latitudes as they erupt through the star's convection zone.

Using a simple dipole theory, Leone, Catanzaro & Catalano (2000) have determined the angle between the rotational and dipole axes, and the polar strength of the field, of several magnetic stars. They have also conducted simultaneous photometry, and have confirmed the importance of effects related to the non-homogeneous distribution of elements on the stellar surface as the origin of the light variability.

12.3
Helium Rich/Weak Stars

The peculiar variable helium-rich star, σ Ori, was observed by Landstreet & Borra (1978) who reported a magnetic field varying between -2300 and $+3100$ G, with a period of $1.^{d}19$, matching that obtained from spectrometric and photometric variations of the star. They interpreted the behaviour in terms of the oblique rotator model that has hot gas trapped in a magnetosphere above the magnetic equator and atmospheric helium enhancement which has occurred preferentially in a zone around the magnetic equator. This notion was pursued by Clarke & McGale (1988) in analysing broadband polarization measurements of Kemp & Herman (1977) to provide a model involving the presence of an off-centred dipole magnetic field, with concentrations of the scattering material occurring at the intersection of the rotational and magnetic equators. In their original paper, Kemp & Herman (1977) modelled the polarimetric behaviour in terms of a binary system containing a highly non-spherical component such as a disc.

The helium strong star HD 184827 (B2V) has been studied under a contemporaneous project involving ultraviolet and optical spectrometry, and Zeeman polarimetry, by Barker, Brown, Bolton, *et al.* (1982). A clear sinusoidally varying magnetic field was detected, the period matching that determined by photometry, and by the changes in the stellar line profiles.

A survey of 27 helium-weak stars was conducted by Borra, Landstreet & Thompson (1983) using an Hβ analyser. With typical measurement errors of ± 100 to ± 400 G, fields were detected in 10 stars. The fraction of He-weak stars showing large fields appeared to be larger than for Ap stars, but smaller than for He-strong stars.

12.4
White Dwarfs

Following the notion that white dwarfs might be expected to possess magnetic fields of the order of 10^6 G, Angel & Landstreet (1970a) designed a polarimeter to investigate the presence of circularly polarized light of opposite senses in the alternate wings of the broad Hγ line, any signature resulting from the Zeeman effect. Their exploratory scheme provided a null result.

The detection of wide-band circularly polarized light (1–3%) from a white dwarf was first reported by Kemp, Swedlund, Landstreet, *et al.* (1970) for the semi-DC 'peculiar' star, Grw $+70°$ 8247. The wavelength dependence of v appeared to correspond to that expected of a projected B field, estimated at 1×10^7 G, based on the theory of gray-body magneto-emissivity (see Kemp, 1970a), this physical mechanism demonstrated in the laboratory by Kemp, Swedlund & Evans (1970). All previous searches providing null results had concentrated on the DA-type white dwarfs with H-lines.

This positive result was followed by the announcement by Landstreet & Angel (1971) of the discovery of circular polarization in G 99–37. They also provided a list of 24 white dwarfs which they had observed, but yielding null results. Angel & Landstreet (1971a) found that a second white dwarf (G 195-19) displayed circular polarization, and this was confirmed by Kemp, Swedlund & Wolstencroft (1971). Angel & Landstreet (1971b) later showed that this object displayed variations with a period of $1.^{\mathrm{d}}34$. Further measurements of G 195–19 were made by Angel, Illing & Landstreet (1972), these revealing a period of $1.^{\mathrm{d}}3309$, with a sinusoidal v-curve for blue/green wavelengths. For a red band, the variation in v was less sinusoidal, with a phase shift in the maximum polarization value relative to the behaviour at shorter wavelengths. The observations are explainable by considering the star's magnetic field as an off-centred dipole, with its axis not passing through the rotation axis.

Following the initial discovery of circular polarization associated with Grw $+70°$ 8247, further observations of this star were made by Angel & Landstreet (1970b) who extended the wavelength coverage, searching also for time-dependent variations, but with a null result. A presence of linear polarization in the blue end of the spectrum, and a sharp drop in the circular component shortward of 4000 Å, was not explainable by the simple theory of magneto-emission. With increased spectral resolution, Angel, Landstreet & Oke (1972) (see Figure 12.4) recorded sharp changes in the dispersion of the circular polarization, these associated with the structure of the Minkowski bands of molecular helium. Bluewards of 6000 Å, the polarization remains constant with time, but redwards of this wavelength there appeared to be changes relative to the previous year. For a star with a pure helium atmosphere, molecules could be formed in sufficient density to give the observed absorption features. According to Angel (1972), the Zeeman effect in molecular helium can explain the observed spectral features in the polarization, and may also be responsible for the continuum polarization. Coyne (1974) undertook a search for linear polarization in the blue spectral region in 15 white dwarfs, but with no intrinsic effects being detectable.

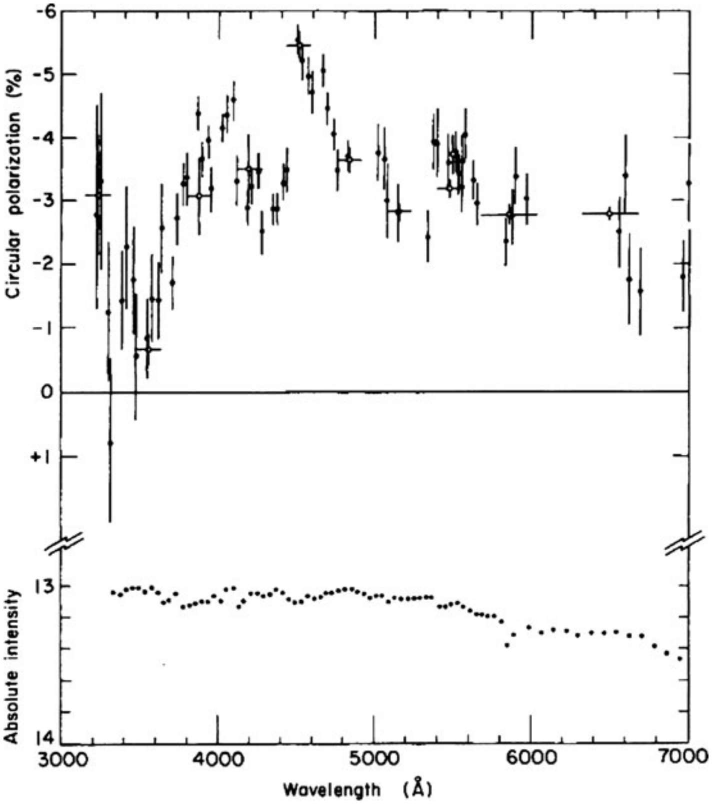

Fig. 12.4 The upper box presents the circular polarization of Grw +70°8247 across the visible spectrum, and shows steps at 4135 and 4470 Å, corresponding to the Minkowski bands of molecular helium; there is also a weaker feature at 3910 Å. Each white dwarf appears to display a unique $\nu(\lambda)$ spectrum, making it difficult to categorize them. (Taken from Angel, Landstreet & Oke, 1972.)

Another white dwarf of interest is GD 229. Following evidence by Swedlund, Wolstencroft, Michalsky, *et al.* (1974) that this peculiar object displayed time-varying circular and linear polarization, Kemp, Coyne, Swedlund, *et al.* (1974) investigated its linear polarization. This paper highlights some of the problems associated with the removal of spurious signals from the background sky polarization. In the blue part of the spectrum the linear polarization is well defined at about 3%, but whether there is variability in the red remains an open question demanding further observational study. The possibility as to whether the major component of the linear polarization has an interstellar origin was not broached. Landstreet & Angel (1974) reported on the wavelength dependence of the circular polarization in this star and, over the period of their observations, concluded there was no evidence of variability in any region of the spectrum.

Berdyugin & Piirola (1999) have made further measurements of GD 229 and G 240–72, with a confirmation that these stars have long-term variations of polarization on time scales of ≥ 10 years, with the suggestion that these objects have rotational periods of about, or longer than, 100 years, the extreme slow rotation probably being a result of magnetic braking.

Circular polarization of several photometrically variable white dwarfs was searched for by Rich & Williams (1973). Although three stars were highlighted as polarimetric suspects, the claims do not carry high confidence. Liebert & Stockman (1980) have also made observational studies by circular polarimetry of 32 white dwarfs with null results.

From spectral measurements of G 99-37, Angel & Landstreet (1974) have considered the strong polarization feature associated with the G-band of CH which is very apparent. They have calculated the magnetic circular dichroism of the band and find that a good fit to the data is achieved by taking an effective field of 3.6×10^8 G. Using this value, an estimate is also made of the wavelength dependence of continuous circular polarization, assuming the dominant opacity to come from He^-, and this is also in agreement with the observations.

The photometric spectrum of GD 90 indicates the presence of absorption features with very broad and distorted Balmer lines. A polarimetric investigation by Angel, Carswell, Strittmatter, *et al.* (1974) clearly demonstrated the resolution of the Zeeman components indicating the presence of magnetic fields $\sim 5 \times 10^6$ G. Angel, Hintzen, Strittmatter, *et al.* (1974) reported that the dispersion of the circular polarization of G 240–72 was unusual in that it exhibited a sign change from blue to red light.

Angel, Hintzen & Landstreet (1975) have made measurements of G 227–35, a white dwarf suspect, with no detectable absorption features. Strong circular polarization with a hump of 3% in the blue was measured and, after falling away across the spectrum, there is a spectacular rise to ~8% at 1 μm. The longitudinal field is probably in excess of 10^7 G.

Continuing the observational study of white dwarfs, Landstreet & Angel (1975) measured a static circular and linear polarization of Grw $+70°$ 8247, the behaviour interpreted as being due to magnetic circular dichroism in a helium atmosphere. The estimated field strength was 5×10^7 to 10^8 G. Earlier, Kemp (1970b) had suggested that structure in the wavelength dependence of the circular polarization was caused by the magneto-emission mode with an intermediate case between that of the weak-field 'gray-body' theory and that of a strong-field, quantum-magnetic limit. The data considered by him included those in the infrared from Kemp & Swedlund (1970).

Remarkable polarimetric behaviour was reported for DQ Her, an old nova likely to contain a DA white dwarf, with a noted 71-second light variation. Swedlund, Kemp & Wolstencroft (1974) found a variable circular polarization, with a period twice that of the light period, from which it was concluded that the object contains an oblique magnetic rotator. The same group (see Kemp, Swedlund & Wolstencroft, 1974) also discovered a periodic linear polarization with the same period of 142 s, a simple model being offered.

The eclipsing white dwarf binary, BD $+16°516$, has been investigated by Kemp & Rudy (1975). A mean level of polarization was detected but assumed to have an interstellar origin. There was also marginal evidence for a polarization component in the ultraviolet which varies with phase.

Piirola & Reiz (1990) have revealed a strong rotationally modulated circular polarization for the white dwarf, PG 1031+234, peaking in the ultraviolet at 17%, and correlated with brightness variations. They suggest that the variations arise from dichroism in the highly magnetic atmosphere with values of opacity being greatly different for the two senses of circular polarization.

From the behaviour of circular polarization in association with the various absorption features, Greenstein (1974) proposed a classification nomenclature. He made comment, however, that no two polarizations of peculiar stars show similar or familiar features. A key to the observed behaviours may be the quadratic Zeeman effect, complicated by the wide range of temperatures, surface compositions and field strengths.

In respect of definitions associated with handedness, the development of the study of white dwarfs highlights some of the difficulties in dealing with the conventions. As discussed earlier in Chapters 4 and 9, differences arise from how the rotation of the electric vector is described according to the viewpoint, whether the discussion is dealing with the remaining light after a polarizational sensitive absorption, and how a mathematical sign is assigned to the definition. In promoting the notion that gray-body magneto-emission might be the source of the observed circular polarization, Kemp (1970b) highlighted a further dilemma associated with 'sign' convention. He noted that in an earlier paper, (see Kemp, 1970a) he had presented the formula for the generated circular polarization as $q(\lambda)[\equiv v(\lambda)] = (eB/4\pi mc)\lambda$, but carrying a minus sign; if e is taken as unsigned, for electrons, the minus sign in the formula is not required. He also noted: – "that positive actual q-values [$\equiv v$-values] mean 'left-handed' polarization in the illogical traditional nomenclature; in my paper I call this right handed, conforming to the right-hand screw conventions." Although this not exactly clear, the sense of his measurements of Grw $+70°8247$, (see Kemp, 1970b) agree with those of Angel & Landstreet (1970b). In the paper describing an instrument used to determine the polarization in the wings of Hγ, Angel & Landstreet (1970a) note that that '+' v in the blue wing corresponds to left-handed polarization; '+' v in the red wing refers to right-handed polarization. They also comment that with this sign convention, '+' polarization corresponds to a +ve field in Babcock's (1958). Again, what is meant by these statements are difficult to interpret with clarity. Future work in this area of white dwarfs still requires care to be taken in understanding the chosen definition for handedness, and any interpretations of sense of direction of the stellar magnetic field.

References

References to Magnetic and Ap Stars

Babcock, H.W. (1947) Zeeman effect in stellar spectra. *ApJ*, **105**, 105–119. [254]

Babcock, H.W. (1949) Magnetic intensification of stellar absorption lines. *ApJ*, **110**, 126–142. [259]

Babcock, H.W. (1951) The magnetically variable star HD 125248. *ApJ*, **114**, 1–36. <?xml-tex [254]

Babcock, H.W. (1954) The magnetic variable HD 188041. *ApJ*, **120**, 66–75. [254]

Babcock, H.W. (1958) A catalog of magnetic stars. *ApJS*, **3**, 141–210. [254]

Babcock, H.W. (1960) The 34-kilogauss magnetic field of HD 215441. *ApJ*, **132**, 521–532. [254]

Babcock, H.W., Burd, S. (1952) The variable magnetic field of α^2 Can Venaticorum. *ApJ*, **116**, 8–17. [254]

Bagnulo, S., Landi Degl'Innocenti, E., Landolfi, M., Leroy, J.L. (1995) Linear polarimetry of Ap stars. III. A diagnostic method for the magnetic structure of rotating stars. *A&A*, **295**, 459–470. [260]

Bagnulo, S., Szeifert, T., Wade, G.A., Landstreet, J.D., Mathys, G. (2001) Detecting magnetic fields of upper-main-sequence stars with FORS1 at ANTU. *The Messenger*, No: **104**, 32–36. [258]

Berdyugin, A., Breger, M., Polosukhina, N. (1992) A search for polarization variability in Babcock's Star. *A&A*, **255**, 149–152. [254]

Bonsack, W.K., Pilachowski, C.A., Wolff, S.C. (1974) The variations of the magnetic Ap Star 49 Camelopardalis. *ApJ*, **187**, 265–270. [255]

Borra, E.F. (1973) 53 Cam and the transverse Zeeman effect in Hβ. *ApJ*, **186**, 959–960. [255]

Borra, E.F. (1974a) The orientation of magnetic axes in Ap stars: An alternative interpretation of the component with small obliquity. *ApJ*, **187**, 271–274. [256]

Borra, E.F. (1974b) On the interpretation of the magnetic curves of the Ap stars as determined by the photographic technique. *ApJ*, **188**, 287–290. [257]

Borra, E.F. (1980a) High-resolution polarization observations inside spectral lines of the Magnetic Ap Stars III: observations of 78 Virginis. *ApJ*, **235**, 911–914. [258]

Borra, E.F. (1980b) The geometry of the magnetic field of 78 Virginis. *ApJ*, **235**, 915–924. [258]

Borra, E.F., Dworetsky, M.M. (1973) The long-term behaviour of the magnetic field of β Coronae Borealis. *ApJ*, **186**, 211–217. [255]

Borra, E.F., Landstreet, J.D. (1973) A search for weak stellar magnetic fields. *ApJ*, **185**, L319–L143. [255]

Borra, E.P., Landstreet, J.D. (1977) The surface magnetic field distributions of 53 Camelpardalis and α^2 Canum Venaticorum. *ApJ*, **212**, 141–148. [257]

Borra, E.F., Landstreet, J.D., Vaughan, Jr., A.H. (1973) High-resolution Zeeman polarimetry. *ApJ*, **185**, L145–L147. [255]

Borra, E.F., Vaughan, A.H. (1977) High-resolution polarization observations inside spectral lines of maagnetic Ap stars. I. Instrumentation and observations of β Coronae Borealis. *ApJ*, **216**, 462–478. [257]

Borra, E.F., Vaughan, A.H. (1978) High-resolution polarization observations inside spectral lines of magnetic Ap stars. II. Observations of α^2 Canum Venaticorum. *ApJ*, **220**, 924–930. [258]

Cameron, A., Donati, J.-F., Semel, M. (1997) *Anglo-Australian Newsletter*, **83**, 8–9. [263]

Conti, P.S. (1970) Zeeman measures of sharp-lined early B stars. *ApJ*, **159**, 723–725. [255]

Demkina, L.B., Obridko, V.N. (1973) Polarization of the radiation of magnetic stars. *Sov. Astron.*, **16**, 853–855. [259]

Donati, J.-F., Cameron, A.C. (1997) Differential rotation and magnetic polarity patterns on AB Doradus. *MNRAS*, **291**, 1–19. [263]

Donati, J.-F., Howarth, I.D., Bouret, J.-C., Petit, P., Catala, C., Landstreet, J. (2006) Discovery of a strong magnetic field on the O star HD 191612: new clues to the future of θ^1 Orionis C. *MNRAS*, **365**, L6–L10. [262]

Donati, J.-F., Semel, M., Carter, B.D., Rees, D.E., Cameron, A.C. (1997) Spectropolarimetric observations of active stars. *MNRAS*, **291**, 658–682. [262]

Donati J.-F., Semel, M., Praderie, F. (1989) Zeeman–Doppler imaging of active stars.

II. Numerical simulation and first observational results. *A&A*, **225**, 467–478. [262]

Finn, G.D., Kemp, J.C. (1974) The linear polarization of 53 Camelopardis. *MNRAS*, **167**, 375–391. [257]

Gjellestad, G., Babcock, H.W. (1953) The magnetically variable star HD 153882. *ApJ*, **117**, 12–20. [254]

Huovelin, J., Tuominen, I., Shcherbakov, Z.A. (1989) The magnetic fields of late-type stars: Measurements from Line Profiles. *104th IAU Colloquium on Solar and Stellar Flares*, August 15–19, 1988, Stanford, CA. Printed in *Sol. Phys.*, **121**, 419–429. [253]

Kemp, J.C., Wolstencroft, R.D. (1973) HD 215441 and 53 Camelopardalis: Intrinsic polarization of Hβ and the continuum. *ApJ*, **179**, L33–L37. [255, 255]

Kemp, J.C., Wolstencroft, R.D. (1974) The intrinsic linear polarization of 53 Camelopardalis and α^2 Canum Venaticorum. *MNRAS*, **166**, 1–18. [257]

Kemp, J.C., Wolstencroft, R.D., Swedlund, J.B. (1972) Circular polarimetry of fifteen interesting objects. *ApJ*, **177**, 177–189. [258]

Landolfi, M., Bagnulo, S., Landi Degl'Innocenti, M., Landi Degl'Innocenti, E, Leroy, J.L. (1997) Constraints on the magnetic configuration of Ap stars from simple features of observed quantities. *A&A*, **322**, 197–201. [261]

Landolfi, M., Landi Degl'Innocenti, E., Landi Degl'Innocenti, M., Leroy, J.L. (1993) Linear polarimetry of Ap stars I. A simple canonical model. *A&A*, **272**, 285–298. [260]

Landstreet, J.D. (1980) The measurement of magnetic fields in stars. *AJ*, **85**, 611–620. [253]

Landstreet, J.D. (1982) A search for magnetic fields in normal upper main sequence stars. *ApJ*, **258**, 639–650. [258]

Landstreet, J.D., Borra, E.F. (1977) Discovery of magnetic fields in three short-period Ap stars. *ApJ*, **212**, L43–L46. [257]

Leone, F., Catanzaro, G., Catalano, S. (2000) Spectropolarimetric measurements of the mean longitudinal magnetic field of chemically peculiar stars. *A&A*, **355**, 315–326. [263]

Leroy, J.L. (1962) Contributions a L'Étude de la Polarisation de la Lumière Solaire. *Ann. d'Astr.*, **25**, 127–164. [259]

Leroy, J.L. (1989) The spectral variation of polarization due to magnetic intensification. *A&A*, **215**, 360–370. [259]

Leroy, J.L. (1990) Broad-band polarization in crowded spectra. *A&A*, **237**, 237–242. [260]

Leroy, J.L. (1995) Linear polarimetry of Ap stars. V. A general catalogue of measurements. *A&AS*, **114**, 79–104. [254, 259, 259, 261, 261, 261]

Leroy, J.L., Bagnulo, S., Landolfi, M., Landi Degl'Innocenti, E., (1994) A long period model for the magnetic star γ Equulei. *A&A*, **284**, 174–178. [260]

Leroy, J.L., Landolfi, M., Landi Degl'Innocenti, E. (1993) Linear polarimetry of Ap stars. II. New observations with a reappraisal of former ones. *A&A*, **270**, 335–344. [260]

Leroy, J.L., Landolfi, M., Landi Degl'Innocenti, E. (1996) Linear polarimetry of Ap stars VI. A modified dipolar model consistent with the observations. *A&A*, **311**, 513–522. [261]

Leroy, J.L., Landolfi, M., Landi Degl'Innocenti, M., Landi Degl'Innocenti, E., Bagnulo, S., Laporte, P. (1995) Linear Polarimetry of Ap Stars. IV. The influence of deviations from a pure dipolar model. *A&A*, **301**, 797–810. [260]

Leroy, J.L., Landstreet, J.D., Bagnulo, S. (1994) 49 Camelopardalis: an uncommon magnetic star. *A&A*, **284**, 491–498. [260]

North, P., Brown, D.N., Landstreet, J.D. (1992) The magnetic field and period of the Ap Si star 108 Aquarii. *A&A*, **258**, 389–396. [258]

Piirola, V., Tuominen, I. (1981) The intrinsic polarization of the magnetic variable HD 71866. pp. 283–288 in *Les étoiles de composition chimique anormale du début de la séquence principale* (Upper main sequence chemically peculiar stars) – 23rd Liège Astrophys. Coll., Université de Liège. [259]

Polosukhina, N.S. (1964) Polarimetric observations of the magnetic variable HD 215441. *Sov. Astron.*, **7**, 498. [254]

Polosukhina, N.S., Lebedeva, L. (1966) Polarization and brightness variations of the magnetic variable HD 215441 *Sov. Astron.*, **10**, 407–410. [254]

Preston, G.W. (1967) A statistical investigation of the orientation of magnetic axes in the periodic magnetic stars. *ApJ*, **150**, 547–550. [256]

Preston, G.W. (1969a) The magnetic field of HD 215441. *ApJ*, **156**, 967–982. [256]

Preston, G.W. (1969b) Partial resolution of Zeeman patterns in the spectrum of 53Camelopardalis. *ApJ*, **157**, 247–251. [255]

Preston, G.W., Kazimierz, S., Wolff, S.C. (1969) The magnetic field and light variations of 17 Comae Berenices and κ Cancri. *ApJ*, **156**, 653–660. [254]

Preston, G.W., Pyper, D.M. (1965) The performance of the Zeeman analyzers of the 120-in. Coudé spectrograph. *ApJ*, **142**, 983–989. [254]

Preston, G.W., Stępień, K. (1968) The magnetic field and light variations of HD 32633. *ApJ*, **151**, 577–581. [254]

Pyper, D.M. (1969) α^2 Canum Venaticorum and the oblique-rotator theory. *ApJS*, **18** (164), 347–378. [257]

Sargent, W.L.W., Sargent, A.I., Strittmatter, P.A. (1967) The existence of magnetic fields in two peculiar B stars in Orion. *ApJ*, **147**, 1185–1188. [255]

Semel M. (1989) Zeeman–Doppler imaging of active stars. I. Basic principles. *A&A*, **225**, 456–466. [262]

Semel, M., Donati, J.-F., Rees, D.E. (1993) Zeeman–Doppler imaging of active stars. III. Instrumental and technical considerations. *A&A*, **278**, 231–237. [262]

Serkowski, K., Chojnacki, W. (1969) Polarimetric observations of magnetic stars with two-channel polarimeter. *A&A*, **1**, 442–448. [258]

Severny, A. (1970) The weak magnetic fields of some bright stars. *ApJ*, **159**, L73–L76. [255]

Stibbs, D.W.N. (1950) A study of the spectrum and magnetic variable Star HD 125248. *MNRAS*, **110**, 395–404. [256]

Stift, M.J. (1986) Theoretical Stokes profiles of magnetic stars – II. An appraisal of statistical methods for magnetic field determination. *MNRAS*, **219**, 203–216. [262]

Thiessen, G. (1961) Über die Polarisation des Sternlichtes, die Strahlung der Sterne, Sowie Bemerkungen zur Galaktiscehn Struktur. *Astr. Abh. Hamburg Stern.*, Band V, No. 9, p 313. [258]

Wade, G.A., Donati, J.-F., Mathys, G., Piskunov, N. (1998) Linear spectropolarimetry of Ap stars: a new degree of constraint on magnetic structure. *Cont. Astron. Obs. Skalnaté Pleso*, **27**, 436–440. [263]

Waite, I., Marsden, S. (2007) Spectropolarimetry of solar-type stars with the AAT. *Anglo-Australian Observatory Newsletter*, Issue **112**, 3–6. [263]

Warwick, J.W. (1951) Absorption-line polarization in magnetic stars. *AJ*, **56**, 50–51. [259]

Wolff, S.C. (1969) The magnetic field variations of HD 188041. *ApJ*, **157**, 253–259. [254]

Wood, H.J., Campusano, L.B. (1975) Zeeman observations of new southern magnetic stars. *A&A*, **45**, 303–305. [255]

Zappala, R.R., Hiltner, W.A. (1966) Polarization of HD 71866. *PASP*, **78**, 337–339. [259]

References to Helium Stars

Barker, P.K., Brown, D.N., Bolton, C.T., Landstreet, J.D. (1982) Magnetospheres and winds of the helium strong stars. *Advances in Ultra-violet Astronomy: Four Years of IUE Research*, Symposium NASA Goddard Flight Center, 1982, March 30–April 1. [263]

Borra, E.F., Landstreet, J.D., Thompson, I. (1983) The magnetic fields of helium-weak B stars. *ApJS*, **53**, 151–167. [263]

Clarke, D., McGale, P.A. (1988) Temporal polarization variations of Be stars IV. The polarimetric behaviour of σ Orionis E. *A&A*, **205**, 207–214. [263]

Kemp, J.C., Herman, L.C. (1977) The polarization of sigma Orionis E: a curious eclipsing binary. *ApJ*, **218**, 770–775. [263, 263]

Landstreet, J.L., Borra, E.F. (1978) The magnetic field of sigma Orionis E. *ApJ*, **224**, L5–L8. [263]

References to White Dwarfs

Angel, J.R.P. (1972) Interpretation of the Minkowski bands in Grw +70° 8247. *ApJ*, **171**, L17–L21. [264]

Angel, J.R.P., Carswell, R.F., Strittmatter, P.A., Beaver, E.A., Harms, R. (1974) Discovery of a magnetic DA white dwarf. *ApJ*, **194**, L47–L50. [266]

Angel, J.R.P., Hintzen, P., Landstreet, J.D. (1975) Identification of G 227–35 as a strongly polarized magnetic white dwarf. *ApJ*, **196**, L27–L29. [266]

Angel, J.R.P., Hintzen, P., Strittmatter, P.A., Martin, P.G. (1974) G240–72: A new magnetic white dwarf with unusual polarization. *ApJ*, **190**, L71–L72. [266]

Angel, J.R.P., Illing, R.M.E., Landstreet, J.D. (1972) New measurements of circular polarization and an ephemeris for the variable white dwarf G195–19. *ApJ*, **175**, L85–L87. [264]

Angel, J.R.P., Landstreet, J.D. (1970a) Magnetic observations of white dwarfs. *ApJ*, **160**, L147–L152. [264, 267]

Angel, J.R.P., Landstreet, J.D. (1970b) Further polarization studies of Grw +70° 8247 and other white dwarfs. *ApJ*, **162**, L61–L66. [264, 267]

Angel, J.R.P., Landstreet, J.D. (1971a) Detection of circular polarization in a second white dwarf. *ApJ*, **164**, L15–L16. [264]

Angel, J.R.P., Landstreet, J.D. (1971b) Discovery of periodic variations in the circular polarization of a white dwarf. *ApJ*, **165**, L71–L75. [264]

Angel, J.R.P., Landstreet, J.D. (1974) A determination by the Zeeman effect of the magnetic field strength in the white dwarf G 99–37. *ApJ*, **191**, 457–464. [266]

Angel, J.R.P., Landstreet, J.D., Oke, J.B. (1972) The spectral dependence of circular polarization in Grw +70° 8247. *ApJ*, **171**, L11–L15. [264, 265]

Babcock, H.W. (1958) A catalog of magnetic stars. *ApJS*, **3**, 141–210. [267]

Berdyugin, A.V., Piirola, V. (1999) Polarization variability in magnetic white dwarfs GD 229 and G 240–72. *A&A*, **352**, 619–622. [266]

Coyne (SJ), G.V. (1974) A search for linear polarization in white dwarfs. *Ric. Astron. Spec. Vaticana*, **8** (27). [264]

Greenstein, J.L. (1974) Spectrophotometry of magnetic degenerate stars. *ApJ*, **194**, L51–L55. [267]

Kemp, J.C. (1970a) Circular polarization of thermal radiation in a magnetic field. *ApJ*, **162**, 169–179. [264, 267]

Kemp, J.C. (1970b) Quantum-magnetic features in the polarized light of Grw +70° 8247. *ApJ*, **162**, L69–L72. [266, 267]

Kemp, J.C., Coyne (SJ), G.V., Swedlund, J.B., Wolstencroft, R.D. (1974) On the linear polarization of GD 229. *ApJ*, **189**, L79–L80. [265]

Kemp, J.C., Rudy, R.J. (1975) The linear polarization of the white dwarf binary BD +16° 516. *PASP*, **87**, 301–303. [267]

Kemp, J.C., Swedlund, J.B. (1970) Large infrared circular polarization of Grw +70° 8247. *ApJ*, **162**, L67–L68. [266]

Kemp, J.C., Swedlund, J.B., Evans, B.D. (1970) Magneto-emission from incandescent bodies. *Phys. Rev. Letters*, **24**, 1211–1214. [264]

Kemp, J.C., Swedlund, J.B., Landstreet, J.D., Angel, J.R.P. (1970) Discovery of circularly polarized light from a white dwarf. *ApJ*, **161**, L77–L79. [264]

Kemp, J.C., Swedlund, J.B., Wolstencroft, R.D. (1971) Confirmation of the magnetic white dwarf G–195–19. *ApJ*, **164**, L17–L18. [264]

Kemp, J.C., Swedlund, J.B., Wolstencroft, R.D. (1974) DQ Herculis: periodic linear polarization synchronous with the rapid light variations. *ApJ*, **193**, L15–L19. [266]

Landstreet, J.D., Angel, J.R.P. (1971) Discovery of circular polarization in the white dwarf G99–37. *ApJ*, **165**, L67–L70. [264]

Landstreet, J.D., Angel, J.R.P. (1974) The wavelength dependence of circular polarization in GD 229. *ApJ*, **190**, L25-L26. [265]

Landstreet, J.D., Angel, J.R.P. (1975) The polarization spectrum and magnetic field strength of the white dwarf Grw +70° 8247. *ApJ*, **196**, 819–825. [266]

Liebert, J., Stockman, H.S. (1980) Circular polarization measurements of selected white dwarfs. *PASP*, **92**, 657–660. [266]

Piirola, V., Reiz, A. (1990) The highly magnetic (B $\sim$ 500 MG) white dwarf PG 1031 +234 : discovery of wavelength dependent polarization and intensity variations. *Astrophys. Space Sci.*, **169**, 231–232. [267]

Rich, A., Williams, W.L. (1973) A search for optical circular polarization in white dwarfs and late-type stars with circumstellar shells. *ApJ*, **180**, L123–L126. [266]

Swedlund, J.B., Kemp, J.C., Wolstencroft, R.D. (1974) DQ Herculis: Periodic circular polarization synchronous with the rapid light variations. *ApJ*, **193**, L11–L13. [266]

Swedlund, J.B., Wolstencroft, R.D., Michalsky, Jr., J.J., Kemp, J.C. (1974) Discovery of time-varying circular and linear polarization in the white-dwarf suspect GD 229. *ApJ*, **187**, L121–L123. [265]

13
Early-type Stars

13.1
Introduction

The origins of polarimetric interest in early-type stars relate to the theory of radiative transfer in their atmospheres through the work of Chandrasekhar, particularly his iconic paper of 1946 (see Chandrasekhar, 1946).For pure scattering, it was suggested that p may be as large as 12% at the limb of the stellar disc. A method for theoretically investigating the polarization of radiation from stellar atmospheres has also been presented by Harrington (1970). The high values of limb polarization predicted by Chandrasekhar were later reassessed by Ruciński (1970), and he put forward arguments to suggest that any polarization would be much smaller. The problem of solving the behaviour of polarized radiation arising in a plane-parallel non-gray atmosphere from Thomson scattering by free electrons was also investigated by Collins (1970). By performing the calculations in respect of early-type stars, it was shown that almost no net polarization is to be expected in the visible part of the spectrum. A similar outcome was arrived at by Loskutov (1987) who also drew attention to the fact that the polarization direction should flip along a projected stellar radius. At the limb, the vibration is tangential to the disc. The magnitude decreases across the disc, becoming zero within a short distance along the radius, but then reappearing again, with the vibration parallel to the stellar radius, before reducing again to zero at the centre of the disc. Such signatures were shown to be more pronounced with increasing temperature, becoming marked at stellar temperatures $>$10 000 K.

Many early-type stars have high $v \sin i$ values, with possible associated global distortions as a result of the fast rotation. Harrington & Collins (1968) demonstrated that the presence of gravity darkening, limb darkening and rotational distortion will affect the symmetry of early-type stars such that the electron scattering should produce detectable polarizations under suitable conditions, or geometries. Some simple rotationally distorted stellar geometries with electron scattering atmospheres have been explored by Cassinelli & Haisch (1974) suggesting that overall polarizations of 2 to 6% might be exhibited. Later, Haisch & Cassinelli (1976) examined the potential of electron scattering using equations of transfer, modified by an absorptive opacity, in extended, distorted atmospheres of early-type stars. The

Stellar Polarimetry. David Clarke

ISBN: 978-3-527-40895-5

explored models, with rotational asymmetry, provided a net polarization, but highly flattened discs were required to obtain values of $p = 1\%$, or higher. The $p(\lambda)$ variations produced by the models matched the observed behaviour of Be stars between the Balmer and Paschen edges. This basic category of early-type star will be discussed first.

13.2
Be Stars

Be stars are loosely defined simply because their Balmer lines are in emission, or have been at some time. They may be divided into three main groups, i. e. (1) Classical – rapidly rotating near main sequence B stars, (2) B spectral types associated within star-forming regions with the emission line character indicating an early age, (3) B[e] stars noted for the presence of forbidden lines, as well as HI emission, in their spectra, accompanied by a strong IR continuum excess, this latter feature also seen in Herbig Be stars. Clear differences in the behaviours of the various stellar categories are revealed when the polarimetry is assessed in terms of correlation with photometry. For example, Yudin (2000) has shown that classical Be stars can exhibit optical polarizations from very low values up to ∼2%, with little photometric colour excess, $E(V - L)$, whereas for Herbig Ae/Be (HAEBE) stars, p can have similar or higher values which are correlated with the colour excess. The polarization associated with Be stars originates from scattering by free electrons, while that from Ae/Be stars may carry a component from dust scattering, the dust also giving rise to a thermal emission providing the colour excess. In a comprehensive survey of classical Be stars, Yudin (2001) has examined the statistical behaviour of 627 stars. He found that the distributions of p are significantly different according to spectral subgroups. In contrast with stars categorized as B5→B9.5, the distribution of those in the range B0→B2 does not peak at p values around zero. The same study examines correlations of p with $v \sin i$ and infrared excess, with an overall conclusion that the circumstellar envelopes for the majority of Be stars are optically thin discs with a range of the half-opening angles given by $10° < \Theta < 40°$.

The first suggestion that stars of B spectral type exhibiting emission in the Balmer lines carry intrinsic polarization appears at the end of a general stellar survey by Hall & Mikesell (1950). A comment is made there in respect of ζ Tau, a well-known Be shell star, on the unexpected high value of p for its small colour excess.

13.2.1
Polarimetric Spectral Behaviour

In a survey of the wavelength dependence of polarization, Coyne & Gehrels (1967) found several early-type stars with variable polarization, while a new tool in identifying early-type stars with intrinsic polarization was introduced by Serkowski (1968), and later extended by him (see Serkowski, 1970 and Figure 13.1). He found that emission-line stars exhibit a peculiar wavelength dependence of polarization,

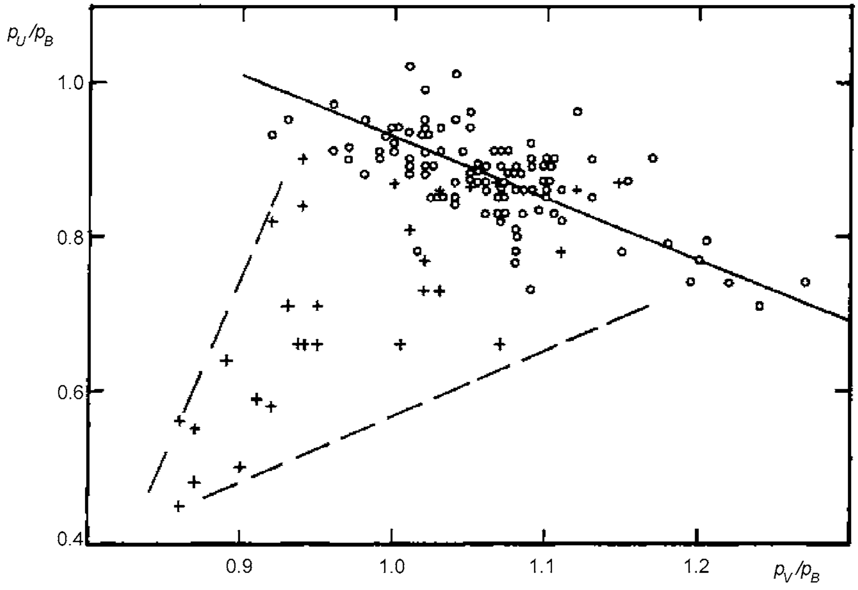

Fig. 13.1 A plot of p_U/p_B against p_V/p_B clearly distinguishes the intrinsic polarization associated with Be stars (+) relative to stars exhibiting interstellar polarization (o) which occupy a band in the upper part of the diagram (After Serkowski, 1970).

with low values in the ultraviolet with respect to the average interstellar $p(\lambda)$ curve. Using a series of broadband filters, Coyne & Kruszewski (1969) and Coyne (1971a) observed the $p(\lambda)$ curve in the region of 3000–10 000 Å in 19 Be stars. Although it was realized that interstellar polarization influenced some of the measurements, no real effort was made to remove its effects from the recorded values. With an observed anti-correlation of the $p(\lambda)$ curve with the bound-free absorption coefficient of hydrogen, and with dips in the polarization at the Balmer and Paschen limits being a fairly common feature, it was immediately apparent that the behaviour could be attributed to electron scattering in an asymmetric circumstellar cloud, modified by polarized radiation from hydrogen recombination and by hydrogen bound-free opacity.

Poeckert & Marlborough (1976) observed the linear polarization of 48 Be stars in two-colour bands near the Hα line, with the aim of exploring the relationship between the intrinsic p and $v \sin i$. It was found that intrinsic polarization depends strongly on $v \sin i$; stars with low $v \sin i$ displayed little, or no, polarization. No apparent difference between pole-on and extreme Be stars was obtained. It was found that from the relationship between the intrinsic p and $v \sin i$, and assuming thin discs, an envelope density of $\leq 5 \times 10^{11}\,\mathrm{cm}^{-3}$ can account for the levels of polarization recorded for all of their observed stars. A review of the status of the polarization associated with Be stars at the time of the mid-1970s was presented by Coyne (1976a). A review of studies of polarimetry of Be stars up to the early 1980s was presented by Coyne & McLean (1982).

Poeckert, Bastien & Landstreet (1979) conducted an intermediate-band survey of 70 Be stars, reducing their values to remove the contaminations of interstellar polarization. About half of the group exhibited intrinsic effects, but there was no single universal wavelength dependence that could be scaled to fit all Be stars. There were marked variations from star to star at the Balmer jump, and for the slope of the Paschen continuum.

A logical step in terms of experimental observations was the investigation of the spectral behaviour of the intrinsic polarization in the region of the Balmer emission lines themselves. In the very early 1960s, Tamburini & Thiessen (1961) had suggested from some observations of bright stars, including two Be types, that polarizational variations may occur within their spectral lines. This work was followed by similar reports by Clarke & Grainger (1965, 1966), but these latter results were prone to misinterpretation as a result of their experimental methodology. In 1972, at the Polarimetry Conference in Tucson, Arizona, Clarke & McLean (1974a) reported on a novel way to undertake polarimetric observations of the emission lines of Be stars using tilted narrow-band interference filters. Their system was applied to a study of γ Cas, and it was found that the intrinsic polarization dropped in the Hβ emission feature (see Clarke & McLean, 1974b and Figure 13.2).

This discovery was immediately followed with similar effects observed by Coyne (1974) in the Hα emission line of another Be star, ζ Tau. Further observations of γ Cas and ζ Tau at Hβ were made by Clarke & McLean (1976). An immediate interpretation was to consider that the emission radiation was unpolarized, and that the reduction of polarization depended on the strength of the emission line. For the Be star, 48 Per, despite the Balmer lines being in emission, no substantial polarimetric changes across Hβ were found. Further measurements at Hα and Hβ of several Be stars were discussed by McLean & Clarke (1976).

Hayes & Illing (1974) conducted polarimetric studies of the Hγ line of 10 stars, recording a decrease in p at the line centre of γ Cas, the only one selected as displaying intrinsic polarization. Other stars, chosen on the basis of being fast rotators, showed no polarimetric structure across the line. Later, Hayes (1975a) recorded a polarization reduction in the Hγ line of ζ Tau, but noted that, in relation to the strength of the emission, and the reduction of p relative to the continuum levels, it could not be ascribed simply to the addition of unpolarized flux.

Twelve Be stars were measured by Poeckert (1975) for polarimetric structure across the Hα line. Shell stars like ζ Tau were found to exhibit a decrease in polarization which was proportional to the strength of the emission component. Stars considered as being *pole-on* were found to have no significant changes in p, nor position angle, across the line. Observations of the polarization at Hα and Hβ were made by Coyne (1976b) of 28 Be stars. Twelve exhibited decreased polarization at these wavelengths, these tending to be stars with a shell spectrum or with large $v \sin i$.

From investigations of Southern Hemisphere Be stars, McLean & Clarke (1979) found that the polarization reductions in Hα and Hβ had a more complicated behaviour in relation to a simple unpolarized emission-line flux model. For η Cen, an increase in polarization was found in the cores of Hβ and Hα, the effect attributed

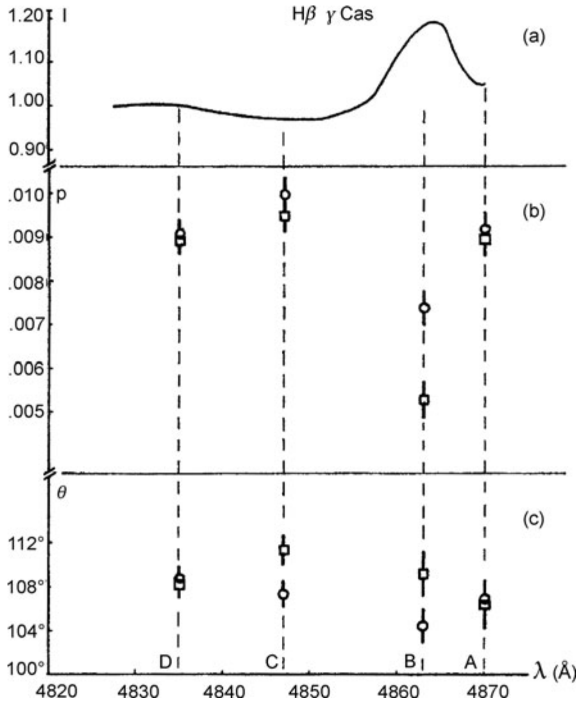

Fig. 13.2 Measurements of an apparent reduction of polarization across the Hβ emission feature in the spectrum of γ Cas made on two different nights in November, 1973 (see Clarke & McLean, 1974b). The upper curve (a) plots the intensity profile of the emission line, while (b) plots four spot measurements of p and (c) the polarization position angle at the selected wavelengths positions.

to shell-line absorption. For the observed stars, various strategies were explored to separate the intrinsic stellar polarization from any subsequent interstellar component, these involving information provided by field stars, the temporal behaviour of p, the application of Serkowski's law to the colour measurements, and the spectral behaviour of p across the Balmer emission lines.

Further attention to the emission line polarization of γ Cas was given by Poeckert & Marlborough (1977) who obtained a more detailed record of the behaviour across the Hα line, the most important feature being a near sinusoidal variation in the position angle across the emission. When plotted in the Stokes parameter plane, the wavelength scan provided a locus in the form of a loop. A model was presented based on a rotating disc, with the absorption along the line of sight dependent on both line and continuum absorption. As a result of Doppler shifts, in the blue wing, the radiation is coming from further within the stellar envelope on the receding side, with the converse for the light of the red wing. The strength of the effect depends on the inclination of the rotation axis, and a value of $i \approx 45°$ matched the behaviour of γ Cas. The sense of position angle change from $+/0/-$, or −/0/+, this also being reflected in the sense of execution with wavelength of the loop in the Stokes parameter plane, indicates the sense of rotation of the star; it may be noted that γ Cas rotates in a clockwise direction as seen from the Earth. With the addition of further polarimetric data, Poeckert & Marlborough (1978a) extended the model in two stages by developing it to fit the Hα line profile and the continuum polarization, giving good agreement for the continuum energy distribution and the Balmer decrement. The number of free parameters in the approach is large, and the sensitivity of their contributions was investigated by Poeckert & Marlborough (1978b). In order to determine the range over which the value of a particular parameter does not significantly affect observable features, and conversely, whether a particular observable can be used to constrain particular model parameters, they explored the effects caused by changes in the inclination, envelope density, envelope temperature, stellar effective temperature, rotation velocity, and expansion velocity. As might be expected, the polarimetric behaviour across emission lines and over the continuum was found to be sensitive to the inclination.

In addition to observations of the Hβ line, Clarke & Brooks (1984) observed several bright Be stars at the Ca II H and K lines. For those objects which exhibited polarization dips at Hβ, there appeared to be an enhancement of p in the calcium lines so revealing stratification in the polarigenic processes within the extended atmospheres.

A classical example of how spectropolarimetric measurements can be used to separate the intrinsic and interstellar components is provided by Coyne & McLean (1975) in connection with the Be star, ϕ Per. This star has since been studied at higher spectral resolution, and with greater spectral coverage, by Clarke & Bjorkman (1998). By combining the resolved elements to provide better polarimetric accuracy, the intrinsic component was again separated from the interstellar effect. The nature of the noted temporal changes suggest that the discs surrounding the component stars of this binary are inclined to the orbital plane. For the record, sample data related to this latter study are presented in Figure 13.3, these providing testament as to how the application of 2D detectors has advanced the information gathering power of spectropolarimetry relative to the earlier sequential scanning techniques as used to produce Figure 13.2.

Spectral resolution of Hβ polarimetry was greatly improved by McLean, Coyne, Frecker, *et al.* (1979) with measurements made of γ Cas, ϕ Per, ψ Per and ζ Tau, using a Digicon detector. In comparing their results, it is obvious that the increased spectral resolution required deeper explanations for the recorded behaviour. For example, the locus of the measurements for γ Cas at Hβ displayed a far more complicated behaviour than that recorded earlier by Poeckert & Marlborough (1977). The wavelength progression of p crosses the intrinsic line at several points, without any coherent sense as to the direction of rotation, so negating any interpretation of the sense of rotation of the star, as suggested by Poeckert & Marlborough (1977). Although the q, u loci of the spectral behaviour across Hβ for the four stars measured by McLean, Coyne, Frecker, *et al.* (1979) are very different, some similarities emerged. The polarization decreases as the line centre is approached from either wing; at the line centre itself, the polarization increases, and has secondary max-

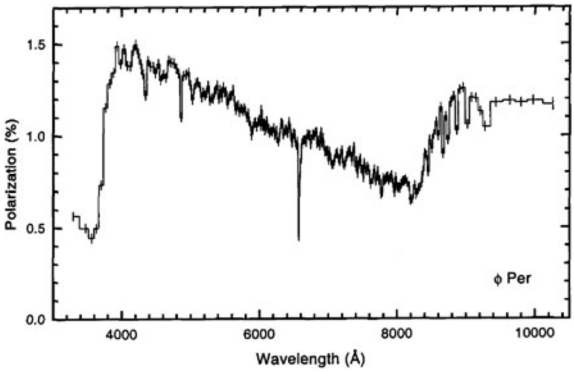

Fig. 13.3 A representative sample of spectropolarimetric data of the Be star, ϕ Per, recorded at the Pine Bluff Observatory of the University of Wisconsin. Note the relatively smooth decline of p across the visible spectrum between the Balmer and Paschen jumps, with polarization reductions at Hα, Hβ and Hγ. (Taken from Clarke & Bjorkman, 1998.)

ima and minima in the wings out to $\Delta\lambda \approx \pm 10$ Å. In addition there are small variations in the intrinsic polarization azimuth across the line. The behaviour of two stars (γ Cas and ϕ Per) is displayed in Figure 13.4.

The basic models involving Thomson scattering predict that the polarization between the Lyman and Balmer limits should have a wavelength dependence similar to that observed in the optical region between the Balmer and Paschen limits. When the first space-borne ultraviolet observations were made of Be stars, Bjorkman, Nordsieck, Code *et al.* (1991) found that the continuum $p(\lambda)$ was close to being flat or slowly declining shortward of the Balmer jump with broad dips around 1700 and 1900 Å, suggesting that they are produced by Fe line attenuation effects. This diagnosis is supported by optical data for ζ Tau with similar polarization drops exhibited across the Fe II lines.

A new dimension to the polarimetric behaviour of Be stars emerged through the infrared survey by the IRAS satellite. From the analysis of 101 objects by Coté & Waters (1987), it was found that the visual (4250 Å) polarization increased according to the colour excess ($V - 12\,\mu$m), but, for any particular value of excess, there was a range of p values that a star might exhibit up to a maximum level. This behaviour is displayed in Figure 13.5 and its form is similar that of the distributions of stars with interstellar polarization and colour excess $E_{(B-V)}$, as in Figure 10.2. In simplistic terms, it might be suggested that the recorded intrinsic p values for Be stars result from the vector addition of the generated polarization from various parts of the extended atmosphere, with the sum depending on the associated vibration azimuths, while the amount of free–free emission is given more simply by the algebraic sum over the atmosphere.

In a follow-up to the observations of infrared excess, Waters & Marlborough (1992) explored a simple model, and concluded that the combination of polarization and infrared excess does not put strong constraints on the geometry of the

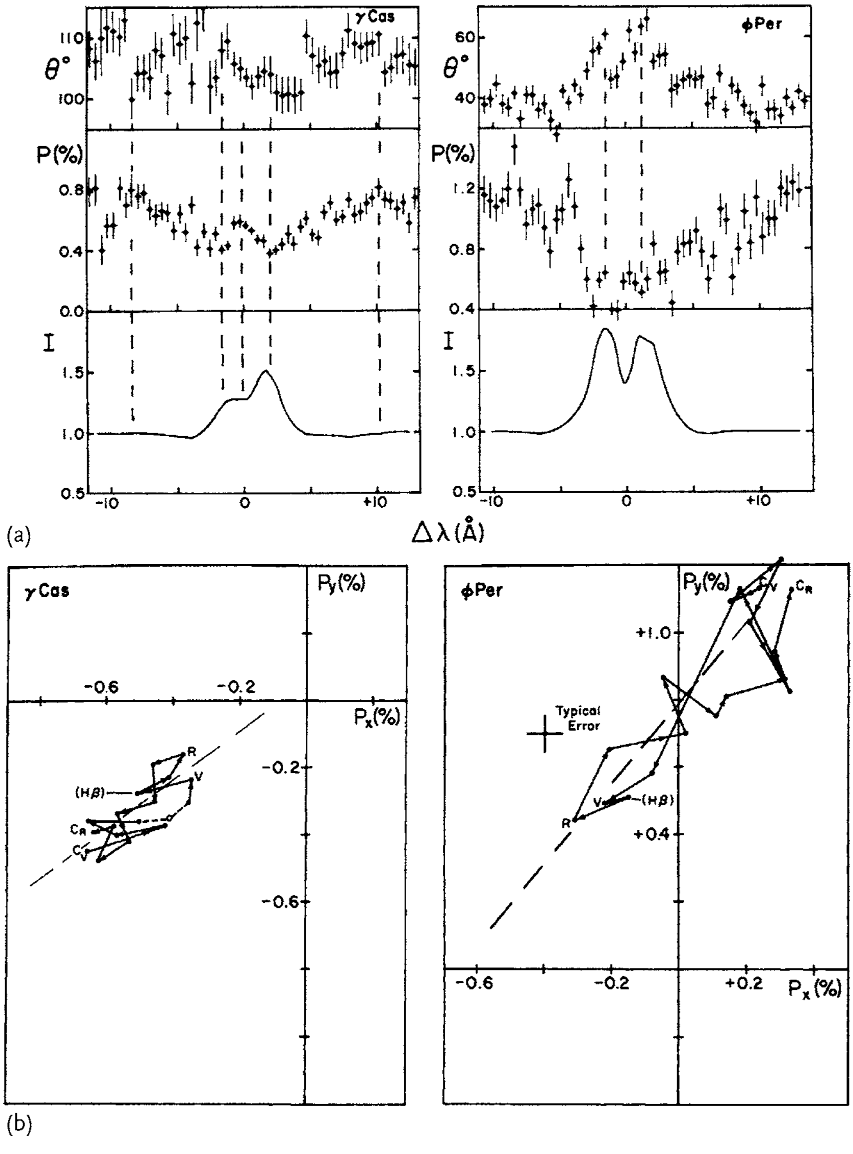

Fig. 13.4 (a) displays the polarimetric behaviour (p and $\theta \equiv \zeta$) of γ Cas and ϕ Per across the Hβ emission line; (b) display this complicated behaviour in the qu-plane; R, V correspond to the dips in the red and violet portions of the emission, and C_R, C_V are the continuum values in the red and violet, respectively. (Taken from McLean, Coyne, Frecker, *et al.*, 1979.)

stellar discs. It was demonstrated that a wide range of opening angles can produce a polarization and infrared excess in agreement with the observations.

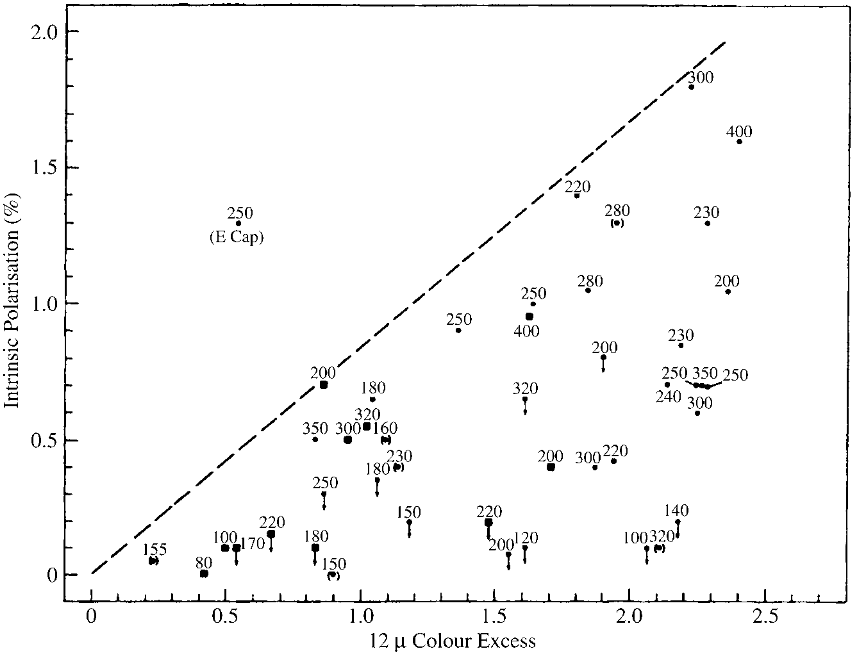

Fig. 13.5 The triangular distribution of Be stars from measurements of colour excess (V — 12 µm) plotted against the intrinsic polarization at 4250 Å; dots (●) indicate B0 to B4 stars, while squares (■) are for B5 to B9.5. The upper limits for p are indicated by the dashed line. (Taken from Coté & Waters, 1987.)

Because of the nature of the spectra of Be stars it is generally impossible to detect the presence of any magnetic field by classical Zeeman splitting diagnostics. However, there is possible scope for field detections by investigating the Hanle effect as outlined by Ignace, Nordsieck & Cassinelli (1997). They found that the integrated line polarization is $\propto \sin^2 i$; in some cases the position angle of the polarization in the line can be rotated by 90° relative to the the zero field case. Based on the Hanle effect, it was concluded that polarimetry of UV and visible resonance lines offers means of detecting fields in the range 1–1000 G in stellar winds. Other references related to this topic can be found in Section 9.2.5.

13.2.2
Temporal Variations

Polarization which is variable must be intrinsic to the star. Behr (1959) was first to observe variable polarization in an early-type emission line star, this being γ Cas (B0 1Ve). Polarization variability was also found for χ Oph (B2 IIIpe) by Shakhovskoi (1962).

Variability on short time scales was confirmed for γ Cas by Piirola (1979) who made observations over three nights, monitoring the changes occurring over intervals of a few hours. These data were later investigated by Clarke (1990) who showed that the three colour measurements provide a well-defined intrinsic line. Setting this as the intrinsic direction, $q_\star$, it was suggested that a period of $0.^{\mathrm{d}}59$ might be present in the $u_\star$ parameter, seen best in the B-band, this corresponding to the rotational period, or perhaps half its value. With much longer observing windows, and hence better accuracy for any deduced period, it may be noted that Smith, Henry & Vishniac (2006) have discovered a photometric light-curve with an amplitude $0.^{\mathrm{m}}006$, giving a rotational period for γ Cas of $1.^{\mathrm{d}}21581 \pm 0.^{\mathrm{d}}00004$, this being twice that suggested by polarimetry.

The time scales on which polarimetry is seen to be variable can be short. For example, Rodriguez (1978) found that γ Cas and ζ Tau varied from night-to-night, and that the former star exhibited significant rapid variations on a time scale of a few minutes.

Confirmation that Be stars are generally polarimetric variables was presented by Coyne (1975). He observed 11 Be stars and found that 6 exhibited variable polarization with an amplitude in the V-band of about 40% on the mean level, the maximum change taking place over an interval of hundreds of days. Superimposed on these changes, there are smaller fluctuations occurring on timescales of a few days.

Polarimetric variations in the V-band for κ Dra have been reported by Arsenijević, Jankov, Djurašević, *et al.* (1986) over a 5-year interval. These data have been analysed by Clarke (1990), and again a well-defined intrinsic line was found. The variability is not just confined to being along this direction, this suggesting that the surrounding envelope does not change simply in a homogeneous manner. An attempt was made to determine a periodicity associated with the rotation of the star; although a period of $\sim 0.^{\mathrm{d}}79$ was suggested, the result does not carry high significance. According to Clarke & Brooks (1983), κ Dra does not display polarimetric variations across the Hβ line, but presents an unusual enhancement of p at the centre of the Ca II K line. The effect can be considered to arise as a result of a shell absorbing more of the direct starlight relative to the light scattered by the extended atmosphere.

The Be star, o And, displays a complex behaviour and has been catalogued as an eclipsing binary. It is known to have lost its shell characteristics several times since 1897. According to Coyne (1976b), the polarization at Hα is the same as in the nearby continuum. Arsenijević, Vince & Kubičela (1979) monitored the star over a 3-year period (1974–1977), suggesting that there was an anti-correlation between the level of polarization and brightness. In 1975, p was at a maximum, and there were some obvious jump-like daily changes. Over a 9-month period in 1979, Hayes & Terrance (1980) found no significant variability in p at the 0.015% level.

From five selected stars chosen by Hayes (1980) as presenting a close to pole-on aspect, only ω Ori displayed variability. The star was later monitored using both photometry and polarimetry by Hayes & Guinan (1984). According to Figure 13.6, the temporal behaviour reveals that the polarization rises dramatically over a few days, and then falls with a slower decay. When the data are plotted in the Stokes parameter plane, the locus follows a well-defined intrinsic line as indicated in Figure 13.7, this being drawn following a least squares fitting to the data. The be-

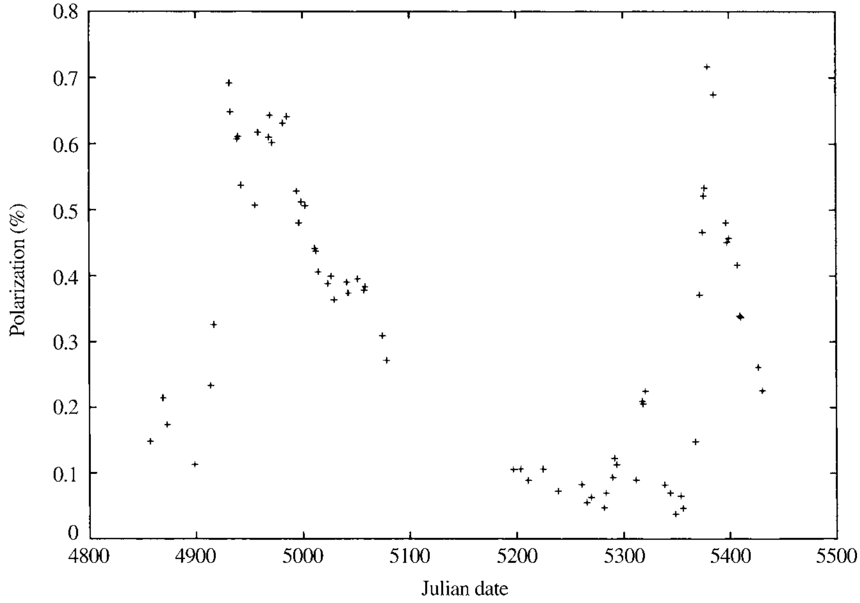

Fig. 13.6 Two mass loss events are displayed for ω Ori showing a rapid rise of the recorded polarization followed by a slow decay. (The JD is 2 440 000+). (Data taken from Hayes & Guinan, 1984 and Sonneborn, Grady, Chi-Chao Wu, *et al.*, 1988.)

haviour was ascribed to effects of mass loss, but with the scattering material preserving axial symmetry. Over a monitored mass loss episode, they found a strong correlation between the variations of continuum photometry and polarimetry, with Hα line photometry also being correlated, but to a lesser extent. The increase in envelope mass during the event was estimated to be $> 6 \times 10^{-11}\ M_{\odot}$. A further mass loss episode was monitored by B-band polarimetry, but with a more comprehensive diagnosis by Sonneborn, Grady, Chi-Chao Wu, *et al.* (1988) involving inclusion of other multi-parameter observational material. Variations in visual colours and continuum fluxes were correlated with p. The lack of correlation between the highly ionized stellar wind, as observed in IUE spectra, and the continuum polarization and flux variations, was interpreted as evidence for the spatial separation of the wind-accelerated zone and the inner portion of the envelope. Similarly, the lack of correlation between the Hα fluxes and continuum changes was interpreted as indicating that the Hα line-formation zone is much more extended than the regions of the envelope where the stellar wind lines and the polarization are formed. A straightforward interpretation of the available data is that the continuum polarization, continuum-magnitude changes, and colour changes are produced in an equatorial disc close to the stellar photosphere.

In an exercise to relate the variable optical polarization and UV narrow absorption lines in Be stars, Brown & Henrichs (1987) considered the data for ω Ori. It was concluded that there are two types of mass loss occurring. One involves ap-

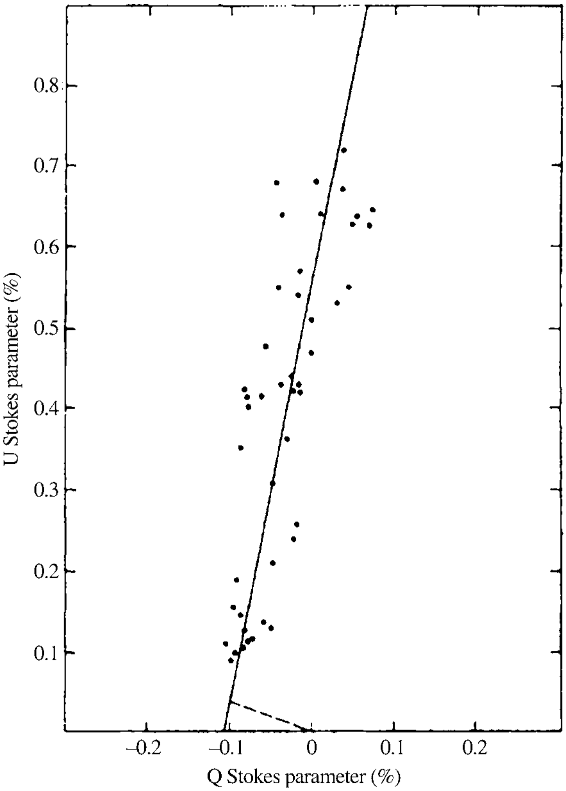

Fig. 13.7 *B*-band polarization measurements of ω Ori over the interval Sep 9, 1981 to Nov 10, 1982 follow a path along an intrinsic line, indicating that the underlying mass loss event has maintained axial symmetry. The dashed line denotes the interstellar polarization deduced from field stars. (Taken from Hayes & Guinan, 1984.)

proximately spherical shell enhancements of the normal wind, these lasting $\lesssim 20$ days and are responsible for narrow UV line transients, but are not sufficiently dense, or aspherical, to give polarimetric signals. The second is in the form of episodic mass ejections lasting $\gtrsim 40$ days, affecting the global distribution of the circumstellar disc material. The polarization grows along the intrinsic line, the direction corresponding to the projection of the stellar equator; both optical and Hα photometry display correlated changes with p. Closer inspection of the $u_\star$ values, as they scatter about the intrinsic line suggest an oscillatory behaviour as the polarization grows and declines along the intrinsic $q_\star$ direction. A period search on the intrinsic $u_\star$ values by the author was inconclusive in relation to the photometric period of $0.^{d}99$, or double light-curve of $0.^{d}525$, discovered by Balona, Marang, Monderen, *et al.* (1987), as the polarization behaviour was sampled with too large a time interval. It would be profitable to conduct polarimetry in a concentrated way over a number of consecutive nights. A careful study of the data behaviour possibly indicates that the decay around JD 5000+ has intrinsic $u_\star$ values providing a local mean that is not zero; the effect can be seen in the mid section of the plot in Figure 13.7 where the data points tend to lie on the left of the intrinsic line. This would indicate that the dispersal of the ejected material is not exactly axisymmetric.

The Be star, X Per = HD 24534, became of particular interest when it was proposed to correspond to the X-ray source 3U 0352 + 30. An extensive observational programme was undertaken by Kemp & Barbour (1983) who obtained 400 measurements on 356 nights during 1977–1982. According to their analysis, part of the polarimetric variability was correlated with a then promoted 580^{d} radial velocity cycle. Later, Clarke & McGale (1988) reworked the data with a variety of reduction methods, and promoted the presence of a very significant and much shorter period of $23.^{\mathrm{h}}95 \pm 0.^{\mathrm{h}}95$, commenting that X Per behaves as an oblique rotator with $i = 50° \pm 10°$, with the scattering source located at high stellar latitude. This short period occurs in the periodogram of Kemp & Barbour (1983), but is not clearly presented, being located at a break in the sectioned graph. Such a period is, of course, awkwardly close to values that can be artificially generated by taking nightly measurements, but care was taken in assessing this potential problem. Possible polarizational changes across Hα and Hβ were investigated by Clarke & McLean (1975) with a null result.

As part of an exercise to measure the polarization of 14 Be stars, Lin & Zihe (1988) made special comment on 8 of them which had been observed on 6 or more nights. It was claimed that all of them exhibited temporal changes, but without any intrinsic lines being obvious. For CX Dra, when the Stokes parameters were phased on a period which is half the known orbital period of this binary system, both q and u presented a clear oscillation.

Annual monitoring of the long-term temporal behaviour of a number of brighter Be stars has been conducted by McDavid (1986, 1990, 1994), his work covering an interval of 9 years. No strong cases of night-to-night variability were discovered, and only π Aqr displayed significant long term variations, with a comment that these could be readily explained by changes in the circumstellar electron number density.

13.3
Disc Orientations

Polarimetry of Be stars can provide information related to the projection angle of the plane of the circumstellar disc on the celestial sphere. With the advancing technology of stellar interferometry being able to resolve extended stellar envelopes, results from the different diagnostic procedures can be compared. If the polarization is produced from the disc with little contribution by scattering from material near the stellar poles, the direction of vibration of the intrinsic polarization, $\zeta_\star$, is perpendicular to the plane of the disc. Hence, the polarimetric position angle will be perpendicular to the position angle of the major axis, ϕ, of the elongated structure as defined by interferometry, i. e., $\phi = \zeta_\star + \pi/2$.

By using long-baseline interferometry at Hα, Quirrenbach, Hummel, Buscher, *et al.* (1993) determined the asymmetry of γ Cas and noted that the elongation was at right angles to the polarization angle supporting the standard interpretation of p generated by electron scattering in a flattened envelope, or disc. Later, Quirrenbach, Buscher, Mozurkewich, *et al.* (1994) reported that they also had resolved the disc of ζ Tau at Hα. Their maximum-entropy map again provided strong evidence for the presence of a disc-like structure. Later, Vakili, Mourard, Stee, *et al.* (1998) recorded developments in the equatorial disc of this star, concluding that it exhibits a prograde one-armed oscillation. The disc itself is inclined at an angle of 122° (N through E). The engendered position angle of the polarization produced by electron scattering would be $122° - 90° \sim 32°$, which matches the observed value.

Interferometry of seven Be stars at Hα with contemporaneous spectropolarimetry was undertaken by Quirrenbach, Bjorkman, Bjorkman, *et al.* (1997) with the aim of relating any non-sphericity in the spatial structure of the image to the position angle of the polarization. Great care was exercised to remove the contaminations of interstellar polarization, in particular using the measurements across the Balmer jump. For the four stars with well-defined intrinsic polarization position angles, their levels of intrinsic polarization were the highest, and they also displayed the largest elongations in their interferometric images. The stars, γ Cas, ϕ Per, ψ Per and ζ Tau, all gave excellent agreement between the elongation directions and position angles of the polarization. Since the interferometric and polarimetric position angles are orthogonal to each other, optically thick and/or geometrically thick envelopes can be ruled out as these would have the polarization position angle parallel to the plane of the disc. An overall conclusion from the study was that the disc paradigm for Be stars is preferred over alternative mildly ellipsoidal scenarios.

Interferometric studies of γ Cas at Hα by Tycner, Hajain, Mozurkewich, *et al.* (2003) provide an axial ratio of 0.79 ± 0.03, with a position angle of the axis at $32° \pm 5°$. According to Quirrenbach, Bjorkman, Bjorkman, *et al.* (1997), the resolved disc axis is set at $19° \pm 2°$, this being closer to the value of $112.°4 - 90° = 22.°4$, as provided from the analysis of polarimetric data by Clarke (1990).

For some young objects, polarization maps have been imaged about the star and the situation has been modelled by Bastien & Ménard (1990) in terms of multiple scattering in flattened, optically thick, structures. The model predicts the presence of circular polarization, and this has been detected in a few of the stars which have been mapped. The size of the optically thick part of the disc is determinable from the observations, as well as the inclination of the disc to the line of sight.

13.4
Be Star Models

As is the case in many areas of astrophysics, modelling of a particular phenomenon is sometimes undertaken on a star by star basis to match particular observations, or is considered in a more general, universal way. Both kinds of approach are evident in the study of Be stars.

For example, relative to the star match approach, an extension of a basic model of Shakhovskoi (1965) was presented by Capps, Coyne & Dyck (1973) to explore the spectral polarimetric behaviour of ζ Tau, with the inclusion of a free-free emission component to explain the decrease of the polarization in the infrared (out to 2.2 μm). Their proposed geometry was simplistic with the star embedded in a homogeneous, isothermal, completely ionized disc of hydrogen, seen edge-on. By assuming the disc radiation to be unpolarized, the observed degree of polarization takes a simple form

$$p_\nu = \frac{f_\mathrm{p} f_\mathrm{s} S_\nu}{S_\nu(\mathrm{e}^{-\tau} + f_\mathrm{s}) + D_\nu} , \tag{13.1}$$

where S_ν is the flux of the star in the absence of the disc, D_ν is the flux for disc resulting from recombination and free-free emission, $f_\mathrm{s} S_\nu$ is the stellar flux scattered towards the observer, f_p is the fraction of the scattered energy which is completely linearly polarized, and τ is the scattering optical depth of the disc.

Considering the disc to be optically thin, and approximating the geometry as a point source illuminating a physically thin disc, the polarization as a function of wavelength reduces to

$$p_\nu = \frac{3\tau}{16(1 + D_\nu/S_\nu) - 7\tau} , \tag{13.2}$$

where $\tau = N_\mathrm{e}\sigma_\mathrm{e}(R_\mathrm{o} - R_\mathrm{i})$, with R_o and R_i being the outer and inner radii of the disc, respectively; N_e is the number density of the electrons, each with a scattering cross-section, σ_e. By exploring this equation with realistic values, the behaviour of p_ν offered an excellent fit to observations of ζ Tau across the visible spectrum.

The basics of the polarigenic process in Be stars is summarized in the scenario presented by Nordsieck, Babler, Bjorkman, *et al.* (1992), as in Figure 13.8. When the unresolved star is observed, the measured light comprises the summation of scattered radiation from elements within the circumstellar atmosphere added to the predominant direct contribution from the star itself. According to the simple cartoon, the polarization generated by a scattering element may be expressed as

$$p = p(\theta)\frac{L_\mathrm{sca}}{L_\star + L_\mathrm{sca}} \approx p(\theta)\frac{L_\mathrm{sca}}{L_\star} , \tag{13.3}$$

where L_sca and $L_\star$ are the fluxes received from the scattering element and directly from the star itself, and $p(\theta)$ the generated polarization at a scattering angle, θ. In turn, this may be written as

$$p \approx \frac{\Omega}{4\pi} p_\mathrm{max} g(\theta)\tau_\mathrm{s}(1 - \tau_\mathrm{a})D(r) , \tag{13.4}$$

where Ω is the solid angle of the elemental scattering volume as seen from the stellar surface, p_max is the maximum polarization that is generated by the scatterers and, for electrons, this occurring at a phase angle of 90°; $g(\theta)$ is the polarization

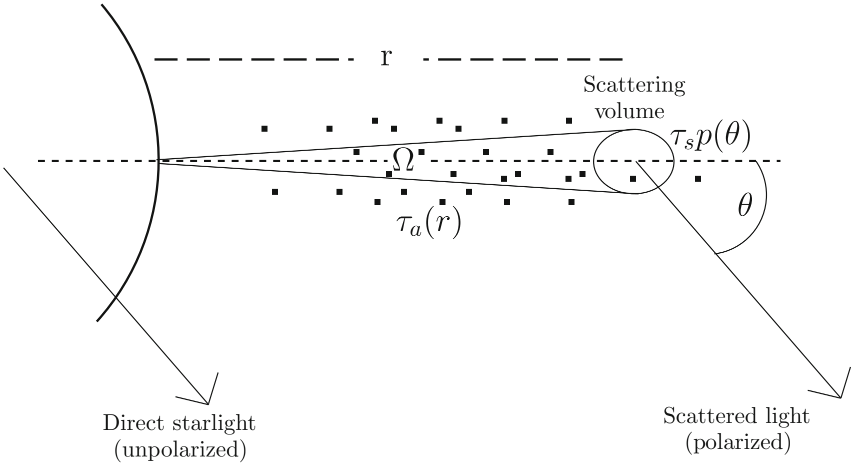

Fig. 13.8 Localized scattering by a volume of electrons within an extended stellar atmosphere shows that, at distance, r, the subtended angle is Ω, with the received illumination being attenuated by the optical depth $\tau_a(r)$ between the star and the volume. The polarized flux of the emerging radiation according to the phase angle, θ, from the volume with optical depth, τ_s, is expressed as $p(\theta)$. (After Nordsieck, Babler, Bjorkman, *et al.*, 1992.)

scattering efficiency at any angle, θ; τ_s is the scattering optical depth, τ_a, the absorptive optical depth between the star and the scattering volume, and $D(r)$ is the geometric dilution factor resulting from the star having a finite size and offering a range of scattering angles for the received radiation entering the scattering volume.

Modelling for the production of the overall intrinsic polarizations of Be stars was first developed to the more general level by Brown & McLean (1977). They considered ionized envelopes surrounding a source star with axial symmetry, this direction set at an inclination, i, to the line of sight. The polarization produced from the scattering is expressed as

$$p = \frac{\sin^2 i}{2\alpha + \sin^2 i}\,, \tag{13.5}$$

with $\alpha = (1+\gamma)/(1-3\gamma)$, where γ is a shape factor defined by the ratio of two moments of the density distribution of the scattering centres (electrons) in spherical coordinates, and relates the oblateness (or prolateness) of the envelope. With the addition of the direct unpolarized radiation from the star, the observed polarization may then be expressed as $\approx 2\bar{\tau}(1-3\gamma)\sin^2 i$, where $\bar{\tau}$ is a mean scattering optical depth, assumed to be small. This immediately shows that the observed behaviour generally depends on the geometric aspect of the star. Maximum polarization for a given geometry is displayed when the inclination is at 90° to the line of sight, i. e. the stellar equator is edge-on. If the star is viewed pole-on, although scattering with subsequent polarization occurs, the directions of vibration from the various portions around the equator present a circular symmetry so that the overall polarization reduces to zero.

For a selection of Be stars observed such that their i values are at random, McLean & Brown (1978) provided an expression for the statistical distribution of the parameter $p = 2\bar{\tau}(1 - 3\gamma)$, after removing the effects of the $\sin^2 i$ term, using a classical inversion technique. At the same time, the distribution of equatorial rotational velocity, v, was investigated by the same process from the values of $v \sin i$. Using data for 67 Be stars, for which the interstellar component had been removed, it was concluded that p is strongly skewed to small values for which the presented polarizations are hardest to measure and to separate from any interstellar component. The effect of the inclination of each individual star can be eliminated by using a parameter defined by the ratio of p to the square of the apparent rotational velocity, i. e.

$$k = \frac{2\bar{\tau}(1 - 3\gamma)}{v^2} \; . \tag{13.6}$$

A wide range of k values ensued, but with a fairly well-defined limit of $k \sim 3 \times 10^{-7}$ (km $\mathrm{s}^{-1})^{-2}$, reflecting the fact that there are few Be stars which have both low equatorial velocity and large intrinsic polarization.

Cassinelli, Nordsieck & Murison (1987) established equations to describe the polarigenic potential of an axially symmetric distribution of electrons around a star. By firstly considering the star as a point source, and then developing the model to allow for the finite size of the star, a factor was derived to correct the bench mark model of Brown & McLean (1977). This was later generalized by Brown, Carlaw & Cassinelli (1989) with the development taking account of the finite size of the stellar disc relative to a point source, and to the effects this has by providing a range of illuminating angles on any point within the envelope.

It was found that, for any Rayleigh/Thomson scattering, a depolarization factor can be derived for any spatial distribution of scatterers with its functional form, $D(\mu_\star)$, depending on the limb darkening law. A correction factor was also derived for the total intensity of Rayleigh scattered light, this depending only on the observer's direction described by i, and on $\mu_\star$. The finite stellar disc factor was found to reduce the polarization to typically less than one half that of the point star predictions.

As well as the depolarizing effect produced by considering the illuminating source to have finite size, the effect of the stellar disc occulting part of the envelope has been considered by Brown & Fox (1989) for a flat envelope viewed edge-on. For the case of an axisymmetric envelope, they showed that, for a wide variety of radial density distributions, any point source model grossly overestimates the resultant polarization by not considering occultation, and the spread in the directions of illumination of the circumstellar material. It was concluded that the observed polarizations ($p \sim 1\%$) of Be stars demand highly flattened, optically thin disc envelopes. For the special case of edge-on viewing, effects of occultation reduce the polarization more than the depolarizing effects caused by the illuminating source having finite size. This work was extended by Fox & Brown (1991) to cover the effects of viewing flat envelopes at arbitrary inclination. For an axisymmetric disc scattering region viewed at low inclination, stellar occultation enhances the expected net polarization, while at high inclination, the polarization is reduced by occultation. Their analysis was also applied to the variation of polarization from binary systems in which the scattering material consists of a rotating one-dimensional plume between the stars, superposed on an axisymmetric disc. They showed that the inclination of the system and the radial structure of the plume can be deduced for sufficiently high inclinations ($i > 60°$). The extent to which the method can be generalized to an arbitrarily distributed two-dimensional scattering region was considered via Fourier analysis. It was found that the inclination of the system is largely insensitive to the density distribution when the distribution function is of a simple power-law form. The question was also raised that for some stars, the polar mass loss will have a greater ionization fraction than the equatorial region, such that the pole might be the dominant source for free electrons.

In the third paper of this series, Fox (1991) considered the effects of occultation and finite sized-source depolarization, concluding that the net polarization has a complicated inclination dependence, and that the simple result of it being $p \propto \sin^2 i$, obtained by Brown & McLean (1977), does not hold. For Be stars with high intrinsic polarizations, the circumstellar envelope must be concentrated either towards equatorial or polar regions, and that a substantial optical depth is required with $\tau > 0.05$.

The possible variability of the observed polarization from an obliquely rotating envelope has been investigated by Fox (1992), such a scenario having been mooted by others as being an alternative interpretation to diagnoses involving binary motion, but with lack of spectroscopic evidence to add weight to such duplicity. The results of the exercise were not too sanguine as it was evident that effects due to rotation about a body axis and binary orbital motion are indistinguishable. It was also found that the physical geometry of the obliquely rotating envelope could not be inferred. When the light source is considered to have finite extent, discrimination between envelope geometries emerges to some degree as a result of the occultation of parts of the envelope by the extended source.

Further modelling by Fox (1993a) has emphasized the effect that an extended light source has on the resulting polarization by scattering in circumstellar envelopes. If the underlying star is non-spherical, as a result of its large rotational velocity say, its photosphere will also generate a net polarization, adding to that which is produced by scattering within the extended atmosphere. This situation has been modelled by Fox (1993a) who found that, in general, the predicted polarization was a factor of 2–3 times larger than what is observed for Be star systems. It was also noted that the theoretical models for Be star envelopes had not yet reached a level of sophistication to estimate by polarimetry the number density of free electrons throughout the circumstellar envelope. The origin of stellar winds in Be stars may be influenced by magnetic fields and Fox (1993b) has considered this additional parameter in polarimetric models. From his analysis, the range of observed values of p can be explained if the stars possess small magnetic fields of $B_0 < 100\,\mathrm{G}$. Observed increases in p during the onset of a shell phase is indicative of an increased magnetic field.

To allow interpretation of synoptic polarimetric measurements of Be stars, Clarke & McGale (1986) have explored the behaviour of a stochastic model whereby small localized scattering clouds, or globules, appear at specific positions defined by stellar polar coordinates, and at various distances from the star for a range of viewing angles according to the stellar inclination. The pseudo-data distributions in the qu-plane showed that globules ejected randomly in stellar azimuth and latitude do not translate to a random data density distribution in the qu-plane. It was proposed that real data might be compared with the simulations to infer the basic geometries and astrophysical processes giving rise to any recorded polarization fluctuations.

The problem of inferring mass loss distributions in time and polar angle have been explored by Brown & Wood (1992) to see how these might be obtained from observed polarimetric and absorption line strength variations. They considered the numerical application of analytic inversions to both simulated and the real data associated with ω Ori.

Using a Monte Carlo radiative transfer code, Wood, Bjorkman, Whitney, *et al.* (1996a) have investigated the effects of multiple scattering within axisymmetric circumstellar envelopes. Contrary to immediate expectation, they found that multiple scattering tends to increase the expected polarization, as the scattering predominantly arises within the optically thick parts of the disc; the orientation of the scattering planes for these multiply scattered photons is biased towards a common direction, that being the plane of the disc. In the absence of any absorptive opacity, which would reduce the number of multiple scatterings, resultant polarization levels of order 3–4% are expected in circumstellar discs. The exercise was also undertaken by considering the stellar source to have finite angular extent. Rather than their being a depolarization effect as appears in single-scattering calculations, an enhancement of polarization also occurs. This happens because more photons enter the disc from a finite star than from the more highly attenuated point source; these additional photons are multiply scattered, raising the polarization for a finite star above that for a point-source star. If multiple scattering occurs in any stellar system, caution must be taken in applying single-scattering, or point-source approximations, to place constraints on circumstellar geometries by polarimetry. Multiple scattering can have a dramatic effect on the predicted polarization levels, possibly producing a 90° flip of the position angle.

The computational scheme above has been extended by Wood, Bjorkman, Whitney, *et al.* (1996b) to include absorptive opacity. According to the level of this parameter, the resultant polarization reduces to become similar to the levels predicted by schemes involving single scattering with attenuation. An important consequence of this relates to wavelengths around an ionization edge such as the Balmer jump. Much larger changes in p are predicted relative to single-scattering plus attenuation approximations. This arises because just shortward of the jump, the absorptive opacity is large and the polarization approaches the level associated with single-scattering plus attenuation; just longward of the jump, where the absorptive opacity a small, multiple scattering is dominant and the polarization is larger than the single-scattering plus attenuation prediction. For these reasons, the combined effects of multiple scattering, plus absorptive opacity, provides much larger polarization discontinuities at the Balmer jump than previous predictions. For geometrically thick equatorial disc-like geometries, a position angle flip of 90° can occur shortward of the Balmer jump as the large hydrogen opacity absorbs the multiply scattered photons in the disc, the polarization dominated by singly scattered photons from the polar regions producing negative values of Q.

Using a Monte Carlo radiative transfer code in respect of spectropolarimetric data, Wood, Bjorkman & Bjorkman (1997) investigated possible geometries for ζ Tau. It turned out that the observations could be mimicked by either a geometrically thin disc, with a half-opening angle of $2.^\circ5$, or a thick disc with a half-opening angle of 56°. Key to determining which option should be preferred is the prediction for the thin disc model to produce a polarization flip at 12 µm, so that it is orthogonal relative to what is recorded in the visible spectrum.

As for interpretations and modelling of $p(\lambda)$ and the intrinsic polarizations associated with the emission lines themselves, McLean (1979) discussed the issues with physical insight. The paper demonstrates that all axisymmetric, quasi-optically thin Be star envelopes have approximately the same form of $p(\lambda)$ in the continuum and that the behaviour is controlled by the average properties of the envelope. The size of the oscillation of the position angle across the emission lines, as well as depending on the optical depths of the envelope, is shown to be proportional to $\cos i$.

A numerical model for the behaviour of γ Cas was presented by Poeckert & Marlborough (1978a) by assuming a density distribution in a rotating, expanding envelope, with the hydrogen level populations determined appropriately at points through the envelope. The Balmer line intensities and polarimetric profiles were then determined by integrating the equation of radiative transfer along the lines of sight, and so including stellar disc occultation effects in the process. The exercise was successful in predicting the observed behaviour across the Hα line.

An investigation of the physical factors that control the behaviour of $p(\lambda)$ and $\zeta(\lambda)$ across emission line profiles has been made by Wood, Brown & Fox (1993) based on Thomson scattering in an optically thin circumstellar cloud which is subject to bulk motions in the form of a rotating and/or expanding disc. The value of p is asymmetric about the line centre and stronger in the red wing unless there is no disc expansion. Changes in ζ across the line occur through the symmetry breaking effects of stellar occultation of the scattering material, and the combination of rotation and expansion of the disc. A symmetric p profile indicates envelope rotation, while profiles which show stronger p in the red wing indicate expansion of a scattering region. The ratio of p in the red and blue wings should lead to information on the ratios of expansion to rotation velocities.

In a later paper, Wood & Brown (1994a) developed the model by considering the star to act as a monochromatic source for scattering by a rotating and expanding disc, the assumption being reasonably realistic, the line broadening being dominated by the scattering rather than in its origins. By assuming certain parametric forms for the disc velocity and density distributions, analytic expressions were obtained for the wavelength dependence of the scattered profiles in terms of the velocity and density model parameters, and of the inclination of the disc. This modelling approach allows potentially powerful diagnostic use of high-resolution spectropolarimetric data. The outcome is, however, effected by the thermal motions of the scattering electrons in the circumstellar disc, as demonstrated by Wood & Brown (1994b). They have shown that the random thermal component of the electron bulk velocity has a smearing effect on the scattered spectral features compared to resultant spectropolarimetric line profiles from electrons moving with only the bulk velocity components of disc rotation, or expansion. This analysis shows that it is not possible to determine the line profile behaviour of the polarization simply be convolving the results of the previous cold electron scattering model with a thermal smearing function. The determination of disc inclinations, as promoted by the previous models, is unaffected by the disc being hot, however.

A generic model based on Monte Carlo techniques, applied to the scattering off rotating discs, and suitable for application to the geometries of several kinds of stellar object, has been presented by Vink, Harries & Drew (2005) for the exploration of polarimetric line profiles. A major finding was that there is a marked difference between scattering of line emission by a disc that reaches to the stellar surface, relative to a disc with an inner hole. For the case of an inner hole, the position angle rotation across the line profile causes a single loop if $p(\lambda)$ is plotted in the qu-plane; for a disc which is uninterrupted up to the stellar surface, the locus of the $p(\lambda)$ variation produces a double loop.

13.5
Herbig Ae/Be Stars

An important astrophysical problem of the day concerns the dynamo generation of magnetic fields in stellar interiors, and the effects such as magnetic braking of young, fast rotating stars. The study of Herbig Ae/Be (HAEBE) stars is especially important in this regard.

The Be star, HD 45677, was found by Coyne & Vrba (1976) to have a peculiar $p(\lambda)$ form, with a rise into the infrared to 1 μm, and with no maximum value being evident. The polarization, particularly in the red, also exhibited temporal variability. With relation to other supporting evidence, the polarimetric behaviour was ascribed to a combination of Thomson scattering with a substantial addition of scattering by circumstellar dust, with a gas-to-dust ratio being an order of magnitude smaller than the interstellar medium. The Be object MWC 349 (= V 1478 Cyg) was noted to have a high value of p by Elvius (1974), and this discovery was followed up by a series of R-band measurements by Yudin (1996). The object displays marked temporal variability, and some of the observed polarization is generated by scattering from a circumstellar dust disc. It is classified as a B[e] star.

Fourteen Herbig Ae/Be stars were measured in five colour bands by Petrova & Shevchenko (1987). Most of the program stars exhibited polarization which was indistinguishable from having an interstellar origin. Four of them [BD +46° 3471, BD +65° 1637, HD 200775 and Lk Hα 234] exhibited temporal changes, however.

A synoptic polarimetric study of some 60 Southern Hemisphere peculiar early-type stars, including Herbig Ae/Be objects, was undertaken by Yudin & Evans (1998) with a view to investigate variability on time scales of minutes... hours... and days. In addition to the presentation of the results, this work provides many references to previous polarimetry of HAEBE stars.

A study of the Herbig Ae star, AB Aur, was undertaken by Catala, Böhm, Donati, *et al.* (1993). Although the lines of Fe II 5018 Å and He I 5876 Å were photometrically spectacularly variable, circular polarization in the former line was surprisingly not detected. An upper limit of 1 kG was assigned to the photospheric magnetic field. The same star was observed by Beskrovnaya, Pogodin, Najdenov, *et al.* (1995) for short-term spectral and polarimetric fluctuations. Particularly from the behaviour of the P Cyg-type profile of Hα, they demonstrated that there were connections to circumstellar inhomogeneities moving in the envelope. Broadband polarimetry showed variations over a few hours and on longer time scales. Pontefract, Drew, Harries, *et al.* (2000) later performed spectropolarimetry at Hα for this star and found that there is an intrinsic linear polarized emission component suggesting scattering in a rotating circumstellar disc. The locus in the qu-plane of the measurements across the emission profile displayed a loop (see Figure 13.9).

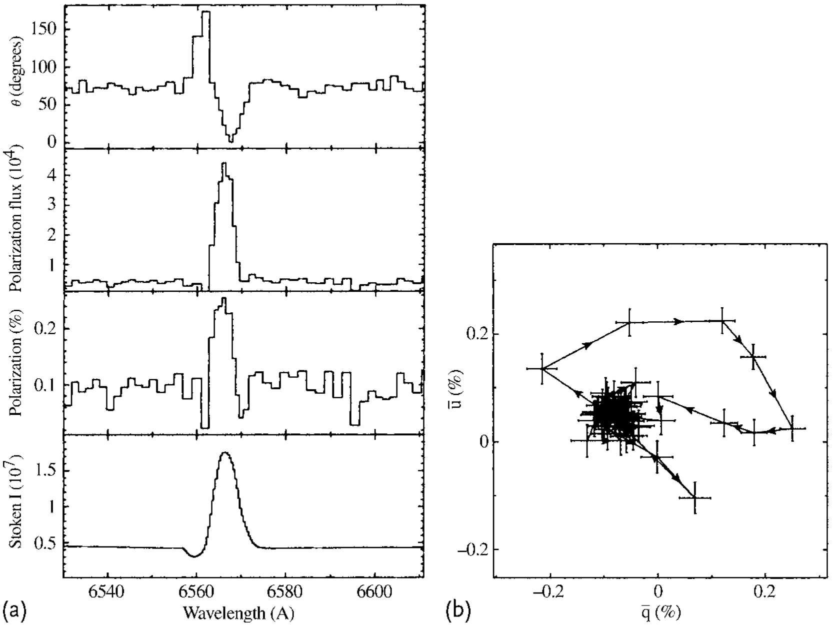

Fig. 13.9 The polarization spectrum of AB Aur around Hα is displayed in (a). The polarization values have been binned with a varying wavelength interval so that each plotted value carries an identical uncertainty of ±0.03%; (b) depicts the NSPs for AB Aur in the region of Hα showing a knot of values corresponding to the continuum. The large loop in the upper portion of (b) is associated with the line emission; the small excursion of lower (b) corresponds to the absorption feature bluewards of the main emission – see the bottom curve of (a). (Both figures are taken from Pontefract, Drew, Harries, *et al.*, 2000.)

There was also a spike-like excursion across the blue-shifted absorption feature, the position of this matching the orientation of a highly inclined disc recorded as a long-wavelength image by other observers.

As part of a spectroscopic campaign of observations of HD 163296 (Herbig Ae), Beskrovnaya, Pogodin, Yudin, *et al.* (1998) reported on Q, U, V polarimetry over a 13 night run. The nightly means for the U parameter for each of three colours (VRI) revealed steady night-to-night increases, but superimposed on this trend, a sinusoidal oscillation with amplitude $\sim$0.1%, and a period of $P = 7.^{\mathrm{d}}5 \pm 0.^{\mathrm{d}}3$, was noted. The variations in the Q parameter were less distinct, but could also be fitted by a sinusoidal curve with the same period, and shifted in phase by $\pi/4$ relative the variation of U. Low levels of circular polarization (V parameter) were claimed seemingly to increase across the spectrum from the B-band to the I-band. Variations of the nightly means were correlated with those of p. These results implied the presence of aligned particles in the circumstellar environment.

Beskrovnaya, Pogodin, Miroshnichenko, *et al.* (1999) have also undertaken a multi-parameter study of the Herbig Ae candidate, HD 36112, including polarimetry. As with other classical Herbig Ae stars, long-term trends and more rapid changes during a single night were recorded. The variations are in accord with the hypothesis of orbital motion of different circumstellar inhomogeneities rotating in the common flattened gaseous-dusty envelope.

A two-colour study by Clarke, Smith & Yudin (1999) of the Herbig Be star, HD 100546, showed polarimetric variability that was likely caused by changes in the distribution of dust within the stellar environment. The young Herbig Ae star, HD 139614, has also been shown to be a polarimetric variable by Yudin, Clarke & Smith (1999) and, in the same paper, comments are made on the differences of polarimetric behaviour of Vega-type stars.

Photopolarimetric activity of the classical Ae/Be star RR Tau has been discussed by Rostopchina, Grinin, Okazaki, *et al.* (1997). This star has a photometric variability of 4^{m} in the V-band. The value of p anti-correlates with brightness changes. In addition, colour–magnitude diagrams display a strange behaviour with the colour index having the same values at maximum and minimum light, this being referred to as the *turnaround* effect. The overall behaviour of RR Tau is classical with respect to a set of young stars exhibiting non-periodic Algol-type minima, UX Ori being the prototype, giving rise to a category of stars referred to as UXORs. The behaviour of p is predicted in the framework of a variable circumstellar extinction model, and is a result of the screening of the young star by opaque fragments, or clouds, in the protoplanetary disc (Grinin's model). After estimating the interstellar component for RR Tau, numerical modelling of the intrinsic polarization together with the colour–magnitude diagrams indicates that the revolving circumstellar disc around this star is strongly flattened, and seen edge on, or under small inclination to the line of sight. The characteristic size of the grains are intermediate between that of interstellar dust and dust in the old protoplantery disc. It is thought to be a young progenitor of a β Pictoris-type star. The disc of this latter star has been imaged with polarization vector maps by Gledhill, Scarrott & Wolstencroft (1991) and Wolstencroft, Scarrott & Gledhill (1995). Modelling of the dust disc has been undertaken by Voshchinnikov & Krügel (1999), with the result that grains have refractive index in the R-band of $m_R = 1.152 - 0.005i$, with size distribution expressed by $n(a) \sim a^{-3.2}$, the decreasing number density with distance from the star being expressed by r^{-3}.

Oudmaijer & Drew (1999) have presented data of the polarization structures across the Hα emission lines in several B[e] and Herbig Be stars. All the B[e] stars showed large changes of p, ζ across the Hα emission features, whereas only about half the Herbig Be objects displayed polarization changes.

A comprehensive analysis of the correlations between the polarimetric and photometric characteristics of Ae/Be stars has been made by Yudin (2000). There is a general relationship between the optical polarization and the infrared colour index $(V - L)_{\rm obs}$, and the colour excess, $E_{(V-L)}$, as a result of circumstellar dust shells. Most young stars have statistically larger values of p in comparison with stars which are at an evolutionary stage prior to their arrival at the main sequence. The notion that the polarimetric behaviours of young stars relate to the evolution of their circumstellar shells has been strongly promoted.

Polarimetric changes across Hα are generally very evident in Herbig Ae/Be stars, as reported in an observational study of a sample of 23 objects by Vink, Drew, Harries, *et al.* (2002). From their observations, they note that the signatures for Ae stars differ from Be objects, with depolarization across Hα in Be stars, and with polarization enhancements in the Ae group. It has been suggested that the differences in behaviour may be an indication that there is a transition in the HR diagram from magnetic accretion at spectral type A, to disc accretion at spectral type B. Alternatively, the interior polarized line emission apparent in Ae stars may be masked in Herbig Be stars, owing to their higher levels of Hα emission.

A search for the presence of magnetic fields in three Ae stars was made by Hubrig, Schöller & Yudin (2004) using circular polarization line wing measurements. A longitudinal field of -450 ± 93 G was measured for HD 139614, and suspected field detections were reported for HD 144432 and HD 144668. For the latter two stars, circular polarization signatures were noted in the Ca II K line.

13.6
Early-Type Supergiants

From repeated measurements of a sample of 20 early-type supergiant stars, Coyne (1971b) presented evidence to show that their $p(\lambda)$ curves differ from Serkowski's law, and also tend to display variable polarization with amplitudes ranging from 0.2% to 0.5%.

Ten emission-line O stars were monitored by Hayes (1975b) over a 7-month period. His measurements revealed that four of them exhibited variable polarization, with a tentative conclusion that the behaviour depended on spectral classification distinctions which attempt to identify the presence of extended envelopes.

A campaign to monitor the polarimetric behaviour of λ Cep was undertaken by Hayes (1978). Over an interval spanning 32 months, 74 observations were made during 31 nights. The measurements indicated evidence for polarization variability on a timescale of about a day, but shorter term sampling during several nights of observation provided no indication of more rapid variability.

Temporal polarization variations of the early-type supergiants, κ Cas (B1 Ia) and α Cam (09.5 Ia), were monitored by Hayes (1984). For both stars, plots of the measurements in the qu-plane provided a fairly random distribution but with 'ordered' changes when the data points of individual observing runs were linked with time arrows. The morphologies of the variations, seen from night to night, suggested that the measurements relate to waxing and waning of non-periodic envelope clumpiness. Over the winter of 1984–1985, Rigel (β Ori A – B8Ia) was observed by Hayes (1986) on 68 occasions over 55 nights. The variable behaviour revealed episodes of substantially enhanced aperiodic activity, with coherent movements in the qu-plane, the excursions having a range of directions. Such temporal patterns are interpreted as manifestations of spatial invariant mass loss.

Low spectral resolution polarimetry has been performed by Lupie & Nordsieck (1987) for 10 OB supergiants and O emission-line stars. Seven of the program stars exhibited random fluctuations at the 0.2–0.4% level, on time scales of several days to months. For the sample, admittedly small, the polarization variations are large for slow rotators and objects with large Hα emission components. The basic interpretation is one involving electron scattering by density enhanced blobs embedded in the stellar wind. The same study has also be presented as a PhD Thesis by Lupie (1983).

The first ultraviolet spectropolarimetric measurements of hot supergiants were reported by Taylor, Code, Nordsieck, *et al.* (1991) for P Cyg and κ Cas. For the former object, its intrinsic polarization remained at a fairly constant level in the Balmer continuum, except for a broad dip between 2600 and 3000 Å, this contrary behaviour to the then current model. This feature was considered in terms of possible Fe line blanketing. The intrinsic polarization of κ Cas is small, most of the observed value being a result of the interstellar medium. The curve, extrapolated from the visual region for the Serkowski law, falls consistently below the values observed in the ultraviolet.

Nine of the brightest northern O stars have been reassessed by McDavid (2000) using $UBVRI$ polarimetry. Comparison with earlier measurements shows no clearly defined long-term variability. For all nine stars, the $p(\lambda)$ behaviour can be fitted by the standard interstellar law. The position angles are also consistent with neighbouring field stars. The simplest conclusion of this work is that the polarization of all the program stars is primarily interstellar. This is somewhat disconcerting in view of claims of variability by other observers, and may well reflect noise problems in their studies which were not identified at the time. Two cases of possible small-amplitude, short-term periodic variability is suggested to correlate with contemporaneous Hα and ultraviolet spectrometry.

The issue of whether O-type stars which, from their spectra, are known to possess variable wind structures has been taken up by Clarke, McDavid, Smith, *et al.* (2002). For ξ Per and λ Cep, analysis of a series of measurements made on single nights with individual uncertainties of $\Delta p \sim \pm 0.0002$, with nightly means carrying uncertainties of $\Delta p \sim \pm 0.00007$, suggested night-to-night variations with $\delta p \sim 0.0002$. It was suggested that such low-level fluctuations might be engendered by structured instrumental polarization in the stellar diffraction pattern, and instrumental depolarization effects that will induce polarimetric noise according to inconsistent target acquisition and/or the action of variable seeing conditions. Reassessment of the older data for λ Cep from Hayes (1978) also suggested that his claims for the detection of variability of this star suffer from the same problems. Whether or not such supergiant stars do exhibit polarization variability requires further observational work, with careful attention being paid to the stability of repeated measurements.

With the advent of CCD spectropolarimetry, Harries & Howarth (1996) have investigated the Hα emission line of ζ Pup (O4 I(n)f). Although data from their instrument suffered from polarizance fringes, a correction procedure was applied with the results showing that there is a polarization signature across the Hα emission of this star. The feature is attributed to an equatorial density enhancement of the wind, their numerical model suggesting a factor of 1.3 for the equator-to-pole density ratio.

Harries (2000) has applied Monte Carlo principles to set up stellar wind radiative-transfer codes. Effects of co-rotating spiral density enhancements and also effects of clumpiness within the wind were investigated. Although the test runs reproduce the observed spectrometric variability of OB supergiants, the suggested polarimetric variability of these models is too weak to explain the observed behaviour of these stars. A predicted spectral line polarization was noted resulting from line absorption of continuum photons in a rotating wind, the effect having a strong resemblance to the Hα polarimetric signal recorded by Harries & Howarth (1996) for ζ Pup. It is suggested that the recorded behaviour stems from this effect, rather than by line dilution of a continuum polarization.

It is of interest to note that an attempt was made by Hanbury Brown, David & Allan (1974) to measure the diameter of the supergiant β Ori with orthogonal polarizations, using the Narrabri stellar intensity interferometer, in an attempt to detect any geometric distortion of the star's corona. No significant changes of correlation were detected for the two polarizations, with no changes in the apparent diameter of the star. An assessment of the possibility of success with this kind of observational technique was undertaken by Sams & Johnston (1974) using stellar models to predict the polarization. It was concluded that the sensitivity would require improvements of 20 times, or more, to detect photospheric polarization in early-type stars. In view of the success of other interferometric observations at Hα in respect of Be stars with disc structures, as described in Section 13.3, neglect of application of the intensity interferometer at this wavelength would seem to have missed out on making a substantial contribution here.

13.7
Wolf–Rayet (WR) Stars

For binary systems, phased-locked variations can be used to determine some of the basic orbital characteristics such as a value for the inclination, this being very important for resolving the mass function. The distribution of scattering material around any system may be established with estimates for the rate of mass loss. Schulte-Ladbeck (1989) discussed the importance of knowing the masses of Wolf–Rayet binaries in respect of their evolution, and she emphasized the role that polarimetry plays in helping to establish a catalogue of values. The appendix of her work provides a summary of 10 such systems. For single stars, polarization variability provides information on asymmetries and inhomogeneities (blobs) in the stellar wind.

As early as 1946, Kopal & Shapley (1946) suggested that the eclipsing Wolf–Rayet, V 444 Cyg, was an ideal system for investigation by polarimetry. From the light curve, they concluded that the main cause of extinction in the semi-transparent envelope surrounding the WR component is scattering by free electrons, and, in turn, this would produce a small polarized flux best seen several hours before and after primary minimum. Monitoring the variation of p should provide an estimate of the proportion of the light scattered, and allow determination of the longitude of the node of the binary system.

Early polarimetric observations of a WR star were those of McLean, Coyne, Frecker, *et al.* (1979) using a spectral resolution of $\sim$50 Å, revealing that the prominent emission lines of HD 50896 = WR 6 = EZ CMa, a WN5-type star, exhibited decreases of polarization relative to the continuum. The behaviour suggested stratification of ionization and excitation in the extended atmosphere, with the recombination lines of He II being formed deeper than those of He I, so that the ionization is decreasing outwards. The continuum polarization is typical of almost pure electron scattering, suggesting that the envelope must be highly ionized and flattened to some degree, or localized. Later, McLean (1980) showed that the system had a polarimetric period of $1.^{d}88$, this being the second harmonic of the $3.^{d}76$ value associated with photometric and spectroscopic modulations. Determination of i was made difficult because of aperiodic instabilities, but a value of $\sim 71^\circ$ was suggested, implying a 1.3 $M_\odot$ companion for the 10 $M_\odot$ primary star. As a result of a photometric and polarimetric campaign, Drissen, Robert, Lamontagne, *et al.* (1989) found that the shapes of both the light curve and the polarimetric curve changed over 2 months, but maintained the periodicity. From high spectral resolution measurements, Schulte-Ladbeck, Nordsieck, Nook, *et al.* (1990) revealed that the position angle of the polarization changed across the emission lines such that loops were executed in the qu-plane. Such behaviour may be explained in terms of there being a rotating, expanding disc in the system.

The behaviour of the emission lines was explored further by Moffat & Piirola (1993) who found their polarization variation $\sim$0.3% was very much less than that of the continuum $\sim$1.6%. For two other non-eclipsing WC7 + O binaries, they found no variation in the emission complex of C III/IV 4650 Å + He II 4685 Å, in contrast to the continuum modulation which provided period determinations. This is perhaps to be expected in such binary systems if the orbital polarization modulation is due mainly to scattering of O-companion light off free electrons in a hot, dense, spherically symmetric WR wind; there is little or no asymmetric distribution of free electrons off which WR emission line and continuum photons can scatter and produce detectable polarization.

The Wolf–Rayet binary system, HD 152270, has been observed by Luna (1982) and, from the phase-locked measurements, an inclination of 35° was calculated, allowing determination of the stellar masses.

St-Louis, Drissen, Moffat, *et al.* (1987) presented the first paper from the group in Montreal discussing the results of polarimetric variability in the complete sample of southern WC stars. Two stars exhibited a double-wave behaviour expected of binary systems with an asymmetric distribution of scattering material within an orbiting system. For HD 97152, an inclination of $i = 43.^\circ5 \pm 5^\circ$ was deduced, while for HD 152270, the determined value was $i = 44.^\circ8 \pm 5^\circ$.

The WN7 binary system of HD 197406 (WR 148) was investigated polarimetrically by Drissen, Lamontagne, Moffat, *et al.* (1986). From analysis of the oscillatory behaviour of the measurements in the qu-plane, they determined an inclination of the orbit of $\approx 67^\circ$, yielding a mass of 12.4 $M_\odot$ for the unseen companion, based on a mass of 60 $M_\odot$ for the primary, with speculation that the secondary is an X-ray quiet black hole.

Drissen, Moffat, Bastien, *et al.* (1986) conducted a concentrated campaign of measurements of the WN7 binary, CQ Cep (HD 214419), which displays large polarization variations $\approx$0.8%. They demonstrated that the second harmonic of the fundamental period was dominant, as can be appreciated by inspection of Figure 13.10. Determination of the Fourier coefficients of the fundamental and second harmonic provided a value of $i \approx 78^\circ \pm 1^\circ$, with masses of 42 $M_\odot$ and 30 $M_\odot$ for the WN7 star and the unseen O star companion, respectively.

From five-colour measurements of CQ Cep and V444 Cyg, Piirola & Linnaluoto (1988) conclude that the polarization is generated by electron scattering in an optically thin envelope with determinations of $i = 78.^\circ1 \pm 1.^\circ7$, and $i = 83.^\circ5 \pm 1.^\circ1$, respectively.

Robert, Moffat, Bastien, *et al.* (1990) have also investigated the polarimetric behaviour of V 444 Cyg and determined a value of $i = 78.^\circ5$, in agreement with Rudy & Kemp (1978) and Piirola & Linnaluoto (1988). Their data also showed rapid fluctuations around phase 0.5 when the O star eclipses the scattering electrons located in the dense inner wind.

As well as discussing binary systems, St-Louis, Drissen, Moffat, *et al.* (1987) described the stochastic behaviour of three single line stars. The randomness of the variability of the WN8 star, HD 96548 = WR 40, is clearly portrayed in Figure 13.11, there being no structure to the time progression of the measurements when plotted in the qu-plane. In an immediate following paper, Drissen, St-Louis, Moffat, *et al.* (1987) presented results of a survey of southern galactic WN stars, all of which displayed apparently random variations with amplitudes from $\Delta p = 0.15$–0.6%. Combining these results with the data on WC stars, they found a general anti-

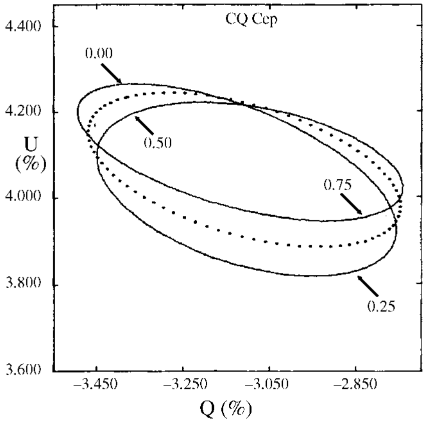

Fig. 13.10 The fitted periodic variation of the polarization of CQ Cep plotted in the qu-plane. The solid curve is based on the best fit of the original data to a Fourier series up to the second harmonic, the arrowed points indicating the phase of the variation; the dotted locus represents only second harmonic terms, these dominating the behaviour of this star. (Taken from Drissen, Moffat, Bastien, *et al.*, 1986.)

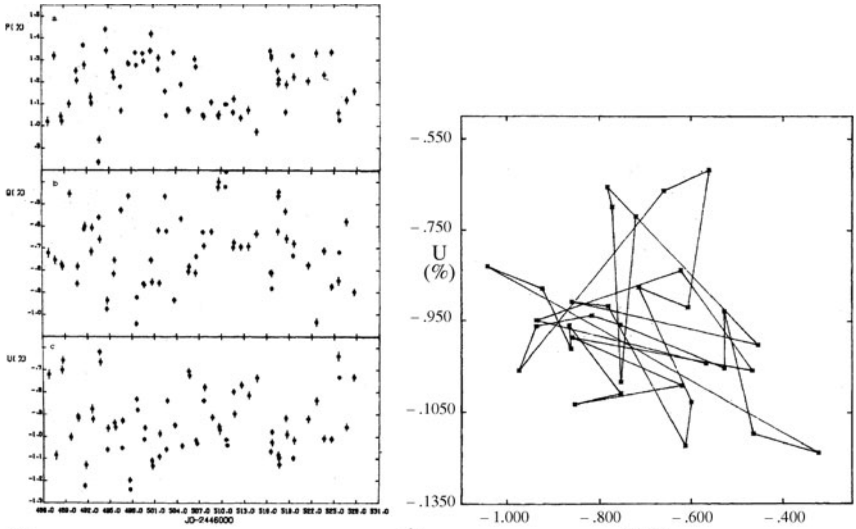

(a) (b)

Fig. 13.11 The spot measurements of p, q and u of the WN8 star, HD 96548 (WR 40) are plotted in (a) and exhibit an apparent random variation with time. The randomness of the polarization variations is clearly apparent in the qu-plane plot in (b) the points joined in time sequence. (Both figures are taken from Drissen, St-Louis, Moffat, *et al.*, 1987.)

correlation between the terminal velocity of the wind and the amplitude of the polarimetric variations.

Robert & Moffat (1989) have presented more evidence of linear polarization variability ∼0.5% in Wolf–Rayet stars, but also report on observations directed to the detection of circular polarization. They obtained a null result at the $\delta v \pm 0.01\%$ level.

Drissen, Robert & Moffat (1992) reported on measurements of three Wolf–Rayet stars thought to be single. Over an interval of a month, WR 14 showed no variation above levels of the experimental noise. For WR 25 and WR 69, small variations seem to appear at random times which may be interpreted as stochastic instabilities in the stellar winds.

Robert, Moffat, Bastien *et al.* (1989) provided data on six WR stars showing random, low-amplitude fluctuations on time scales of hours to days. In combination with data for previously measured stars, they confirm that the degree of scatter in the polarization is correlated with spectral sub-class and terminal velocity of the wind. They propose the presence of propagating 'blobs' which form, survive, and/or grow more easily in slower winds, especially for WN stars (compared with WC stars). A simple 'blob scenario' was also investigated by Fox & Henrichs (1994) who showed that the generated polarization would be more readily detectable than any associated changes in the UV spectrum.

Brown, Richardson, Antokhin, *et al.* (1995) have considered the effects of the blobs in the stellar winds of WR stars. After establishing the observational effects that the blobs have on photometry, spectrometry and polarimetry, they suggest how coordinated observations would help to unravel the ambiguities that the simple approach of applying just one of the experimental disciplines introduces. It is known that observations reveal that the ratio of the rms fluctuations on the photometric and polarimetric signals is $\simeq 0.05$, whereas it would be expected to be ~ 1 if the localized enhancements are in the form of individual optically thin packages of electrons which scatter some fraction of the star's light in the observer's direction. The reduction of the ratio can be achieved by considering that the observed polarization might be reduced by the vector addition of the polarizations accruing from enhancements, with a range of phase angles associated with the geometry of the scattering. Richardson, Brown & Simmons (1996) have investigated the statistics of the problem and arrive at the conclusion that multiple inhomogeneities or blobs cannot explain the discrepancy.

13.8
Luminous Blue Variables

The luminous B2 supergiant, HD 80077, was monitored by Knoechel & Moffat (1982) using spectroscopy, photometry and polarimetry. From data of the latter diagnostic, a period of $21.^{d}1$ was determined, the star being highlighted as among the brightest known B-type supergiant in the Galaxy.

Following a visual brightness increase, Schulte-Ladbeck, Clayton & Meade (1993) undertook spectropolarimetry of the luminous blue variable (LBV) star, AG Car, and the LMC variable, R 127. For AG Car, the position angle of the intrinsic polarization is aligned with a major axis of the ring nebula and perpendicular to the 'jet'. In R 127, the polarization is perpendicular to two bright features of the local material. These observations provide strong evidence that the asymmetries seen in the surroundings of these LBVs originate in the underlying stars.

AG Car became the subject of a more detailed paper by Schulte-Ladbeck, Clayton, Hillier, *et al.* (1994). The Hα emission line profile exhibits very extended wings that are differently polarized in amount and position angle relative to both the line core and the continuum, suggesting an origin by electron scattering in a dense wind. The polarization exhibits large temporal variations indicating significant variations in the envelope opacity. The general polarization varies along a preferred position angle of $\sim 145°$, this direction interpreted as a symmetry axis of the stellar wind. Its direction is co-aligned with the major axis of the AG Car ring nebula and perpendicular to the star's jet. The temporal polarization variability of AG Car was confirmed by Leitherer, Allen, Altner, *et al.* (1994), who also extended the polarimetry of this object into the ultraviolet.

Schulte-Ladbeck, Leitherer, Clayton, *et al.* (1993) undertook colour filter measurements of R 127 in the Large Magellanic Cloud. The polarization at Hα decreased with respect to the continuum. They assumed that Hα line is recombination dominated, and thus intrinsically unpolarized, so allowing the interstellar polarization to be estimated. The intrinsic polarization was determined to be of the order of 1% → 1.5%, implying both the presence of copious free electrons and a considerable asphericity in their distribution.

Parthasarathy, Jain & Bhatt (2000) have made *UBVRI* measurements of HR Car, and noted large temporal changes in the level of p, and also in the form of $p(\lambda)$. Spectropolarimetry of this object was also conducted by Clampin, Schulte-Ladbeck, Nota, *et al.* (1995). Changes of polarization across the Hα emission line were noted. Both these papers imply that the scattering material close to the star does not have a spherically symmetrical distribution, and that the behaviour is consistent with the bi-polar geometry imaged by others using a coronographic technique.

Spectropolarimetry has been undertaken of LBVs in our Galaxy and in the Magellanic Clouds by Davies, Oudmaijer & Vink (2005). They showed that many of their selected objects exhibit polarimetric signatures across the Hα emission line, indicating that the light from the stars is intrinsically polarized, and that asphericity already exists at the base of the wind. Four of the target stars displayed polarization variability with three of them, AG Car, HR Car and P Cyg, providing temporal position angle changes which appeared random. Such behaviour can be explained by the presence of strong wind-inhomogeneities, or 'clumps' within the wind. Only one star, R 127, exhibited p variations along an intrinsic line, with evidence of axial symmetry, as well as clumpiness. However, if viewed at low inclination, and with limited temporal sampling, such a wind would produce a seemingly random polarization of the type observed in the other three stars.

Modelling of the polarimetric behaviour of hot stellar winds has been undertaken by Davies, Vink & Oudmaijer (2007) with the conclusion that the variability can be reproduced by either of two regimes. The first is summarized by the action of one or a small number of massive, optically thick clumps; the second relates to a very large number of low-mass clumps. The predicted polarization scales linearly with mass-loss rate, and the study suggests that all hot stars with very large mass-loss rates should display polarimetric variability. This is consistent in that intrinsic polarizations are more common in stars with strong Hα emission.

References

References to Introduction

Cassinelli, J.P., Haisch, B.M. (1974) Polarization by rotationally distorted electron scattering atmospheres. *ApJ*, **188**, 101–104. [273]

Chandrasekhar, S. (1946) On the radiative equilibrium of a stellar atmosphere. X. *ApJ*, **103**, 351–370. [273]

Collins II, G.W. (1970) Intrinsic polarization on nongray atmospheres. *ApJ*, **159**, 583–591. [273]

Haisch, B.M., Cassinelli, J.P. (1976) Theoretical wavelength dependence of polarization in early-type stars. *ApJ*, **208**, 253–266. [273]

Harrington, J.P. (1970) Polarization of radiation from stellar atmospheres. The grey case. *Astrophys. Space Sci.*, **8**, 227–242. [273]

Harrington, J.P., Collins II, G.W. (1968) Intrinsic polarization of rapidly rotating early type stars. *ApJ*, **151**, 1051–1056. [273]

Loskutov, V.M. (1987) Polarization of the emission of hot stars. *Sov. Astron.*, **31**, 395–398. [273]

Ruciński, S.M. (1970) An upper limit to the Chandrasekhar polarization in early-type stars. *Acta Astron.*, **20**, 1–12. [273]

References to Be Stars

Arsenijević, J., Vince, I., Kubičela, A. (1979) Some light polarization changes of o And. Proceedings of the III National Conference of Yugoslav astronomers, Belgrade, 1977. Union of Societies of Mathematicians, Physicists and Astronomers of Yugoslavia, Belgrade, 1979. *Publ. Astron. Opseratorije Beogr.*, **26**, 125–132. [282]

Arsenijević, J., Jankov, S., Djuraševič, G., Vince, I. (1986) Variations of the linear optical polarization of κ Draconis. *Bull. Obs. Astron. Belgrade*, **136**, 6–11. [282]

Balona, L.A., Marang, F., Monderen, P., Reitermann, A., Zickgraf, F.-J. (1987) The short-period photometric variability of four Be stars. *A&AS*, **71**, 11–24. [284]

Behr, A. (1959) Die interstellare Polarisation des Sternlichts in Sonnennumgebung. *Veröff. der Univ.-Sternwarte zu Göttingen*, **7**, (Nr. 126), pp. 199–256. [281]

Bjorkman, K.S., Nordsieck, K.H., Code, A.D., Anderson, C.M., Babler, B.L., Clayton, G.C., Magalhães, A.M., Meade, M.R., Nook, M.A., Schulte-Ladbeck, R.E., Taylor, M., Whitney, B.A. (1991) First ultra-violet spectropolarimetry of Be stars from the Wisconsin ultraviolet photo-polarimeter experiment. *ApJ*, **383**, L67–L70. [279]

Brown, J.C., Henrichs, H.F. (1987) The relation between the visual polarization and UV narrow absorption lines in irregular Be star variations. *A&A*, **182**, 107–114. [283]

Clarke, D. (1990) Temporal polarization variations of Be Stars V. Comments, similar behaviour of γ Cassiopeiae and κ Draconis. *A&A*, **227**, 151–155. [282, 282]

Clarke, D., Bjorkman, K.S. (1998) On the polarization of ϕ Persei. *A&A*, **331**, 1059–1065. [278, 279]

Clarke, D., Brooks, A. (1983) Enhanced polarization in the CaII K line in the Be Star κ Dra. *MNRAS*, **205**, 9P–13P. [282]

Clarke, D., Brooks, A. (1984) Polarization measurements of Be Stars at Hβ and CaII H and K. *MNRAS*, **211**, 737–752. [278]

Clarke, D., Grainger, J.F. (1965) Polarization effects on the profile of the Hβ line in the light from the star γ Ursae Majoris. *Nature*, **207**, 1180. [276]

Clarke, D., Grainger, J.F. (1966) Polarization effects in stellar absorption lines. *Ann. d'Astr.*, **29**, 355–359. [276]

Clarke, D., McGale, P.A. (1988) Temporal polarization variations of Be stars. III. The polarimetric behaviour of X Persei. *A&A*, **190**, 93–102. [285]

Clarke, D., McLean, I.S. (1974a) Polarization measurements within stellar line profiles. pp. 752–761 in *Planets, Stars and Nebulae studied with Photopolarimetry*, Ed. T. Gehrels, University of Arizona, Tucson, AZ. [276]

Clarke, D., McLean, I.S. (1974b) Observations of the linear polarization in the Hβ emission feature of γ Cas. *MNRAS*, **167**, 27P–30P. [276, 277]

Clarke, D., McLean, I.S. (1975) Polarimetric measurements at Hα and Hβ of X Per. *MNRAS*, **173**, 21P–24P. [285]

Clarke, D., McLean, I.S. (1976) Linear polarization measurements at Hβ of early-type emission line studies. *MNRAS*, **174**, 335–343. [276]

Coté, J., Waters, L.B.F.M. (1987) IRAS observations of Be Stars. I. Statistical study of the IR excess of 101 Be stars. *A&A*, **176**, 93–106. [279, 281]

Coyne, (SJ) G.V. (1971a) Polarization of Be stars at high galactic latitudes. *Ric. Astron. Spec. Vaticana*, **8**, No:11, 201–210. [275]

Coyne, (SJ) G.V. (1974) Polarimetry in the emission lines of shell stars. *MNRAS*, **169**, 7P–11P. [276]

Coyne, (SJ) G.V. (1975) Variable polarization in Be stars. *Ric. Astron. Spec. Vaticana*, No:28 **8**, 533–541. [282]

Coyne, G.V. (1976a) Polarization in Be stars. pp. 233–260 in *IAU Symp. No: 70, Be and Shell Stars*, Ed. A. Slettebak, Reidel, Dordrecht, The Netherlands. [275]

Coyne, G.V. (1976b) Polarization in emission lines of Be stars. *A&A*, **49**, 89–96. [276, 282]

Coyne, (SJ) G.V., Gehrels, T. (1967) Wavelength dependence of polarization. X. Interstellar polarization *AJ*, **72**, 887–898. [274]

Coyne, G.V., Kruszewski, A. (1969) Wavelength dependence of polarization. XVII. Be-type stars. *AJ*, **74**, 528–532. [275]

Coyne, G.V., McLean, I.S. (1975) Wavelength dependence of polarization XXX. Intrinsic polarization in Phi Persei. *AJ*, **80**, 702–710. [278]

Coyne, (SJ) G.V., McLean, I.S. (1982) Polarimetry and physics of Be star envelopes. pp. 77–93 in *Be Stars – IAU Symp No:98.* (eds M. Jaschek and H.-G. Grott). Reidel, Dordrecht. [275]

Hall, J.S., Mikesell, A.H. (1950) Polarization of light in the galaxy as determined from observations of 551 early-type stars, *Publications of the US Naval Observatory* – Second Series, Vol. XVII – Part I. [274]

Hayes, D.P. (1975a) Detection of a linear polarization decrease in the Hγ line of ζ Tauri. *PASP*, **87**, 609–611. [276]

Hayes, D.P. (1980) A search for linear polarization in pole-On Be-stars. *PASP*, **92**, 661–665. [282]

Hayes, D.P., Illing, R.M.E. (1974) Linear polarization in the Hγ line of γ Cas and other stars. *AJ*, **72**, 1430–1432. [276]

Hayes, D.P., Guinan, E.F. (1984) The morphology of a mass loss episode of the Be star ω Orionis. *ApJ*, **279**, 721–728. [282, 283, 284]

Hayes, D.P., Terrance, T.N. (1980) Lack of recent linear polarization variability in the shell star o Andromedae. *PASP*, **92**, 89–90. [282]

Ignace, R., Nordsieck, K.H. Cassinelli, J.P. (1997) The Hanle effect as a diagnostic of magnetic fields in stellar envelopes: I. Theoretical results for integrated line profiles. *ApJ*, **486**, 550–570. [281]

Kemp, J.C., Barbour, M.S. (1983) X Persei: Optical polarization variation on the 580 day binary-like period. *ApJ*, **264**, 237–250. [285, 285]

Lin, H., Zihe, G. (1988) Measurements of linear polarization of fourteen Be stars. *Vistas Astron.*, **31**, 293–296. [285]

McDavid, D. (1986) Multicolor Polarimetry of selected Be stars: A long-term analysis. *PASP*, **98**, 572–576. [285]

McDavid, D. (1990) Multicolor Polarimetry of selected Be stars: 1986–89. *PASP*, **102**, 773–782. [285]

McDavid, D. (1994) Multicolor Polarimetry of selected Be stars 1990–93. *PASP*, **106**, 949–963. [285]

McLean, I.S., Clarke, D. (1976) Polarization measurements across the Balmer lines of Be and shell stars. pp. 261–275 in *IAU Symp. No: 70, Be and Shell Stars*, Ed. A. Slettebak, Reidel, Dordrecht, The Netherlands. [276]

McLean, I.S., Clarke, D. (1979) Separation of the intrinsic and interstellar linear polarization components of Southern Hemisphere early-type emission-line stars. *MNRAS*, **186**, 245–263. [276]

McLean, I.S., Coyne, G.V., Frecker, J.E., Serkowski, K. (1979) High resolution polarization structure of Hβ in Be-shell stars measured with a new digicon spectropolarimeter. *ApJ*, **228**, 802–808. [278, 278, 280]

Piirola, V. (1979) Rapid variations in the polarization of the Be star γ Cas. *A&AS*, **38**, 193–196. [281]

Poeckert, R. (1975) Linear polarization of Hα in Be stars. *ApJ*, **196**, 777–787. [276]

Poeckert, R., Bastien, P., Landstreet, J.D. (1979) Intrinsic polarization of Be stars. *ApJ*, **84**, 812–830. [276]

Poeckert, R., Marlborough, J.M. (1976) Intrinsic linear polarization of Be stars as a function of $V \sin i$. *ApJ*, **206**, 182–195. [275]

Poeckert, R., Marlborough, J.M. (1977) Linear polarization of Hα in the Be star Gamma Cassiopeia. *ApJ*, **218**, 220–226. [277], [278], [278]

Poeckert, R., Marlborough, J.M. (1978a) A model for γ Cassiopeiae. *ApJ*, **220**, 940–961. [278]

Poeckert, R., Marlborough, J.M. (1978b) Be star models: observable effects of model parameters. *ApJS*, **38**, 229–252. [278]

Rodriguez, M.G. (1979) Rapid linear polarization variability in Be stars. *Astrometica & Astrofisika*, **39**, 3–8. (In Russian). [282]

Serkowski, K. (1968) Correlation between the regional variations in wavelength dependence of interstellar extinction and polarization. *ApJ*, **154**, 115–134. [274]

Serkowski, K. (1970) Intrinsic polarization of early-type stars with extended atmospheres. *ApJ*, **160**, 1083–1105. [274], [275]

Shakhovskoi, N.M. (1962) *Astr. Circ. (USSR)* **228**, 16. [281]

Smith, M.A., Henry, G.W., Vishniac, E. (2006) Rotational and cyclical variability in γ Cassiopeia. *ApJ*, **647**, 1375–1386. [282]

Sonneborn, G., Grady, C.A., Chi-Chao Wu, Hayes, D.P., Guinan, E.F., Barker, P.K., Henrichs, H.F. (1988) Mass loss in a B2IIIe star: ω Orionis 1978–1984. *ApJ*, **325**, 784–794. [283, 283]

Tamburini, T., Thiessen, G. (1961) On the existence of a new polarization effect in stellar spectral lines. *Accad. Naz. dei Lincei*, Ser VIII, Vol. XXX, fasc. 4, 492–496. [276]

Waters, L.B.F.M., Marlborough, J.M. (1992) Constraints on Be star wind geometry by linear polarization and IR excess. *A&A*, **256**, 195–204. [279]

Yudin, R.V. (2000) Analysis of correlations between polarimetric and photometric characteristics of young stars. *A&AS*, **114**, 285–306. [274]

Yudin, R.V. (2001) Statistical analysis of intrinsic polarization, IR excess and projected velocity distributions of classical Be stars. *A&A*, **368**, 912–931. [274]

References to Disc Orientations

Bastien, P., Ménard, F. (1990) Parameters of disks around young stellar objects from polarization observations. *ApJ*, **364**, 232–241. [286]

Clarke, D. (1990) Temporal polarization variations of Be stars V. Comments, similar behaviour of γ Cassiopeiae and κ Draconis. *A&A*, **227**, 151–155. [286]

Quirrenbach, A., Buscher, D.F., Mozurkewich, D., Hummel, C.A., Armstrong, J.T. (1994) Maximum-entropy maps of the Be shell star ζ Tauri from optical long-baseline interferometry. *A&A*, **283**, L13–L16. [286]

Quirrenbach, A., Bjorkman, K.S., Bjorkman, J.E., Hummel, C.A., Buscher, D.F., Armstrong, J.T., Mozurkewich, D., Elias Ii, N.M., Babler, B.L. (1997) Constraints on the geometry of circumstellar envelopes: optical interferometric and spectropolarimetric observations of seven Be stars. *ApJ*, **479**, 477–496. [286, 286]

Quirrenbach, A., Hummel, C.A., Buscher, D.F., Armstrong, J.T., Mozurkewich, D., Elias II, N.M. (1993) The asymmetric envelope of γ Cassiopeiae observed with the Mk III optical interferometer. *ApJ*, **416**, L25–L28. [286]

Tycner, C., Hajain, A.R., Mozurkewch, D., Armstrong, J.T., Benson, J.A., Gilbreath, G.C., Hutter, D.J., Pauls, T.A., Lester, J.B. (2003) A method for internal calibration of optical interferometer data and application to the circumstellar envelope of γ Cassiopeiae. *AJ*, **125**, 3378–3388. [286]

Vakili, F., Mourard, D., Stee, Ph., Bonneau, D., Berio, P., Chesneau, O., Thureau, N., Morand, F., Labeyrie, A., Tallon-Bosc, I. (1998) Evidence for one-armed oscillations in the equatorial disk of ζ Tau from GI2T spectrally resolved interferometry. *A&A*, **335**, 261–265. [286]

References to Be Star Models

Brown, J.C., Carlaw, V.A., Cassinelli, V.A. (1989) Finite source depolarization factors for circumstellar scattering. *ApJ*, **344**, 341–349. [289]

Brown, J.C., Fox, G.K. (1989) Stellar occultation of polarized light from circumstellar electrons: I. Flat envelopes viewed edge on. *ApJ*, **347**, 468–478. [289]

Brown, J.C., McLean, I.S. (1977) Polarisation by Thomson scattering in optically thin stellar envelopes. I. Source star at centre axisymmetric envelope. *A&A*, **57**, 141–149. [288, 289, 290]

Brown, J.C., Wood, K. (1992) Derivation of episodic mass loss functions for hot stars from polarimetric and absorption line data. *A&A*, **265**, 663–668. [291]

Capps, R.W., Coyne, G.V., Dyck, H.M. (1973) A model for the observed polarization flux for Zeta Tauri. *ApJ*, **184**, 173–179. [287]

Cassinelli, J.P., Nordsieck, K.H., Murison, M.A. (1987) Polarization of light scattered from the winds of early-type stars. *ApJ*, **317**, 290–302. [289]

Clarke, D., McGale, P.A. (1986) Temporal polarization variations of Be Stars. I. Models based on stochastic behaviour. *A&A*, **169**, 251–258. [291]

Fox, G.K. (1991) Stellar occultation of polarized light from circumstellar electrons: III. General axisymmetric envelopes. *ApJ*, **379**, 663–675. [290]

Fox, G.K. (1992) The theoretical polarisation from the obliquely rotating envelopes of single stars. *Astrophys. Space Sci.*, **187**, 219–239. [290]

Fox, G.K. (1993a) The scattering of polarized radiation through optically thin circumstellar envelopes. *MNRAS*, **260**, 513–524. [290, 290]

Fox, G.K. (1993b) A polarimetric investigation of a magnetically driven Be star wind. *MNRAS*, **260**, 525–528. [290]

Fox, G.K., Brown, J.C. (1991) Stellar occultation of polarize light from circumstellar electrons: II. Flat envelopes viewed at arbitrary angle. *ApJ*, **375**, 300–313. [289]

McLean, I.S. (1979) Interpretation of the intrinsic polarizations of early-type emission-line stars. *MNRAS*, **186**, 265–285. [292]

McLean, I.S., Brown, J.C. (1978) Polarisation by Thomson scattering in optically thin stellar envelopes. III. A statistical study of the oblateness and rotation of Be star envelopes. *A&A*, **69**, 291–296. [289]

Nordsieck, K.H., Babler, B., Bjorkman, K.S., Meade, M.R., Schulte-Ladbeck, R.E., Taylor, M.J. (1992) Stellar Spectropolarimetric Monitoring at The University of Wisconsin. pp. 114–117 in *Nonisotropic and Variable Outflows from Stars – ASP Conf. Ser.*, No: **22**, (eds L Drissen, C. Leitherer & A. Nota), San Francisco. [287, 288]

Poeckert, R., Marlborough, J.M. (1978a) A model for γ Cassiopeiae. *ApJ*, **220**, 940–961. [292]

Shakhovskoi, N.M. (1965) Polarization in variable stars. II. Eclipsing binaries. *Sov. Astron.*, **8**, 833–842. [287]

Vink, J.S., Harries, T.J., Drew, J.E. (2005) Polarimetric line profiles for scattering off rotating disks. *A&A*, **430**, 213–222. [293]

Wood, K., Bjorkman, J.E., Whitney, B.A., Code, A.D. (1996a) The effect of multiple scattering on the polarization from axisymmetric circumstellar envelopes. I. Pure Thomson scattering envelopes. *ApJ*, **461**, 828–846. [291]

Wood, K., Bjorkman, J.E., Whitney, B.A., Code, A.D. (1996b) The effect of multiple scattering on the polarization from axisymmetric circumstellar envelopes. II. Thomson scattering in the presence of absorptive opacity sources. *ApJ*, **461**, 847–857. [291]

Wood, K., Bjorkman, K.S., Bjorkman, J.E. (1997) Deriving the geometry of Be star circumstellar envelopes from continuum spectropolarimetry I. The case of ζ Tauri. *ApJ*, **477**, 926–939. [292]

Wood, K., Brown, J.C., Fox, G.K. (1993) Polarimetric line profiles from optically thin Thomson scattering circumstellar envelopes. *A&A*, **271**, 492–500. [292]

Wood, K., Brown, J.C. (1994a) Parametric determination of the inclination, velocity and density structure of circumstellar discs from spectropolarimetric profiles of scattered lines. *A&A*, **285**, 220–228. [292]

Wood, K., Brown, J.C. (1994b) Effect of electron thermal motions on Thomson scattered line profiles from hot circumstellar envelopes. *A&A*, **291**, 202–208. [293]

References to Herbig Ae/Be Stars

Beskrovnaya, N.G., Pogodin, M.A., Najdenov, I.D., Romanyuk, I.I. (1995) Short-term spectral and polarimetric variability in the Herbig Ae star AB Aurigae as an indicator of the circumstellar inhomogeneity. *A&A*, **298**, 585–593. [294]

Beskrovnaya, N.G., Pogodin, M.A., Yudin, R.V., Franco, G.A.P., Vieira, S.L.A., Evans, A. (1998) Cyclic phenomena in the circumstellar gaseous envelope of the candidate Herbig A0e star HD 163296. *A&AS*, **127**, 243–249. [295]

Beskrovnaya, N.G., Pogodin, M.A., Miroshnichenko, A.S., Thé, P.S., Shakovskoy, N.M., Rostopchina, A.N., Kozlova, O.V., Kuratov, K.S. (1999) Spectroscopic, photometric, and polarimetric study of Cyclic phenomena in the Herbig Ae candidate HD 36112. *A&A*, **343**, 163–174. [295]

Catala, C., Böhm, T., Donati, J.-F., Semel, M. (1993) Circular polarization and variability in the spectrs of Herbig Ae/Be stars I. The Fe II 5018 Å and He I 5876 Å lines of AB Aurigae. *A&A*, **278**, 187–198. [294]

Clarke, D., Smith, R.A., Yudin, R.V. (1999) Polarimetric variability of the Herbig Be Star HD 100546. *A&A*, **347**, 590–593. [295]

Coyne, (SJ) G.V., Vrba, F.J. (1976) Polarization from a dust ring surrounding the peculiar Be star HD 45677. *ApJ*, **207**, 790–798. [293]

Elvius, A. (1974) Polarization of light from the peculiar Be star MWC 349. *A&A*, **34**, 371–374. [293]

Gledhill, T.M., Scarrott, S.M., Wolstencroft, R.D. (1991) Optical polarization in the disc around β Pictoris. *MNRAS*, **252**, 50P–54P. [295]

Hubrig, S., Schöller, M., Yudin, R.V. (2004) Magnetic fields in Herbig Ae stars. *A&A*, **428**, L1–L4. [296]

Oudmaijer, R.D., Drew, J.E. (1999) Hα spectropolarimetry of B[e] and Herbig Be stars. *MNRAS*, **305**, 160–180. [296]

Petrova, N.N., Shevchenko, V.S. (1987) Polarization in the light from Herbig Ae/Be stars. *Sov. Astron. Letters*, **13 (4)**, 289–293. [293]

Pontefract, M., Drew, J.E., Harries, T.J., Oudmaijer, R.D. (2000) Hα spectropolarimetry of the Herbig Ae star AB Aurigae. *MNRAS*, **319**, L19–L23. [294, 294]

Rostopchina, A.N., Grinin, V.P., Okazaki, A., Thé, P.S., Kikuchi, S., Minikhulov, N.Kh. (1997) Dust around young stars – Photopolarimetric activity of the classical Herbig Ae/Be star RR Tauri, *A&A*, **327**, 145–154. [295]

Voshchinnikov, N.V., Krügel, E. (1999) Circumstellar disc of β Pictoris: constraints on grain properties from polarization. *A&A*, **352**, 508–516. [296]

Vink, J.S., Drew, J.E., Harries, T.J., Oudmaijer, R.D. (2002) Probing the cicumstellar structure of Herbig Ae/Be stars. *MNRAS*, **337**, 356–368. [296]

Wolstencroft, R.D., Scarrott, S.M., Gledhill, T.M. (1995) *Astrophys. Space Sci.*, **224**, 395–398. [295]

Yudin, R.V. (1996) Quasisimultaneous polarimetry and photometry of peculiar early-type stars. I. Circumstellar environment of a B[e] star: MWC 349 (= V 1478 Cyg). *A&A*, **312**, 234–242. [293]

Yudin, R.V. (2000) Analysis of correlations between polarimetric and photometric characteristics of young stars. *A&AS*, **114**, 285–306. [296]

Yudin, R.V., Evans, A. (1998) Polarimetry of southern peculiar early-type stars. *A&AS*, **131**, 401–429. [294]

Yudin, R.V., Clarke, D., Smith, R.A. (1999) Polarimetry of the young Herbig Ae star HD 139614 – Differences in polarimetric behaviour of Vega-type stars. *A&A*, **345**, 547–552. [295]

References to Early-Type Supergiants

Clarke, D., McDavid, D., Smith, R.A., Henrichs, H.F. (2002) On the polarimetric variability of bright O-type stars. *A&A*, **383**, 580–590. [298]

Coyne, (SJ) G.V. (1971b) Intrinsic polarizations in the atmospheres of supergiant stars. *Specola Vaticana, Cont. No: 53 – Proc. of the Third Trieste Colloquium in Astrophysics* (Ed. M. Hack) Osservatario di Trieste, 93–107. [296]

Hanbury Brown, R., Davis, J., Allen, L.R. (1974) An attempt to detect a corona around beta Orionis with an intensity interferometer using and linearly polarized light. *MNRAS*, **168**, 93–100. [298]

Harries, T.J. (2000) Synthetic line profiles of rotationally distorted hot-star winds. *MNRAS*, **315**, 722–734. [298]

Harries, T.J., Howarth, I.D. (1996) Linear spectropolarimetry of the Hα emission line of ζ Puppis. *A&A*, **310**, 533–546. [298, 298]

Hayes, D.P. (1975b) Detection of intrinsic linear polarization in emission-line O stars. *ApJ*, **197**, L55–L56. [296]

Hayes, D.P. (1978) Linear polarization variability in the emission line O star λ Cephei. *ApJ*, **219**, 952–955. [297, 298]

Hayes, D.P. (1984) Variable polarization observations of the early type supergiants κ Cas and α Cam. *AJ*, **89**, 1219–1228. [297]

Hayes, D.P. (1986) Rigel's circumstellar envelope structure. *ApJ*, **302**, 403–409. [297]

Lupie, O.L. (1983) Visible and infrared continuum spectropolarimetric observations of ten OB supergiant and O emission line stars, PhD Thesis, The University of Wisconsin (Madison). [297]

Lupie, O.L., Nordsieck, K.H. (1987) Visible and infra-red spectropolarimetric observations of ten OB supergiant and O emission-line stars. *AJ*, **92**, 214–230. [297]

McDavid, D. (2000) A search for intrinsic polarization in O stars with variable winds. *AJ*, **119**, 352–364. [297]

Sams, D.C., Johnston, I.D.S. (1974) On the possibility of detecting photospheric polarization with an interferometer. *MNRAS*, **168**, 463–467. [298]

Taylor, M., Code, A.D., Nordsieck, K.H., Anderson, C.M., Babler, B.L., Bjorkman. K.S., Clayton, G.C., Magalhães, A.M., Meade, M.R., Schulte-Ladbeck, R.E., Whitney, B.A. (1991) The first ultraviolet spectropolarimetry of hot supergiants. *ApJ*, **382**, L85–L88. [297]

References to Wolf–Rayet (WR) Stars

Brown, J.C., Richardson, L.L., Antokhin, I., Robert, C., Moffat, A.F.J., St-Louis, N. (1995) Combined spectrometric, photometric and polarimetric diagnostics for 'blobs' in WR star winds. *A&A*, **295**, 725–735. [302]

Drissen, L., Lamontagne, R., Moffat, A.F.J., Bastien, P., Segvin, M. (1986) Spectroscopic and polarimetric parameters of the runaway WN7 binary system HD 197406. Is the secondary an X-ray-quiet black hole? *ApJ*, **304**, 188–200. [300]

Drissen, L., Moffat, A.F.J., Bastien, P., Lamontagne, R. (1986) Polarimetric observations of the WN7 binary CQ Cephei. *ApJ*, **306**, 215–224. [300, 301]

Drissen, L., Robert, C., Lamontagne, R., Moffat, A.F.J., St-Louis, N., van Weeren, N., van Genderen, A.M. (1989) Photometry and polarimetry of the unusual WN5 star EZ Canis Majoris. *ApJ*, **343**, 426–436. [299]

Drissen, L., Robert, C., Moffat, A.F.J. (1992) Polarization variability among the Wolf–Rayet stars VII. The single stars WR 14, WR 25 and WR 69. *ApJ*, **386**, 288–292. [302]

Drissen, L., St-Louis, N., Moffat, A.F.J., Bastien, P. (1987) Polarization variability among Wolf–Rayet stars. II linear polarization of a complete sample of Southern Galactic WN stars. *ApJ*, **322**, 888–901. [300, 301]

Fox, G.K., Henrichs, H.F. (1994) The theoretical correlation between UV discrete absorption components and the polarization of ejected blobs in the winds of early-type stars. MNRAS, **266**, 945–952. [302]

Kopal, Z., Shapley, M.B. (1946) A study of the extended envelope surrounding the Wolf–Rayet component of V444 Cygni. *ApJ*, **104**, 160–176. [299]

Luna, H.G. (1982) Polarimetric determination of the inclination of the Wolf–Rayet binary system HD 152270. *PASP*, **94**, 695–699. [300]

McLean, I.S. (1980) Periodic variations in the linear polarization of HD 50896: A new Wolf–Rayet binary? *ApJ*, **236**, L149–L153. [299]

McLean, I.S., Coyne (SJ), G.V., Frecker, J.E., Serkowski, K. (1979) Detection of polarization structure across the emission lines of the Wolf–Rayet star HD 50896. *ApJ*, **231**, L141–L145. [299]

Moffat, A., Piirola, V. (1993) Polarization variability among Wolf–Rayet stars VIII. Emission lines versus continuum in WR + O binaries. *ApJ*, **413**, 724–734. [299]

Piirola, V., Linnaluoto, S. (1988) Multicolour Polarimetry of Wolf–Rayet binaries. pp. 655–666 in *Polarized Radiation of Circumstellar Origin* – Vatican Observatory Conference Proceedings: (eds G.V. Coyne, A.M. Magalhães, A.F.J. Moffat, R.E. Schulte-Ladbeck, S. Tapia & D.T. Wickramasinghe). University of Arizona Press, Tucson, AZ. [300, 300]

Richardson, L.L., Brown, J.C., Simmons, J.F.L. (1996) Polarimetric versus photometric variability and the density of WR star wind inhomogeneities. *A&A*, **306**, 519–526. [302]

Robert, C., Moffat, A.F.J. (1989) Polarization variability among Wolf–Rayet stars IV. A complete lack of circular polarization in the optical continuum. *ApJ*, **343**, 902–908. [302]

Robert, C., Moffat, A.F.J., Bastien, P., Drissen, L., St-Louis. (1989) Polarization variability among Wolf–Rayet stars V. Linear polarization of the bright Cygnus stars and an anticorrelation with wind speed. *ApJ*, **347**, 1034–1054. [302]

Robert, C., Moffat, A.F.J., Bastien, P., St-Louis, N., Drissen, L. (1990) Polarization variability among Wolf–Rayet stars VI. Linear polarization of the eclipsing binary V 444 Cygnii. *ApJ*, **359**, 211–218. [300]

Rudy, R.J., Kemp, J.C. (1978) A polarimetric determination of binary inclinations. *ApJ*, **221**, 200–210. [300]

Schulte-Ladbeck, R.E. (1989) Masses and the evolution of Wolf–Rayet binaries. *AJ*, **97**, 1471–1479. [299]

Schulte-Ladbeck, R.E., Nordsieck, K.H., Nook, M.A., Magalhães, A.M., Taylor, M.,Bjorkman, K.S., Anderson, C.M. (1990) A rotating, expanding disk in the Wolf–Rayet star EZ Canis Majoris? *ApJ*, **365**, L19–L22. [299]

St-Louis, N., Drissen, L., Moffat, A.F.J., Bastien, P., Tapia, S. (1987) Polarization variability among Wolf–Rayet stars. I. Linear polarization of a complete sample of Southern Galactic WC Stars. *ApJ*, **322**, 870–887. [300, 300]

References to Luminous Blue Variables

Clampin, M., Schulte-Ladbeck, R.E., Nota, A., Robberto, M., Paresce, F., Clayton, G.C. (1995) High resolution coronographic imaging and spectropolarimetry of the HR Carinae Nebula. *AJ*, **110**, 251–258. [303]

Davies, B., Oudmaijer, R.D., Vink, J.S. (2005) Asphericity and clumpiness in the winds of luminous blue variables. *A&A*, **439**, 1107–1125. [303]

Davies, B., Vink, J.S., Oudmaijer, R.D. (2007) Modelling the clumping-induced polarimetric variability of hot star winds. *A&A*, **469**, 1045–1056. [304]

Knoechel, G., Moffat, A.F.J. (1982) Mass loss, linear polarization variability and duplicity of the luminous B2 supergiant HD 80077. *A&A*, **110**, 263–271. [302]

Leitherer, C., Allen, R., Altner, B., Daminelli, A., Drissen, L., Idiart, T., Lupie, O., Nota, A., Robert, C., Schmutz, W., Shore, S.N. (1994) Geometry and physical conditions in the stellar wind of AG Carinae. *ApJ*, **428**, 292–318. [303]

Parthasarathy, M., Jain, S.K., Bhatt, H.C. (2000) Polarization measurements of the luminous blue variable HR Carinae. *A&A*, **355**, 221–226. [303]

Schulte-Ladbeck, R.E., Leitherer, C., Clayton, G.C., Robert, C., Meade, M.R., Drissen, L., Nota, A., Schmutz, W. (1993) The asymmetric wind of R 127. *ApJ*, **407**, 723–732. [303]

Schulte-Ladbeck, R.E., Clayton, G.C., Meade, M.R. (1993) Spectropolarimetry of the luminous blue variables AG Carinae and R 127. pp. 237–239 in *Massive Stars: Their Lives in the Interstellar Medium – ASP Conf. Ser.*, No: **35**, (eds J.P. Cassinelli & E.B. Churchwell), San Francisco. [303]

Schulte-Ladbeck, R.E., Clayton, G.C., Hillier, D.J., Harries, T.J., Howarth, I.D. (1994) The asymmetric stellar wind of AG Carinae. *ApJ*, **429**, 846–856. [303]

14
Late-type Stars

14.1
Introduction and Surveys

Being in the lower temperature domain of the HR diagram, late-type stars have attributes that lend themselves to carry polarigenic mechanisms, giving rise to observable intrinsic polarization. In the case of single stars, polarization may be produced by scattering from grains within their relatively cool atmospheres, particularly if there is clumpiness in the distribution of the dust. Asymmetry of the radiation field produced by a star's convective photosphere, with localized hot/cool-spots, may also engender an overall polarization. This might ensue either from variations in the localized radiative transfer at the stellar surface, or by the outer scattering shells being illuminated in a non-uniform way.

As is the case for other spectral types, the fact that the wide variety of late-type stars display intrinsic polarization is evident either by temporal variability, or by the wavelength-dependent variation being very much different to that produced by the interstellar medium. Many late-type stars are known to be photometric variables and, as a consequence, if they display intrinsic polarization, this parameter is also likely to display temporal changes.

From a multi-colour study of 55 cool stars, Dyck & Jennings (1971) explored the location in the HR diagram of stars, which exhibit intrinsic polarization. The tendency was high among K and M supergiants, but with no correlation with temperature. For luminosity class-III stars, the frequency was high for stars of spectral type M4 or later. From the general behaviour, and the wavelength dependence of p, it was argued that the polarization in giants and supergiants must be of circumstellar origin, and that the mechanism for it is one of scattering by solid particles. By comparing polarization measurements with emission core intensities of the CaIIK line, Dyck & Johnson (1969) suggested that the stronger the intensity of the CaIIK2 peak, the smaller are the temporal polarization variations. This is in accord with the association of CaII emission cores with stellar chromospheric heating, and polarization with the presence of molecules, or particles, in a cool outer atmosphere.

A spectral survey of 23 red variables was undertaken by Kruszewski, Gehrels & Serkowski (1968) who found that the polarization rises steeply into the ultraviolet, but with carbon stars differing in their $p(\lambda)$ behaviour relative to M-type stars.

Stellar Polarimetry. David Clarke

ISBN: 978-3-527-40895-5

Simple explanations were proposed to explain the high values in the UV, and the flat values between blue and yellow for the carbon stars, in terms of scattering by different particle types.

A sample of 18 very cool stars was observed by Kruszewski & Coyne (1976) over a wide spectral range. Large values of p ($\sim$8%) were recorded for two stars at 1 μm; large variations on time scales of a few days were also apparent. Among objects with the largest photometric excesses at 10 μm, there is a striking absence of stars with small values of p, this result possibly having implications for the interpretation of the origin of polarization in very cool stars.

From a selection of 25 local cool giant stars, with spectral types of K0 to M3, narrow-band measurements at CaIIK and Hβ by Schwarz (1985) demonstrated the general growth of p as the stellar temperature falls, the general behaviour being accounted for by the influence of large convection cells, these also being related to photospheric temperature.

A review of polarimetry with respect to the observational work related to cool giants and supergiants to round about 1985 has been provided by Schwarz (1986). Another work of interest is by Arsenijević (1986).

Many of the observations of late-type stars point to the presence of dust as the source for the scattering, which produces the polarization. Most explored models generally cover the behaviours of the different subgroups, and some of them might be mentioned here. In a paper presenting models related to the wavelength dependence of polarization, and the reddening produced by dust in circumstellar envelopes, Shawl (1975) considered scattering by spherical silicate, graphite and iron grains, and by the hydrogen molecule. Various geometries, density distributions and particle size distributions were explored for inter-comparison in terms of the produced polarization and reddening. Modelling of circumstellar envelopes was developed by Simmons (1982) with greater mathematical sophistication. By considering a star as a point source, the engendered polarization was calculated for optically thin circumstellar envelopes involving arbitrary spherical symmetric scattering mechanisms. The resulting normalized Stokes parameters were expressed in terms of series expressions. For the special case of Thomson and Rayleigh scattering, these take a particularly simple form with the results obtained for axisymmetric envelopes being readily derived. Analogous expressions from the study were obtained for general spherically symmetric atmospheres, with the produced polarization and reddening by envelopes of cool stars discussed in detail by considering Mie scattering. To a first-order approximation, it was shown that the form of $p(\lambda)$ is independent of the specific density distribution of scatterers in the envelope, and that the position angle is independent of the specific scattering mechanism. This treatment was later extended by Simmons (1983) to scattering in co-rotating envelopes of arbitrary form associated with binary stars.

Multiple scattering within circumstellar dust shells of moderate optical thickness has been investigated by Voshchinnikov & Karjukin (1994) using the Monte Carlo approach. They have studied the scattering by dust grains in prolate and oblate spheroidal shells as viewed at various angles. The numerical code has been applied to Rayleigh and Mie scattering. The resulting values of p usually did not exceed 1–

2%, with a weak colour dependence in the visual and red regions. Code & Whitney (1995) have developed a Monte Carlo method for calculating p due to scattering in various geometries. They have applied their method to the case of scattering in a spherical cloud illuminated by parallel rays. The value of p is largest in small optical depths, but decreases as the optical depth increases until a limit is reached at which scattering occurs on the surface. The applications are discussed in relation to the polarization in supergiants and R CrB stars, and scattering in a clumpy interstellar medium.

Many of the polarimetric surveys performed on late-type stars contain information on a mixed bag of spectral types involving a broad range of astrophysical circumstance and mechanisms for producing any observed polarization. For the presentation here, where most appropriate, the material is discussed according to the more regular nature and classification of the stars. In addition, some infrared objects, not normally referred to as late-type stars, will also be described in terms of their polarimetric behaviour.

14.2
Late-Type Supergiants

Early evidence of polarimetric variability associated with late-type supergiants was provided by Grigoryan (1958) for the semi-irregular supergiant, μ Cep. Sparodic notes on the variability of this star have since been provided by Arsenijević, Kubicela & Vince (1980) and Hayes (1981a, 1982). Using broadband filters, the behaviour of $p(\lambda)$ for the star was investigated by Coyne & Kruszewski (1968). In addition to the strong decrease of polarization towards longer wavelengths, they recorded complex temporal changes indicating that the intrinsic polarization is not confined to a constant plane, suggesting that the polarigenic zones occur in different regions of the stellar atmosphere or stellar envelope.

In an observational study, 14 high-galactic semi-regular supergiants and Mira variables were investigated by Zappala (1967); he found that seven displayed temporal variability, and that an additional four had values of p above those expected from the line of sight interstellar medium, according to their location in the Galaxy. He noted that μ Cep displayed substantial temporal changes and there were no obvious correlations between the brightness and the polarization variations for the group of observed stars. Red supergiants have also been measured by Abramyan (1981, 1982).

From observations over the 1979–1980 seasons, Hayes (1980) recorded secular and ordered polarization changes for α Ori (Betelgeuse). He suggested that they resulted either through changes in the photoscattering regime, or indirectly through changes in the illumination of circumstellar material via the waxing and waning of large-scale convection cells. By monitoring α Ori and α Sco (Antares), Tinbergen, Greenberg & de Jager (1981) qualitatively linked their behaviours to the development and movement of large convective cells with the polarization engendered by atomic and dust scattering. The polarimetric behaviour of α Ori was monitored by

Hayes (1984) over four consecutive seasons. The smooth, secular changes drawn out in the qu-plane suggested that they were the manifestation of the waxing and waning of large-scale convection cells. Using the data of Hayes (1980, 1981b), a model was proposed by Schwarz & Clarke (1984) based on the effects of a hotspot, with the polarization generated by the action of the locally enhanced radiation field on the photospheric scattering immediately above it. For a given density of optically thin scatterers, the observed p depends on the spot's size, location and temperature. The form of $p(\lambda)$ is a convolution of the characteristics of the scattering process and the spot's parameters. It was also demonstrated that the observed behaviour of the secular $p(\lambda)$ form could be generated solely by the spot's parameters rather than by the wavelength dependence of the efficiency of scattering, being a result of the spectral emissivity difference between the spot and the general photosphere.

For α Ori, Clarke & Schwarz (1984) reported on measurements across the spectrum from 4000 to 8500 Å, with spectral resolution of 50 Å, displaying changes across the TiO bands (see Figure 14.1). The hotspot model, involving two or more photospheric disturbances, allows both p and the position angle to change with wavelength. Changes in p and ζ across the TiO features can be accounted for by

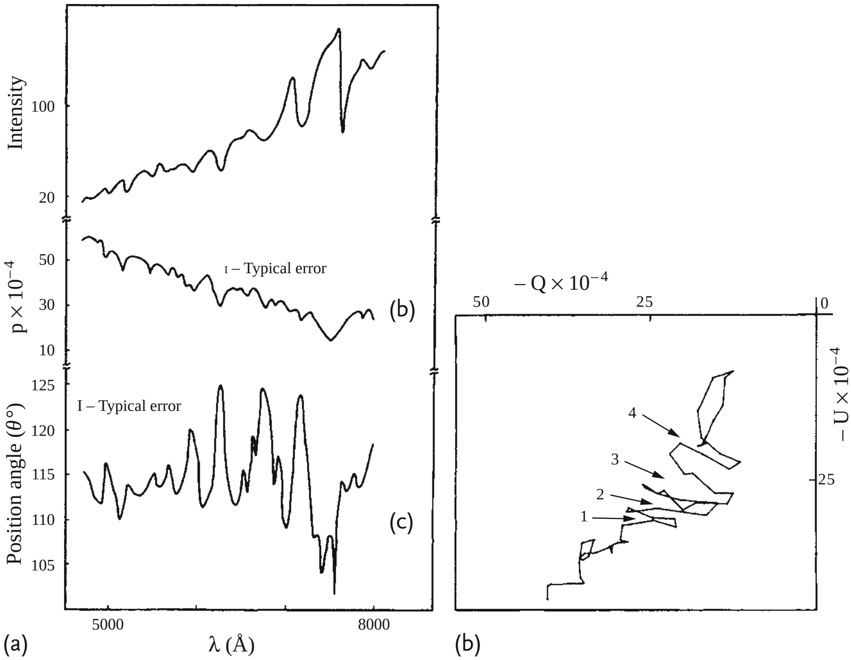

Fig. 14.1 (a) displays the intensity spectrum, $p(\lambda)$ and the spectral variation of the position angle for α Ori in Dec 1979. When the same data are plotted in the qu-plane (b), the continuum appears to follow an intrinsic line, with departures marked 1 to 4 corresponding to TiO bandheads at 5947, 6159, 6651, 7054 Å, respectively, with the variations across these features suggesting a point of convergence towards the right of the diagram. (Taken from Clarke & Schwarz, 1984.)

differential limb darkening. A more sophisticated model has been presented by Doherty (1986) suggesting that the polarization behaviour can be explained in terms of the combined effects of Rayleigh scattering in the photosphere and scattering by circumstellar dust in the presence of one or more photospheric hot spots. Assessment of models involving asymmetric distributions of circumstellar dust, alignments of dust by the stellar magnetic field, or photospheric structures was made by Marcondes-Machado (1987). In his proposal, he demonstrated that good fits to data, including wavelength variations of the position angle, could be produced by a model based on paramagnetic grains which are aligned by a stellar magnetic field, with the grain size and magnetic field geometry varying with distance from the star, and with the effective stellar radius changing with wavelength.

Le Borgne, Mauron & Leroy (1986) have performed polarimetry of the resolved dust shell surrounding α Ori. Using UBV filters, they found that the dust density falls off according to r^{-2}, and that no significant departures in spherical symmetry could be found. Further modelling of the situation was undertaken by Mauron & Le Borgne (1986) to explore the rate of mass loss, with values that depend on the grain type solutions which provide satisfactory fits to the measured polarization. The possibility that circular polarization may be generated in the immediate dusty nebulosities surrounding late-type supergiants has been promoted through the modelling by Shafter & Jura (1980). Observations in this area appear to be absent, although circular polarization has been detected in some Mira variables (see below).

Intrinsic polarizations have been recorded by White, Shawl & Coyne (1984) for 15 out of 39 measured red giants in the globular clusters NGC 5272 (M3) and NGC 6205 (M13). Possible mechanisms for producing the polarization were discussed in terms of dust in circumstellar envelopes, and from photospheric effects such as surface magnetic fields.

If localized surface brightness variations are the root cause of the polarization for stars such as α Ori, then it should be possible to link the observed position angle to brightness maps produced by high-resolution interferometry. An attempt to do this has been described by Tuthill (1994) with some success. The relationship of polarimetry to the mapping of hotspots has also been mentioned by Tuthill, Hanhiff & Baldwin (1997). Further interdisciplinary observations along these lines are only to be recommended.

14.3
Mira Variables

For Mira variables, Harrington (1969) suggested they might display larger values of p than expected from the ‘classical’ values predicted for a pure scattering atmosphere, the enhancement depending on temperature variations over the stellar surface.

A list of measurements of some long-period variables has been provided by Serkowski (1966a); a table of measurements of Miras has also been given by Serkowski (1966b). He noted that some stars reached maximum polarization at minimum brightness, while others were least polarized at maximum brightness. From simultaneous photometry and polarimetry of 21 late-type stars, Dyck (1968) found that, for the Mira variables, there was a correlation between changes in brightness and p; an increase in brightness corresponds to a decrease in p, and vice-versa. Immediately following the discovery of intrinsic Mira polarizations, Donn, Stecher, Wickramasinghe, *et al.* (1966) proposed that the polarigenic mechanism was graphite dust, this being very efficient in its effect. A further study by Dyck & Sanford II (1971) of 21 Mira variables generally showed the large increase of polarization in the blue end of the spectrum indicating that it must originate in the circumstellar envelope, rather than in the stellar atmosphere.

Shawl (1975b) later presented data for 25 red variables and discussed models which suggest that a large number of small particles are produced with each light cycle, but growing in size on dispersion. For *o* Cet and V CVn, the polarization increases at the time when the hydrogen emission lines become visible. From a study by Materne (1976) of three Miras, whose intrinsic polarizations were corrected for interstellar effects, it was concluded that, following the triggered eruption of small particles, the grain size grows as they disperse, thus confirming Shawl's study. Hayes & Russo (1981) noted that the position angles at maximum light of *o* Cet differ greatly from cycle to cycle; some further measurements have been provided by Hayes (1982).

Synoptic multi-colour measurements of three Miras have been made by Yudin & Evans (2002). They suggest that the polarimetric variability which is more evident in the blue, rather than in the more stable red end of the spectrum, is consistent with episodic mass ejections with the formation of small dust particles in the circumstellar environment.

Attempts to detect circular polarization in a sample of late-type stars was made by Rich & Williams (1973), with a possible detection only for the star Z Eri. For the others including *o* Cet, null results were obtained. Circular polarization had previously been recorded in VY CMa (0.4% at 1 μm, < 0.5% with a *V* filter) by Gehrels (1972), and in NML Cyg (maximum, 0.6% at 1.7 μm) and VY CMa by Serkowski (1973).

Narrow- and intermediate-band measurements were made by Coyne & Magalhães (1977) of a number of Mira variables and also the semi-irregular variable, V CVn. They suggested from the increase in p around Hβ, and the relative decrease near the Balmer discontinuity, any polarizing dust must be well mixed in the extended atmosphere of the latter star, and that the behaviour may be explained by a shock wave passing through the envelope. Further observations by Coyne & Magalhães (1979), particularly of the TiO bands of μ Cep and V CVn, confirm the model of a pulsating molecular scattering atmosphere in which the polarization is linked to the pulsation cycle, and the polarization changes across the TiO bands are due to changes in the ratio of absorption to scattering with optical depth.

By using narrow-band filters, McLean (1979) supported the discovery that long-period (regular) variable stars exhibited significant linear polarization variations across some of their molecular bands and atomic lines. Variations in p and position angle were found across the stronger molecular (TiO) absorption bands in the yellow and red spectral regions of μ Cep and R Tri.

The temporal behaviour of V CVn has been monitored by Magalhães, Coyne & Benedetti (1986) systematically over a complete cycle. The observations across the 4955 AA TiO band give further evidence for the notion of a photospheric origin for most of the optical polarization, with the existence of an intermediate scattering layer in the stellar photosphere.

A fall in polarization at Hβ was noted by McLean & Clarke (1977) for the Mira variable R Carinae near maximum light, with other spectral structures, suggested as being related to TiO molecular absorptions. For the case of Mira (*o* Ceti) itself, a large effect of polarized Balmer emission was reported by McLean & Coyne (1978), again with decreases in p in the TiO bands. Further spectropolarimetry was performed by Tomaszewski, Landstreet, McLean, *et al.* (1980) of Mira at maximum light in 1978 with polarization dips showing well in the TiO bands, but with increases in the emission lines of Hγ and Hδ and the absorption line of CaI at 4226 Å. The behaviour of $p(\lambda)$ was provisionally interpreted as resulting from the effects of scattering in an atmosphere which is not uniformly bright. Spectropolarimetry with resolution between 20 and 160 Å was performed by Landstreet & Angel (1977) on five Mira variables and the RV Tauri star, R Sct. Strong polarization changes were noted in lines associated with molecules such as TiO and ZrO

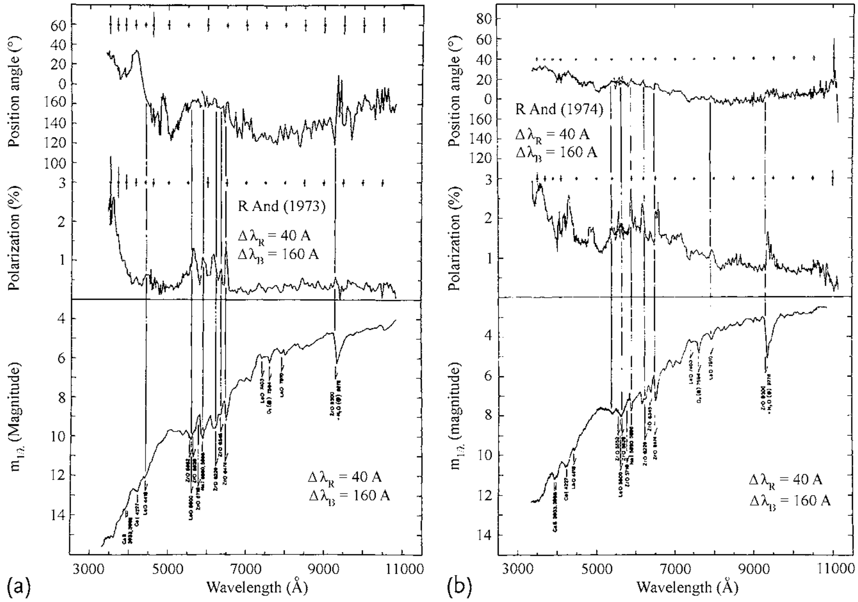

Fig. 14.2 The two figures display the position angle, degree of polarization and the continuum brightness of R And on 1973 June 22 (a) and 1974 September 6 (b). Enhancements in p are clearly visible across the complex of absorption lines around 6000 Å, with marked structure for the position angle on the first date. (Both figures are taken from Landstreet & Angel, 1977.)

for all the Miras. Little or no line effects were noted for R Sct. An example of these data is presented in Figure 14.2 for R And.

Using narrow-band filters to isolate strong features such as the TiO bands and the CaI line at 4226 Å, Codina-Landaberry & Magalhães (1980) have observed four Miras in the Southern Hemisphere, and the semi-irregular variable L_2 Pup. Variability was found in the TiO bands in all of the target stars. The behaviour is thought to be controlled by the variation of the source function, and the ratio of absorption to scattering, as a function of optical depth in the stellar photosphere. For L_2 Pup, there were polarization changes across the calcium line, indicating that CaI is unevenly distributed across a stellar surface.

Further narrow-band measurements were made of L_2 Puppis by Magalhães, Coyne, Codina-Landaberry, *et al.* (1986) over a 3-year period. Systematic changes were recorded in both p and ζ, being most noteworthy for the CaI 4226 Å atomic line. The behaviour was best explained by a combination of photospheric effects including a non-uniform distribution of *Ca* across the stellar disc, and scattering from dust grains in an asymmetric cloud about the star, in which there is a systematic time variation in grain size with distance from the star.

A sample of Mira-type variables was monitored by Boyle, Aspin, Coyne, *et al.* (1986) with 20 Å resolution over the blue end of the spectrum. The most remarkable feature of the study was the behaviour of the resonance line, CaI 4226 Å. Many of the surveyed stars, but not all, showed enhanced p in this atomic line, with several revealing rotation of the direction of vibration relative to measurements of the nearby continuum. For some stars, there is a decrease in p across the TiO bands, whereas for others there is an increase. It is argued that these behavioural features require more than one polarigenic mechanism, and that both photospheric and circumstellar processes are important.

Spectropolarimetric studies have been made by Bieging, Schmidt, Smith, *et al.* (2006) for a selection of asymptotic giant branch (AGB) and post-asymptotic giant branch stars. Most of the objects exhibited intrinsic polarization with features being detectable in the various molecular lines. Effects were recorded in the TiO bands of three M-type Mira variables, in the CN bands of the carbon stars R Lep and V 384 Per, and in the Swan bands of C_2 in R CrB and two proto-planetary nebulae. Polarization effects in the molecular bands appear to be more common, and the effects are larger, in O-rich rather than C-rich objects.

14.4
AGB and R Cor Bor Stars

Asymptotic giant branch (AGB) and R CrB stars display spectra indicating that they are carbon rich. Serkowski & Kruszewski (1969) found that for RY Sag during its photometric minimum, both p and ζ changed quite markedly. The overall behaviour is in keeping with the notion of the occasional condensing of graphite particles within a carbon-rich atmosphere.

The temporal variation of $p(\lambda)$ of R CrB itself was observed by Coyne & Shawl (1973) during a photometric minimum. Very significant developments in the spectral behaviour were recorded, these being interpreted as 'dramatic' changes in the distribution of particles of different sizes associated with the 'discrete cloud model'. Further observations were presented by Coyne (1974), which supported the model.

Spectropolarimetric observations have been made of V 854 Cen by Kameswara Rao & Raveendran (1993). They noted that the $p(\lambda)$ variation was much steeper during the light minimum. During the brightness decline phase, the polarized flux was attenuated by the same factor as the flux directly from the star, this implying that the obscuring cloud affects both the radiation from the photosphere and the scattering centres, suggesting a restriction to the geometrical extent of the scattering region.

In an observational study of the global values of p in a collection of objects in the stages of evolution from red giant to planetary nebula, Johnson & Jones (1991) noted that polarization is a characteristic of the majority of these stars. When arranged on an evolutionary sequence, a clear trend in p was found. A maximum of polarization was observed within an evolutionary stage. The value of p was found to increase with age from mildly dusty Mira variables, through to protoplanetary nebulae for which the highest polarization is found; the polarization then decreases as the star evolves into an old planetary nebula.

Spectropolarimetry of 31 post-asymptotic giant branch (post-AGB) stars were observed by Trammell, Dinerstein & Goodrich (1994), these objects believed to be in the first phases of the transition from the AGB to the planetary nebula stage. Their survey suggested that the objects might be placed into one of four types depending on the recorded behaviour of $p(\lambda)$ and $\zeta(\lambda)$. Type [1] objects display higher levels of polarization and large position angle rotations; Type [2] have polarizations too large to be attributed to interstellar material, but without large position angle changes; Type [3] objects show position angle rotations and polarization changes across TiO absorption features; Type [4] are objects for which the observed polarization can be entirely attributed to interstellar effects. Twenty four objects displayed evidence for aspherical geometry, with an implication that asymmetry begins very early in the transition from AGB to the planetary nebula phase. Their schematic model involves bipolar lobes giving rise to polarization in the blue part of the spectrum as a result of scattering of photospheric light by the contained dust grains. Orthogonal to these lobes is an obscuring torus, and the polarization in the red is the result of scattering of photospheric light or transmission polarization in this torus.

Likkel, Morris, Kastner, *et al.* (1994) have obtained maps of IRAS 21282+5050 revealing that the polarization is not centro-symmetric close into the stellar source. It was concluded that there is not a large component of scattered light in the near-infrared. The emission at 2.2 μm may arise from transiently heated dust. In a polarimetric study of IRC +10216, a carbon-rich infrared evolved star on the AGB of the HR diagram, Kastner & Weintraub (1994) found elliptical symmetry in a *J*-band map endorsing other photometric maps, all these providing evidence of axial symmetry of the envelope, with the equatorial plane of the star lying perpendicular to the major axis of the surrounding inner envelope of the nebula. The axisymmetric

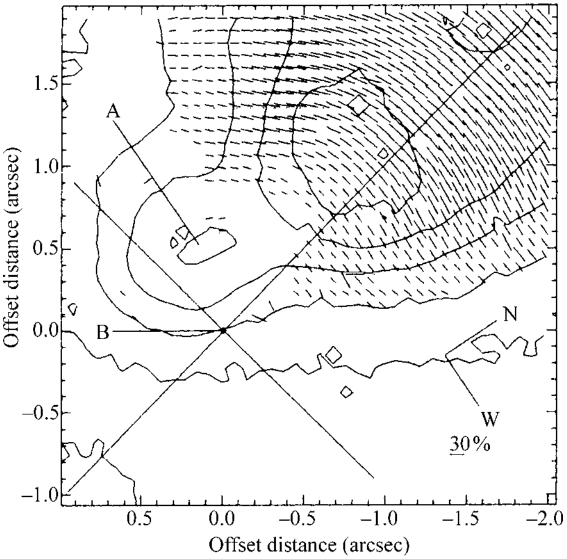

Fig. 14.3 The vector map of the central region of RAFGL 2688, or the Egg nebula, with values of $p \geq 0.15$ indicated, provides a polarimetric centroid at B. The '+' sign at this point indicates the 1σ uncertainty of its calculated position. (Taken from Weintraub, Kastner, Hines, *et al.*, 2000.)

near-infrared intensity and polarization morphologies are best understood in terms of enhanced mass loss in the equatorial plane.

One of the sources of highest polarization is the Egg nebula, or RAFGL 2688, the level being detectable at the telescope simply by eye and a *polaroid*. The object is a rapidly evolving pre-planetary nebula, with a thick dust torus blocking direct radiation from the central object, while scattering from the dust shells and other material in the bipolar flow produce the highly polarized radiation. The directions of vibration of this are normal to the scattering plane and by imaging the nebulosity in the form of a polarization map, the vectors can be used to determine the location of the obscured 'stellar' source as has been performed by Weintraub, Kastner, Hines, *et al.* (2000). A central portion of their map made at 2 μm is presented in Figure 14.3. The inferred position of the central star corresponds to the geometric centre of the tips of four principle lobes of near-infrared H_2 emission. The polarimetric and imaging data suggest that the infrared peak intensity is a self-luminous source and is likely to be a distant binary companion of the obscured illuminating star. Although consensus theory predicts that bipolar structure in pre-planetary and planetary nebulae is a consequence of binary evolution, the separation of the two components here is too large for the presence of the infrared companion to have influenced the structure of the RAFGL 2688 nebula.

R Cor Bor stars produce dust at regular intervals, with the apparent brightness of the central star falling by several magnitudes as a result of the extinction. During a deep decline of 8.2 mag of V 854 Centauri, Whitney, Clayton, Schulte-Ladbeck, *et al.*

(1992) performed spectropolarimetry revealing a polarization of 14% at 4200 Å to about 4% at 6500 Å, the position angle remaining constant. It was noted that the polarization decreased across the emission lines, but that the polarized flux remained constant, indicating that the line light is unpolarized. The emission probably arises in a region unobscured by dust.

During an extinction event of R CrB itself, Clayton, Bjorkman, Nordsieck, *et al.* (1997) made a spectropolarimetric study. The position angle of the continuum polarization was almost constant from 1 µm to 7000 Å, but then changed markedly by $\sim 60°$ between 7000 and 4000 Å. It was noted that this behaviour was strikingly similar to that displayed in AGB stars having an obscuring torus and bipolar dust lobes. The observations strengthen the suggestion that there is a preferred direction to the dust ejections in R CrB. Dust ejections seem to occur predominantly along two roughly orthogonal directions, consistent with a bipolar geometry. If confirmed, this finding will reinforce the relationship between the RCB stars and other post-AGB stars.

Yudin, Evans, Barrett, *et al.* (2003) measured five RCB stars using broadband polarimetry. It was concluded that there is a presence of permanent clumpy nonspherical dust shells about these stars, and that neutral extinction must be significant in their atmospheres.

14.5
Symbiotic Stars

Symbiotic stars exhibit simultaneously the signatures of a cool giant and an ionized nebulosity – binary systems comprising a red giant and a hot radiation source $T \approx 100\,000$ K. The nebulosity is thought to be ionized material from the mass-losing giant. According to a set of colour measurements over a six night interval made by Efimov (1979), the symbiotic star HM Sge displayed an intrinsic polarization, which was variable. The near monotonic decline of p with wavenumber resembled the behaviour of typical reflection nebulae, with the polarization arising in an asymmetric dust envelope comprising dielectric (silicate) grains $\sim$0.2 µm in radius. Schulte-Ladbeck (1985) made multi-colour observations of 16 symbiotic stars establishing that intrinsic polarization was detectable in 8 out of 18 such objects, indicating that a lack of spherical symmetry appears to be a common feature. The polarization did not appear to change across the TiO band at 6159 Å, relative to the continuum, indicating that photospheric polarization was not the origin of the intrinsic component.

Very marked spectral variations in p were discovered by Aspin, Schwarz, McLean, *et al.* (1985) for the peculiar symbiotic star R Aquarii. By using a small field stop, the measurements concentrated on the stellar source with the minimum of contamination from its associated nebulosity. Strong polarization enhancements were displayed across the TiO absorption features, with large rotations of the direction of vibration. Noteworthy, too, was the secular wavelength variation, the direction of vibration changing by about 10° from 4500 to 6250 Å, followed by a jump $\approx 40°$

over an interval of 500 Å, with a fairly flat behaviour from thereon to 8500 Å. Again, the structures in the $p(\lambda)$, $\zeta(\lambda)$ records require a combination of two or more polarigenic mechanisms, with the detailed variations in the molecular absorption bands explained by the existence of photospheric hotspots (convection cells) on the cool stellar component of the system. Later, Schwarz & Aspin (1987) noted that both p and ζ displayed large temporal variations with a change of $\sim$1% to $\sim$10% in the U-band. The significant p dip at the OIII emission line, previously noticed in earlier data, is also commented on as being subject to dramatic changes according to the Mira phase of this object. The value of p was found to have a maximum at minimum light, the sense of the correlation being opposite to that of *o* Ceti, as reported by Shawl (1974).

A very remarkable discovery was made related to the 6825 and 7082 Å emission features in the spectra of symbiotic stars when they were diagnosed by Schmid (1989) as resulting from a Raman scattering process. This involves the absorption of radiation at some wavelength with re-emission at another. The process of remission is dipole in nature, and consequently the redirected energy is likely to exhibit polarization. The concepts of the scenario have been briefly described by Schild & Schmid (1992). A simple geometric model, which allowed its exploration by Monte Carlo simulations, was presented by Schmid (1992).

The basic model suggests that the variation of p may be simply expressed as

$$p = p_{\max} \sin^2 \alpha \,, \tag{14.1}$$

where α is the angle between the line of sight and the binary axis connecting the two stars. This in turn may be expressed as

$$p = p_{\max} \left(\cos^2 \varphi \cos^2 i + \sin^2 \varphi\right) , \tag{14.2}$$

with the orbital phase, φ, being given by the photometric phase. The temporal variations of the polarization signatures of the Raman lines at 6825 and 7082 Å thus provide unique information on the geometry of the orbit such as the inclination, i, the orientation of the line of nodes, ω, and the sense of its description. The geometry requires strong O VI radiation produced in the ionized region near the hot component, and converted by neutral hydrogen into Raman photons in the extended atmosphere and wind of the cool giant. As the binary orbit is executed, the scattering geometry rotates relative to the line of sight. A phase-locked rotation of the position angle, ζ, is expected. For an orbit with inclination, the rotation of ζ is faster near conjunction and slower nearer quadrature. The values of p are expected to be at a minimum near conjunction, being closest to a forward or backward scattering situation; higher values of p will occur at the quadratures which offer scattering nearer to 90°. In addition, information on the geometric structure of the nebular O VI region, and on absorbing particles in the outer atmosphere of the red giant, may be obtained.

The orientation of the orbital plane can be determined from measurements of ζ, particularly in the blue wing of the Raman lines. The reason for this is that these photons originate predominantly from scattering close to the binary axis where the neutral hydrogen atoms in the giant's wind move towards the O VI source, introducing a blueward Doppler shift. The red wing emission originates from the receding (relative to the O VI source) outer part of the giant wind, which is geometrically less defined, and where geometric cancellation of the polarimetric signal is important. Thus, the orientation of the line of nodes may be determined from ζ measured at the orbital quadrature phase.

Based on such a scenario, monitoring of the Raman lines allows determinations of orbital parameters such as period, inclination and orientation of the orbital plane. In addition, information on the geometric structure of the nebular O VI region and on absorbing particles in the outer atmosphere of the red giant may be obtained. As a result of a survey of 15 symbiotic stars, Schmid & Schild (1994) found high values of p across the noted Raman lines with effects integrated over the emission profiles of about 5%. Three types of structure seem to present themselves: I. Profiles with constant p across the lines. II. Profiles with decreasing p towards the red line wing and constant direction of vibration. III. Profiles with two components and a rotating or flipping vibration angle. The morphological differences in the profile polarization structures can be accounted for by the simple geometric model.

Spectropolarimetric observations were made by Schild & Schmid (1996) of the symbiotic Mira, V 1016 Cygni, covering the broad emission features at 6825 and 7082 Å. A data record is depicted in Figure 14.4 showing these features in emission, with q and u signatures on an otherwise flat polarimetric continuum. They found that p increased over a 3-year interval, and that the azimuth of the polarization in the blue wing of the lines rotates clockwise at a constant rate of 8° ± 2° per year. From these data, it was concluded the binary system has a period of 80 ± 25 years and that the orbit inclination is 60° ± 20°. In August 1991, the binary axis projected on the celestial sphere was at position angle 81°, but had rotated to 58°

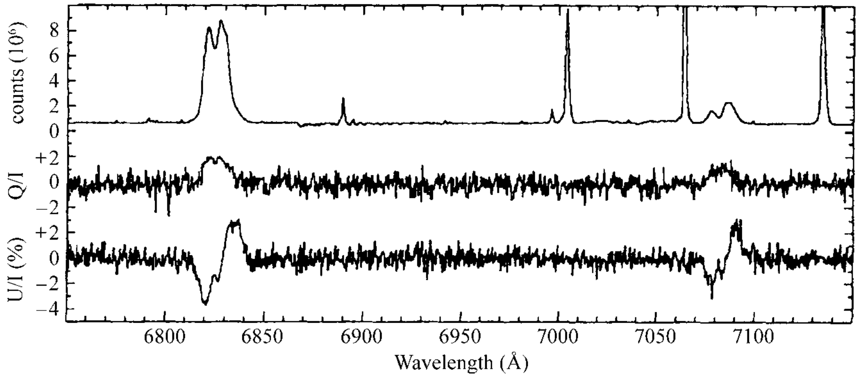

Fig. 14.4 In the upper section, spectral records of V 1016 Cygni in Sep 1994 reveal the strong emission features at 6825 and 7082 Å. The lower records for q and u indicate that the same two emissions are the only features carrying a polarimetric signature. (Taken from Schild & Schmid, 1996.)

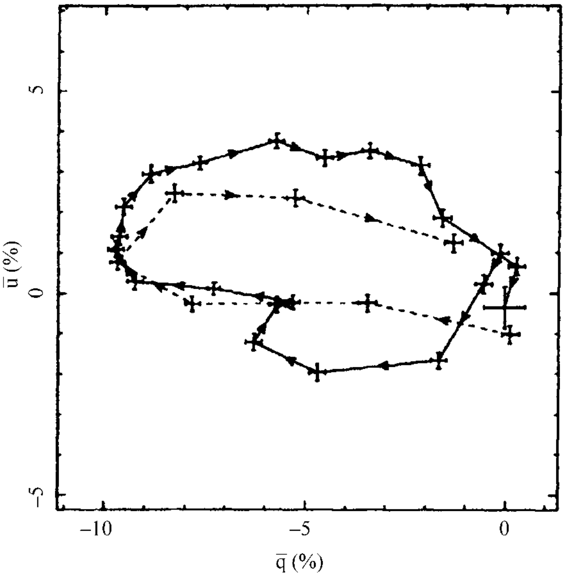

Fig. 14.5 The polarization rotations across the structure of the Raman lines at 6825 Å (solid locus) and 7082 Å (dashed locus) for the star, H2-38, clearly show the form of loops when data are plotted in the *qu*-plane; the progression of the loops, marked as arrows, runs from blue to red. (Taken from Harries & Howarth, 1996a.)

by September 1994. From the modelling, it is proposed that the system comprises a Mira variable with a radially symmetric neutral wind region, which is terminated on the hot component's side by an ionization front, warped by the relative binary and wind motions.

A Southern Hemisphere survey of 23 stars has also been undertaken by Harries & Howarth (1996a, 1997a) with reports that the Raman lines displayed a variety of morphologies, but with the intensity and polarization profiles basically appearing to be triple-peaked. One of the common characteristics is a rotation of the direction of vibration across the profile, this being clearly seen when the data are plotted in the *qu*-plane; the loci of the data tend to form closed loops as the emission line is scanned. An example of this behaviour is illustrated in Figure 14.5 for the star, H2-38. The observational work was followed up by Harries & Howarth (1997b) with the development of a numerical model which successfully reproduced the observed line ratios, velocities, polarizations and the viewing-angle (orbital) dependence of the line strengths and polarized intensities. In principle, the structure of the position angle variation in resolved Raman lines provides a diagnostic of the extent of the ionized region in symbiotic systems and the conditions in the red-giant wind, particularly if the observations are undertaken over the complete orbital path.

For symbiotic star systems, Harries & Howarth (1996b) have shown, using SY Mus as an example, how a data series can lead to the determination of the orbital parameters. The same principle of establishing orbital information by polarimetry has also been applied to AG Dra by Schmid & Schild (1997a), and to Z And by Schmid & Schild (1997b) who emphasised the fact that a value for i may be determined to help resolve the mass function of these systems. For Z And, they obtained values of $i = 47° \pm 12°$ and $\omega = 72° \pm 6°$. A value of $0.6M_\odot$ was obtained for the hot stellar component, typical of a white dwarf, and indicating the sources luminosity as being due to thermonuclear reactions, rather than accretion onto a main sequence star.

The star R Aqr exhibits the spectral characteristics of a symbiotic star, but Svatoš & Šolc (1981) have suggested that its polarization behaviour has characteristics akin to that of *o* Ceti, and that it may be a single star system rather than possessing a binary nature.

The peculiar M6 giant, CH Cygni, was monitored by Piirola (1988) during one of its outbursts when its quiescent spectrum developed into being more like a classical symbiotic star. Over a 5-year interval, the direction of vibration rotated by $\approx 120°$. It is suggested that over the outburst, the observations have covered the formation, growth and disappearance of dust particles in the circumstellar material.

14.6
Carbon Stars/RV Tauri Stars

The carbon rich RV Tauri star, AR Pup, with a photometric period $\sim$ 75 days, was observed by Raveendran, Kameswara Rao, Deshpande, *et al.* (1985) to display very large changes in $p(\lambda)$ and $\zeta(\lambda)$ over an interval of a few months.

Broadband ($BVRI$) polarimetry has been undertaken by Raveendran (1991a) for a variety of carbon stars. Although there is significant scatter in the data, it was concluded that carbon stars show a flatter wavelength dependence than oxygen-rich objects. Circumstellar grain scattering appears to be the main mechanism for the intrinsic polarization of the observed objects.

Numerical computations have been performed by Raveendran (1991b) on the polarization generated by circumstellar dust envelopes. He concluded that any non-uniform surface brightness distribution was likely to cause the greatest effects on the normalized wavelength dependence of the polarization and also changes across spectral features. The envelope geometry has little effect on the normalized $p(\lambda)$ behaviour, and radial pulsation of the star does not significantly affect the net polarization. In terms of possible grain types, the polarimetric behaviour of carbon stars is inconsistent with scattering by graphite grains.

14.7
FK Comae Stars

These stars are oddities in that they are late-type fast-rotating giants. In this category, Piirola & Vilhu (1982) undertook polarimetry of HD 199178 with classification of G5 III–IV or G5p. They recorded a behaviour of $p(\lambda) \propto \lambda^{-4}$, with a temporal variation of p which matched the suggested photometric period of $\sim$ 4 days. It was proposed that the star has magnetic active regions distributed with a range of longitudes, with the polarigenic mechanism being either Rayleigh scattering and/or saturation of the transverse Zeeman effect, varying with the stellar rotation period.

Using ZDI techniques, magnetic regions have been monitored across the surface of YY Men by Donati, Semel, Carter, *et al.* (1997). It was found, in common with all the other stars measured in the same observational run, that the magnetic regions were several hundred degrees cooler than the surrounding photosphere.

14.8
Infrared Stars

For two extremely red stars, NML Cyg and NML Tau, Forbes (1967) measured their polarization in the infrared. The former object displayed high polarization, while the latter provided levels hardly different from the instrumental values. In the visual part of the spectrum, Appenzeller & O'Dell (1967) found NML Taurus to have a high level of polarization. The wavelength dependence of 11 infrared objects was investigated by Kruszewski (1971). For NML Cyg, in addition to a large interstellar polarization, a variable intrinsic polarization was noted. Both NML Tau and CIT 6 exhibited large amplitude variations with maximum p at light minimum.

Early infrared polarimetry was undertaken by Dyck, Forbes & Shawl (1971), expanding the spectral coverage of measurements for some 64 red and infrared stars over 1–4 µm. It was shown that large polarization in this part of the spectrum is usually associated with extreme circumstellar characteristics among cool stars. Many of the sources from the Caltech 2-µm survey were found to be intrinsically polarized and particular attention was paid to VY CMa, with a model developed involving a circumstellar shell containing two discrete particle sizes – 0.1 and 1 µm. Satisfactory agreement with the observations was achieved considering spherical grains with refractive index corresponding to $(Mg,Fe)SiO_3$. Observations at 10 µm were conducted by Capps & Dyck (1972) on a selection of cool stars with circumstellar shells. Generally the values of p were small ($\sim$1%) and barely detectable. For the three most interesting stars (IRC+10216, VY CMa, and NML Cyg), the recorded polarization at 10 µm appears to be a simple extension of the mechanism producing the polarization in these stars at shorter wavelengths. With respect to NML Cyg, Penston (1967) proposed an intriguing model suggesting that the behaviour of $p(\lambda)$ was in keeping with the presence of a high magnetic field associated with the source being a protostar, exchanging angular momentum with its surroundings by magnetic torques, rather than an alternative view that it comprises a highly reddened M-type supergiant.

Polarization measurements in the visual region have been linked to infrared excess at 11 µm by Dyck, Forrest, Gillett, *et al.* (1971) for a sample of 60 late-type stars. A theory was also developed which explains how the relationship comes about through the scattering and absorption optical depth of circumstellar clouds containing solid particles. Both NML Cyg and VY CMa display circular polarization in the infrared as described by Serkowski (1973). Maximum v occurs near the wavelength of minimum linear polarization, as expected from Mie scattering theory.

VY CMa may be classified as a hypergiant. Being the largest known star, and also one of the most luminous, it has attracted much observational attention as an OH emission source. Large polarization was detected by both Shawl (1969) and Serkowski (1969a), together with a strong wavelength dependence of the position angle. The UBV measurements suggested that Rayleigh scattering by circumstellar dust grains produces the polarization, rather than synchrotron radiation being present. Hashimoto, Maihara, Okuda, *et al.* (1970) made observations of this object in the infrared H- and K-bands finding the values to follow an extrapolation of measurements made previously by others in the visual part of the spectrum. Forbes (1971) extended the polarization measurements of VY CMa into the infrared, confirming a near-linear rise of p with wavenumber.

Extremely high values of polarization in the blue spectrum region have been observed by Serkowski (1969b) in the nebulae associated with VY CMa and R CrA. For the former object, the value of p was ~40%. Both stars also showed significant changes in p over an interval of a few weeks. By exploring the polarization structure associated with the nebulosity surrounding VY CMa, Herbig (1972) suggested that the temporal variability of the integrated radiation can be explained by the photometric variability of the star, or of portions of the nebula. The dispersion of the polarization position angle can be explained by a wavelength variation of the relative brightness of the star and various parts of the nebula.

Remarkable structure in the spectral range 4000–8250 Å, with reductions in $p \sim 1\%$ and rotations of direction of vibration $\sim 10°$ across the TiO bands, have been recorded by Aspin, Schwarz & McLean (1985) for VY CMa. Using a 'cell hotspot model', they reproduced the characteristics of the observed behaviour, providing possible values for the sizes of the hotspots and their temperatures. The difference in behaviour between VY CMa and α Ori can be accounted for by an increase in the amount of scattering material, or by taking the effective temperature as 2700° K, compared with 3900° K.

The Becklin–Neugebauer (BN) object in the Orion nebula has also attracted polarimetric attention. Breger & Herdorp (1973) made observations at 1.6 µm and found a polarization of 25%. In addition, they also investigated NU Ori, also near to the Orion Nebula, with a range of passbands, and noticed that there was a significant rotation of the position angle across the spectrum. Loer, Allen & Dyck (1973) extended the infrared polarization measurements of the BN object to 2.2 and 3.5 µm. The polarization displayed a minimum between 4 and 8 µm encouraging circular polarization measurements to be attempted by Serkowski & Rieke (1973) with positive results. Some part of the polarization appears to have its source in a dense cloud, with mean alignment of particles changing along the line of sight. Dyck, Capps, Forrest, *et al.* (1973) found this same object to be highly polarized in the 5–11 µm spectral range. From 8 to 11 µm, the polarization is strongly correlated with the optical depth in the 10 µm absorption feature, and reaches a maximum of about 15% at 10 µm. The observations are consistent with the polarization being produced by a cloud of cool, absorbing, elongated, aligned dust particles in front of the object.

By using the discrete dipole approximation method, the polarization engendered by porous-spherical dust grains has been explored by Henning & Stognienko (1993) to mimic the observed behaviour associated with the silicate features in the infrared. They found that compact oblate grains give a better fit to the polarization in the 10 and 18 μm features of the massive young stellar object, AFGL 2591, rather than oblate, or porous grains. An increase of porosity results in an increase of the 18 μm to 10 μm peak polarization ratio, as desired for fitting the observed polarization of the BN object, but also there is a shift of the peak polarization to longer wavelengths.

The infrared source IRC + 10216 was observed by Shawl & Zellner (1970) to have high p (∼20%) in the I-band. The polarization appears to be generated in an ellipsoidal or disc-shaped envelope surrounding a low-temperature dust cloud.

Near-infrared polarimetry of a variety of cool stars, including M giants, supergiants, Mira variables and carbon stars, was undertaken by McCall & Hough (1980). Significant values were found for most objects. Temporal variability of p and position angle were a common property. In some oxygen-rich stars, there is evidence of polarization reversals or 90° step-like rotations, as might occur for Mie scattering associated with certain sized particles.

Daniel (1982) suggested that to achieve the relatively high values of polarization in cool stars, the circumstellar envelope cannot be considered as optically thin. To deal with this situation, he promoted models involving multiple scattering within various geometries, using a Monte Carlo technique to follow the emergence of the radiation through the shell. In his paper, he applied the model to mimic behaviour of about 12 stars whose polarization, some with sudden rotations of position angle at a particular wavelength, have been well recorded.

The Galactic nucleus has been observed for infrared polarization at 10.2 μm by Low, Kleinmann, Forbes, *et al.* (1969) with inconclusive results.

14.8.1

Molecular Clouds

Polarimetry has been extended by Novak, Gonatas, Hildebrand, *et al.* (1987) to the 100 μm spectral region. Positive detections from the cores of the molecular clouds of the Kleinmann-Low (KL) nebula in Orion, Mon R2 and Sgr A have been made, allowing vector maps to be produced. The polarization is attributed to continuum thermal emission from magnetically aligned grains. The inferred field directions lie along the observed rotational axes of the cores of these clouds.

Initial results of submillimetre polarimetric observations of a variety of objects, including dust clouds have been presented by Flett & Murray (1991). Polarimetry at 800 μm by Vallée & Bastien (1996) of the dust cloud, M17-SW, has provided vector maps, which suggest that the cloud's magnetic field is mainly perpendicular to the cloud's elongation.

14.9
Red dwarfs/BY Dra Stars

Following reports of polarization activity in late-type dwarfs, Zappala (1969) conducted a survey of 10 dM and dMe stars but found that none could be identified as having intrinsic polarization. The flare star, BY Dra, was observed by Koch & Pfeiffer (1976) who reported that polarization variability in the red, with time scales on the order of months, had been detected at the 99% confidence level, but with no links made to the rotational photometric modulation of $3.^{d}8$, nor to the spectroscopic binary period of $5.^{d}97$. With this encouragement, Mullan & Bell (1976) modelled the effects of magnetic intensification, suggesting that the observed polarization was a possible evidence of magnetic fields of order of 10 kG in this star. Pettersen & Hsu (1981) conducted a survey of 19 solar neighbourhood flare stars and spotted stars and obtained null detections, however, for all of them, including BY Dra. A similar observational programme by Clayton & Martin (1981) found no evidence for intrinsic polarization of five UV Ceti stars also including the spotted flare star BY Dra. Much earlier, Efimov (1968) had drawn attention to the importance of undertaking polarimetry during flare episodes of UV Ceti stars, but discussed the practical difficulties of obtaining the required accuracy over the very short time scales of such events.

Positive results of high-dispersion spectrographic observations in the region of Hα for BY Dra, however, have been presented by Anderson, Hartmann & Bopp (1976). A Zeeman spectrogram obtained with the starspot near the limb shows obvious differences between the Hα emission profile seen in the two senses of circular polarization. If this is interpreted as a longitudinal Zeeman effect, a field of 40 kG is implied. The photospheric absorption-line spectrum shows no gross evidence of large magnetic fields, but the sensitivity of these observations is such that fields of several kilogauss cannot be ruled out.

A high-resolution infrared spectrum of the dM3.5e flare star, AD Leo, obtained by Saar & Linsky (1985) with the Kitt Peak 4 m Fourier transform spectrometer, clearly shows the presence of strong magnetic fields. Although polarimetry was not used directly, advantage of the proportionality to λ^2 of magnetic Zeeman splitting, and the near-infrared peak in stellar flux, was taken in this study. Five absorption lines in the 4400–4600 cm^{-1} region (2.17–2.27 µm) have been modelled, and it was inferred that $73\% \pm 6\%$ of the surface of AD Leo is covered by active regions, outside of dark spots, containing a mean field strength of 3800 ± 260 G. If these active regions are brighter than the quiet photosphere, the surface filling factor will be somewhat smaller. Since simultaneous Hα observations exhibited no evidence of flares, the observations probably represent the quiescent magnetic flux level. The large observed filling factor is consistent with efficient dynamo generation of magnetic flux in this rapidly rotating star.

14.10
Non-Extreme Late-Type Stars

The results of a survey of solar neighbourhood stars by Tinbergen & Zwaan (1981) suggested that intrinsic linear polarization begins to appear in stars later than F1. They proposed its origins to the presence of differential saturation of the Zeeman components associated with transverse magnetic fields. Solar-types of course should be included under this wide umbrella, but reference to such stars is postponed to the following chapter.

The possibilities of detecting polarization are more likely if chromospheric activity is detected say by the presence of Ca II H and K in emission. An early investigation on the possibility of detecting polarization in these emission features themselves was undertaken by Chen (1982) for the stars λ And, σ Gem, μ Gem, ϵ Gem, η Gem and α Her. By using photography, the level of detectivity at $\sim$10% was low and a null result ensued.

Measurements at the Hβ and Ca II K lines of a sample of 25 late-type stars (mainly K type) were made by Clarke, Schwarz & Stewart (1985). Enhancements of p were found in these lines for a few of the monitored objects. A similar study was made by Clarke & Brooks (1985), mainly of Southern Hemisphere stars, with suspicions that α CMi and α Sco display polarization changes across the Ca II K line at detection levels $\sim \pm 0.01\%$.

Long term and accurate monitoring in the B-band of the K2 III giant α Boö (Arcturus) by Kemp, Henson, Kraus, *et al.* (1986) indicated variations with amplitude in p of about 0.005%, with a period or semi-period of around 45 days. Three different processes were explored for the polarigenic mechanism; pulsation modulation appeared to be ruled out, the more likely cause being related to the rotation of the star.

Based on the mechanism of magnetic intensification, Landi Degl'Innocenti (1982) modelled the possible periodic variability of the linear polarization gener-

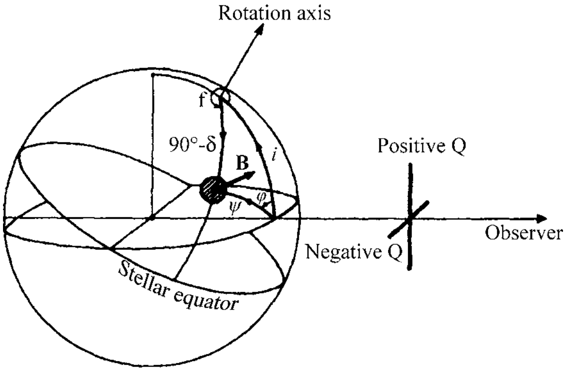

Fig. 14.6 The model of Landi Degl'Innocenti depicts a magnetic region at latitude, δ, relative to the rotational axis of the star, with the local magnetic field direction defined by the polar angles, ψ and ϕ. The polarigenic mechanism is based on magnetic intensification. (Taken from Landi Degl'innocenti, 1982.)

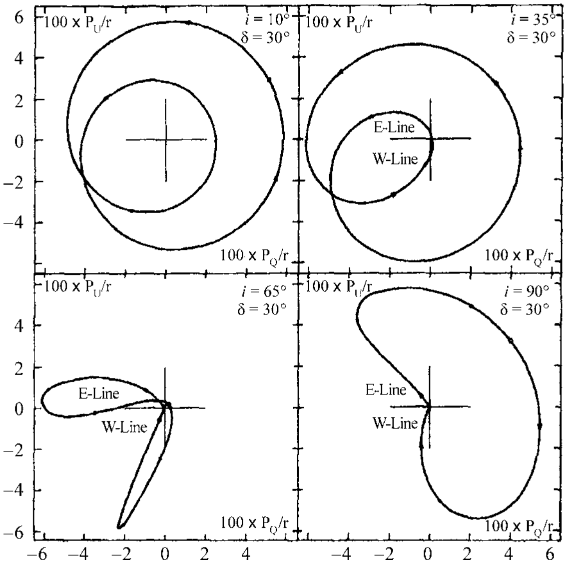

Fig. 14.7 Examples of the expected polarimetric behaviour of a star with a magnetic spot with the emitted radiation from the active area suffering magnetic intensification. These diagrams relate to the magnetic zone being at latitude 30° for various angles of inclination, *i*. (Taken from Landi Degl'innocenti, 1982.)

ated from cool stars with magnetic structures. The loci of the expected behaviour is presented according to the inclination of the star for random distributions of magnetic regions in two activity belts, equidistant from the stellar equator. The geometry associated with a single spot is depicted in Figure 14.6. A sample of the expected polarimetric behaviour is illustrated in Figure 14.7 for a spot at latitude 30°, with the star viewed with a range of inclinations.

Modelling to describe broadband linear polarization was advanced by Huovelin & Saar (1991) with a treatment involving integrations over the stellar surface to describe the spatial structures. This approach demonstrated the inadequacies of simple scaling predictions of simple spot models when the magnetic region filling factors are larger than ≈1% of the visible hemisphere, the discrepancies being particularly marked when the region is close to the stellar limb.

References

References to Introduction and Surveys

Arsenijević, J. (1986) Polarization of radiation from some cool supergiants. *Pubs. Obs. Astron. Beograd.* No: 28, 55pp (In Croation). [312]

Code, A.D., Whitney, B.A. (1995) Polarization from scattering blobs. *ApJ*, **441**, 400–407. [313]

Dyck, H.M., Jennings, M.C. (1971) Intrinsic polarization in K and M giants and supergiants. *AJ*, **76**, 431–444. [311]

Dyck, H.M., Johnson, H.R. (1969) Chromospheres and polarization in late-type stars. *ApJ*, **156**, 389–392. [311]

Kruszewski, A., Coyne, G.V. (1976) Wavelength dependence of polarization. XXXI. Cool stars. *AJ*, **81**, 641–649. [312]

Kruszewski, A., Gehrels, T., Serkowski, K. (1968) Wavelength dependence of polarization. XII. Red Variables. *AJ*, **73**, 677–687. [311]

Schwarz, H.E. (1985) Narrow band polarimetry of a sample of cool giants and supergiants. *A&A*, **147**, 111–114. [312]

Schwarz, H.E. (1986) Polarimetry of cool giants and supergiants. *Vistas Astron.*, **29**, 253–280. [312]

Shawl, S.J. (1975) Wavelength dependence of polarization XXVIII. Circumstellar scattering: polarization and reddening models. *AJ*, **80**, 595–601. [312]

Simmons, J.F.L. (1982) Analytic treatment of polarization by arbitrary scattering mechanisms in circumstellar envelopes – I. Single Stars. *MNRAS*, **200**, 91–113. [312]

Simmons, J.F.L. (1983) Analytic treatment of polarization by arbitrary scattering mechanisms in circumstellar envelopes – II. Binary Stars. *MNRAS*, **205**, 153–170. [312]

Voshchinnikov, N.V., Karjukin, V.V. (1994) Multiple scattering of polarized radiation in circumstellar dust shells. *A&A*, **288**, 883–896. [312]

References to Late-Type Supergiants

Abramyan, G.V. (1981) Polarimetric investigations of red supergiants. *Soob. Byurakan Obs.*, **52**, 24–43. [313]

Abramyan, G.V. (1982) The interstellar component of linear polarization of 12 red supergiants. *Soob. Byurakan Obs.*, **53**, 40–76. [313]

Arsenijević, J., Kubičela, A., Vince, I. (1980) Surprisingly high polarization of μ Cephei. *IBVS*, No: 1859, Budapest. [313]

Clarke, D., Schwarz, H.E. (1984) The polarization of α Orionis II. Interpretation of narrow-band measures. *A&A*, **132**, 375–380. [314, 314]

Coyne, (SJ) G.V., Kruszewski, A. (1968) Wavelength dependence of polarization. XI. Mu Cephei. *AJ*, **73**, 20–25. [313]

Doherty, L.R. (1986) On the polarization of alpha Orionis. *ApJ*, **307**, 261–268. [315]

Grigoryan, K.A. (1958) Polarization observations of μ Cep. *Soob. Byurakan Obs.*, **28**, 45–48. [313]

Hayes, D.P. (1980) Ordered linear polarization changes in Betelgeuse. *ApJ*, **241**, L165–L168. [313, 314]

Hayes, D.P. (1981a) B-filter linear polarization measurements of μ Cep in the Autumn of 1980. *IBVS*, No: 1984, Budapest. [313]

Hayes, D.P. (1981b) Lower atmosphere changes inferred from variations in Betelgeuse's linear polarization. *PASP*, **93**, 752–755. [314]

Hayes, D.P. (1982) Linear polarization of the late-type variable stars μ Cep and Mira in year 1981. *IBVS*, No: 2064, Budapest. [313]

Hayes, D.P. (1984) Variations of Betelgeuse's optical linear polarization over four consecutive observing seasons: 1974–1983. *ApJS*, **55**, 179–188. [314]

Le Borgne, J.F., Mauron, N., Leroy, J.L. (1986) The polarized dust shell around α Orionis. I. New UBV measurements. *A&A*, **168**, 211–216. [315]

Marcondes-Machado, J.A. (1987) A model for the intrinsic linear polarization of cool giant and supergiant stars. *A&A*, **188**, 131–136. [315]

Mauron, N., Le Borgne, J.F. (1986) The polarized dust shell around α Orionis. II. The silicon fractional condensation, mass-loss rate and grain radius. *A&A*, **168**, 217–224. [315]

Schwarz, H.E., Clarke, D. (1984) The polarization of α Orionis I: Interpretation of broadband measures. *A&A*, **132**, 370–374. [314]

Shafter, A., Jura, M. (1980) Circular polarization from scattering by circumstellar grains. *AJ*, **85**, 1513–1519. [315]

Tinbergen, J., Greenberg, J.M., de Jager, C. (1981) Multicolor linear polarimetry of Betelgeuse and Antares. *A&A*, **95**, 215–220. [313]

Tuthill, P.G. (1994) PhD Thesis: "Imaging Stars Through the Atmosphere", Chapter 4, University of Cambridge, Cambridge. [315]

Tuthill, P.G., Hanhiff, C.A., Baldwin, J.E. (1997) Hotspots on late-type supergiants. *MNRAS*, **285**, 529–539. [315]

White, R.E., Shawl, S.J., Coyne (SJ), G.V. (1984) Discovery of intrinsic polarization in the apparent light of globular cluster red giant stars. *AJ*, **89**, 480–486. [315]

Zappala, R.R. (1967) Fluctuating polarization in long-period variable stars. *ApJ*, **148**, L81-L85. [313]

References to Mira Variables

Bieging, J.H., Schmidt, G.D., Smith, P.S., Oppenheimer, B.D. (2006) Optical spectropolarimetry of asymptotic giant branch and post-asymptotic giant branch stars. *ApJ*, **639**, 1053–1068. [318]

Boyle, R.P., Aspin, C., Coyne, G.V., McLean, I.S. (1986) CCD spectropolarimetry of a sample of cool variable stars. *A&A*, **164**, 310–320. [318]

Codina-Landaberry, S.J., Magalhães, A.M. (1980) Narrowband polarimetry of southern red long-period variables. *AJ*, **85**, 875–881. [318]

Coyne, G.V. (S.J.), Magalhães, A.M. (1977) Wavelength dependence of polarization. XXXII. Narrow-band polarization effects in cool stars. *AJ*, **82**, 908–915. [316]

Coyne, G.V. (S.J.), Magalhães, A.M. (1979) Wavelength dependence of polarization. XXXVI. Changes in polarization across TiO Bands in cool stars. *AJ*, **84**, 1200–1210. [316]

Donn, B., Stecher, T.P., Wickramasinghe, N.C., Williams, D.A. (1966) Comments on the intrinsic polarization of Mira variables. *ApJ*, **145**, 949–951. [316]

Dyck, H.M. (1968) Photometric polarimetry of late-type stars. *AJ*, **73**, 688–696. [316]

Dyck, H.M., Sanford II, M.T. (1971) Multicolor polarimetry of some Mira variables. *AJ*, **76**, 43–49. [316]

Gehrels, T. (1972) On the circular polarization of HD 226868, NGC 1068, NGC 4151, 3C 273, and VY Canis Majoris. *ApJ*, **173**, L23–L25. [316]

Harrington, J.P. (1969) The intrinsic polarization of Mira Variables. *Astrophys. Lett.*, **3**, 165–168. [315]

Hayes, D.P. (1982) Linear polarization of the late-type variable stars μ Cep and Mira in year 1981. *IBVS*, No: 2064, Budapest. [316]

Hayes, D.P., Russo, R.A. (1981) Mira's linear polarization near the 1980 light maximum. *IBVS*, No: 1910, Budapest. [316]

Landstreet, J.D., Angel, J.R.P. (1977) Detection of polarization variation across absorption features in Mira variables. *ApJ*, **211**, 825–835. [317, 317]

Magalhães, A.M., Coyne, G.V. (S.J.), Benedetti, E.K. (S.J.) (1986) Time dependent spectropolarimetry of the red variable V CVn. *AJ*, **91**, 919–924. [317]

Magalhães, A.M., Coyne, G.V., Codina-Landaberry, S.J., Gneiding, C. (1986) Polarimetric evidence for an evolving circumstellar cloud in L_2 Puppis. *A&A*, **154**, 1–7. [318]

Materne, J. (1976) The wavelength dependence of polarization of Mira stars compared with the interstellar polarization in a field near the galactic equator. *A&A*, **47**, 53–58. [316]

McLean, I.S. (1979) Narrow-band polarimetry of the Mira variable R Tri and the semi-regular variable μ Cep. *MNRAS*. **186**, 21–30. [316]

McLean, I.S., Clarke, D. (1977) Narrow-band structure in the intrinsic linear polarization of the Mira variable R Carinae. *MNRAS*, **179**, 293–301. [317]

McLean, I.S., Coyne, G.V. (S.J.) (1978) Spectropolarimetry of o Ceti (Mira): discovery of polarized Balmer emission. *ApJ*, **226**, L145–L148. [317]

Rich, A., Williams, W.L. (1973) A search for optical circular polarization in white dwarfs and late-type stars with circumstellar shells. *ApJ*, **180**, L123–L126. [316]

Serkowski, K. (1966a) Long period variable stars with large intrinsic polarizations. *IBVS*, No: 141, Budapest. [315]

Serkowski, K. (1966b) Intrinsic polarization of the Mira variables. *ApJ*, **144**, 857–859. [315]

Serkowski, K. (1973) Infrared circular polarization of NML Cygni and VY Canis Majoris. *ApJ*, **179**, L101–L106. [316]

Shawl, S.J. (1975) Wavelength dependence of polarization. XXIX. Observations of red variable stars. *AJ*, **80**, 602–624. [316]

Tomaszewski, L., Landstreet, J.D., McLean, I.S., Coyne, G.V. (1980) Spectropolarimetry of Omicron Ceti around the 1978 Maximum. *ApJ*, **238**, 935–940. [317]

Yudin, R.V., Evans, A. (2002) Polarimetry of evolved stars. *A&A*, **386**, 916–925. [316]

References to AGB and R Cor Bor Stars

Clayton, G.C., Bjorkman, K.S., Nordsieck, K.H., Zellner, N.E.B., Schulte-Ladbeck, R.E. (1997) Evidence for a bipolar geometry in R Coronae Borealis. *ApJ*, **476**, 870–874. [321]

Coyne, G.V., (1974) Polarimetric observations of R Coronae Borealis stars. *IBVS* No: 914, Budapest. [319]

Coyne, G.V., Shawl, S.J. (1974) Polarimetry of R Coronae Borealis at visual light minimum. *ApJ*, **186**, 961–966. [319]

Johnson, J.J., Jones, T.J. (1991) From red giant to planetary nebula: Dust, asymmetry, and polarization. *AJ*, **101**, 1735–1751. [319]

Kameswara Rao, N., Raveendran, A.V. (1993) UBVR Polarimetry of the peculiar R CrB star V 854 Centauri. *A&A*, **274**, 330–334. [319]

Kastner, J.H., Weintraub, D.A. (1994) Broken symmetry: The structure of the dust envelope of IRC +10216. *ApJ*, **434**, 719–732. [319]

Likkel, L., Morris, M., Kastner, J.H., Forveille, T. (1994) Radio and near-infrared images of IRAS 21282+5050: a transitional planetary nebula. *A&A*, **282**, 190–196. [319]

Serkowski, K., Kruszewski, A. 1969. Changes in polarization of the R Coronae Borealis star RY Sagittarii. *ApJ*, **155**, L15–L16. [318]

Trammell, S.R., Dinerstein, H.L., Goodrich, R.W. (1994) Evidence for the early onset of aspherical structure in the planetary nebula formation process: spectropolarimetry of post-AGB stars. *AJ*, **108**, 984–997. [319]

Weintraub, D.A., Kastner, J.H., Hines, D.C., Sahai, R. (2000). Pinpointing the position of the post-asymptotic giant branch star at the core of RAFGL 2688 using polarimetric imaging with NICMOS. *ApJ*, **531**, 401–406. [320, 320]

Whitney, B.A., Clayton, G.C., Schulte-Ladbeck, R.E., Meade, M.R. (1992) Spectropolarimetry of V 854 Centauri at minimum light: clues to the geometry of the dust and emission-line region. *AJ*, **103**, 1652–1657. [321]

Yudin, R.V., Evans, A., Barrett, P., Albinson, J.S., Davies, J.K., Hutchinson, M.G. (2003) Polarimetry of evolved stars III, RV Tau and R CrB stars. *A&A*, **412**, 405–416. [321]

References to Symbiotic Stars

Aspin, C., Schwarz, H.E., McLean, I.S., Boyle, R.P. (1985) Discovery of polarization structure in the optical spectrum of the peculiar symbiotic star R Aquarii. *A&A*, **149**, L21–L23. [321]

Efimov, Y.S. (1979) Polarimetry of HM Sge in 1977-79. *Sov. Astron. Lett.*, **5**, 352–454. [321]

Harries, T.J., Howarth, I.D. (1996a) Raman scattering in symbiotic stars. I. Spectropolarimetric observations. *A&AS*, **119**, 61–90. [324, 324]

Harries, T.J., Howarth, I.D. (1996b) Spectropolarimetric orbits of symbiotic stars: SY Muscae. *A&A*, **310**, 235–238. [324]

Harries, T., Howarth, I. (1997a) Raman scattering in symbiotic stars. *Anglo-Australian Newsletter* July 97, No: 82, 5–7. [324]

Harries, T.J., Howarth, I.D. (1997b) Raman scattering in symbiotic stars. II. Numerical models. *A&AS*, **121**, 15–44. [324]

Piirola, V. (1988) Monitoring circumstellar dust formation in CH Cygni: Multicolour Polarimetry in 1977–1984. pp. 261–279 in *Polarized Radiation of Circumstellar Origin* (eds G.V. Coyne (SJ), A.M. Magalhães, A.F.J. Moffat, R.E. Schulte-Ladbeck, S. Tapia, W. Wickramasinghe). University of Arizona, Tucson, AZ. [325]

Schild, H., Schmid, H.M. (1992) Raman scattering, spectropolarimetry and symbiotic stars. *Gemini*, No: 37, September, pp. 4–7. [322]

Schild, H., Schmid, H.M. (1996) Spectropolarimetry and symbiotic stars – On the binary orbit and the geometric structure of V 1016 Cygni. *A&A*, **310**, 211–220. [323, 323]

Schmid, H.M. (1989) Identification of emission bands $\lambda\lambda$ 6830, 7088. *A&A*, **211**, L31–L34. [322]

Schmid, H.M. (1992) Monte Carlo simulations of Raman scattered OVI emission lines in symbiotic stars. *A&A*, **254**, 224–240. [322]

Schmid, H.M., Schild, H. (1994) Raman scattered emission lines in symbiotic stars: a spectropolarimetric survey. *A&A*, **281**, 145–160. [323]

Schmid, H.M., Schild, H. (1997a) Spectropolarimetry of symbiotic stars: AG Draconis. *A&A*, **321**, 791–802. [325]

Schmid, H.M., Schild, H. (1997b) The polarimetric orbit of Z Andromedae. *A&A*, **327**, 219–223. [325]

Schulte-Ladbeck, R. (1985) Linear polarization of symbiotic stars. *A&A*, **142**, 333–340. [321]

Schwarz, H.E., Aspin, C. (1987) Spectroscopy and polarimetry of the R Aquarii System. pp 471–473 in – 122nd IAU Symp – Circumstellar Matter (Heidelberg – 1986). (eds I. Appenzeller, C. Jordan. D. Reidel) Pubs. Co., Dortrecht. [322]

Shawl, S.J. (1974) Polarimetry of late-type stars. pp 821–844 in *Planets, Stars and Nebulae studied with Photopolarimetry*. Ed. T. Gehrels. University of Arizona Press, AZ [322]

Svatoš, J., Šolc, M. (1981) Intrinsic polarization variations of the symbiotic star R Aqr and the single star hypothesis. *Astrophys. Space Sci.*, **78**, 503–506. [325]

References to Carbon Stars/RV Tauri Stars

Raveendran, A.V., Kameswara Rao, N., Deshpande, M.R., Joshi, U.C., Kuleshrestha, A.K. (1985) Dramatic changes in the polarization of AR Pup. *IBVS*, No: 2713, Budapest. [325]

Raveendran, A.V. (1991a) *BVRI* polarimetry of carbon stars. *A&A*, **243**, 453–457. [325]

Raveendran, A.V. (1991b) An investigation of polarization produced by circumstellar dust envelopes. *A&A*, **243**, 445–452. [325]

References to FK Comae Stars

Piirola, V., Vilhu, O. (1982) Polarimetric observations of HD 199178 – an FK Comae type star. *A&A*, **110**, 351–354. [325]

Donati, J.-F., Semel, M., Carter, B.D., Rees, D.E., Cameron, A.C. (1997) Spectropolarimetric observations of active stars. *MNRAS*, **291**, 658–682. [326]

References to Infrared Stars/Molecular Clouds

Appenzeller, I., O'Dell, C.R. (1967) Polarization of the Taurus infrared source. *ApJ*, **149**, L5–L6. [326]

Aspin, C., Schwarz, H.E., McLean, I.S. (1985) Polarization structure and variability in the optical spectrum of VY Canis Majoris. *A&A* **151**, 169–173. [327]

Breger, M., Hardorp, J. (1973) Infrared polarimetry of very young objects including the Becklin–Neugebauer source. *ApJ*, **183**, L77–L79. [327]

Capps, R.W., Dyck, H.M. (1972) The measurement of polarized 10-micron radiation from cool stars with circumstellar shells. *ApJ*, **175**, 693–697. [326]

Daniel, J.Y. (1982) Monte Carlo study of highly polarized cool stars. *A&A*, **111**, 58–70. [328]

Dyck, H.M., Capps, R.W., Forrest, W.J., Gillett, F.C. (1973) Discovery of large 10-micron linear polarization of the Becklin–Neugebauer source in the Orion Nebula. *ApJ*, **183** L99–L102. [327]

Dyck, H.M., Forrest, W.J., Gillett, F.G., Stein, W.A., Gehrz, R.D., Woolf, N.J., Shawl, S.J. (1971) Visual intrinsic polarization and infrared excess of cool stars. *ApJ*, **165**, 57–66. [326]

Dyck, H.M., Forbes, F.F., Shawl, S.J. (1971) Polarimetry of red and infrared stars at 1 to 4 microns. *AJ*, **76**, 901–915. [326]

Flett, A.M., Murray, A.G. (1991) First results from submillimetre polarimeter on the James Clerk Maxwell Telescope. *MNRAS*, **249**, 4P–6P. [328]

Forbes, F.F. (1967) The infrared polarization of the infrared star in Cygnus. *ApJ*, **147**, 1226–1229. [326]

Forbes, F.F. (1971) The infrared polarization of Eta Carinae and VY Canis Majoris. *ApJ*, **165**, L83–L86. [327]

Hashimoto, J., Maihara, T., Okuda, H., Sato, S. (1970) Infrared polarization of the peculiar M-type variable VY Canis Majoris. *Pub. Astron. Soc. Japan*, **22**, 335–340. [327]

Henning, Th., Stognienko, R. (1993) Porous grains and polarization of light: The silicate features. *A&A*, **280**, 609–616. [328]

Herbig, G.H. (1972) VY Canis Majoris III: Polarization and structure of the nebulosity. *ApJ*, **172**, 375–381. [327]

Kruszewski, A. (1971) Wavelength dependence of polarization. XXIV. Infrared objects. *AJ*, **76**, 576–580. [326]

Loer, S.J., Allen, D.A., Dyck, H.M. (1973) 2.2 and 3.5-Micron polarization measurements of the Becklin–Neugebauer object in the Orion Nebula. *ApJ*, **183**, L97–L98. [327]

Low, F.J., Kleinmann, D.E., Forbes, F.F., Aumann, H.H., (1969) The infrared spectrum, diameter, and polarization of the galactic nucleus. *ApJ*, **157**, L97–L101. [328]

McCall, A., Hough, J.H. (1980) Near infrared polarimetry of cool stars. *A&AS*, **42**, 141–154. [328]

Novak, G., Gonatas, D.P., Hildebrand, R.H., Platt, S.R., Dragovan, M. (1989) Polarization of far-infrared radiation from molecular clouds. *ApJ*, **345**, 802–810. [328]

Penston, M.V. (1967) The polarization of NML Cygnus. *The Observatory*, **87**, 276–280. [326]

Serkowski, K. (1969a) Large optical polarization of the OH emission source VY Canis Majoris. *ApJ*, **156**, L139–L140. [327]

Serkowski, K. (1969b) Polarization of the reflection nebula associated with VY Canis Majoris and R Coronae Austrinae. *ApJ*, **158**, L107-L110. [327]

Serkowski, K. (1973) Infrared circular polarization of NML Cygni and VY Canis Majoris. *ApJ*, **179**, L101–L106. [327]

Serkowski, K., Rieke, G.H. (1973) Circular polarization of the Becklin-Neugebauer infrared sources in the Orion Nebula. *ApJ*, **183**, L103–L104. [327]

Shawl, S.J. (1969) Strong optical polarization observed in VY Canis Majoris. *ApJ*, **157**, L57–L58. [327]

Shawl, S.J., Zellner, B. (1970) Polarization of IRC + 10216. *ApJ*, **162**, L19–L20. [328]

Vallée, J.P., Bastien, P. (1996) Magnetic fields in the dust cloud M17-SW from extreme-infrared (800 μm) polarimetry. *The JCMT Newsletter*, No:7, September 1996, 19–21. [328]

References to Red Dwarfs/BY Dra Stars

Anderson, C.M., Hartmann, L.W., Bopp, B.W. (1976) Zeeman observations of the Hα region in BY Draconis. *ApJ*, **204**, L51–L54. [329]

Clayton, G.C., Martin, P.G. (1981) On the intrinsic polarization of red dwarfs. *AJ*, **86**, 1518–1519. [329]

Efimov, Yu. S. (1968) On the polarimetric study of UV Ceti type star flares. *IAU Coll. Budapest*. Non-periodic phenomena in variable stars, pp. 169–171. [329]

Koch, R.H., Pfeiffer, R.J. (1976) The linear polarization of BY Draconis. *ApJ*, **204**, L47–L49. [329]

Mullan, D.J., Bell, R.A. (1976) Possible evidence for the occurrence of magnetic fields of order of 10 kilogauss in the red dwarf star BY Draconis. *ApJ*, **204**, 818–829. [329]

Pettersen, B.R., Hsu, J-C. (1981) Search for linear polarization in solar neighborhood flare stars and spotted stars. *ApJ*, **247**, 1013–1023. [329]

Saar, S.H., Linsky, J.L. (1985) The photospheric magnetic field of the dM3.5 flare star AD Leonis. (1985) *ApJ*, **299**, L47–L50. [329]

Zappala, R.R. (1969) Polarimetric observations of late-type dwarfs. *PASP*, **81**, 433–437. [329]

References to Non-Extreme Late-Type Stars

Chen, P.C. (1982) A search for resonance polarization in stars with enhanced CaII H and K emission. *PASP*, **94**, 948–949. [330]

Clarke, D., Brooks, A. (1985) Narrow-band polarization measurements of late-type stars. *MNRAS*, **212**, 211–218. [330]

Clarke, D., Schwarz, H.E., Stewart, B.G. (1985) Polarization measurements of late-type stars at Hβ and Ca II K. *A&A*, **145**, 232–240. [330]

Huovelin, J., Saar, S.H. (1991) Broad-band linear polarization in cool stars. I. Models and spatial effects for magnetic and scattering regions. *ApJ*, **374**, 319–329. [331]

Kemp, J.C., Henson, G.D., Kraus, D.J., Beardsley, I.S., Carrol, L.C., Duncan, D.K. (1986) Variable polarization and activity in Arcturus. *ApJ*, **301**, L35–L38. [330]

Landi Degl'Innocenti, E. (1982) Expected broadband linear polarization from cool stars with magnetic structures. *A&A*, **110**, 25–29. [330, 330, 331]

Tinbergen, J., Zwaan, C. (1981) Magnetic structure in cool stars II. Observational evidence for transverse magnetic fields. *A&A*, **101**, 223–225. [330]

15
General Stellar Variability

15.1
Introduction

As photoelectric polarimeters were developed in the 1950s and 1960s, their application to stars known to be photometric and/or spectroscopic variables was natural and automatic. Each type of stellar variable was examined, and frequently found to exhibit polarimetric signals. Kris Serkowski was key to the promotion of such studies, and he provided many 'firsts' in the establishment of polarimetry of variable stars (see, for example, Serkowski, 1971). It should also be put on record that he brought to the West knowledge of the substantial polarimetric researches undertaken by astronomers in the East.

Intrinsic polarization associated with stars can only be produced if symmetry is broken. This would be the case if a star possesses a non-spherical radiation field as the result of some geometric distortion, or if it has a non-uniform photospheric surface brightness, say in the form of spots, or there is clumpiness in the outer atmosphere where scattering takes place.

Any polarimetric variability, as with any other observational diagnostic, is usually investigated for periodicity. Care must be exercised, however, in using periods obtained by other means to act as the template for exploration to see if polarimetry follows the same period. In a simple exercise of considering the effects of a spot traversing the stellar disc and producing a rotational modulation, Clarke (2003) has shown the differences in periodograms that may result according to whether photometry, radial velocity or polarimetry are used as the measurement diagnostic. Analysis of the signals from the three basic observations revealed the dangers of simply using a single measurement parameter alone to investigate stellar temporal cyclic behaviour, and how analysis of polarimetric data is likely to provide strong power in the harmonics of the fundamental rotational period.

Stellar Polarimetry. David Clarke

ISBN: 978-3-527-40895-5

15.2
X-Ray Sources

Following the observational search by Angel, Novick, Vanden Bout, *et al.* (1969), for the presence of polarization of X-rays in the 6–18 keV range from Sco X-1, Angel (1969) demonstrated that polarization of a few per cent may arise for non-spherically symmetric thermal X-ray sources as a result of Thomson scattering. Many X-ray binary objects have been investigated for optical polarization signatures with positive outcomes.

Reports by Nikulin, Kuvshinov, Severny (1971) and Gnedin & Shulov (1971) suggested that the X-ray source Sco X-1 displayed substantial circular polarization ($\sim$1%). This was later followed by a discussion by Dolginov, Gnedin & Silant'ev (1973) on some astrophysical reasons why some other observers might have obtained null results because of wavelength passband differences. By improving accuracies by an order of magnitude to $\sim \pm 0.05\%$, Kemp & Wolstencroft (1972) and Illing & Martin (1972) showed that the early claims were spurious. With their higher level of detectivity and accuracy, a null result was obtained. Kemp (1972), however, still raised questions about the presence of a circular polarization. He made special checks on the possible disturbing influence of sky background contamination affecting the observations. He also noted that Gnedin & Shulov (1971) referred to the effect occurring in the red, and at a flare event. Kemp's data also suggested a flare event, but with the overall data set agreeing with expected fluctuations; an indication remained, however, of a non-Gaussian noise which was not typical of his many polarization measurements made of other objects. Gehrels (1972) also commented on the erroneous claims of Nikulin, Kuvshinov & Severny (1971) in respect to variable circular polarization from HD 226868, the optical counterpart of Cyg X-1. He also presented measurements of $p(\lambda)$ for this star, showing that its origin was essentially interstellar. Michalsky, Swedlund & Avery (1975) also presented results showing a definite circular polarization for HD 226868, but noted that a case for an interstellar origin was strong. Severny & Kuvshinov (1975) later revised the instrumentation used by Nikulin, Kuvshinov, Severny (1971), and made extensive measurements of Sco X-1, Cyg X-1 and 3C273, suggesting that all three objects exhibited an occasional appearance of appreciable circular polarization.

In a search for the Zeeman effect in the X-ray star candidates, θ^2 Orionis and X Persei, and the X-ray source Cygnus X-1, Borra (1975) investigated circular polarization in the wings of the He I line at 6678 Å, but obtained null results.

Following the possible identification of X Per with the X-ray source 2ASE 0352 +30, Baud & Tinbergen (1972) undertook circular polarimetry, but obtained a null result at a detection level of $\pm 0.02\%$. This was later followed with observations by Stokes, Avery & Michalsky (1973) who made three-colour measurements to uncertainties of $\pm 0.0006\%$. Although the *BVR* measurements provided the same sense of handedness, no firm detections were realised and, in any case, it was not possible to rule out the origin as being interstellar. In a later paper, the same research team (Avery, Michalsky & Stokes, 1973) detected a wavelength dependence of circular polarization in the star, showing no temporal variability over a 3-month period, both behaviours indicating an interstellar origin.

On its discovery, A0620-00 (= Nova Monocertis 1975) was noted as being an X-ray transient. It is a binary system, the primary of which is an X-ray emitter, and is a degenerate object whose mass has been inferred from the spectroscopic mass function. By measuring a polarimetric variation over its 8-hour binary period, Dolan & Tapia (1989) determined an inclination of $i = 57^\circ\ (+20^\circ/-50^\circ)$. They concluded that the large uncertainty limits associated with the derived value were too large to consider that the object was a black hole.

Again, following the suggestion that HZ Her was the optical counterpart of a pulsating X-ray binary system, modelled as an accreting neutron star with its magnetic axis inclined at a large angle to its rotation axis, the possibility of the presence of cyclotron emission was investigated by Stokes, Avery, Michalsky, *et al.* (1973) by circular polarimetry. A null result ensued, with no variation of v detectable related to the $1.^{\rm d}7$ X-ray period, or even a detection of v itself.

The $H\beta$ line was used for the investigation of the Zeeman effect by Kemp & Wolstencroft (1973a) in the then X-ray star candidates HD 77581 (=4U 0900-40) and θ^2 Ori. By applying line wing circular polarimetry to the X-ray candidate, HD 153919 (=4U 1700-37), Kemp & Wolstencroft (1973b) found evidence of magnetic fields which fluctuated on time scales as short as 10 minutes, but showing smaller average values over intervals of 1–3 h. The fluctuations were largest on the peak and trailing parts of the X-ray amplitude.

Polarimetry was undertaken by van Paradijs (1980) of two massive X-ray binaries, HD 77581 and HD 153919, and they noted that p was significantly variable with amplitudes $\sim 2 \times 10^{-3}$. Korhonen & Piirola (1980) also made measurements of HD 77581, again finding polarimetric variations, but with no clear periodicity from observations covering 1/2 of the orbital cycle. Östreicher & Schulte-Ladbeck (1982) made UBV polarimetric measurements of three X-ray binaries, and noted that they all displayed variations. In particular, the power spectrum for HD 153919 (4U 1700-37) displayed a conspicuous maximum at the expected frequency corresponding to the orbital semi-period. Narrow-band circular polarization observations were undertaken by Angel, McGraw & Stockman (1973) of the X-ray binaries, HD 77581 and HD 153919, mentioned immediately above, with the hope of finding indications of Zeeman splitting. The measurements provided null results.

Variable polarization was detected by Dolan & Tapia (1984) in the X-ray binaries HD 153919 and HD 152667 (= OAO 1653-40?), with correlations associated with their orbital phases, but with the polarimetric curve displaying variations from year to year. Orbital and physical parameters of the binary systems were derived from the polarimetric data. From polarimetric measurements, Dolan & Tapia (1988) determined the inclination of the X-ray binary, HD 77581, providing a value of $i = 76^\circ\ (+5^\circ/-9^\circ)$.

Polarimetric data for the X-ray transient, AO 538–66, were analysed by Simmons & Boyle (1984). Assuming the system to comprise a neutron star orbiting a Be star, they showed that the variability can be modelled by the neutron object having a highly eccentric orbit.

15.2.1
SS433

The enigmatic object, SS 433, the optical counterpart of the X-ray source, A 1909+04, stands alone in terms of its general behaviour, and in its model interpretations. Its unique structure was implied initially from the behaviour of its spectrum, and of its photometric variations. Periods of ~ 164 days and ~ 13 days are associated with the optical behaviour, the longer value related to the cyclic variation of spectral emission features, with amplitudes corresponding to relativistic velocities. The shorter period is associated with the binary nature of the system. The optical source is embedded in an extended radio object, with its main form comprising a pair of lobes. The system is suggested as being a supernova remnant, with a remaining binary component shedding material into a disc surrounding a neutron star. The general dynamics of the system have been modelled in terms of a disc and high-velocity outflow in the form of jets precessing relative to the normal of the binary plane. Overfeed into the disc promotes additional material release into the jets, these dynamics being noisy, give rise to clumpiness in the material flows, the effects being seen as short-term optical bursts.

Following the initial interest in the spectral line features exhibiting simultaneous redshifts and blueshifts, Liebert, Angel, Hege, *et al.* (1979) undertook circular spectropolarimetry to investigate the possibility of there being Zeeman signatures. Their observations provided a null result. Michalsky, Stokes, Szkody, *et al.* (1980) made some broadband polarimetric measurements but, without making a strong claim that the object might exhibit intrinsic polarization, they suggested that it displayed an unusual interstellar component.

McLean & Tapia (1980) reported on observations which revealed that the linear polarization of the optical radiation from SS433 exhibited a long-term variation, as well as large night-to-night changes. This established that a substantial fraction of the observed polarization is intrinsic to SS 433, although there is also a large interstellar component. In a later paper, McLean & Tapia (1981) explored a basic model for their data, clearly demonstrating the effect of the 164-day precessional period of the jets, being consistent with electron scattering in the jets. Kundt (1985) has also examined the data of McLean & Tapia (1981) and, from linking the successive measurements in the qu-plane, demonstrated that the effects of the orbit tend to provide a noisy oscillatory movement generally along directions parallel to a position angle ~ 10°, at the fundamental period, and also at twice this value. The whole data set have been examined by the author and phased on the orbital period of 13 days; a doubling of the variation is not seen and it cannot be confirmed that the second harmonic is present. It is difficult to decide if the windowing of observations prevents the harmonic being seen in a continuous way. Variations caused by the precessional motion of the jets appear to be approximately orthogonal to the orbit in the qu-plane, i. e., the polarization associated with jets is at an angle ~ 45° to the orbital plane.

A model describing the polarization engendered by a precessing, electron-scattering accretion disc has been developed by Bochkarëv & Karitskaya (1983), and they have considered it in relation to the behaviour of SS 433. Their work suggests that the plane of the disc is perpendicular to the mean direction of the relativistic jets indicated by both radio and X-ray observations.

Efimov, Piirola & Shakhovskoy (1984) undertook *UBVRI* measurements which allowed a value for the interstellar polarization to be assessed. A value of $p \sim 4.7\%$ was obtained. A check on nearby field stars made by the author was inconclusive, but such a high value is likely as a result of the exhibited extinction. The recorded variations assignable to the orbital period are approximately orthogonal to the interstellar direction. The variation related to the precessional period roughly follows a direction parallel to the direction of the radio jets.

Brown & Fletcher (1992) have suggested that polarization of at least 0.2% should be generated by wind heating of 'bullets' within the red- and blue-shifted jet components of the Hα line, as a result of the impact polarization principle, and have urged that attempts be made to follow their proposal by spectropolarimetry.

15.3
T Tauri Stars

T Tauri stars have spectral types running from F to M, and are pre-main sequence objects displaying optical activity and strong chromospheric lines. They are normally embedded in molecular clouds and radiate by virtue of energy released from their gravitational contraction, rather than by hydrogen fusion at their centres.

The reporting of polarimetric variability in T Tauri stars has had a checkered history. Using a very basic kind of polarimeter, Hunger & Kron (1957) suggested that NX Mon displayed large variations in polarization. These results were echoed by RHG (1958a) as an exciting development in the study of the continuous emission in the ultraviolet which is exhibited by some T Tauri stars, indicating the presence of a source of strongly polarized ultraviolet radiation, superposed on the ordinary Balmer continuum. With the suggestion that the origin of the polarization might be synchrotron radiation, Hilter & Iriarte (1958) made more careful observations of NX Mon, and blue galaxies, with negative results. It was noted that the original observations might have suffered from variable contamination from the light of the star's brighter companion. The issue was again summarized by RHG (1958b).

Polarization changes in T Tauri stars were first established by Vardanian (1964) who measured T Tau itself and RY Tau. Standard *UBV* measurements were later made by Serkowski (1969) again of T Tau, and also of AK Sco. The colour dependence of p suggested that both stars were subject to interstellar components, but the changes in the blue and yellow spectral regions were coherent. As well as temporal changes in p, large fluctuations in ζ were recorded.

Following a rapid increase of brightness of some 5 mags, Rieke, Lee & Coyne (1972) investigated the polarization of V 1057 Cyg, a T Tauri-type star associated with NGC 7000, the North American Nebula. Although photometry provides a large infrared excess from circumstellar dust, the recorded polarization was ascribed entirely to the interstellar medium. The star, R Mon, at the head of Hubble's Variable

Nebula, NGC 2261 has a T Tauri-like spectrum, and has been promoted as a protoplanetary system. It was found by Zellner (1970) to display variable polarization. The $p(\lambda)$ curve was generally flat but, on occasion, rose in the infrared. Electron scattering as the polarigenic mechanism was ruled out in favour of scattering by large dust grains. An analysis by Bastien (1981) of earlier data showed that the position angle of the intrinsic polarization is a function of both wavelength and time. Interpretation of this requires complex geometrical distributions for the scattering dust grains in an extended circumstellar envelope. The strong variations in the wavelength dependence of the polarization suggest large variations in the grain size in the dust scattering regions. High-resolution polarimetric maps of the Hubble's variable nebulosity itself have been obtained by Ageorges & Walsh (1997).

Observations of six T Tauri stars were made by Schulte-Ladbeck (1983), two of the objects already known to display intrinsic polarization, but four new ones were added to the list. The behaviour of $p(\lambda)$ was found to be consistent with the presence of dust grains, with a large range of sizes, in asymmetric circumstellar envelopes. Temporal variations were also found on time-scales on the order of days, but periodicity was not detected. For RY Tau, the position angle rotates in the qu-plane, suggesting that the scattering material is in orbit about the star.

Drissen, Bastien & St-Louis (1989) observed 21 Southern Hemisphere T Tauri stars. Some displayed obvious variability while others appeared to be more quiescent. The star RY Lup which previously had been reported as having periodic polarization variability, failed to reveal its periodicity during this later monitoring. A survey of all T Tauri stars brighter than 13th magnitude north of −30° was carried out by Bastien (1982) over a 3-year period. On the basis of a few synoptic measurements of each star, 35% of the sample exhibited polarimetric variability. Bastien's paper (his Table IV) also provides a list of 23 references of polarization observations related to his program stars and other T Tauri stars. Correlations were found between p and colour excess, $E_{(B-V)}$, between p and the average infrared colour indices, especially $\langle V \rangle - \langle L \rangle$, and between p and the positions in the HR diagram. The correlations with the infrared colour indices indicate that the excess at 3.5 μm, and longward, can be attributed to absorption of stellar radiation by dust and re-emission in the infrared for at least 25% of the stars. Further work by Bastien (1985) extended the study to T Tauri stars in the Southern Hemisphere, concluding that the rapid p variations in some stars are best explained by changes in the illumination of the dust. Correlations were found for p with IR excess, and He I, O I equivalent widths. This work was followed by another survey by Ménard & Bastien (1992) of T Tauri stars fainter than 13th magnitude with the conclusion that at least 43% and, perhaps all T Tauri stars, are polarimetric variables. On a statistical basis they showed that the data are compatible with the model of optically thick circumstellar discs.

The star, V 410 Tau, has little infrared excess and displays weak Hα emission, properties giving it membership of the naked T Tauri group, also referred to as 'weak emission T Tauri stars' (WTTS). Mekkaden (1999) confirmed its periodic photometric behaviour ($P = 1.^{d}872$), and also found small amplitude periodic variations in p and ζ linked to the light-curve, but with a small phase difference.

The variable polarization of the system has been modelled in terms of the presence of two adjacent spots on the photosphere, with changing illumination of a thin scattering circumstellar dust envelope as the star rotates.

Following the analysis of observations of T Tauri stars performed during 1979–1985, the characteristics of brightness and polarization variability have been interpreted on the basis of a hydromagnetic model of Red'kina, Tarasov, Kiselev, *et al.* (1989). The polarization parameter changes are interpreted as being due to the effect of the variable magnetic field of the star. For the case of a spherical envelope, the value of the dipole field of the star may be determined. This approach was furthered by Wood, Kenyon, Whitney, *et al.* (1996) to establish the cause of the underlying photopolarimetric behaviours of T Tauri stars. They considered a dynamical model whereby material from a magnetically truncated Keplerian disc creeps along magnetic field lines onto the stellar surface at high latitudes, producing 'hot spots' on the stellar photosphere. These spots act as the origin of the UV excesses in T Tauri stars. As the star rotates, the observed UV excess varies, as will the polarization arising from the spot from which the radiation is scattered in the circumstellar disc. The model predicts correlations between the brightness and polarization that can be tested by synoptic observations. The magnetic accretion model has been developed by Stassun & Wood (1999) who employed a Monte Carlo radiation transfer code to investigate the behaviour produced by spotted stars surrounded by dusty circumstellar discs, according to the rotational phase.

In an analysis of correlations between polarimetric and photometric characteristics of young stars, Yudin (2000) demonstrated the statistical differences between T Tauri types and Ae/Be stars. Both categories generally display an intrinsic polarization, but T Tauris offer a narrower distribution, tending not to exhibit the large values (>5%), displayed by some of the Ae/Be types.

Spectropolarimetry at Hα of 10 bright T Tauri stars has been undertaken by Vink, Drew, Harries, *et al.* (2005). Polarization signatures were recorded for nine of them, with the interpretation in terms of a model involving a compact source, with line photons being scattered off a rotating accretion disc. There is consistency between the position angle of the polarization and the axes of discs, as imaged by infrared and millimetre cameras. Comparisons were made with a similar study of Herbig AeBe stars such as AB Aur, MWC 480 and CQ Tau, which show the position angle of the polarization to be perpendicular to the imaged disc, as expected from single scattering; for the T Tauri stars DR Tau, SU Aur and the star, FU Ori, the polarization aligns with the outer disc, conforming to the effects of multiple scattering. This difference can be explained if the inner discs of Herbig Ae stars are optically thin, whilst those around T Tauri stars and FU Ori are optically thick.

By using high-resolution circular polarimetry, Symington, Harries, Kurosawa, *et al.* (2005) observed seven classical T Tauri stars. Magnetic fields were detected for BP Tau, DF Tau and DN Tau. For the former two stars, their measurements were consistent in terms of both sign and magnitude of previous studies, suggesting that the characteristics of T Tauri magnetospheres are persistent over several years. By modelling to a dipole, they determined a polar field for BP Tau of $\sim$3 kG, with a dipole offset of 40°, while the polar field for DF Tau was ~ -4.5 kG, with the dipole offset by 10°. An overall conclusion of this study is that many classical T Tauri stars have circumstellar magnetic fields that are both strong enough and sufficiently globally ordered to sustain large-scale magnetospheric accretion flows.

Further and more comprehensive data have been obtained for BP Tau by Donati, Jardine, Gregory, *et al.* (2008). The magnetospheric accretion was monitored throughout most of the rotation period for the star at two epochs. They report that the rotational modulation dominates the temporal variations of both unpolarized and circularly polarized spectral proxies which trace the photosphere and the footprints of accretion funnels. Tomographic imaging techniques were applied to construct the locations of the accretion spots. They concluded that the magnetic behaviour of BP Tau can be described by a 1.2 kG dipole field in combination with a 1.6 kG octupole, both slightly tilted with respect to the rotation axis. The accretion spots coincide with the two main magnetic poles, and overlap with dark photospheric spots, covering about 2% of the stellar surface. The scenario suggests that the magnetic fields of fully convective T Tauri stars, such as BP Tau, are not likely to be fossil remnants, but rather result from vigorous dynamo action operating within the bulk of their convection zones. The modelling suggests that the magnetosphere of BP Tau extends to distances of at least $4R_\star$ to ensure that accretion spots are located at high latitudes, and is not blown open near the surface by a putative stellar wind. It apparently succeeds in coupling to the accretion disc as far out as the co-rotation radius, and could possibly explain the slow rotation of this star.

15.4
Solar-Type Stars

It is expected that any intrinsic polarization from solar-type stars integrated over the complete globe is likely to be very small. Using a simple model based on the presence of spots co-rotating with a star, Fox (1995) has provided insight on the experimental requisites of polarimetry to detect rotational modulations. The prospect of detecting polarization associated with solar-type stars is not sanguine. Kemp, Henson, Steiner, *et al.* (1987) conducted experiments of polarimetry for the whole Sun, and large sectors of the disc, at high levels of detectivity. Upper limits for the intrinsic global solar linear polarization towards solar minimum were 0.2×10^{-6} in the *V*-band, and 0.8×10^{-6} in *B*. Circular polarization was discovered, however, with the polar sections showing $v = -1 \times 10^{-6}$ to -6×10^{-6} for the north zone, and 0 to $+2 \times 10^{-6}$ for the south. The spectral dependence of v rises steeply towards the blue. The whole disc had a net v of -0.1×10^{-6} to -1.0×10^{-6} from red to blue, the negative sign emerging from the magnetically dominant north pole. The spectral dependence of the global broadband circular polarization resembles that of sunspots, and of local non-spot regions with magnetic flux tubes. Later, when the Sun was more active, Clarke (1991) monitored the whole solar disc with a specially designed observational arrangement and showed that the observed value of p increased with the solar activity index, with changes of $\Delta p \sim 0.0002$ (see

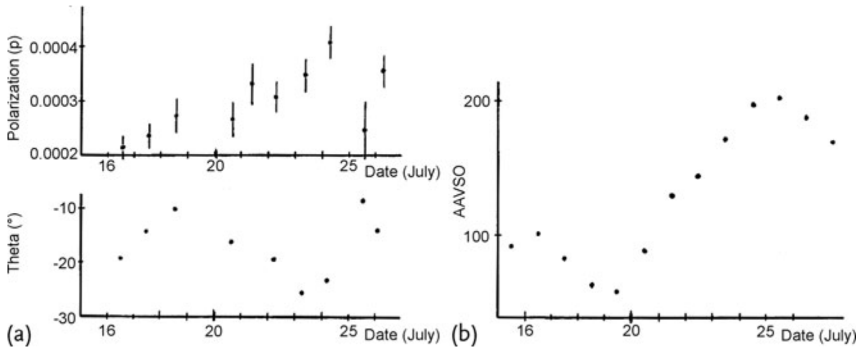

Fig. 15.1 The growth of p and the changes of ζ during a 10-day interval in July 1991 are depicted in (a) and may be compared with the increasing AAVSO activity index in (b). (Taken from Clarke, 1991.)

Figure 15.1). Clarke & Fullerton (1996) also monitored polarimetric variations between $p \sim 0.00001$ and 0.0001 in the global light during a time when the Sun was close to sunspot maximum, with the effects of the passage of a large sunspot group moving across the disc being detectable.

Coyne (1974) has described a preliminary investigation of faint stars in the Pleiades, these being young solar-types. His work suggested a number of them exhibited intrinsic polarization by the fact that the value of p is largest in the ultraviolet. At the time, the discussion was related to elementary structure of the nebulosity within the Pleiades. It may be possible that some polarization may be engendered by flare-like and spot activity which many of the early solar-type stars in the Pleiades are known to exhibit.

Ellias II & Dorren (1990) recorded polarimetric variability for the young ~70 Myr solar-type star HD 129333, probably a member of the Pleiades moving group. Broadband measurements indicated that p remained virtually constant at ~0.1%, but with the position angle rotating smoothly with a period of about 14 days. The same star also exhibited circular polarization of about 1%, but the data were insufficient to reveal periodicity, if any. Subjecting these data on the star's photometric period of 2.^{d}7, or on its harmonic (1.^{d}35), an exercise not reported in the paper, provides phased curves with no structure, suggesting that the variations are not related to the spots co-rotating with the star and giving rise to the photometric period. Elias II & Dorren (1990) discussed the possibility of the star being a binary system, but the polarimetric variation remains an enigma.

Reports by a Finnish group, including papers by Huovelin, Linnaluoto, Piirola, *et al.* (1985a, 1985b), Huovelin, Saar & Tuominen (1988), Huovelin, Linnaluoto, Tuominen, *et al.* (1989) and Huovelin & Saar (1990), announcing polarimetric variability of solar-type stars, and linked to chromospheric activity, now appear to have been abandoned, the results, particularly those for the *U*-band, being susceptible to contamination by scattered moonlight. In a Workshop Paper, Leroy (1990) discussed the net polarization that can be generated by the plethora of metal lines subject to differential saturation of the Zeeman components in the presence of a transverse magnetic field and, at the time, had reservations on its detection in the *B*-band for late-type dwarfs with magnetic spots. The results of the Finnish team were not confirmed by the careful work of Leroy & LeBorgne (1989). Huovelin & Pirrola (1990) contested the criticism related to problems of moonlight contamination. Whether or not there is rotationally modulated polarization present in late-type dwarf stars requires further study, involving measurements with improved signal-to-noise.

15.5
RS Can Ven (CVn) Stars

RS CVn stars are usually close binary systems with late- to middle-type stars showing chromospheric emission lines, radio emissions and X-ray flaring. Early polarimetric observations of such stars generally provided null results. In respect of RS CVn itself, Pfeiffer (1979) recorded an intrinsic polarization which displayed a trend of secularly declining variability over 5 years. The observed polarization variation was interpreted as a result of scattering from cool, transient circumstellar material, probably ejected in clouds or streams from the active chromosphere of the K0 component.

With observational accuracies $\sim \pm 0.01\%$, Barbour & Kemp (1981) established that the polarization in the *U*-band for HR 5110 varies synchronously on the known binary period of $2.^{d}6132$, with a peak-to-peak amplitude of $p = 0.03\%$. At the time, the promoted polarigenic mechanism was suggested to be reflection of light by the cooler star, or to be Rayleigh-type scattering by a plasma concentration in the system. The results of photometric and polarimetric observations of HR 5110 and λ And have been presented by Barbour & Kemp (1982)

A few years later, Kemp, Henson, Kraus, *et al.* (1987) discovered broadband variability of circular polarization with amplitude of $v = 0.002–0.004\%$ for λ And. The basic period associated with the variation appeared to be that of the stellar rotation period of 54 days, but there were marked differences from year to year, with a double-peaked (27 days) pattern developing, this being explainable in terms of the presence of either one or two major spots on the star. The light-curves also displayed changes in their pattern matching the developments of the curves for circular polarization, but with a curious form of anti-correlation. In their first observing season (1982), the low amplitude $v(t)$ provides a good fit to a 27-day sine wave, and contrasts with the strong 54-day light variation. Four years later, the circular polarization variation was much larger, while the light-curve had reduced its amplitude, and displaying a poorer form. These behaviours are displayed in Figure 15.2. The overall behaviour may be described by a qualitative model with two magnetic spots with opposite polarities at a high latitude ($\sim 70°$) in the hemisphere tilted towards the Earth with a small inclination of $i \approx 25°$, as sketched in Figure 15.3.

Multi-colour measurements of 15 RS CVn systems were made by Scaltriti, Piirola, Coyne *et al.* (1993). Generally any variation of polarization had small amplitude,

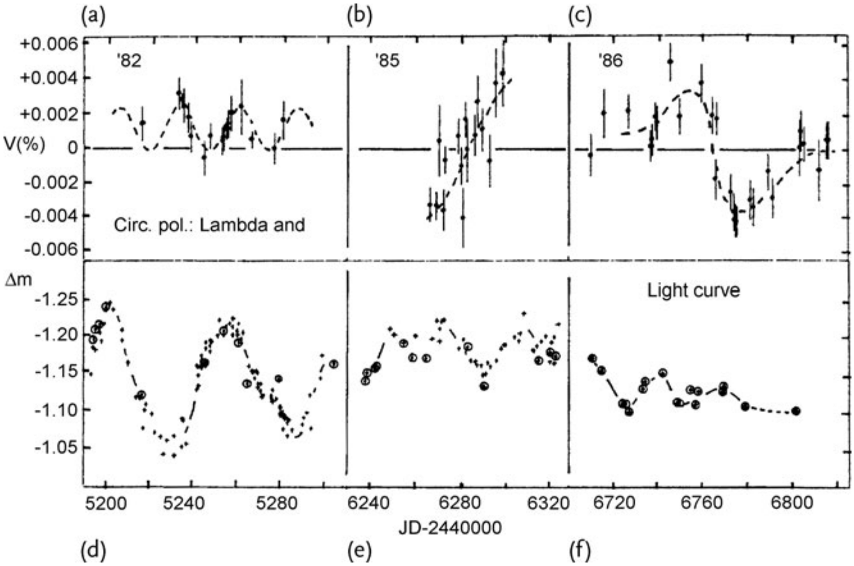

Fig. 15.2 Broadband circular polarization and brightness changes have been measured for λ And in three seasons. In (a) ν data have been regression-fitted to the first harmonic of the star's rotation period; all the other curves (b–f) are simply hand drawn. (Taken from Kemp, Henson, Kraus, *et al.*, 1987.)

but the data for four of the binaries (II Peg, DK Dra, GK Hya, UX Ari) allowed Fourier analysis to the second order. The phase-locked polarimetric behaviour of II Peg clearly indicated that the polarization is due to scattering by circumstellar material in the binary system. Analysis of the data for the other mentioned binaries was less productive and, in general, the intrinsic polarization of RS CVn binary systems is small, being $<$ 0.02 to 0.05%. Three of the systems, II Peg, UX Ari and DK Dra exhibited mean polarizations whose colour dependence differed from that of the interstellar polarization law.

Zeeman–Doppler imaging (ZDI) has proved to be a successful technique for producing both temperature and magnetic field maps of stellar photospheres, particularly of the active components of RS CVn systems. Pioneers of the technique were Donati, Semel & Rees (1992) who undertook studies of some 9 objects. Four of their target stars gave detections of magnetic fields on their cool active components, with evidence that the field structure of one of them, HR 1099, varied significantly over an interval of $1.^y3$. A concentrated programme of ZDI has been directed to this star by Donati, Brown, Semel, *et al.* (1992). This system is a non-eclipsing spectroscopic binary with an orbital period of $2.^d837$, the primary (brighter) component being active and the main source of the Ca II and Hα emission. The basic Doppler imaging of late 1988 provided maps of large spots covering the polar region of this component with temperatures some 1000 K cooler than the photosphere. Two warm regions, ~300 K hotter than the photosphere, were noted as being just above the

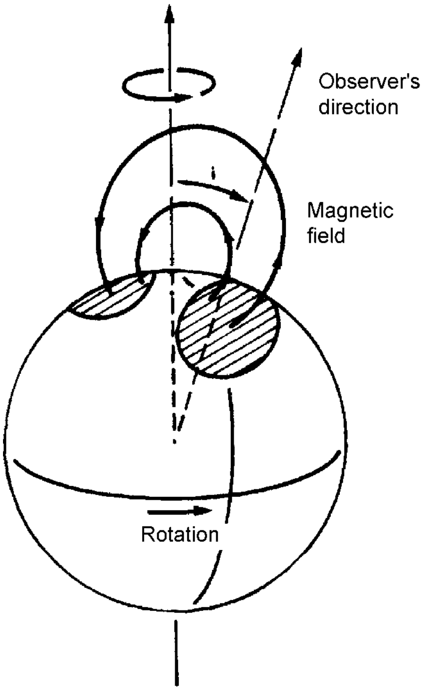

Fig. 15.3 A simple geometric model for λ And, comprising two high-latitude magnetic spots with ~ kG field strengths, with their aspect such that $i \approx 15°$, giving rise to broadband circular polarization variations. (Taken from Kemp, Henson, Kraus, *et al.*, 1987.)

equator. Two years later the pattern had evolved with significant changes in shape of the polar spot and a cool region, ~400 K below that of the photosphere, had developed on the equator. In 1988, sample spectra split into circularly polarized components indicated that the star's magnetic field lines were emerging radially and/or poloidally from an equatorial warm region. Two years later, a set of circularly polarized spectra, obtained over a full rotation cycle, allowed a maximum entropy image of the photospheric field to be constructed for the K1 subgiant. The magnetic field map revealed a concentration of the magnetic flux in two main regions where it is toroidally directed. A ring of clockwise field of ≈ −300 G appeared to surround the polar spot, while a region of counterclockwise field of ≈700 G was detected slightly above the equator and very close to the equatorial cool spot appearing on the corresponding temperature map.

The technique of ZDI has now been developed to allow the extraction of information from many lines simultaneously, thus enhancing the S/N ratios for the detection of spotted structures associated with stellar magnetic fields of active stars. HR 1099 was again observed by Donati, Semel, Rees, *et al.* (1997) together with field detections in seven other RS CVn stars.

Synoptic multi-colour measurements of three RS CVn stars have been made by Yudin & Evans (2002). For IM Peg, $p(\lambda)$ corresponded well with Rayleigh's law with $p \propto \lambda^{-4}$, while for UV Psc, the form of $p(\lambda)$ was less pronounced.

15.6
RV Tauri Stars

RV Tauri stars are yellow supergiants, not well understood, but generally known for displaying both photometric variations, with two minima, one deep and one shallow, and spectroscopic variations with periods $\sim$ 100 days, but with behaviours that are not exactly repeatable from one cycle to the next. Shakhovskoi (1963) discovered p variations for AC Her and R Sct, but was reserved on the behaviour of U Mon. The latter two stars were later comprehensively monitored by Serkowski (1970) who made 51 and 56 *UBV* polarimetric observations, respectively, although not all three colours were used for measurement on each night. Data related to U Mon are portrayed in Figure 15.4, with the variations of p and ζ phased on the photometric period of this star.

The polarimetric behaviour of both these stars is similar, with variations both in p and ζ, producing ellipse-like loci in the qu-plane, the patterns being largest in the U-band. Without quantitative detail for the proposed model, the large difference in

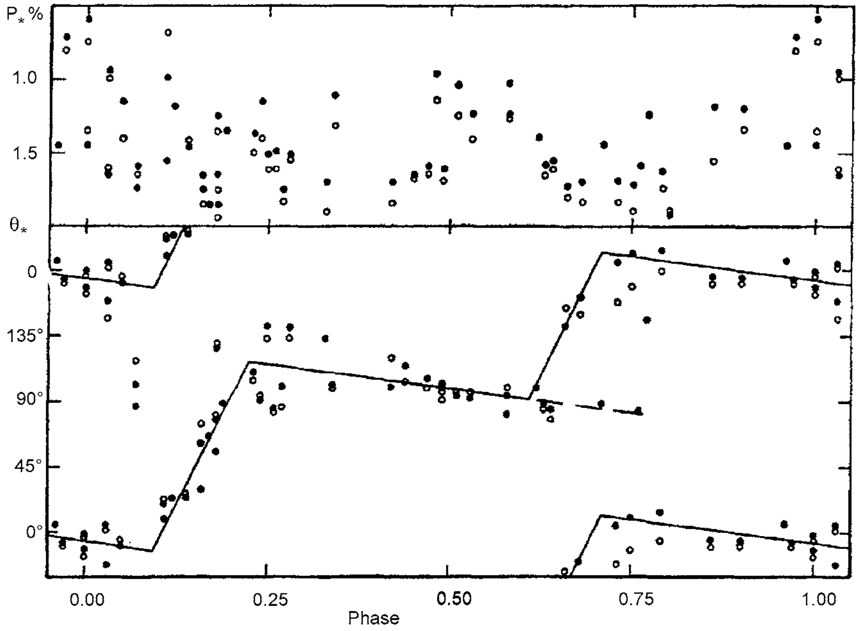

Fig. 15.4 The variations of p and ζ of U Mon for yellow (○) and blue (●) light phased on a photometric period of 92 days. (Taken from Serkowski, 1970.)

the value of ζ at the deep and shallow light minima suggest the presence of non-spherical oscillations, with the surface of the star being described as an ellipsoid with axes a, b and c. The polarization is engendered by a large source function gradient in the photosphere with an opacity dominated by Rayleigh scattering (see Harrington, 1969). The polarization increases rapidly from the centre of the stellar disc towards the limb, the direction of vibration being parallel to the limb.

At the deep minima $a > b \approx c$, whereas at the shallow minima, $a \approx b < c$. The hottest parts of the stellar surface are along the plane defined by the two shorter axes of the ellipsoid. This plane, different at deep light minima than at the shallow ones, is perpendicular to the direction of the polarization vibrations averaged over the stellar disc. The differences in ζ observed at different cycles of the light variation, particularly for R Sct, may be explained by rotation of the star, with a period not commensurable with that of the pulsations.

Alternative notions as to the basic polarization production mechanism are related to scattering by dust envelopes (see Raveendran, 1990). RV stars have infrared excess. Of the several stars monitored by Indian astronomers, AR Pup appears to have the most dramatic behaviour. The $p(\lambda)$ curve exhibits a wide variety of shapes depending on the level of polarization; at times when p increases, $p(\lambda)$ becomes very steep towards the UV with a variation in p_U of some 14%, as described by Raveendran & Kameswara Rao (1988) and Raveendran, Kameswara Rao & Ananderan (1989a). The polarization increases occur close to the epochs of light minima, during the ascent of the light-curve. It is suggested that the localized grain condensations provide the source for the polarigenic scattering and that during each pulsation, matter is ejected along a preferred plane from which dust condensation occurs. A similar conclusion by Raveendran, Kameswara Rao & Ananderan (1989b) is arrived at from a study of AC Her. According to their interpretation, the observed polarization probably results from a combination of pulsation-related asymmetry in the star and circumstellar grain scattering; its variation during the light cycle is not caused by changes in the dust envelope, but rather by the changes in the asymmetry of the star. Yudin, Evans, Barrett, *et al.* (2003) have made broadband measurements of 8 RV Tau stars and concluded that these stars provide evidence of permanent clumpy, non-spherical dust shells around them.

15.7
Pulsating Stars

If the geometry of the radiation field is changed during the pulsation of any star during its cycle, there is a likelihood that polarization will be engendered. The best candidates for investigation are stars which, from studies using other diagnostic observational tools, appear to suffer non-radial pulsations.

The question as to whether Cepheid stars have been detected for polarimetric variability has a somewhat checkered history. According to Polyakova & Sudakov (1981), three different types of Cepheid (RR Lyr, W Vir and Z Lac) all exhibited polarization modulations that appear to be related to spectral variations, as is the case of the RV Tau variable U Mon. For RR Lyr, Piirola (1981) was unable to detect variability in either p or ζ. Later Polyakova (1984) reported that data of Cepheids, when plotted in the qu-plane occupy 'rosette' envelopes with the base at a position corresponding to the star's interstellar value. These findings have not been followed up by other observers.

The first quantitative predictions of the effects due to the distortion of the stellar globe dominated by electron scattering opacity were made by Odell (1979) and Stamford & Watson (1980a), the models suggesting that the largest effects should be in the ultraviolet, rather than in the optical region. It was shown that analysis of the patterns of cyclic behaviour in the qu-plane allows deduction of the vibration modes and the viewing aspect of the star. Stamford & Watson (1980b) also made predictions for the polarimetric behaviour of 12 Lac based on its model atmosphere; their estimates for polarization effects in the visual spectrum are down by a factor of 15 relative to those made at 1500 Å. The application of polarimetry as a diagnostic on mode identification has been presented more fully by Watson (1983).

The first observations of classical β Cep or β CMa stars appear to have been made by Serkowski (1970), but without any attempt to follow the stars through their cycles. Schafgans & Tinbergen (1979) followed β Cep through its cycle but were unable to detect any variability in p at the ~ 0.0005 level. The only claimed detection of polarization associated with the non-radial pulsation in these stars is by Odell (1981) for BW Vul, with a variation of semi-amplitude $\sim$0.004%. From the behaviour in the qu-plane, the data are consistent with a model of the $l = 2$, $m = \pm 2$ mode, viewed at $i = 90°$. As this result stands alone in respect of this type of pulsating star, its observation bears repeating with modern instrumentation; this and other stars should also be made targets for satellite polarimetry in the UV.

Clarke (1986) made measurements of three Southern Hemisphere β Cep stars with null results, indicating that any pulsation variability had amplitudes of p less than 0.0001. It was noted that because of the photometric periods associated with these stars, spurious detections of polarization variability are likely to arise if observational windows are limited to just a few consecutive nights.

Nine β Cep stars were investigated for the presence of magnetic fields by Rudy & Kemp (1978) who measured circular polarization in the wings of Balmer lines, with results suggesting that fields of the order of 1000 G might be present in β Cep and γ Peg, or even more generally in this class of star.

15.8

Novae

The first nova to be measured polarimetrically appears to have been Nova Herculis 1960 by Grigoryan & Vardanian (1961), who found no temporal variations. Clarke (1964) obtained a similar result for Nova Herculis 1963 and suggested that the static values reflected an interstellar component which could be used, in comparison with field stars, to provide a distance estimator for use in absolute magnitude determinations. After concluding that Nova Cygni 1975 displayed no intrinsic component, and that the recorded values were wholly interstellar, McLean (1976) pursued such an analysis more thoroughly. A distance was determined as 1.14 kpc, thus providing an absolute magnitude at maximum brightness of $-10.^{\mathrm{m}}1$, a value consistent with its temporal photometric behaviour.

Zellner & Morrison (1971) reported polarimetric colour measurements of the very slow outburst of Nova HR Delphini 1967, and also for Nova Vulpeculae No. 1 1968 and Nova Serpentis 1970. For HR Del 1967, after making correction for its interstellar component, p was 0.6% in the red during the first 120 days following the outburst. In the later phases, the intrinsic component was generally small and irregularly variable. The same authors also found variations in p of 1% for Nova Serpentis 1970, but no variations for Nova Vulpeculae No. 1 1968. According to Zellner (1971), Mie theory suggests that the polarization of HR Del 1967 can be explained by scattering from grains of iron or graphite within an asymmetric circumstellar cloud, and definitely not pure silicate. Such non-volatile matter may be the condensation of material ejected at the outburst, or may be the debris remaining from a previous outburst event.

Zellner (1971) also commented on the infrared excesses seen in Novae Ser 1970 and Aquilae 1970, attributing them to thermal radiation from grains in the dust shell. Noting that the strong infrared fluxes did not appear during Epoch I for Nova Del, nor for Nova Ser, during the early stages when the variable polarization was seen, Zellner suggested two distinct generations of circumstellar grains. It is perhaps possible that the high ejection velocities of the fast novae prevent the formation of small grains, at least in the initial stages, or the lack of intrinsic polarization may simply indicate no source dust in the system. Zellner proposed that the small grains responsible for the production of the polarization are precursors of condensation nuclei for the accretion of much larger particles of radius $\geq 1\,\mu\mathrm{m}$. For future fast novae, it is important to combine polarimetry with infrared photometry to follow the suggested grain developments.

Pirrola & Korhonen (1979) made observations of Nova Cygni 1978 and noted an increase in polarization from 1.6% to 1.9% over a period of a week. The change correlated with infrared observations promotes a notion of there being a dust forming stage.

Combined with photometry which revealed short-term flickering in Nova Cygni 1978, Blitzstein, Bradstreet, Hrivnak, *et al.* (1980) also reported on polarimetric measurements made in the early phase of the outburst, prior to the time of dust formation. After consideration of the interstellar component, a residual intrinsic polarization of 0.23% was deduced, attributable to non-spherical scattering of Hα emission. A rough estimate of the distance was obtained by considering the interstellar component.

Variable, and hence intrinsic polarization, was observed by Eggen, Mathewson & Serkowski (1967) for Nova Pyxidis in the very early stages of its outburst in 1966–1967. Little comment was made except that the lack of significant changes in the Hγ line suggest that the polarization was generated in the outer shell of the nova.

Kemp & Rudy (1976) observed Nova Cygni 1975 over a wide range of wavelengths, including narrow-band studies of the Hα emission. No structure in $p(\lambda)$, or $\zeta(\lambda)$, was seen across this intense feature and the general form of $p(\lambda)$ corresponded to the behaviour expected of Serkowski's Law. It was concluded that the recorded polarization was clearly interstellar. Intrinsic circular polarization, however, was detected with a Zeeman-like structure across the Hα emission. The estimated field in the emission region was $\approx$100 G. If the system is interpreted as being a pair of dwarf stars, this implies an impossibly large field, $\sim 10^{17}$ G, at the nucleus, say at the white dwarf surface. The situation is reconcilable by considering the outburst to be highly asymmetrical, taking the form of conical and polar plumes such that geometry requires very high, but reasonable, fields on the surface of the central star.

This scenario was revealed more dramatically by Stockman, Schmidt & Lamb (1988) when the same nova had declined by late 1987 to magnitude 17 and relabelled as V 1500 Cygni. Circular polarization was detected and interpreted as high harmonic optical cyclotron emission from an accreting, magnetic white dwarf primary. They recorded a periodic variation of v at $P = 0.^{\mathrm{d}}137154$, with a semi-amplitude of $\pm1.5\%$, corresponding to the rotation period of a star with a large dipolar field. The suggestion is that the pre-nova system was a synchronised AM Her magnetic variable. During the outburst and subsequent dense wind phase, coupling between the white dwarf and expanded envelope produced the change in period first noted by photometry.

Substantial polarization variation during minimum light at the eclipse stage of DQ Her was monitored by Dibai & Shakhovskoi (1967), thus allowing determination of the position for the orbital plane of the close binary system, this being very similar to the direction of the major axis of the envelope after the 1934 nova outburst. Perhaps the most remarkable polarimetric discovery related to the same object displaying a remarkable 71-second light variation, is that of Swedlund, Kemp & Wolstencroft (1974) who found variable circular polarization with a period of 142 s, or twice that of the light period. It was concluded that the object contains an oblique magnetic rotator. The same research group (Kemp, Swedlund & Wolstencroft, 1974) also discovered a periodic linear polarization with the same period of 142 s, and offered a simple model.

The nova-like system V 3885 Sgr, sometimes referred to as Bond's star, was observed in 1983 by Metz (1989) to investigate the 'binary character of the system'. The standard deviations of the measurements were 'surprisingly' in accordance with photon statistics, with no periodicity detectable. Phase diagrams were constructed around various assumed values, but no periodic variation was significant, with the conclusion that the study of polarization does not help the understanding of this object.

Nova Cassiopeiae 1993, or V 705 Cas was monitored by Okazaki, Kurihara, Hirata, *et al.* (1996) in its early stages and was found to display irregular variations of p on time scales of several days, and it was suggested that its intrinsic polarization in the early decline phase was caused by dust scattering. The observations were modelled by Kawabata, Seki, Matsumuru *et al.* (1996) who suggested that that the dust size distribution was quite narrow in the early stages of the outburst, but became wider later.

Spectropolarimetry has been undertaken by Ikeda, Kawabata & Akitaya (2000) on three outburst objects. No evidence was found for intrinsic polarization in CI Cam and Nova Sag 1998. For U Sco, depolarization effects were noted in the emission lines and there were rapid temporal variations in the continuum.

Polarimetry of several novae in outburst has been undertaken by Evans, Yudin, Naylor, *et al.* (2002), with polarigenic mechanisms by inhomogeneities in dust ejection, electron scattering and the effects of resonance lines being suggested for different objects. Schmid, Corradi, Krautter, *et al.* (2002) performed spectropolarimetry of the symbiotic nova, HM Sge. Various effects are noted related to the red giant component with polarization structures covering the TiO bands. The Raman scattered line at 6825 Å exhibits strong p of 3.4% with a variation of ζ across the feature, indicating an axisymmetric geometry with the distribution of the neutral hydrogen in the inner binary system not being strongly perturbed by the binary motion.

15.9
Supernovae

Just a year after the supernova event of 1987 in the Large Magellanic Cloud, Sparks, Parasce & Macchetto (1989) recorded an arc of emission at $\approx 8.''3$, exhibiting a polarization of $p = 0.15 \pm 0.04$. The observation indicated that the reflecting material is confined in a thin sheet or shell of column density $\simeq 10^{18}$–10^{19} atoms cm^{-2} located at $\simeq$ 3 to 5 pc from the supernova which may have arisen from a previous red giant phase of the SN progenitor.

Wang, Wheeler, Li, *et al.* (1996) measured five supernovae with the aim of investigating possible asymmetries in their explosive events with a preliminary conclusion that no significant polarization is associated with three type Ia objects, and that the two type II objects exhibit polarization $\sim$1%. These results depend very much on allowing the contributions of interstellar polarization. Advances have since been made in the subject area by the application of the new larger telescopes and improved detector systems with better quality results presented by Wang, Baade, Hölich, *et al.* (2002).

15.10
Pulsars

The optically brightest pulsar, NP 0532, is embedded in the Crab Nebula which itself displays high levels of polarization (see, for example, McLean, Aspin & Rietsema, 1983). As for the light of the pulsar itself, Kristian, Visvanathan, Westphal, *et al.* (1970) found that the degree of polarization changed smoothly through the pulse from zero up to a level of 25%, with the direction of vibration sweeping through 150° during 60° of the pulsar's rotation. Similar results were also obtained by Cocke, Disney, Muncaster, *et al.* (1970). The time behaviour was similar in the

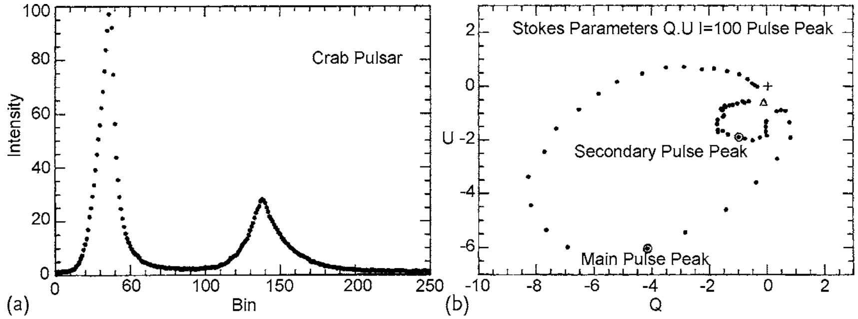

Fig. 15.5 (a) The intensity variation of the Crab Pulsar shows a smooth double-peaked structure over its period. In (b), the variation of the polarization intensities, Q, U are plotted with the scale normalized so that the $I = 100$ for the pulse peak; the positions corresponding to the primary and secondary pulse peaks are marked as ⊙. (Both figures are taken from Smith, Jones, Dick, *et al.*, 1988.)

main pulse and the subpulse. The model suggests that the observed pulses are due to a fixed, polarized emission pattern which is azimuthally scanned as the object rotates, and the sweep of the direction of vibration is interpreted in terms of a very general geometrical model; the projection of the axis of rotation is readily determined but with an ambiguity of 90°. Observations by Cocke, Muncaster & Gehrels (1971) failed to detect any circular polarization at the ±0.07% level.

A more detailed record of the polarization behaviour and deeper discussion of the model has been given by Smith, Jones, Dick, *et al.* (1988). Figure 15.5 shows the double-peaked periodic intensity variation, and the behaviour of a double-looped locus in the QU-plane. A symmetry is revealed showing that the intensity peaks correspond to the same position angle direction of the varying polarization. The observations support a model in which optical and other high-energy radiation is emitted from close to the light cylinder, the two pulses corresponding to the magnetic poles in a nearly orthogonal rotator.

15.11
Stars within Nebulosities and Stellar Discs

One of the most spectacular stellar nebulosities is associated with η Carina. Spectropolarimetry at Hβ of the Homunculus nebula surrounding this nebula was undertaken by Meaburn, Walsh & Wolstencroft (1993). The spectral profiles were complex with structure dependent on position over the Homunculus. The level of polarization was very high with p achieving 35%. Scattering by dust with an outflow velocity of ~650 km s^{-1} is invoked. Further spectropolarimetry with a wavelength coverage of the optical with UV measurements from the Astro-2 Space Shuttle Mission was undertaken by Schulte-Ladbeck, Hillier, Clampin, *et al.* (1997)

Herbig-Haro objects have also had polarimetry directed to them. Measurements by Strom, Strom & Kinman (1974) supported the idea that they are essentially reflection nebulae illuminated by heavily obscured young stars. A study of H-H 100 by Vrba, Strom & Strom (1975) linked this reflection nebula to illumination by an infrared source.

The relationships of polarization and the presence of stellar discs has been mentioned earlier under several different category of stars. In relation to young stellar objects, Scarrott, Gledhill & Rolph (1990) obtained vector polarization maps of the central regions of the associated reflection nebulae. Based on the behaviour expected by scattering from illumination by a point source, deviations were apparent indicating the presence of circumstellar discs. Bastien & Ménard (1990) also obtained linear polarization maps, with patterns of aligned polarization vectors recorded close to the central objects. The patterns have been interpreted in terms of multiple scattering in flattened, optically thick structures. These patterns provide direct evidence of circumstellar discs around young stellar objects. The distribution of the inclinations of the discs is consistent with what is expected from modelling, and inclination angles and disc sizes compare well with values obtained by other means.

Imaging polarimetry has also been applied to pre-main sequence binaries by Monin, Ménard & Peretto (2001), with their results determining the orientation of discs, particularly in T Tauri stars of which a large fraction are binary, or multiple stars.

Simulated polarization maps have been generated by Fischer, Henning & Yorke (1994) for two time windows of a $1 M_\odot$ rotating molecular clump evolving into a protostar, surrounded by a disc and envelope. The computed maps agree with the typical features of the observed polarization maps of circumstellar regions around young stellar objects.

15.12
Gravitational Lensing

Simmons, Willis & Newsam (1995) have considered the polarimetric signals that might be produced by gravitational microlensing events for a star, which displays a polarization variation across its disc, from the centre to its limb. They comment that the rise in polarization generally takes place later than the rise of the total flux and that any suspected amplification of flux could be immediately monitored to provide confirmation of it being a lensing event. By the nature of the generally low levels of limb polarization, and the fact that only a small fraction of this is involved in the lensing, any polarimetric signal will be very small.

15.13
Extra-Solar Planets

In some circumstances the scattered light from a gas planet may be substantially polarized. As a consequence, the prospect of gaining image contrast between itself and its parent star is being considered. Work on the development of such schemes involving polarimetric differential imaging has been presented by Brandner, Apai, Lenzen, *et al.* (2005), Schmid, Gisler, Joos, *et al.* (2005) and Stuik, Tinbergen, Joos, *et al.* (2005)

The possibility of detecting the scattered light of a planet orbiting a parent star, within the total brightness, has been considered by Seager, Whitney & Sasselov (2000). They have shown that polarimetric signals are highly dependent on the sizes and types of condensates in the planetary atmosphere. The amplitudes of the variations have been predicted to be of the order of a few parts in 10^6, being much lower than the regular instrumental detection limits. Partly in response to such predictions, Hough, Lucas, Bailey, *et al.* (2006) have developed a highly sensitive arrangement to investigate the possibility of detecting extra solar planets by polarimetry.

One successful technique, requiring a fortuitous geometry and viewing aspect, involves high-cadence photometry to monitor the brightness changes at the time of a transit of the planet on the stellar disc, with ingress and egress recorded. In the case of HD 209458, Charbonneau, Brown, Latham, *et al.* (2000) recorded brightness changes of 2% at these times.

Although it does not seem to have been aired, it may be noted that if the parent star of any such system exhibits limb polarization, then the transits will generate polarimetric signals. Asymmetries in the behaviours of q and u between ingress and egress would allow determination of the inclination of the orbit as indicated in Figure 15.6. If a Stokes parameter reference frame is established such that '+ve' q is parallel to the radius between the star centre and the point of contact of ingress, then the limb polarization being normal to the radius will have a '−ve' q value. From circular symmetry, the overall intrinsic polarization associated with the star will be zero. As the transit begins, some '−ve' q will be blocked, causing a '+ve' value of q to emerge. This signal will fall quickly as the planet's path crosses the stellar disc, but, at egress, a mirror image of the earlier variation would be apparent. Over the complete transit event, the value of u should remain constant and zero.

For a viewing aspect which is not exactly in the orbital plane, the path of the planet across the stellar disc will not run along a projected diameter. Such a scenario is sketched as (b) in Figure 15.6. At ingress, the behaviour of q will be much the same as for the earlier description. At egress, however, the last contact point occurs where the limb polarization will have both q and u components, i. e., the position angle of the polarization signal will be different to that at ingress. As sketched in the figure, a situation has been depicted showing that most of the signal corresponds to a '+ve' u value, with little or no contribution associated with q. In this case there

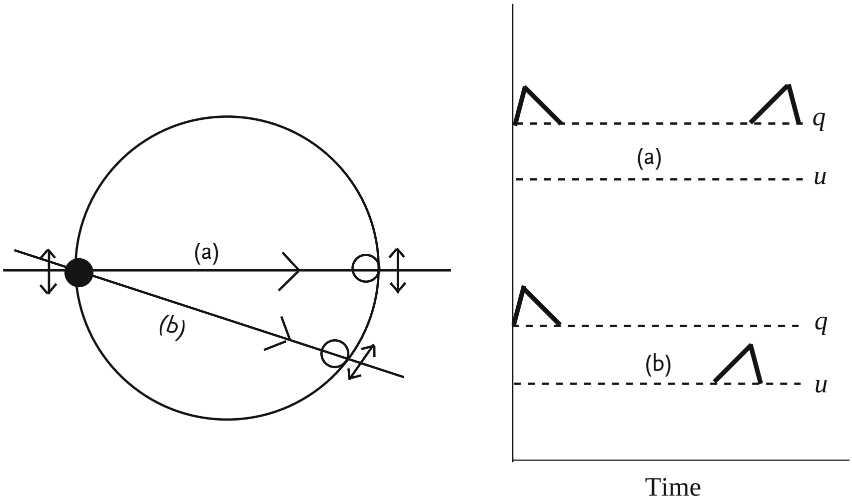

Fig. 15.6 By setting the reference frame such that horizontal polarization is defined as '+ve' *q* for a planetary orbit set at an inclination of 90° as sketched in (a), the ingress (•) disturbs the disc symmetry by removing a '−ve' element of *q* (marked as ↕), producing an overall '+ve' *q* signal as indicated in the right hand panel; a mirror image of the signal is produced at egress (○). The transit has no effect on the *u* values. For the case of tilted orbit with the path not cutting across a diameter as in (b), the ingress produces a signal predominantly in the *q* parameter; at egress, the signal predominantly appears in *u*.

is a position angle difference of 45° between the ingress and egress signals. In principle, the recorded differences for the two events offer a unique diagnostic for determining the trajectory across the disc, allowing the orbital inclination to be calculated.

As to the possible magnitudes of the signals, a crude estimate can be made by assuming a limb polarization of 0.001, and by using a figure that 1% of the stellar disc is occulted, the observed amplitude of p would be of the order of 1 part in 10^5.

It is remarkable to note that the exciting prediction of polarization signals caused by planetary transits is essentially the same as that of Chandrasekhar (1946) in respect of eclipsing binaries. In some sense, it might be said that it has taken just over 60 years for the discipline of *Stellar Polarimetry* to come full circle.

References

References to Introduction

Clarke, D. (2003) Period determinations of spotted stars. *A&A*, **407**, 1029–1037. [337]

Serkowski, K. (1971) Polarization of variable stars. pp 11–31 in *New Directions and New Frontiers in Variable Star Research* – IAU Coll. No:15, Bamberg. [337]

References to X-Ray Sources

Angel, J.R.P. (1969) Polarization of thermal X-ray sources. *ApJ*, **158**, 219–224. [338]

Angel, J.R.P., McGraw, J.T., Stockman, Jr., H.S. (1973) Magnetic observations of the X-ray binaries HD 77581 and HD 153919. *ApJ*, **184**, L79–L83. [339]

Angel, J.R.P., Novick, R., Vanden Bout, P., Wolff, R. (1969) Search for X-ray polarization in Sco X-1. *Phys. Rev. Lett.*, **22**, 861–865. [338]

Avery, R.W., Michalsky, J.J., Stokes, R.A. (1973) Circular polarization in the B stars X Persei, 5 Persei, 55 Cygni and 30 Pegasi. *ApJ*, **180**, L127–L128. [338]

Baud, B., Tinbergen, J. (1972) Optical polarization of X Per. *Nature*, **237**, 29–30. [338]

Bochkarëv, N.G., Karitskaya, E.A. (1983) Intrinsic polarization of a precessing electron scattering accretion disk, with applications to SS 433. *Sov. Astron. Lett.*, **9**, 6–9. [340]

Borra, E.F. (1975) A search for the Zeeman effect in the X-ray star candidates θ^2 Orionis and X Persei, the X-ray source Cygnus X-1, and the B2 Ib star HD 31327. *ApJ*, **196**, L109–L111. [338]

Brown, J.C., Fletcher, L. (1992) Hα polarization of wind-heated optical bullets in S 433. *A&A*, **259**, L43–L45. [341]

Dolan, J.F., Tapia, S. (1988) Variable polarization in X-ray binaries: HD 77581 *A&A*, **202**, 124–132. [339]

Dolan, J.F., Tapia, S. (1984) Variable polarization in X-ray binaries: HD 153919 (= 4U 1700–37) and HD 152667 (= OAO 1653–40?). *A&A*, **139**, 249–257. [339]

Dolan, J.F., Tapia, S. (1989) The orbital inclination of A 0620-00 measured polarimetrically. *PASP*, **101**, 1135–1139. [339]

Dolginov, A.Z., Gnedin, Yu. N., Silante'v, N.A. (1973) Polarization of optical radiation and magnetic field of X-ray stars. *Astrophys. Lett.*, **13**, 85–87. [338]

Efimov, Y.S., Piirola, V., Shakhovskoy, N.M. (1984) The linear polarization of SS 433 = V 1343 Aql. *A&A*, **138**, 62–70. [341]

Gehrels, T. (1972) On the circular polarization of HD 226868, NGC 1068, NGC 4151, C 273, and VY Canis Majoris. *ApJ*, **173**, L23–L25. [338]

Gnedin, Yu. N., Shulov, O.S. (1971) Observation of variable circular polarization in the optical emission of the X-ray source Sco X-1. *JETP Lett.*, **14**, 348–350. [338, 338]

Illing, R.M.E., Martin, P.G. (1972) Scorpius X-1: A search for optical circular polarization. *ApJ*, **176**, L113–L114. [338]

Kemp, J. (1972) Sco X-1 circular polarization of source and nearby sky. *Nature (Phys. Sci.)*, **240**, 103–104. [338]

Kemp, J.C., Wolstencroft, R.D. (1972) NGC 1068, 3C 273, and Scorpius X-1: circular polarization disputed. *ApJ*, **173**, L113–L118. [338]

Kemp, J.C., Wolstencroft, R.D. (1973a) Zeeman effect in the X-ray star candidates HD 77581 and θ^2 Orionis. *ApJ*, **182**, L43–L46. [339]

Kemp, J.C., Wolstencroft, R.D. (1973b) Fluctuating magnetic fields in HD 153919. *ApJ*, **185**, L21–L25. [339]

Korhonen, T., Piirola, V. (1980) Variable linear polarization of the X-ray binary HD 77581. *A&A*, **91**, 372–373. [339]

Kundt, W. (1985) SS 433 revisited. *A&A*, **150**, 276–280. [340]

Liebert, J., Angel, J.R.P., Hege, E.K., Martin, P.G., Blair, W.P. (1979). The moving emission features in SS 433 require a dynamical interpretation. *Nature*, **279**, 384–387. [340]

McLean, I.S., Tapia, S. (1980) Discovery of intrinsic linear polarization in SS 433. *Nature*, **287**, 703–705. [340]

McLean, I.S., Tapia, S. (1981) Intrinsic polarization of SS 433: an electron scattering model. *Vistas Astron.*, **25**, 45–50. [340]

Michalsky, J.J., Stokes, G.M., Szkody, P., Larson, N.R. (1980) Broad-band polarization observations of SS 433. *PASP*, **92**, 654–656. [340]

Michalsky, J.J., Swedlund, J.B., Avery, R.W. (1975) Circular polarization of HDE 226868. *Nature*, **254**, 39–40. [338]

Nikulin, N.S., Kuvshinov, V.M., Severny, A.B. (1971) On the circular polarization of some peculiar objects. *ApJ*, **170**, L53–L58. [338, 338, 338]

Östreicher, R., Schulte-Ladbeck, R. (1982) UBV-polarimetry of the X-ray binaries HD 77581 (4U 0900–40), HD 153919 (4U 1700-37) and of HD 152667. (1982) *A&A*, **114**, 328–336. [339]

Severny, A.B., Kuvshinov, V.M. (1975) Circular polarization of the X-ray sources Scorpius X-1, Cygnus X-1 and 3C273. *ApJ*, **200**, L13–L17. [338]

Simmons, J.F.L., Boyle, C.B. (1984) Interpretation of the variable linear polarization of X-ray transient AO 538–66. *A&A*, **134**, 368–372. [339]

Stokes, R.A., Avery, R.W., Michalsky Jr., J.J. (1973a) Optical circular polarization of X Persei. *Nature (Phys. Sci.)*, **241**, 5. [338]

Stokes, R.A., Avery, R.W., Michalsky Jr., J.J., Swedlund, J.B. (1973) Circular polarization observations of HZ Herculis. *ApJ*, **185**, L17–L19. [339]

van Paradijs, J. (1980) Polarimetric observations of the massive X-ray binaries HD 77581 (4U 0900–40) and HD 153919 (4U 1700-37). *A&A*, **87**, 210–212. [339]

References to T Tauri Stars

Ageorges, N., Walsh, J.R. (1997) Examples of high-resolution imaging and polarimetry of R Monocerotis and NGC 2261. The Messenger, No: 87, 39–43. [342]

Bastien, P. (1981) The wavelength dependence of linear polarization in T Tauri stars. *A&A*, **94**, 294–298. [342]

Bastien, P. (1982) A linear polarization survey of T Tauri stars. *A&AS*, **48**, 153–164. [342]

Bastien, P. (1985) A linear polarization survey of southern T Tauri stars. *ApJS*, 59, 277–291. [342]

Donati, J.-F., Jardine, M.M., Gregory, S.G., Petit, P., Paletou, F., Bouvier, J., Dougados, C., Ménard, F., Cameron, A.C., Harries, T.J., Hussain, G.A.J., Unruh, Y., Morin, J., Marsden, S.C., Manset, N., Aurière, M., Catala, C., Alecian, E. (2008) Magnetospheric accretion on the T Tauri star BP Tauri. *MNRAS*, **386**, 1234–1251. [344]

Drissen, L., Bastien, P., St-Louis, N. (1989) Linear polarization of T Tauri stars. I. Variability of southern stars. *AJ*, **97**, 814–821. [342]

Hiltner, W.A., Iriarte, B. (1958) Polarization in blue galaxies and T Tauri stars. *ApJ*, **127**, 510–512. [341]

Hunger, K., Kron, G.E. (1957) Polarization in a bright UV T Tauri star. *PASP*, **69**, 347–350. [341]

Mekkaden, M.V. (1999) Polarimetric and spectroscopic study of the weak-emission T Tauri star V 410 Tauri. *A&A*, **344**, 111–116. [342]

Ménard, F., Bastien, P. (1992) Linear polarization observations of T Tauri stars II. A sample of objects fainter than 13th magnitude. *AJ*, **103**, 564–572. [342]

Red'kina, N.P., Tarasov, K.V., Kiselev, N.N., Chernova, G.P. (1989) Analysis of combined photometric and polarimetric observations of T Tauri stars. *Akademiia Nauk Tadzhikskoi SSR, Institut Astrofiziki, Biulleten, (ISSN 0321-4885)*, No:**78**, 37–46. (In Russian). [343]

RHG (1958a) Polarization in NX Mon. *The Observatory*, **78**, 42. [341]

RHG (1958b) Polarization of T Tauri stars. *The Observatory*, **78**, 178. [341]

Rieke, G., Lee, T., Coyne, G.V. (1972) Photometry and polarimetry of V 1057 Cygni. *PASP*, **84**, 37–45. [341]

Schulte-Ladbeck, R. (1983) Linear polarization variations of six T Tauri stars. *A&A*, **120**, 203–214. [342]

Serkowski, K. (1969) Changes in polarization of T Tauri stars. *ApJ*, **156**, L55–L57. [341]

Stassun, K., Wood, K. (1999) Magnetic accretion and photopolarimetric variability in classical T Tauri stars. *ApJ*, **510**, 892–904. [343]

Symington, N.H., Harries, T.J., Kurosawa, R., Naylor, T. (2005) T Tauri stellar magnetic fields: He I measurements. *MNRAS*, **358**, 977–984. [343]

Vardanian, R.A. (1964) Polarization in the light of T and RY Tauri. *Soob. Byurakan Obs.*, **35**, 3–23. [341]

Vink, J.S., Drew, J.E., Harries, T.J., Oudmaijer, R.D., Unruh, Y. (2005) Probing the circumstellar structures of T Tauri stars and their relationship to those of Herbig stars. *MNRAS*, **359**, 1049–1064. [343]

Wood, K., Kenyon, S.J., Whitney, B.A., Bjorkman, J.E. (1996) Magnetic accretion and photopolarimetric variability in T Tauri stars. *ApJ*, **458**, L79–L82. [343]

Yudin, R.V. (2000) Analysis of correlations between polarimetric and photometric characteristics of young stars. *A&AS*, **114**, 285–306. [343]

Zellner, B. (1970) Wavelength dependence of polarization. XXI. R Monocerotis. *AJ*, **75**, 182–185. [342]

References to Solar Type Stars

Clarke, D. (1991) The solar-stellar connection – polarimetry. *Vistas Astron.*, **34**, 303–324. [344, 345]

Clarke, D., Fullerton, S.R. (1996) The Sun as a polarimetric variable star. *A&A*, **310**, 331–340. [345]

Coyne (SJ), G.V. (1974) Intrinsic polarization of faint members of the Pleiades. *Mem. della Soc. Astronomica Italiana*, **45**, 445–455. [345]

Elias II, N.M., Dorren, J.D. (1990) Detection of variable elliptical polarization of HD 129333. *AJ*, **100**, 818–824. [345, 345]

Fox, G.K. (1995) Can the variability of solar-like spotted stars be detected polarimetrically? *ApJ*, **441**, 408–413. [344]

Huovelin, J., Linnaluoto, S., Piirola, V., Tuominen, I., Virtanen, H. (1985a) Polarimetric observations of solar-type stars. *A&A*, **152**, 357–360. [345]

Huovelin, J., Linnaluoto, S., Piirola, V., Tuominen, I., Virtanen, H. (1985b) Linear polarization and activity in late-type stars. Lecture Notes in Physics. **254**, 333–335. *Proceedings of 4th Conference Workshop in Cool Stars, Stellar Systems and the Sun*. Santa Fe, October 1985. (eds M. Zeilik & D.M. Gibson). [345]

Huovelin, J., Linnaluoto, S., Tuominen, I., Virtanen, H. (1989) Observations on the variability of linear polarization in late-type dwarf stars. *A&AS*, **78**, 129–139. [345]

Huovelin, J., Piirola, V. (1990) A note on stellar ultraviolet linear polarization observations. *A&A*, **231**, 588–590. [346]

Huovelin, J., Saar, S.H. (1990) Results of coordinated multiwavelength observations of solar-type stars. pp 443–446 in *Solar photosphere: structure, convection and magnetic fields* IAU Symp. **138**. Ed. J.O.Stenflo. [345]

Huovelin, J., Saar, S.H., Tuominen, I. (1988) Relations between broad-band polarization and Ca II H and K emission in late-type dwarf stars. *ApJ*, **329**, 882–893. [345]

Kemp, J.C., Henson, G.D., Steiner, C.T., Powell, E.R. (1987) The optical polarization of the Sun measured at a sensitivity of parts in ten million. *Nature*, **326**, 270–273. [344]

Leroy, J.L. (1990) Broadband linear polarization measurements: The Sun and F-G-K dwarf stars. pp 330–337 in *11th Summer Workshop*. Sac Peak Obs., 27–31 August 1990. Ed. L. November. [345]

Leroy, J.-L., Le Borgne, J.F. (1989) Polarimetry of solar-type stars and magnetic field diagnostics. *A&A*, **223**, 336–342. [346]

References to RS Can Ven Stars

Barbour, M.S., Kemp, J.C. (1981) Discovery of phase-locked variable polarization in an RS Canum Venaticorum – like star, HR 5110. *ApJ*, **246**, 203–207. [346]

Barbour, M.S., Kemp, J.C. (1982) Polarimetry and Photometry of two RS CVn stars. pp 255–259 in *Second Cambridge Workshop on Cool Stars, Stellar Systems and the Sun*, Vol 1. (eds M.S. Giampapa and L. Golub). (Smithson. Astrophys. Obs. Special Report No: 392). [346]

Donati, J.-F., Brown, S.F., Semel, M., Rees, D.E., Dempsey, R.C., Matthews, J.M., Henry, G.W., Hall., D.S. (1992). Photospheric imaging of the RS CVn system HR 1099. *A&A*, **265**, 682–700. [347]

Donati, J.-F., Semel, M., Rees, D.E. (1992) Circularly polarized spectroscopic observations of RS CVn systems. *A&A*, **265**, 669–681. [347]

Donati, J.-F., Semel, M., Rees, D.E., Cameron, A.C. (1997) Spectropolarimetric observations of active stars. *MNRAS*, **291**, 658–682. [348]

Kemp, J.C., Henson, G.D., Kraus, D.J., Dunaway, M.H., Hall, D.S., Boyd, L.J., Genet, R.M., Guinan, E.F., Wacker, S.W., McCook, G.P. (1987) Discovery of optical circular polarization in Lambda Andromeda. *ApJ*, **317**, L29–L32. [347, 346, 348]

Pfieffer, R.J. (1979) Intrinsic linear polarization of the eclipsing binary RS Canum Venaticorum. *ApJ*, **232**, 181–189. [346]

Scaltriti F., Piirola, V., Coyne (SJ), G.V., Koch, R.H., Elias, N.M., Holenstein, B.D. (1993) UBVRI Linear and circular polarization of RS CVn-type binaries. *A&AS*, **102**, 343–360. [346]

Yudin, R.V., Evans, A. (2002) Polarimetry of evolved stars. *A&A*, **386**, 916–925. [349]

References to RV Tauri Stars

Harrington, J.P. (1969) The intrinsic polarization of Mira variables. *Astrophys. Lett.*, **3**, 165–168. [350]

Raveendran, A.V. (1990) Dust Envelopes around RV Tauri stars. *Q. Newsl. Ind. Inst. Astrophy.*, **5** (4), 21–23. [350]

Raveendran, A.V., Kameswara Rao, N. (1988) Polarimetric observations of the RV Tauri star AR Puppis. *A&A*, **192**, 259–263. [350]

Raveendran, A.V., Kameswara Rao, N., Ananderan, M.N. (1989a) Polarimetric and photometric study of the RV Tauri Star AR Puppis. *MNRAS*, **240**, 823–831. [350]

Raveendran, A.V., Kameswara Rao, N., Ananderan, M.N. (1989b) Polarimetric study of the RV Tauri star AC Herculis. *Bull. Astron. Soc. India*, **17**, 95–100. [350]

Serkowski, K. (1970) Polarimetric observations of the RV Tauri stars U Monocertis and R Scuti. *ApJ*, **160**, 1107–1116. [349, 349]

Shakhovskoi, N.M. 1963. Investigation of the polarization radiation of variable stars. I. *Sov. Astron.*, **7**, 806–812. [349]

Yudin, R.V., Evans, A., Barrett, P., Albinson, J.S., Davies, J.K., Hutchinson, M.G. (2003) Polarimetry of evolved stars III, RV Tau and R CrB stars. *A&A*, **412**, 405–416. [350]

References to Pulsating Stars

Clarke, D. (1985) Polarization measurements of β Cep stars. *A&A*, **161**, 412–416. [351]

Odell, A.P. (1979) Possible polarization effects in β Cephei stars. *PASP*, **91**, 326–328. [351]

Odell, A.P. (1981) Nonradial pulsation detected through polarization variation in BW Vulpeculae. *ApJ*, **246**, L77–L80. [351]

Piirola, V. (1981) A search for polarimetric variations in RR Lyrae. *Peremennye Zvezdy Prilozhenie – Astr. Sov. ANNSSR*, **4**, No: 19, 31–34. [351]

Polyakova, T.A. (1984) Interstellar polarization from Cepheid polarimetry. *Sov. Astron. Lett.*, **10**, 312–315. [351]

Polyakova, T.A., Sudakov, S.V. (1981) Variable linear polarization in three Cepheids. *Sov. Astron. Lett.*, **7**, 58–60. [350]

Rudy, R.J., Kemp, J.C. (1978) A survey of nine beta Cephei stars for magnetic fields. *MNRAS*, **183**, 595–603. [351]

Schafgans, J.J., Tinbergen, J. (1979) An attempt to detect non-radial pulsation in beta Cephei. *A&AS.*, **35**, 279–280. [351]

Serkowski, K. (1970) Intrinsic polarization of early-type stars with extended atmospheres. *ApJ*, **160**, 1083–1105. [351]

Stamford, P.A., Watson, R.D. (1980a) Polarization models for Hot nonradial pulsators. *Acta Astron.*, **30**, 193–214. [351]

Stamford, P.A., Watson, R.D. (1980b) A polarization model for 12 Lacertae. *Proc. Astron. Soc. Australia*, **4**, 83–85. [351]

Watson, R.D. (1983) Mode constraints on nonradial pulsations from polarization data. *Astrophys. Space Sci.*, **92**, 293–306. [351]

References to Novae and Supernovae

Blitzstein, W., Bradstreet, D.H., Hrivnak, B.J., Hull, A.B., Koch, R.H., Pfeiffer, R.J., Galatola, A.P. (1980) Multifilter photometry and polarimetry of nova Cygni 1978 (V1668 Cygni). *PASP*, **92**, 338–344. [352]

Clarke, D. (1964) The polarization of nova Herculis (1963). *The Observatory*, **84**, 28–29. [351]

Dibai, E.A., Shakhovskoi, N.M. (1967) Polarization observations of DQ Herculis (Nova Herc 1934). *Sov. Astron.*, **10**, 1059–1060. [353]

Eggen, O.J., Mathewson, D.S., Serkowski, K. (1967) Changes in polarization, light and colour during the outburst stage of the recurrent nova T Pyxidis. *Nature*, **213**, 1216–1217. [352]

Evans, A., Yudin, R.V., Naylor, T., Ringwald, F.A., Koch Miramond, L. (2002) Broadband polarimetry of novae in outburst. *A&A*, **384**, 504–512. [354]

Grigoryan, K.A., Vardanian, R.A. (1961) Photometric, Colourimetric and polarimetric studies of nova Her 1960. *Soob. Byurakan Obs.*, **29**, 39–50. [351]

Ikeda, Y., Kawabata, K.S., Akitaya, H. (2000) The spectropolarimetric observations of three outburst objects, CI Camelopardalis, Nova Sagittarii 1998, and U Scorpii. *A&A*, **355**, 256–260. [354]

Kawabata, K., Seki, M., Matsumuru, M., Okazaki, A., Kikuchi, S., Hirata, R. (1996) Large variations in the polarization properties of nova Cassiopeiae 1993. pp. 186–190 in *Polarimetry of the Interstellar Medium – ASP Conf. Ser.*, No: **97**, (eds W.G. Roberge & D.C.B. Whittet), San Francisco. [353]

Kemp, J.C., Swedlund, J.B., Wolstencroft, R.D. (1974) DQ Herculis: Periodic linear polarization synchronous with the rapid light variations. *ApJ*, **193**, L15–L19. [353]

Kemp, J.C., Rudy, R.J. (1976) Nova Cygni 1975: Narrow-band polarimetry and photometry 0.36–1.7 microns. *ApJ*, **203**, L131–L135. [352]

McLean, I.S. (1976) Optical Polarimetry and distance estimate for nova Cygni 1975. *MNRAS*, **176**, 73–80. [352]

Metz, K. (1989) A search for variable polarization in V3885 Sgr. *IBVS*, No: 3385, Budapest. [353]

Okazaki, A., Kurihara, J., Hirata, R., Kikuchi, S., Satoh, H., Yoshioka, K., Saijo, K., Seki, M., Kawabata, K., Hayashi, K., Matsumuru, M. (1996) Multichannel polarimetry of nova Cassiopeiae 1993. pp. 178–182 in *Polarimetry of the Interstellar Medium – ASP Conf. Ser.*, **97**, (eds W.G. Roberge & D.C.B. Whittet), San Francisco. [353]

Piirola, V., Korhonen, T. (1979) The linear polarization of Nova Cygni 1978. *A&A*, **79**, 254–255. [352]

Schmid, H.M., Corradi, R., Krautter, J., Schild, H. (2002) Spectroplarimetry of the symbiotic nova HM Sge. *A&A*, **355**, 261–270. [354]

Sparks, W.B., Paresec, F., Macchetto, D. (1989) Polarization and visual intensity of the inner light echo around SN 1987A. *ApJ*, **347**, L65–L68 (with plates) L11–L12. [354]

Stockman, H.S., Schmidt, G.D., Lamb, D.Q. (1988) V1500 Cygni: Discovery of a magnetic Nova. *ApJ*, **332**, 282–286. [353]

Swedlund, J.B., Kemp, J.C., Wolstencroft, R.D. (1974) DQ Herculis: Periodic circular polarization synchronous with the rapid light variations. *ApJ*, **193**, L11–L13. [353]

Wang, L., Wheeler, J.C., Li, Z., Clocchiatti, A. (1996) Broadband polarimetry of supernovae: SN 1994D, SN 1994Y, SN 1994ae, SN 1995D, and SN 1995H. *ApJ*, **467**, 435–445. [354]

Wang, L. Baade, D., Hölich, P., Wheeler, J.C. (2002) Supernova polarimetry with the VLT: Lessons from asymmetry. *The Messenger*, No:109 (Sept), 47–51. [354]

Zellner, B. (1971) Wavelength dependence of polarization. XXIII. dust grains in novae. *AJ*, **76**, 651–654. [352, 352]

Zellner, B., Morrison, N.D. (1971) Wavelength dependence of polarization. XXII. Observations of novae. *AJ*, **76**, 645–650. [352]

References to Pulsars

Cocke, W.J., Disney, M.J., Muncaster, G.W., Gehrels, T. (1970) Optical polarization of the Crab Nebula pulsar. *Nature*, **227**, 1327–1329. [354]

Cocke, W.J., Muncaster, G.W., Gehrels, T. (1971) Upper limit to circular polarization of optical pulsar NP 0532. *ApJ*, **169**, L119–L121. [355]

Kristian, J., Visvanathan, N., Westphal, J.A., Snellen, G.H. (1970) Optical polarization and intensity of the pulsar in the Crab Nebula. *ApJ*, **162**, 475–484. [354]

McLean, I.S., Aspin, C., Rietsema, H. (1983) High-resolution polarization images of Crab Nebula with a charge-coupled device camera. *Nature*, **304**, 243–246. [354]

Smith, F.G., Jones, D.H.P., Dick, J.S.B., Pike, C.D. (1988) The optical polarization of the Crab Pulsar. *MNRAS*, **233**, 305–319. [355]

References to Stars With Discs

Bastien, P., Ménard, F. (1990) Parameters of disks around young stellar objects from polarization observations. *ApJ*, **364**, 232–241. [356]

Fischer, O., Henning, Th., Yorke, H.W. (1994) Simulation of polarization maps. *A&A*, **284**, 187–209. [356]

Meaburn, J., Walsh, J.R., Wolstencroft, R.D. (1993) The outflowing dust around η Carinae. *A&A*, **268**, 283–293. [355]

Monin, J.-L., Ménard, F., Peretto, N. (2001) Disk orientations in PMS binary systems determined through polarimetric imaging with UT1/FORS. *The Messenger*, No: 104, 29–31. [356]

Scarrott, S.M., Gledhill, T.M., Rolph, C.D. (1990) Polarization studies of nebulae associated with young stars and outflow regions. *Q. J. R. Astron. Soc.*, **31**, 47–52. [356]

Schulte-Ladbeck, R.E., Hillier, D.J., Clampin, M., Pasquali, A., Lupie, O.L., Nota, A. (1997) The structure of η Carina's Homunculus for imaging polarimetry and spectropolarimetery. pp. 260–266 in *Luminous Blue Variables: Massive Stars in Transition – ASP Conf. Ser.* No: **120**, (eds A. Nota & H.J.G.L.M. Lamers), San Francisco. [355]

Strom, K.M., Strom, S.E., Kinman, T.D. (1974) Optical polarization of selected Herbig-Haro objects. *ApJ*, **191**, L93–L94. [356]

Vrba, F.J., Strom, S.E., Strom, K.M. (1975) Optical polarization of a Herbig-Haro object in Corona Austrina. *PASP*, **87**, 337–339. [356]

References to Gravitational Lensing

Simmons, J.F.L., Willis, J.P., Newsam, A.M. (1995) Polarisation as a tool for gravitational microlensing surveys. *A&A*, **293**, L46–L48. [356]

References to Extra-Solar Planets

Brandner, W., Apai, D., Lenzen, R., Felt, M. (2005) Polarimetric differential imaging studies of stellar environments: disks and planets. pp. 75–76 in *Astronomical Polarimetry: Current Status and Future Directions – ASP Conf. Ser.*, No: **343**, (eds A. Adamson, C. Aspin, C.J. Davis & T. Fujiyoshi), San Fransisco. [357]

Chandrasekhar, S. (1946) On the radiative equilibrium of a stellar atmosphere. X. *ApJ*, **103**, 351–370. [358]

Charbonneau, D., Brown, T.M., Latham, D.W., Mayor, M. (2000) Detection of planetary transits across a sun-like star. *ApJ*, **529**, L45–L48. [357]

Hough, J.H., Lucas, P.W., Bailey, J.A., Tamura, M., Hirst, E., Harrison, D., Bartholomew-Biggs, M. (2006) PlanetPol: A very high sensitivity polarimeter. *PASP*, **118**, 1302–1318. [357]

Schmid, H.M., Gisler, D., Joos, F., Povel, H.P., Stenflo, J.O., Feldt, M., Lenzen, R., Brandner, W., Tinbergen, J., Quirrenbach, A., Stuik, R., Gratton, R., Turatto, M., Neuhäuser, R. (2005) ZIMPOL/CHEOPS: a polarimetric imager for the direct detection of extra-solar planets. pp. 89–91 in *Astronomical Polarimetry: Current Status and Future Directions – ASP Conf. Ser.*, No: **343**, (eds A. Adamson, C. Aspin, C.J. Davis & T. Fujiyoshi), San Fransisco. [357]

Seager, S., Whitney, B.A., Sasselov, D.D. (2000) Photometric light curves and polarization of close-in extrasolar giant planets. *ApJ*, **540**, 504–520. [357]

Stuik, R., Tinbergen, J., Joos, F., Schmid, H.M. (2005) Instrumental polarization in CHEOPS: exoplanet detection and characterization. pp. 94–95 in *Astronomical Polarimetry: Current Status and Future Directions – ASP Conf. Ser.*, No: **343**, (eds A. Adamson, C. Aspin, C.J. Davis & T. Fujiyoshi), San Fransisco. [357]

Appendices

Stellar Polarimetry. David Clarke

ISBN: 978-3-527-40895-5

Appendix A
The Fresnel Laws

A.1
Introduction

Various texts and papers presenting the Fresnel laws reveal disparities in respect of the assigned 'signs' of the amplitude reflection and transmission coefficients when electromagnetic waves interact with an optical interface. There are also problems in describing phase changes that the waves suffer. For reference to the understanding of the behaviour of various optical devices, and for establishing consistent definitions within stellar polarimetry, the essence of Fresnel's laws is provided here. Based on this presentation, the appropriate Mueller matrices required to describe the behaviour of reflections within optical instruments are derived.

A.2
Optical Interfaces

The behaviour of reflections and refractions of beams of light at interfaces is generally covered in undergraduate courses on optics. Inspection of the standard optical texts, however, reveals differences in the presentation of the Fresnel laws which describe the electromagnetic behaviour of radiation when it meets a boundary, with a change of refractive index. The optical literature shows that there are disparities with sign conventions associated with the description of the Fresnel coefficients. Generally these are of little consequence, but they are very important in situations involving interference phenomena and phase changes occurring when light beams are reflected. A proper understanding of the nature of phase changes is very necessary to the description of the effects of reflections by telescope mirrors, or within optical devices such as the Fresnel rhomb. Without this, misinterpretations of the handedness of any circular polarization in the original collected light may ensue.

In the presentation of Clarke & Grainger (1971), the behaviour of light at reflection has been discussed in terms of nodality and phase changes, allowing appreciation of polarizational changes that occur. To provide the means for determining the reflection and transmission properties of any optical device with respect to po-

Stellar Polarimetry. David Clarke

ISBN: 978-3-527-40895-5

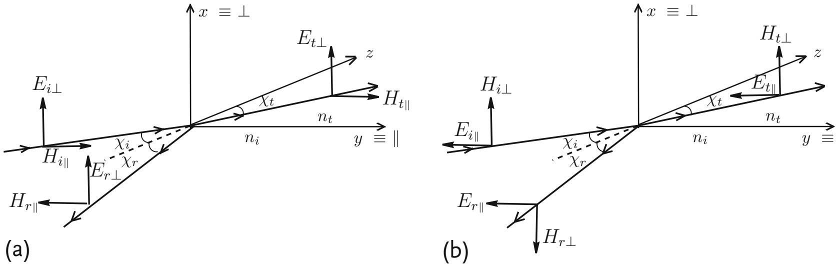

Fig. A.1 The electric and magnetic vectors of the incident, transmitted and reflected beams at the point of incidence on a dielectric interface (xy-plane) with refractive discontinuity from n_{i} to n_{t}, with $n_{\mathrm{t}} > n_{\mathrm{i}}$. (a) relates to polarized light with direction of vibration perpendicular to the the plane of incidence (parallel to the x-axis), while (b) depicts the situation for polarized light in the plane of incidence (parallel to the y-axis). (NB: The $x \equiv \perp$, $y \equiv \|$, z frame is right handed and the E and H vectors have been drawn according to Poynting's theorem).

larized light, from the telescope, to instruments that are appended such as spectrometers, and for completeness here, the important features of the Fresnel laws are summarized in the following sections.

A.2.1
Reflection at a Denser Medium

Consider the situation of classical electromagnetic waves impinging on a dielectric boundary, with a change in refractive index from n_{i} to n_{t}, the latter being larger than the former. As is normal practice, the incident and reflected beams define a plane of incidence, and the electric fields are resolved with components vibrating perpendicular to or parallel to this plane; the angles of incidence and of refraction (transmission) are designated χ_{i} and χ_{t} respectively; the angle of reflection is defined as χ_{r} and equals χ_{i}. In Figure A.1, instantaneous vectors are depicted for the electric, $E_{\perp}$, $E_{\|}$, and magnetic, $H_{\perp}$, $H_{\|}$, oscillations at the point of contact of a beam impinging on the boundary. As drawn in Figure A.1a, related to the polarization being parallel to the x-axis, $E_{\mathrm{i}\perp}$, $E_{\mathrm{t}\perp}$ and $E_{\mathrm{r}\perp}$ are shown with their vectors pointing in the same direction, as though they are all in phase. Similarly, in Figure A.1b, the electric vectors, $E_{\mathrm{i}\|}$, $E_{\mathrm{t}\|}$ $E_{\mathrm{r}\|}$, are depicted as pointing in the same direction and being in phase. The directions of all the H vectors have been assigned by applying Poynting's theorem so that the flux carried by the electromagnetic wave is described by the vector product of the E and H components, this providing the direction of propagation.

To deduce the amplitude reflection coefficients, two pieces of information are utilized, namely

1. The components of E and H parallel to the boundary are continuous across it.
2. Since $E/H = Z = \sqrt{\mu\mu_0/\epsilon\epsilon_0}$, and the refractive index $= \sqrt{\epsilon}$ (see Chapter 2), it follows that $H = E \times$ (refractive index) $\times \sqrt{\epsilon_0/\mu\mu_0}$.

Provided that μ may be taken as unity for both media, as is usually the case in the optical region of the spectrum, the relationship between H and E may be written as

$$H = E \times \text{refractive index} \times C \ ,$$

where C is a constant, and equal to $\sqrt{\epsilon_0/\mu_0}$.
Consider first the case of the polarization being parallel to the x-axis as depicted in Figure A.1a. By using the boundary condition, referred to as (1) above

$$E_{\mathrm{i}\perp} + E_{\mathrm{r}\perp} = E_{\mathrm{t}\perp} \ , \tag{A1}$$

$$H_{\mathrm{i}\|} \cos\chi_{\mathrm{i}} - H_{\mathrm{r}\|} \cos\chi_{r} = H_{\mathrm{t}\|} \cos\chi_{\mathrm{t}} \ . \tag{A2}$$

By using the relationship of (2) above, (A2) may be rewritten as

$$n_{\mathrm{i}} E_{\mathrm{i}\perp} \cos\chi_{\mathrm{i}} - n_{\mathrm{i}} E_{r\perp} \cos\chi_{\mathrm{r}} = n_{\mathrm{t}} E_{t\perp} \cos\chi_{\mathrm{t}} \ . \tag{A3}$$

The amplitude reflection coefficient is $E_{\mathrm{r}\perp}/E_{\mathrm{i}\perp} \equiv r_{\perp}$ and, by manipulating (A1) and (A3), together with the law of reflection ($\chi_{\mathrm{i}} = \chi_{\mathrm{r}}$), it may be expressed as

$$r_{\perp} = \frac{n_{\mathrm{i}} \cos\chi_{\mathrm{i}} - n_{\mathrm{t}} \cos\chi_{t}}{n_{\mathrm{i}} \cos\chi_{\mathrm{i}} + n_{\mathrm{t}} \cos\chi_{\mathrm{t}}} \ . \tag{A4}$$

Using the law of refraction that $n_{\mathrm{i}} \sin\chi_{\mathrm{i}} = n_t \sin\chi_{\mathrm{t}}$, (A4) reduces to

$$r_{\perp} = -\frac{\sin(\chi_{\mathrm{i}} - \chi_{\mathrm{t}})}{\sin(\chi_{\mathrm{i}} + \chi_{\mathrm{t}})} \ . \tag{A5}$$

It may be noted that value of $r_{\perp}$ is negative for all angles of incidence from $\chi_{\mathrm{i}} = 0$ to $\pi/2$, this corresponding to there being a phase change of π. With respect to the depiction of $E_{\mathrm{r}\perp}$ in Figure A.1, this vector should be re-drawn to point in the opposite direction.

For polarized radiation in the plane of incidence, with the vibration parallel to the y-axis, as in Figure A.1b, application of the continuity conditions as before, provides the identities

$$E_{\mathrm{i}\|} \cos\chi_{\mathrm{i}} + E_{\mathrm{r}\|} \cos\chi_{r} = E_{\mathrm{t}\|} \cos\chi_{\mathrm{t}} \ , \tag{A6}$$

$$H_{\mathrm{i}\perp} - H_{\mathrm{r}\perp} = H_{\mathrm{t}\perp} \ . \tag{A7}$$

Using again the relationship of (2) above, (A7) may be rewritten as

$$n_{\mathrm{i}} E_{\mathrm{i}\|} - n_{\mathrm{i}} E_{\mathrm{r}\|} = n_{\mathrm{t}} E_{\mathrm{t}\|} \ . \tag{A8}$$

Combining (A6) and (A8), and using $\chi_{\mathrm{i}} = \chi_{\mathrm{r}}$, the reflection coefficient, $r_{\|}$, for the polarization parallel to the plane of incidence is given by

$$r_{\|} = -\frac{n_{\mathrm{t}} \cos\chi_{\mathrm{i}} - n_{\mathrm{i}} \cos\chi_{\mathrm{t}}}{n_{\mathrm{t}} \cos\chi_{\mathrm{i}} + n_{\mathrm{i}} \cos\chi_{\mathrm{t}}} \ . \tag{A9}$$

Using the law of refraction again as defined earlier, (A9) reduces to

$$r_{\parallel} = -\frac{\tan(\chi_\mathrm{i} - \chi_\mathrm{t})}{\tan(\chi_\mathrm{i} + \chi_\mathrm{t})} \,. \tag{A10}$$

For angles of incidence not very different from zero, the two tangent functions are both positive, and so the '−ve' sign indicates that the reflected wave undergoes a phase shift of π with respect to the depiction of Figure A.1, i. e. $E_{\mathrm{r}\parallel}$ should be depicted to point in the opposite direction. For $(\chi_\mathrm{i} + \chi_\mathrm{t}) = \pi/2$, the value of $r_{\parallel}$ falls to zero, and so the reflected beam can only contain a perpendicularly vibrating component. It is easy to show that for $(\chi_\mathrm{i} + \chi_\mathrm{t}) = \pi/2$, the value of χ_i corresponds to $\arctan(n_\mathrm{t}/n_\mathrm{i})$. This angle of incidence is known as *Brewster's angle*. For angles of incidence greater than this, $\tan(\chi_\mathrm{i} - \chi_\mathrm{t})$ has a negative value and $r_{\parallel}$ changes sign and numerically becomes positive, and the relative phases of the incoming and reflected beams, as portrayed in Figure A.1, are correct.

Comparison of (A5) and (A10) shows that for small angles of incidence, both formulas tend to give the same value, both predicting that the electric vector suffers a phase change of π; no phase difference is introduced between the two resolved components. At normal incidence the parallel and perpendicular components are indistinguishable, but their phase changes of π are important to the description of situations involving interference. They explain the presence of the dark spot at the centre of the classical Newton's ring experiment and the dark fringe in Lloyd's mirror arrangement. It may be noted that for $r_{\perp}$, there is no change in the sign as χ_i increases and becomes larger than Brewster's angle.

The reflection coefficients, $r_{\perp}$ and $r_{\parallel}$, are known as the Fresnel amplitude reflection coefficients, their derivation originally based on the elastic solid theory of the ether. Similar amplitude coefficients for transmission are readily established. Confusion has arisen from time to time in the way that the Fresnel coefficients have been presented. Fresnel's original paper of 1823 (see p. 777 in Fresnel, 1876) gives the expressions exactly as the (A5) and (A10). Yet, as pointed out by Lord Kelvin in 1884 (see p. 402 in Lord Kelvin, 1904) in a footnote by Verdet, an editor of Fresnel's work (see p. 789 in Fresnel, 1876), the formulas are changed with the '−ve' sign associated with the 'tangent formula' being omitted. Lord Kelvin surmises:

> It obvious that … the … two expressions must have the same sign, because at very nearly normal incidences the tangents are approximately equal to the sines, and at normal incidence, the two formulas mean precisely the same thing … Yet, notwithstanding the manifest absurdity of giving different signs to the 'tangent formula' and the 'sine formula' of Fresnel we find … the formulas changed … in consequence of certain 'considérations' set forth by Fresnel. I hope sometime to return to these 'considérations' and to give a diagram showing the displacements … by which Fresnel's 'petite difficulté' is explained, and the erroneous change from his originally correct formulas is obviated.

By adopting a consistent notation, and interpreting it correctly, no ambiguities concerning phase change arise for reflection at an interface of a less-dense medium to one of greater density; both the perpendicular and parallel components suffer a phase change of π. However, the incorrect '+ve' sign for the 'tangent formula' is carried in some optical texts. Lord Kelvin (1904) remarked (see p. 402): 'The falsified formulas have been repeated by some subsequent writers; avoided by others'.

Perhaps one reason why a '+ve' sign is erroneously used in the 'tangent formula' by some workers might relate to the well-known fact that, for near normal incidence, circular polarization changes its sense of handedness on reflection. This can be readily expressed mathematically by considering there to be a phase difference of π introduced between the two resolved components on reflection. Mathematically this might be described by using a '+ve' sign for the 'tangent formula' (parallel component) but keeping the '−ve' sign for the sine formula (perpendicular component). Doing this, however, masks the real underlying physical processes. The flip of handedness is not caused by the physical behaviour of the electromagnetic wave disturbances in respect of reflecting surface material, but results from the effect of the mirror changing the direction of propagation, as explained in the following argument.

Consider a classical beam of radiation arriving close to normal incidence on a dielectric surface as sketched in Figure A.1. A coordinate frame can be established so that the incident and reflected beams are contained in a plane defined by x and y with the z-axis being the normal to the surface, the system being defined as right handed. At the surface, the electromagnetic disturbances of the waves are resolvable in the two directions, x and y, these equivalent to the electric vibrations being perpendicular ($x \equiv \perp$) and parallel ($y \equiv \|$) to the plane of incidence respectively. An instrument of some kind designed to record the electric disturbances, looking at the incoming radiation, may be set so that its reference axes correspond to x and y. The oscillatory behaviour would be recorded as

$$E_\perp = E_{\perp 0} \cos(\omega t + \delta_\perp) \,, \tag{A11}$$

$$E_\| = E_{\| 0} \cos(\omega t + \delta_\|) \,. \tag{A12}$$

Immediately after the reflection these disturbances would be modified to

$$E_\perp = |r_\perp| \, E_{\perp 0} \cos(\omega t + \delta_\perp + \pi) \,, \tag{A13}$$

$$E_\| = \left|r_\|\right| \, E_{\| 0} \cos(\omega t + \delta_\| + \pi) \,, \tag{A14}$$

or

$$E_\perp = r_\perp \, E_{\perp 0} \cos(\omega t + \delta_\perp) \,, \tag{A15}$$

$$E_\| = r_\| \, E_{\| 0} \cos(\omega t + \delta_\|) \,, \tag{A16}$$

with the appropriate signs applied to $r_\perp$ and $r_\|$, according to the evaluations of (A5) and (A10), respectively.

In order to assess the resultant behaviour of the modified electric disturbances, the viewing instrument, with its right-hand coordinate frame, needs to be brought

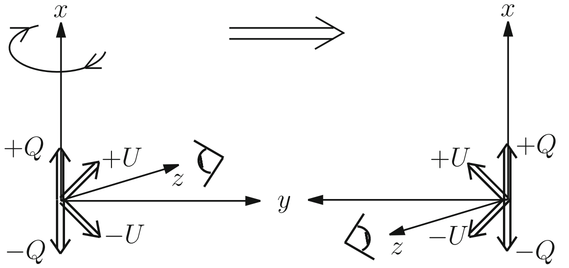

Fig. A.2 An instrument (eye) receiving the radiation prior to the reflection in the *xy*-plane provides a reference frame as depicted in the left-hand side of the diagram. Rotating the instrument about the *x*-axis by 180° to receive the reflected radiation causes the sign of the *y*-axis to flip, as sketched in the right-hand side of the figure. The directions defining the Stokes parameters, $\pm Q$, $\pm U$, are indicated for the reference frame prior to, and following reflection.

around the interface to receive the reflected beam. It can be done by rotating it about the *x*-axis, this being perpendicular to the plane of incidence. As can be seen in Figure A.2, on reflection the *x*-axis remains the same but the *y*-axis points oppositely to its original direction. For the reflected radiation to be described in this new frame, a sign change is required for the vibration parallel to *y*. Hence the description of the electric disturbances in the new reflected right-handed coordinate frame requires to be written as

$$E_\perp = r_\perp E_{\perp 0} \cos(\omega t + \delta_\perp) \,, \tag{A17}$$

$$E_{\|} = -r_{\|} E_{\|0} \cos(\omega t + \delta_{\|}). \tag{A18}$$

Thus, it is the '−ve' sign caused by reflecting the coordinate frame and carried by (A18) that causes the handedness flip, and not any physical phase change brought about by the dielectric material. Using a descriptive approach involving matrices, the incoming beam may be expressed in the form of a Jones column vector (see Chapter 3) given by $\{E_\perp e^{i\delta_\perp}, E_{\|} e^{i\delta_{\|}}\}$, or if beam can be expressed with a relative phase between the components, the vector can be written as $\{E_\perp e^{i(\delta_\perp - \delta_{\|})}, E_{\|}\}$. The effect of a reflection may therefore be summarized as

$$\begin{bmatrix} E'_\perp e^{i(\delta'_\perp - \delta'_{\|})} \\ E'_{\|} \end{bmatrix} = \begin{bmatrix} 1 & 0 \\ 0 & -1 \end{bmatrix} \begin{bmatrix} r_\perp & 0 \\ 0 & r_{\|} \end{bmatrix} \begin{bmatrix} E_\perp e^{i(\delta_\perp - \delta_{\|})} \\ E_{\|} \end{bmatrix} , \tag{A19}$$

with the appropriate signs being taken for $r_\perp$ and $r_{\|}$.

To confirm the accuracy of this description, consider a reflection of some circularly polarized light which requires the incoming resolved amplitudes, *E*, to be identical and with a phase difference, $(\delta_\perp - \delta_{\|})$, equal to either $+\pi/2$ or $-\pi/2$, according to the selected handedness. For example here $(\delta_\perp - \delta_{\|}) = \pi/2$ is selected, and, with reference to Figure A.1, this would correspond to an anti-clockwise rotation of *E* as seen in the receiving interface. At normal incidence, $r_\perp$ and $r_{\|}$ can be considered as identical, both being negative and taking a value of $-r$, say. Thus the reflective transformation may be summed up as

$$E\begin{bmatrix}1 & 0\\ 0 & -1\end{bmatrix}\begin{bmatrix}-r & 0\\ 0 & -r\end{bmatrix}\begin{bmatrix}\mathrm{e}^{\mathrm{i}\frac{\pi}{2}}\\ 1\end{bmatrix}, \tag{A20}$$

leading to

$$rE\begin{bmatrix}1 & 0\\ 0 & -1\end{bmatrix}\begin{bmatrix}-\mathrm{e}^{\mathrm{i}\frac{\pi}{2}}\\ -1\end{bmatrix}, \tag{A21}$$

in turn leading to

$$rE\begin{bmatrix}-\mathrm{e}^{\mathrm{i}\frac{\pi}{2}}\\ 1\end{bmatrix} = rE\begin{bmatrix}\mathrm{e}^{-\mathrm{i}\frac{\pi}{2}}\\ 1\end{bmatrix}. \tag{A22}$$

Thus, the phase of the emerging perpendicular component has been shifted by π relative to its input phase, thus describing a handedness change. It may be noted from earlier that, for angles of incidence greater than Brewster's angle, the 'tangent' formula given by (A5) provides a positive value for $r_{\|}$; application of Jones matrices as above for this situation shows that there is no handedness change on reflection.

A similar analysis for the refracted beam provides amplitude transmission coefficients of

$$t_{\perp} = \frac{2\cos\chi_{\mathrm{i}}\sin\chi_{t}}{\sin(\chi_{\mathrm{i}}+\chi_{t})}, \tag{A23}$$

and

$$t_{\|} = \frac{2\cos\chi_{\mathrm{i}}\sin\chi_{t}}{\sin(\chi_{\mathrm{i}}+\chi_{t})\cos(\chi_{\mathrm{i}}-\chi_{t})}. \tag{A24}$$

It may be noted that these coefficients are positive for all values of χ_{i}, and no sign changes are required to describe the progress of the refracted beam,

For more general situations, it is usually the intensity reflection and transmission coefficients that are of interest. They can be readily derived from the Fresnel amplitude coefficients, and a Mueller matrix can be established to describe the behaviour of an interface. For example, the basic matrix for reflection by a dielectric is similar to that of a partial polarizer, and may be written as

$$\frac{1}{2}\begin{bmatrix}(r_{\perp}^{2}+r_{\|}^{2}) & (r_{\perp}^{2}-r_{\|}^{2}) & 0 & 0\\ (r_{\perp}^{2}-r_{\|}^{2}) & (r_{\perp}^{2}+r_{\|}^{2}) & 0 & 0\\ 0 & 0 & 2r_{\perp}r_{\|} & 0\\ 0 & 0 & 0 & 2r_{\perp}r_{\|}\end{bmatrix}. \tag{A25}$$

The terms $r_{\perp}^{2}$ and $r_{\|}^{2}$ are automatically positive, while the resulting sign of the product, $r_{\perp}r_{\|}$, contained in elements, [3,3] and [4,4], depends on whether the angle of incidence is smaller (+ve) or larger (−ve) than Brewster's angle. In addition, consideration must again be given to the axial frame change caused by reflection. The effect of this is readily appreciated from the sketch in Figure A.2. When an instrument designed to record the Stokes parameters receives the radiation prior to reflection, the directions of both positive and negative Q and U may be projected against the xy-plane as shown. It may be noted that $+U$ is set at $+45°$ (rotated from x to y) relative to $+Q$. Following the reflection, to assess the modified Stokes parameters, the instrument must be rotated about the normal to the plane of incidence to receive the radiation. As a result, while $+Q$ and $-Q$ remain the same, the apparent directions of $+U$ and $-U$ are flipped by $90°$, as indicated in the right-hand side of the figure. The reversal of the direction of propagation also induces a handedness change. These two effects may be summarized by the application of a Mueller matrix given by

$$\begin{bmatrix} 1 & 0 & 0 & 0 \\ 0 & 1 & 0 & 0 \\ 0 & 0 & -1 & 0 \\ 0 & 0 & 0 & -1 \end{bmatrix}. \tag{A26}$$

It may be noted that this matrix is equivalent to one describing a phase change of π between the resolved components. It is, however, not a real physical change, but is simply the effect of the coordinate flip that a reflection imposes.

Overall, the reflection at a dielectric interface may therefore be expressed by

$$\begin{bmatrix} 1 & 0 & 0 & 0 \\ 0 & 1 & 0 & 0 \\ 0 & 0 & -1 & 0 \\ 0 & 0 & 0 & -1 \end{bmatrix} \begin{bmatrix} (r_\perp^2 + r_\parallel^2) & (r_\perp^2 - r_\parallel^2) & 0 & 0 \\ (r_\perp^2 - r_\parallel^2) & (r_\perp^2 + r_\parallel^2) & 0 & 0 \\ 0 & 0 & 2r_\perp r_\parallel & 0 \\ 0 & 0 & 0 & 2r_\perp r_\parallel \end{bmatrix} \tag{A27}$$

$$= \begin{bmatrix} (r_\perp^2 + r_\parallel^2) & (r_\perp^2 - r_\parallel^2) & 0 & 0 \\ (r_\perp^2 - r_\parallel^2) & (r_\perp^2 + r_\parallel^2) & 0 & 0 \\ 0 & 0 & -2r_\perp r_\parallel & 0 \\ 0 & 0 & 0 & -2r_\perp r_\parallel \end{bmatrix}. \tag{A28}$$

By considering the signs of the values of $r_\perp$ and $r_\parallel$, for insertion in this matrix, it is clearly apparent that, for angles of incidence from zero up to Brewster's angle, there is a handedness change for reflected circularly polarized light. For angles of incidence greater than Brewster's angle, there is no handedness reversal.

By using intensity reflection coefficients, $R_\perp$, $R_\parallel$, this Mueller matrix may be written as

$$\begin{bmatrix} (R_\perp + R_\parallel) & (R_\perp - R_\parallel) & 0 & 0 \\ (R_\perp - R_\parallel) & (R_\perp + R_\parallel) & 0 & 0 \\ 0 & 0 & -2\sqrt{R_\perp R_\parallel} & 0 \\ 0 & 0 & 0 & -2\sqrt{R_\perp R_\parallel} \end{bmatrix}, \tag{A29}$$

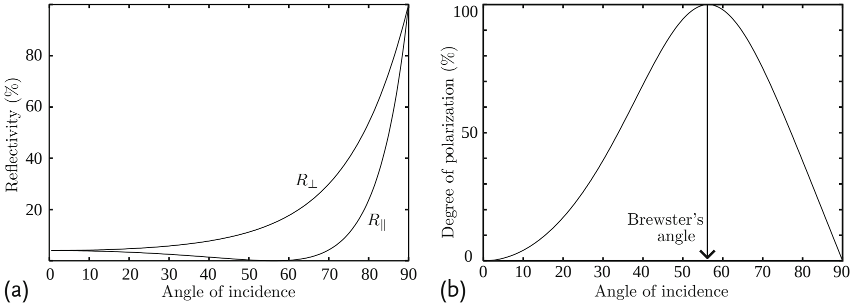

Fig. A.3 The intensity reflection coefficients, $R_\perp$, $R_\parallel$, for the directions of vibration perpendicular and parallel to the plane of incidence are plotted as a function of the angle of incidence for a dielectric interface with a refractive index ratio $n_t/n_\mathrm{i} = 1.5$ (a); (b) displays the degree of polarization produced by reflection. At Brewster's angle the reflected light is 100 per cent polarized, with a direction of vibration perpendicular to the plane of incidence.

but it must be remembered that the value of $\sqrt{R_\perp}$ carries a negative sign, and for $\sqrt{R_\parallel}$ the sign may be either '+ve', or '−ve', depending on the angle of incidence. The variation with angle of incidence of the numerical values of the resolved intensity coefficients, together with the engendered degree of polarization given by $p = (R_\perp - R_\parallel)/(R_\perp + R_\parallel)$ is depicted in Figure A.3 for a refractive index ratio of $n_t/n_\mathrm{i} = 1.5$.

The Mueller matrix for the change in polarization affecting the transmitted beam may be written as

$$\begin{bmatrix} (t_\perp^2 + t_\parallel^2) & (t_\perp^2 - t_\parallel^2) & 0 & 0 \\ (t_\perp^2 - t_\parallel^2) & (t_\perp^2 + t_\parallel^2) & 0 & 0 \\ 0 & 0 & 2t_\perp t_\parallel & 0 \\ 0 & 0 & 0 & 2t_\perp t_\parallel \end{bmatrix}. \tag{A30}$$

A.3
Reflection at a Dense- to Less-Dense Medium

If the refractive index of the first medium is higher than that of the second ($n_\mathrm{i} > n_t$), then the behaviour of the reflected wave becomes complicated above a certain angle of incidence referred to as the *critical angle*. Rewriting (A4) and (A9) in terms of the relative refractive index $n = n_t/n_\mathrm{i}$ gives

$$r_\perp = \frac{\cos\chi_\mathrm{i} - n\cos\chi_t}{\cos\chi_\mathrm{i} + n\cos\chi_t}, \tag{A31}$$

$$r_\parallel = \frac{\cos\chi_t - n\cos\chi_\mathrm{i}}{\cos\chi_t + n\cos\chi_\mathrm{i}}\ . \tag{A32}$$

Using the law of refraction, namely: $\sin\chi_{\mathrm{i}} = n\sin\chi_t$, the term $\cos\chi_t$ may be expressed as $\pm(1/n)\sqrt{n^2-\sin^2\chi_{\mathrm{i}}}$, allowing (A31) and (A32) to be rewritten as

$$r_{\perp} = \frac{\cos\chi_{\mathrm{i}} - (\pm\sqrt{n^2-\sin^2\chi_{\mathrm{i}}})}{\cos\chi_{\mathrm{i}} + (\pm\sqrt{n^2-\sin^2\chi_{\mathrm{i}}})}\,, \tag{A33}$$

$$r_{\parallel} = \frac{\pm\sqrt{n^2-\sin^2\chi_{\mathrm{i}}} - n^2\cos\chi_{\mathrm{i}}}{\pm\sqrt{n^2-\sin^2\chi_{\mathrm{i}}} + n^2\cos\chi_{\mathrm{i}}}\,. \tag{A34}$$

Since $n < 1$, for values of $\chi_{\mathrm{i}} \leqslant \arcsin(n)$, the square root is real, and there is no difficulty in deciding which of the alternative signs should be chosen, as χ_t is less than $\pi/2$, and $\cos\chi_t$ must be positive. For $\chi_{\mathrm{i}} > \arcsin(n)$, however, the square root, and hence $\cos\chi_t$, becomes imaginary, and care must be taken to resolve the sign ambiguity. This is a troublesome point as the literature bears testament. Many workers simply choose the positive sign, without considering the problem, and this has led to incorrect assessment of the phase changes on total internal reflection. In fact, Astronomer Royal Airy (1831), using an incorrect '+ve' sign for the Fresnel 'tangent' formula, accidentally obtained the correct answer to the Fresnel rhomb (Chapter 6) by arbitrarily and, as we shall see, incorrectly by choosing the '+ve' sign for the above square root.

The problem can be solved by considering the disturbance in the second medium. At some point, (y, z), with both values being positive (see Figure A.1) in the medium of the refractive index, n_t, the transmitted wave may be written in the form

$$E_{\mathrm{t}} = E_{\mathrm{t0}}\exp\left[i\omega\left(t - \frac{n_t}{c}\left(y\sin\chi_t + z\cos\chi_t\right)\right)\right], \tag{A35}$$

where E_{t0} is the amplitude of the transmitted disturbance. Since $\cos\chi_t$ is imaginary, and $\sin\chi_t$ real, but greater than one, (A35) can be rewritten as

$$\begin{aligned} E_{\mathrm{t}} = E_{\mathrm{t0}}&\exp\left[-i n_t\frac{\omega}{c}\cdot i\left(\pm\frac{1}{n}\sqrt{\sin^2\chi_t - n^2}\right)z\right] \\ &\times\exp\left[i\omega\left(t - \left(\frac{n_t}{c}\sin\chi_t\right)y\right)\right], \end{aligned} \tag{A36}$$

i. e. a disturbance oscillatory in y, and varying with z, according to

$$E_{\mathrm{t}}(z) = E_{\mathrm{t0}}\exp\left[\frac{\omega}{c}\frac{n_t}{n}\left(\pm\sqrt{\sin^2\chi_t - n^2}\right)z\right]. \tag{A37}$$

Depending on whether the positive or negative sign for the square root is selected, there will be an exponential increase, or decrease, in the amplitude of the disturbance. As it turns out, there is no energy in this transmitted wave, as the reflection coefficients for both parallel and perpendicular components are unity. The 'transmitted' E and H vectors are in quadrature, in fact, and the Poynting vector is consequently zero. The behaviour needs to be explored, however, for a situation in which the wave has travelled a small finite distance, z_1, at which point the refractive index reverts to n_i again. To do this, the boundary conditions at the second interface cannot be satisfied without the existence of an ordinary, energy-carrying wave proceeding into the second region of refractive index, n_i. This wave will have an amplitude of $E_\mathrm{t}(z_1)$, given by (A37), and therefore the negative sign for the square root must represent reality as, otherwise, by allowing larger and larger values of z_1, the energy flow would arbitrarily increase through the point. The disturbance in n_t must be attenuated with z, and consequently the 'minus' sign must be applied wherever the square root occurs.

Thus, for $\chi_t > \arcsin(n)$, (A33) and (A34) must be rewritten as

$$r_\perp = \frac{\cos\chi_\mathrm{i} + i\sqrt{\sin^2\chi_\mathrm{i} - n^2}}{\cos\chi_\mathrm{i} - i\sqrt{\sin^2\chi_\mathrm{i} - n^2}} = \frac{a + ib}{a - ib}\,, \tag{A38}$$

$$r_\parallel = \frac{-n^2\cos\chi_t - i\sqrt{\sin^2\chi_\mathrm{i} - n^2}}{n^2\cos\chi_t - i\sqrt{\sin^2\chi_\mathrm{i} - n^2}} = -\frac{a' + ib}{a' - ib}\,, \tag{A39}$$

where $a = a'/n^2$, $a' = n^2\cos\chi_\mathrm{i}$ and $b = \sqrt{\sin^2\chi_\mathrm{i} - n^2}$.

Both these complex reflection coefficients have a modulus of unity, since they are the ratios of complex conjugates, and so all the incident energy is reflected. They do, however, differ in phase as discussed later.

When the angle of incidence, χ_i, is *less than* the critical angle the positive alternative for the square root in (A33) and (A34) must be taken to give

$$r_\perp = \frac{\cos\chi_\mathrm{i} - \sqrt{n^2 - \sin^2\chi_\mathrm{i}}}{\cos\chi_\mathrm{i} + \sqrt{n^2 - \sin^2\chi_\mathrm{i}}}\,, \tag{A40}$$

$$r_\parallel = \frac{\sqrt{n^2 - \sin^2\chi_\mathrm{i}} - n^2\cos\chi_\mathrm{i}}{\sqrt{n^2 - \sin^2\chi_\mathrm{i}} + n^2\cos\chi_\mathrm{i}}\,. \tag{A41}$$

Both these reflection coefficients are real and, at $\chi_\mathrm{i} = 0$, they have the same sign, as they must. However, for $\chi_\mathrm{i} > \arctan(n)$, $r_\parallel$ becomes negative, i. e. it suffers a phase change of π. Thus from $\chi_\mathrm{i} > \arctan(n)$ up to the critical angle, the two components are out of phase by π.

For $\chi_\mathrm{i} > \arcsin(n)$, the real and imaginary parts of $r_\perp$ and $r_\parallel$ need to be determined from (A38) and (A39) in the following form

$$r_\perp = \left(\frac{a^2 - b^2}{a^2 + b^2}\right) + i\left(\frac{2ab}{a^2 + b^2}\right), \tag{A42}$$

$$r_\parallel = \left(\frac{b^2 - a'^2}{a'^2 + b^2}\right) + i\left(\frac{-2a'b}{a'^2 + b^2}\right). \tag{A43}$$

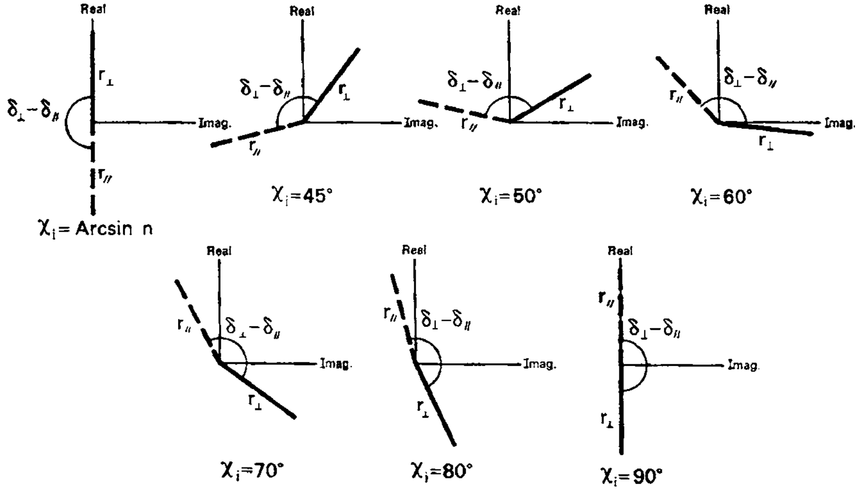

Fig. A.4 Amplitudes and phases of the reflection coefficients at total internal reflection in a dielectric as a function of the angle if incidence, χ_i, calculated for $n = 2/3$.

Since a, b and a' are all positive, it follows that the imaginary part of $r_\perp$ is always positive, whereas that of $r_\|$ is always negative. In Figure A.4 the behaviours of $r_\perp$ and $r_\|$ are plotted in the complex plane, for various values of χ_i above the critical angle. As χ_i increases, the *phase difference* between the reflected components falls below π passes through a minimum (and not a maximum, as is often stated) and then rises again to π at $\chi_\mathrm{i} = 90°$. The perpendicular component is, however, always ahead of the parallel one, and is *advanced* relative to the incident wave. The opposite is often stated and arises from the incorrect choice of sign for the square root.

The actual values of the phases, $\delta_\perp$ and $\delta_\|$, of the perpendicular and parallel components are easily determined from the real and imaginary parts as

$$\delta_\perp = 2\arctan\left(\frac{\sqrt{\sin^2\chi_\mathrm{i} - n^2}}{\cos\chi_\mathrm{i}}\right), \tag{A44}$$

$$\delta_\| = 2\arctan\left(\frac{\sqrt{\sin^2\chi_\mathrm{i} - n^2}}{n^2\cos\chi_\mathrm{i}}\right) - \pi\ . \tag{A45}$$

Any ambiguities arising from the nature of 'tangent' in these equations are resolved by using Figure A.4. An example of the behaviour of the phase difference $(\delta_\perp - \delta_\|)$ is shown in Figure A.5. For $\chi_\mathrm{i} < \arctan(n)$ the phase difference is zero; from $\chi_\mathrm{i} = \arctan(n)$ to $\chi_\mathrm{i} < \arcsin(n)$ the phase difference jumps to π and for $\chi_\mathrm{i} > \arcsin(n)$ up to $\pi/2$ it follows a smooth variation, with a minimum value occurring at an

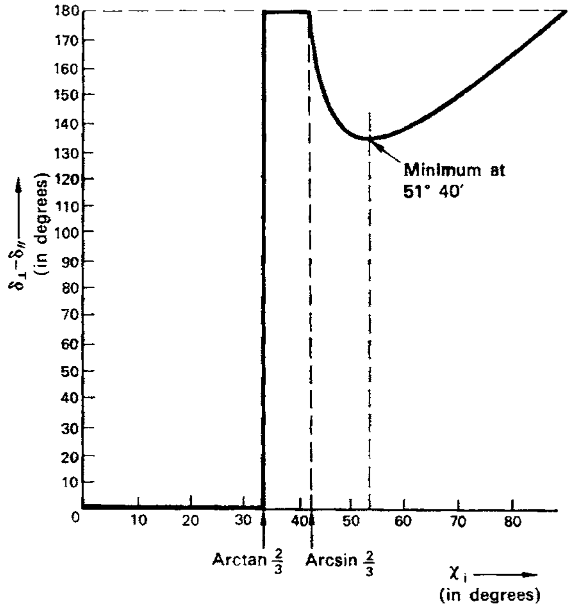

Fig. A.5 The variation of the phase difference, $\delta_\perp - \delta_\parallel$, at total internal reflection for a dielectric with $n = 2/3$.

angle of incidence given by

$$\cos \chi_i = +\sqrt{\frac{1-n^2}{1+n^2}} \, . \tag{A46}$$

The value of this minimum phase difference is given by

$$(\delta_\perp - \delta_\parallel)_{\min} = 4 \arctan(n) \, . \tag{A47}$$

The phase difference $(\delta_\perp - \delta_\parallel)$ is greater than $\pi/2$ for all values of n greater than $\left(\sqrt{2}-1\right)$, i. e. for all dielectrics with refractive indices less than $\left(\sqrt{2}+1\right)$. It is interesting to note that Lord Kelvin (1904) (see p. 388) commented on this as follows:

> We see that the phasal differences for internal reflection in glasses and all known transparent bodies of refractive index less than 2.414, are obtuse for all angles of incidence through the whole range of total internal reflection. This conclusion was very startling to myself, because for eighty years we have been taught that, for total internal reflection in glass, the phasal difference was an acute angle in a single reflection.

Inspection of the current literature frequently shows that some teaching still carries this error and ‘lessons have not been learned’.

A.4
Metallic Reflection

To describe metal reflection, the optical properties of the material require its refractive index to be considered as being complex. The classical texts show that alternative expressions are used with '+ve' and '−' being applied to the complex component. The two forms may be summarized by the expression:

$$\hat{n} = n(1 \pm i\kappa) , \tag{A48}$$

where n is the real part of the complex index, and κ is the attenuation index, or *extinction coefficient*. Rather than presenting all the arcane and laborious details for the determination of the amplitude reflection coefficients, with either the '*plus*' or '*minus*' sign being used, it may be assumed that their behaviour must be similar to that for a dielectric surface, particularly for small values of κ. Values of $r_\perp$ and $r_\parallel$ are always negative for the complete range of χ_i, from 0° to π/2. Unlike the behaviour of a dielectric, $r_\parallel$ is never zero, although its modulus displays a minimum at some angle of incidence, χ_p, referred to as the *principal angle of incidence*. In addition, each resolved component suffers a phase change from π to zero, but with differing values, according to the angle of incidence; a phase difference, $\varDelta = (\delta_\perp - \delta_\parallel)$, grows from zero to π as χ_i increases from 0° to π/2. At the principal angle, we have $\varDelta = \pi/2$.

Unless interference effects are under consideration, it is simply the intensity coefficients that need to be determined, together with the generated phase difference, to describe the behaviour of a metallic reflection. Overall a metallic reflection may be represented by

$$\begin{bmatrix} 1 & 0 & 0 & 0 \\ 0 & 1 & 0 & 0 \\ 0 & 0 & -1 & 0 \\ 0 & 0 & 0 & -1 \end{bmatrix} \times$$
$$\begin{bmatrix} (R_\perp + R_\parallel) & (R_\perp - R_\parallel) & 0 & 0 \\ (R_\perp - R_\parallel) & (R_\perp + R_\parallel) & 0 & 0 \\ 0 & 0 & 2\sqrt{R_\perp R_\parallel}\cos\varDelta & 2\sqrt{R_\perp R_\parallel}\sin\varDelta \\ 0 & 0 & -2\sqrt{R_\perp R_\parallel}\sin\varDelta & 2\sqrt{R_\perp R_\parallel}\cos\varDelta \end{bmatrix} , \tag{A49}$$

where the first matrix relates to the reflection of the axes, and the second describes the basic electromagnetic behaviour of the metallic reflection in the original coordinate frame. By multiplying out (A49), the final matrix may be written as

$$\begin{bmatrix} (R_\perp + R_\parallel) & (R_\perp - R_\parallel) & 0 & 0 \\ (R_\perp - R_\parallel) & (R_\perp + R_\parallel) & 0 & 0 \\ 0 & 0 & -2\sqrt{R_\perp R_\parallel}\cos\varDelta & -2\sqrt{R_\perp R_\parallel}\sin\varDelta \\ 0 & 0 & +2\sqrt{R_\perp R_\parallel}\sin\varDelta & -2\sqrt{R_\perp R_\parallel}\cos\varDelta \end{bmatrix} . \tag{A50}$$

It may be noted that as $r_\perp$ and $r_\parallel$ both carry the same sign (−ve), the numerical value of $\sqrt{R_\perp R_\parallel}$ is always positive. As $\varDelta$ takes values from zero to $\pi/2$, $\cos\varDelta$ and $\sin\varDelta$ are also always positive. Elements [3,3], [3,4] and [4,4] of the matrix in (A49) therefore carry negative values, while [4,3] is always positive.

According to Ditchburn (1952) the values of $R_\perp$ and $R_\parallel$, and their dependence on the angle of incidence, may be written as

$$R_\perp = \frac{n^2(1+\kappa^2)\cos^2\chi_\mathrm{i} - 2n\cos\chi_\mathrm{i} + 1}{n^2(1+\kappa^2)\cos^2\chi_\mathrm{i} + 2n\cos\chi_\mathrm{i} + 1}\,, \tag{A51}$$

$$R_\parallel = \frac{n^2(1+\kappa^2)\cos^2\chi_\mathrm{i} - 2n\cos\chi_\mathrm{i} + \cos^2\chi_\mathrm{i}}{n^2(1+\kappa^2)\cos^2\chi_\mathrm{i} + 2n\cos\chi_\mathrm{i} + \cos^2\chi_\mathrm{i}}\,. \tag{A52}$$

From knowledge of the values of n and κ, values of $R_\perp$ and $R_\parallel$ can be calculated for any angle of incidence.

The refractive index is given by

$$n \approx \frac{\sin\chi_\mathrm{i}\tan\chi_\mathrm{i}\cos 2\psi}{1+\sin 2\psi\cos\varDelta}\,, \tag{A53}$$

where ψ is equal to $\arctan(R_\perp/R_\parallel)$.

The extinction coefficient, κ, is given by

$$\kappa \approx \tan 2\psi \sin\varDelta\,. \tag{A54}$$

In determining the values of n and κ by experiment, the principal angle of incidence, χ_p, is generally sought by determining the angle of incidence which gives a maximum for the linear polarization produced from unpolarized light. As seen from the example of Figure A.6, at the principal angle, the value of $\varDelta = \pi/2$ so that

$$n = \sin\chi_p\tan\chi_p\cos 2\psi_p \quad \text{and} \quad \kappa \approx \tan 2\psi_p\,, \tag{A55}$$

where ψ_p is given by $\arctan(R_\perp/R_\parallel)$, determined from values of the two intensity reflection coefficients at χ_p.

In the presentation of metallic mirror reflection by Capitani, Cavallini, Ceppatelli, *et al.* (1989), they define X^2 as being equal to $R_\perp/R_\parallel$. The value of X^2, according to the angle of incidence, may be written as

$$X^2 = \frac{f^2+g^2-2f\sin\chi_\mathrm{i}\tan\chi_\mathrm{i}+\sin^2\chi_\mathrm{i}\tan^2\chi_\mathrm{i}}{f^2+g^2+2f\sin\chi_\mathrm{i}\tan\chi_\mathrm{i}+\sin^2\chi_\mathrm{i}\tan^2\chi_\mathrm{i}}\,, \tag{A56}$$

and the accompanying phase difference, $\varDelta$, between the orthogonal vibrations expressed by

$$\tan\varDelta = \frac{2g\sin\chi_\mathrm{i}\tan\chi_\mathrm{i}}{\sin^2\chi_\mathrm{i}\tan^2\chi_\mathrm{i}-(f^2+g^2)}\,, \tag{A57}$$

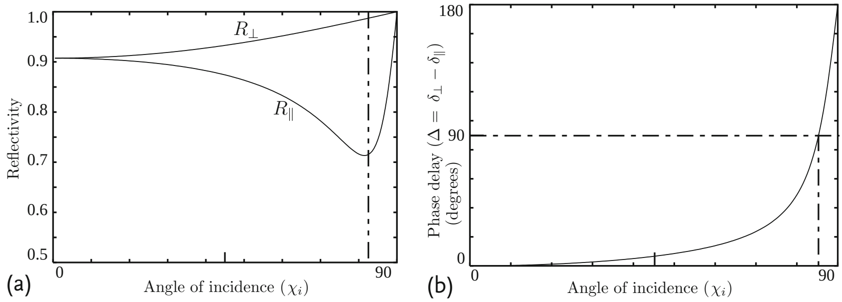

Fig. A.6 The behaviour of the intensity reflection coefficients, $R_\perp$ and $R_\parallel$, (a) and the phase delay, $\varDelta$, (b) with angle of incidence for a metallic surfaced coelostat mirror with $n = 1.036$ and $\kappa = 5.89$, these values determined experimentally by Capitani, Cavallini, Ceppatelli, *et al.* (1989). The vertical dashed line corresponds to the principal angle of incidence, χ_p, for which $R_\parallel$ is a minimum and $\varDelta = 90°$.

with the values of f and g given by

$$f^2 = \frac{1}{2}\left[n^2 - \kappa^2 - \sin^2\chi_\mathrm{i} + \left\{(n^2 - \kappa^2 - \sin^2\chi_\mathrm{i})^2 + 4n^2\kappa^2\right\}^{\frac{1}{2}}\right], \tag{A58}$$

$$g^2 = \frac{1}{2}\left[\kappa^2 - n^2 + \sin^2\chi_\mathrm{i} + \left\{(n^2 - \kappa^2 - \sin^2\chi_\mathrm{i})^2 + 4n^2\kappa^2\right\}^{\frac{1}{2}}\right]. \tag{A59}$$

They write the reflection matrix as

$$\frac{R_\perp}{2}\begin{bmatrix} X^2+1 & X^2-1 & 0 & 0 \\ X^2-1 & X^2+1 & 0 & 0 \\ 0 & 0 & 2X\cos\varDelta & 2X\sin\varDelta \\ 0 & 0 & -2X\sin\varDelta & 2X\cos\varDelta \end{bmatrix}. \tag{A60}$$

Expression (A60) differs from that of (A50) in terms of the signs of elements [3,3], [3,4], [4,3] and [4,4]. It may be noted, however, that Capitani, Cavallini, Ceppatelli *et al.* (1989) have defined $\varDelta$ to run from π to 0° for angles of incidence from 0° to $\pi/2$. As a consequence of their definition, $\varDelta$, corresponding to $(\pi - \varDelta)$, expressions (A50) and (A60) are equivalent; the former formulation is to be preferred, however, as at normal incidence, $\varDelta$ must be zero as the resolved components are indistinguishable.

A.5
Handedness Calibration

Finally, a comment may be made on the handedness of the circular polarization generated when linear polarized light is incident on a metal surface. As mentioned in Chapter 4, Swindell (1971) noted that when the **E**-vector of some incident linearly

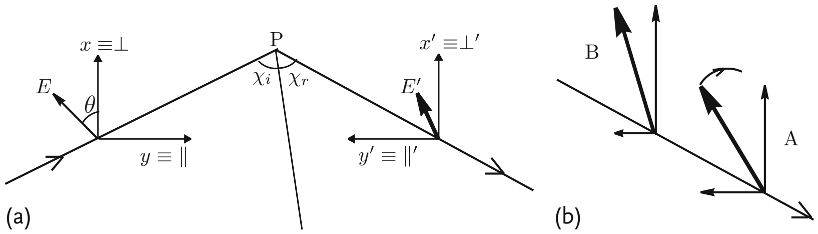

Fig. A.7 (a) depicts a beam of linear polarization, set at an angle, θ, in a clockwise direction as seen from the point P on the mirror surface, with the angle of incidence, χ_i, equal to the angle of reflection, χ_r. The xy- and $x'y'$-frames are right handed, and define the incoming and reflected beams; (b) depicts the temporal rotation of the E' vector of the reflected beam (see the text for fuller description).

polarized light is oriented in a direction given by a clockwise rotation, θ $(0 < \theta < \pi/2)$, from the plane of incidence when looking back into the source, then the reflected light is right-elliptically polarized.

This outcome can be readily investigated in a similar fashion to the establishment of (A19), using the Jones matrix approach. The described situation is sketched in Figure A.7 with the polarization vibration set at θ to the x-axis, the angle being clockwise as seen looking against the source, say from point, P, at which the beam is incident on the reflecting surface. In the depicted coordinate frame, the vibrations of the wave with amplitude, E, may be resolved into components in the $x \equiv\perp$ and $y \equiv\|$ directions. They may be described by a column vector in the form $\{E_\perp, E_\|\} = \{+E\cos\theta, -E\sin\theta\}$; for $\theta = 45°$, this may be rewritten as $E/\sqrt{2}\{1, -1\}$. The outcome of the reflection may be summarized by combining the effects of three matrices as follows

$$\frac{E}{\sqrt{2}}\underbrace{\begin{bmatrix}1 & 0\\ 0 & -1\end{bmatrix}}_{\text{Axis}}\underbrace{\begin{bmatrix}\mathrm{e}^{-\mathrm{i}\Delta} & 0\\ 0 & 1\end{bmatrix}}_{\text{Phase}}\underbrace{\begin{bmatrix}r_\perp & 0\\ 0 & r_\|\end{bmatrix}}_{\text{Reflection}}\begin{bmatrix}1\\ -1\end{bmatrix}. \tag{A61}$$

The reflection matrix holds the values of the orthogonal amplitude reflection coefficients. Both these are numerically negative, although this does not affect the outcome; the important thing is that they have the same sign. The phase matrix is written expressing the differential phase delay as $\Delta = (\delta_\perp - \delta_\|)$, its value being positive; the perpendicular component suffers a greater retardance, $\delta_\perp$, relative to that of the parallel component, $\delta_\|$. For small angles of incidence, the value of Δ is small, but grows very quickly for $\chi_i > 45°$. Finally, the axis matrix describes the effect of the change of reference frame as a result of the reflection. By multiplying the three matrices, a description of the emergent component vectors can be written as

$$\begin{bmatrix}E'_\perp\\ E'_\|\end{bmatrix} = \frac{E}{\sqrt{2}}\begin{bmatrix}r_\perp \mathrm{e}^{-\mathrm{i}\Delta}\\ r_\|\end{bmatrix}. \tag{A62}$$

The behaviour of the disturbances in an xy-plane, as seen against the reflected direction of propagation, can be appreciated by considering a particular time when the parallel component is at a maximum with the perpendicular component lagging, according to its larger phase retardation. In Figure A.7b, the depiction 'A' represents a time when the E' vector has components with $E'_{\|}$ at its maximum, say, and $E'_{\perp}$ approaching its maximum, as it is more delayed in phase relative to the parallel component; the sketch shows $E'_{\perp}$ to be larger than $E'_{\|}$, this simply reflecting the fact that the magnitude of $r_{\perp}$ is larger than $r_{\|}$. The depiction marked 'B' corresponds to a moment later with $E'_{\|}$ reduced from its maximum, and $E'_{\perp}$ increasing towards its maximum, causing their vector addition to rotate as indicated. As can be appreciated, a snapshot picture of the behaviour of the compounded vector of E' along the direction of propagation would be in the form of a right-handed helix. As time progresses, the helix advances without rotation, and in a given plane, E', rotates with its locus executing an ellipse in a clockwise direction as seen by the observer (see page 2.2 in Chapter 2). This sense of rotation, within the general optical arena is defined as *right-handed polarization*. The outcome is the same if the values of the amplitude reflection coefficients had both been positive.

If originally the linear polarization had been set with $\theta = -45°$, the incoming electric disturbances would have been written as $1/\sqrt{2}\{+E, +E\}$, with the resultant being written as

$$\begin{bmatrix} E'_{\perp} \\ E'_{\|} \end{bmatrix} = \frac{E}{\sqrt{2}}\begin{bmatrix} r_{\perp}\mathrm{e}^{-\mathrm{i}\Delta} \\ -r_{\|} \end{bmatrix} \equiv \frac{E}{\sqrt{2}}\begin{bmatrix} r_{\perp}\mathrm{e}^{-\mathrm{i}(\Delta+\pi)} \\ r_{\|} \end{bmatrix}, \tag{A63}$$

with the executed ellipse being drawn out in an anti-clockwise direction.

A.5.1
IAU Definitions

The earlier exercise provides confirmation for the definitions associated with position angle of linear polarization, and of handedness of elliptical polarization, as adopted by the IAU (see page 4.5 in Chapter 4). With reference to Figure 4.6, a value of $\theta = -45°$, as above, corresponds to a positive value of $\zeta = +45°$, North through East, with P in Figure A.7 acting as the viewing point of the observer. The electric vector of the reflected radiation seen by the observer's new position looking against P, would rotate anti-clockwise, this being equivalent of ζ increasing positively, North through East. Such a rotational sense is defined by the IAU as being *right-handed*.

References

Airy, G.B. (1831) See p. 364 in *Mathematical Tracts*, Cambridge. [376]

Capitani, C., Cavallini, F., Ceppatelli, G., Landi Degl'innocent, E., Landi Degl'innocent, M., Landolfi, M., Righini, A. (1989) Polarization properties of a 'Zeiss-Type' coelostat: the case of the olar tower in Arcetri. *Sol. Phys.*, **120**, 173–191. [382, 381, 382]

Clarke, D., Grainger, J.F. (1971) *Polarized Light and Optical Measurement*. Pergamon, Oxford. [367]

Ditchburn, R.W. (1952) *Light*. Blackie & Son, London and Glasgow. [381]

Fresnel, A.J. (1876) *Œuvres Complètes d'Augustin Fresnel*, Vol 1, (eds Henri de Senarmont, Émile Verdet and Léonor Fresnel), Imprimerie Impériale, Paris. [370, 370]

Lord Kelvin (1904) *Baltimore Lectures – 1884*, Cambridge University Press, Cambridge. [370, 371, 379]

Swindell, W. (1971) Handedness of polarization after metallic reflection of linearly polarized light. *J. Opt. Soc. Am.*, **61**, 212–215. [382]

Appendix B
Papers of the *AJ* Series

For some 20 years the *Astronomical Journal* ran a series of papers with the comprehensive title of (*The*) *Wavelength Dependence of Polarization*. Forty works were published under this heading. Although some of them were devoted to lunar and planetary matters, a full listing of all of them is provided below in numerical order.

Gehrels, T. (1960) The wavelength dependence of polarization. I. Instrumental polarization. *AJ*, **65**, 466–469.

Gehrels, T. (1960) The wavelength dependence of polarization. II. Interstellar polarization. *AJ*, **65**, 470–472.

Gehrels, T., Coffeen, T., Owings, D. (1964) Wavelength dependence of polarization. III. The lunar surface. *AJ*, **69**, 826–852.

Gehrels, T., Coffeen, T., Owings, D. (1965) Erratum: wavelength dependence of polarization. III. The lunar surface. *AJ*, **70**, 447.

Coffeen, D.L. (1965) Wavelength dependence of polarization. IV. Volcanic cinders and particles. *AJ*, **70**, 403–413

Gehrels, T., Silvester, A.B. (1965) Wavelength dependence of polarization. V. Position angles of interstellar polarization. *AJ*, **70**, 579–580.

Gehrels, T. (1966) Wavelength dependence of polarization. VI. Molecular scattering at the skin of interstellar particles. *AJ*, **71**, 62–63.

Gehrels, T., Meltzer, A.S. (1966) Wavelength dependence of polarization. VII. Interstellar polarization. *AJ*, **71**, 111–113.

Coyne (SJ), G.V., Gehrels, T. (1966) Wavelength dependence of polarization. VIII. Interstellar polarization. *AJ*, **71**, 355–362

Gehrels, T. (1967) Wavelength dependence of polarization. IX. Interstellar particles. *AJ*, **72**, 631–641

Coyne (SJ), G.V., Gehrels, T. (1967) Wavelength dependence of polarization. X. Interstellar polarization. *AJ*, **72**, 887–898.

Coyne (SJ), G.V., Kruszewski, A. (1968) Wavelength dependence of polarization. XI. MU Cephei. *AJ*, **73**, 20–25.

Kruszewski, A., Gehrels, T., Serkowski, K. (1968) Wavelength dependence of polarization. XII. Red variables. *AJ*, **73**, 677–687.

Serkowski, K., Gehrels, T., Wiśniewski, W. (1969) Wavelength dependence of polarization. XIII. Interstellar extinction and polarization correlations. *AJ*, **74**, 85–90.

Stellar Polarimetry. David Clarke

ISBN: 978-3-527-40895-5

Gehrels, T., Herman, B.M., Owen, T. (1969) Wavelength dependence of polarization. XIV. Atmosphere of Jupiter. *AJ*, **74**, 190–199.

Coffeen, D.L., Gehrels, T. (1969) Wavelength dependence of polarization. XV. Observations of Venus. *AJ*, **74**, 433–445.

Coffeen, D.L. (1969) Wavelength dependence of polarization. XVI. Atmosphere of Venus. *AJ*, **74**, 446–460.

Coyne (SJ), G.V., Kruszewski, A. (1969) Wavelength dependence of polarization. XVII. Be-type stars. *AJ*, **74**, 528–532.

Coyne (SJ), G.V., Wickramasinghe, N.C. (1969) Wavelength dependence of polarization. XVIII. Interstellar polarization. *AJ*, **74**, 1179–1190.

Pellicori, S.F. (1969) Wavelength dependence of polarization. XIX. Comparison of the lunar surface with laboratory samples. *AJ*, **74**, 1066–1072.

Coyne (SJ), G.V., Pellicori, S.F. (1970) Wavelength dependence of polarization. XX. The integrated disk of the Moon. *AJ*, **75**, 54–60.

Zellner, B. (1970) Wavelength dependence of polarization. XXI. R Monocerotis. *AJ*, **75**. 182–185.

Zellner, B., Morrison, N.D. (1971) Wavelength dependence of polarization. XXII. Observations of novae. *AJ*, **76**, 645–650.

Zellner, B. (1971) Wavelength dependence of polarization. XXIII. Dust grains in novae. *AJ*, **76**, 651–654.

Kruszewski, A. (1971) Wavelength dependence of polarization. XXIV. Infrared objects. *AJ*, **76**, 576–580.

Coyne, G.V. (1974) Wavelength dependence of polarization. XXV. Rotation of the position angle by the interstellar medium. *AJ*, **79**, 565–580.

Coyne (SJ), G.V., Gehrels, T., Serkowski, K. (1974) Wavelength dependence of polarization. XXVI. The wavelength of maximum polarization as a characteristic parameter of interstellar grains. *AJ*, **79**, 581–589.

Gehrels, T. (1974) Wavelength dependence of polarization. XXVII. Interstellar polarization from 0.22 to 2.2 micron. *AJ*, **79**, 590–593.

Shawl, S.J. (1975) Wavelength dependence of polarization. XXVIII – Circumstellar scattering: Polarization and reddening models. *AJ*, **80**, 595–601.

Shawl, S.J. (1975) Wavelength dependence of polarization. XXIX. Observations of red variable stars. *AJ*, **80**, 602–624.

Coyne, G.V., McLean, I.S. (1975) Wavelength dependence of polarization. XXX. Intrinsic polarization in phi Persei. *AJ*, **80**, 702–710.

Kruszewski, A., Coyne, G.V. (1976) Wavelength dependence of polarization. XXXI. Cool stars. *AJ*, **81**, 641–649.

Coyne, G.V., Magalhães, A.M. (1977) Wavelength dependence of polarization. XXXII. Narrow-band polarization effects in cool stars. *AJ*, **82**, 908–915.

Coyne, G.V., Tapia, S., Vrba, F.J. (1979) Wavelength dependence of polarization. XXXIII – The Alpha Persei star cluster. *AJ*, **84**, 356–369.

Gehrels, T., Gradie, J.C., Howes, M.L., Vrba, F.J. (1979) Wavelength dependence of polarization. XXXIV – Observations of Venus. *AJ*, **84**, 671–682.

Lane, W.A. (1979) Wavelength dependence of polarization. XXXV – Vertical structure of scattering layers above the visible Venus clouds. *AJ*, **84**, 683–691.

Coyne (SJ), G.V., Magalhães, A.M. (1979) Wavelength dependence of polarization. XXXVI – Changes in polarization across TiO bands in cool stars. *AJ*, **84**, 1200–1210.

Dollfus, A., Auriére, M., Santer, R. (1979) Wavelength dependence of polarization. XXXVII – Regional observations of Venus. *AJ*, **84**, 1419–1436.

Santer, R., Herman, M. (1979) Wavelength dependence of polarization. XXXVIII – Analysis of ground-based observations of Venus. *AJ*, **84**, 1802–1810.

Santer, R., Dollfus, A. (1980) Wavelength dependence of polarization. XXXIX – Venus UV cloud model from polarimetry. *AJ*, **85**, 564–572.

Santer, R., Dollfus, A. (1980) Wavelength dependence of polarization. XXXX – Venus upper atmosphere aerosol layers from polarimetry. *AJ*, **85**, 751–764.

Appendix C
Reference Abbreviations

In the Reference Citations, abbreviations have been used for identifying the source Journals and origins of publication. Those which are not common within the literature should be sufficiently self-explicit as to be readily identifiable. For the record, most of them, but not all, are listed below.

A&A Astronomy and Astrophysics
A&AS Astronomy and Astrophysics Supplement (Series)
Abastumanskaya Astrofiz. Obs. Byull Abastumanskaia Astrofizicheskaia Observatoriia Biulleten
Accad. Naz. dei Lincei Accademia Nazionale dei Lincei
Acta Astron. Acta Astronomica
AJ Astronomical Journal
Am. J. Phys. American Journal of Physics
Ann. Acad. Sci. Fennicae Annales Academiæ Scientiarum Fennicæ
Ann. d'Astr. Annales d'Astrophysique
Ann. de Chimie et de Physique Annales de chimie et de physique
Ann. Phys. Annalen der Physik
ApJ Astrophysical Journal
ApJS Astrophysical Journal Supplement (Series)
Appl. Opt. Applied Optics
Ark. för Astron. Arkiv for Astronomi
Astr. Abh. Hamburg Stern. Astronomische Abhandlungen der Hamburger Sternwarte
Astr. Circ. USSR Astronomical Circular of the USSR
Astron. Gesellschaft Abstract Series Astronomische Gesellschaft Abstract Series
Astrophys. Lett. Astrophysical Letters
Astrophys. Space Sci. Astrophysics and Space Science
Bell Systems Tech. J. Bell System Technical Journal
Bull. Astron. Inst. Czech. Bulletin of the Astronomical Institutes of Czechoslovakia
Bull. Astron. Soc. India Bulletin of the Astronomical Society of India
Bull. Obs. Astron. Belgrade Bulletin de l'Observatoire Astronomique de Belgrade

Stellar Polarimetry. David Clarke

ISBN: 978-3-527-40895-5

ChemPhysChem A Journal of Chemical Physics and Physical Chemistry – Published by Wiley
Cont. Astron. Obs. Skalnaté Pleso Contributions of the Astronomical Observatory Skalnate Pleso
CR Comptes Rendus de l'Académie des sciences
Edinburgh New Philos. J. Edinburgh New Philosophical Journal
Indian Inst. Astrophys. Newsl. Indian Institute of Astrophysics Newsletter
JETP Lett. Letters to Journal of Experimental and Theoretical Physics
J. Atmos. Terr. Phys. Journal of Atmospheric and Terrestrial Physics
JBAS Journal of the British Astronomical Society
J. Chem. Phys. Journal of Chemical Physics
J. Opt. Soc. Am. (A) Journal of the Optical Society of America (A)
J. Quant. Spectrosc. Radiat. Transf. Journal of Quantitative Spectroscopy & Radiative Transfer
J. R. Astron. Soc. Can. Journal of the Royal Society of Canada
J. Sci. Inst. Journal of Scientific Instruments
Mem. della Soc. Astronomica Italiana Memorie della Societa Astronomica Italiana
Mem. R. Astron. Soc. Memoirs of the Royal Astronomical Society
MNRAS Monthly Notices of the Royal Astronomical Society
Naturwiss. Naturwissenschaften
Nauch. Inf. Ser. Astrofiz. Nauchnye Informatsii Informatsii – Astronomicheskij Soviet Akademii Nauk SSSR
PASP Publications of the Astronomical Society of the Pacific
Philos. Mag. Philosophical Magazine
Philos. Trans. R. Soc. Philosophical Transactions of the Royal Society
Phys. Rev. Physical Review
Phys. Rev. Lett. Physical Review Letters
Phys. Zeitschr. Physikalische Zeitschrift
Planet. Space Sci. Planetary and Space Science
Proc. Astron. Soc. Australia Proceedings of the Astronomical Society of Australia
Proc. Indian Acad. Sci. Proceedings of the Indian Academy of Science
Proc. IRE Proceedings of the Institute of Radio Engineers
Proc. Phys. Soc. London Proceedings of the Physical Society of London
Proc. R. Soc. London Proceedings of the Royal Society London
Pub. Astron. Soc. Japan Publications of the Astronomical Society of Japan
Publ. Astron. Opseratorije Beogr. Publications de l'Observatoire Astronomique de Beograd
Pubs. Obs. Astron. Beograd. Publications de l'Observatoire Astronomique de Beograd
Q. J. R. Astron. Soc. Quarterly Journal of the Royal Astronomical Society
Q. Newsl. Indian Inst. Astrophys. Quarterly Newsletter of the Indian Institute of Astrophysics
Rev. d'Opt. Revue d'Optique
Ric. Astron. Spec. Vaticana Richerche Astronomiche Specola Vaticana
Sci. Proc. R. Soc. Dublin Scientific Proceedings of the Royal Society of Dublin

Sol. Phys. Solar Physics
Soob. Byurakan Obs. Soobshcheniya Byurakanskoj Observatorii
Sov. Astron. Soviet Astronomy – AJ
Sov. Astron. Lett. Soviet Astronomy Letters
Stockholms Obs. Ann. Stockholms Observatoriums Annaler
Tokyo Astron. Bull. Tokyo Astronomical Bulletin
Trudy Astron. Obs. Leningrad Trudy Astronomicheskoj Observatorii Leningrad
Vat. Obs. Pubs. Vatican Observatory Publications
Veröff. Astr. Rechen-Inst. Heidelberg Veroeffentlichungen des Astronomischen Rechen-Instituts Heidelberg
Veröff. der Univ.-Sternwarte zu Göttingen Veröffentlichungen der Universitäts-Sternwarte zu Göttingen
Vistas. Astron. Vistas in Astronomy
Zeit. für Astrophysik Zeitschrift für Astrophysik
Zeit. Optik Zeitschrift Optik
Zeit. Phys. Zeitschrift für Physik

Acknowledgements

Many of the figures have been prepared by the author but some are taken directly from Journals and due acknowledge is made here to the Editors and original Authors of the papers.

Permission for reproduction of material from *Monthly Notices of the Royal Astronomical Society*, related to Figures: 1.4, 8.4, 13.9, 15.4, has been granted by Wiley-Blackwell.

Figures: 5.2, 5.3, 5.4, 5.9, 9.3, 9.4, 9.6, 11.1, 12.2, 12.3, 13.3, 13.5, 14.1, 14.4, 14.5, 14.6, 14.7, originally published in *Astronomy & Astrophysics*, are reproduced with permission © ESO.

For material from the *Astrophysical Journal*, agreements were obtained from the various authors, where appropriate, and through IOP Publishing Limited, and the following Figures are "Reproduced by permission of the AAS": 10.1, 10.2, 10.3, 12.4, 13.1, 13.4, 13.7, 13.10, 13.11, 14.2, 14.3, 15.2, 15.3, 15.4.

In addition, Figure: 8.3 is reproduced with permission of IOP Publishing Limited.

Stellar Polarimetry. David Clarke

ISBN: 978-3-527-40895-5

Author Index

Stellar Polarimetry. David Clarke
Copyright © 2010 WILEY-VCH Verlag GmbH & Co. KGaA, Weinheim
ISBN: 978-3-527-40895-5

Cited Stars/Objects

Stellar Polarimetry. David Clarke

ISBN: 978-3-527-40895-5

General Index

Stellar Polarimetry. David Clarke

ISBN: 978-3-527-40895-5